Geochemistry of Northeast China Cenozoic Basalts and Experimental Study on Crystal Dissolution

by

Yang Chen

A dissertation submitted in partial fulfillment
of the requirements for the degree of
Doctor of Philosophy
(Geology)
in The University of Michigan
2008

Doctoral Committee:

Professor Youxue Zhang, Chair
Professor James R. Barber
Professor Eric J. Essene
Professor Rebecca A. Lange
Professor Samuel B. Mukasa

To my grandpa

Acknowledgements

My Ph.D. work summarized in this dissertation lies upon the effort and help of many people. As my advisor, Dr. Youxue Zhang had the most profound influence, with his intelligent ideas and the courage and persistence to pursue them. My thesis committee members, Drs. Eric Essene, Becky Lange and Sam Mukasa, provided valuable inspirations, suggestions, questions and criticisms through very different personal styles. Dr. James Barber's help on my specific science questions was always timely and comprehensive. As a cognate member in my committee, he introduced me the beauty of a quite different science subject, containing stress, strain and complicated mathematics. I must mention that sitting in my committee members' classes was a great experience. The enthusiasm they conveyed during their teaching is one important driving force to me. The merits I saw in them and all the things I gained from them will certainly strongly affect my future science path.

Field trips to Northeast China were helped by Bolu Jin, Jianbo Shao and other colleagues at Shenyang Geological Academy, Ruishan Li, Yaoqi Zhou, Shiyong Yan, Zhicong Zhang, Qitao Lv, Baoshu Piao, and Xiaochen Han. As being in the same research group, I learned about piston-cylinder experiments and Fourier transform infrared spectroscopy from Zhengjiu Xu, Hejiu Hui and Huaiwei Ni. Discussion on various science and technique problems with them is a vital research activity for me. I learned microbeam usage from Carl E. Henderson and Zeb Page. The effort and help

from the above people enabled me to produce the data reported in this dissertation. In addition, Zeb Page wisely foresaw that someone (as me) would use his dissertation as formatting guideline and kindly put encouragement to following students in his acknowledgements.

Lastly, I would like to thank all the people who indirectly contributed to my thesis work, including my parents, Ji Chen and Yuansheng Yang, my girlfriend, Jing Zhou, my friends and my graduate students colleagues.

Table of Contents

List of Figures

List of Tables

List of Appendices

Chapter I

Introduction

Intraplate (i.e., not along plate boundaries) volcanism is important, but it is much less well understood than volcanism along plate boundaries. Within the framework of plate tectonics theory and with the understanding of the geochemistry and thermodynamics of the mantle, volcanism along plate boundaries is explained mostly by mantle partial melting and occasionally by slab melting, triggered by the relative motion of the plates and the resultant physical and chemical processes. At divergent plate boundaries (i.e., mid-ocean ridges and continental rift zones), the plates move apart and the mantle upwells. As the temperature of the upwelling material intercepts its solidus temperature, partial melting occurs. At convergent plate boundaries when an oceanic crust is subducted beneath another oceanic or continental crust (i.e., subduction zone), volatiles (H_2O, CO_2, and others) are delivered to the mantle, lowering its solidus and causing partial melting in or above the subducted slab. Crisp (1984) compiled a global dataset on long-term averaged volumetric rates (km^3yr^{-1}) of magma emplacement and volcanic output. Her data showed that 75% of the total rate averaged over the last 180 Ma is contributed by magmatism along mid-ocean ridges, and about 20% from subduction zones. Hence, plate boundary settings contribute volumetrically about 95% of the

volcanism on the Earth. The remaining 5% comes from intraplate settings, with oceanic intraplate settings contributing more than continental intraplate settings. The dominant role of mid-ocean ridges in contributing to the long-term global volcanism, however, is due to its large geographic magnitude (65,000 km long × a few km wide volcanic belt at present) and continuous magmatic activity, in contrast to intraplate volcanism. Taking the volcanic active surface area into account, intraplate volcanism can also be very vigorous. Intraplate volcanism may contribute a strong disturbance to the Earth's surface environment. For example, Self et al. (2008) estimated that eruptions of Deccan flood basalt province might have released 3.6×10^3 to 5.4×10^3 Tg of SO_2 to the atmosphere over time periods of years to decades. The annual release rate is estimated to be several times larger than recent anthropogenic emissions of SO_2 (80 Tg of S). Intraplate volcanism as in this extreme case may have a severe impact on global climate.

Intraplate volcanism provides the opportunity to study the mantle chemistry far from plate boundaries. It produces a wide range of rock compositions, which carry unique chemical characteristics and involve complex igneous evolution processes. Furthermore, direct mantle samples are often brought to the surface by intraplate basaltic eruptions. A wealth of information about the mantle source and the pathway to the surface can be obtained from study of these samples. An example is the helium isotope ratio $^3He/^4He$. The $^3He/^4He$ ratio in mid-ocean ridge basalts (MORB) is between 6 to 10 times the atmospheric ratio (Graham 2002). In contrast, mantle samples from oceanic intraplate settings such as Hawaii display $^3He/^4He$ ratios in a wide range, up to about 40 times the atmospheric ratio (Kurz et al., 1983; Hilton et al., 1999). The high ratios are

usually considered to reflect a relative ^{3}He enrichment in less degassed and presumably deeper mantle sources (e.g., Kurz et al. 1983; Class and Goldstein 2005).

Chapter II studies the intraplate volcanism in Northeast China. The origin of intraplate volcanism has been the subject of continued controversy. Two commonly proposed mechanisms are (i) mantle plumes and hot spots (i.e., thermal anomalies in the mantle), such as at Hawaii and Yellowstone; (ii) continental rift, such as at the East African Rift. Intraplate volcanism occurred in Northeast China from about 80 Ma to 300 years ago. About 590 volcanoes and 50000 km^2 volcanic rocks have been documented (Liu, 1999). Numerous studies have been conducted on various aspects of the volcanism, and its origin remains under debate. In addition to the above two commonly invoked mechanisms, other hypothesis include: (1) back-arc extension caused by subduction of Kula-Pacific plate (e.g., Basu et al., 1991; Liu et al., 2001; Ren et al., 2002); (2) mantle upwelling while crossing from a thick lithosphere to a thin lithosphere (Niu, 2005), and (3) thinning/delamination of the lithosphere beneath the northeast portion of mainland Asia (e.g., Griffin et al., 1998; Menzies and Xu, 1998; Wilde et al., 2003). The goal of this study is to test these hypotheses using the geochemistry of the basalts and entrained mantle xenoliths. This chapter was published in Chen et al. (2007).

The interaction between the xenocrysts and xenoliths and hosting magma is a subject closely related to intraplate volcanism, because xenocrysts and xenoliths commonly occur in volcanic rocks from intraplate settings. The interaction is an important process in magma evolution. Depending on the thermodynamic stauts of the system, crystal may grow or dissolve. Dissolution of one mineral may lead to growth of another mineral. If the thermodynamics is understood, constrains about the thermal

history of the system may be inferred from the reaction textures between xenocrysts and xenoliths and hosting magma. Furthermore, if the kinetics of the reaction is understood, the magnitude of the reaction textures can be used to infer the time scale of the magma evolution. Chapters III and IV are experimental and theoretical studies on crystal dissolution with applications to the thermal history and evolution time scale of basalts in Northeast China.

Dissolution involves interface reaction (components detaching from the crystal) and mass transfer in the melt (dissolved components migrating away from the interface). Mass transfer is necessary when the compositions of the crystal and the melt are different, which is generally the case in nature. Mass transfer is likely accomplished with convection arising from the relative motion between the crystal and the melt driven by the density contrast. A theory to calculate the dissolution or growth rate in this condition was initially proposed by Kerr (1995) and later expanded and applied to some geologically interesting problems by Zhang and Xu (2003, 2008), Zhang (2005), Zhang and Kling (2006). To apply this theory to crystal dissolution in silicate melts, it is critical to know the diffusivity of the dissolving components in the melt and the interface melt composition.

Experiments were conducted on two minerals: olivine and clinopyroxene. Chapter III is devoted to olivine dissolution (Chen and Zhang, 2008), and Chapter IV is devoted to clinopyroxene dissolution. Olivine is the most abundant mineral in the upper mantle, and it is a major phase in mantle xenoliths. Clinopyroxene is also an abundant mantle mineral. Furthermore, clinopyroxene is more compatible to incompatible elements compared to other mantle minerals such as olivine and orthopyroxene. It is an important

reservoir for the imcompatible elements. The reaction between clinopyroxene and hosting magma may significantly affect the geochemistry of the magma.

References

Basu A.R., Wang J.-W., Huang W.-K., Xie G.-H., Tatsumoto M. (1991) Major element, REE, and Pb, Nd and Sr isotopic geochemistry of Cenozoic volcanic rocks of eastern China: implications for their origin from suboceanic-type mantle reservoirs. *Earth and Planetary Science Letters* **105**, 149-169.

Chen Y., Zhang. Y., Graham, D., Su, S., Deng, J. (2007) Geochemistry of Cenozoic basalts and mantle xenoliths in Northeast China. *Lithos* **96**, 108-126.

Chen Y., Zhang Y. (2008) Olivine dissolution in basaltic melt. *Geochim. Cosmochim. Acta*. doi 10.1016/j.gca.2008.07.014.

Class C., Goldstein S.L. (2005) Evolution of helium isotopes in the Earth's mantle. *Nature* **436**, 1107-1112.

Crisp J.A. (1984) Rates of magma emplacement and volcanic output. *Journal of Volcanology and Geothermal Research* **20**, 177-211.

Graham D.W., (2002) Noble gas isotope geochemistry of mid-ocean ridge and ocean island basalts: characterization of mantle source reservoirs. *Reviews in Mineralogy & Geochemistry* **47**, 247-317.

Griffin W.L., Zhang A., O'Reilly S.Y., Ryan C.G. (1998) Phanerozoic evolution of the lithosphere beneath the Sino-Korean Craton. In: Flower, M.F.J., Chung, S.-L., Lo, C.-H., Lee, T.-Y., (eds.), Mantle dynamics and plate interactions in east Asia 27, American Geophysical Union.

Hilton D.R., Gronvold K., Macpherson C.G., Castillo P.R. (1999) Extreme $^{3}He/^{4}He$ ratios in northwest Iceland: constraining the common component in mantle plumes. *Earth and Planetary Science Letters* **173**, 53-60.

Kerr R.C. (1995) Convective crystal dissolution. *Contrib Mineral Petrol* **121**, 237-246.

Kurz M.D., Jenkins W.J., Hart S.R., Clague D. (1983) Helium isotopic variations in volcanic rocks from Loihi Seamount and the island of Hawaii. *Earth and Planetary Science Letters* **66**, 388-406.

Liu J.-Q. (1999) Chinese Volcanoes (in Chinese), Science Press, Beijing.

Liu J.-Q., Han J.-T., Fyfe W.S. (2001) Cenozoic episodic volcanism and continental rifting in northeast China and possible link to Japan Sea development as revealed from K-Ar geochronology. *Tectonophysics* **339**, 385-401.

Menzies M.A., Xu Y.-G. (1998) Geodynamics of the North China Craton. In: Flower M.F.J., Chung S.-L., Lo C.-H., Lee T.-Y., (eds.), Mantle dynamics and plate interactions in east Asia 27, American Geophysical Union.

Niu Y.-L. (2005) Generation and evolution of basaltic magmas: some basic concepts and a new view on the origin of Mesozoic-Cenozoic basaltic volcanism in Eastern China. *Geological Journal of China Universities* **11**, 9-46.

Ren J.-Y., Tamaki K., Li S., Zhang J.-X. (2002) Late Mesozoic and Cenozoic rifting and its dynamic setting in Eastern China and adjacent areas. *Tectonophysics* **344**, 175-205.

Self S., Blake S., Sharma K., Widdowson M., Sephton S. (2008) Sulfur and chlorine in late Cretaceous Deccan magmas and eruptive gas release. *Science* **319**, 1654-1657.

Wilde S.A., Zhou X.-H., Nemchin A.A., Sun M. (2003) Mesozoic crust-mantle interaction beneath the North China craton: a consequence of the dispersal of Gondwanaland and accretion of Asia. *Geology* **31**, 817-820.

Zhang Y., Xu Z. (2003) Kinetics of convective crystal dissolution and melting, with applications to methane hydrate dissolution and dissociation in seawater. *Earth and Planetary Science Letters* **213**, 133-148.

Zhang Y. (2005) Fate of rising CO_2 droplets in seawater. *Environmental Science & Technology* **39**, 7719-7724.

Zhang Y., Xu Z. (2008) "Fizzics" of bubble growth in beer and champagne. *Elements* **4**, 47-49.

Chapter II

Geochemistry of Cenozoic basalts and Mantle Xenoliths in Northeast China

Abstract

Volcanic activity in Northeast China and adjacent regions is widespread, with eruption ages ranging from Late Cretaceous (80 Ma) to about 300 years ago. Volcanic rock types are principally basanite, alkali olivine basalt, and tholeiite, with minor evolved trachyte and rhyolite. Ultramafic xenoliths, mainly spinel lherzolite and harzburgite, are common in alkali olivine basalt and basanite.

New major and trace element data from 11 volcanic fields and helium isotope data from ultramafic xenoliths of three of those fields are reported. The $^{3}He/^{4}He$ ratio ranges from 5 to 7 times the atmospheric ratio, indicating that previously reported high $^{3}He/^{4}He$ ratios are likely due to the contamination by cosmogenic ^{3}He. There is currently no evidence for a high-$^{3}He/^{4}He$ mantle plume component beneath NE China. The Sr-Nd-Pb isotopic data from the literature do not support a significant degree of crustal contamination, and are here interpreted to result from mixing between a FOZO end-member and a LoMu end-member. The LoMu end-member appears to reside within continental lithosphere. Major and trace elements do not indicate significant contributions from a subducted slab. Differences in depth and the extent of partial melting in the asthenosphere, both within individual fields and between the different

volcanic fields, explain most of the correlations between major and trace elements observed in this study, with deeper melting usually associated with a smaller degree of melting. Highly potassic basalts are associated with the LoMu end-member and are interpreted to be the products of lithosphere melting.

2.1. Introduction

The origin of intraplate volcanism is diverse and not always well understood. Although volcanism at intraplate setting is less common than along mid-ocean ridges and subduction zones, it is of significant importance, for both preventing geological hazards and understanding mantle geochemistry.

One notable area of intraplate volcanism is Northeast China and adjacent regions, as part of the larger volcanic belt along the eastern Asian continental margin. This area lies on two tectonic units: 1) North North China-Korea Craton (NCKC) and 2) Central Asian Orogenic Belt (CAOB, Sengor and Natal'in, 1996). The NCKC formed during the Archean and early Proterozoic. The CAOB is interpreted to be an intercontinental fold belt that underwent collision and subduction among Siberian Craton, NCKC and other smaller Mongol-Okhotsk blocks. The NCKC and CAOB became part of Eurasian plate as the Mongolo-Okhotsk Ocean closed during the early Cretaceous. This closure event may account for the widespread calcalkaline series volcanism in Daxing'anling in late Jurassic and early Cretaceous (e.g., Yin and Harrison, 1996). During the late Cretaceous, volcanic rocks in NE China changed composition from dominantly cal-calkaline series to dominantly alkali series (Ma et al., 2002). In the late Mesozoic to Cenozoic, the tectonic evolution of East Asia is controlled by indentation of Indian plate and subduction of

Pacific plate and Philippine Sea plate. These Cenozoic alkali volcanic rocks are the focus of this work.

Cenozoic basalts in Northeast China surrounding NE China Plain is widespread although volumetrically small. In an area of about two million square kilometers, there are over 590 volcanoes with volcanic rocks covering about 50000 km^2 (Liu, 1999). The ages of tholeiitic and alkali basalts vary from about 80 Ma to about 300 years ago. For brevity, the volcanic area will be referred to as the Greater NE China (Fig. 2-1); volcanic rocks south of this region (e.g., Zou et al., 2000) are not the focus of this work. The activity of each volcanic field varies significantly. Some large volcanic fields were active for tens of million years, while some small ones lasted for less than 1 Myr. The major types of the volcanic rocks are basanite, alkali olivine basalt, and tholeiite, with minor evolved trachyte and alkaline to peralkaline rhyolite. Ultramafic xenoliths, mainly spinel lherzolite and harzburgite, are common in basanite and alkali olivine basalt (e.g., Fan and Hooper, 1989).

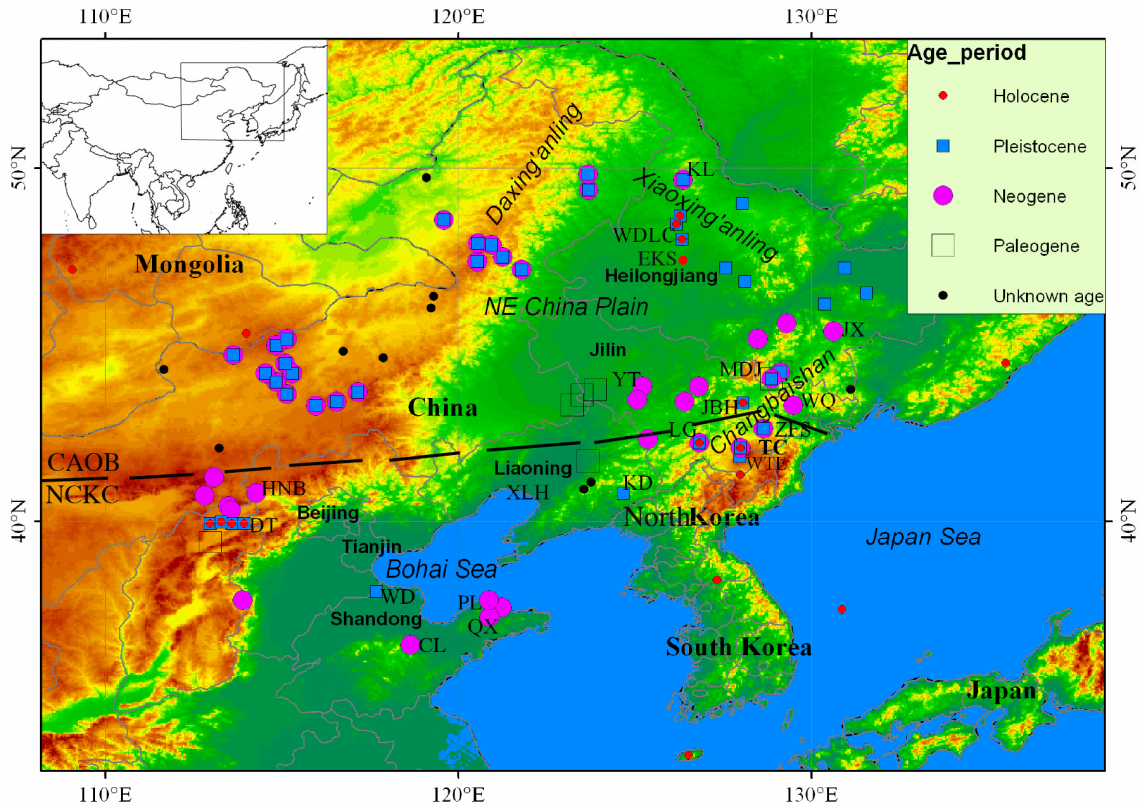

Figure 2-1. Volcanic fields in Northeast China. Dashed line is the approximate boundary between North China-Korea Craton and Mongol-Okhotsk Tectonic Belt. Abrreviations of volcanic fields are as follows: KL (Keluo), **WDLC (Wudalianchi)**, **EKS (Erkeshan)**, **JX (Jixi)**, **MDJ (Mudanjiang)**, WQ (Wangqing), YT (Yitong), **JBH (Jingbohu)**, **CBS (Changbaishan**, including TC (Tianchi), ZFS (Zengfengshan) and WTE (Wangtian'e)), **LG (Longgang)**, **KD (Kuandian)**, XLH (Xialiaohe, borehole samples), **CL (Changle), WD (Wudi)**, PL (Penglai), QX (Qixia), HNB (Hannuoba), and **DT (Datong)**. Bold-face type indicates that the volcanic field has been sampled in this work. Ages are from: Zhou and Armstrong (1982), Wang et al. (1983, 1988), Chen and Peng (1985), Jin (1985), Liu (1987, 1999), Luo and Chen (1990), Liu (1992), Liu et al. (2001), Jin and Zhang (1994), Zhang et al. (1998, 2002), Liu et al. (2001).

In addition to field studies and geochronology, numerous geochemical investigations on the volcanic rocks have been carried out, including major element, trace element and isotope analyses. The rocks are highly enriched in incompatible elements (e.g., Zhou & Armstrong, 1982; Basu et al., 1991; Liu, 1992, 1995, 1999; Zhi and Feng, 1992; Jin and Zhang, 1994). Based on Sr-Nd-Pb isotopic data (Zhou and Armstrong, 1982; Peng et al., 1986; Basu et al., 1991; Zhang et al., 1991; Tu et al., 1992; Xu et al., 1998b), significant contamination by continental crust was ruled out, Basu et al., 1991 suggested that the mantle may be viewed as a mixture between a depleted mantle and an enriched mantle EM1. Helium isotope data (Xu et al., 1998a, 2003; Li et al., 2002; Xu and Liu, 2002; Wu et al., 2003; Lai et al., 2005) are scattered, and some seem to indicate a possible high-$^{3}He/^{4}He$ plume component. The most extreme helium data are those of Li et al. (2002), with $^{3}He/^{4}He$ ratio varying widely from 0.1 to 700 times the atmospheric ratio.

The origin of intraplate volcanism in this region is under debate. Numerous hypotheses used to explain the diffuse volcanism in the Greater NE China, include but are not limited to, a mantle plume/hotspot (e.g. Deng et al., 1996, 1998, 2004), back-arc extension caused by subduction of Kula-Pacific plate (e.g., Liu, 1987a; Liu et al., 2001; Ren et al., 2002), mantle upwelling while crossing from a thick lithosphere to a thin lithosphere (Niu, 2005), and thinning/delamination of the lithosphere beneath northeast mainland Asia from a thickness of about 200 km in the Paleozoic to about 80 km in the present (e.g., Menzies et al., 1993; Griffin et al., 1998; Menzies and Xu, 1998; Wilde et al., 2003). The widely distributed volcanic rocks provide an opportunity to study the

mantle characteristics of this large area, which in turn can provide some new constraints on the origin of the volcanism.

2.2. Samples and analytical methods

2.2.1. Samples

The samples come from eleven volcanic fields. From North to South, they are Wudalianchi (WDLC), Erkeshan (EKS), Mudanjiang (MDJ), Jixi (JX), Jingbohu (JBH), Changbaishan (CBS), Longgang (LG), Kuandian (KD), Datong (DT), Wudi (WD), and Changle (CL) (Fig. 1). Because of compositional similarities, WDLC and EKS are often combined, so are MDJ and JX, and WD and CL. No attempt was made to map and sample every volcanic field systematically. The samples are mainly Quaternary in age, except for those from MDJ, JX, and CL, and some from CBS).

The 14 Quaternary cinder cones of the WDLC volcanic field (Heilongjiang Province) cover about 800 km^2. Basaltic rocks in this volcanic field are highly potassic, which distinguishes them from the other fields in NE China. EKS is a single cinder cone about 50 km to its south. The most recent eruptions in WDLC occurred about 300 years ago.

The JBH volcanic field (Heilongjiang Province) consists of one volcanic plateau, several cinder cones and some exposed small lava flows. The samples are Quaternary basanite, hawaiite and phonotephrite. Mantle xenoliths, commonly spinel lherzolite, are widely distributed.

The MDJ and JX (Heilongjiang Province) comprise several large basaltic bodies (total area >3000 km^2) lying to the north of JBH. The eruption sequence is not clear. Available K-Ar age data range from about 40 Ma to 0.5 Ma (Liu, 1987b, 2002).

The CBS (Jinin Province) consists of three large volcanic centers: Tianchi (TC), Wangtian'e (WTE) and Zengfengshan (ZFS), each of which has a long eruption history. TC and WTE are stratovolcanos. TC volcano has been most extensively studied in literature. It was active from about 20 Ma to 800 yrs ago (Jin and Zhang, 1994). Eruption products evolved from basalt to hawaiite, mugearite, basaltic andesite to peralkaline rhyolite. Mantle xenoliths are only found in early basalts. Samples from WTE are mainly trachyte and rhyolite and similar to the products of the final stages of TC. Only basaltic samples were reported for ZFS. Although there are evolved rocks, the focus in this work is to understand mantle characteristics and the origin of volcanism, and hence on basaltic rocks.

The LG volcanic field (Jinin Province) comprises many calderas/maars, lava flow units and cinder cones, spreading an area of about 2000 km^2 (Xu et al., 2003). Most age data are <2 Ma. Rock types range from basalt, hawaiite, mugearite to basaltic andesite. Harzburgite xenoliths are commonly found.

There are about 20 cinder cones in KD volcanic field in Liaoning Province (Liu, 1992). Limited age data show that they were active in the last 2 Ma. Rock types are mainly basanite, hawaiite and mugearite. Mantle xenoliths are abundant in the alkali basalt of Huangyishan cinder cone.

The WD (Shandong Province) is made of only one cinder cone of 0.3~0.8 Ma. The CL is part of the Changle-Linqu volcanic field with many cinder cones from 20 Ma to 10 Ma.

The DT volcanic field is in Shanxi Graben System, to the west of North China Plain. There are more than 10 cinder cones and some lava flows, with ages ranging from 1.3 Ma to 0.2 Ma. Rocks are mainly basalt and basaltic andesite.

Basalt samples were collected from fresh outcrops including quarries and road cuts. Most basaltic samples are aphyric with microphenocrysts (≤0.2 mm) of olivine, plagioclase and clinopyroxene. Fe-Ti oxides occur in some samples. Major and trace element analyses were carried out on basalts. In order to avoid cosmic ray contribution of ^{3}He, mantle xenolith samples for $^{3}He/^{4}He$ isotope analyses are collected from quarries, fresh road cuts and deep gullies. No other isotopic data were obtained, but literature data will be used in exploring mantle characteristics.

2.2.2. Major and trace element analyses

Fresh samples are cut and cleaned for major and trace elements analysis. Major elements plus Rb, Sr and Zr are analyzed by X-ray fluorescence method (XRF). Other trace elements were analyzed by inductively coupled plasma mass spectrometry (ICP-MS). Most samples were analyzed at Michigan State University following the procedures of Hannah et al. (2002). In order to crosscheck the accuracy of the analyses, selected samples were re-analyzed at Washington State University-Pullman following the procedures of Knaack et al. (1994). The results are listed in Appendix A - Table 1b.

Standards BCR-2, BHVO-2, K1919, NKT-1 are measured as unknowns and are compared with reference values from USGS and literature in Appendix A - Table 1a.

The quality of the analyses is assessed in several ways: (1) by comparisons between standards analyzed as unknowns and published reference values; (2) by comparison between MSU and WSU analyses of the same rocks; and (3) by repeated analyses of the same rock. Furthermore, when trace element relations show peculiarity, attempts were made to check the data. For example, some data from the MSU lab showed a significant positive Yb anomaly. Some of the same samples were sent to WSU and such anomalies are found not present. Based on these assessments, the accuracy is within 3% relative for SiO_2, TiO_2, Al_2O_3, MgO, and CaO; 5% for P, Mn, Y, Cu, and Zn; 10% for Fe_2O_3, K, Sr, Nb, La, and Ce; 15% for Nd, Zr, Ba, Th, Ta, Pr, Sm, Ho, Er, and Hf; 20% for Eu, Na, Tb, Dy, V, Sc, and Ga; and 25% for Ho and Gd. The uncertainty for Tm is not known, but repeated analyses agree well. Other elements (Ni, Cr, Rb, Yb, Lu, Pb, and U) may be in error by much more and are not reported in Table 1b.

2.2.3. Helium isotope analyses

In order to test whether a mantle plume component with high-$^3He/^4He$ is present, mantle xenoliths were collected and He isotopes were analyzed on 8 mantle xenoliths from JBH (2 samples), KD (3 samples) and LG (3 samples) volcanic fields. Spinel lherzolite samples from KD have the freshest appearance of the xenoliths studied here, and bear little rust-colored iddingsite or other signs of alteration, and typically contain large (1-4 mm diameter) and transparent olivine grains. Spinel lherzolites from JBH are also fresh but relatively small and only a limited amount of olivine crystals could be

obtained from each xenolith. Harzburgites from LG are large (10's of centimeters in diameter) but show a larger extent of rust-colored alteration both on the surface and along cracks inside the crystals.

Large and relatively fresh olivine crystals, typically about 1 mm in maximum size, were picked from crushed xenolith samples under a binocular microscope. The range of sample sizes analyzed was between 0.4 and 0.5 gram. To avoid possible contamination from adhering groundmass of the host basalt or from dust, olivine grains were first ultrasonically cleaned in 1 M HCl for 15 to 30 minutes, and then rinsed successively by deionized water and ethanol. The final products were re-examined under the microscope to ensure the absence of foreign material.

The helium isotope analyses were performed at NOAA/PMEL in Newport, OR following procedures described previously (Graham et al., 1998). All gas extractions were performed by crushing in vacuum to release helium trapped in melt and fluid inclusions. After loading the sample into a stainless steel chamber together with a magnetic piston, the piston was lifted and dropped about 200 times under vacuum using a system of external solenoids, crushing the sample to a powder. Non-condensable, reactive gases were gettered over hot Ti; Ar, Kr and Xe were trapped on activated charcoal using liquid N_2; and neon was separated onto a cryogenically-controlled charcoal trap at 38 K. The helium was admitted directly to the mass spectrometer for isotope ratio and peak height (concentration) determination. The vacuum line blank for crushing was $<1\times10^{-10}$ ccSTP for ^{4}He, and line blanks were run before and after all samples. Simultaneous measurement of ^{3}He and ^{4}He was performed on a double collector mass spectrometer especially designed for high precision helium isotope analysis by J.E. Lupton. The

instrument is equipped with a Baur-Signer ion source (manufactured by ETH, Zurich) that contributes to its high sensitivity, high linearity, and low mass discrimination. The collector section is fitted with a Johnston electron multiplier attached to ion counting electronics and a Faraday cup. The sensitivity for helium is $>10^{-4}$ A/Torr, while the absolute detection limit is $<5\times10^{4}$ atoms ^{3}He. The He isotope data are reported in Table 2-1.

In summary, care was taken during both sample collection and analyses to avoid cosmogenic ^{3}He. (1) Because cosmic ray spallation may produce ^{3}He in old exposed surface rocks (about 1 m depth), samples were collected in quarries, fresh road cuts and deep gullies (presumably rapidly cut), and hence may be assumed to contain only negligible amount of cosmogenic ^{3}He. (2) For helium isotope analyses, the crushing technique that releases ^{3}He in fluid inclusions is used, instead of the melting technique that releases ^{3}He in both inclusions and the lattice. Because most cosmogenic ^{3}He would be inside the lattice instead of fluid inclusions in olivine, the crushing method minimizes the contribution from cosmogenic ^{3}He.

Table 2-1. Helium isotope data in mantle xenoliths from NE China

Location and Sample name	Lat (°N)	Long (°E)	Weight (mg)	^{4}He 10^{-9} cc/g	^{3}He 10^{-14} cc/g	$^{3}He/^{3}He$ (Ra)±2σ
KD-HY-2a-2	40.72339	124.76103	470.6	9.53	9.33	7.00±0.17
KD-HY-2b-1	40.72339	124.76103	500.9	2.30	1.82	5.67±0.40
KD-HY-4d	40.72194	124.76117	485.3	0.433	0.291	4.80±1.55
LG-DLW-1d-1	42.33611	126.41672	452.1	4.13	3.18	5.50±0.29
LG-DLW-1f	42.33611	126.41672	477.4	6.98	5.61	5.75±0.18
LG-DLW-1q	42.33611	126.41672	393.6	3.26	2.74	6.01±0.38
JBH-3i-1	44.19588	128.52737	460.0	1.95	1.69	6.21±0.52
JBH-3i-5	44.19588	128.52737	393.6	0.289	0.292	7.23±2.60

All analyses were performed on hand-picked olivine grains from lherzolite (KD and JBH) or harzburgite (LG) by in vacuo crushing using ~200 high impact strokes. Uncertainties are the quadrature sum of in run statistics plus uncertainties associated with air standards and blanks. The sample names are as follows: KD-HY-2 means fieldwork stop 2, Huangyishan (HY) in the Kuandian (KD) volcanic field, and LG-DLW-1 means fieldwork stop 1, Dalongwan (DLW) in the Longgang (LG) volcanic field.

2.3. Results

2.3.1. Major oxides

Major oxide concentrations from this work are shown in Fig. 2-2 in a diagram of total alkalis versus SiO_2. Also shown are literature data. As recognized by previous authors and shown in Fig. 2-2, the volcanic rocks in NE China are diverse, ranging from tholeiitic to alkaline to peralkaline. Specifically, Wudalianchi and Erkeshan basalts are highly potassic (Fig. 2-3), Wudi rocks are mostly foidite, and the rest are more "normal" alkali and tholeiitic basalts.

Fig. 2-4 shows major oxides plotted against MgO concentration. SiO_2 is negatively and CaO is positively correlated with MgO. The upper limit of K_2O decreases linearly with MgO. For each volcanic field, Al_2O_3 is linearly anticorrelated with MgO (Fig. 2-4). At a given MgO, Al_2O_3 concentration is lowest at WDLC&EKS, and highest at LG. The difference in Al_2O_3 at the same MgO probably reflects difference in melting conditions. At a given MgO, WDLC-EKS and WD display the highest K_2O, and DT and CBS show the lowest K_2O. WD samples also exhibit high Na_2O and P_2O_5 for its very high MgO concentration.

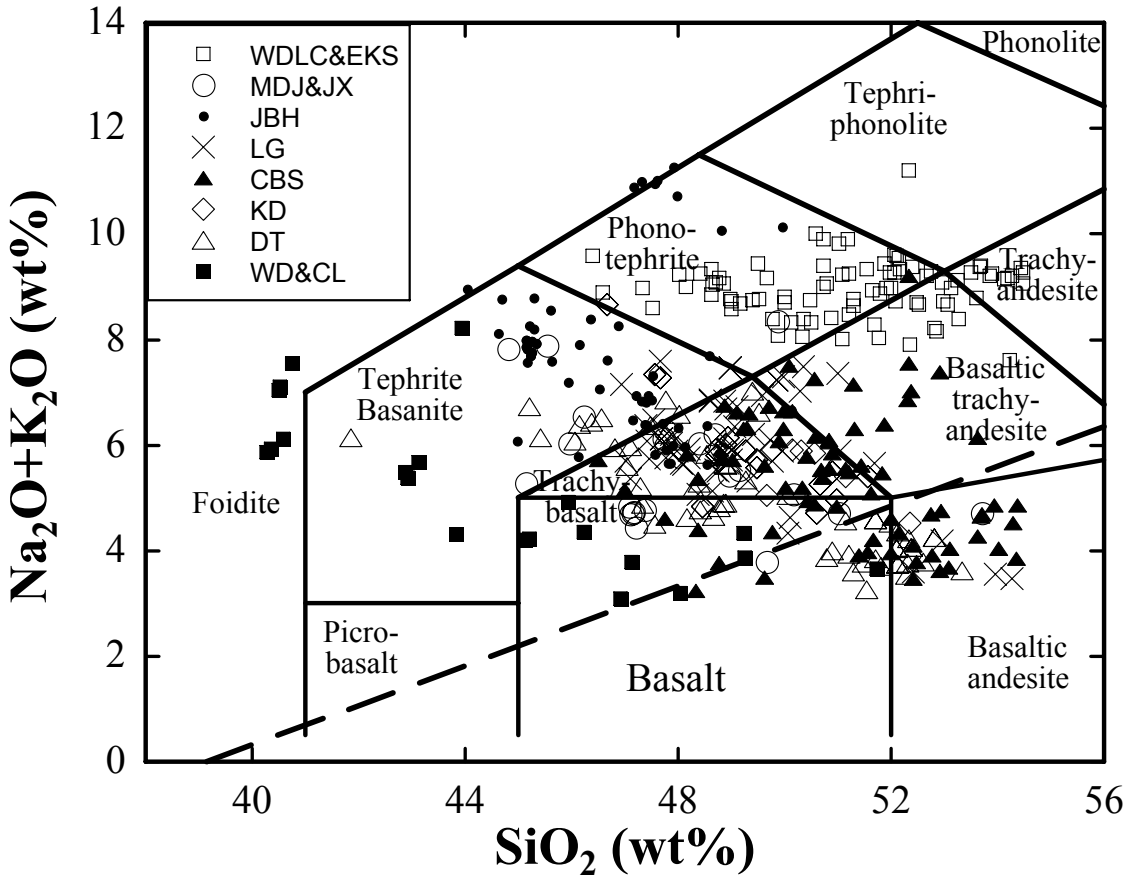

Figure 2-2. Total alkalis versus SiO_2. Data sources: Wang and Guo (1982), Zhou and Armstrong (1982), Zhang (1984), Chen and Peng (1985), Jin (1985), Xia et al. (1986), Tian and Tang (1989), Fan and Hooper, 1991; Zhang et al. (1991, 2002), Liu (1992), Fan et al. (1998, 1999a,b), Zhi and Feng (1992), Jin and Zhang (1994), Hsu and Chen (1998), Li et al. (1998), Liu (1999), Sui et al. (1999), Hsu et al. (2000), and this work.

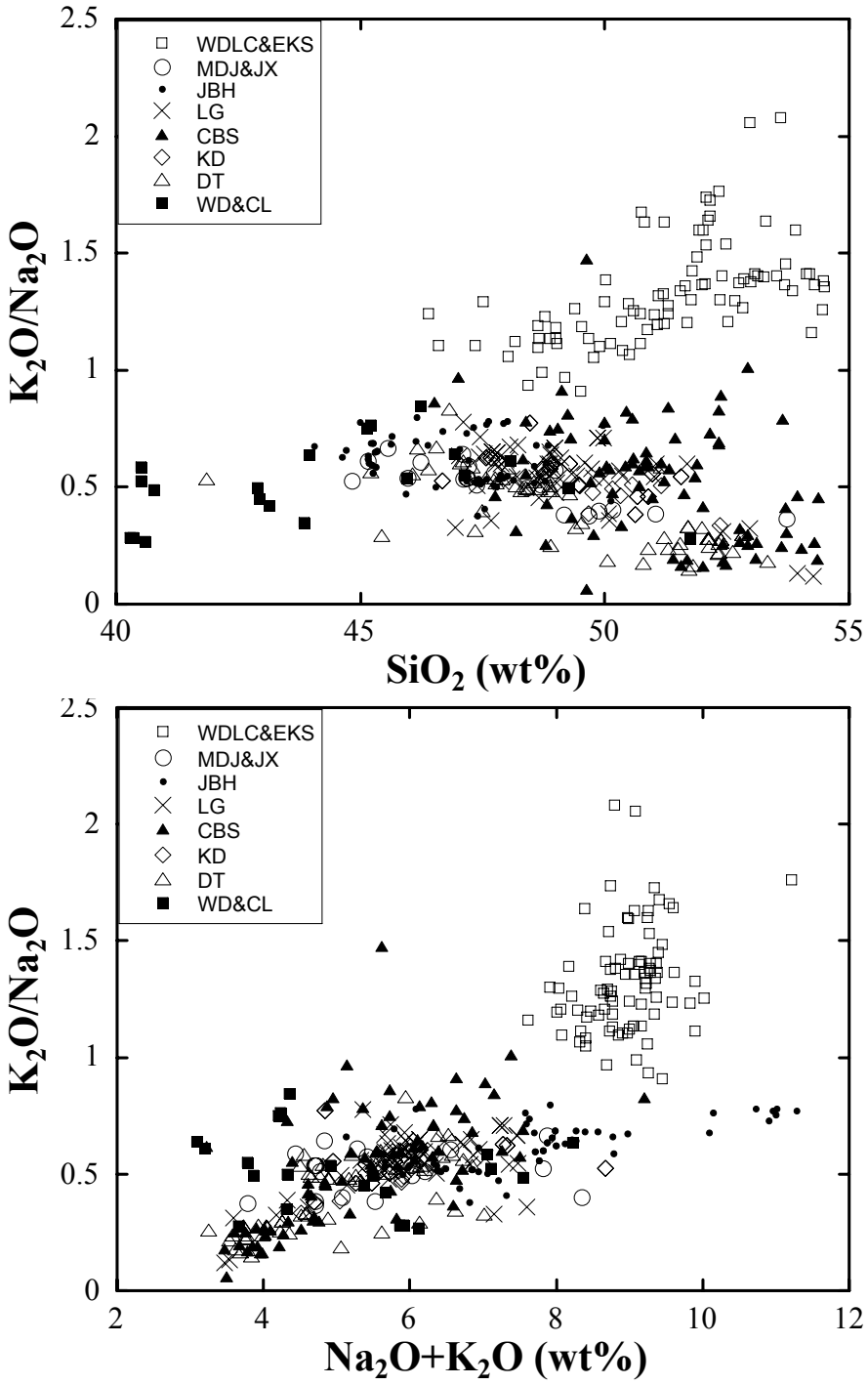

Figure 2-3. K_2O/Na_2O ratio versus SiO_2 and total alkalis for Greater NE China volcanic rocks with $SiO_2 < 55\%$. See Figure 2-1 for abbreviations of the volcanic fields. Data source see Figure 2-2.

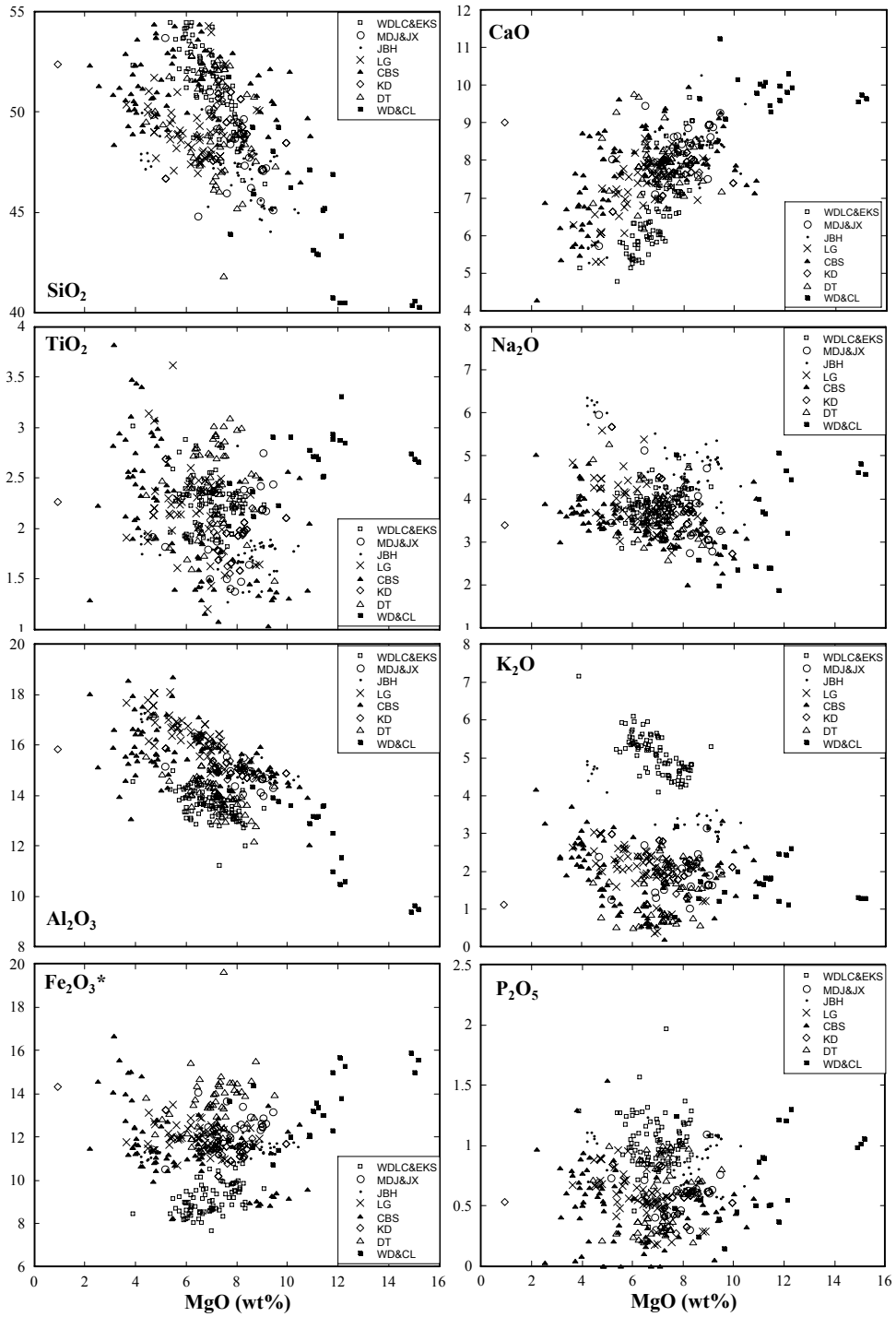

Figure 2-4. SiO_2, TiO_2, Al_2O_3, Fe_2O_3*, CaO, Na_2O, K_2O, and P_2O_5 versus MgO. See Fig. 2-1 for abbreviations of the volcanic fields. Data sources see Fig. 2-2.

2.3.2. Trace elements

Trace element concentrations are reported in Appendix A - Table 1b. Selected trace elements and major elements are plotted in Fig. 2-5. Some trace elements are well correlated. Hf and Zr are well correlated with Hf/Zr ratio slightly below chondrite ratio (Fig. 2-5c). Figure 5d shows that Ta and Nb are well correlated with Nb/Ta ratio of 17.3 (scatter of ±25%, roughly the analytical uncertainty), in agreement with the chondritic ratio of 17.8 (McDonough and Sun, 1995).

In K_2O versus SiO_2 (Fig. 2-5a), WD, CL, JBH, WDLC and EKS form a positive correlation trend, whereas MD, JX, DT, CBS, and KD show a negative correlation trend. Each volcanic field seems to trend toward a focal zone of (46±2) wt% SiO_2 and (2.8±0.5) wt% K_2O. Nb and some other trace elements (Ta, La, Ce, Th) are in general negatively correlated with SiO_2 (Fig. 2-5b). This will be addressed in the Discussion.

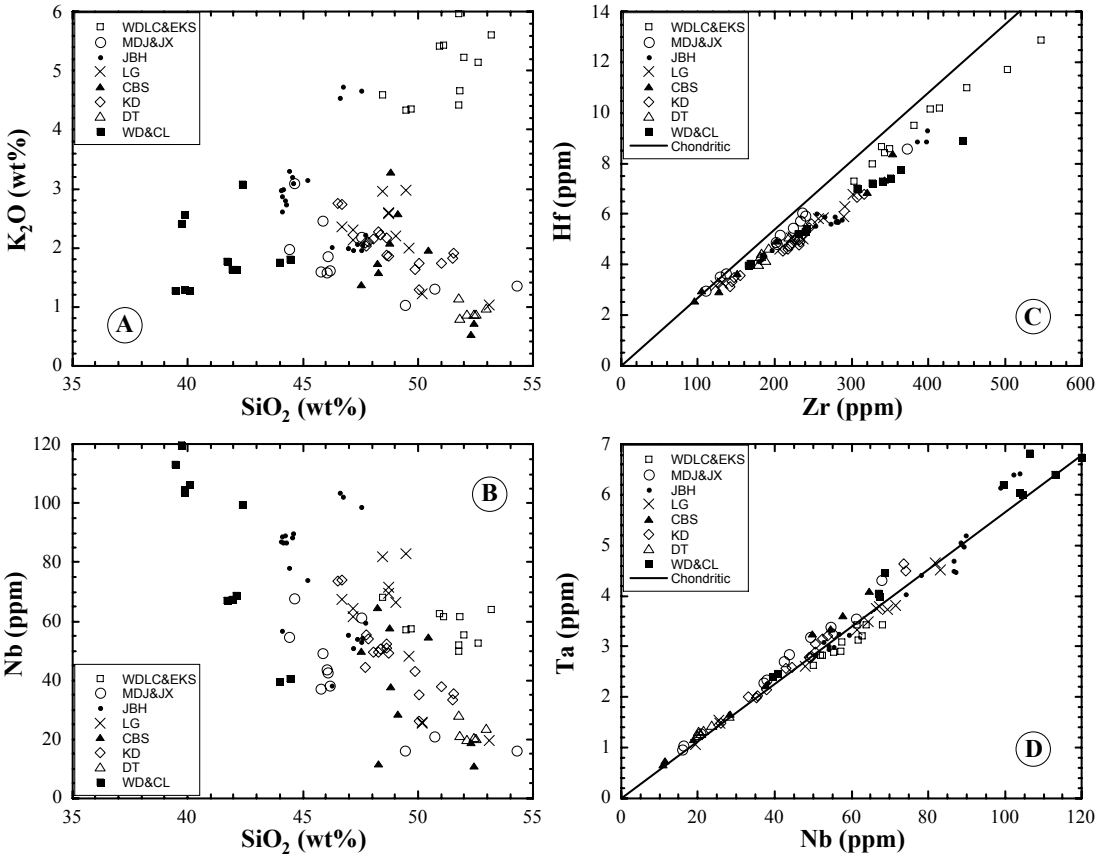

Figure 2-5. Selected elemental plots. See Fig. 2-1 for abbreviations of the volcanic fields. Data are from this work.

Most trace element data are shown in Fig. 2-6 as "spidergrams" by normalizing to concentrations in the bulk silicate Earth (BSE) (McDonough and Sun, 1995). Elements with compatibility in between REE (such as Zr, Hf, P, Ti, and Y) are not plotted so that the REE part is clearly shown in Fig. 2-6, eliminating the need for a separate REE plot. Lu concentration data have large uncertainties (as high as 40% relative) and are not reported in Appendix A - Table 1. Nevertheless, Lu is still shown in the spidergrams to complete the REE pattern. (Yb is not shown because the measurement uncertainty is even larger.) Not all the patterns are identical in shape. One general feature is the strong enrichment in LREE and other incompatible elements in recent basalts from Greater NE China. There is more enrichment in LREE in WDLC, EKS, and JBH, than in DT. When the LREE enrichment is less strong, the absolute concentration of HREE is slightly higher, leading to cross patterns (Fig. 2-6g), suggesting that partial melting occurred at different depths with different partition coefficients. There is no excess enrichment of large ion lithophile elements (LILE) such as Ba and K, except for both enrichment and depletion of K in CBS, and depletion of K in CL and WD. In some volcanic fields, there are depletions of K, Ba and Th compared to the extrapolated REE patterns. No depletion in high field strength elements (HFSE) such as Nb and Ta is observed, except for WDLC and EKS regions. The difference between the volcanic fields will be discussed later.

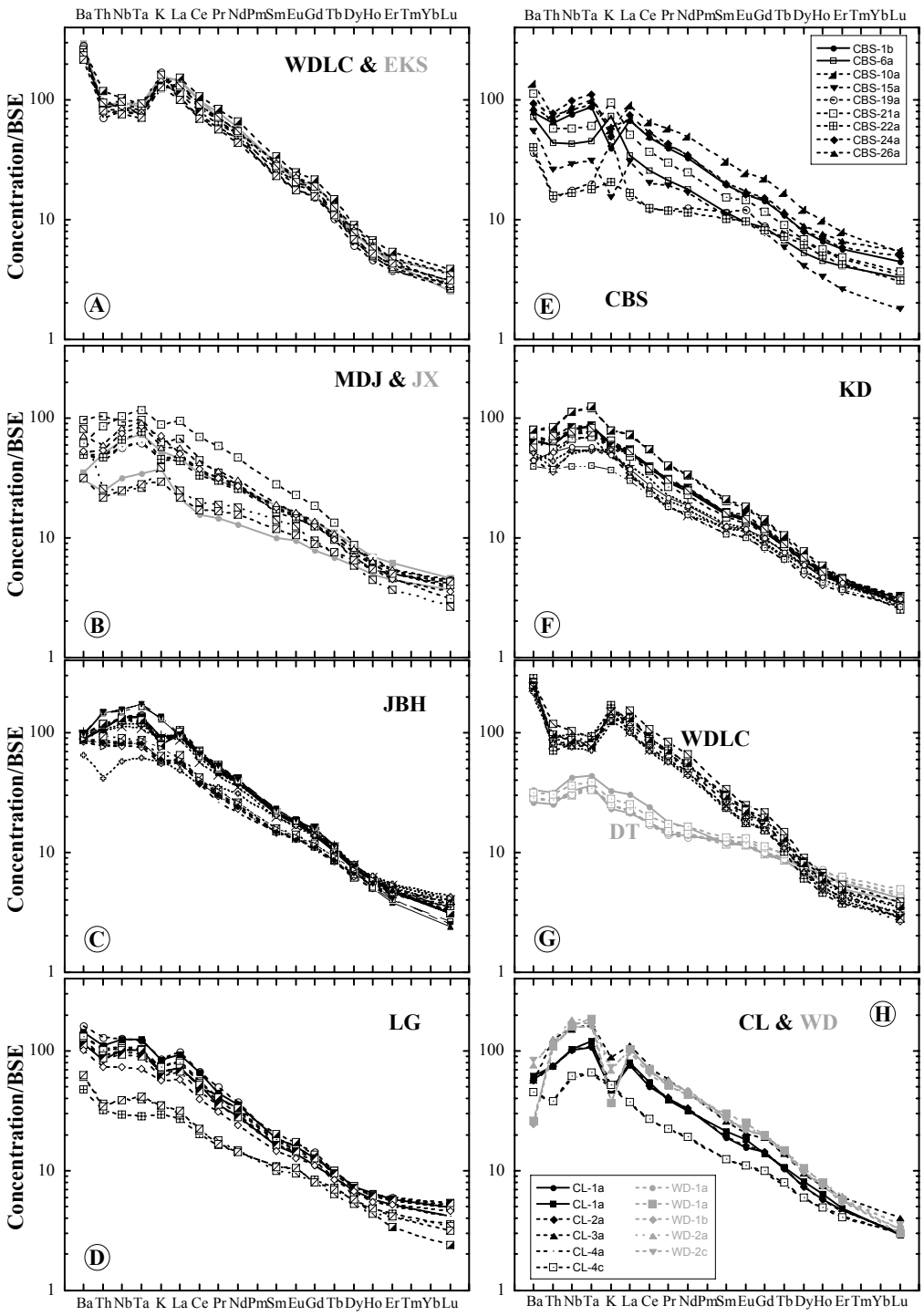

Figure 2-6. Spidergram normalized to the concentration of bulk silicate Earth (McDonough and Sun, 1995). See Fig. 2-1 for abbreviations of the volcanic fields. Data are from this work.

2.3.3. Helium isotopic data

$^{3}He/^{4}He$ ratios in xenoliths from three of the volcanic fields (Kuandian, Longgang, and Jingbohu) are relatively uniform, ranging from 4.8±1.6 R_A to 7.0±0.2 R_A times the atmospheric ratio (R_A) at KD (reported analytical uncertainties are 2s), from 5.5±0.3 to 6.0±0.4 at LG, and from 6.2±0.5 to 7.2±2.6 at JBH. There is no systematic correlation with helium abundance, although the two analyses with the largest uncertainties are for samples with [He] below $5x10^{-10}$ ccSTP/g. Based on these data there does not appear to be a difference in $^{3}He/^{4}He$ between these 3 localities. Most significantly, no high $^{3}He/^{4}He$ ratios have been measured in this study, in which samples were collected from freshly exposed surfaces and all gas extractions were performed by crushing to minimize the effects of any possible cosmogenic ^{3}He that might have been present.

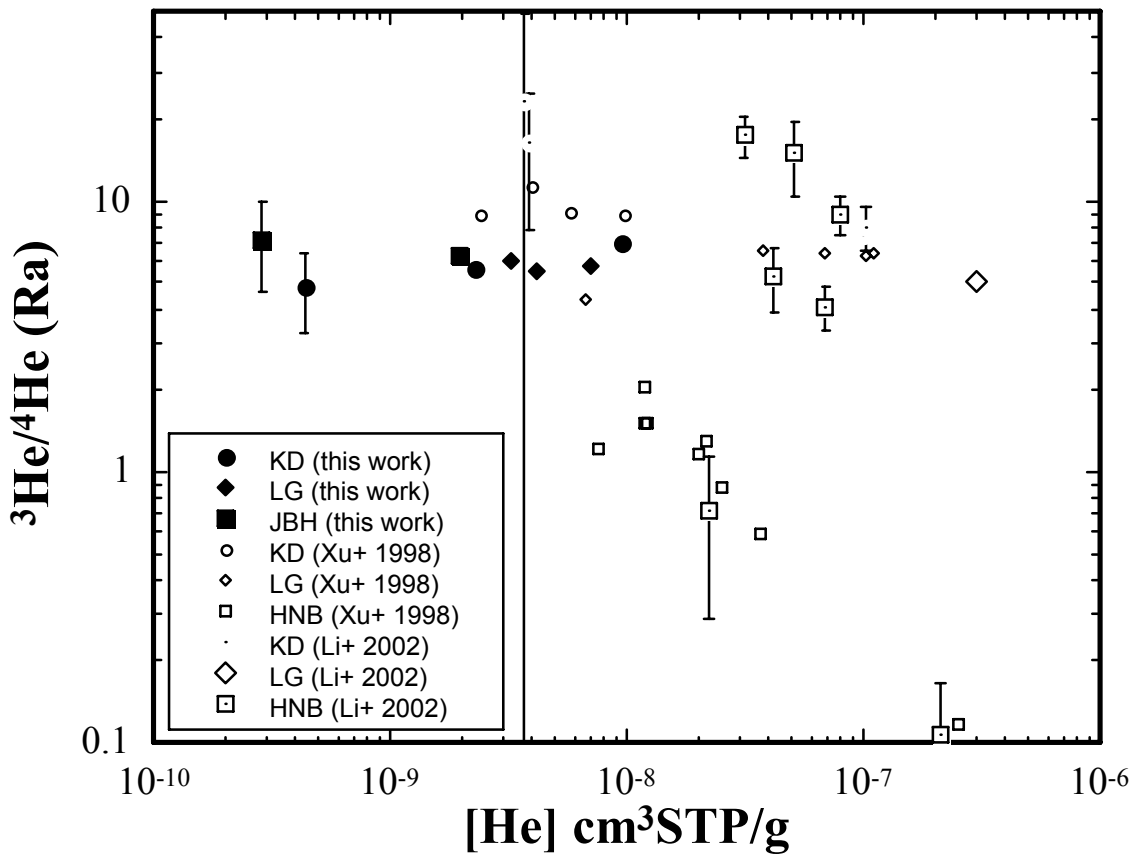

Figure 2-7. Helium isotopic data. Solid symbols are data from this work with ^{3}He/^{4}He analyzed by crushing. Open symbols are literature data from Xu et al. (1998a) and Li et al. (2002) with ^{3}He/^{4}He analyzed by melting. Two data points from Li et al (2002) with ^{3}He/^{4}He ratio of about 700 times Ra are not shown so that the vertical axis is not too compressed. Error bars are shown at 2σ when the error is larger than the size of the symbol.

2.4. Discussion

In this section, we first discuss more certain signals of basalts from Greater NE China using our data and literature data. Then we investigate less clear trends and speculate.

2.4.1. Helium isotope characteristics

Helium isotopic ratios are a useful tracer of mantle source regions. The $^{3}He/^{4}He$ ratio in the mantle, as sampled by basalts, mantle xenoliths and volcanic gases, is greater than that in the atmosphere or the crust, due to primordial ^{3}He still trapped in the mantle and rapid ^{3}He escape from the atmosphere (Clarke et al., 1969). The $^{3}He/^{4}He$ ratio in mid-ocean ridge basalts away from the influence of ocean island hotspots is relatively uniform, between 6 to 10 times the atmospheric ratio (Graham 2002). The highest $^{3}He/^{4}He$ in the source regions of island arcs is typically at the low end of the MORB range (Poreda and Craig 1989; Porcelli et al. 1992), and ranges to considerably lower ratios (Hilton and Craig 1989) due to the presence of radiogenic helium derived either from shallow levels in the crust or from subducted material. In contrast, mantle plumes sampled at ocean islands such as Hawaii and Iceland display $^{3}He/^{4}He$ ratios higher than those in MORB (Kurz et al., 1983; Hilton et al., 1999). Such high ratios are usually considered to reflect a relative ^{3}He enrichment in less degassed and presumably deeper mantle sources of the plumes (e.g., Kurz et al. 1982; Class and Goldstein 2005).

A possible complication of $^{3}He/^{4}He$ isotopic analyses of subaerial rocks is the presence of cosmogenic ^{3}He, is produced primarily via spallation reactions on O, Mg and Si in silicates due to the penetration of secondary neutrons that were ultimately produced

by cosmic rays in the atmosphere. The characteristic (e-folding) penetration distance is about 0.5 m, and results in a ^{3}He production rate of 100 atoms·g^{-1}·yr^{-1} in silicates exposed at the Earth's surface (Kurz 1986). While cosmogenic ^{3}He is useful in determining exposure ages, it needs to be avoided in understanding mantle ^{3}He/^{4}He characteristics from rocks exposed at the Earth's surface.

Previous ^{3}He/^{4}He results for mantle xenoliths from Greater Northeast China basalt are complicated by the possible presence of cosmogenic ^{3}He. Porcelli et al. (1987) reported a ^{3}He/^{4}He ratio in a spinel lherzolite from Northeast China of (49±16) R_A. They assumed that the initial ratio before exposure to cosmic ray bombardment to be 8 R_A, and found that the excess ^{3}He was consistent with derivation from in situ cosmic ray spallation. Shangguan et al. (1998) reported ^{3}He/^{4}He ratios in Changbaishan hot springs to be (5.6±0.3) R_A, consistent with the xenolith results reported here. Xu et al. (1998a) analyzed ^{3}He/^{4}He by melting of samples, and found ratios ranging from 8.9 to 11.3 R_A for pyroxenite and lherzolite xenoliths from Kuandian basalts, and 4.3 to 6.6 R_A for xenoliths from Longgang (also called Huinan) basalts. Li et al. (2002) also analyzed samples by the melting technique, and reported ^{3}He/^{4}He between 7.5 and 24 (±26) R_A for megacrysts from Kuandian, and 0.11 to 5.3 R_A for xenoliths, and 4.1 to 694 (±13) R_A for megacrysts from Hannuoba. Xu et al. (1998a) discussed the issue of cosmogenic ^{3}He inconclusively, and mentioned that analyses of the samples by crushing would resolve the issue. Li et al. (2002) did not address the presence of cosmogenic ^{3}He at all. The ^{3}He/^{4}He results for Longgang by Xu et al. (1998a) are in agreement with our results, but those for Kuandian by Xu et al. (1998a) and Li et al. (2002) differ from ours (Fig. 2-7) and may be explained by the presence of small amounts of cosmogenic ^{3}He in those

earlier analyses. Wu et al. (2003) measured $^3He/^4He$ ratios in augite megacryst, peridotite and alkali basalts in Kuandian using the melting technique, and obtained ratios of 10 R_A for augite megacryst, 2.6 to 4.5 R_A for peridotite, and 0.5 to 0.6 R_A for alkali basalts. Lai et al. (2005) determined $^3He/^4He$ ratios in olivine, orthopyroxene and clinoperoxene of mantle xenoliths from both Kuandian and Wudalianchi using the crushing technique, and found the ratio to be between 4.5 and 7.5 R_A, similar to our data for Kuandian, Longgang and Jingbohu. Because we have taken care to avoid cosmogenic ^3He in both sample collection and analyses, we interpret our crushing results to reflect mantle characteristics, whereas the higher $^3He/^4He$ ratios (>8 R_A) in some previous papers likely reflect some unknown amount of contamination by cosmogenic ^3He, and the lower ratios reflect crustal contamination.

In summary, $^3He/^4He$ ratios in the mantle xenoliths of the 3 volcanic fields we have studied in Northeast China range from 5.5 to 7.0 R_A. This range is significantly below the high $^3He/^4He$ ratios of mantle plumes such as those beneath Hawaii and Iceland. It overlaps the range for the MORB mantle, and is also similar to values in some island arc and ocean island regions. The small variation in the $^3He/^4He$ ratio could be attributed to in-growth of ^4He. There is presently no clear evidence for a high-$^3He/^4He$ mantle plume component contributing to the volcanism in NE China, although the data coverage is still limited. Another earlier claims for the presence of high $^3He/^4He$ ratios beneath part of Japan (proximal to NE China) were recently revisited by Yokochi et al. (2005), who also concluded that those high ratios are most likely to be cosmogenically derived.

The He isotopes were measured in mantle xenoliths instead of basalt (sub-aerial eruption) because subaerial basalt cannot maintain its original helium (e.g., Lai et al., 2005). Because mantle xenoliths are entrained as deep-sourced magma erupted, the xenoliths do not necessarily come from the same depth or the same source as the basalt. Hence the absence of high $^{3}He/^{4}He$ ratios in mantle xenoliths does not completely rule out the presence of high-$^{3}He/^{4}He$ in the source region of the basalt.

2.4.2. Sr-Nd-Pb isotopes

There is already a significant body of isotopic data for Cenozoic NE China basalts (Zhou and Armstrong, 1982; Peng et al., 1986; Liu et al., 1989; Basu et al., 1991; Zhang et al., 1991; Tu et al., 1992; Fan et al., 2001) and there are no special concerns about the quality of the data. In this section available literature isotopic data are examined. Zhou and Armstrong (1982) carried out the first Sr-Nd isotopic study on recent basalts from North and Northeast China, and recognized mantle heterogeneity in eastern China. Peng et al. (1986) identified a distinct mantle component with time-integrated low U/Pb ratio. Liu et al. (1989) first proposed the presence of a LoMu component in NE China mantle. Basu et al. (1991) and Zhang et al. (1991) suggested that recent basalts in eastern China can be attributed to mixing between a MORB-like reservoir and an EM1 endmember (and with significant Dupal signature). Later authors (e.g., Tu et al., 1992; Choi et al., 2005) mostly followed the interpretation of Basu et al. (1991) and Zhang et al. (1991).

Fig. 2-8 compares literature isotopic data in recent NE China basalts with various mantle end-members (see figure caption for references). On Sr-Nd-Pb isotopic plots, NE China basalts show linear trends, attributable to mixing between two end-members, as

suggested by Basu et al. (1991). However, the end-member with low Pb isotopic ratios in NE China differs from the EM1 end-member in $^{208}Pb/^{204}Pb$: in EM1, $^{208}Pb/^{204}Pb$ is about 38.2, but in NE China, $^{208}Pb/^{204}Pb$ is as low as 36.2, indicating a LoMu component (e.g., Doe et al., 1982; Liu et al., 1989; Zhou and Zhu, 1992; Zhou et al., 1992; O'Brien et al., 1995; Mahoney et al., 1996; Douglass et al., 1999; Douglass and Schilling; 2000). In literature, the end-member of low Pb isotopic ratios is often confused with the EM1 end-member. For example, Douglass and Schilling (2000) explicitly defined a LoMu endmember as $^{206}Pb/^{204}Pb$ = 16.50, $^{207}Pb/^{204}Pb$ =15.70, and $^{208}Pb/^{204}Pb$ =38.5. However, this definition is similar to EM1 with fairly high $^{207}Pb/^{204}Pb$ and $^{208}Pb/^{204}Pb$ ratios, significantly higher than the LoMu end-member in NE China and in Smoky Butte, Western US (Fig. 2-8). In Fig. 2-8, it can be seen that there is an end-member with low $^{206}Pb/^{204}Pb$ (16.00), low $^{207}Pb/^{204}Pb$ (15.20), and low $^{208}Pb/^{204}Pb$ (36.1), as exemplified by Smoky Buttes and pointed to by NE China basalts. This end-member, together with $^{87}Sr/^{86}Sr$ = 0.706 and $^{143}Nd/^{144}Nd$ = 0.5113, is hereafter defined as the LoMu end-member (Table 2-2). We suggest that one isotopic end-member for NE China basalts is this LoMu, instead of EM1.

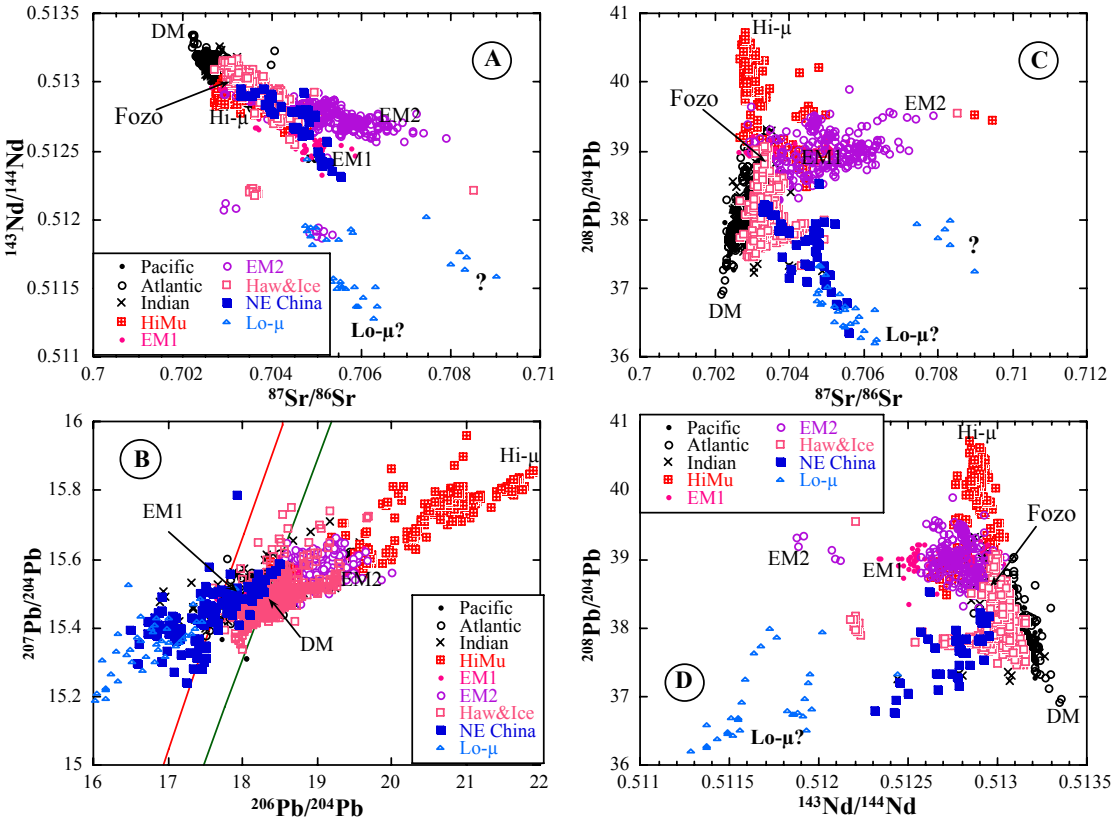

Figure 2-8. Sr-Nd-Pb isotopic data. The two lines in (b) are 4.55 Ga and 4.45 Ga geochrons. Data for Pacific, Atlantic and Indian MORB are from the PETDB database (http://petdb.ldeo.columbia.edu). Data for HiMu, EM1, EM2, and Haw&Ice (Hawaii and Iceland) are from GEOROC database (http://georoc.mpch-mainz.gwdg.de) (Hofmann, 2003). Lo-μ data are from Fraser et al. (1985), Meen and Eggler (1987), Dudas et al. (1987), Dudas (1991), and O'Brien et al. (1995). Isotopic data for NE China basalts are from Zhou and Armstrong (1982), Peng et al. (1986), Song et al. (1990), Basu et al. (1991), Zhang et al. (1991), Tatsumoto et al. (1992), Tu et al. (1992), Han et al. (1999), Fan et al. (2001).

Table 2-2. Isotopic end-members

	$^{206}Pb/^{204}Pb$	$^{207}Pb/^{204}Pb$	$^{208}Pb/^{204}Pb$	$^{87}Sr/^{86}Sr$	$^{143}Nd/^{144}Nd$
LoMu, ref. 1	16.5	15.7	38.5	0.710	0.51125
LoMu, this work	16.0	15.2	36.1	0.706	0.5122
EM1, ref. 2	17.6	15.48	39	0.7055	0.5124
EM2, ref. 2	19.2	15..6	39.6	0.708	0.5126
HiMu, ref. 2	22	16	40.8	0.7028	0.5128
FOZO, ref. 3	19	15.6	39	0.7035	0.5129
DMM, ref. 2	17.5	15.38	36.9	0.7022	0.5134

References: 1. Douglass and Schilling (2000); 2. See references for Figure 2-8; 3. Hauri et al., (1994), Stracke et al. (2005).

The other endmember, with higher Pb isotopic ratios, lower $^{87}Sr/^{86}Sr$ and higher $^{143}Nd/^{144}Nd$, was interpreted to be a MORB-like reservoir (or DMM, depleted MORB mantle) by Basu et al. (1991). This does not seem to be the best interpretation either: (i) The isotopic ratios in Greater NE China basalts are never as depleted as in MORB. Fig. 2-8c shows both MORB isotopic trend and NE China trend point to and roughly meet at FOZO (Hart, 1992; Stracke et al., 2005). The concept of FOZO (Focal zone) was introduced by Hart (1992), and post-date the work of Basu et al. (1991). (ii) Trace elements in NE China basalts exhibit a strongly enriched signature, opposite to strongly depleted signature of MORB. In summary, (a) DMM could be one end-member for the Nd-Sr isotope data, but it is not the only choice; (b) DMM could not explain the Pb isotopic data, especially $^{208}Pb/^{206}Pb$ ratios; (c) DMM's contribution to trace elements features is negligible, Hence, the other isotopic end-member in NE China basalts is suggested to be FOZO instead of DMM. One end-member of Greater NE China basalts is FOZO is consistent with the notion that the FOZO component is the focal zone from which most mantle mixing arrays emanate (Hart, 1992).

The LoMu isotopic feature is encountered in potassic basalts in continental setting. Commonly invoked LoMu source is sub-continental lithosphere (e.g., Douglass and Schilling, 2000) with the presence of a potassic phase such as phlogopite and/or amphibole (Hawkesworth et al., 1990), which may produce Ta depletion during partial melting (Class and Goldstein, 1997). These are consistent with data for WDLC&EKS (potassic rocks with Ta depletion).

Another interesting observation is that in $^{207}Pb/^{204}Pb$-$^{206}Pb/^{204}Pb$ diagram, data from NE China basalts are on both sides of the 4.55-Ga geochron, whereas literature data

on MORB and OIB are mostly on the right hand side of the geochron because of the absence of the LoMu end-member in oceanic basalts. If there is enough LoMu material, then average $^{207}Pb/^{204}Pb$ and $^{206}Pb/^{204}Pb$ ratios of the bulk silicate Earth might lie on the 4.55-Ga geochron.

2.4.3. Major and trace elements

Trace element data quality: Numerous publications are available on trace element data on Greater NE China basalts (see references on Fig. 2-9). However, the quality of literature data is not always easy to assess. Goldstein et al. (2003) published an editorial and suggested the standards for publication of chemical data. Previous workers might not know the standards and might not have followed them. Because reanalyzing the same samples reported in literature is not a practical option, below rough assessment is made using concentration plots of two elements known to have similar compatibility. In such plots, excellent correlations are expected if data quality is high. Fig. 2-9a shows Ta versus Nb (literature data and data from this study). The concentrations of these two elements are essential for assessing whether there is significant HFSE depletion using "spidergrams", which is a characteristic of island arc basalts. Fig. 2-5d and 2-9 show that with data from this study Ta and Nb are highly correlated as expected. Literature data are of variable quality and there is no relation between data quality and year of publication. For example, the quality of data by Zhi and Feng (1992) is about the same as this study. However, Nb/Ta ratio of recent data by Zhang Z. et al. (2002) ranges from 15 to 128, and that of data by Fan et al. (2002) ranges from 10.7 to 15.1, deviating significantly from Nb/Ta ratio established by other analyses. Fig. 2-9a also shows basalt data from E.

Australia (Zhang M. et al., 2001) with quality and mean Nb/Ta ratio about the same as this study.

Fig. 2-9b shows Ho versus Y. Excellent correlation is clear. Data from this study again show excellent correlation between Ho and Y with Y/Ho ratio at 28.1 (similar to the BSE ratio of 28.9, McDonough and Sun, 1995), and the total deviation is ≤20%. Literature data, although with more scatter than this study, show less scatter than that on the Ta versus Nb diagram. Total deviation is ≤40%.

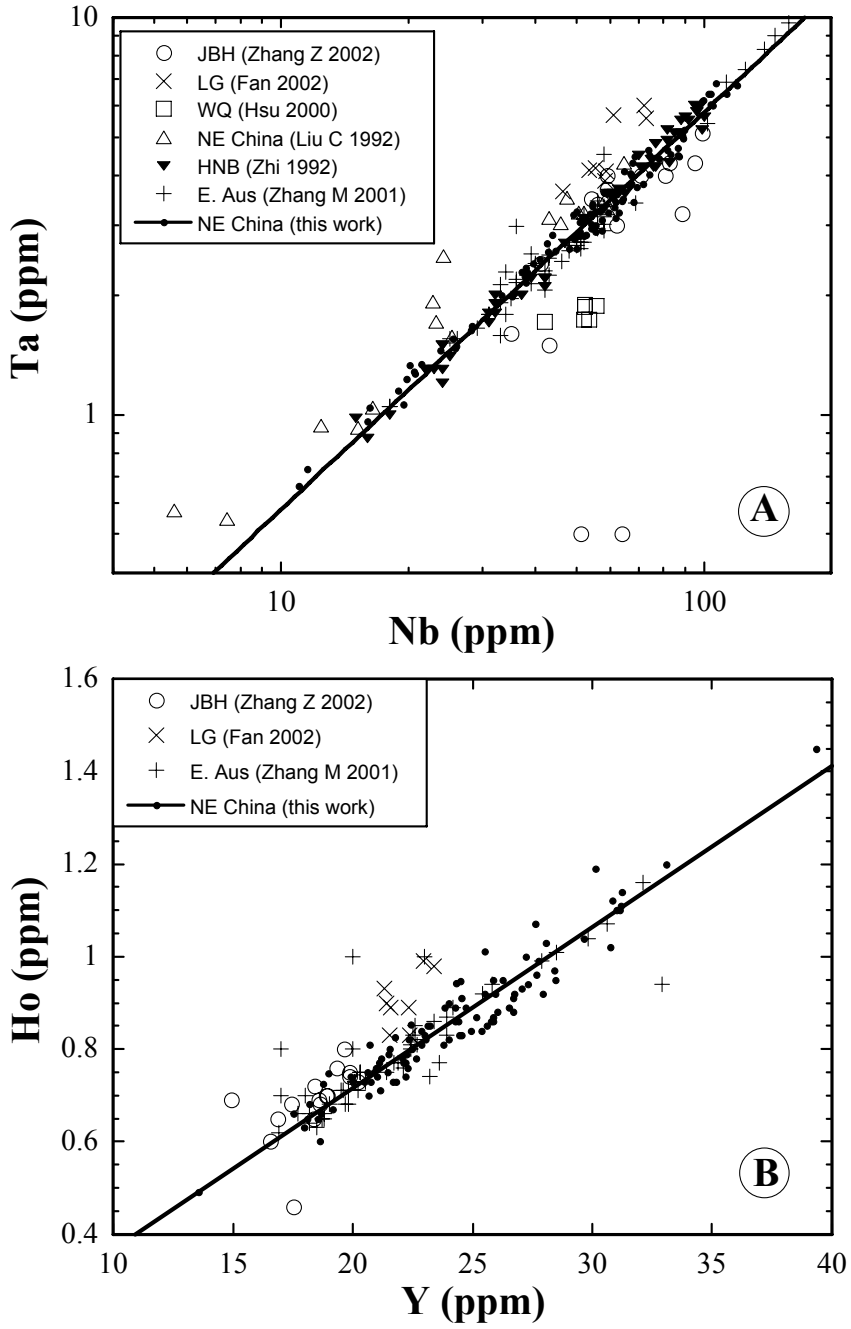

Figure 2-9. (a) Ta versus Nb concentration plot (log-log scale to show large variations). (b) Ho versus Y concentration plot. Data sources are: Clague and Frey (1982) for the Honolulu series; Zhang M. et al. (2001) for E. Australia; the rest are from Liu et al. (1992), Zhi and Feng (1992), Hsu et al. (2000), Fan et al. (2002), Zhang et al. (2002), and this work.

Because literature data (even very recent data) are of variable quality and it is difficult to evaluate the quality *a priori*, one cannot simply compile literature data to examine the enrichment or depletion of specific elements (such as Nb, Ta, Ba, and Rb). In the future it will be important for authors to acquire more trace element data and to follow the standard procedures (Goldstein et al., 2003) in presenting geochemical data. In discussion below, trace element data from this study (although limited) is emphasized to investigate source characteristics and address the origin of volcanic rocks in NE China.

Trace element characteristics from spidergrams: Trace element abundances normalized to BSE (McDonough and Sun, 1995) are plotted in spidergrams in Fig. 2-6. For all samples, there is no significant (meaning beyond analytical uncertainty) Eu anomaly, and there is Th depletion to various degrees. Although Zr and Hf are not included, examination of the data shows that there is no depletion. In the spidergram sequence, Nb is on the left-hand side of Ta, meaning Nb is slightly more incompatible than Ta. However, basaltic data from Greater NE China show that the ratio is essentially constant. There is occasional depletion of Ba and K in some samples, which is opposite to enrichment of large ion lithophile elements in subduction-related basalts, but is largely consistent with other intraplate volcanic rocks, such as East Australia basalts.

In summary, there is no depletion of high field strength elements (except for WDLC and EKS, which will be addressed later) and no enrichment of large ion lithophile elements in most basalts from Greater NE China. Hence, there is no geochemical evidence for the involvement of subduction slab in the production of Greater NE China

basalts. Zhao et al. (2004) showed that subducted slab is at a depth of 400 to 600 km in the transition zone of the mantle in NE China volcanic region. Combining both geophysical and geochemical observations, the subduction slab in the transition zone does not seem to contribute fluids or materials to the partial melting zone. Whether the slab and the subduction process are causing a corner flow in the big mantle wedge (Chen, personal communication) cannot be evaluated from geochemistry.

2.4.4. Variations among different volcanic fields

In this section, major and trace elements are used to further infer the partial melting conditions in the mantle and examine difference among volcanic fields. In order to infer the partial melting conditions in the mantle, shallow level fractionation was corrected by adding olivine incrementally to a basalt until the Mg# of the basalt is 73% (e.g., Hart et al., 1997). The correction is applied to basalt with MgO $\geq$ 6 wt% so that olivine is the dominant mineral of low-pressure fractionation. Before correction, the ferric Fe content is assumed to be 10% of total Fe and major oxide total is normalized to 100%. $K_{D,Fe/Mg}$ and $K_{D,Mn/Mg}$ between olivine and melt are assumed to be 0.33 and 0.25 respectively (e.g., Roeder and Emslie, 1970; Hanson and Langmuir, 1978; Jones, 1984). Samples that require more than 30 wt% additional olivine to reach Mg# 73 are removed from the corrected data. In plots discussed below, although plotting the corrected data changes the details, the overall trends are the same as plotting original data. Furthermore, correction does not change ratios of incompatible trace elements. That is, correction does not significantly affect the diagrams and conclusions below, but makes it self-consistent to treat these melts as mantle-derived.

The information to infer about the mantle and partial melting process includes mantle composition (trace elements) and the degree and depth of partial melting. If the partition coefficients are constant during partial melting and the mantle is homogeneous for a given volcanic field, in principle it is possible to carry out inverse modeling to obtain trace element ratios and relative degree of partial melting (e.g., Shaw, 1970; Allegre et al., 1977; Zou & Zindler, 1996; Hart et al., 1997; Zou, 2000). However, it will be seen below that the depth of melting, the percentage of garnet in the source region, and hence the partition coefficients are variable.

Because there are significant variations in Sr-Nd-Pb isotopic ratios in basalts (Fig. 2-8), mantle composition in NE China is not strictly homogeneous. (There are even larger variations in mantle xenoliths, e.g., Song and Frey, 1989; Xu, 2002; and Zhou et al. 2002.) Nevertheless, for the purpose of understanding the systematics of mantle partial melting, major and trace elements in the source mantle (mostly asthenospheric mantle) are assumed to be homogeneous to the first order, and variations in the basalts are ascribed to variations in the depth and degree of partial melting, except for the positive or negative anomalies in Figure 6 (mainly Nb, Ta and Th in WDLC and EKS, K and Ba in WD and CL), which are addressed separately (e.g., WDLC and EKS basalts can be accounted for by invoking melting in the lithospheric mantle of different mineralogy). It is further assumed that trace element pattern of the mantle before partial melting is similar to that of bulk silicate earth (McDonough and Sun, 1995; Chen et al., 2001).

If the mantle is homogeneous and partial melting conditions are similar, elements with (i) different incompatibility and (ii) partition coefficients independent of source mineralogy (such as proportion of garnet) are expected to correlate. Plotting C_1/C_2

versus C_1 (C refers to concentration, and subscripts 1 and 2 indicate two elements) would result in a straight line (Allegre et al., 1977; Hofmann et al., 1986):

$$\frac{C_1}{C_2} = \left[D_2 - D_1 \left(\frac{1-P_2}{1-P_1} \right) \right] \frac{C_1}{C_2^0} + \frac{C_1^0}{C_2^0} \left(\frac{1-P_2}{1-P_1} \right) \qquad (2\text{-}1)$$

where D is the bulk partition coefficient of the minerals weighted in the proportions in the source, P is the bulk partition coefficient of the minerals weighted in the proportions in which they melt, superscript 0 represents original value in the source.

Fig. 2-10a shows (La/Sm) ratio normalized to chondrite versus La concentration. For most volcanic fields (such as WDLC&EKS, MDJ&JX, JBH, LG, KD, and DT), La/Sm versus La is roughly a straight line. However, when all volcanic fields in Greater NE China are viewed together, recent Greater NE China basalts roughly follow a curved trend. East Australia basalts (Zhang M. et al., 2001) and Honolulu peralkaline basalts (Clague and Frey, 1982) also follow curved trends. East Australia basalts follow similar trend as Greater NE China, but Honolulu basalts follow a different trend. The observations suggest that for a given volcanic field, the variation in the partition coefficients of La and Sm is small enough so that a linear trend is produced from a homogeneous source mantle. However, for the whole volcanic province (11 volcanic fields), the partition coefficients vary so that the overall trend is curved. The variation in the partition coefficients is attributed to the variation in mineralogy as well as mineral proportions in the source mantle. Other figures show similar relations, and the relation can be more curved if the difference in the degrees of incompatibility of the two elements is large. Furthermore, there can be more scatter if one of the elements shows anomalies in the spidergram.

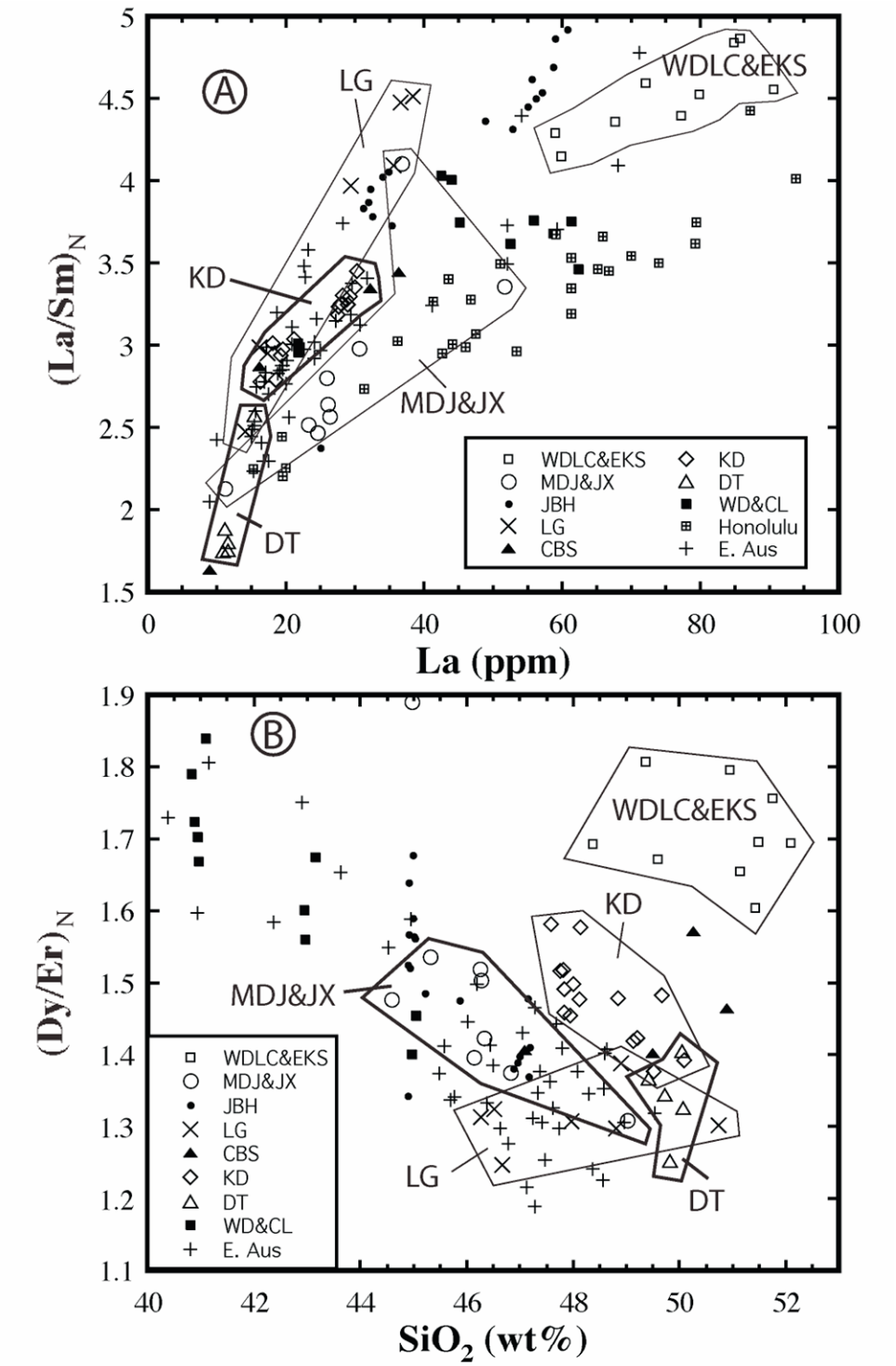

Figure 2-10. (a) Normalized La/Sm ratio versus corrected La concentration. (b) Normalized (Dy/Er) ratio versus corrected SiO_2. Data are from this work.

The fractionation-corrected concentrations of incompatible elements such as Th and La, as well as trace element ratios such as La/Sm, increase with decreasing degree of partial melting assuming the mantle has roughly the chondritic pattern of trace elements. The SiO_2 activity of mantle partial melts decreases with increasing depth of partial melting (e.g. Carmichael et al., 1970; Carmichael, 2004) assuming olivine and orthopyroxene are coexisting in the mantle (very robust). Because calculation of SiO_2 activity requires knowledge of H_2O content in the melt (Carmichael, 2004) in equilibrium with the mantle, which is not available, SiO_2 content is used to be a rough indicator of SiO_2 activity.

Heavy rare earth elements may indicate the percentage of garnet in the mantle, which in turn is roughly correlated with depth of melting. Because Yb and Lu concentrations are not well analyzed in this work, Dy/Er ratio is used for this exercise. In Fig. 2-11, normalized (Dy/Er) ratio is plotted against (La/Sm) ratio, together with calculated grids of the degree of partial melting and the percentage of garnet in the source region using forward modeling. This diagram is constructed by analogy to (Dy/Yb) versus (La/Sm) diagrams used by Fram and Lesher (1995) and Mayborn and Lesher (2004). One difference is the use of proportion of garnet here instead of depth on constructing the grids because relating proportion of garnet with depth requires additional assumptions. The partition coefficients are from Donnelly et al. (2004). The diagram shows that the degree of partial melting ranges from 0.5% to 10% with lower degree of partial melting at WDLC, EKS, JBH, LG and KD, and higher degree of partial melting at MDJ, JX, DT, and CBS (highest degree of melting). The high degree of partial melting at CBS suggests high temperature or high water content in the mantle, and is consistent

with CBS being the largest volcano in the Greater NE China. Because the variation in (Dy/Er) ratio is small, and 2σ error bar for (Dy/Er) ratio is about 25%, the proportion of garnet in the source region is not well resolved, but roughly in the range of 0 to 10%.

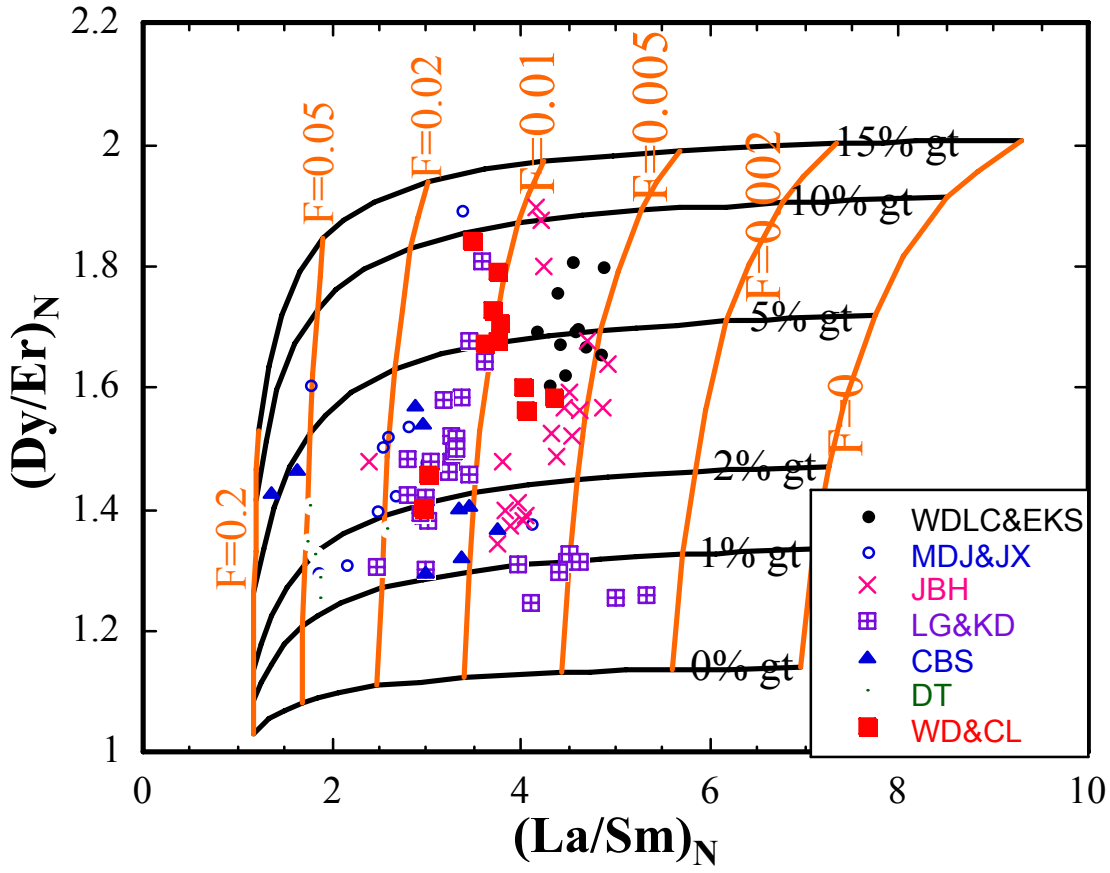

Figure 2-11. Normalized (Dy/Er) ratio versus (La/Sm) ratio. The 2σ relative errors for La/Sm and (Dy/Er) ratio are 18% and 25% respecitively. Data are from this work.

Fig. 2-10b shows normalized (Dy/Er) ratio versus corrected SiO_2. Both are related to the depth of mantle partial melting. A low SiO_2 means melting at greater depth. A high (Dy/Er) ratio means more garnet in the source and hence greater depth. Hence there should be a negative correlation between (Dy/Er) ratio and corrected SiO_2. This is indeed so in Fig. 2-10b, with subparallel and nearly identical trends for NE China and East Australia basalts, except for WDLC and EKS region. The small differences in the lines in Figure 10b may be attributed to uncertainty in Dy/Er ratio.

Fig. 2-12 shows corrected La concentration and normalized La/Sm ratio versus corrected SiO_2 (roughly related to the depth of melting). There is negative correlation between La and SiO_2, as well as La/Sm and SiO_2 for recent NE China basalts as well as East Australia basalts and Honolulu peralkaline basalts. (Again, WDLC and EKS are off the general trend.) The observed negative correlation can be explained by different degree of partial melting at different depth, with smaller degree at greater depth. Furthermore, at a given volcanic field, there is large variation in corrected La and SiO_2 content, as well as La/Sm ratio, indicating a large range of depth and degree of partial melting, and minimal mixing of melts generated at different depths.

The negative correlation cannot be attributed to different degrees of partial melting from a homogeneous mantle at the same depth. If melting occurred at the same depth and same source mineral compositions, a smaller degree of melting would produce greater SiO_2 content (Baker et al., 1995) and incompatible element concentrations, leading to positive correlations.

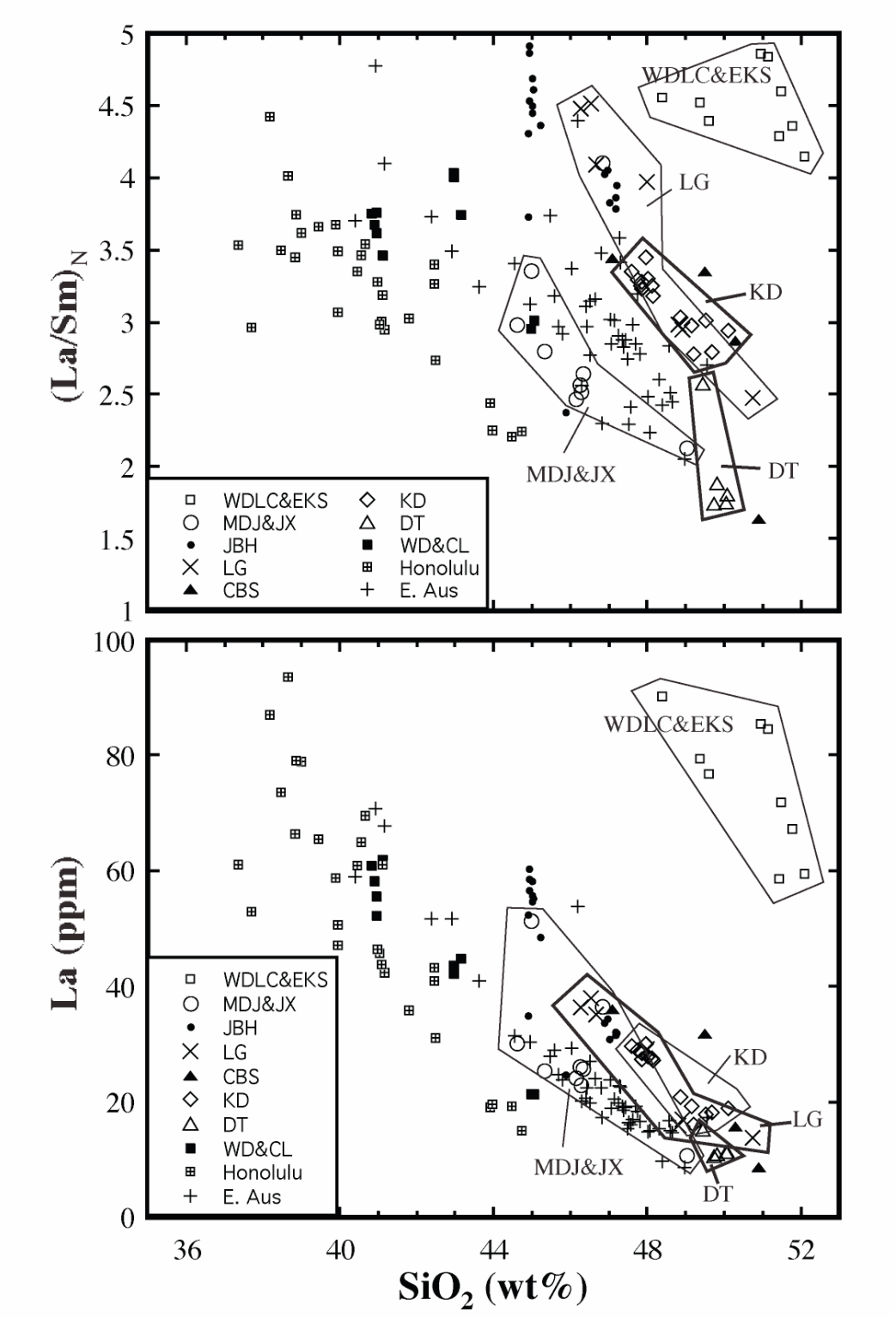

Figure 2-12. Corrected La concentration and normalized (La/Sm) ratio versus corrected SiO_2. Data are from this work.

The slightly different trends for various volcanic fields in Fig. 2-12 probably reflect different degrees of partial melting at a given depth (or a given SiO_2). That is, at a given depth (such as 70 km), the degree of partial melting is highest at WD, CL, MDJ, and JX, followed by DT, LG, CBS, KD, and JBH. WDLC and EKS are outliers, and have the highest SiO_2 content at the same (La/Sm) ratio or the same corrected La concentration. The results imply that there is some regional difference in geothermal gradient or in volatile contents in the mantle, which led to the difference in the degrees of partial melting.

2.4.5. WDLC and EKS

Basalts of WDLC and EKS are different in many aspects from the rest of recent basalts in Greater NE China. The differences are summarized below:

(i) Basalts of WDLC and EKS are potassic. Nevertheless, on trace element spidergram, there is no additional K enrichment. Hence the highly potassic nature is attributable to very small degree of partial melting.

(ii) SiO_2 content in WDLC and EKS basalts is high especially relative to the incompatible trace element concentrations (Fig. 2-12), suggesting shallow depth of melting.

(iii) Dy/Er ratio is high, suggesting garnet presence in the source region.

(iv) La concentration and La/Sm ratios are high, suggesting very small degree of melting.

(v) Depletion of Nb, Ta and Th suggests melting of continental lithosphere (Turner and Hawkesworth, 1995)

(vi) Isotopically, WDLC and EKS are near the extreme end of the LoMu isotopic end-member, similar to Smoky Buttes lamproites.

The above characteristics are best explained by small degrees of partial melting of the continental lithosphere at shallow depth in the presence of phlogopite and/or amphibole (Class and Goldstein, 1997). The inferred presence of garnet in the source region is difficult to reconcile with shallow depth, but might be due to garnet-bearing eclogite veins. If the mantle source region contains high water content, partial melting of the relatively cold lithosphere would be facilitated.

2.4.6. Depletion of large ion lithophile elements

Basalts from WD and CL show significant depletion (by about a factor of 2) of large ion lithophile elements (K and Ba). Furthermore, basalts from CBS display both depletion and enrichment of large ion lithophile elements. Because K and Ba are easily mobilized in fluid, the depletion (as well as occasional enrichment) may be attributed to fluid activity in the source mantle. Removal of fluid (dehydration) would deplete the large ion lithophile elements, and addition of fluid would enrich these elements. It is hence important in the future to investigate water content in the mantle source region or in pre-eruptive basalt.

2.4.7. Summary and synthesis

Plume/hotspot volcanism? He isotopic data presented in this work suggest that there is no high-$^3He/^3He$ mantle plume involved in NE China volcanism. Furthermore, seismic tomographic images of Zhao et al. (2004) show that the seismic velocity anomalies beneath volcanic fields are shallow, without any deep roots that would be consistent with a deep-seated hotspot or mantle plume. Hence, the plume or hot spot hypothesis for recent NE China volcanism does not have strong support.

Back-arc volcanism? Seismic tomography (Zhao et al., 2004) shows that the Pacific plate subducts from Japan trench and gradually becomes flat at a depth of 400 to 600 km (in the transition zone). The horizontal slab underlies the volcanic fields in greater NE China, consistent with the suggestion that recent NE China basalts are related to back-arc extension (e.g. Basu et al., 1991; Liu et al., 2001; Ren et al., 2002). The linear volcanic belt along Changbaishan is roughly parallel to Japan Trench, also consistent with the suggestion. However, there is no slab signature in recent NE China basalts. Classical back-arc basalts show affinities with island arc basalts with LILE enrichment and HFSE depletion, and this signature diminishes as the distance of back-arc spreading center to the island or continental arc increases (Taylor and Martinez, 2003). Therefore, the complete absence of slab signature may be attributed to the great distance (> 1000 km) between NE China volcanic fields and Japan Arc. Hence, the back-arc extension hypothesis cannot be ruled out by geochemistry. Because there is no evidence for the involvement of slab fluid, partial melting in the mantle of NE China is not helped by water from dehydrated Pacific slab even if the volcanism is due to back-arc extension.

Volcanism due to asthenosphere upwelling when cross the Gravity Gradient Line? This hypothesis was advanced by Niu (2005). In Figure 1, one can see a sharp topographic boundary between the low-lying East China and high-lying West China. The boundary is slightly to the east of Daxing'anling in its north segment, and to the east of Erdos in its south segment. The boundary was referred to as the Gravity Gradient Line by Niu (2005). Niu (2005) argues that because the lithosphere thickness changes rapidly across the boundary, from about 150 km west of the boundary to about 80 km east of the boundary, the volcanism in the Greater NE China is due to decompression from 150 km depth to 80 km depth when asthenospheric flow crosses the boundary from west to east. Although this model can explain the few volcanic activities on the immediate east of the Gravity Gradient Line, it does not explain volcanic activities on the west of the Line, nor does it explain the volcanic activities about 700 km to the east of the boundary.

Volcanism due to delamination of continental lithosphere? Based on the presence of diamondiferous kimberlitic rocks, thermobarometry of mantle xenoliths found in kimberlites, and other lines of argument, the lithosphere thickness of the NCKC was about 200 km during Paleozoic (e.g., Menzies et al., 1993; Griffin et al., 1998; Menzies and Xu, 1998). At present, the lithosphere is thinnest (about 60 km) in Bohai region, and thickens outward to about 120 km (Liu, 1987a; Xu et al., 1998b; Ma et al, 2002). The thinning of the lithosphere brought hot asthenosphere closer to the surface and hence might lead to widespread decompressional melting. The localized distribution of the volcanic fields on the borders of NE China Plain may be attributed to the pathways for magma to come to the surface.

Although the data from this study cannot pin down the exact origin, the various lines of evidence, including the absence of high $^{3}He/^{4}He$ ratios, the lack of HFSE depletion and LILE enrichment, the diffuse distribution of volcanic rocks, the strongly alkaline nature of the volcanic rocks, the strong enrichment of incompatible elements, and the involvement of both asthenospheric and lithospheric mantle in mantle partial melting, seems to be most easily reconciled by diffuse volcanism due to lithosphere thinning. Nevertheless, it is possible that subduction played a role in thinning the lithosphere. For example, the current pile-up of subducted slab at 400-700 km depth would eventually avalanche into the lower mantle (Tackley et al., 1993). When this happens, mantle convection would be significantly enhanced, which might lead to rapid erosion or delamination of a thick lithosphere. Similar pile-up and avalanche could have happened in the past and led to lithosphere thinning of North China Craton. This speculation may be evaluated through geodynamic mantle convection models.

There is a difficulty (or paradox) to account for volcanism in Greater NE China by delamination because delamination occurred mostly in NCKC, but most of the volcanism in this region is north of NCKC. Whether and how delamination in NCKC could affect NE China require future studies.

2.4.8. Future research directions

Accurate and detailed mapping the volcanic rocks is the first and critical step for all subsequent investigations. Detailed geochronological investigations on volcanic history of individual volcanic fields based on mapping in this vast volcanic province will

be necessary to reveal the spatial-time evolution of volcanic activities. Both mapping and dating should be intensified in the future.

To further understand partial melting that produced the volcanos in Greater NE China, it will be important to determine the pre-eruptive water content in various volcanic fields. From the pre-eruptive water content in basalts, it may be possible to estimate H_2O/K_2O ratio in the mantle source, and the role of H_2O in controlling the depth and degree of partial melting. The regions with anomalous trace element patterns may be related to water and hydrous minerals in the mantle. For example, high water content in the mantle source would be consistent with and help to explain partial melting at relatively low temperatures in the lithospheric mantle in WDLC and EKS. Loss of a fluid component from the mantle source could explain the depletion of large ion lithophile elements in WD and CL.

The preliminary modeling indicates that some CBS basalts formed by high degree of mantle partial melting, which is consistent with CBS being the largest volcano in the Greater NE China. More systematic sampling and comprehensive investigation of major and trace elements is necessary to check whether this is true for the basement building stage of Mount Changbai. Furthermore, whether the high degree of partial melting is related to high water content in the mantle, or whether it is due a hotter mantle may be resolved by thermobarometry and determination of water content in the mantle.

A broader spatial coverage of the volcanic fields for $^3He/^4He$ analyses is clearly needed to rule out any role for a high $^3He/^4He$ mantle plume in the volcanism of NE China. Particular attention needs to be paid to sample collection and analyses aimed at minimizing the contribution of cosmogenic ^3He.

Because reliable trace element data are still scarce, it will be important in the future to obtain high-quality trace element data for all volcanic fields. Accurate mapping of crustal and lithospheric thickness might help to relate compositional characteristics to geophysical properties.

Acknowledgments

We thank Bolu Jin, Jianbo Shao and other colleagues at Shenyang Geological Academy, Ruishan Li, Yaoqi Zhou, Shiyong Yan, Zhicong Zhang, Qitao Lv, Baoshu Piao, and Xiaochen Han for assistance in fieldwork. Informal discussion with Yigang Xu, Xinhua Zhou, and Haibo Zou was very helpful. Constructive reviews by Xinhua Zhou and Haibo Zou are greatly appreciated. The editor Yaoling Niu helped in manuscript revision and instructed us to shorten the manuscript and reference list. This work is supported by the US National Science Foundation, a Sokol International Summer Research Fellowship to Yang Chen by the University of Michigan, and the Chinese Natural Science Foundation.

References

Allegre C.J., Treuil M., Minster J.F., Minster B. and Albarede F. (1977) Systematic use of trace-element in igneous process. Part I. Fractional crystallization processes in volcanic suites. *Contributions to Mineralogy and Petrology* **60**, 57-75.

Baker M.B., Hirschmann M.M., Ghiorso M.S. and Stolper E.M. (1995) Composition of near-solidus peridotite melts from experiments and thermodynamic calculations. *Nature* **375**, 308-311.

Basu A.R., Wang J.-W., Huang W.-K., Xie G.-H. and Tatsumoto M. (1991) Major element, REE, and Pb, Nd and Sr isotopic geochemistry of Cenozoic volcanic rocks of eastern China: implications for their origin from suboceanic-type mantle reservoirs. *Earth and Planetary Science Letters* **105**: 149-169.

Carmichael I.S.E. (2004) The activity of silica, water, and the equilibration of intermediate and silicic magmas. *American Mineralogist* **89**: 1438-1446.

Carmichael I.S.E., Nicholls J. and Smith A.L. (1970) Silica activity in igneous rocks. *American Mineralogist* **55**, 246-263.

Chen D.-G. and Peng Z.-C. (1985) K-Ar ages and Pb, Sr isotopic characteristics of Cenozoic volcanic rocks in Shandong. *China. Geochimica* **4**, 293-303 (in Chinese).

Chen S., O'Reilly S.Y., Zhou X.-H., Griffin W.L., Zhang G., Sun M., Feng J. and Zhang M. (2001) Thermal and petrological structure of the lithosphere beneath Hannuoba, Sino-Korean Craton, China: evidence from xenoliths. *Lithos* **56**, 267-301.

Choi S.H., Kwon S.-T., Mukasa S.B. and Sagong H. (2005) Sr-Nd-Pb isotope and trace element systematics of mantle xenoliths from Late Cenozoic alkaline lavas, South Korea. *Chemical Geology* **221**, 40-64.

Clague D. and Frey F.A. (1982) Petrology and trace element geochemistry of the Honolulu volcanics, Oahu: Implications for the oceanic mantle below Hawaii. *Journal of Petrology* **23**, 447-504.

Clarke W.B., Beg M.A. and Craig H. (1969) Excess ^{3}He in the sea: evidence for terrestrial primordial helium. *Earth and Planetary Science Letters* **6**, 213-220.

Class C. and Goldstein S.L. (2005) Evolution of helium isotopes in the Earth's mantle. *Nature* **436**, 1107-1112.

Deng J.-F., Zhao H.-L., Mo X.-X., Wu Z.-S. and Luo Z.-H. (1996) Continental roots-plume tectoncis: a key to continental dynamics. Geology Press, p. 110 (in Chinese).

Deng J.-F., Zhao H.-L., Luo Z.-H., Guo Z.-F. and Mo X.-X. (1998) Mantle plumes and lithosphere motion in east Asia. In: Flower M.F.J., Chung S.-L., Lo C.-H., Lee T.-Y. (Eds.) Mantle dynamics and plate interactions in east Asia. American Geophysical Union. 27, p. 59-65.

Deng J.-F., Mo X.-X., Zhao H.L., Wu Z.X., Luo Z.H. and Su S.G. (2004) A new model for the dynamic evolution of Chinese lithosphere: 'continental roots-plume tectonics'. *Earth-Science Reviews* **65**, 223-275.

Doe B.R., Leeman W.P. and Christiansen R.L. (1982) Lead and strontium isotopes and related trace-elements as genetic tracers in the upper Cenozoic rhyolite-basalt

association of the Yellowstone Plateau volcanic field. *Journal of Geophysical Research* **87**, 4785-4806.

Donnelly K.E., Goldstein S.L., Langmuir C.H. and Spiegelman M. (2004) Origin of enriched ocean ridge basalts and implications for mantle dynamics. *Earth and Planetary Science Letters* **226**, 347-366.

Douglass J., Schilling J.-G. and Fontignie D. (1999) Plume-ridge interactions of the Discovery and Shona mantle plumes with the southern Mid-Atlantic Ridge 40°-55°S. *Journal of Geophysical Research* **104**, 2941-2962.

Douglass J. and Schilling J.-G. (2000) Systematics of three-component, pseudo-binary mixing lines in 2D isotope ratio space representations and implications for mantle plume-ridge interaction. *Chemical Geology* **163**, 1-23.

Fan Q.-C. and Hooper P.R. (1989) The mineral chemistry of ultramafic xenoliths of Eastern China: implications for upper mantle composition and the Paleogeotherms. *Journal of Petrology* **30**, 1117-1158.

Fan Q.-C., Sui J.-L. and Liu R.-X. (2001) Sr-Nd isotopic geochemistry and magmatic evolutions of Wudalianchi volcano, Tianchi volcano and Tengchong volcano. *Acta Petrologica et Mineralogica* **20**, 233-238 (in Chinese).

Fan Q.-C., Sui J.-L., Liu R.-X., Wei H.-Q., Li D.-M., Sun Q. and Li N. (2002) Periods of Quarternary volcanic activity in Longgang area, Jilin province. *Acta Petrologica Sinica* **18**, 495-500 (in Chinese).

Fram M.S. and Lesher C.E. (1993) Geochemical constraints on mantle melting during creation of the North Atlantic basin. *Nature* **363**, 712-715.

Goldstein S.L., Deines P., Oelkers E.H., Rudnick R.L. and Walter L.M. (2003) Standards for publication of isotope ratio and chemical data in Chemical Geology. *Chemical Geology* **202**, 1-4.

Graham D.W. (2002) Noble gas isotope geochemistry of mid-ocean ridge and ocean island basalts: characterization of mantle source reservoirs. *Reviews in Mineralogy & Geochemistry* **47**, 247-317.

Graham D.W., Larsen L.M., Hanan B.B., Storey M., Pedersen A.K. and Lupton J.E. (1998) Helium isotope composition of the early Iceland mantle plume inferred from the Tertiary picrites of West Greenland. *Earth and Planetary Science Letters* **160**, 241-255.

Griffin W.L., Zhang A., O'Reilly S.Y. and Ryan C.G. (1998) Phanerozoic evolution of the lithosphere beneath the Sino-Korean Craton. In: Flower M.F.J., Chung S.-L., Lo C.-H., Lee T.-Y. (Eds.) Mantle dynamics and plate interactions in east Asia. American Geophysical Union. 27.

Hannah R.S., Vogel T.A., Patino L.C., Alvarado G.E., Perez W. and Smith D.R. (2002) Origin of silicic volcanic rocks in Central Costa Rica: a study of a chemically variable ash-flow sheet in the Tiribi Tuff. *Bulletin of Volcanology* **64**, 117-133.

Hanson G.N. and Langmuir C.H. (1978) Modelling of major elements in mantle-melt systems using trace element approaches. *Geochimica et Cosmochimica Acta* **42**, 725-741.

Hart S.R. (1992) Mantle plumes and entrainment: isotopic evidence. *Science* **256**, 517-520.

Hart S.R., Blusztajn J., LeMasurier W.E. and Rex D.C. (1997) Hobbs Coast Cenozoic volcanism: implications for the West Antarctic rift system. *Chemical Geology* **139**, 223-248.

Hauri E.H., Whitehead J.A. and Hart S.R. (1994) Fluid dynamic and geochemical aspects of entrainment in mantle plumes. *Journal of Geophysical Research* **99**, 24275-24300.

Hawkesworth C.J., Kempton P.D., Rogers N.W., Ellam R.M. and van Calsteren P.W. (1990) Continental mantle lithosphere, and shallow level enrichment processes in the Earth's mantle. *Earth and Planetary Science Letters* **96**, 256-268.

Hilton D.R. and Craig H. (1989) A helium isotope transect along the Indonesian archipelago. *Nature* **342**, 906-908.

Hilton D.R., Gronvold K., Macpherson C.G. and Castillo P.R. (1999) Extreme $^{3}He/^{4}He$ ratios in northwest Iceland: constraining the common component in mantle plumes. *Earth and Planetary Science Letters* **173**, 53-60.

Hofmann A.W., Jochum K.P., Seufert M. and White W.M. (1986) Nb and Pb in oceanic basalts: new constraints on mantle evolution. *Earth and Planetary Science Letters* **79**, 33-45.

Jin B.-L. and Zhang X.-Y. (1994) Researching Volcanic Geology in Mount Changbai. Dongbei Chaoxianminzu Jiaoyu Press.

Jones J.H. (1984) Temperature- and pressure- independent corrleations of olivine/liquid partition coefficients and their application to trace element partitioning. *Contributions to Mineralogy and Petrology* **88**, 126-132.

Kelley K.A., Plank T., Ludden J. and Staudigel H. (2003) Composition of altered oceanic crust at ODP Sites 801 and 1149. *Geochemistry Geophysics Geosystems* **4**, Art. No. 8910 Jun 27.

Knaack C., Cornelius S.B. and Hooper P.R. (1994) Trace element analyses of rocks and minerals by ICP-MS. Lab Technical Notes, GeoAnalytical Lab, Washington State University, http://www.wsu.edu/~geology/geolab/note/icpms.html.

Kurz M.D., Jenkins W.J. and Hart S.R. (1982) Helium isotopic systematics of oceanic islands and mantle heterogeneity. *Nature* **297**, 43-47.

Kurz M.D., Jenkins W.J., Hart S.R. and Clague D. (1983) Helium isotopic variations in volcanic rocks from Loihi Seamount and the island of Hawaii. *Earth and Planetary Science Letters* **66**, 388-406.

Kurz M.D. (1986) In situ production of terrestrial cosmogenic helium and some applications to geochronology. *Geochimica et Cosmochimica Acta* **50**, 2855-2862.

Lai Y., Liu Y.L., Huang B.L. and Chen Y.J. (2005) The characteristics of noble gases in mantle-derived xenoliths in Wudalianchi and Kuandian, NE China: MORB-like mantle and metasomatized mantle. *Acta Petrol. Sinica* **21**(5), 1373-1381 (in Chinese).

Le Bas M.J., LeMaitre R.W., Streckeisen A. and Zanettin B. (1986) A chemical classification of volcanic rocks based on the Total Alkali-Silica diagram. *Journal of Petrology* **27**, 745-750.

Li Y.-H., Li J.-C., Song H.-B. and Guo L.-H. (2002) Helium isotope studies of the mantle xenoliths and megacrysts from the Cenozoic basalt in the eastern China. *Science in China* **45**, 174-183.

Liu G.-D. (1987a) The Cenozoic rift system of the North China Plain and the deep internal process. *Tectonophysics* **133**, 727-285.

Liu J.-Q. (1987b) Geochronology study on Cenozoic volcanic rocks in northeast China. *Acta Petrologica Sinica* **4**, 21-30 (in Chinese).

Liu J.-Q., Han J.-T. and Fyfe W.S. (2001) Cenozoic episodic volcanism and continental rifting in northeast China and possible link to Japan Sea development as revealed from K-Ar geochronology. *Tectonophysics* **339**, 385-401.

Liu J.-Q. (1999) Chinese Volcanoes. Beijing, Science Press (in Chinese).

Liu R.-X. (Editor) (1992) Geochoronlogy and Geochemistry of Cenozoic Volcanic Rocks in China. Beijing, Dizhen Chubanshe (in Chinese).

Liu R.-X. (Editor) (1995) Volcanic Activities and Human Environment. Seismology Press, Beijing.

Ma L.-F., Qiao X.-F., Min L.-R., Fan B.-X. and Ding X.-Z. (Editors) (2002) Geology Maps of China. Geology Press, Beijing, 348 pp.

Mahoney J.J., White W.M., Upton B.G.J., Neal C.R. and Scrutton R.A. (1996) Beyond EM-1: lavas from Afanasy-Nikitin Rise and the Crozet Archipelago, Indian Ocean. *Geology* **24**, 615-618.

Mayborn K.R. and Lesher C.E. (2004) Paleoproterozoic mafic dike swarms of northeast Laurentia: products of plumes or ambient mantle? *Earth and Planetary Science Letters* **225**, 305-317.

McDonough W.F. and Sun S.-S. (1995) The composition of the Earth. *Chemical Geology* **120**, 223-253.

Menzies M.A., Fan W. and Zhang M. (1993) Paleozoic and Cenozoic lithoprobes and the loss of >120 km of Archean lithosphere, Sino-Korean craton, China. In: Prichard H.M., Alabaster T., Harris N.B.W., Neary C.R. (Eds.) Magmatic processes and Plate Tectonics. Geological Society Special Publications, p. 71-81.

Menzies M.A. and Xu Y.G. (1998) Geodynamics of the North China Craton. In: Flower M.F.J., Chung S.-L., Lo C.-H., Lee T.-Y. (Eds.) Mantle Dynamics and Plate Interactions in East Asia. Geodynamics Series. American Geophysical Union, Washington, D.C., p. 155-165.

Niu Y.-L. (2005) Generation and evolution of basaltic magmas: some basic concepts and a new view on the origin of Mesozoic-Cenozoic basaltic volcanism in Eastern China. *Geological Journal of China Universities* **11**, 9-46.

O'Brien H.E., Irving A.J., McCallum I.S. and Thirlwall M.F. (1995) Strontium, neodymium, and lead isotopic evidence for the interaction of post-subduction asthenospheric potassic mafic magmas of the Highwood Mountains, Montana, USA, with ancient Wyoming craton lithospheric mantle. *Geochimica et Cosmochimica Acta* **59**, 4539-4556.

Peng Z.-C., Zartman R.-E., Futa K. and Chen D.-G. (1986) Pb-, Sr- and Nd- isotopic systematics and chemical characteristics of Cenozoic basalts, Eastern China. *Chemical Geology* **59**, 3-33.

Porcelli D.R., O'Nions R.K., Galer S.J.G., Cohen A.S. and Mattey D.P. (1992) Isotopic relationships of volatile and lithophile trace elements in continental ultramafic

xenoliths. *Contributions to Mineralogy and Petrology* **110**, 528-538.

Porcelli D.R., Stone J.O.H. and O'Nions R.K. (1987) Enhanced $^{3}He/^{4}He$ ratios and cosmogenic helium in ultramafic xenoliths. *Chemical Geology* **64**, 25-33.

Poreda R. and Craig H. (1989) Helium isotope ratios in circum-Pacific volcanic arcs. *Nature* **338**, 473-478.

Ren J.-Y., Tamaki K., Li S. and Zhang J.-X. (2002) Late Mesozoic and Cenozoic rifting and its dynamic setting in Eastern China and adjacent areas. *Tectonophysics* **344**, 175-205.

Roeder P.L. and Emslie R.F. (1970) Olivine-liquid equilibrium. *Contributions to Mineralogy and Petrology* **29**, 275-289.

Sengor A.M.C. and Natal'in B.A. (1996) Paleotectonics of Asian: fragments of a synthesis. In: Yin A., Harrison T.M. (Eds.) The Tectonic Evolution of Asian, Cambridge University Press, New York, p. 486–640.

Shangguan Z.-G., Du J.-K. and Zang W. (1998) Modern hot spring geochemistry at the Tanlu fault and Jiaoliao block in eastern China. *Science in China Series D* **41**, 87-94.

Shaw D.M. (1970) Trace element fractionation during anatexis. *Geochimica et Cosmochimica Acta* **34**, 237-243.

Song Y. and Frey F.A. (1989) Geochemistry of peridotite xenoliths in basalt from Hannuoba, Eastern China: implications for subcontinental mantle heterogeneity. *Geochimica et Cosmochimica Acta* **53**, 97-113.

Stracke A., Hofmann A.W. and Hart S.R. (2005) FOZO, HIMU, and the rest of the mantle zoo. *Geochemistry Geophysics Geosystems* **6**, Art. No. Q05007 May 19.

Tackley P.J., Stevenson D.J., Glatzmaier G.A. and Schubert G. (1993) Effects of an endothermic phase transition at 670 km depth in a spherical model of convection in the Earth's mantle. *Nature* **361**, 699-704.

Taylor B. and Martinez F. (2003) Back-arc basin basalt systematics. *Earth and Planetary Science Letters* **210**, 481-497.

Tu K., Xie G.-H., Zhang M., Wang J.-W., Flower M.F.J. and Carlson R.W. (1992) Sr, Nd and Pb isotopic compositions of Cenozoic basalt in East China. In: Liu R.-X. (Ed.) Cenozoic basalt in China: geochronology and geochemistry. Seismology Press, Beijing, pp. 330-338 (in Chinese).

Turner S. and Hawkesworth C. (1995) The nature of the sub-continental mantle: constraints from the major-element composition of continental flood basalts. *Chemical Geology* **120**, 295-314.

Wilde S.A., Zhou X.-H., Nemchin A.A. and Sun M. (2003) Mesozoic crust-mantle interaction beneath the North China craton: a consequence of the dispersal of Gondwanaland and accretion of Asia. *Geology* **31**, 817-820.

Wu M.B., Wang X.B., Ye X.R. and Zhang M. J. (2003) Noble gas isotopic compositions of Cenozoic volcanics and mantle-derived xenoliths from Kuandian in Liaoning Province and their significance. *Acta Petrol. Mineral.* **22**, 254-258 (in Chinese).

Xu S. and Liu C.-Q. (2002) Noble gas abundances and isotopic compositions in mantle-derived xenoliths, NE China. *Chinese Science Bulletin* **47**, 755-760.

Xu S., Nagao K., Uto K., Wakita H., Nakai S. and Liu C.-Q. (1998a) He, Sr and Nd isotopes of mantle-derived xenoliths in volcanic rocks of NE China. *Journal of Asian Earth Sciences* **16**, 547-556.

Xu Y.-G. (2002) Evidence for crustal components in the mantle and constraints on crustal recycling mechanisms: pyroxenite xenoliths from Hannuoba, North China. *Chemical Geology* **182**, 301-322.

Xu Y.-G., Menzies M.A., Thirlwall M.F., Huang X.-L., Liu Y. and Chen X.-M. (2003) Reactive harzburgites from Huinan, NE China: products of the lithosphere-asthenosphere interaction during lithospheric thinning? *Geochimica et Cosmochimica Acta* **67**, 487-505.

Xu Y.-G., Menzies M.A., Vroon P., Mercier J.C. and Lin C. (1998b) Texture-temperature-geochemistry relationship in the upper mantle as revealed from spinel peridotite xenoliths from Wangqing, N.E. China. *Journal of Petrology* **39**, 469-493.

Yin A. and Harrison M. (Editors) (1996) The Tectonic Evolution of Asia. Cambridge University Press, Cambridge, England, 666 pp.

Yokochi R., Marty B. and Pik R. (2005) High He-3/He-4 ratios in peridotite xenoliths from SW Japan revisited: evidence for cosmogenic He-3 released by vacuum crushing. *Geochemistry Geophysics Geosystems* **6**, Art. No. Q01004 Jan 21.

Zhang M., Menzies M.A., Suddaby P. and Thirlwall M.F. (1991) EM1 signature from within the post-Archaean subcontinental lithospheric mantle: Isotopic evidence from the potassic volcanic rocks in NE China. *Geochemical Journal* **25**, 387-398.

Zhang M., Stepehson P.J., O'Reilly S.Y., McCulloch M.T. and Norman M. (2001) Petrogenesis and geodynamic implications of late Cenozoic basalt in North Queensland, Australia: Trace-element and Sr-Nd-Pb isotope evidence. *Journal of Petrology* **42**, 685-719.

Zhang Z.-C., Feng C.-Y., Li Z.-N., Li S.-C., Xin Y., Li Z.-M. and Wang X.-Z. (2002) Petrochemical study of the Jingpohu Holocene alkali basaltic rocks, northeastern China. *Geochemical Journal* **36**, 133-153.

Zhao D.-P., Lei J.-S. and Tang R.-Y. (2004) Origin of the Changbai intraplate volcanism in Northeast China: Evidence from seismic tomography. *Chinese Science Bulletin* **49**, 1401-1408.

Zhi X.C. and Feng J.L. (1992) Geochemistry of Hannuoba basalt. In: Liu, R.-X. (Ed.), Geochoronlogy and Geochemistry of Cenozoic Volcanic Rocks in China. Beijing, Dizhen Chubanshe: 114-148 (in Chinese).

Zhou X.H. and Armstrong R.L. (1982) Cenozoic volcanic rocks of eastern China - secular and geographic trends in chemistry and strontium isotopic composition. *Earth and Planetary Science Letters* **58**, 301-329.

Zhou X.H. and Zhu B.Q. (1992) Cenozoic basalts in eastern China: Isotopic systematics and mantle geochemical zoning. In: Liu R.-X. (Ed.) Geochronology and Geochemistry of Cenozoic Volcanic Rocks in Eastern China, Seismological Press, Beijing (in Chinese), p. 366-391.

Zhou X.H., Sun M., Zhang G. and Chen S. (2002) Continental crust and lithospheric mantle interaction beneath North China: isotopic evidence from granulite xenoliths in Hannuoba, Sino-Korean cration. *Lithos* **62**, 111-124.

Zou H.-B. (2000) Modeling of trace element fractionation during non-modal dynamic melting with linear variations in mineral/melt distribution coefficients. *Geochimica et Cosmochimica Acta* **64**, 1095-1102.

Zou H.-B. and Zindler A. (1996) Constraints on the degree of dynamic partial melting and source composition using concentration ratios in magmas. *Geochimica et Cosmochimica Acta* **60**, 711-717.

Zou H.-B., Zindler A., Xu X. and Qi Q. (2000) Major, trace element, and Nd, Sr and Pb isotope stuides of Cenozoic basalts in SE China: mantle sources, regional variations, and tectonic significance. *Chem. Geol.* **171**, 33-47.

Chapter III

Olivine Dissolution in Basaltic Melt

Abstract

The main purpose of this work is to understand and quantify diffusive and convective olivine dissolution in basaltic melt. Crystal dissolution and growth in a magma chamber is often accompanied by the descent or ascent of the crystal in the chamber due to gravity. The motion induces convection that enhances mass transport. Such convective dissolution and growth rates have not been quantified before. MgO diffusivity in the melt (D_{MgO}), MgO concentration of the interface melt (C_0) and the effective thickness of the compositional boundary layer (δ) are necessary parameters to model the convective dissolution. Experiments of non-convective olivine dissolution in a basaltic melt were conducted at 1271-1480°C and 0.47-1.42 GPa in a piston-cylinder apparatus. At specific temperature and pressure conditions, multiple experiments of different durations show that the interface melt reaches near-saturation within 2 minutes. Therefore, diffusion, not interface reaction, is the rate-controlling step for non-convective olivine dissolution in basaltic melt. The compositional profile length and olivine dissolution distance are proportional to the square root of experimental duration, consistent with diffusive dissolution. D_{MgO} and C_0 are obtained from the experimental

results. D_{MgO} displays Arrhenian dependence on temperature, but the pressure dependence is small and not resolved. C_0 increases with increasing temperature and decreases with increasing pressure. Comparison with literature data shows that D_{MgO} depends strongly on the initial melt composition, while C_0 does not. δ is estimated from fluid dynamics. D_{MgO}/δ, which characterizes the kinetic and dynamic aspects of convective crystal dissolution, is parameterized as a function of temperature, pressure, and olivine composition. Convective olivine dissolution rate in basaltic melt can be conveniently calculated from the model results. This model may be applied to convective olivine dissolution in mantle xenoliths and to convective olivine growth, with limitations.

3.1. Introduction

Crystal dissolution in silicate melts is an essential process in igneous petrology. It is often encountered in treating xenolith and xenocryst digestion, magma contamination and some other magmatic processes. The theoretical and experimental methods utilized to attack this problem and the data obtained are also helpful for other problems, such as multi-component diffusion in silicate melts, crystal melting, crystal growth in silicate melts, and crystal growth and dissolution in aqueous solutions.

Numerous studies on crystal dissolution have been carried out (see Kerr, 1995 for brief reviews of early works; recent works include Shaw et al., 1998; Liang, 1999, 2000, 2003; Shaw, 2000; Acosta-Vigil et al., 2002; Morgan and Liang, 2003; Zhang and Xu, 2003; Shaw, 2004; Acosta-Vigil et al., 2006; Morgan et al., 2006; Shaw, 2006). Crystal dissolution in silicate melts can be controlled by interface reaction and mass transfer. Heat transfer is often considered not the rate-controlling mechanism because it is faster

than mass transfer in silicate melts. Mass transfer can be either diffusive (e.g. Zhang et al., 1989; Liang, 1999) or convective (e.g. Kerr, 1995; Liang 2003; Zhang and Xu, 2003). These two types of mass transfer must be treated by different experimental and mathematical methods. For diffusive and convective crystal dissolution, the interface melt is not at exact saturation but at near-saturation. At exact saturation no dissolution (or growth) would occur. From numerical calculation perspective, however, the difference between melt compositions at near-saturations and exact saturation is negligible. For crystal growth, nucleation is an important process in addition to interface reaction and mass transfer.

Convection can arise from motion induced by crystal settling (e.g., Martin and Nokes, 1988) due to the density difference between the crystal and melt, or from density difference between the interface melt and far-field melt. In some earlier experimental works on crystal dissolution in silicate melts, convection was not specifically suppressed and was likely present. Those experiments yield direct measurement of convective dissolution rate. However, as pointed out by Zhang et al. (1989), the results cannot be used to quantify chemical diffusivities, and the application of the measured dissolution rate is limited to natural systems of similar convection regimes. Theory on convective crystal dissolution rate has been developed by Kerr (1995) for Reynolds number ≤ 1. Recently, Zhang and Xu (2003) expanded this theory to Reynolds number up to 10^5. To estimate convective dissolution rate based on this theory, it is necessary to know the diffusivity of the equilibrium-determining component in the melt and the interface melt composition, which can be obtained from diffusive crystal dissolution experiments. The interface melt composition may also be extracted from convective dissolution

experiments. Crystal growth experiments often involve nucleation and are more complicated than crystal dissolution experiments, hence not suitable for diffusivity measurement. Many authors investigated non-convective dissolution (e.g., Watson, 1982; Zhang et al., 1989; Finnila et al., 1994; Liang, 1999, 2000; Shaw, 2000, 2004, 2006; Morgan et al., 2006). In particular, Shaw (2000) showed experimentally that the dissolution rate of quartz dissolving in basanite melt depends strongly on the mass transfer mechanism.

Zhang et al. (1989) numerically examined the relative role of the interface reaction and diffusive mass transfer. Using the interface reaction rate of diopside (Kuo and Kirkpatrick, 1985), Zhang et al. (1989) concluded that the interface melt reaches near-saturation within a few seconds, and convection-free crystal dissolution is controlled by diffusive mass transfer afterwards. That is, non-convective crystal dissolution in silicate melts is practically diffusive. This conclusion is consistent with experimental results of olivine, diopside, spinel, quartz and rutile dissolution in andesitic melt (Zhang et al., 1989), and quartz in haplodacitic melt (Liang, 1999), among others. However, Acosta-Vigil et al. (2002) and Shaw (2004) suggested that interface reaction plays a role in corundum and andalusite dissolution in haplogranitic melt, and quartz dissolution in synthetic melts (43-60 wt% SiO_2), respectively. Therefore, it is of interest to further address the relative role of interface reaction and diffusion in non-convective dissolution.

Olivine is commonly found in mantle xenolith or as single xenocryst in basalts. Olivine dissolution in silicate melts has been extensively investigated in early experimental works, but the relative role of diffusive and convective mass transfer was not well characterized, and the application of the experimental results are limited. Zhang

et al. (1989) carried out diffusive olivine dissolution experiments. However, this work was on andesitic melt, and did not systematically examine the pressure effect on the interface melt composition (i.e., the saturation state).

With these issues in mind, we report an experimental study on diffusive olivine dissolution in a mid-ocean ridge basalt at 1271 to 1480°C and 0.47 to 1.42 GPa. The tholeiitic melt composition is chosen because it is the most common basalt and good quality natural glass samples are available. The applicability of the model result to other types of basaltic melts (such as alkali basalt) is discussed in Section 3.5.7. The experimental results are used to (i) characterize interface melt composition at different temperature and pressure; (ii) examine if the interface melt composition depends on the experimental duration to assess the role of interface reaction; (iii) determine diffusion rate in the basaltic melt at different temperature and pressure; and (iv) model convective olivine dissolution in basaltic melt using the theoretical framework by Kerr (1995) and Zhang and Xu (2003).

3.2. Theoretical Background

Below we briefly introduce the theories on crystal dissolution, with emphasis on the practical calculation methods employed in this study.

3.2.1. Interface Reaction

Based on the transition state theory, interface reaction rate can be expressed as follows (simplified from Eqn. (31) in Kirkpatrick, 1981):

$$u = ATe^{-E/(RT)}(1-w), \tag{3-1}$$

where u is the melt growth rate (m/s in SI units), A is a constant depending on the crystal and melt structure and the nature of the activated transition complex (m s^{-1} K^{-1}), T is the absolute temperature (K), E is the activation energy for detachment of atoms from the crystal surface (J/mol), R is the gas constant (J K^{-1} mol^{-1}), and w (dimensionless) is the degree of saturation of the interface melt, which may be expressed as:

$$w = \mathrm{e}^{-\Delta G/(RT)} \approx \frac{C}{C_\mathrm{e}}, \tag{3-2}$$

where ΔG is the Gibbs free energy change of the dissolution reaction (J/mol), and C and C_e are the concentration and saturation concentration of the crystalline component in the melt (for a one-component crystal, or for a principal equilibrium-determining component). The crystal dissolution rate equals the melt growth rate u multiplied by the density ratio of melt to crystal.

3.2.2. Convection-Free Crystal Dissolution

Interface reaction and diffusion are two necessary sequential steps for convection-free crystal dissolution, when the crystal and melt compositions are different (i.e. when mass transfer is necessary). Atoms are detached from the crystal surface into the melt and the interface melt is modified towards the saturation composition. Compositional gradient in the melt develops and diffusive mass transport occurs. If diffusion is rapid compared to interface reaction, compositional gradient would be eliminated and the interface melt would remain near its initial composition. In this end-member case, the rate-limiting step is interface reaction. In the other end-member case, interface reaction is rapid compared to diffusion, the interface melt reaches near-saturation rapidly, and the rate-controlling step is diffusion. This is referred to as diffusive crystal dissolution. If the rates of

diffusion and interface reaction are comparable, the interface melt approaches the near-saturation composition in some finite time. This finite time is referred to as the "transition stage" hereafter. In the transition stage, both interface reaction and diffusion affect the dissolution rate. After this transition stage, saturation is nearly reached and diffusion becomes the only rate-controlling process. The duration of the transition stage depends on the rate of diffusion and interface reaction, and therefore may depend on temperature.

For diffusive crystal dissolution, the interface melt cannot be simply treated by crystal-melt equilibrium. First, the interface melt is not at exact saturation but at near-saturation (e.g., Fig. 1 in Zhang et al. 1989). At exact saturation no dissolution (or growth) would occur. Hence, "near-saturation" is used to refer such a state. From numerical calculation perspective, however, the difference between melt compositions at near-saturations and exact saturation is negligible. Second, the near-saturated melt is not necessarily in near-equilibrium with the dissolving crystal if the crystal is a solid solution (Fig. 19 in Zhang et al. 1989) because the crystal composition during crystal dissolution is fixed (and randomly picked). In other words, the liquidus crystal composition may be different from the dissolving crystal.

In a reference frame fixed at the crystal-melt interface, one dimensional reaction-diffusion equation in the melt for crystal dissolution in an infinite melt reservoir can be written as:

$$\frac{\partial w}{\partial t} = \frac{\partial}{\partial x}(D\frac{\partial w}{\partial x}) - u\frac{\partial w}{\partial x}, \tag{3-3a}$$

with initial condition: $w\big|_{t=0} = w_\infty$ at $x > 0$, (3-3b)

boundary condition 1: $w\big|_{x=\infty} = w_\infty$ at $t > 0$, (3-3c)

and boundary condition 2: $D\frac{\partial w}{\partial x}\big|_{x=0} = u(w_0 - w_c)$ at $t > 0$, (3-3d)

where t is time (s), x is the distance in the melt from the interface (m), D is effective binary diffusivity of the principal-equilibrium-determining component (m^2/s), w is the degree of saturation (Eqn. 3-2), w_∞ is w of the initial melt, w_0 is w of the interface melt (w_0 approaches 1 for diffusive dissolution), and w_c is the degree of saturation of a hypothetical melt that has the same composition of the crystal. The initial condition means that the melt is initially homogeneous. Boundary condition 1 states that the far-field melt composition is unchanged over the duration of the dissolution process (infinite reservoir assumption). Boundary condition 2 is the mass balance condition at the interface, i.e., dissolved extra component equals the diffusive mass flux. This study implements an approximate approach using effective binary diffusion and equilibrium-determining component. More sophisticated models based on multiple component equilibrium and diffusion may be constructed when enough data are available for natural silicate melts.

If interface reaction is fast, the transition stage can be ignored, and the interface melt composition is practically a constant. The dissolution can be treated as purely diffusion controlled. We have (Crank, 1975, p 298-308):

$$u = \alpha\sqrt{\frac{D}{t}}, \tag{3-4}$$

where parameter α is to be determined from:

$$\sqrt{\pi}\alpha e^{\alpha^2}\,\mathrm{erfc}(-\alpha) = (w_0 - w_\infty)/(w_c - w_0). \tag{3-5}$$

Substitute Eqn. (3-4) in Eqn. (3-3a), the solution for the composition profile in the melt is:

$$w = w_\infty + (w_0 - w_\infty)\,\mathrm{erfc}\left(\frac{x}{2\sqrt{Dt}} - \alpha\right) \Big/ \mathrm{erfc}(-\alpha). \qquad (3\text{-}6)$$

If the interface reaction rate is slow such that the transition stage cannot be ignored (i.e., the interface melt composition changes significantly), Eqn. (3-6) cannot be applied. If the necessary parameters in Eqn. (3-1) are known, Eqn. (3-3) can be combined with Eqn. (3-1) and solved numerically.

Whether to consider the transition stage or not depends on the time scale of interest. For example, if the interface reaction takes several hours to reach saturation, it must be considered if a dissolution experiment of several hours is under question, but can be ignored if a natural process of several years or longer is under question.

3.2.3. Convective Dissolution

Two types of convection relevant to crystal dissolution have been discussed in the literature (Kerr, 1995). In free convection the interface melt detaches from the interface and sinks or rises through the bulk melt due to their density difference. Forced convection refers to the removal of the interface melt as the crystal moves relative to the melt, which might be due to the buoyant descent or ascent of the crystal in the melt, or magma flow against the magma chamber wall. Far away from the crystal, convection maintains a homogeneous and constant melt composition. A compositional gradient exists within a melt layer around the crystal, which is called the compositional boundary layer. Within this boundary layer, mass is transported by diffusion. The strength of convection determines the boundary layer thickness.

If the interface reaction is rapid so that the interface melt is near saturation, the dissolution is referred to as convective dissolution. In this study, for simplicity the

diffusion across the boundary layer is treated as effective binary diffusion for the principal equilibrium-determining component (multi-component treatment may be applied as in Liang, 1999, 2000, 2003; Morgan et al., 2006). To model the convective dissolution rate using the effective binary approach, one needs to know the diffusivity in the melt, the concentrations of the principal equilibrium-determining component in interface melt, and the boundary layer thickness. The diffusivity and the interface melt composition can be obtained from diffusive crystal dissolution experiments, which is one of the purposes of this study. The boundary layer thickness needs to be estimated from fluid dynamics.

For one specific case of convective dissolution: a single spherical crystal falling or rising in an infinite melt reservoir due to density difference, the following calculation method is used to obtain the effective boundary layer thickness δ and the dissolution rate (Kerr, 1995; Zhang and Xu, 2003):

(1) Assign initial conditions, including melt composition, density (ρ_m), viscosity (η), cation diffusivity in the melt (D), and crystal composition, density (ρ_c) and radius (a).

(2) Use the following three equations to solve for Reynolds number (Re), crystal falling or rising velocity (U, m/s) and drag coefficient (C_D):

$$\mathrm{Re} = \frac{2aU\rho_m}{\eta}, \tag{3-7a}$$

$$U = \sqrt{\frac{8ga|\rho_c - \rho_m|}{3\rho_m C_D}}, \tag{3-7b}$$

$$C_D = \frac{24}{\mathrm{Re}}(1 + 0.15\mathrm{Re}^{0.687}) + \frac{0.42}{1 + 42500\mathrm{Re}^{-1.16}}. \tag{3-7c}$$

Eqn. (3-7a) is the definition of the Reynolds number Re. Eqn. (3-7b) is the general equation to calculate the falling or rising velocity of a rigid spherical particle in a fluid (Turcotte and Schubert, 1982). Eqn. (3-7c) is from Clift et al. (1978) and has a relative error of ~ ±5% for Re ≤ 3× 10^5.

(3) Calculate compositional Peclet number (Pe) as (definition of Pe):

$$\mathrm{Pe} = 2aU/D. \tag{3-8}$$

(4) Calculate the Sherwood number (Sh) as following, for Re ≤ 10^5 (Zhang and Xu, 2003):

$$\mathrm{Sh} = 1 + (1+\mathrm{Pe})^{1/3}\left(1 + \frac{0.096\mathrm{Re}^{1/3}}{1+7\mathrm{Re}^{-2}}\right). \tag{3-9}$$

(5) Calculate the effective boundary layer thickness δ (m) as (definition of the Sherwood number Sh):

$$\delta = 2a/\mathrm{Sh}. \tag{3-10}$$

(6) Use equilibrium data to calculate the concentration (wt%) of the equilibrium-determining component at the interface (C_0), and then determine dimensionless parameter β as:

$$\beta = \frac{\rho_m(C_0 - C_\infty)}{\rho_c(C_c - C_0)}. \tag{3-11}$$

(7) Calculate the crystal dissolution rate u:

$$u = \beta D/\delta. \tag{3-12}$$

When a crystal is very small (e.g. <100 μm), free convection may be more important than the forced convection described above. In this case, rather than using Eqns. (3-7) to (3-9) to calculate Sh, one uses:

$$\mathrm{Sh} = 2 + 0.6\mathrm{Ra}^{1/4}, \tag{3-13}$$

where Ra is the Rayleigh number defined as:

$$\mathrm{Ra} = \frac{8ga^3\Delta\rho}{\eta D}, \tag{3-14}$$

where $\Delta\rho$ is the density difference between the interface melt and far-field melt. Eqn. (3-13) works when $\mathrm{Ra} \leq 10^{10}$. In our calculation, Sh for the forced convection and free convection are both calculated and the larger one (i.e., the thinner boundary layer) is used in Eqn. (3-10).

Note that the above calculation scheme deals with forced convection due to relative motion between the crystal and the melt driven by the density difference, regardless of the absolute motion of the melt body. The crystal may travel upward together with the erupting magma, and olivine would still be falling relative to the melt and the calculation method is applicable. The relative motion between the crystal and the melt determines the boundary layer thickness, whereas the overall motion of the melt-crystal system does not affect it. Walker and Kiefer (1985) conducted two sets of experiments on convective NaCl dissolution in water. In the first set, water was stationary in laboratory-fixed reference frame and NaCl crystal was falling freely in water. In the second set, water flowed upward at a velocity roughly the same as the falling velocity of NaCl crystal, leading to roughly stationary NaCl crystal. The dissolution rates obtained from these two sets of experiments were consistent (except for a slight temperature effect), indicating that it is the relative motion between the crystal and fluid, not the overall motion of water, that affects the dissolution rate. On the other hand, if the crystal is fixed to the magma chamber wall, roof or floor, the relative velocity U between the crystal and the melt would be the magma flow velocity but not the crystal sinking or rising velocity due to gravity, and estimation of crystal dissolution rate requires different

equations (e.g., Eqn. 10 in Zhang and Xu, 2003).

3.3. Experimental and Analytical Methods

Experiments were conducted using a 1/2-inch piston-cylinder apparatus at the University of Michigan. At some *T-P* conditions, series of experiments of different durations were conducted to examine how the interface melt composition changes with time and whether the dissolution distance is proportional to the square root of time.

The basalt sample is from Juan de Fuca Ridge, with <1% phenocrysts (plagioclase, augite and olivine) and <0.5% vesicles (Dixon et al., 1986, 1988). It contains ~0.4 wt% of water (Zhang and Stolper, 1991). The starting olivine crystals are from San Carlos, AZ. The compositions of the basalt and olivine are listed in Table 3-1.

Table 3-1. Starting material compositions.

	San Carlos olivine (wt%)	Basalt (wt%)	Error in glass measurement (2σ)	Standard*
SiO_2	41.33	50.23	0.40	K-feldspar
TiO_2		1.94	0.08	geikielite
Al_2O_3		13.61	0.16	K-feldspar
FeO	9.16	12.06	0.19	ferrosilite
MnO	0.18	0.22	0.11	rhodonite
MgO	49.72	7.05	0.12	olivine
CaO	0.11	10.75	0.19	clinopyroxene
Na_2O		2.73	0.10	albite
K_2O		0.17	0.05	K-feldspar
P_2O_5		0.10	0.09	apatite
H_2O		0.25-0.40**		
Total	100.49	99.16		

*: beam condition: 15 kV, 5 nA, 5×5 or 15×15 μm raster. Typical counting times are 20 s with the exception of SiO_2 (60 s), TiO_2 (30 s), FeO (60 s) and CaO (30 s).

**: Fourier transform infrared (FTIR) spectrometry measurement

Olivine grains were cut and ground into 2.4 mm diameter rods, sliced into ~0.5 mm thick discs, and doubly-polished. The discs were examined under an optical microscope, and those chosen for experiments were inclusion free and usually cracks free. Occasionally, samples with very small cracks that do not intercept the interface were accepted. The initial thickness of the olivine disc was measured by a digital micrometer. Basaltic glass was cut and ground into 2 mm diameter rods, sliced into ~1.6 mm thick discs, and doubly-polished. The olivine disc was larger in diameter than the glass, such that the rim of the olivine disc was not in contact with the melt and can be used as a reference position to measure dissolution distance after experiments (Fig. 3-1). Glass was placed above olivine in a graphite capsule to suppress convection, because the melt produced by olivine dissolution is denser than the initial melt. The graphite capsule was fit into MgO pressure medium, which was placed inside a graphite heater, and then into $BaCO_3$ pressure medium. To minimize the temperature gradient inside the capsule and to improve the accuracy of temperature determination, relatively short samples were used, with total olivine+glass thickness of ~2.2 mm. To optimize the consistency in the actual temperature of multiple experiments at a given nominal temperature-pressure condition, we used the same sample size and capsule geometry for all experiments.

Experimental procedures are as follows. The experimental assembly is first pressurized to the target pressure by piston-out procedure, i.e., pressurized to about 5 to 10% higher than the target pressure and then relaxed back to target pressure. To improve the pressure reliability, we let the assembly relax at 150°C for ~4 hours. The assembly is heated up to the target temperature at a programmed rate of ~15ºC/second. The liquidus temperature calculated by the MELTS program (Ghiorso and Sack, 1995; Asimow and

Ghiorso, 1998) is ~1243ºC at 0.47 GPa, ~1322ºC at 0.95 GPa and ~1392ºC at 1.42 GPa. Olivine is the liquidus phase at 0.5 GPa, and a near-liquidus phase at 1.0 and 1.5 GPa. The target temperature is always higher than the liquidus temperature of the melt to ensure olivine dissolution. The sample is maintained at the pressure and temperature for a planed duration (nominal duration), and then quenched down by turning off the power.

Nominal "zero-time" experiments were conducted by turning off the power once the thermocouple recording reached the planed experimental temperature. These "zero-time" experiments have nominal durations of several seconds. The main purpose of the "zero-time" experiments is to quantify the extent of reaction and diffusion during the heating up and quenching (Zhang and Stolper, 1991; Zhang, 1994).

A Eurotherm temperature controller is used with a type-S thermocouple at the top of the graphite capsule to monitor and control the temperature. The thermocouple tip was covered by alumina cement, and separated from the graphite capsule by an MgO disc (~0.6 mm thick). The thermal history is recorded by a computer. Variation at the target temperature is typically ±1 ºC. Overshooting is < 6°C and lasts < 6 seconds. The pressure is monitored and adjusted manually, with an uncertainty of ~7 MPa.

The distance from the thermocouple tip to the olivine-melt interface after experiments is ~2 mm. The temperature at the olivine-melt interface is corrected based on the thermal gradient calibrated by Hui et al. (2008). For our capsule geometry, the temperature correction varies from ~20ºC at about 1250ºC to ~26ºC at about 1450ºC. The temperature uncertainty is estimated to be about 10 to 15°C. The nominal pressures are 0.5, 1.0 and 1.5 GPa. Pressure calibration using quartz-coesite transition indicates the real

pressure is lower than the nominal pressure by ~5.5% (Hui et al., 2008, Ni and Zhang, 2008). The real pressures are hence 0.47, 0.95 and 1.42 GPa.

After the experiments, samples were embedded in epoxy mounts and prepared for electron microprobe analysis. Composition profiles were measured by a Cameca SX100 electron microprobe at Electron Microbeam Analysis Laboratory of the University of Michigan. Analytical details are listed in Table 3-1. Some samples were doubly-polished for FTIR measurement. Olivine dissolution distance was measured by three different methods: (1) subtracting the final thickness from the initial thickness (L_1 in Table 3-2); (2) measurement under microscope (L_2 in Table 3-2); and (3) measurement under electron microprobe (L_3 in Table 3-2).

Table 3-2. Summary of experimental conditions and results

Exp#	P (GPa)	T_1 (ºC)	T_2 (ºC)	Duration (s)		Olivine dissolution distance (μm)			
				t_1	t_2	L_1	L_2	L_3	L_4
15	0.47	1271	1287	721	730	1±11	10±7	11±6	9±1
16	0.47	1270	1351	1798	1806	21±14	18±11	12±10	16±1
18	0.47	1270	1315	3594	3602	23±10	23±6	20±5	23±2
20	0.47	1270	1297	302	310	-1±16	5±12	3±12	5±1
21	0.47	1270	1394	721	729	11±12	13±8	13±7	12±1
22*	0.47	1273		6	14	3±9	5±6	3±5	
23	0.47	1373	1359	303	312	29±12	26±8	28±7	23±1
24*	0.47	1370		2	12	8±14	4±11	3±10	
25	0.47	1376	1363	123	133	24±8	24±4	22±4	16±1
26	0.47	1370	1301	721	731	45±9	41±6	42±5	39±3
29	0.47	1372	1360	123	132	11±11	17±8	22±7	19±1
33	0.47	1368	1432	1200	1209	56±11	46±7	47±6	48±2
34	0.47	1473	1363	245	255	67±9	62±5	59±4	73±3
35*	0.47	1470		6	16	-4±11	4±7	2±6	
37	0.47	1476	1422	602	615	106±11	98±8	95±7	108±3
38	0.47	1477	1434	66	76	34±13	39±9	36±9	39±1
39	0.94	1374	1483	245	252	18±11	17±7	13±6	14±1
40	0.94	1376	1409	963	970	36±13	33±9	30±8	30±1
41	0.94	1379	1436	484	491	20±11	21±8	20±7	21±1
43	0.94	1480	1418	242	253	57±12	60±9	65±8	64±2
44	1.42	1374	1256	243	251	8±11	9±7	5±6	9±1
45	1.42	1422	1395	243	252	29±10	32±6	32±5	28±1
46	1.42	1425	1375	704	713	38±17	43±13	44±13	44±1

Note: P is the corrected pressure; T_1 is the corrected temperature; T_2 is the liquidus temperature by the model of Gaetani and Watson (2002); t_1 is the nominal duration, t_2 is the corrected duration; L_1 is the dissolution distance obtained from measured initial distance (using a digital micrometer) minus final distance (measured under optical microscope), L_2 is the thickness of dissolved olivine (against reference olivine edge) measured by optical microscope, L_3 is that measured by electron microprobe, and L_4 is calculated by Eqn. (3-18). The errors are at 2σ level.

*: “zero-time" experiment

3.4. Experimental Results

Table 3-2 shows the run conditions of all successful experiments. Experimental durations are corrected following Zhang and Behrens (2000). Fig. 3-1 shows a back-scattered electron (BSE) image of a polished experimental charge (Exp#43). Cracks are always present in the glass and olivine after experiments. The cracks in glass are mostly sub-parallel to the interface. The cracks in olivine can be divided into two types: those filled by graphite or unfilled and those filled by glass. The latter is avoided when measuring diffusion profiles in the melt. The part of the olivine in contact with melt is dissolved and indented, while the rim (not in contact with melt) remains intact.

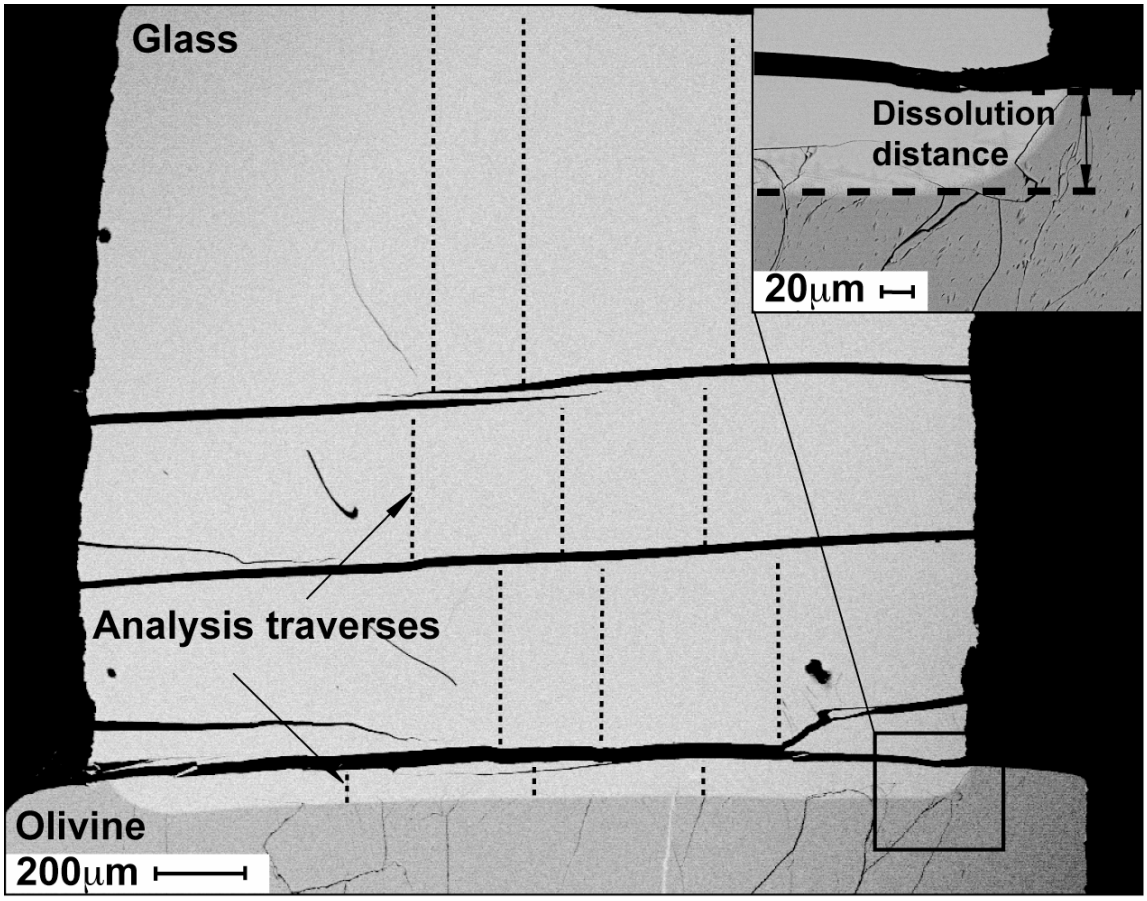

Figure 3-1. Back-scattered electron (BSE) image of the cross-section of Exp#43. Olivine disc is at the bottom of the image. The inset shows a magnified view of the interface, where the olivine dissolution distance is clearly shown and can be measured directly.

The olivine-melt interface is straight unless disrupted by cracks in the olivine. For experiments at ~1272ºC and 0.47 GPa, the olivine-melt interface is crystal-free. For experiments at ~1372ºC, 0.47 GPa and ~1376ºC, 0.95 GPa, sparse needle-shaped crystals can be seen near the interface, extending a few micrometers into the glass. For the other experiments, cluster of crystals with dendritic texture extends up to ~250 μm away from the interface (Fig. 3-2). The extent of the crystals in Exp#43 and 44 is marked in Figs. 3-7 and 3-8. The crystal texture shows no dependence on experimental duration. The composition of the crystals cannot be measured accurately because they are too thin. Energy dispersive spectrometer analysis suggests that they are olivine and clinopyroxene.

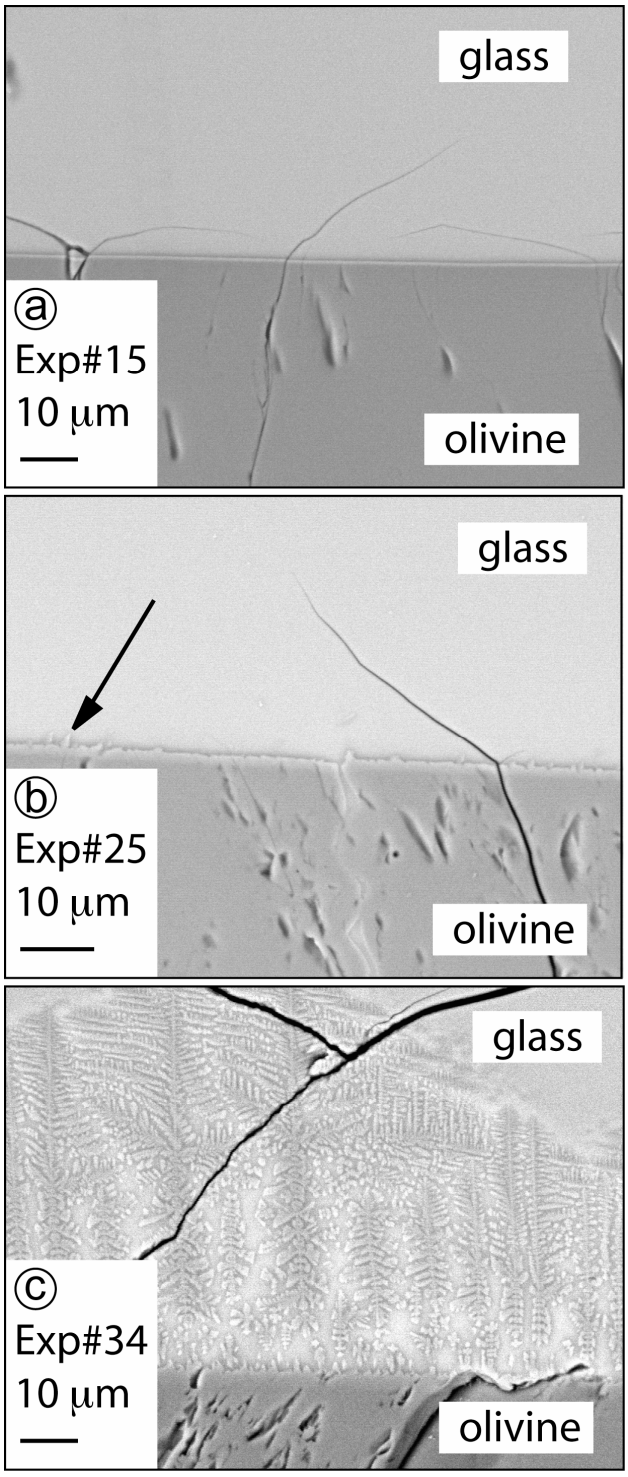

Figure 3-2. Olivine-melt interface and quench crystals. a: Exp#15, 0.47 GPa, 1271°C. b: Exp#25, 0.47 GPa, 1372°C. The arrow points to a quench crystal extending from the interface into the glass. c: Exp#34: 0.47 GPa, 1474°C.

Olivine dissolution distance is listed in Table 3-2. Measurement of the final olivine thickness under microscope has an error of ±5 μm. Measurement of the dissolution distance between the rim and the center has an error of ±1.25 μm under microscope, and ±0.5 μm under electron microprobe. An additional error is due to the heterogeneity in the initial olivine thickness, which on average is about ±5 μm (2σ).

At least three compositional profiles were measured for each experiment (example traverses are shown in Fig. 3-1). Profiles across cracks are re-connected smoothly. When working in crystal-free zone, the electron beam size was 5×5 μm. When working within the cluster of crystals near the olivine-melt interface, a larger beam size was used (15×15 μm). Profiles within the cluster of crystals are consistent with those in crystal-free zone, although with larger scatters. Time-series counting on Na x-ray intensity shows no sign of Na loss under these beam conditions. If the multiple profiles of one experiment are not consistent, the experiment is considered as being failed. Three experiments are classified as failed by this criterion and are not reported. Compositional profiles of all successful experiments are shown in Figs. 3-3 to 3-9, with the crystal-melt interface at x=0. All electron microprobe data of the concentration profiles are in the Appendix B. The far-field melt composition is in close agreement with the initial composition (Table 3-1). The profiles of different durations are in good agreement after normalization by square root of time. Data scatters in the profiles are discussed in Section 3.5.3. FeO shows strong uphill diffusion toward the interface, and Na_2O and K_2O display uphill diffusion toward high SiO_2 melt. For example, in Fig. 3-3, the Na_2O profile has a concentration maximum at $x/t^{1/2} \approx 10$. The profiles bend abruptly within 10 to 40 μm of the interface (SiO_2, TiO_2, Al_2O_3, CaO and Na_2O increase while FeO and MgO decrease

toward the interface), which are opposite to the overall trend defined by the major part of each profile. This feature is attributed to olivine overgrowth during quench and discussed further in Section 3.5.1.

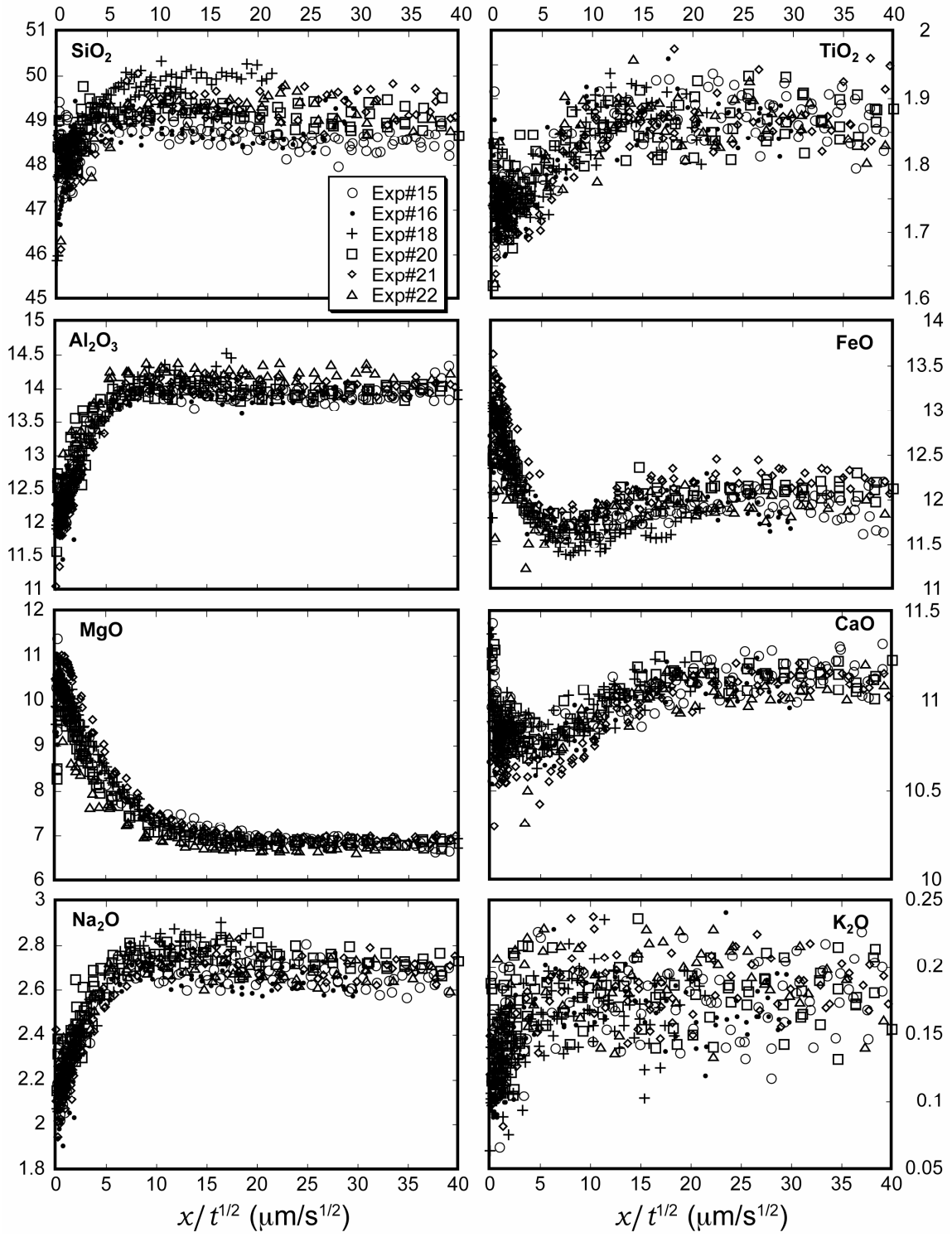

Figure 3-3. Concentration profiles at ~1271ºC and 0.47 GPa. The vertical axes are oxide wt%. Olivine-melt interface sets at x=0.

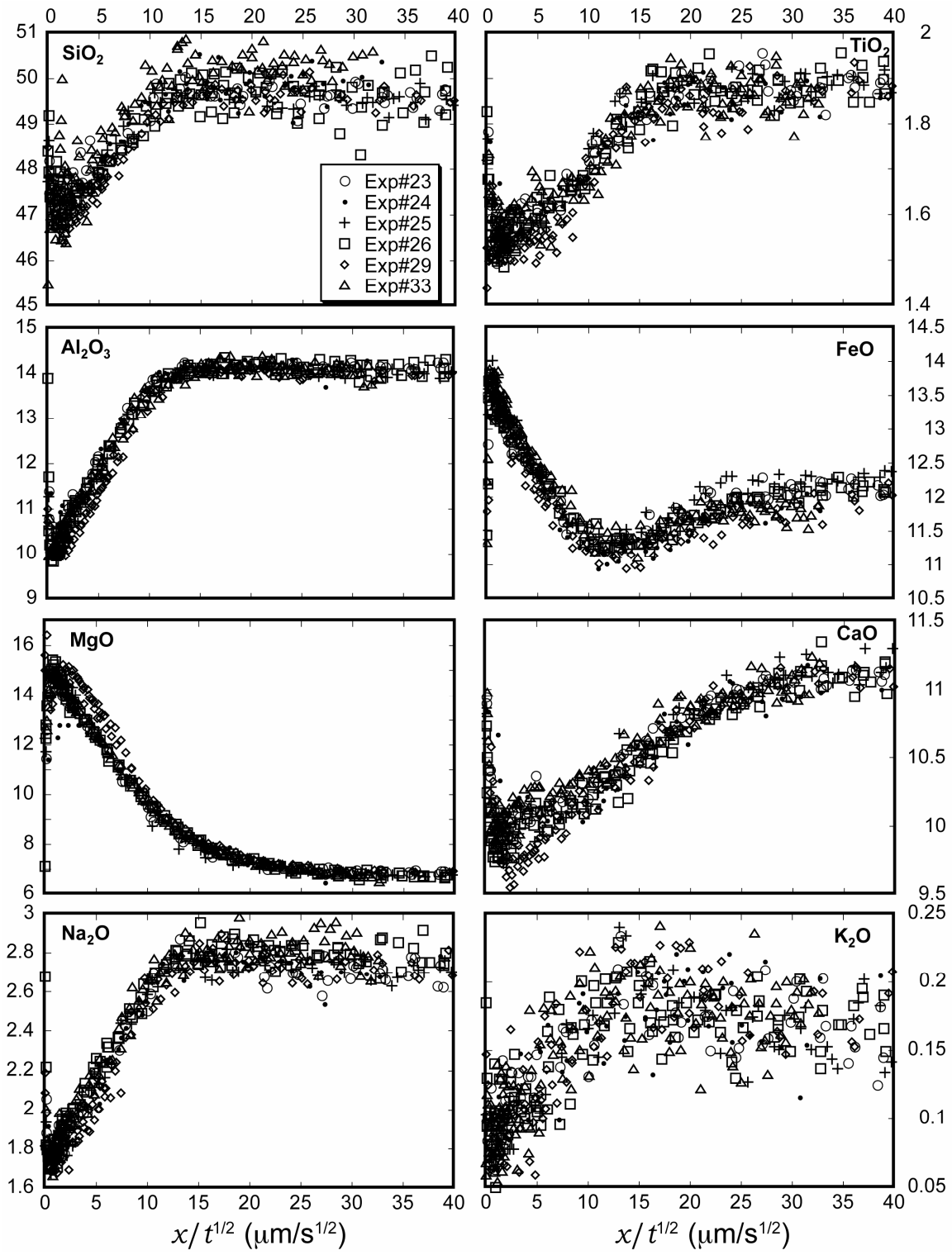

Figure 3-4. Concentration profiles at ~1372ºC and 0.47 GPa. The vertical axes are oxide wt%. Olivine-melt interface sets at x=0.

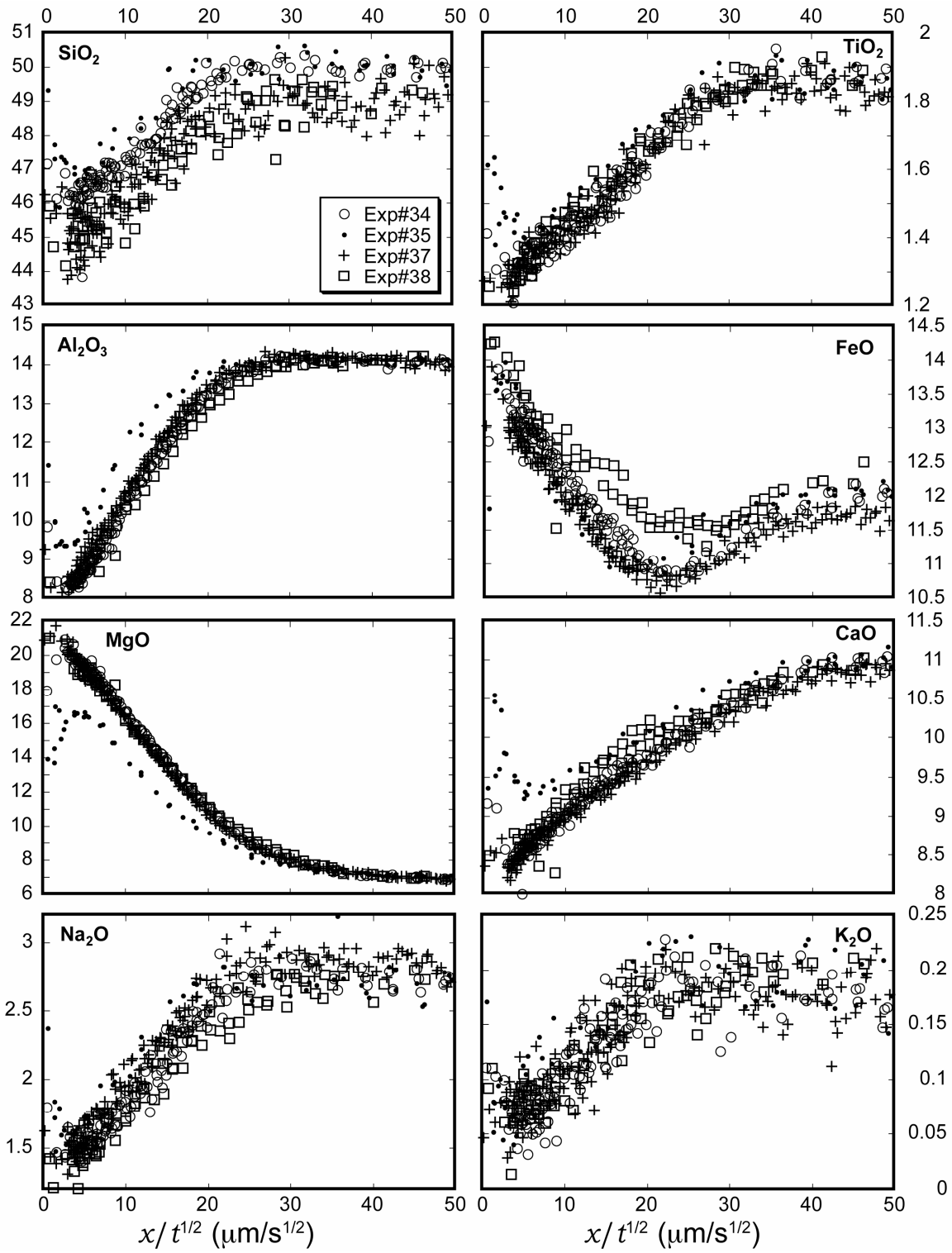

Figure 3-5. Concentration profiles at ~1474ºC and 0.47 GPa. The vertical axes are oxide wt%. Olivine-melt interface sets at x=0.

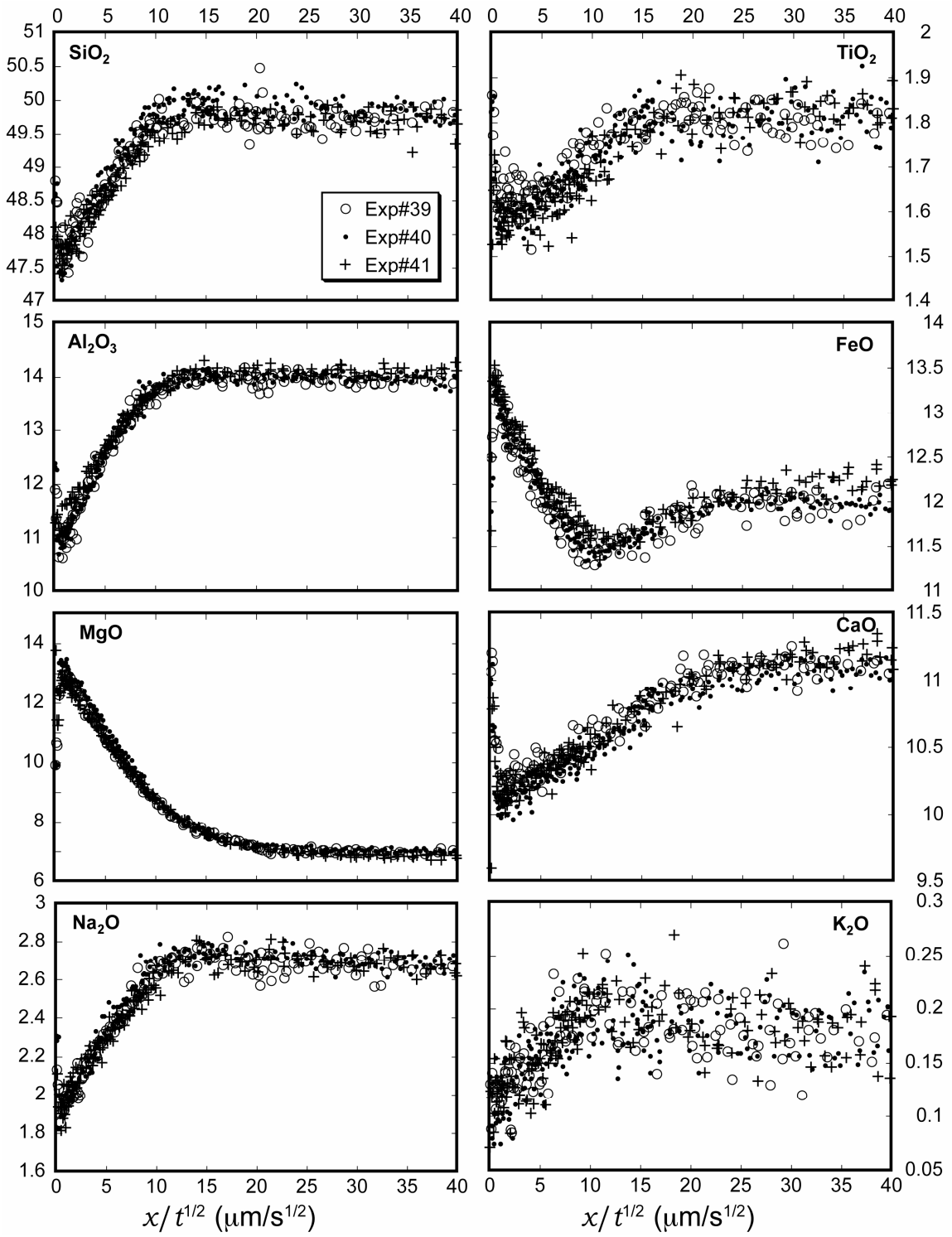

Figure 3-6. Concentration profiles at ~1376ºC and 0.95 GPa. The vertical axes are oxide wt%. Olivine-melt interface sets at x=0.

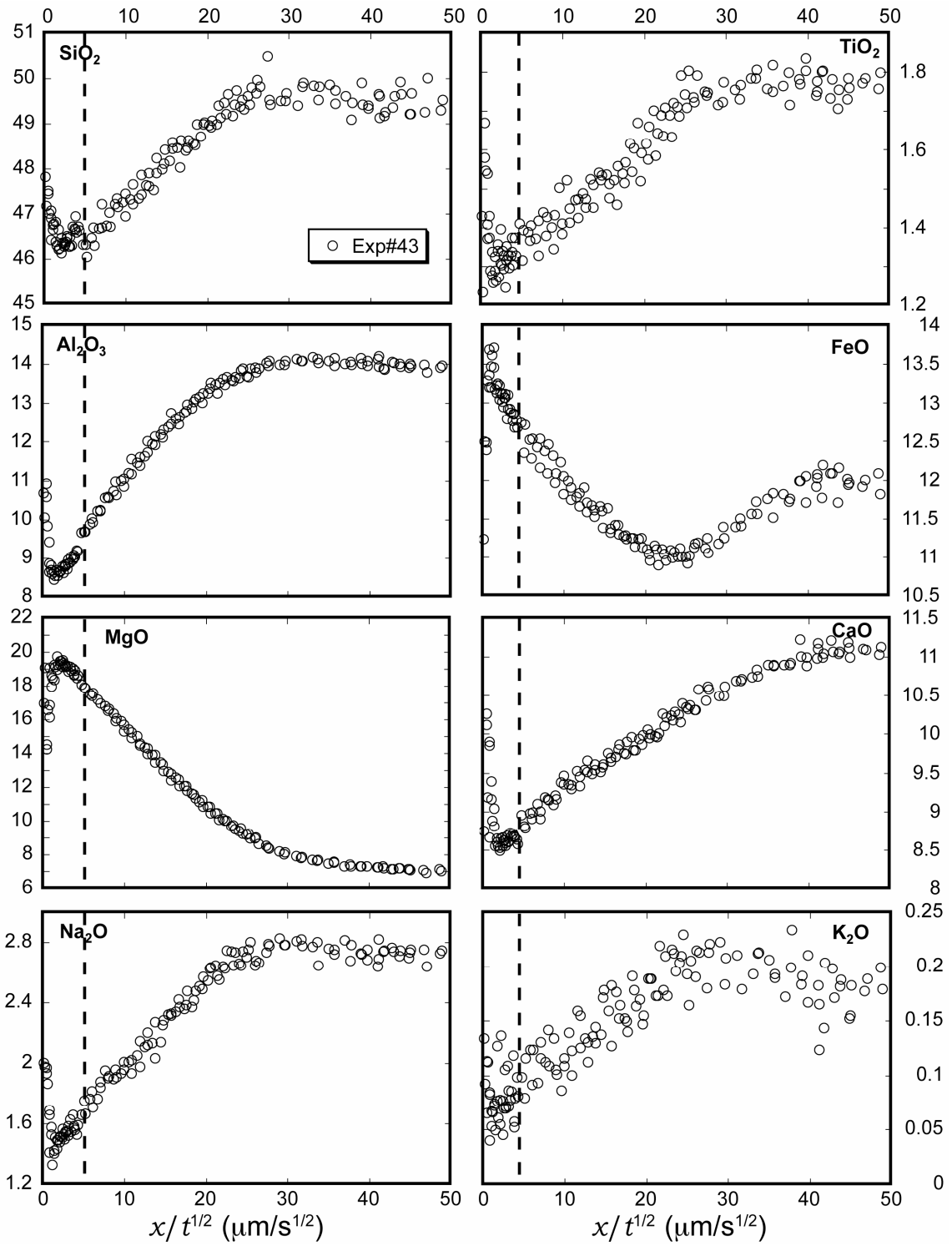

Figure 3-7. Concentration profiles at 1480ºC and 0.95 GPa. The vertical axes are oxide wt%. Olivine-melt interface sets at x=0. Extent of quenching crystals is marked as the dashed vertical line.

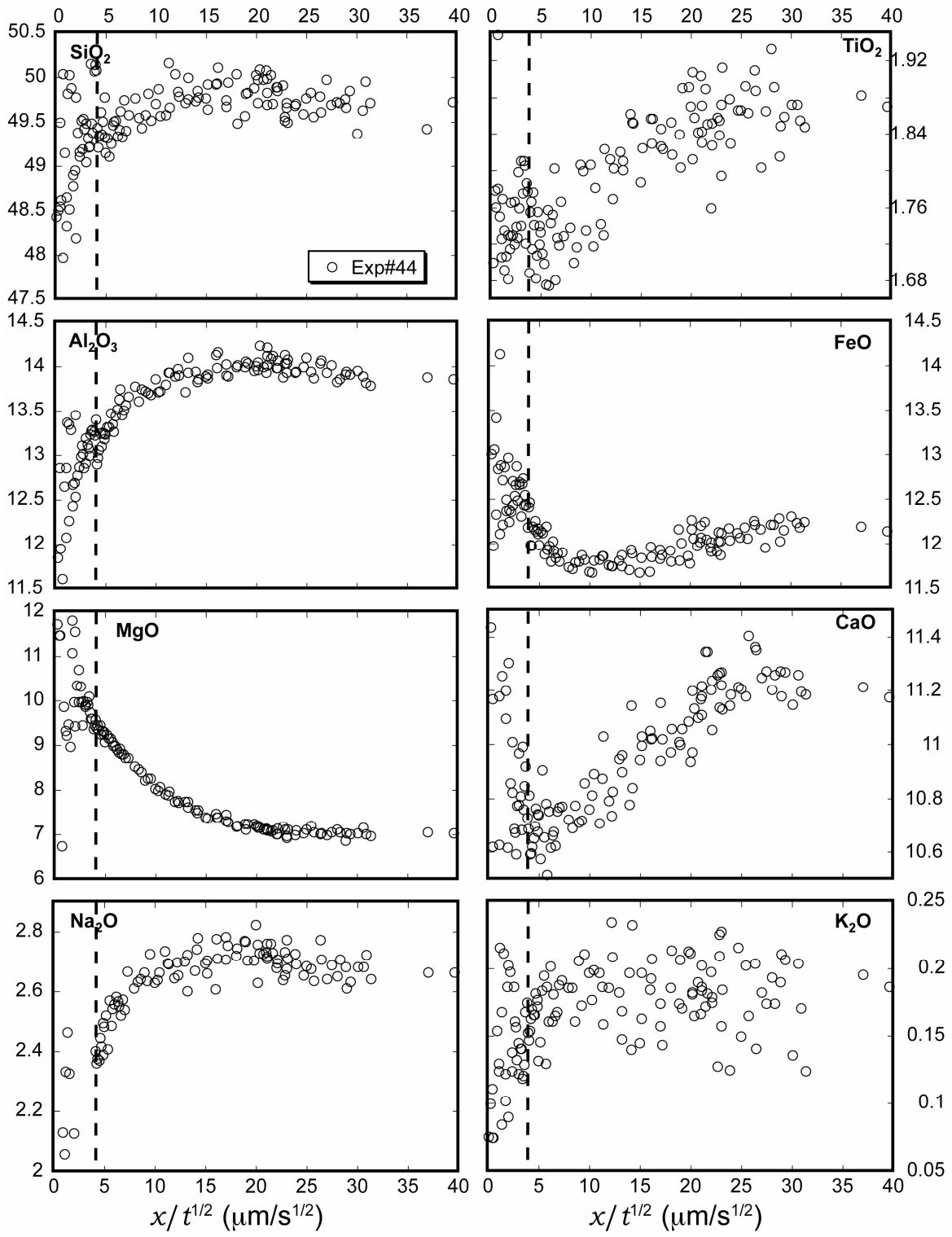

Figure 3-8. Concentration profiles at 1374ºC and 1.42 GPa. The vertical axes are oxide wt%. Olivine-melt interface sets at x=0. Extent of quenching crystals is marked as the dashed vertical line.

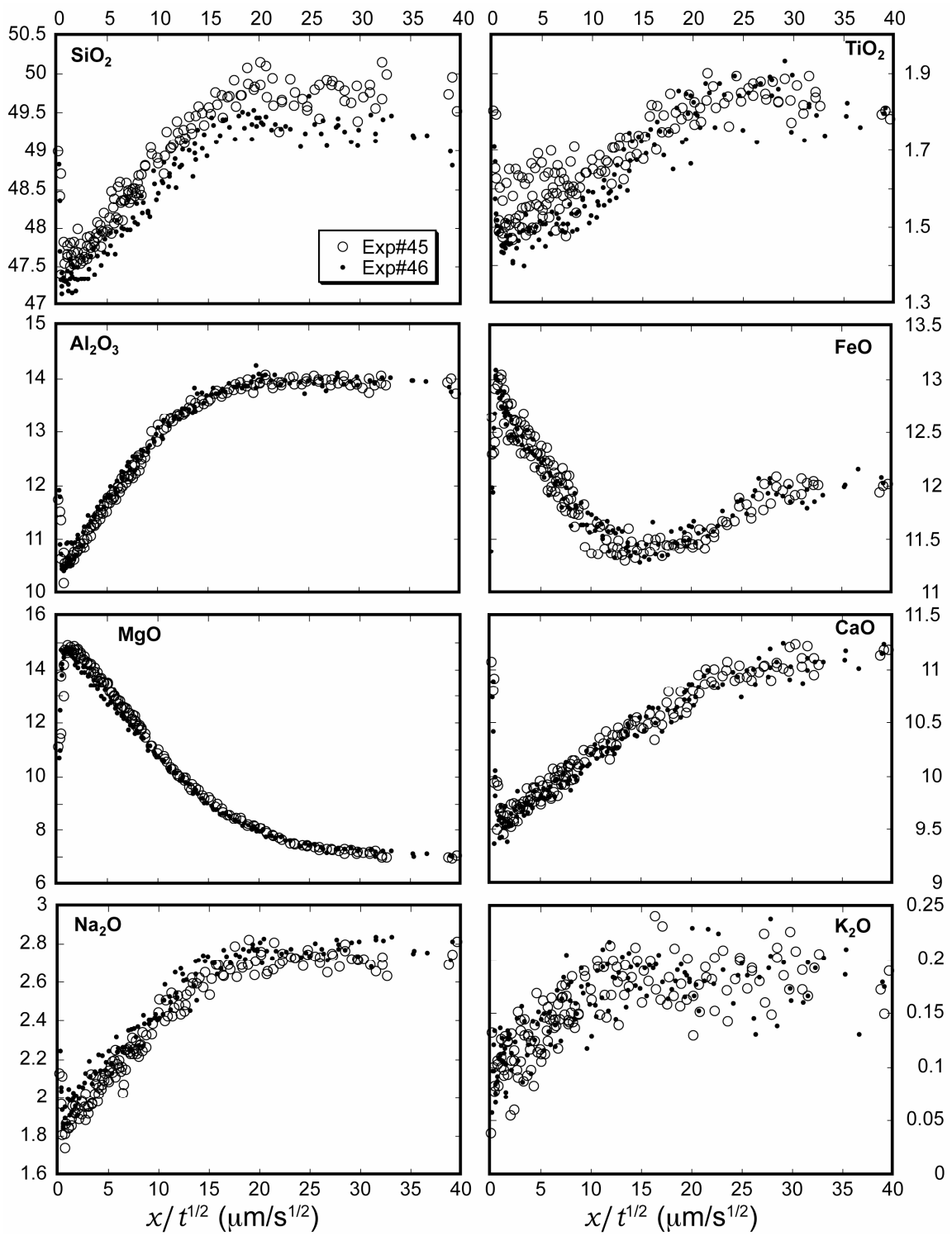

Figure 3-9. Concentration profiles at 1424ºC and 1.42 GPa. The vertical axes are oxide wt%. Olivine-melt interface sets at x=0.

3.5. Discussions and Applications

3.5.1. Quench Effects

Clusters of crystals in the melt near the interface are often present. Measured oxide concentrations within the clusters of crystals using a 15 by 15 μm beam are consistent with those in crystal-free zone, although with larger scatter (Figs. 3-7 and 3-8). The olivine-melt interface is straight, whether or not there are clusters of crystals nearby. The texture of the clusters of crystals depends on the experimental temperature, but not on the experimental duration. All these observations, plus the needle-shape and dendritic texture of the crystals, suggest that the tiny crystals in the melt near the interface are quench crystals. The crystals do not disturb the dissolution process, and their disturbance to the compositional profiles can be minimized using a broad electronic beam in microprobe analyses.

The bent of concentration profiles close to the interface (typically within 10-40 μm of the interface) was commonly attributed to overgrowth of the olivine crystal and resultant diffusion during quench (e.g. Zhang et al., 1989; Shaw, 2004). It cannot be explained by uphill diffusion or by mixed x-ray signal from olivine (e.g., MgO would increase rather than decrease toward the interface if it were due to mixed signal). During experiments, the interface melt is nearly saturated with respect to olivine. As the temperature decreases during quench, the interface melt becomes supersaturated with olivine, leading to olivine overgrowth on the existing olivine surface. At a cooling rate of about 100 K/s (as recorded), the time window for crystal growth is several seconds. The depletion of MgO and FeO and enrichment of all other major oxides is consistent with overgrowth of olivine. Mass balance calculation shows that the typical depletion can be

accounted for by < 1 μm thick olivine overgrowth. Although the MELTS program predicts the liquidus phase of the interface melt at 0.95 and 1.42 GPa to be pyroxene, olivine is also a near-liquidus phase and may grow readily at the olivine surface during quenching because there is no need for nucleation. Hence, we concur with the literature that the bent profiles near the interface are caused by olivine overgrowth at the olivine-basalt interface during quench.

The quench crystals and the olivine overgrowth are different, although they both happen during quenching. The quench crystals occur only in high T and P experiments, while the bent profiles are observed in all experiments. The quench crystals do not disturb the diffusion profiles (although they increase the data scatter), while the olivine overgrowth does.

One purpose of our non-convective dissolution experiments is to determine the interface melt composition. However, it cannot be measured directly because of (i) olivine overgrowth during quench, which disturbs the profile close to the interface; and (ii) the spatial resolution limit of microbeam technique. The interface melt composition must be obtained by fitting experimental profiles using Eqn. (3-6), excluding the part of the profile due to diffusion owing to the overgrowth of olivine during quench. The length of the profiles to be excluded is chosen as $4(\int_{t_0}^{t_1} D\mathrm{d}t)^{1/2}$, where t_0 is the time when the power is turned off, and t_1 is the time when the sample cools to room temperature. This formula yields cutting-off lengths of ~20 μm for ~1271ºC experiments to ~50 μm for ~1474ºC experiments for MgO profiles. The apparent concentration maximum of the

MgO profiles always lies within the excluded segment. The fitting results do not vary much with the choice of cutting-off length changing from 3× to 6× ($\int_{t_0}^{t_1} D\mathrm{d}t)^{1/2}$.

3.5.2. Effective Binary Diffusivity

MgO, FeO and SiO_2 are the major oxides in olivine. Previous olivine-melt equilibrium models usually involve MgO and FeO only (e.g. Langmuir and Hanson, 1980; Gaetani and Watson, 2002) or MgO only (e.g., Niu et al, 2002) without SiO_2. Because FeO plays a minor role compared MgO for MgO-rich olivine, for effective binary treatment in this work, the effect of FeO on olivine saturation is not considered. Consideration of FeO is further complicated by the uphill diffusion behavior of FeO. As discussed in Section 3.5.3, the interface MgO concentration during olivine dissolution is roughly the same for andesitic melt and basaltic melt, while the interface SiO_2 concentration varies from ~47 wt% in basaltic melt to ~53 wt% in andesite melt. Hence, MgO concentration alone almost determines the saturation of olivine, and SiO_2 concentration does not affect the saturation significantly. In this study, the saturation of olivine in basalt is treated as being controlled by MgO (principal equilibrium-determining component).

The concentration profile of MgO is fit by (Eqn. 3-6):

$$C = C_\infty + (C_0 - C_\infty)\,\mathrm{erfc}\left(\frac{x}{2\sqrt{D_{\mathrm{MgO}}t}} - \alpha\right) \Big/ \mathrm{erfc}(-\alpha), \qquad (3\text{-}15a)$$

where α satisfies $$\sqrt{\pi}\alpha e^{\alpha^2}\,\mathrm{erfc}(-\alpha) = (C_0 - C_\infty)/(C_\mathrm{c} - C_0). \qquad (3\text{-}15b)$$

In the above equations, C_c (MgO wt% in the olivine), C_∞ (MgO wt% in the initial melt) and t are known. The parameters we want to obtain from the fitting are the MgO

concentration in the interface melt (C_0) and the MgO effective binary diffusivity (D_{MgO}). To fit a profile, we first estimate the approximate C_0 from the profile, and use Eqn. (3-15b) to solve for α. Then substitute α into Eqn. (3-15a) and fit the profile, obtaining C_0, C_∞ and D_{MgO}. A new α value is then calculated from the new C_0 and C_∞ values and the calculation iterates. After about three iterations the fitting parameters become stable. Fig. 3-10a shows an example MgO profile and fitting results. The bent part of the profile near the interface is excluded. Diffusivities of SiO_2, TiO_2, Al_2O_3 and CaO are also extracted by fitting and reported in Table 3-3. The individual fitting figures are included in the Appendix C. Among the data reported in Table 3-3, D_{MgO} are best constrained. The effective binary diffusivities of SiO_2 are roughly the same as those of Al_2O_3, and are about 1/3 of D_{MgO} at 1270°C and 1/2 of D_{MgO} at 1470°C. Although TiO_2 and CaO profiles are roughly monotonic, the apparent effective binary diffusivities are unexpectedly large, which may be due to the tendency of uphill diffusion toward olivine-melt interface. For example, CaO profiles during olivine dissolution in andesitic melt show clear uphill diffusion (Zhang et al., 1989). Furthermore, CaO profile in Fig. 3-3 is similar to that of Fig. 3-5e of Zhang (1993), which is affected by uphill diffusion. The concentrations of MnO, K_2O and P_2O_5 are low, and the profiles are scattered and hence not treated. FeO and Na_2O profiles are measured well but show uphill diffusion. Treating the uphill diffusion profiles requires either approximate methods such as Zhang (1993) or the diffusion matrix approach, neither of which is attempted here because our focus is on quantifying mineral dissolution rate.

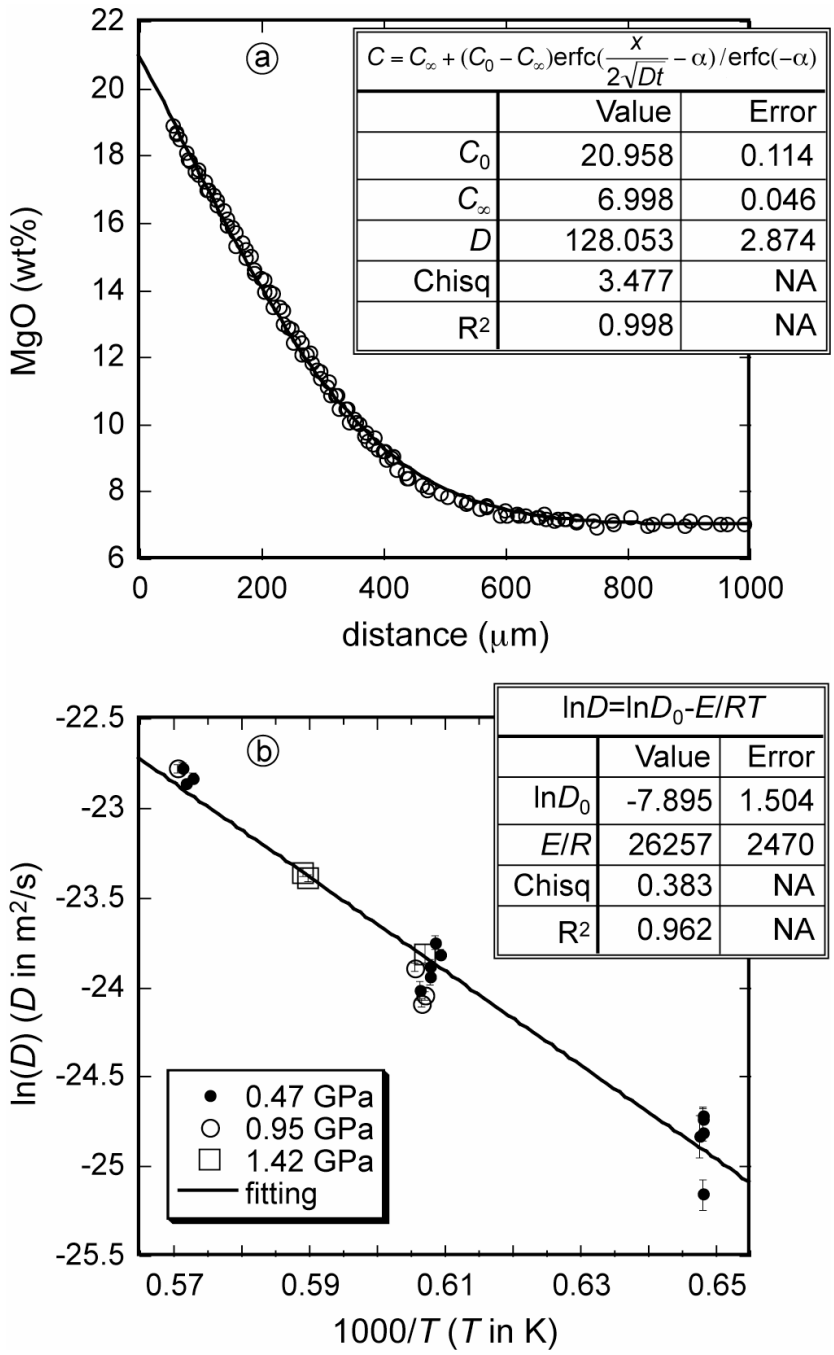

Figure 3-10. MgO diffusivity. a: An example of MgO profile and the fit (Exp#43). The part of the profile close to the interface is modified by quench growth and not shown. b: D_{MgO} as a function of temperature. 2σ error bars are shown. Experiments at different pressures are shown by different symbols, but there is no clear pressure dependence. In the legend of the equation, D and D_0 are in m^2/s, E/R is in K.

Table 3-3. Interface MgO concentration and effective binary diffusivities

Exp #	Interface MgO (wt%)	EBD ($\mu m^2/s$)				
		MgO	SiO_2	TiO_2*	Al_2O_3	CaO*
15	10.41±0.08	16.6±1.9	--	--	4±1	--
16	10.85±0.03	16.9±0.9	--	--	5±1	34±13
18	10.75±0.03	18.5±0.9	8±2	--	7±1	--
20	10.31±0.08	11.9±1.0	--	--	4±1	38±15
21	11.44±0.06	18.2±1.0	--	30±12	7±1	46±12
23	15.44±0.12	40.2±1.9	15±5	49±14	18±2	144±26
25	16.19±0.28	37.1±2.0	14±6	44±9	16±1	126±19
26	15.40±0.10	48.4±1.8	21±6	56±12	20±2	205±40
29	17.23±0.14	42.5±1.6	20±3	55±11	20±2	124±13
33	15.46±0.05	45.6±1.3	20±6	66±19	20±2	289±142
34	22.71±0.12	121.7±3.2	61±4	161±22	61±3	252±16
37	22.39±0.09	118.0±2.6	54±8	144±17	58±2	262±19
38	22.10±0.13	129.0±2.8	60±14	127±15	70±3	230±18
39	13.55±0.06	36.1±0.9	16±3	36±12	13±1	94±14
40	14.01±0.05	34.6±0.8	14±1	43±9	14±1	108±13
41	13.27±0.05	42.2±1.0	20±3	82±18	18±1	123±16
43	20.96±0.11	128.1±2.9	78±9	138±21	63±2	224±14
44	10.62±0.08	45.6±2.3	13±13	84±32	13±3	99±26
45	15.94±0.05	69.6±1.3	38±5	61±20	32±1	117±10
46	15.26±0.06	71.9±1.8	40±6	93±23	33±2	131±16

Note: The error bars are 2σ fitting errors, not including errors due to temperature uncertainty.

* The effective binary diffusivities of TiO_2 and CaO are unexpectedly large and highly scattered, which are attributed to effects of the tendency of uphill diffusion. Extra caution should be exercised when using these data.

Duration correction does not affect the fitting result of C_0. For long-duration (≥2 minutes) experiments, the effect of duration correction on D_{MgO} is small. For short duration (1-2 minutes) experiments, the effect of duration correction on D_{MgO} is significant (up to 15%). For "zero-time" experiments, D_{MgO} and C_0 cannot be reliably extracted. Furthermore, thermal equilibrium may not have been reached for "zero-time" experiments, meaning that the actual run temperatures are less well constrained. Because of the above reasons, D_{MgO} and C_0 of "zero-time" experiments are not reported.

The variation of D_{MgO} with temperature and pressure is shown in Fig. 3-10b. The temperature dependence is well described by the Arrhenian relation. The pressure dependence in this temperature range is small and cannot be clearly resolved from our experimental data, indicating a small activation volume. Hence, D_{MgO} data are fit as:

$$\ln D_{MgO} = \ln D_0 - \frac{E}{RT} = -7.895 - \frac{26257}{T}, \quad (3\text{-}16)$$

where D_{MgO} is in m^2/s and T is in K. The activation energy is 218±21 kJ/mol (2σ error hereafter). The above equation can reproduce the $\ln D_{MgO}$ values to within 0.28 natural logarithm units. Because the pressure dependence is small, error in applying the above equation to the pressure range of 0 to 2.0 GPa is expected to be small (no more than 0.5 units in terms of $\ln D_{MgO}$).

Effective binary diffusion is a simplified and approximate approach. The D_{MgO} values reported in this study can be applied to Mg-rich olivine dissolution in basaltic melt or in similar compositional range and gradient. Because effective binary diffusivities depend on composition as well as the directions of concentration gradients (Cooper, 1968; Zhang, 1993), caution should be exercised when applying to other melt

compositions or different compositional gradients. Fig. 3-11 compares our data with effective binary diffusivities of MgO in various silicate melts. The strong dependence on melt composition is clearly shown. D_{MgO} in basaltic melt is roughly two orders of magnitude higher than in rhyolitic melt.

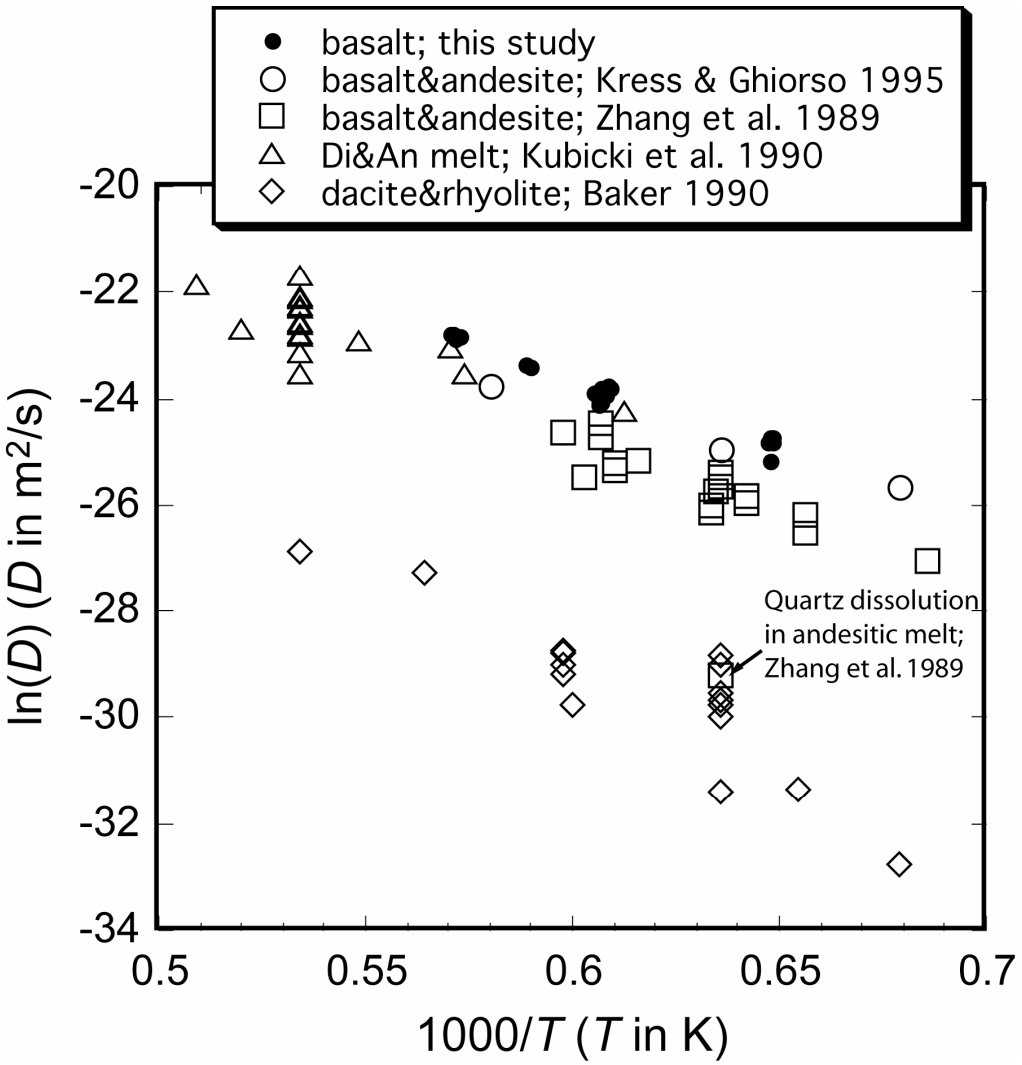

Figure 3-11. Comparison of MgO diffusivity in various silicate melts. Data at different pressures are grouped because the pressure effect is small compared to the effect of temperature and melt composition. Data sources: Kress and Ghiorso (1995): T=1200~1450°C, P=1 bar, diffusion couple; Zhang et al. (1989): T=1185~1400°C, P=0.5~2.15 GPa, olivine, diopside and quartz dissolution in andesitic melt. Note that quartz dissolution produces SiO_2-rich melt, such that the diffusivity falls in the data range of dacite and rhyolite; Kubicki et al. (1990): T=1360~1600°C, P=1 bar~2 GPa, diffusion couple; Baker (1990): T=1200~1600°C, P=1 bar~1 GPa, diffusion couple.

3.5.3. Far-field and Interface Melt Compositions

The interface and far-field melt compositions are listed in Tables 3-4 and 3-5. The far-field composition profiles are flat within analytical uncertainty, and are in close agreement with the initial melt composition. Scatters between different experiments beyond the analytical uncertainty are attributed to small heterogeneity in the starting glass.

Table 3-4. Interface melt compositions (wt%)

Exp#	SiO_2		TiO_2		Al_2O_3		FeO	MgO		CaO		Na_2O
15	47.56	0.16	1.72	0.02	12.35	0.06	13	10.41	0.08	10.75	0.05	2.2
16	47.50	0.25	1.62	0.04	11.74	0.12	13.1	10.85	0.03	10.35	0.20	2
18	48.12	0.09	1.72	0.01	11.97	0.05	13.1	10.75	0.03	10.58	0.11	2.1
20	47.69	0.27	1.71	0.02	11.88	0.15	13.2	10.31	0.08	10.50	0.12	2.2
21	47.75	0.22	1.69	0.02	11.58	0.07	13.6	11.44	0.06	10.14	0.14	1.9
23	46.69	0.21	1.51	0.02	9.93	0.09	13.8	15.44	0.12	9.85	0.04	1.6
25	46.77	0.26	1.46	0.03	9.37	0.12	14	16.20	0.28	9.63	0.06	1.6
26	46.51	0.31	1.48	0.03	9.88	0.12	14	15.40	0.10	9.75	0.05	1.6
29	46.11	0.16	1.44	0.02	9.10	0.12	13.5	17.23	0.14	9.50	0.04	1.6
33	46.87	0.22	1.50	0.02	9.76	0.06	14	15.46	0.05	9.96	0.03	1.7
34	45.17	0.16	1.20	0.02	6.84	0.10	13.8	22.71	0.13	8.14	0.04	1.3
37	44.06	0.25	1.17	0.02	7.22	0.08	14	22.39	0.09	8.12	0.03	1.2
38	43.96	0.47	1.20	0.03	6.98	0.14	14	22.10	0.13	8.34	0.07	1.2
39	47.51	0.13	1.58	0.02	10.51	0.08	13.5	13.55	0.06	10.08	0.04	1.9
40	47.36	0.08	1.53	0.02	10.54	0.06	13.5	14.01	0.05	9.98	0.03	1.9
41	47.52	0.08	1.54	0.02	10.99	0.05	13.5	13.27	0.05	10.05	0.03	1.9
43	45.81	0.14	1.25	0.02	8.02	0.05	13.6	20.96	0.11	8.39	0.04	1.4
44	49.00	0.26	1.66	0.02	12.24	0.12	13.5	10.62	0.08	10.41	0.07	2.2
45	47.23	0.09	1.46	0.03	10.17	0.05	13.2	15.94	0.05	9.46	0.04	1.8
46	47.08	0.08	1.39	0.02	10.32	0.06	13.2	15.26	0.06	9.44	0.04	1.8

Note: SiO_2, TiO_2, Al_2O_3, MgO and CaO concentrations with 2σ errors are from diffusion profile fitting. Other oxides are approximately estimated from the profiles. MnO≈0.2 wt%, K_2O≈0.1 wt%, P_2O_5≈0.1 wt%, H_2O≈0.3 wt%.

Table 3-5. Far-field melt compositions (wt%)

Exp#	SiO_2		TiO_2		Al_2O_3		FeO	MgO		CaO		Na_2O
15	48.61	0.06	1.88	0.01	13.92	0.02	12	6.96	0.04	11.20	0.06	2.7
16	48.80	0.10	1.87	0.01	13.94	0.04	12	6.88	0.03	11.12	0.04	2.7
18	49.85	0.07	1.88	0.02	14.10	0.03	11.7	6.89	0.03	11.21	0.17	2.8
20	49.09	0.05	1.87	0.01	13.95	0.03	12.2	6.86	0.02	11.16	0.01	2.7
21	49.38	0.08	1.88	0.01	14.04	0.02	12.3	6.96	0.03	11.12	0.02	2.7
23	49.63	0.08	1.88	0.01	14.17	0.04	12.1	6.87	0.04	11.14	0.04	2.7
25	49.53	0.06	1.89	0.01	13.99	0.03	12.4	6.76	0.03	11.17	0.03	2.7
26	49.74	0.11	1.89	0.01	14.15	0.04	12.1	6.75	0.05	11.22	0.07	2.8
29	49.63	0.04	1.87	0.01	14.03	0.03	12	6.87	0.03	11.13	0.02	2.7
33	50.51	0.17	1.90	0.02	14.17	0.04	11.8	6.86	0.04	11.41	0.28	2.8
34	50.14	0.08	1.87	0.02	14.13	0.04	12	6.81	0.07	11.08	0.03	2.7
37	49.04	0.15	1.86	0.02	14.18	0.04	11.8	6.77	0.06	11.06	0.06	2.8
38	48.76	0.14	1.88	0.01	14.16	0.04	12.4	6.78	0.04	11.07	0.03	2.7
39	49.79	0.04	1.80	0.01	13.96	0.02	12	7.00	0.01	11.13	0.02	2.7
40	49.91	0.03	1.82	0.01	14.01	0.02	12	7.03	0.02	11.12	0.03	2.7
41	49.76	0.03	1.84	0.01	14.08	0.02	12.2	6.84	0.02	11.20	0.02	2.7
43	49.62	0.08	1.78	0.01	14.06	0.03	12	7.00	0.05	11.17	0.03	2.7
44	49.75	0.05	1.88	0.01	13.96	0.03	12.2	7.03	0.02	11.25	0.03	2.7
45	49.76	0.04	1.80	0.02	13.94	0.02	12.2	7.04	0.02	11.13	0.03	2.7
46	49.35	0.06	1.84	0.02	14.00	0.03	12	7.08	0.04	11.16	0.05	2.7

Note: SiO_2, TiO_2, Al_2O_3, MgO and CaO concentrations with 2σ errors are from diffusion profile fitting. Other oxides are average concentrations of the flat part of the profiles. MnO≈0.2 wt%, K_2O≈0.2 wt%, P_2O_5≈0.1 wt%, H_2O≈0.3 wt%.

At a given T and P excluding “zero-time” experiments, the interface melt composition does not correlate with experimental duration (Fig. 3-12). The "zero-time" experiments always have lower extrapolated C_0 than longer duration experiments, but are not shown in the figure because of their large error bars and because thermal equilibrium may not have been reached in those experiments. Shorter duration experiments are necessary to better resolve the interface melt evolution from its initial composition towards the saturation composition. However, shorter duration experiments are less reliable, hindering this purpose.

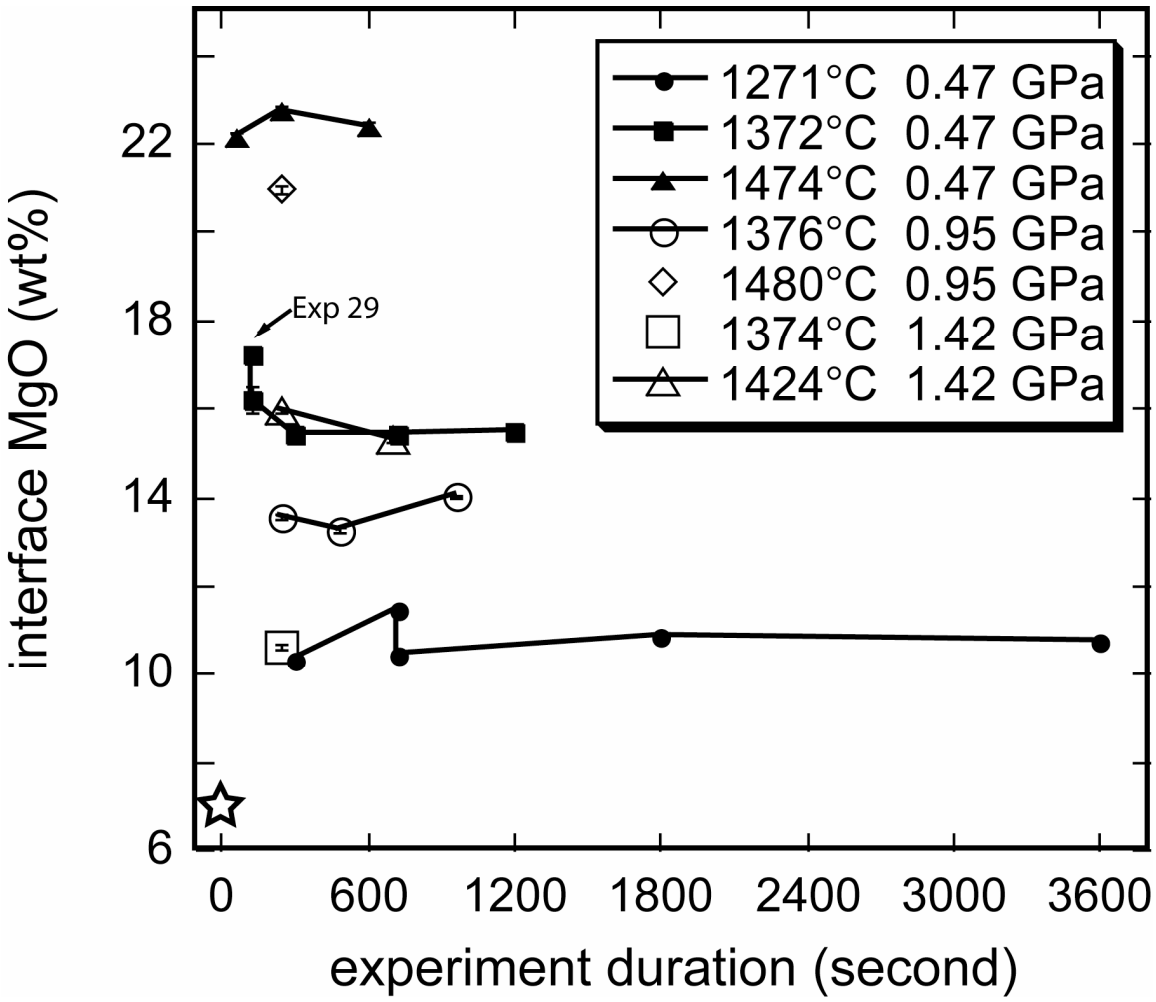

Figure 3-12. Interface MgO concentration versus experimental duration. 2σ error bars of the interface MgO concentration are about the same size as or smaller than the size of the point symbols. Initial melt composition is shown as a star at (t=0, MgO=7 wt%).

At a given *T* and *P*, some interface melt compositions show scatter larger than the analytical error (e.g., MgO at 0.47 GPa and 1372°C, see Fig. 3-12, SiO_2 at 0.95 GPa and 1376°C, see Table 3-4). Four potential causes are discussed below:

(1) In a finite melt reservoir, the interface melt composition would vary as a function of time (Liang, 2003). Because in our experiments the melt was semi-infinite (the far-field composition profiles are still flat and do not change during an experiment), this explanation does not apply here.

(2) The effect of different initial melt composition. One might expect the interface melt composition to correlate with the initial (far-field) melt composition. Because the variation in the initial melt composition is small in this study, we include data from olivine dissolution in andesitic melts (Zhang et al., 1989) to better investigate this correlation. In Fig. 3-13a, at a given *T* and *P*, no correlation is found between the interface and far-field melt MgO concentrations. For non-equilibrium-determining components such as SiO_2, some positive correlation is observed (Fig. 3-13b). Therefore, sample heterogeneity may contribute to the scatter of non-equilibrium-determining components in the interface melt, but cannot explain the variation in the interface MgO concentration at a given *T* and *P*.

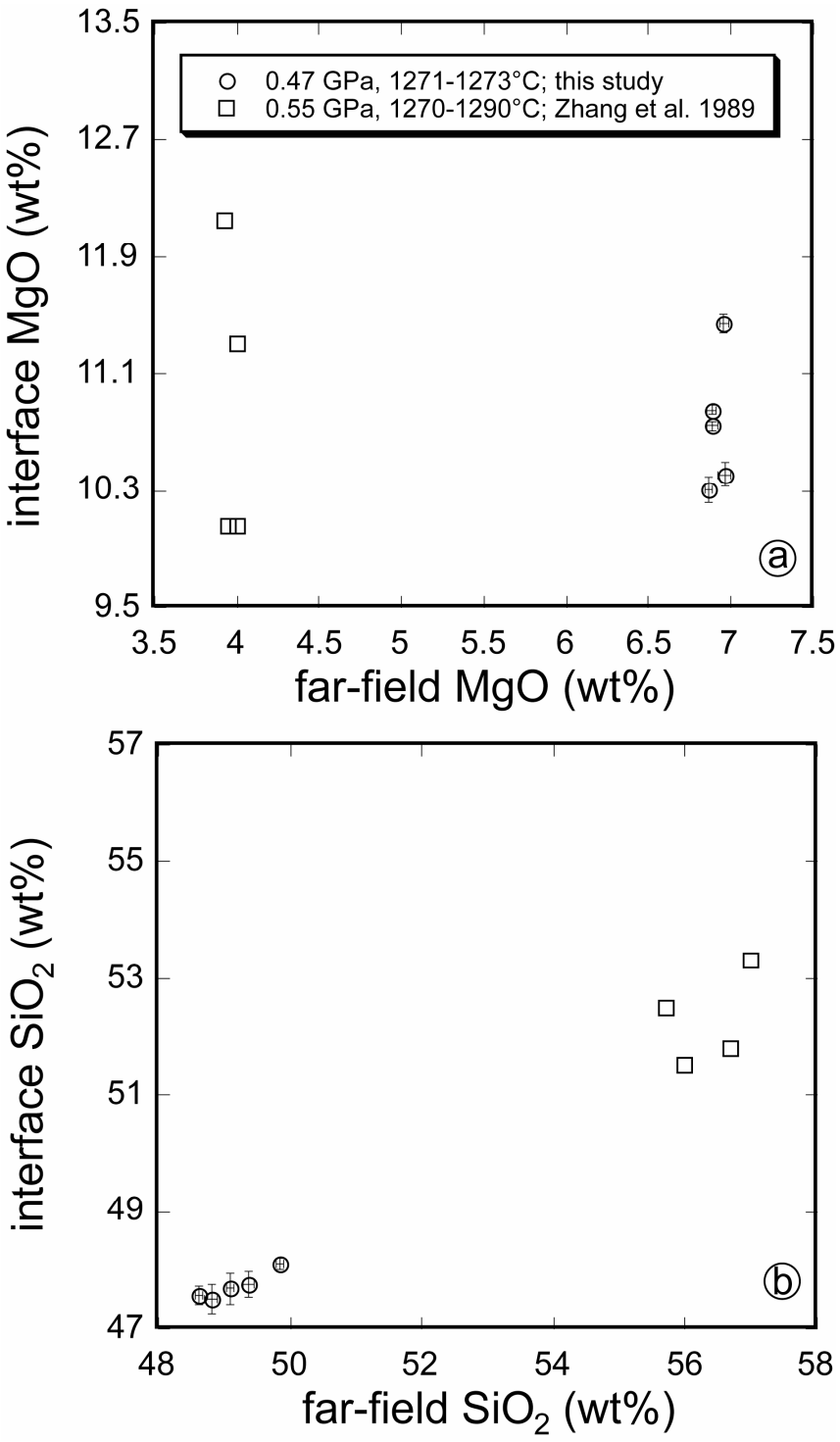

Figure 3-13. Far-field melt vs. interface melt. a: MgO. b: SiO_2. 2σ fitting errors are shown. The interface MgO concentrations show variations larger than analytical uncertainty and do not correlate with far-field MgO concentrations. The interface SiO_2 concentrations show variations larger than analytical uncertainty and correlate with far-field SiO_2 concentrations.

(3) Uncertainty in temperature. All experimental capsules were designed to be of the same geometry. However, small difference still exists during sample preparation and charge compression, which may cause some unknown difference in real experimental temperature. At 0.47 GPa, C_0 changes from ~ 10.7 to ~ 22.4 wt% as temperature changes from ~1270 to 1475°C. On average, a 10°C temperature difference would cause roughly 0.5 wt% MgO variation. At the experimental temperatures of about 1300°C, due to temperature gradient in the assembly, an increment of 1 mm (from 2 to 3 mm) in the distance between the thermal couple tip and the olivine-melt interface would increase the temperature at the olivine-melt interface by about 24°C, which corresponds to a ~1.2 wt% increment in C_0. The scatter in C_0 shown in Figure 3-12 can be attributed to a temperature uncertainty of <20°C, except for exp# 29, which may reflect a temperature uncertainty of 30°C. As can be seen later, the reproducibility of C_0 in our piston-cylinder experiments is much improved over literature data because we adopted a short experimental charge and tried to maintain consistent capsule size. If the capsule geometry was not designed consistently, the error in interface melt composition would be more severe, and the interface melt composition at a given nominal T and P would be less reproducible.

(4) Uncertainty in pressure. Compare the experiments at ~1371 and ~1376°C in Fig. 3-12, C_0 decreases by ~1.5 wt% for a 0.47 GPa pressure increment. A pressure uncertainty of 10 MPa is roughly equivalent to 0.03 wt% MgO difference. This uncertainty is negligible.

In summary, sample heterogeneity may contribute to the scatter of non-equilibrium-determining component concentrations in the interface melt at a given T and

P. For the equilibrium-determining component MgO, the most likely explanation is temperature uncertainty.

In Fig. 3-14, the compositions of the interface melt at 0.47 GPa are roughly consistent with olivine-saturated melt at 1 bar (Mysen, 2007). The liquidus temperature of the interface melt calculated using the model by Gaetani and Watson (2002) is listed in Table 3-2. The model results do not agree well with the corrected experimental temperatures. For similar interface melt compositions at a given *T* and *P*, this model yields liquidus temperatures either too high or too low, with difference up to 128°C. The estimated uncertainty in the corrected experimental temperatures of this study is <20°C (with only one experiment exceeding this uncertainty). The rest of the inconsistency may be due to (i) difference between the interface melt composition and the true saturation composition (Section 3.2.2) and (ii) uncertainty in the model of Gaetani and Watson (2002).

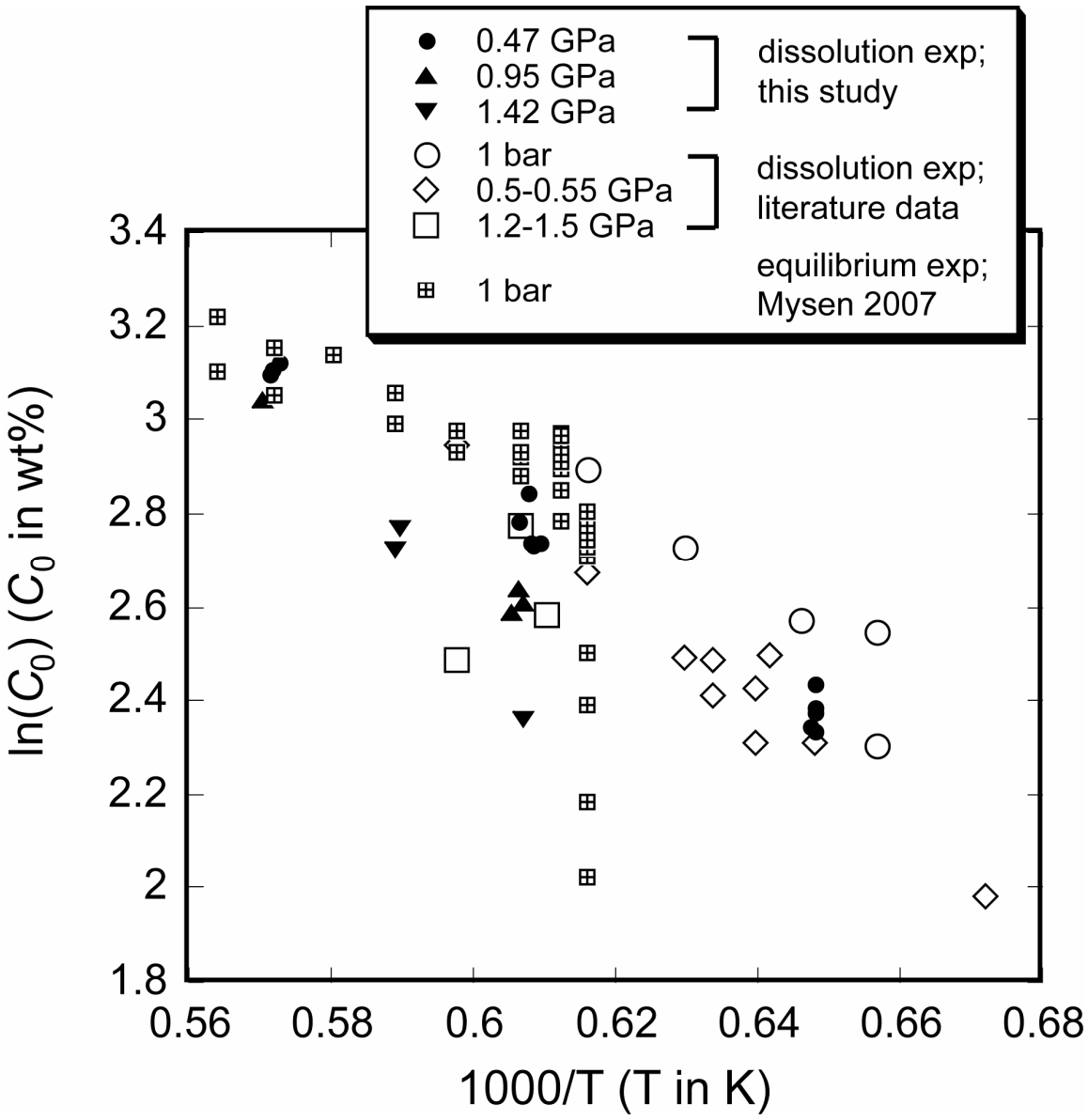

Figure 3-14. C_0 at different P versus 1000/T. Literature data are from: Donaldson (1985): 1250°C, 1 bar, olivine (Fo91.5) dissolution in a tholeiite basaltic melt; Thornber and Huebner (1985): 1250-1350°C, 1 bar, olivine (Fo92) dissolution in a lunar basaltic melt; Brearley and Scarfe (1986): 1400°C, 1.2 GPa, olivine (~Fo90) dissolution in an alkali basaltic melt; Zhang et al. (1989): 1215-1400°C, 0.5-1.5 GPa, olivine (Fo90 and Fo100) dissolution in an andesitic melt; Mysen (2007): olivine-melt equilibrium, 1350-1500°C, 1 bar.

Because the interface melt compositions do not depend on experimental duration at a given T and P, and they roughly agree with the olivine-saturated melt compositions, we conclude that the interface melt reaches near-saturation shortly for olivine dissolution in basaltic melt (in no more than 2 minutes). Interface reaction is not the rate-controlling step in our experiments, and the dissolution is controlled by diffusion.

Fig. 3-14 shows the dependence of C_0 on temperature and pressure. C_0 data from other diffusive or convective olivine dissolution studies are also included (one data point from Donaldson, 1985; four from Thornber and Hueber, 1985; one from Brearley and Scarfe, 1986; and thirteen from Zhang et al., 1989). It increases with increasing temperature, and decreases with increasing pressure. The effect of 1 GPa increase in pressure is roughly equivalent to 50 K decrease in temperature. For the literature data, the one data point from Donaldson (1985) and that of Brearley and Scarfe (1986) turned out to be outliers, as well as two out of the thirteen from Zhang et al. (1989). The outliers are likely due to either uncertainty in temperature at the olivine-melt interface or the quench effect that alters the MgO concentration at the interface.

Data by Zhang et al. (1989) are for olivine dissolution in andesitic melt (56.5 wt% SiO_2, 3.96 wt% MgO). The consistence between most of their data and this study suggests that C_0 does not depend strongly on the initial melt composition, which reinforces the notion that olivine saturation is primarily controlled by MgO, and is consistent with the result shown in Fig. 3-13a. Other non-equilibrium-determining components, such as SiO_2, depend on the initial melt composition. Interface SiO_2 is typically 52-53 wt% in Zhang et al. (1989), but 46-48 wt% in this study.

Furthermore, the data of Zhang et al. (1989) also show that C_0 does not depend strongly on olivine composition. For example, for dissolution of Fo90 olivine (MgO ≈ 50 wt%) and Fo99.6 olivine (MgO ≈ 57 wt%), C_0 is constantly 12.1 wt%. This constancy is probably related to the surface equilibrium between olivine and melt. A very thin olivine surface layer can deviate the initial olivine composition and reach near equilibrium with the melt (Liang 2000; Zhang, 2008).

Since C_0 does not depends strongly on melt or olivine composition, it is approximated by:

$$\ln C_0 = A + BP + \frac{\Delta G_{P=0} + P\Delta V}{RT} = 7.82 + 0.00266P - \frac{8040}{T} - \frac{4.96P}{T}, \qquad (3\text{-}17)$$

where C_0 is in wt%, $\Delta G_{P=0}$ is in J/mol, ΔV is in cc/mol, T is in K, and P is in MPa. The 2σ errors for A, B, $\Delta G_{P=0}/R$ and $\Delta V/R$ are 0.96, 0.00160 MPa^{-1}, 1540 K and 2.63 K/MPa, respectively. The multiple linear correlation coefficient r is 0.9812. Fig. 3-15a shows the prediction by this formula compared to our experiments and literature data. The 2σ error of Eqn. (3-17) in predicting C_0 is 0.79 wt% for our data, 0.86 wt% for our data and the literature data except the four outlier points, and 1.81 wt% if the outliers are included. Inversely, when one is interested in predicting T from given C_0, the 2σ error is 20°C for our data, 24°C for our data and the literature data except the four outliers, and 40°C if the outliers are included. Note that the literature data cover temperature from 1215 to 1400°C, pressure from 1 bar to 1.5 GPa, and melt composition from various basalts to an andesite, suggesting that Eqn. (3-17) is applicable, although with some error, to a broader range of conditions beyond the experiments in this study. Models on melt-olivine equilibrium from Sugawara (2000) and Niu et al. (2002) are shown in comparison in Fig.

3-15b. The model of Niu et al. (2002) was developed for low pressures, hence only applied to data with $P \leq 0.5$ GPa. Overall, their models give good predictions at low C_0's. However, at high C_0's, their models predict consistently lower values for both our data and literature data. This difference may be related to the fact that the near-saturation interface melt during crystal dissolution is not exactly the equilibrium melt with the dissolving olivine (Section 3.2.2).

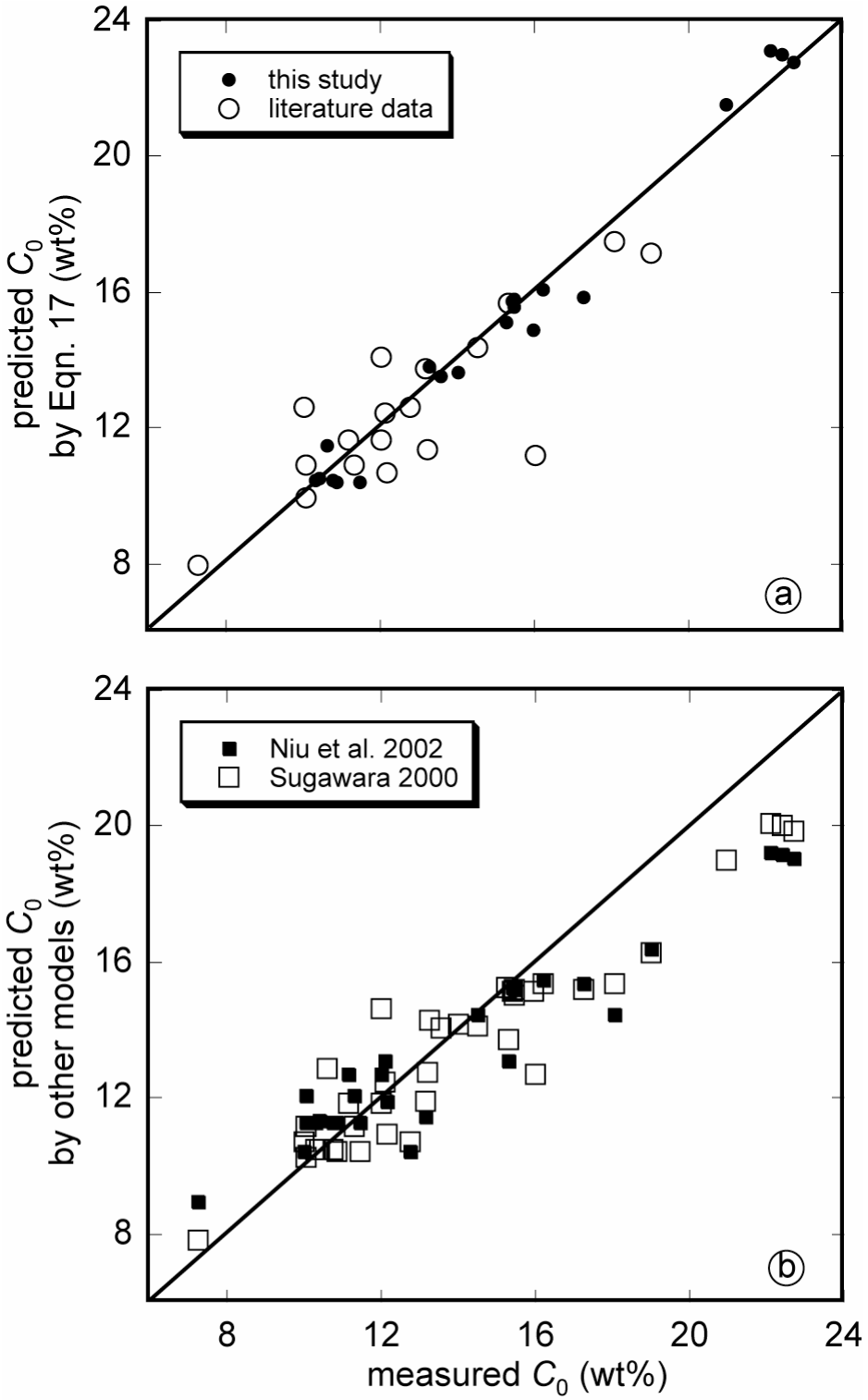

Figure 3-15. C_0 model. a: Comparison between the prediction by Eqn. (3-17) and the experimental C_0. b: Comparison between the prediction by two published models and the measured C_0 in olivine dissolution experiments. 1:1 line is shown as reference.

3.5.4. Diffusive Olivine Dissolution Distance

Diffusion controlled olivine dissolution distance L can be expressed as:

$$L = 2\alpha\rho_m\sqrt{D_{MgO}t}\,/\,\rho_c, \tag{3-18}$$

where α is defined in Eqn. (3-15b). Glass density (ρ_m) is taken as 2.77 g/cc (Tilley, 1922), and olivine density (ρ_c) is taken as 3.34 g/cc (Liu and Li, 2006). With the fitting results, olivine dissolution distance can be calculated. The calculation results are listed in Table 3-2 as L_4. Error in L_4 is obtained by letting D_{MgO} and C_0 vary within their error bounds. The errors in melt and olivine densities, and density variation along the compositional profiles are ignored. Hence, this error estimation is the lower limit. Because the fitting results are based on compositional profiles in the melt and do not incorporate the directly measured olivine dissolution distance, L_4 is independent of the direct measurements. The comparison provides crosscheck to our experiments.

3.5.5. Convective Olivine Dissolution in Basaltic Melt

The experiment results are used to model convective olivine dissolution in basaltic melt using the procedures in Section 3.2.3. In Eqn. (3-12), calculating D_{MgO} and δ involves kinetics and dynamics but not the phase equilibrium condition of the system under discussion, while β depends on the degree of undersaturation, which reflects the thermodynamic aspect of this problem. We calculate D_{MgO}/δ for MgO-rich olivine in basaltic melt and summarize the results for the convenience of applications.

To calculate D_{MgO}/δ, it is necessary to know D_{MgO}, melt density, olivine density and melt viscosity. The melt composition in our calculation is chosen to be the same as in our experiments. Melt density at 1 bar is calculated by the model of Lange and

Carmichael (1987) and Ochs and Lange (1999). Melt density up to 2 GPa is calculated by combining the 1 bar density with the Birch-Murnaghan equation of state by Agee (1998) and Ohtani and Maeda (2001). The two Birch-Murnaghan models yield consistent results (<0.1% relative difference). Olivine density is calculated by the model of Liu and Li (2006). Melt viscosity is calculated by the model of Hui and Zhang (2007). Based on these models and our experiment result, D_{MgO}/δ is calculated for 1150 to 1450°C, 1 bar to 2 GPa and olivine composition from Fo80 to Fo100. The Re and Pe numbers depend on the grain size. For single olivine crystal with 1 mm radius, the Re and Pe numbers are 9.5×10^{-9} to 3.4×10^{-3}, and 4.0×10^{2} to 2.0×10^{4}, at 1150°C and 1450°C respectively. For a xenolith with 100 mm radius, the Re and Pe numbers are 9.4×10^{-3} to 3.5×10^{2}, and 4.0×10^{8} to 3.6×10^{9}, at 1150°C and 1450°C respectively. D_{MgO}/δ depends on the diffusivity and melt viscosity, both of which depend strongly on temperature. D_{MgO}/δ depends weakly on melt and crystal densities, which in turn depend on temperature, pressure, melt and crystal compositions. Kerr (1995) showed that the boundary layer thickness (hence D_{MgO}/δ) does not depend much on grain size at small Re and large Pe. Our calculations show that even for Re > 1 the boundary layer thickness does not depend much on grain radius. For example, when radius changes from 1 to 100 mm at 1300°C, Re increases from 1.9×10^{-5} to 11, but δ only increases by ~10%. Note that D_{MgO} and melt viscosity in our calculation do not depend on pressure. For convenience, the model calculation result is re-cast into the following equation:

$$\ln\left(\frac{D_{MgO}}{\delta}\right) = 6.42 - \frac{32765}{T} - 0.076P - 1.19X_{Fo}, \qquad (3\text{-}19)$$

where D_{MgO}/δ is in m/s, T in K, P in GPa, and X_{Fo} is the mole fraction of Fo in olivine (for pure forsterite, $X_{Fo} = 1$). The 2σ errors for the four coefficients (from left to right) are 0.05, 60 K, 0.004 GPa^{-1} and 0.04, respectively. Eqn. (3-19) can reproduce the model results with a 2σ error of 0.04. The D_{MgO}/δ values calculated from Eqn (3-19) are applicable to olivine in basaltic melts. More broadly, it is also roughly applicable to dissolution or growth of other crystals with similar density and with MgO being the equilibrium-determining component, such as MgO-rich orthopyroxene and clinopyroxene, or mantle xenolith in general, as long as the melt composition is similar to the tholeiite used in this study. The applicability to alkali basalt is discussed in Section 3.5.7.

The theory to calculate convective dissolution rate of a falling or rising particle in a liquid as outlined in Section 3.2.3 has been tested by halide dissolution in aqueous sodium carboxymethyl cellulose solutions (Kerr, 1995), halide dissolution in water (Zhang and Xu, 2003), CO_2 droplet dissolution in seawater (Zhang, 2005), and bubble growth in beer (Zhang and Xu, 2008). Based on these studies, the uncertainty in the calculated convective dissolution rate is about 15% relative if all the parameters (fluid viscosity, diffusivity, interface concentration, and densities of the fluid and crystal) are well known. For D_{MgO}/δ in this study, the uncertainty mainly comes from the errors of: (1) 0.5 in $\log D_{MgO}$; and (2) 0.61 in $\log\eta$ (Hui and Zhang, 2007). The errors in melt and olivine densities and the error in the calculation scheme (e.g. error in Eqn. 3-7c) are much smaller than the above errors. To assess the uncertainty in D_{MgO}/δ, we allowed D_{MgO} and η to vary in their corresponding error bounds. Fig. 3-16 shows $\ln(D_{MgO}/\delta)$ as a function of temperature and the error bounds resulted from the uncertainties in D_{MgO} and η. The

value of $\ln(D_{MgO}/\delta)$ varies by ± 0.34 as $\log(D_{MgO})$ varies by ± 0.5, and ∓ 0.44 as $\log\eta$ varies by ± 0.61. Assuming the errors in D_{MgO} and η are not correlated, the overall uncertainty in $\ln(D_{MgO}/\delta)$ is roughly $\sqrt{0.34^2 + 0.44^2} \approx 0.56$ (a factor of 1.7 in D_{MgO}/δ).

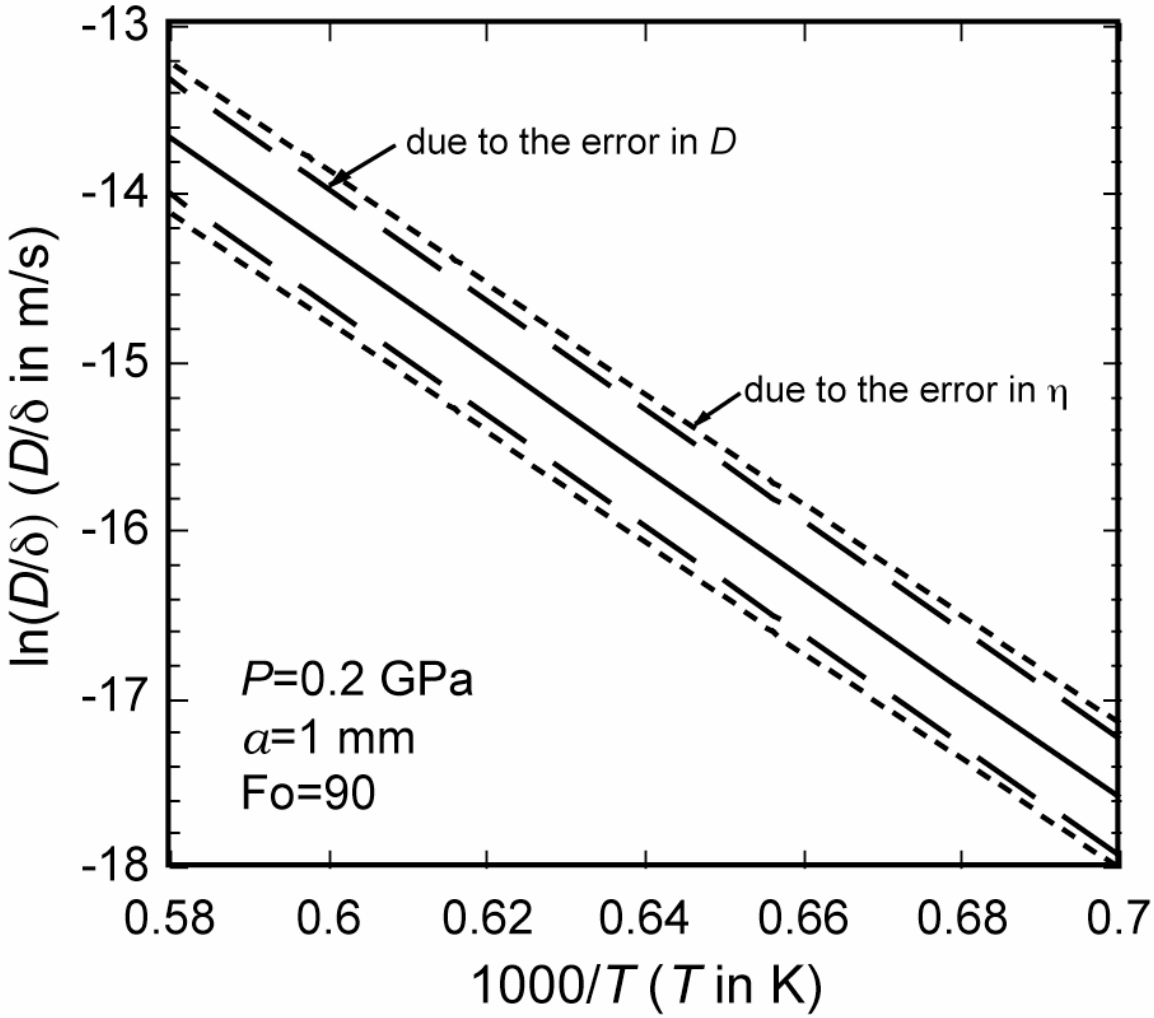

Figure 3-16. Kinetic parameter D_{MgO}/δ as a function of temperature. Its error bounds (dashed lines) due to error in D_{MgO} and viscosity η are shown

The parameter β (Eqn. 3-11) depends on the degree of undersaturation, which can be inferred by various ways. In this study, C_0 is modeled as a function of temperature and pressure in Eqn. (3-17), which is simple but not thermodynamically rigorous (e.g. activity should be preferred than mass fraction). To treat the saturation melt composition rigorously is beyond the scope of this study. Empirically, C_0 can be readily estimated using Eqn. (3-17) for the dissolution of MgO-rich olivine in basaltic melt. If a more rigorous thermodynamics model is constructed for C_0, it can also be combined with D_{MgO}/δ to obtain the convective dissolution or growth rate.

The error in β comes mainly from the error in predicting C_0 (0.86 wt%). The relative error of β becomes unbounded as C_0 approaches C_∞ (the system approaches the liquidus temperature of the melt). This results in large relative error (but absolute error stays roughly the same) when we calculate the convective dissolution rate close to the liquidus temperature.

Combining β with D_{MgO}/δ yields the convective dissolution rate for a given condition. An example of calculation is as follows. Consider the convective dissolution rate of an olivine crystal (Fo90, MgO ≈ 50 wt%) in a basaltic melt with 6 wt% MgO at 1250°C and 0.1 MPa. First estimate $C_0 \approx 12.66$ wt% from Eqn. (3-17). Then $\beta \approx 2.693*(12.66-6)/(50-12.66)/3.153 = 0.1523$. The densities used here are based on the models used earlier in this section. Eqn. (3-19) yields $D_{MgO}/\delta = 0.096$ μm/s. Hence the convective dissolution rate is 52.6 μm/hr. If the radius of the olivine crystal is 2 mm, it would take 1.6 days for the olivine crystal to completely dissolve.

For dissolution in some time interval (with temperature and/or pressure variation), finite time integration method can be applied to find the remaining size of the crystal.

Fig. 3-17 shows the calculated survival time and falling distance of a sinking spherical olivine crystal in an infinite basalt reservoir at a given temperature and 0.2 GPa. For 8 mm radius (maximum grain size in Figure 3-17), the corresponding Re and Pe numbers are 1.3×10^{-5} to 1.0×10^{-3}, and 6.0×10^{5} to 1.6×10^{6}, at 1150°C and 1450°C respectively. The survival time for an olivine crystal (Fo90) of 1 to 8 mm radius varies from about one day to a few hundred days. The falling distance relative to the magma body varies from negligible up to about two kilometer. For larger olivine grains, the temperature and pressure variation needs to be considered because the falling distance becomes very large. The result shown in Fig. 3-17 can be helpful to constrain the ascent rate of the hosting magma. Suppose 1 mm radius olivine xenocrysts are observed in an erupted magma with eruption temperature of 1200°C. If the initial crystal radius was 4 mm, the time interval for the dissolution process would be roughly 20 – 5 = 15 days. The falling distance would be less than 100 m. If the initial crystal radius was 2 mm, the dissolution time interval would be roughly 10 – 5 = 5 days. The falling distance in this case would be less than 10 m. If the starting magma chamber was at 5 km depth, the ascent rate would be roughly 0.3 – 1 km/day.

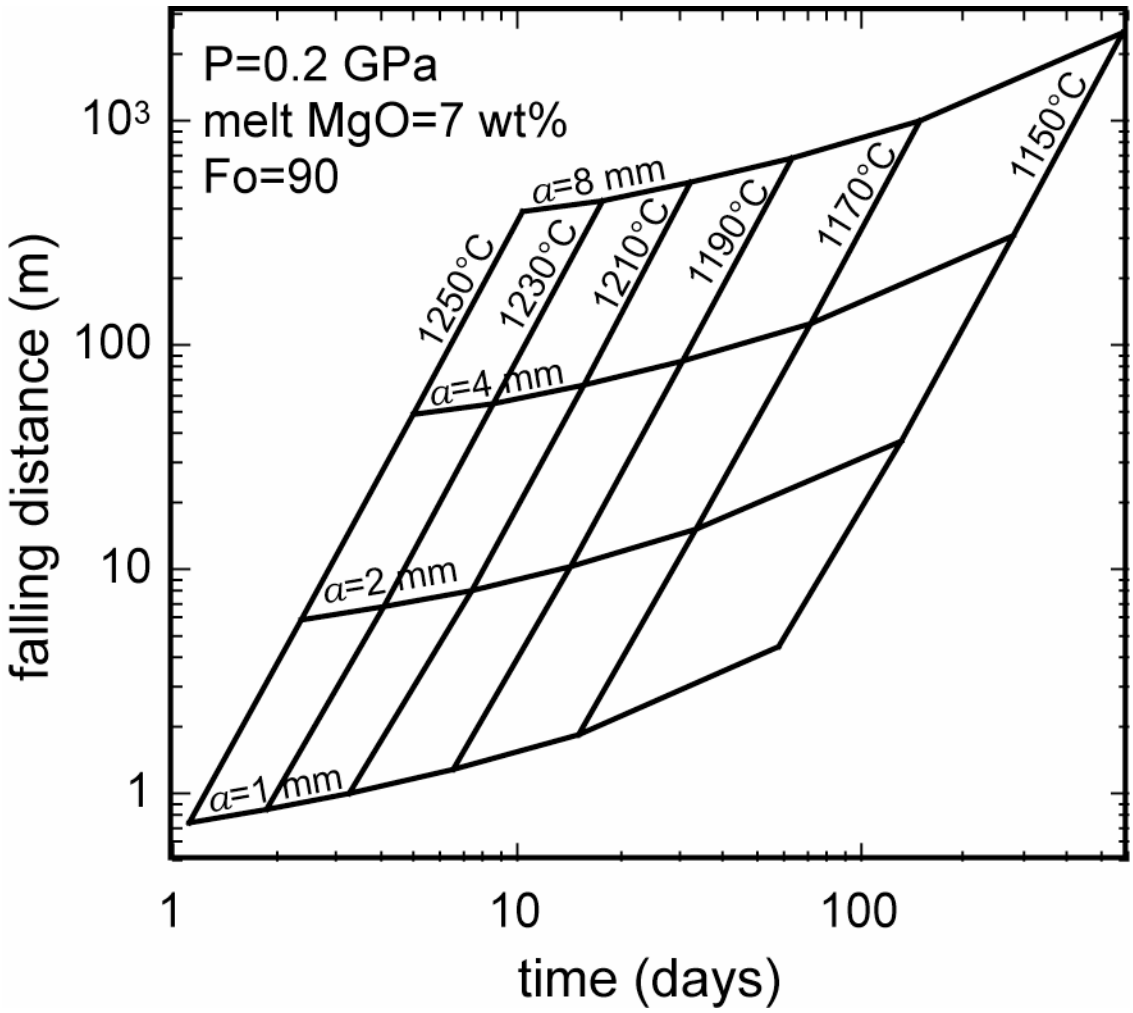

Figure 3-17. Survival time and falling distance for a single olivine grain falling in an infinite basaltic magma chamber. The liquidus temperature of the melt is 1136°C.

3.5.6. Convective Olivine Growth in Basaltic Melt

Some critical differences between crystal growth and dissolution restrict the applicability of our theory. Nucleation is an important process for crystal growth but not for dissolution. Multiple crystals may nucleate and grow simultaneously. Their compositional boundary layers may overlap. When the degree of oversaturation is high, interplay between nucleation and growth can lead to dendritic growth. The macro-scale magma crystallization process cannot be treated without considering nucleation. If the degree of oversaturation is extremely small (such as 10^{-8}), interface reaction is slow and can control the growth rate. In this case, growth rates depend on the crystal faces. The above complexities are not treated in our model. Nonetheless, crystal growth and dissolution share many characteristics. For example, both processes involve interface reaction and mass and heat transfer. A growing olivine in a magma chamber can undergo falling due to density contrast. When the degree of supersaturation is intermediate, not too small and not too large (i.e., dendritic growth or interface reaction is not significant), the convective overgrowth rate of a single olivine grain can be estimated similarly as convective dissolution. Suppose a basaltic melt contains 11 wt% MgO at 1240°C and 200 MPa. The saturation MgO concentration is 10.81 wt% (Eqn. 3-17). The equilibrium MgO and FeO concentration in olivine can be estimated from the MgO and FeO content in the melt (Roeder and Emslie, 1970; Langmuir and Hanson, 1980). Suppose the equilibrium MgO concentration in olivine is 47 wt%, then $\beta = 2.723*(10.81-11)/(47-10.81)/3.163 = -0.004520$. The negative sign means olivine would grow rather than dissolve. From Eqn. (3-19), $D_{MgO}/\delta = 0.085$ μm/s. Hence the convective olivine growth rate is roughly 1.4 μm/hr or 1 mm/month. If the degree of oversaturation is doubled or

halved, the growth rate roughly doubles or halves. 1 mm/month is a fairly high growth rate. Typical olivine growth in a magma chamber probably occurs at smaller degree of saturation.

3.5.7. Dissolution of Olivine in a Mantle Xenolith in Basaltic Melt

In nature, olivine is often found in mantle xenoliths brought up by alkali basalt. As a xenolith falls relatively to the melt, the boundary layer thickness is thin on the leading side of the xenolith and thick on the trailing side (Levich, 1962; Zhang, 2008). Hence, crystals on the leading side dissolve more rapidly than the ones on the trailing side. Nonetheless, the average convective dissolution rate of olivine crystals in the xenolith may be estimated using the average boundary layer thickness surrounding the whole xenolith. The kinetic parameter D_{MgO}/δ obtained earlier is suitable for this case too, but on an average sense. Olivine on the leading side dissolves more rapidly than the calculated average dissolution rate, while olivine on the trailing side dissolves slower. Furthermore, because only one side of an olivine crystal is exposed to the melt, the average survival time of the olivine crystal in a mantle xenolith is two times that of a stand-alone olivine crystal in a melt.

Mantle xenolith may dissolve incongruently. Some minerals may reprecipitate while the others dissolve. Because xenolith consists of different minerals, the interface melt along a xenolith surface may be heterogeneous and diffusion may occur. These complexities are not included in this simple model.

Most magmas that bring mantle xenoliths to the surface are alkali, not typically tholeiitic. The uncertainties introduced by applying our model to alkali basalt are evaluated as following:

(1) As discussed in Section 3.5.3, C_0 does not depend much on the initial melt composition.

(2) As shown in Fig. 3-18, the viscosity of an alkali basalt is about 0.2 logη units lower than the tholeiite used in this study, based on the viscosity model by Hui and Zhang (2007). The compositions of the two basalts are also listed in Fig. 3-18. The alkali basalt is from Chen et al. (2007), which contains abundant mantle xenoliths. The 0.2 logη units difference is within the 0.61 logη units uncertainty of the model by Hui and Zhang (2007). The density difference between the alkali basalt and the tholeiite is <1% and can be neglected.

(3) No suitable MgO diffusivity data is available to evaluate the difference of D_{MgO} between alkali and tholeiitic basalts. Even though the Eyring relation and the Einstein equation predict that diffusivity is inversely proportional to viscosity, many studies have shown that the diffusivity difference between different melts is smaller than the viscosity difference (e.g., Mungall, 2002; Ni and Zhang, 2008). Even if we take the diffusivity difference to be the same as the viscosity difference, a higher D_{MgO} in alkali basalt by 0.2 log units than tholeiitic basalt is small and within the error of our treatment.

Based on the above assessments, we conclude that the calculated olivine dissolution rate in tholeiitic basalt is roughly applicable to alkali basalt within the uncertainty of known magma properties (viscosity and diffusivity).

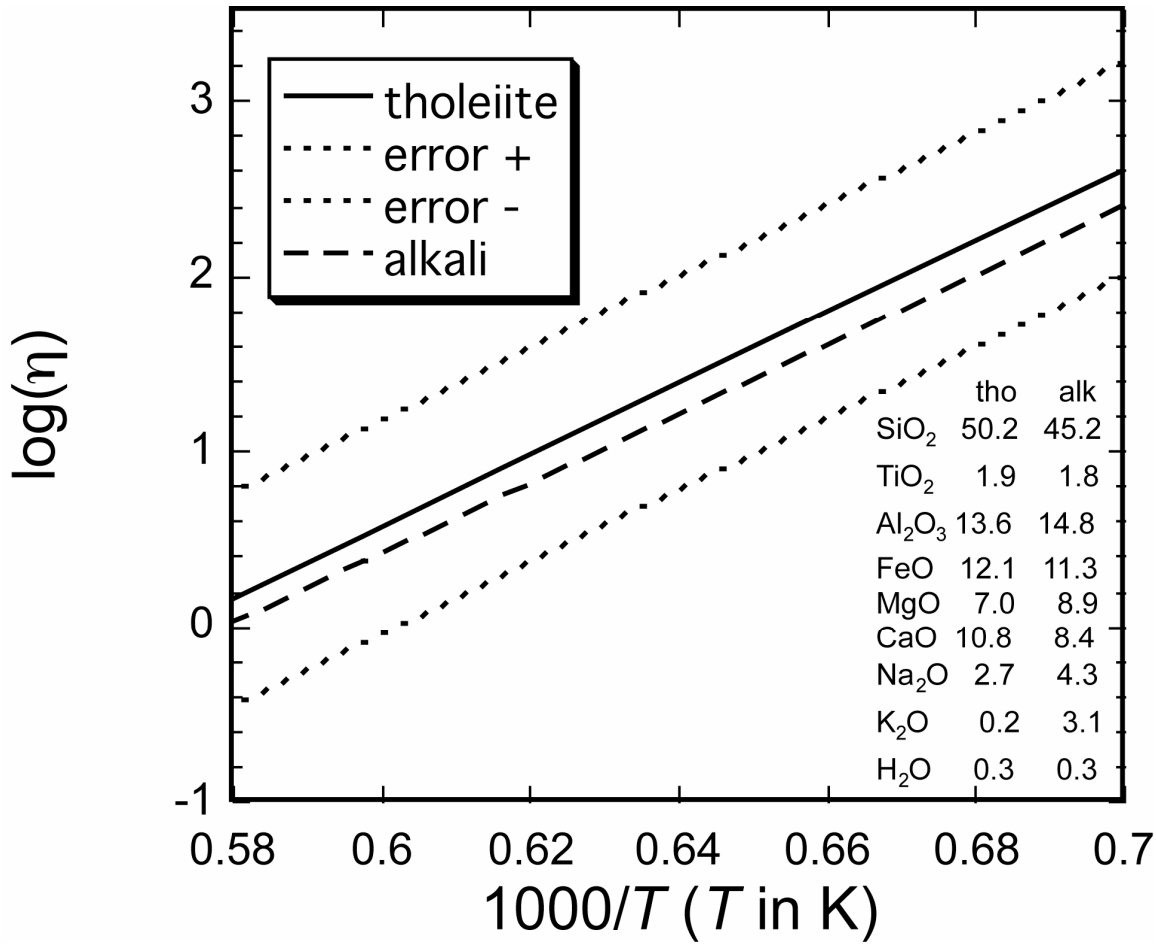

Figure 3-18. Viscosity of tholeiitic (solid line) and alkali (long dashed line) basalt. Model uncertainty for the tholeiite is also shown.

3.6. Conclusions

In our experiments, dissolution rapidly reaches diffusion control. Interface reaction does not significantly limit the rate of olivine dissolution in basaltic melt. The effective binary diffusivity of MgO shows Arrhenian dependence on temperature. The pressure dependence is small and not resolved within 0.47-1.42 GPa. Combining literature data with this study shows that the effective binary diffusivity of MgO depends strongly on the melt composition. MgO concentration in the melt at the olivine-melt interface depends on temperature and pressure, but not on the initial melt composition within basalt and andesite regime. We modeled the MgO concentration in the interface melt as a function of temperature and pressure (Eqn. 3-17).

Convective dissolution rate of a crystal falling or rising in a melt by gravity can be calculated by $\beta D/\delta$, where D is the diffusivity of the principle equilibrium-determining component, δ is the boundary layer thickness, and β depends on the composition of the crystal, the interface melt, and the initial melt. For easy quantitative calculation of convective olivine dissolution rate in basaltic melt, the D_{MgO}/δ values for Fo80-100 olivine are calculated within 1150-1450°C and 1 bar-2 GPa and are given in Eqn. (3-19) as a function of T, P, and X_{Fo}. The uncertainty in D_{MgO}/δ is $\overset{\times}{\div}1.7$ due to the uncertainties in diffusivity and viscosity. For olivine dissolution, β can be estimated based on our model of MgO concentration in the interface melt. The model can also be applied to convective crystal growth and xenolith digestion, with limitations.

Acknowledgements

We thank Peter Ulmer, Ross Kerr, Cliff Shaw and Yan Liang for insightful and constructive comments, and Glenn Gaetani for help with olivine-melt equilibrium model. Y. Chen thanks Zhengjiu Xu, Hejiu Hui and Huaiwei Ni, for training and help on piston-cylinder experiment and FTIR measurement, and Eric J. Essene, Carl Henderson and Zeb Page, for training and help on electron microprobe. This work is supported by NSF grants EAR-0537598 and EAR-0711050. Electron microprobe work is carried out on a Cameca SX100 instrument at Electron Microbeam Analysis Laboratory of the University of Michigan, which is supported by NSF grant 9911352.

References

Acosta-Vigil A., London D., Dewers T.A., Morgan VI G.B. (2002) Dissolution of corundum and andalusite in H_2O-saturated haplogranitic melts at 800C and 200 MPa: constraints on diffusivities and the generation of peraluminous melts. *J. Petrol.* **43**, 1885-1908.

Acosta-Vigil A., London D., Morgan VI G.B., Dewers T.A. (2006) Dissolution of quartz, albite, and orthoclase in H_2O-saturated haplogranitic melt at 800C and 200 MPa: diffusive transport properties of granitic melts at crustal anatectic conditions. *J. Petrol.* **47**, 231-254.

Agee C.B. (1998) Crystal-liquid density inversions in terrestrial and lunar magmas. *Phys. Earth Planet. Interiors* **107**: 63-74.

Asimow P.D. and Ghiorso M.S. (1998) Algorithmic modifications extending MELTS to calculate subsolidus phase relations. *Am. Mineral.* **83**, 1127-1131.

Baker D.R. (1990) Chemical interdiffusion of dacite and rhyolite: anhydrous measurements at 1 atm and 10 kbar, application of transition state theory, and diffusion in zoned magma chambers. *Contrib. Mineral. Petrol.* **104**, 407-423.

Brearley M. and Scarfe C.M. (1986) Dissolution rates of upper mantle minerals in an alkali basalt melt at high pressure: an experimental study and implications for ultramafic xenolith survival. *J. Petrol.* **27**, 1157-1182.

Chen Y., Zhang Y., Graham D., Su S. and Deng J. (2007) Geochemistry of Cenozoic basalts and mantle xenoliths in Northeast China. *Lithos* **96**, 108-126.

Crank J. (1975) *The Mathematics of diffusion*. Oxford Univ. Press, Oxford, pp 414.

Clift R., Grace J.R. and Weber M.E. (1978) *Bubbles, Drops, and Particles.* Academic Press, New York.

Cooper A.R. (1968) The use and limitations of the concept of an effective binary diffusion coefficient for multi-component diffusion. In: *Mass transport in oxides* (eds. J.B. Wachtman Jr and A.D. Franklin). *Nat. Bur. Stand. Spec. Publ.* **296**, 79-84.

Dixon J.E., Clague D.A. and Eissen J.-P. (1986) Gabbroic Xenoliths and Host Ferrobasalt From the Southern Juan de Fuca Ridge. *J. Geophys. Res.* **91**, 3795-3820.

Dixon J. E., Stolper E. and Delaney J.R. (1988) Infrared spectroscopic measurements of CO_2 and H_2O in Juan de Fuca Ridge basaltic glasses. *Earth Planet. Sci. Lett.* **90**, 87-104.

Donaldson C.H. (1985) The rates of dissolution of olivine, plagioclase, and quartz in a basalt melt. *Mineral. Mag.* **49**: 683-693.

Finnila A.B., Hess P.C., Rutherford M.J. (1994) Assimilation by lunar mare basalts: Melting of crustal material and dissolution of anorthite. *J. Geophys. Res.* **99**, 14677-14690.

Gaetani G.A., Watson E.B. (2002) Modeling the major-element evolution of olivine-hosted melt inclusions. *Chem. Geol.* **183**, 25-41.

Ghiorso M. S. and Sack R.O. (1995) Chemical mass transfer in magmatic processes. IV. A revised and internally consistent thermodynamic model for the interpolation and extrapolation of liquid-solid equilibria in magmatic systems at elevated temperatures and pressures. *Contrib. Mineral. Petrol.* **119**, 197-212.

Hui H. and Zhang Y. (2007) Toward a general viscosity equation for natural anhydrous and hydrous silicate melts. *Geochim. Cosmochim. Acta* **71**, 403-416.

Hui H., Zhang Y., Xu Z. and Behrens H. (2008) Pressure dependence of the speciation of dissolved water in rhyolitic melts. *Geochim. Cosmochim. Acta* **72**, 3229-3240.

Kerr R.C. (1995) Convective crystal dissolution. *Contrib. Mineral. Petrol.* **121**, 237-246.

Kirkpatrick R.J. (1981) Kinetics of crystallization of igneous rocks. In *Reviews in Mineralogy: Kinetics of Geochemical Processes, vol. 8* (eds. A.C. Lasaga and R.J. Kirkpatrick). Mineralogical Society of America, Washington, D.C.

Kress V.C. and Ghiorso M.S. (1995) Multicomponent diffusion in basaltic melts. *Geochim. Cosmochim. Acta* **59**: 313-324.

Kubicki J.D., Muncill C.E. and Lasaga A.C. (1990) Chemical diffusion in melts on the $CaMgSi_2O_6$-$CaAl_2Si_2O_8$ join under high pressures. *Geochim. Cosmochim. Acta* **54**: 2709-2715.

Kuo L.-C. and Kirkpatrick R.J. (1985) Kinetics of crystal dissolution in the system diopside-forsterite-silica. *Am. J. Sci.* **285**: 51-90.

Lange R.A. and Carmichael I.S.E. (1987) Densities of Na_2O-K_2O-CaO-MgO-FeO-Fe_2O_3-TiO_2-SiO_2 liquids: new measurements and derived partial molar properties. *Geochim. Cosmochim. Acta* **51**, 2931-2946.

Langmuir C.H. and Hanson G.N. (1980) An evaluation of major element heterogeneity in the mantle sources of basalts. *Phil. Trans. Roy. Soc. (London)*, **A297**, 383-407.

Levich V.G. (1962) *Physicochemical Hydrodynamics.* Prentice-Hall, Englewood Cliff, N.J.

Liang Y. (1999) Diffusive dissolution in ternary systems: analysis with applications to quartz and quartzite dissolution in molten silicates. *Geochim. Cosmochim. Acta* **63**, 3983-3995.

Liang Y. (2000) Dissolution in molten silicates: effects of solid solution. *Geochim. Cosmochim. Acta* **64**, 1617-1627.

Liang Y. (2003) Kinetics of crystal-melt reaction in partially molten silicates: 1. Grain scale processes. *Geochem. Geophys. Geosyst.* **4**, 1045, doi:10.1029/2002GC000375.

Liu W. and Li B. (2006) Thermal equation of state of $(Mg_{0.9}Fe_{0.1})_2SiO_4$ olivine. *Phys. Earth Planet. Interiors* **157**: 188-195.

Martin D., Nokes R. (1988) Crystal settling in a vigorously convecting magma chamber. *Nature* **332**: 534-536

Morgan Z. and Liang Y. (2003) An experimental and numerical study of the kinetics of harzburgite reactive dissolution with applications to dunite dike formation. *Earth Planet. Sci. Lett.* **214**, 59-74.

Morgan Z., Liang Y. and Hess P. (2006) An experimental study of anorthosite dissolution in lunar picritic magmas: implications for crustal assimilation processes. *Geochim. Cosmochim. Acta* **70**, 3477-3491.

Mungall J.E. (2002) Empirical models relating viscosity and tracer diffusion in magmatic silicate melts. *Geochim. Cosmochim. Acta* **66**, 125-143.

Mysen B. (2007) Partitioning of calcium, magnesium, and transition metals between olivine and melt governed by the structure of the silicate melt at ambient pressure. *Am. Mineral.* **92**, 844-862.

Ni H. and Zhang Y. (2008) H_2O diffusion models in rhyolite with new high pressure data. *Chem. Geol.* **250**, 68-78.

Niu Y., Gilmore T., Mackie S., Greig A. and Bach W. (2002) Mineral chemistry, whole-rock compositions and petrogenesis of ODP Leg 176 gabbros: Data and discussion. *Proc. Ocean Drill. Prog. Sci. Results* **176**, 1-60.

Ochs III F.A. and Lange R.A. (1999) The Density of Hydrous Magmatic Liquids. *Science* **283**, 1314-1317.

Ohtani E and Maeda M. (2001) Density of basaltic melt at high pressure and stability of the melt at the base of the lower mantle. *Earth Planet. Sci. Lett.* **193**, 69-75.

Roeder P.L. and Emslie R.F. (1970) Olivine-liquid equilibrium. *Contrib. Mineral. Petrol.* **29**, 275-289.

Shaw C.S.J., Thibault Y., Edgar A.D. and Lloyd F.E. (1998) Mechanisms of orthopyroxene dissolution in silica-undersaturated melts at 1 atmosphere and implications for the origin of silica-rich glass in mantle xenoliths. *Contrib. Mineral. Petrol.* **132**, 354-370.

Shaw C.S.J. (2000) The effect of experiment geometry on the mechanism and rate of dissolution of quartz in basanite at 0.5 GPa and 1350C. *Contrib. Mineral. Petrol.* **139**, 509-525.

Shaw C.S.J. (2004) Mechanisms and rates of quartz dissolution in melts in the CMAS (CaO-MgO-$Al2O_3$-SiO_2) system. *Contrib. Mineral. Petrol.* **148**, 180-200.

Shaw C.S.J. (2006) Effects of melt viscosity and silica activity on the rate and mechanism of quartz dissolution in melts of the CMAS and CAS systems. *Contrib. Mineral. Petrol.* **151**, 665-680.

Sugawara T. (2000) Empirical relationships between temperature, pressure, and MgO content in olivine and pyroxene saturated liquid. *J. Geophys. Res.* **105**, 8457-8472.

Tilley C.E. (1922) Density, refractivity, and composition relations of some natural glasses. *Mineral. Mag.* **19**, 275-294.

Turcotte D.L. and Schubert G. (1982) *Geodynamics: Applications of Continuum Physics to Geological Problems.* Wiley & Sons, New York, NY. pp. 450.

Thornber C.R. and Huebner J.S. (1985) Dissolution of olivine in basaltic liquids: experimental observations and applications. *Am. Mineral.* **70**, 934-945.

Walker D. and Kiefer W.S. (1985) Xenolith digestion in large magma bodies. *J. Geophys. Res.* **90 supplement**, C585-C590.

Watson E.B. (1982) Basalt contamination by continental crust: some experiments and models. *Contrib. Mineral. Petrol.* **80**, 73-87.

Zhang Y. (1993) A modified effective binary diffusion model. *J. Geophys. Res.* **98**, 11901-11920.

Zhang Y. (1994) Reaction kinetics, geospeedometry, and relaxation theory. *Earth Planet. Sci. Lett.* **122**, 373-392.

Zhang Y. (2005) Fate of rising CO_2 droplets in seawater. *Environmental Science & Technology* **39**, 7719-7724.

Zhang Y. (2008) *Geochemical Kinetics.* Princeton University Press. Princeton, NJ.

Zhang Y. and Behrens H. (2000) H_2O diffusion in rhyolitic melts and glasses. *Chem. Geol.* **169**, 243-262.

Zhang Y. and Stolper E.M. (1991) Water diffusion in a basaltic melt. *Nature* **351**, 306-309.

Zhang Y. and Xu Z. (2003) Kinetics of convective crystal dissolution and melting, with applications to methane hydrate dissolution and dissociation in seawater. *Earth Planet. Sci. Lett.* **213**, 133-148.

Zhang Y. and Xu Z. (2008) "Fizzics" of bubble growth in beer and champagne. *Elements* **4**, 47-49.

Zhang Y., Walker D. and Lesher C.E. (1989) Diffusive crystal dissolution. *Contrib. Mineral. Petrol.* **102**, 495-513.

Chapter IV

Clinopyroxene Dissolution in Basaltic Melt

Abstract

The history of magmatic systems may be inferred from the reactive textures between mantle xenoliths and hosting basalt, if the thermodynamic and kinetic aspects of crystal dissolution are quantified. To study diffusive and convective clinopyroxene dissolution in silicate melts, experiments were conducted at 1236-1517 °C and 0.47-1.90 GPa in a piston-cylinder apparatus. Clinopyroxene saturation is treated as being determined by MgO and CaO. The effective binary diffusivities, D_{MgO} and D_{CaO}, and the interface melt compositions, C_0^{MgO} and C_0^{CaO}, are extracted from diffusive clinopyroxene dissolution experiments. D_{MgO} and D_{CaO} show Arrhenian dependence on temperature. The pressure dependence is small and not resolved within 0.47-1.90 GPa. The parameter $C_0^{\mathrm{MgO}} \times C_0^{\mathrm{CaO}}$ increases with increasing temperature, but decreases with increasing pressure. Convective clinopyroxene dissolution rate responses more strongly to superheating than that of olivine, which is mainly because of the difference in the thermodynamic aspect of olivine and clinopyroxene dissolution. The kinetic aspects of the two dissolution processes are quite similar. This model and a previous model on olivine dissolution are applied to xenoliths digestion in a basalt at Kuandian, Northeast

China. The eruption temperature is estimated to be within 1160 to 1310 °C, depending on the the pressure at which the dissolution of clinopyroxene is assumed to start. The residence time of the xenoliths is very short, within a few hours to a few days. The ascent rate is within 26 m/hour to ~6.3 km/hour. Only a small amount of xenolith was digested and the composition of the hosting basalt was not significantly affected.

4.1. Introduction

Reactive textures are commonly found along the interface between mantle xenoliths and hosting melt. Dissolution or growth may happen depending on the saturation status of the xenolith minerals in the melt. The magnitude of the dissolution or growth depend the kinetics of the reactions, which may be controlled by crystal-melt interface reaction and/or mass transfer in the melt. The history of the system may be inferred if the thermodynamic and kinetic aspects are quantified. Clinopyroxene is a common mineral in mantle xenoliths, hence an important component in the xenolith-melt reaction process. Furthermore, clinopyroxene is a main reservoir for incompatible elements in mantle rocks. For example, the partitioning coefficient of rare earth elements between clinopyroxene and melt is on the magnitude of 0.1-0.01, 10 times higher than that of olivine and orthopyroxene. Clinopyroxene can contain up to 0.3 wt% of water under certain conditions (Gavrilenko and Keppler, 2007). Its reaction with the hosting melt may affect the budget of trace elements and volatiles.

Crystal dissolution in nature often occurs under convective conditions, where convection can be driven by the density difference between the crystal and melt (e.g., Martin and Nokes, 1988), or between the interface melt and far-field melt. Because the

interface reaction of clinopyroxene dissolution is fast (Kuo and Kirkpatrick, 1985), the interface melt reaches near saturation rapidly (Zhang et al., 1989). Hence, naturally occurring clinopyroxene dissolution is controlled by convective mass transfer. Theory on convective crystal dissolution has been developed by Kerr (1995) for Reynolds number $\leq$ 1, and later expanded by Zhang and Xu (2003) to Reynolds number up to 10^5. This approach has been tested by halide dissolution in aqueous sodium carboxymethyl cellulose solutions (kerr, 1995), halide dissolution in water (Zhang and Xu, 2003), CO_2 droplet dissolution in seawater (Zhang, 2005), and CO_2 bubble growth in beer (Zhang and Xu, 2008). Application of this theory requires two key parameters: the saturation condition (i.e. the interface melt composition at given *T* and *P*) and the diffusivity in the hosting melt, which can be obtained by diffusive crystal dissolution experiments.

Experimental studies on clinpyroxene dissolution are limited. Scarfe et al. (1980) and Brearley and Scarfe (1986) considered clinopyroxene dissolution in alkali basalt at 1.25-2 and 0.5-3 GPa, respectively. Convection was not specifically controlled in those experiments and likely affected the dissolution process, causing inaccuracy in the extracted diffusion coefficients (Zhang et al., 1989). Kuo and Kirkpatrick (1985) studied diopside dissolution in its own melt at 1 atm and measured the interface reaction rate. Zhang et al. (1989) investigated non-convection clinopyroxene dissolution in andesitic melt at 1.05-2.15 GPa. Based on the results by Kuo and Kirkpatrick (1985), Zhang et al. (1989) showed that the interface melt reaches near saturation within 0.0002-0.2 s. Therefore, the interface reaction is expected not to play a rate-controlling role, and non-convective clinopyroxene dissolution is controlled by diffusion. Van Orman and Grove (2000) examined convection-free clinopyroxene dissolution in lunar basalt at 1-1.3 GPa

and reported the saturation condition and diffusivity in the melt, which are key parameters to model convective crystal dissolution. More data systematically covering a *P* and *T* range are necessary to construct a model for convective clinopyroxene dissolution.

In this study, non-convective clinopyroxene dissolution experiments were carried out in a mid-ocean ridge basalt at 1236-1517 °C and 0.47-1.90 GPa. This is a sister study of our recent work on olivine dissolution in basalt (Chen and Zhang, 2008). The tholeiitic melt composition is chosen because it is the most common basalt and natural glass samples are available. The experimental and model results in this melt can be applied to alkali basalts (Chen and Zhang, 2008). Natural clinopyroxene has a wide range of chemical components. In this study, one clinopyroxene crystal close to diopside end-member was used. The experimental results, i.e., the interface melt composition and the diffusivity, are applied to model convective clinopyroxene dissolution, where the clinopyroxene crystal either exists as individual xenocrysts or coexists with olivine crystals in mantle xenoliths. This model and the model on olivine dissolution (Chen and Zhang, 2008) are applied to the xenolith-basalt reaction at Kuandian, Northeast China. The thermal history is constrained and the residence time and upwelling rate are estimated.

4.2. Theoretical Analysis

This study follows the theoretical approach to crystal dissolution in Chen and Zhang (2008). Key difference exists between the models for olivine and clinopyroxene saturation. Models on olivine saturation typically only consider MgO and FeO, while models on clinopyroxene saturation may include SiO_2, Al_2O_3, MgO, CaO, FeO and Na_2O

(e.g. Putirka, 1999). The complexity of clinopyroxene imposes difficulty to applying the equilibrium-determining component and effective binary diffusion approach. In this study, for MgO and CaO-rich clinopyroxene, the saturation is considered as being determined by $C_0^{\mathrm{MgO}} \times C_0^{\mathrm{CaO}}$, where C_0^{MgO} and C_0^{CaO} are MgO and CaO concentrations in the interface melt. $C_0^{\mathrm{MgO}} \times C_0^{\mathrm{CaO}}$ is modeled as a function of T and P based on experimental results. The model is empirical. SiO_2 is another major components that may affect clinopyroxene saturation, but not included in the saturation model. Based on trial-and-error, including SiO_2 in the saturation model does not yield simpler or better models within the melt composition range investigated (including tholeiitic basalt, alkali basalt and andesite).

For diffusive clinopyroxene dissolution, the following equations are used:

$$L = 2\alpha_{\mathrm{MgO}}\rho_{\mathrm{m}}\sqrt{D_{\mathrm{MgO}}t}\,/\rho_{\mathrm{c}}, \tag{4-1a}$$

$$L = 2\alpha_{\mathrm{CaO}}\rho_{\mathrm{m}}\sqrt{D_{\mathrm{CaO}}t}\,/\rho_{\mathrm{c}}, \tag{4-1b}$$

$$\sqrt{\pi}\alpha_{\mathrm{MgO}}e^{\alpha_{\mathrm{MgO}}^2}\mathrm{erfc}(-\alpha_{\mathrm{MgO}}) = (C_0^{\mathrm{MgO}} - C_\infty^{\mathrm{MgO}})/(C_{\mathrm{c}}^{\mathrm{MgO}} - C_0^{\mathrm{MgO}}), \tag{4-1c}$$

$$\sqrt{\pi}\alpha_{\mathrm{CaO}}e^{\alpha_{\mathrm{CaO}}^2}\mathrm{erfc}(-\alpha_{\mathrm{CaO}}) = (C_0^{\mathrm{CaO}} - C_\infty^{\mathrm{CaO}})/(C_{\mathrm{c}}^{\mathrm{CaO}} - C_0^{\mathrm{CaO}}), \tag{4-1d}$$

$$C_0^{\mathrm{MgO}} \times C_0^{\mathrm{CaO}} = f(T,P), \tag{4-1e}$$

where L is diffusive dissolution distance; α_{MgO} and α_{CaO} are diffusive dissolution parameters defined in Eqn. (4-1c) and (4-1d); ρ_{m} and ρ_{c} are melt and crystal densities, respectively; D_{MgO} and D_{CaO} are effective binary diffusivities of MgO and CaO in the melt; t is time; C_∞^{MgO} and $C_{\mathrm{c}}^{\mathrm{MgO}}$ are MgO concentrations in the initial/far-field melt and clinopyroxene, respectively; C_∞^{CaO} and $C_{\mathrm{c}}^{\mathrm{CaO}}$ are CaO concentrations in the initial/far-

field melt and clinopyroxene, respectively. When D_{MgO}, D_{CaO} and $f(T,P)$ are determined from experiments, L, C_0^{MgO}, C_0^{CaO}, α_{MgO} and α_{CaO} can be solved from Eqn. (4-1).

For convective clinopyroxene dissolution the following equations are used:

$$u = \beta_{\mathrm{MgO}} D_{\mathrm{MgO}} / \delta_{\mathrm{MgO}}, \tag{4-2a}$$

$$u = \beta_{\mathrm{CaO}} D_{\mathrm{CaO}} / \delta_{\mathrm{CaO}}, \tag{4-2b}$$

$$\beta_{\mathrm{MgO}} = \rho_{\mathrm{m}} (C_0^{\mathrm{MgO}} - C_\infty^{\mathrm{MgO}}) \big/ (C_{\mathrm{c}}^{\mathrm{MgO}} - C_0^{\mathrm{MgO}}) / \rho_{\mathrm{c}}, \tag{4-2c}$$

$$\beta_{\mathrm{CaO}} = \rho_{\mathrm{m}} (C_0^{\mathrm{CaO}} - C_\infty^{\mathrm{CaO}}) \big/ (C_{\mathrm{c}}^{\mathrm{CaO}} - C_0^{\mathrm{CaO}}) / \rho_{\mathrm{c}}, \tag{4-2d}$$

$$C_0^{\mathrm{MgO}} \times C_0^{\mathrm{CaO}} = f(T,P), \tag{4-2e}$$

where u is the convective dissolution rate; β_{MgO} and β_{CaO} are convective dissolution parameters defined in Eqn. (4-2c) and (4-2d); δ_{MgO} and δ_{CaO} are effective thicknesses of the compositional boundary layer, and are calculated based on fluid dynamics shown below. When D_{MgO}, D_{CaO} and $f(T,P)$ are determined from experiments, u, C_0^{MgO}, C_0^{CaO}, β_{MgO} and β_{CaO} can be solved.

The parameters δ_{MgO} and δ_{CaO} are estimated as follows (Kerr, 1995; Zhang and Xu, 2003):

(1) Use the following three equations to solve for Reynolds number (Re), crystal falling or rising velocity (U) and drag coefficient (C_{D}):

$$\mathrm{Re} = \frac{2aU\rho_{\mathrm{m}}}{\eta}, \tag{4-3a}$$

$$U = \sqrt{\frac{8ga|\rho_{\mathrm{c}} - \rho_{\mathrm{m}}|}{3\rho_{\mathrm{m}} C_{\mathrm{D}}}}, \tag{4-3b}$$

$$C_{\mathrm{D}} = \frac{24}{\mathrm{Re}}(1 + 0.15\,\mathrm{Re}^{0.687}) + \frac{0.42}{1 + 42500\,\mathrm{Re}^{-1.16}}, \qquad (4\text{-}3c)$$

where a is the crystal radius and η is the melt viscosity. Eqn. (4-3a) is the definition of the Reynolds number Re. Eqn. (4-3b) is the general equation to calculate the falling or rising velocity of a rigid spherical particle in a fluid (Turcotte and Schubert, 1982). Eqn. (4-3c) is from Clift et al. (1978) and has a relative error of ~ ±5% for $\mathrm{Re} \le 3\times 10^5$.

(2) Calculate compositional Peclet number (Pe) as (definition of Pe):

$$\mathrm{Pe} = 2aU/D. \qquad (4\text{-}4)$$

(3) Calculate the Sherwood number (Sh) as following, for $\mathrm{Re} \le 10^5$ (Zhang and Xu, 2003):

$$\mathrm{Sh} = 1 + (1 + \mathrm{Pe})^{1/3}\left(1 + \frac{0.096\,\mathrm{Re}^{1/3}}{1 + 7\,\mathrm{Re}^{-2}}\right). \qquad (4\text{-}5)$$

(4) Calculate the effective boundary layer thickness δ as (definition of the Sherwood number Sh):

$$\delta = 2a/\mathrm{Sh}. \qquad (4\text{-}6)$$

4.3. Experimental and Analytical Methods

The experimental and analytical procedures follow those in Chen and Zhang (2008). This section emphasizes the differences. Chen and Zhang (2008) carried out time-series experiments on olivine dissolution to examine how the interface melt composition and the compositional profile in the melt evolve with experimental duration. Because the interface reaction of clinopyroxene dissolution is rapid (Kuo and Kirkpatrick, 1985), and the experimental design is proved to suppress convection effectively (Zhang et al., 1989), time-series experiments were not conducted. The duration of the experiments is designed

to be long enough to generate a measurable diffusion profile, but short enough to maintain the melt as an infinite reservoir.

The basaltic glass is the same as in Chen and Zhang (2008). The clinopyroxene is a natural sample from American Museum of Natural History. Its composition is listed in Table 4-1. The clinopyroxene crystals have two sets of well-developed cleavages and break easily, posing some machining difficulties. Hence, thick clinopyroxene discs (~1.1 mm) were used in experiments. Minor cracks in the clinopyroxene were difficult to avoid. Efforts were made to minimize cracks in the samples used in experiments.

The interface melt produced by clinopyroxene is actually less dense than the initial basaltic melt (higher SiO_2 concentration) based on the density model of Ochs and Lange (1999). This was not realized (i.e., the calculation was not carried out) until a few experiments were done. Hence, in early experiments (Exp# 1, 5, 6 and 7) the clinopyroxene was placed under the glass, while in later experiments it was placed on the top. For the early experiments, no evidence for convection was found (e.g., multiple analysis traverses show consistent compositional profiles, and earlier and later data are consistent).

Table 4-1. Starting clinopyroxene and glass composition (wt%)

	Clinopyroxene (wt%)	Basalt (wt%)	Error in glass measurement (2σ)	Standard
SiO_2	54.15	50.23	0.40	K-feldspar
TiO_2		1.94	0.08	geikielite
Al_2O_3	0.60	13.61	0.16	K-feldspar
FeO	0.91	12.06	0.19	ferrosilite
MnO		0.22	0.11	rhodonite
MgO	17.90	7.05	0.12	olivine
CaO	25.40	10.75	0.19	clinopyroxene
Na_2O	0.41	2.73	0.10	albite
K_2O		0.17	0.05	K-feldspar
P_2O_5		0.10	0.09	apatite
H_2O		0.25-0.40**		
Total	99.37	99.16		

*: typical beam condition: 15 kV, 5 nA, 5×5 or 15×15 μm raster. Typical counting times are 20 s with the exception of SiO_2 (60 s), TiO_2 (30 s), FeO (60 s) and CaO (30 s).

**: Fourier transform infrared (FTIR) spectrometry measurement

Nine experiments were conducted at *T* and *P* shown in Fig. 4-1. The feasible *T*-*P* conditions are limited by two factors. First, the temperature must be higher than the liquidus temperature of the basalt. Otherwise crystallization occurs. Based on MELTS program calculation (Ghiorso and Sack, 1995; Asimow and Ghiorso, 1998), the liquidus phase is olivine at low pressure, and clinopyroxene at high pressure. Crystallization in the bulk melt must be avoided because it disturbs the diffusion and dissolution processes. This limit also applies to olivine dissolution experiments. Second, the temperature must be lower than the melting temperature of the clinopyroxene. The clinopyroxene used in the experiments is not a pure diopside. At 0.47 GPa, the melting point for pure diopside is ~1460 °C (Boyd and England, 1963; Williams and Kennedy, 1969), but the clinopyroxene used in this study was partially melted at 1380 °C. This limit is severe to clinopyroxene but not to olivine, because the solidus temperature for Mg-rich olivine is significantly higher. The suitable temperature range at given pressure is limited to a window of ~200 °C by these two factors. In order to better constrain the temperature dependence of the dissolution parameters, experiments were tried at temperatures slightly lower than the predicted liquidus by MELTS program. It turned out that dissolution experiments were successful up to ~30 °C below the predicted liquidus by MELTS. The experimental products were analyzed by electron microprobe following the method in Chen and Zhang (2008).

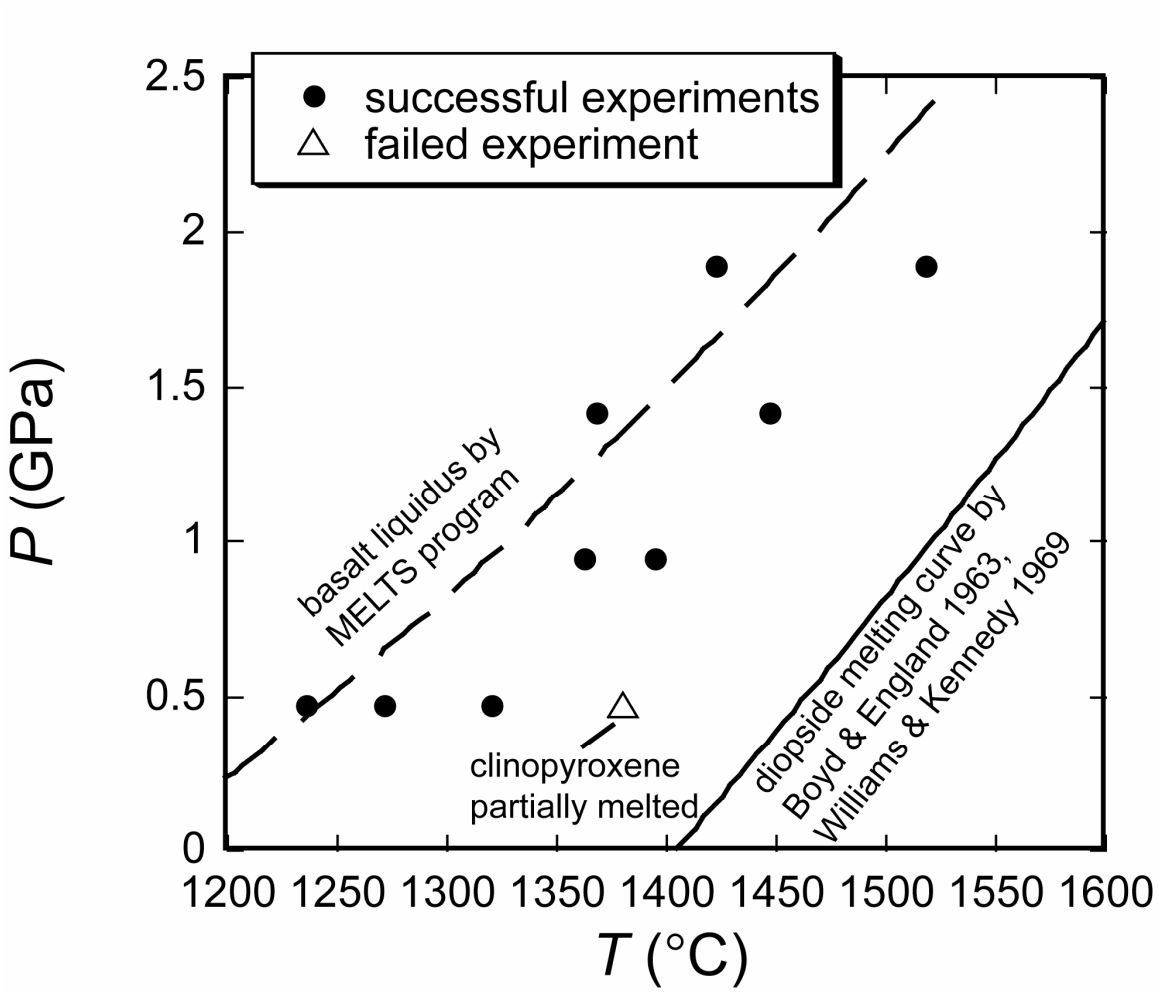

Figure 4-1. Experimental conditions and related limits.

4.4. Experimental Results

Table 4-2 shows the run conditions of all successful experiments. Fig. 4-2 shows a BSE image of a polished experimental charge. The center part of the clinopyroxene crystal is in contact with the melt and was dissolved and indented. The rim part remains intact. The clinopyroxene crystal and glass are always cracked after exposure. The cracks in glass are sub-parallel to the interface and are unfilled, meaning that they were formed during quench. Some cracks in clinopyroxene crystal are unfilled or filled by graphite; the others are filled by glass. The latter cracks are avoided when measuring diffusion profiles.

Shown in Fig. 4-3a and 4-4a, the interface between clinopyroxene and melt is not as flat as that between olivine and melt (Chen and Zhang, 2008). Examining the clinopyroxene-melt interface under reflective and transmit light shows that the interface intersects cleavages in the clinopyroxene (Fig. 4-4b). When a cleavage intersects the interface, the interface indents more. Every major indentation is correlated with a major cleavage in the clinopyroxene. Those major indentations are avoided in dissolution distance and compositional profile measurements.

Table 4-2. Summary of experimental conditions and dissolution distances

Exp#	T_1 (ºC)	T_2 (°C)	P (GPa)	Duration (s)		Diopside dissolution distance (μm)			
				t_1	t_2	L_1[a]	L_2	L_3	L_4
1	1271	1282	0.47	1799	1807	37±10	37±6	38±6	31±2
5	1362	1381	0.95	725	732	<81	49±16	50±15	51±3
6	1446	1470	1.42	720	732	<198	158±7	155±6	163±4
7	1321	1351	0.47	605	613	<89	67±8	65±7	94±10
8	1394	1421	0.95	721	733	<247	138±10	138±9	141±6
11	1422	1475	1.90	482	494	<92	44±13	44±12	41±3
12	1368	1407	1.42	721	732	<118	31±13	30±12	28±2
14	1236	1244	0.47	2397	2404	<22	11±10	7±9	8±1
15[b]	1517	1524	1.90	356	378	<236			147±8

Note: T_1 is corrected temperature; T_2 is the liquidus temperature of the interface melt calculated using MELTS program (interface melt compositions are listed in Table 4-4); P is the corrected pressure; t_1 is the nominal duration, t_2 is the corrected duration; L_1 is the dissolution distance obtained from measured initial distance (using a digital micrometer) minus final distance (measured under optical microscope), L_2 is the dissolution distance measured by optical microscope against reference olivine edge, L_3 is that measured by electron microprobe, L_4 is calculated by Eqn. (4-1). The errors are at 2σ level.

a: For most experiments a small melt reservoir existed on the other side of the clinopyroxene disc opposite to the major melt reservoir, and consumed some clinopyroxene. Hence L_1 values for most experiments are only upper limites.

b: The rim of the clinopyroxene crystal in the cross section of Exp#15 is dissolved, hence L_2 and L_3 are not measured.

All experiments except for Exp#15 were heated up by single stage of fixed heating rate of 900 °C/mins. Exp#15 was conducted in a different piston-cylinder apparatus. Type-D thermocouple was used instead of type-S. The sample was heated up through multiple stages of different heating rates to minimize temperature overshooting.

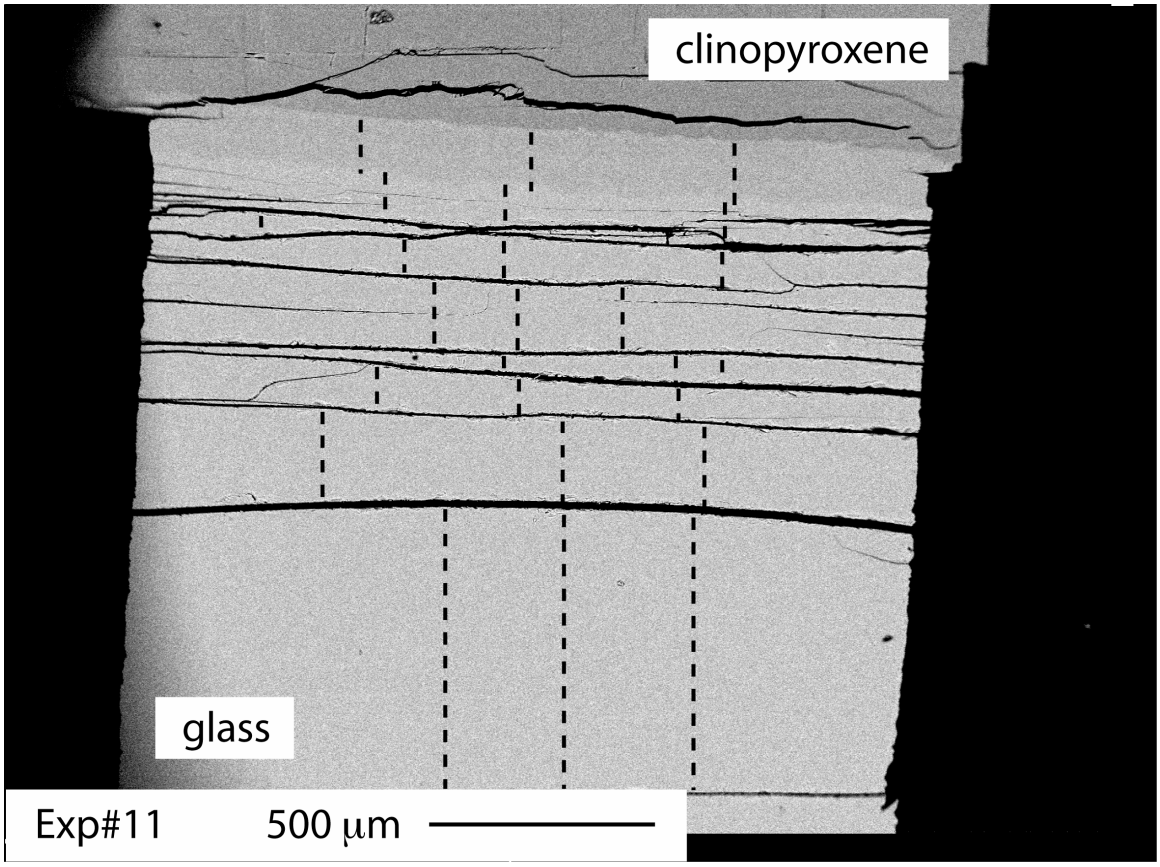

Figure 4-2. BSE image of the cross-section of Exp#11. Clinopyroxene disc is on the top. Electron microprobe analysis traverses are shown as dashed lines.

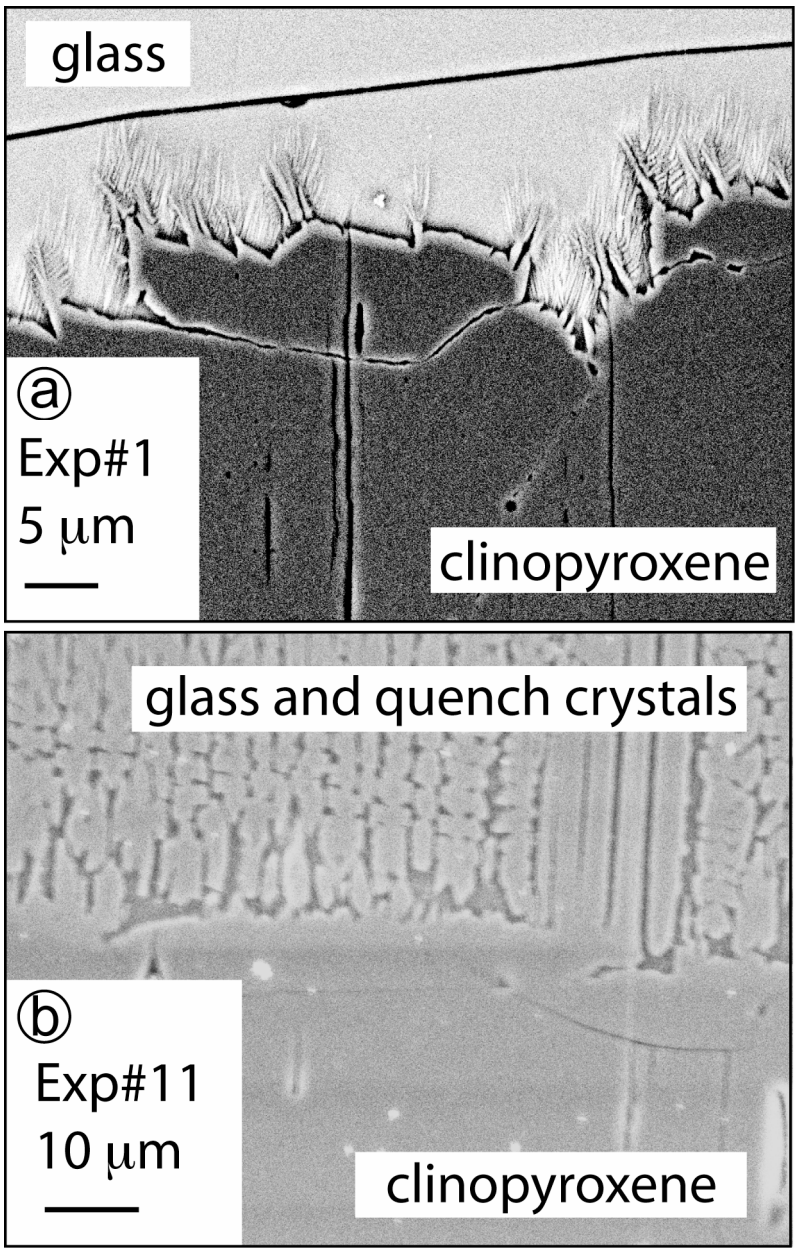

Figure 4-3. BSE images of two different types of quench crystal morphology. a: in a low temperature experiment (<1271ºC). b: in a high temperature experiment (>1271ºC).

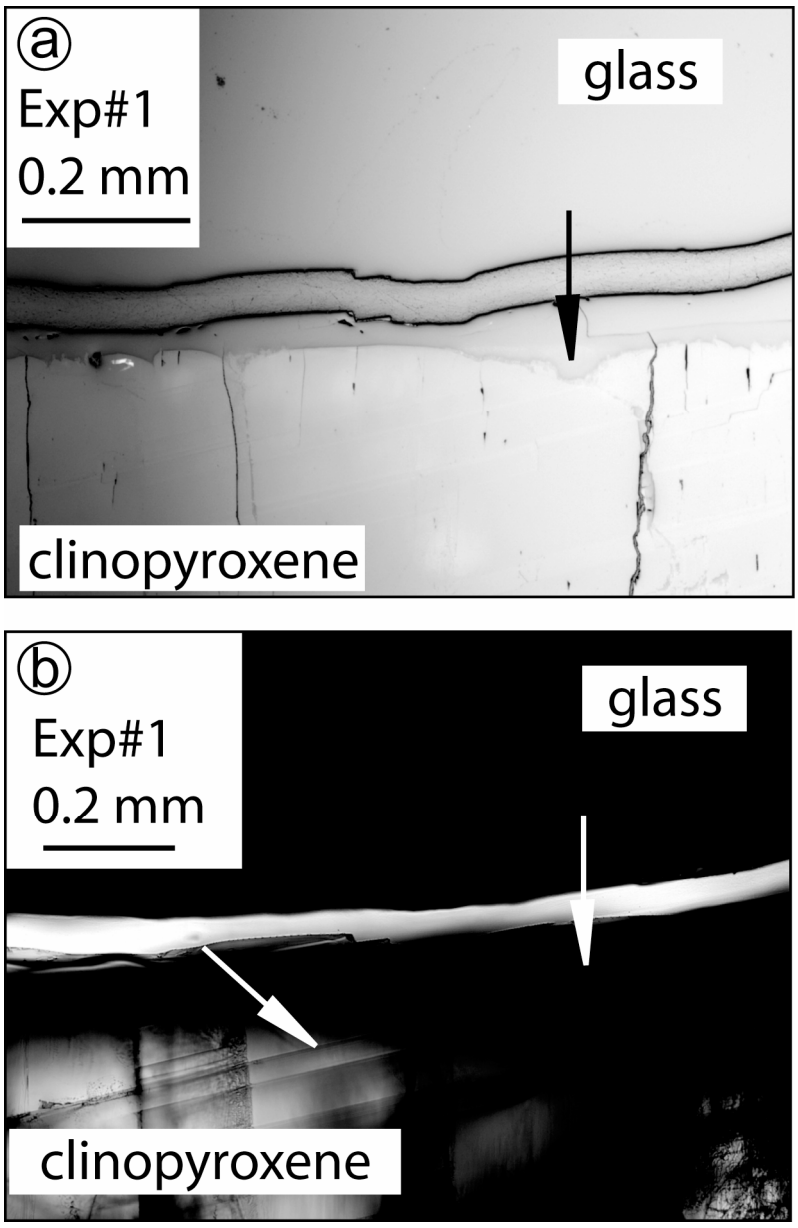

Figure 4-4. Optical microscope images of Exp#1. a: reflective light. Black arrow points to a major indentation in the interface. b: transmitted light on the same area as in (a). The white arrow on the right points to the position of the major indentation shown in a. The white arrow on the left points to a cleavage that intersects the interface at the position of the indentation.

Quench crystals are observed in all experiments. They fall into two categories based on their morphology and the related experimental conditions. At temperatures lower than 1271 ºC (Exp#1 and 14), a few needle-shaped or dendritic crystals extend from the interface into the glass (Fig. 4-3a). At temperatures higher than 1271 ºC, cluster of crystals with dendritic texture extends up to 270 μm away from the interface (Fig. 4-3b). Crystals of both types are attached to the crystal-melt interface. No crystals are found in other regions in the glass. The composition of the crystals cannot be measured accurately because they are too thin. EDS analysis suggests they are clinopyroxenes. The composition profiles within the crystalline zone were measured with 20×20 μm electron beam size, as opposed to 5×5 μm used for crystal-free zone.

Clinopyroxene dissolution distance is listed in Table 4-2. Measurement of the final clinopyroxene thickness under microscope has an error of ±5 μm. Measurement of the dissolution distance between the rim and the center has an error of ±1.25 μm under microscope, and ±0.5 μm under electron microprobe. An additional error is due to the heterogeneity in the initial clinopyroxene thickness (e.g., variation of the thickness from the rim to the center), which on average is about ±9 μm (2σ).

Compositional profiles are measured and treated following Chen and Zhang (2008). They are shown in Fig. 4-5 to 4-13. The far-field melt composition agrees well with the initial composition (Table 4-1). FeO shows uphill diffusion toward the interface in Exp#1, 12 and 14. The profiles bend abruptly close to the interface: TiO_2, Al_2O_3, FeO, Na_2O and K_2O increase while SiO_2, MgO and CaO decrease toward the interface. This trend is opposite to the overall trend defined by the major part of the profiles. This feature

is not clearly resolved in all experiments. It is attributed to clinopyroxene overgrowth during quench and discussed further in section 4.5.1.

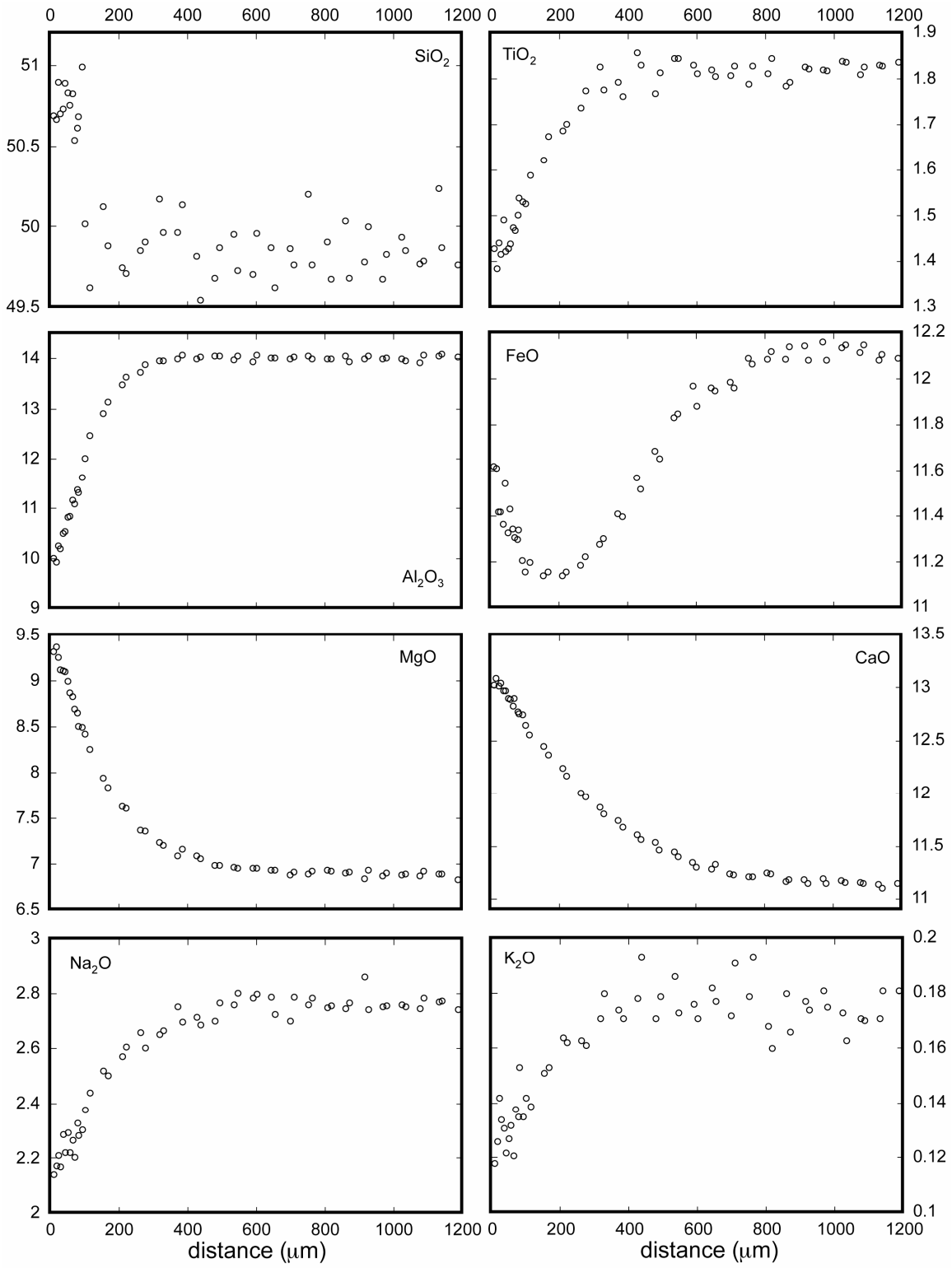

Figure 4-5. Composition profiles of Exp#1 (1271 ºC, 0.47 GPa, 30 minutes). The vertical axes are oxide wt%. Clinopyroxene-melt interface sets at x=0.

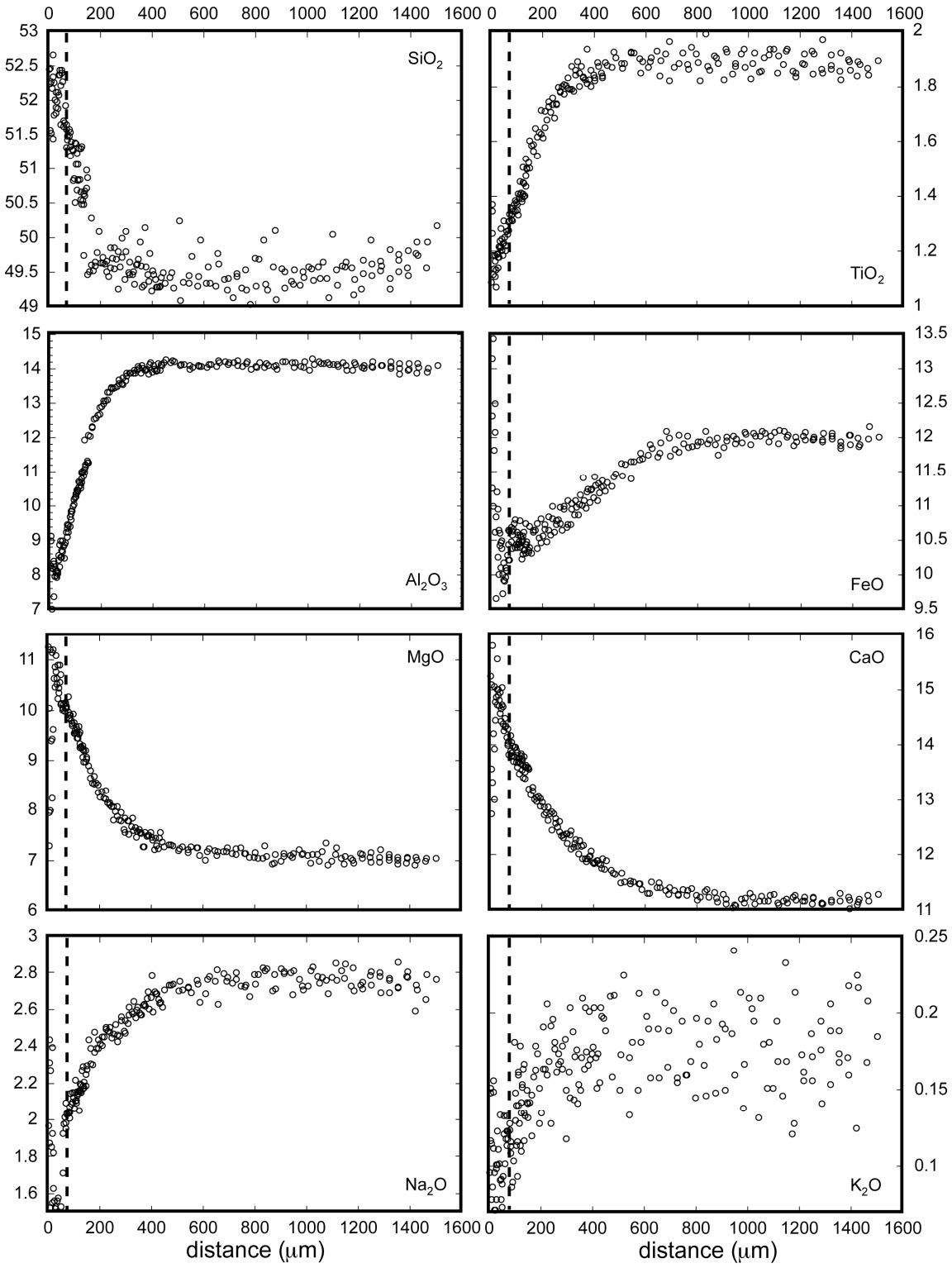

Figure 4-6. Composition profiles of Exp#5 (1362 ºC, 0.95 GPa, 12 minutes). The vertical axes are oxide wt%. Maximum extent of quench crystals is shown as dashed vertical line.

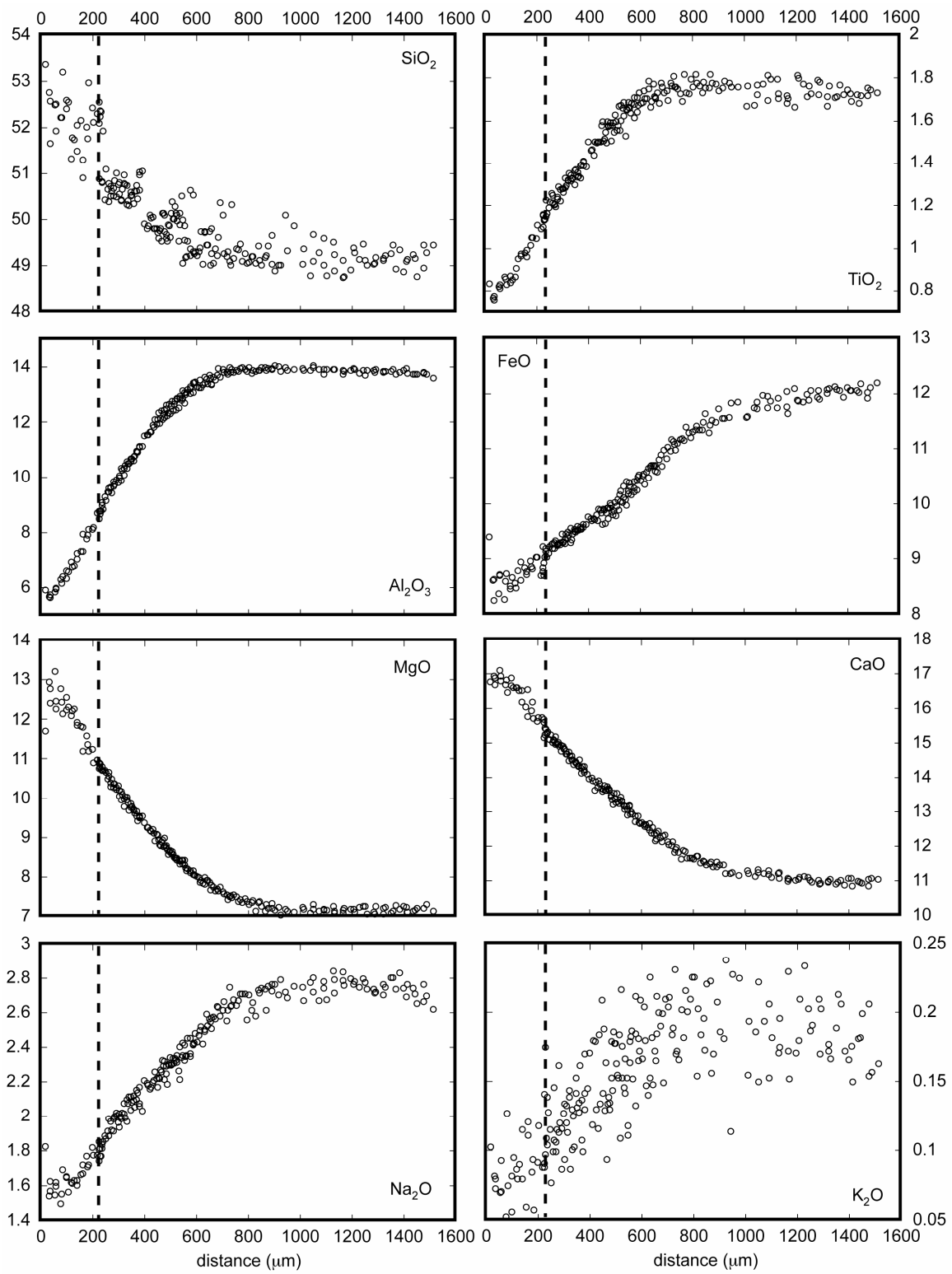

Figure 4-7. Composition profiles of Exp#6 (1446 ºC, 1.42 GPa, 12 minutes). The vertical axes are oxide wt%. Maximum extent of quench crystals is shown as dashed vertical line.

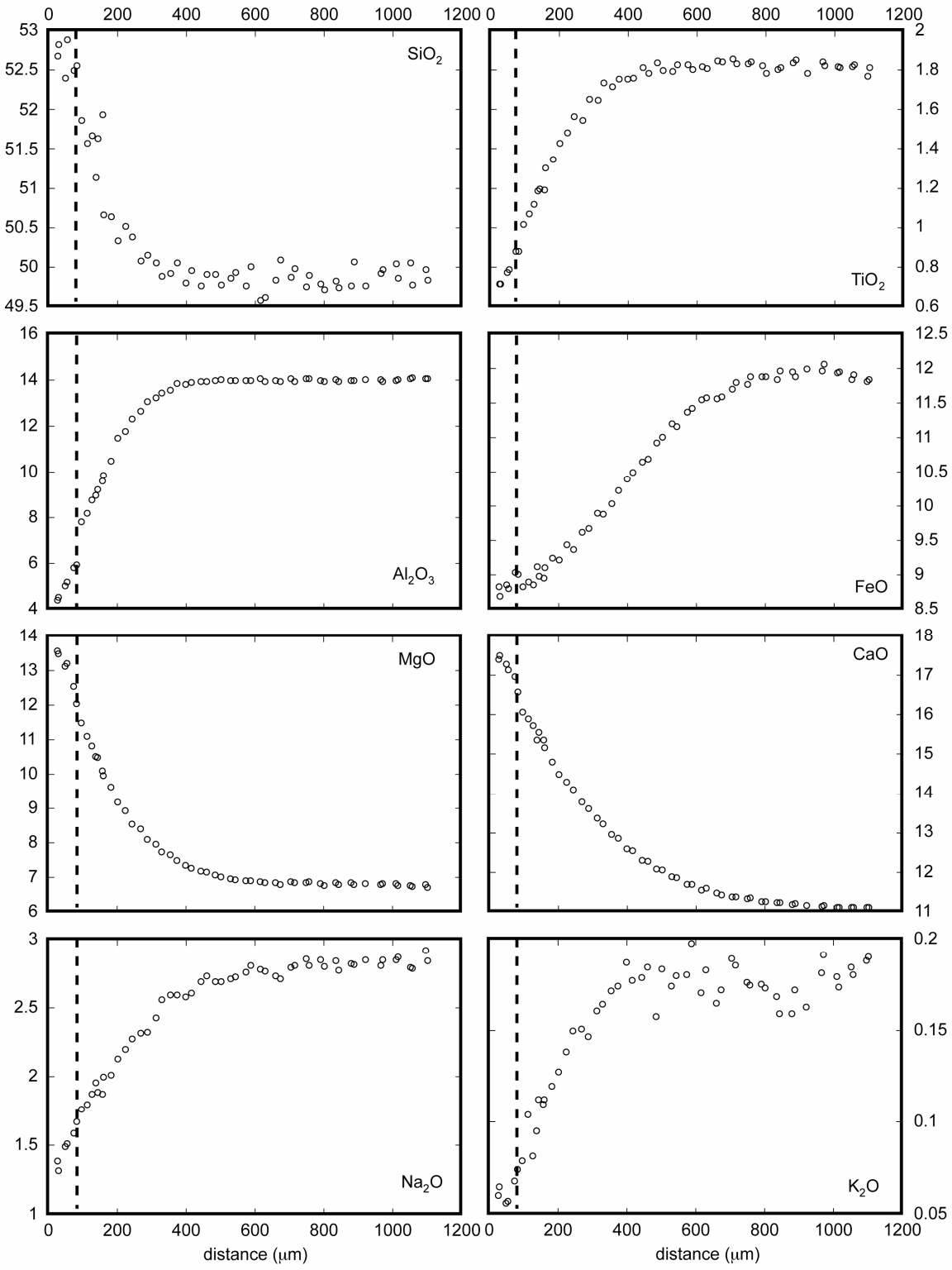

Figure 4-8. Composition profiles of Exp#7 (1321 ºC, 0.47 GPa, 10 minutes). The vertical axes are oxide wt%. Maximum extent of quench crystals is shown as dashed vertical line.

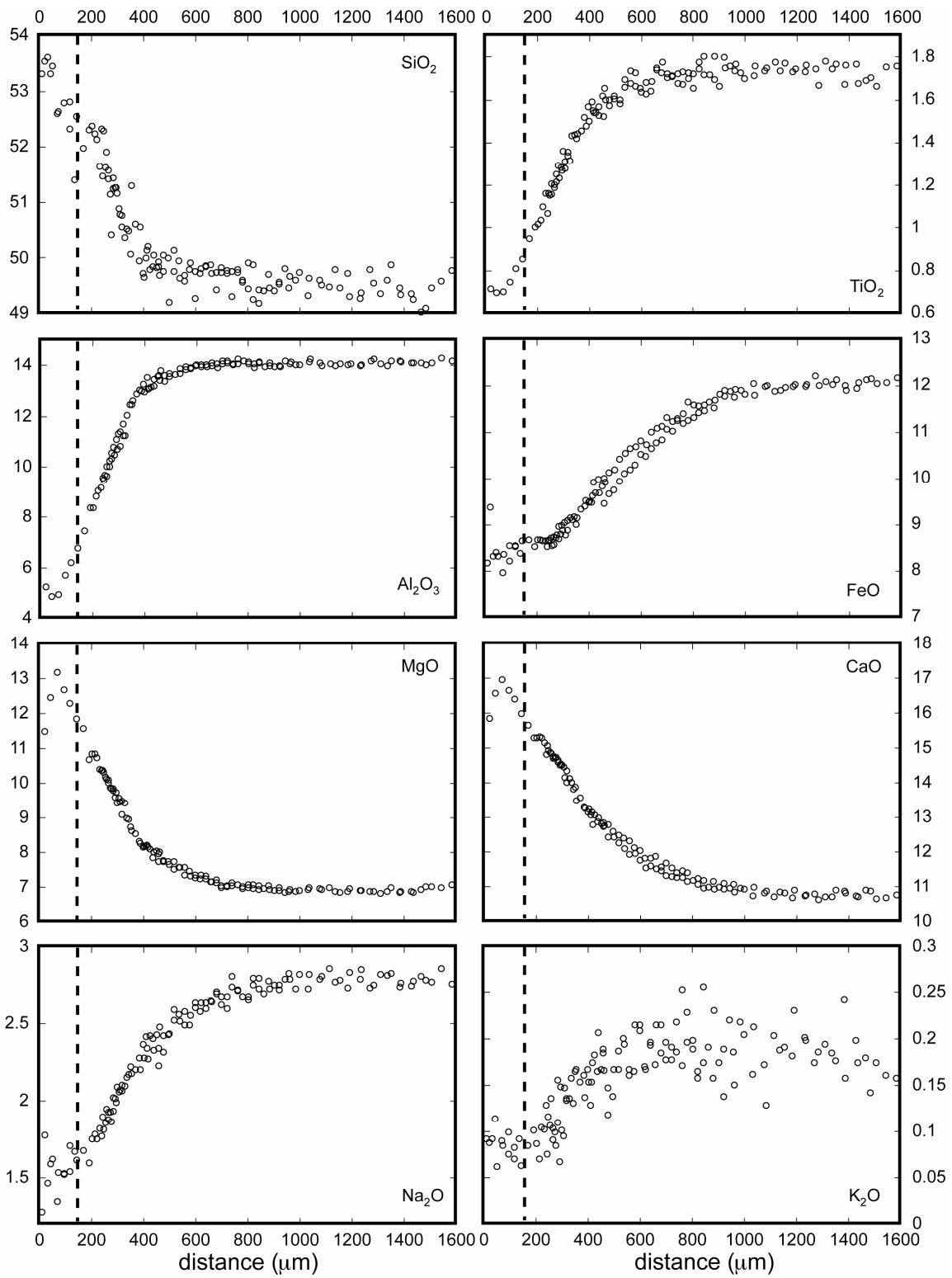

Figure 4-9. Composition profiles of Exp#8 (1394 ºC, 0.95 GPa, 12 minutes). The vertical axes are oxide wt%. Maximum extent of quench crystals is shown as dashed vertical line.

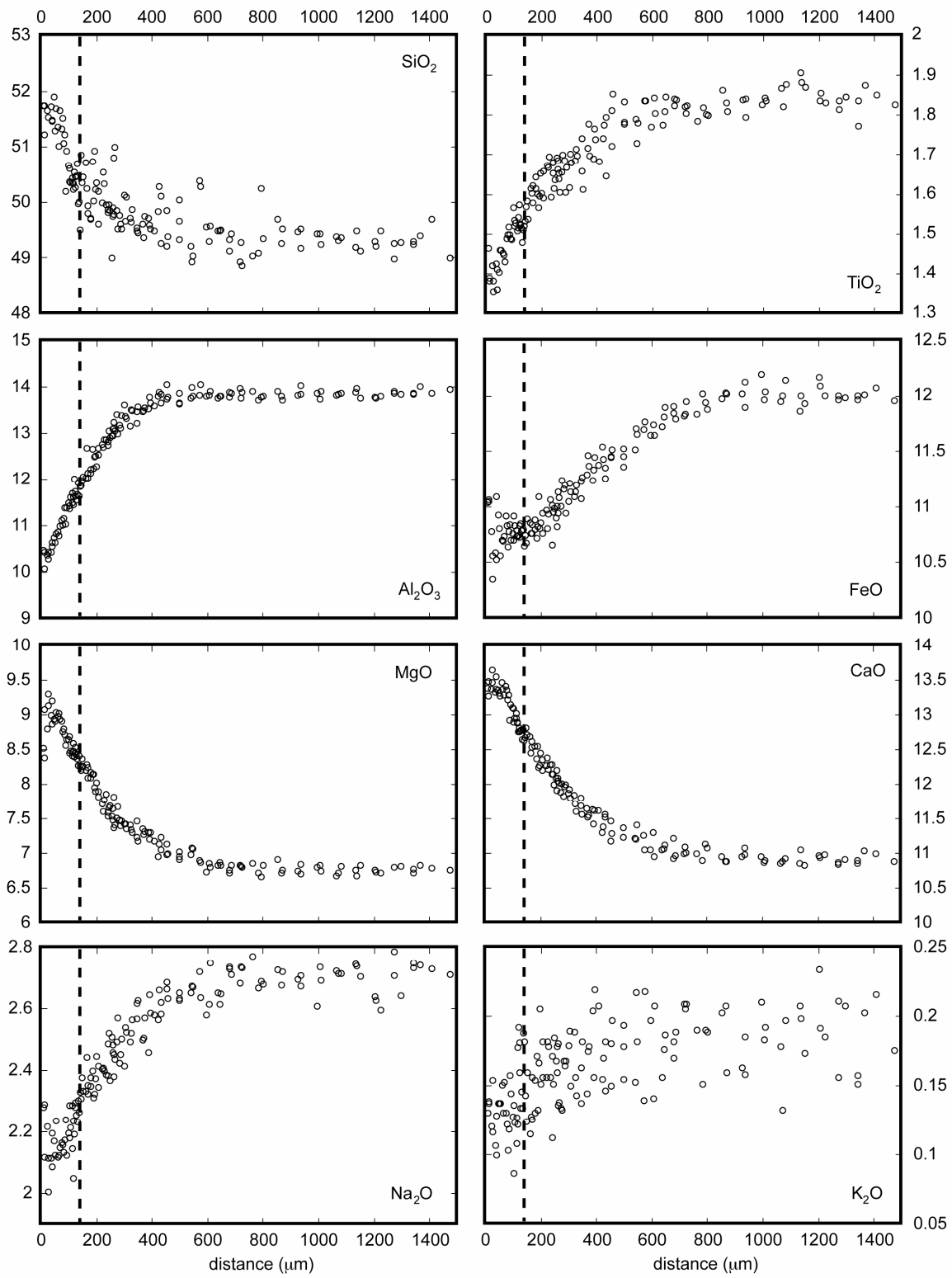

Figure 4-10. Composition profiles of Exp#11 (1422 ºC, 1.90 GPa, 6 minutes). Maximum extent of quench crystals is shown as dashed vertical line.

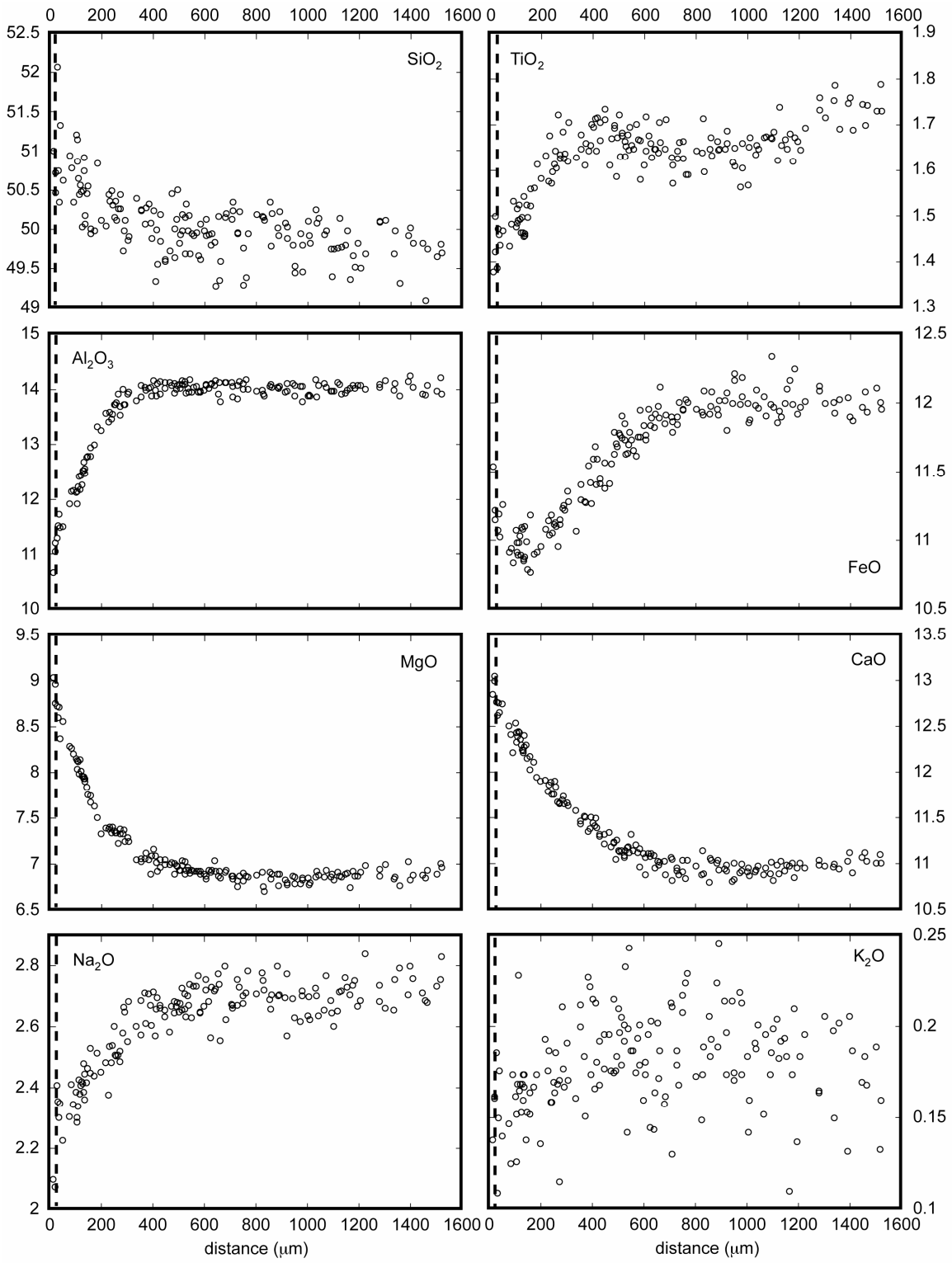

Figure 4-11. Composition profiles of Exp#12 (1368 ºC, 1.42 GPa, 12 minutes). Maximum extent of quench crystals is shown as dashed vertical line.

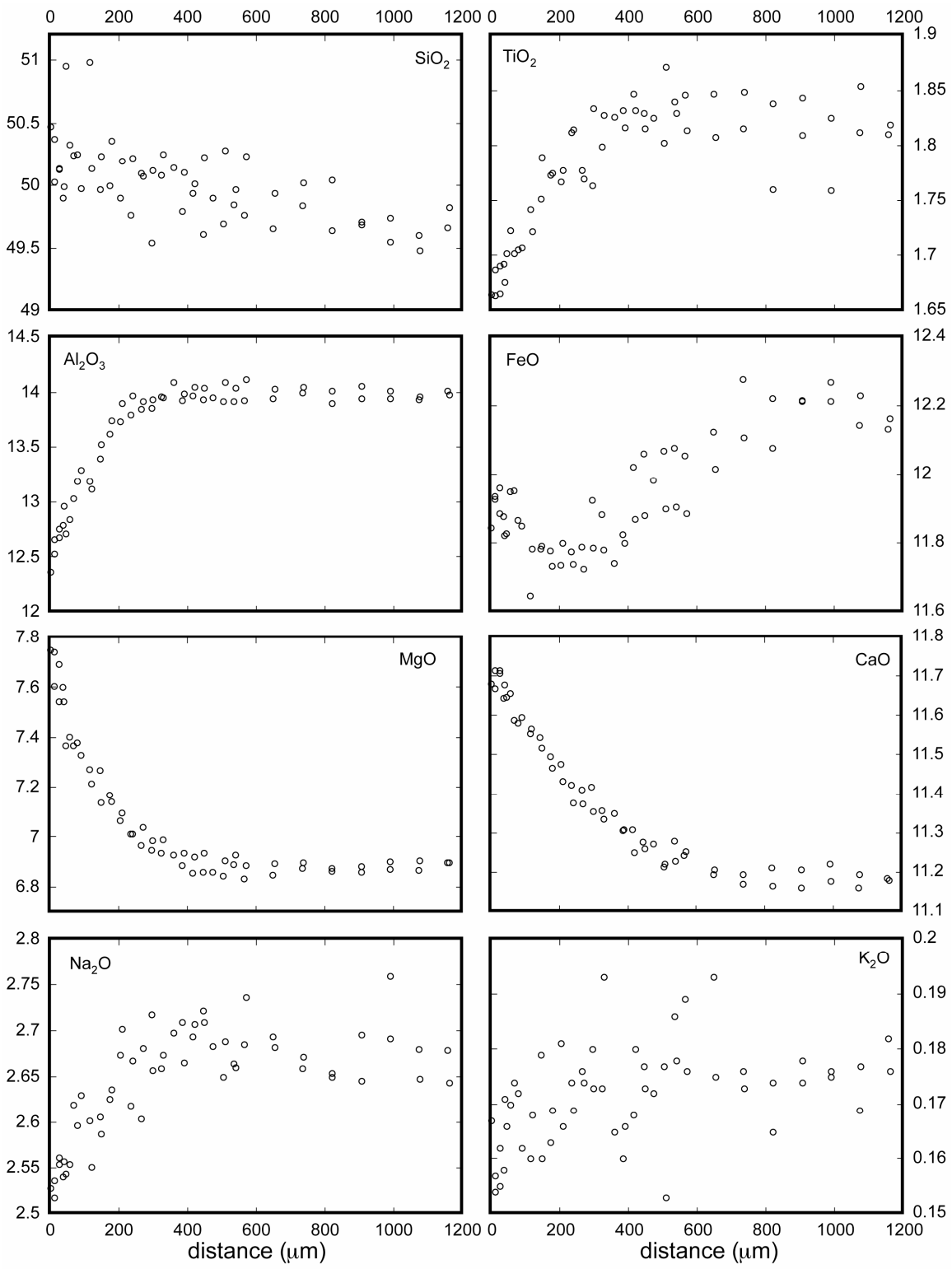

Figure 4-12. Composition profiles of Exp#14 (1236 ºC, 0.47 GPa, 40 minutes).

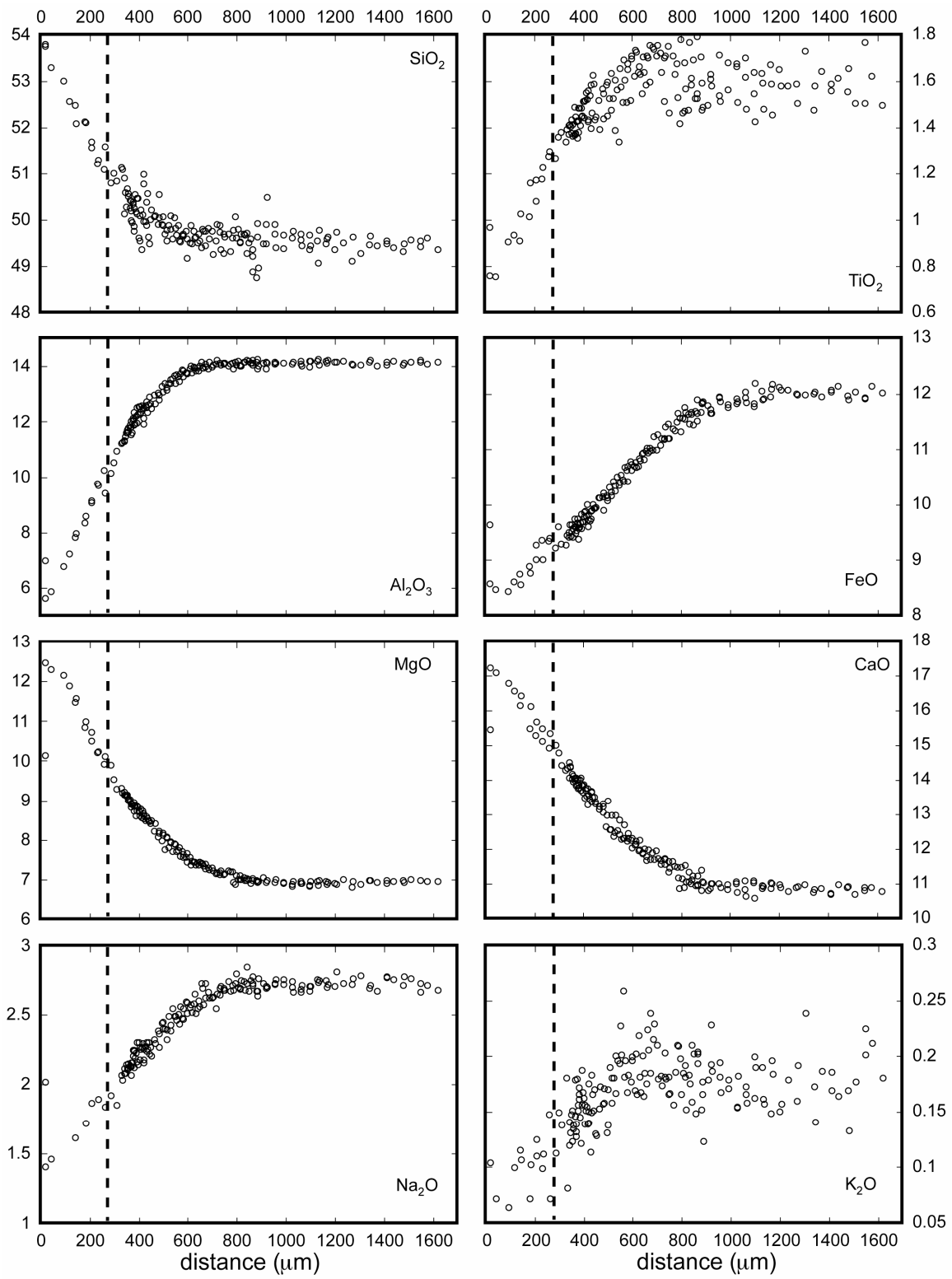

Figure 4-13. Composition profiles of Exp#15 (1517ºC, 1.90 GPa, 5 minutes). Maximum extent of quench crystals is shown as dashed vertical line.

4.5. Discussions and Applications

4.5.1. Interface Crystals and Quench Effect

Although the melt near the interface contain numerous tiny crystals, the composition profiles do not show any inconsistence across from the crystalline zone to non-crystalline zone (Fig 4-6 to 4-11, 4-13). (The data points in the crystalline zone are more scarce due to the larger electron beam size and consequently longer step lengths between data points.) This feature and the dendritic texture of the crystals suggest that the crystals are quenching crystals rather than precipitation during clinopyroxene dissolution.

The bent profiles very close to the interface are attributed to clinopyroxene overgrowth on the existing crystal surface during quench. The exact composition of the overgrowing clinopyroxene cannot be measured because the layer is too thin. MELTS program calculation with the interface melt composition inferred from the profile fittings (section 4.5.2) suggest that clinopyroxene is always a liquidus phase, enriched in diopside and clinoenstatie end-members. The calculation result is consistent with the depletions of SiO_2, MgO and CaO close to the interface. The bent profiles are not clearly resolved in all experiments, and are less significant compared to the feature in olivine dissolution experiments (Chen and Zhang, 2008). This may be because the composition difference between clinopyroxene and melt is smaller than between olivine and melt.

The bent profiles close to the interface are excluded for profile fitting, following the same procedure discussed in Chen and Zhang (2008). The cutting-off lengths varies from ~16 μm for ~1236 ºC experiments to ~50 μm for ~1517 ºC experiments. The apparent concentration maximum of the MgO profiles always lies within the excluded segment.

4.5.2. Effective Binary Diffusivity

Experimental durations are corrected for the effect of heating up and quenching following Zhang and Behrens (2000). The corrections are ~7-12 seconds for Exp#1-14, and 22 seconds for Exp#15 (Table 4-2).

SiO_2, TiO_2, Al_2O_3, MgO, CaO and Na_2O profiles are fit to obtain the effective binary diffusivities following Chen and Zhang (2008). The fitting figures are shown in Appendix E. The effective binary diffusivities are listed in Table 4-3. D_{CaO} is the highest and D_{SiO2} is the lowest. Using D_{Al2O3} as a reference and on an average sense, $D_{SiO_2} \approx 0.9D_{Al_2O_3}$, $D_{TiO_2} \approx 1.6D_{Al_2O_3}$, $D_{MgO} \approx 1.8D_{Al_2O_3}$, $D_{CaO} \approx 4.4D_{Al_2O_3}$, and $D_{Na_2O} \approx 2.4 D_{Al_2O_3}$. The fact that Na_2O diffusivity is smaller than CaO diffusivity may indicate complicated multicomponent effect in the effective binary diffusion of the components.

D_{MgO} and D_{CaO} as functions of temperature are shown in Fig. 4-14. The temperature dependence is well described by the Arrhenian relation. The pressure dependence is small and not resolved. D_{MgO} and D_{CaO} are modeled as:

$$\ln D_{MgO} = \ln D_0 - \frac{E}{RT} = -6.664 - \frac{28897}{T}, \quad (4\text{-}7a)$$

and

$$\ln D_{CaO} = \ln D_0 - \frac{E}{RT} = -10.517 - \frac{21205}{T}, \quad (4\text{-}7b)$$

where the diffusivities are in m^2/s and T is in K. The activation energy is 240±20 kJ/mol and 176±25 kJ/mol for MgO and CaO, respectively. Eqn. (4-7a) can reproduce D_{MgO} within 0.09 natural logarithm units. Eqn. (4-7b) can reproduce D_{CaO} within 0.17 natural logarithm units.

The above equations can be applied to MgO and CaO diffusion in similar melt composition and concentration gradient. Comparison with literature data shows that the effective binary diffusivities depend strongly on melt composition (Fig. 4-15). For example, D_{MgO} in a lunar basalt (Van Orman and Grove, 2000) is about 2 ln$D$ units above that in the basalt used in this study. Note that some data in Fig. 4-15 were obtained from diffusion couple experiments, not crystal dissolution experiments.

Table 4-3. Effective binary diffusivities with 2σ fitting errors (μm^2/s).

	SiO_2		TiO_2		Al_2O_3		MgO		CaO		Na_2O	
Exp#	*D*	2σ	*D*	2σ	*D*	2σ	*D*	2σ	*D*	2σ	*D*	2σ
1			8.1	1.6	3.8	0.3	8.9	0.7	29.7	1.6	9.9	2.1
5	5.4	0.9	16.1	1.4	10.0	0.4	24.0	1.4	52.9	3.0	28.9	2.9
6	46.4	7.1	49.2	2.5	45.1	1.0	72.3	2.0	134.1	4.2	94.7	5.4
7	6.6	1.1	17.2	1.2	10.4	0.6	18.6	1.5	56.2	4.0	34.4	3.2
8	24.7	3.1	30.7	1.9	19.3	0.6	35.0	1.0	81.5	3.3	55.8	3.7
11	29.3	10.6	92.0	15.8	35.5	2.4	59.2	4.3	84.4	6.2	67.9	10.1
12			17.1	5.8	16.1	1.5	28.2	2.5	69.4	6.0	37.7	9.6
14			6.4	3.0	4.3	0.8	6.3	1.2	20.2	2.8	6.0	4.0
15	50.4	5.8	62.2	10.8	71.6	2.0	111.9	3.0	197.4	9.6	123.6	9.1

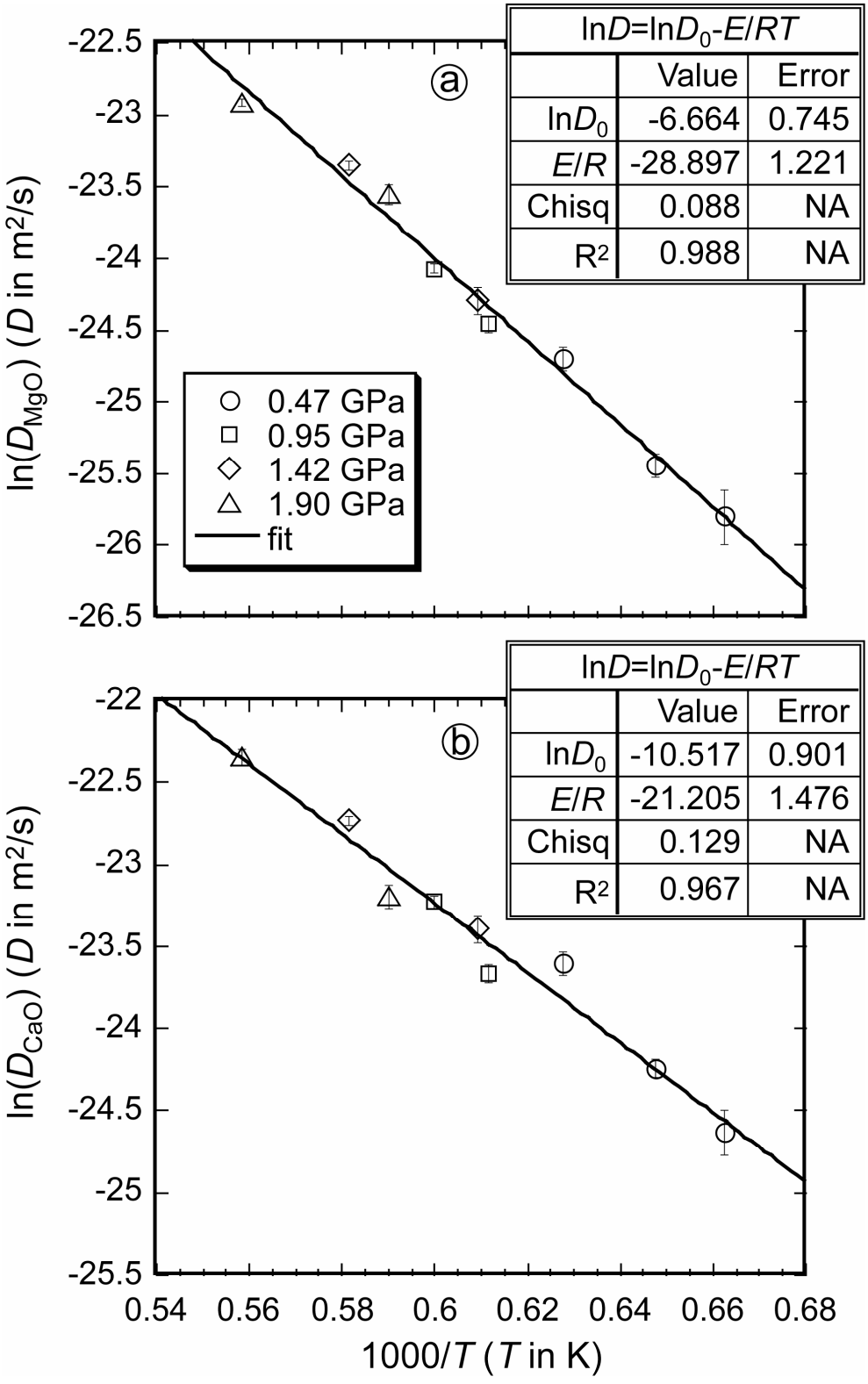

Figure 4-14. a: D_{MgO} vs. T. b: D_{CaO} vs. T. The 2σ error bars are fitting errors (not including experimental errors in temperature fluctuation, etc). In the legend of the equations, D and D_0 are in m^2/s, E/R is in $K/1000$.

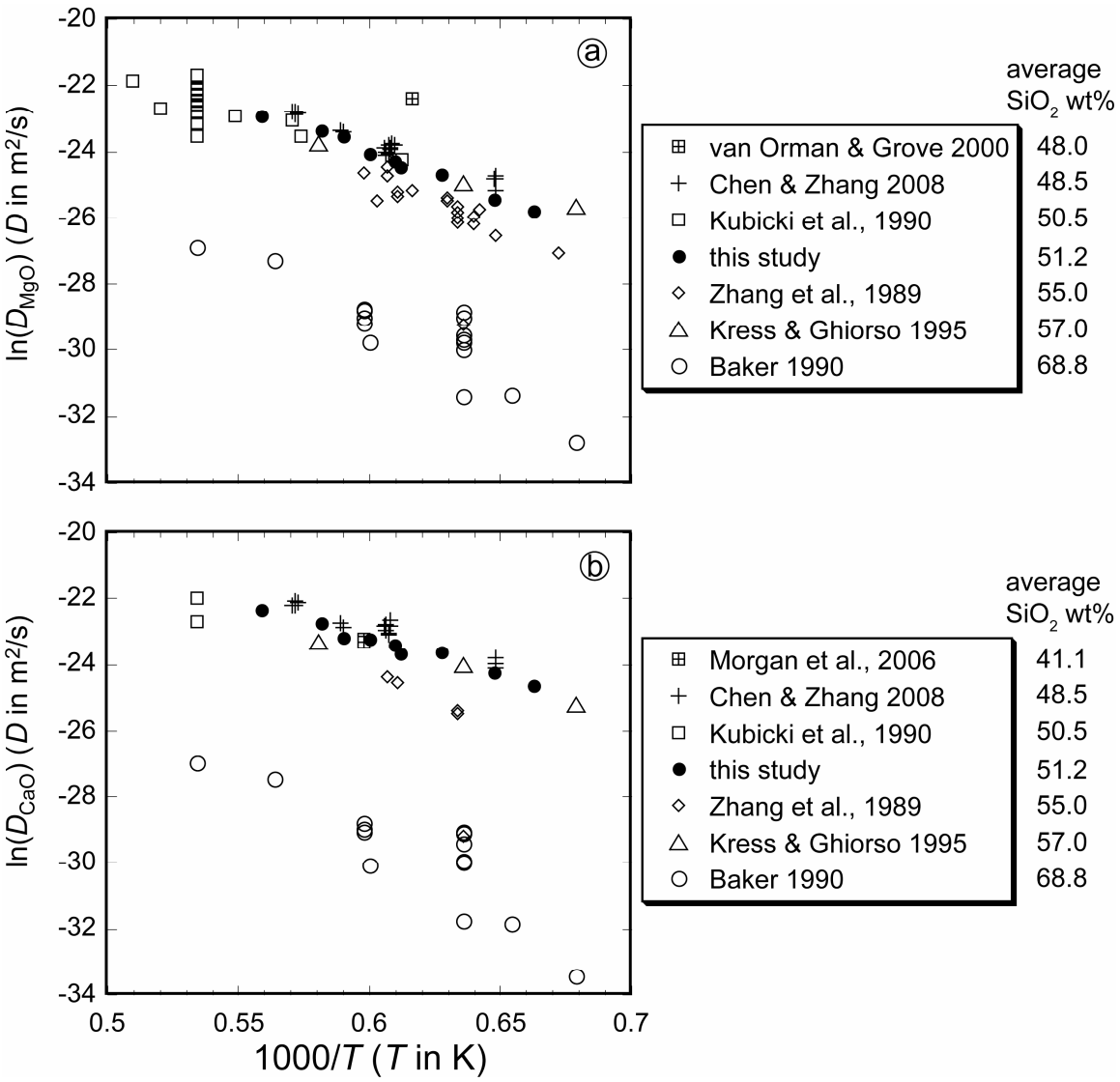

Figure 4-15. D_{MgO} and D_{CaO} in silicate melts. The average SiO_2 concentration of the silicate melts are listed. Data sources: Chen and Zhang (2008): olivine dissolution in a basaltic melt; van Orman and Grove (2000): 1350 °C, 1.3 GPa, diopside dissolution in basaltic melt; Kubicki et al. (1990): 1360~1600 °C, 1 bar~2 GPa, diffusion couple; Zhang et al. (1989): 1215~1400 °C, 0.5~2.15 GPa, olivine, diopside and quartz dissolution in andesitic melt. Note that quartz dissolution produces SiO_2-rich melt, such that the diffusivity falls in the data range of dacite and rhyolite by Baker (1990); Kress and Ghiorso (1995): 1200~1450 °C, 1 bar, diffusion couple; Baker (1990): 1200~1600 °C, 1 bar~1 GPa, diffusion couple; Morgan et al. (2006): 1400, 0.6 GPa, anorthosite dissolution in basaltic melt.

4.5.3. Interface and Far-field Melt Compositions

The interface and far-field melt compositions are listed in Tables 4-4 and 4-5. The concentrations of SiO_2, TiO_2, Al_2O_3, MgO, CaO and Na_2O are obtained by profile fitting except for Exp#14, of which SiO_2 profile was not treated. The others are approximately estimated from the profiles.

MELTS program calculation using the interface melt compositions yields liquidus temperatures within ~50 °C of the corresponding experimental temperatures, with clinopyroxene being the liquidus phase. This result shows that the interface melts is close to clinopyroxene saturation, which is expected as Kuo and Kirkpatrick (1985) showed that interface melt of clinopyroxene dissolution is fast.

As discussed in Zhang et al. (1989), the saturation conditions of dissolution experiments cannot be treated by crystal-melt equilibrium. First, the interface melt is not at exact saturation, but at near-saturation. This difference, however, may be insignificant considering errors in experiments and models. Second and more importantly, the interface melt may not be in near-equilibrium with the dissolving crystal if the crystal is a solid solution.

Table 4-4. Interface melt composition with 2σ fitting errors (wt%).

Exp#	SiO_2		TiO_2		Al_2O_3		FeO[b]	MgO		CaO		Na_2O	
1	51.21	0.31	1.37	0.02	9.57	0.10	11.6	9.40	0.05	13.12	0.02	2.14	0.03
5	52.73	0.33	1.07	0.03	7.10	0.14	10.5	10.92	0.08	14.64	0.06	1.85	0.03
6	52.81	0.23	0.69	0.02	5.08	0.08	8.5	13.13	0.06	17.40	0.06	1.40	0.03
7	53.05	0.26	0.62	0.03	3.71	0.26	8.7	13.84	0.21	17.58	0.14	1.39	0.05
8	53.78	0.33	0.52	0.04	3.40	0.22	8.5	13.98	0.12	17.66	0.11	1.25	0.05
11	51.54	0.30	1.42	0.02	10.10	0.10	10.7	9.31	0.06	13.68	0.06	2.06	0.03
12	50.95	0.25	1.36	0.05	10.86	0.14	11.2	8.78	0.07	12.84	0.05	2.23	0.04
14	50.50		1.66	0.02	12.50	0.09	12.0	7.64	0.04	11.71	0.02	2.54	0.03
15	53.51	0.34	0.68	0.12	5.31	0.17	8.5	12.87	0.09	17.77	0.15	1.28	0.07

a: MnO is ~0.2 wt%, K_2O and P_2O_5 are ~0.1 wt%.
b: FeO profiles are not fitted. The interface FeO concentrations are approximately estimated.

Table 4-5. Far-field melt composition with 2σ fitting errors (wt%).

Exp#	SiO_2		TiO_2		Al_2O_3		FeO[b]	MgO		CaO		Na_2O	
1	49.85	0.07	1.82	0.01	14.03	0.03	12.0	6.93	0.02	11.17	0.02	2.76	0.01
5	49.52	0.05	1.89	0.01	14.11	0.03	12.0	7.12	0.02	11.22	0.03	2.76	0.01
6	49.22	0.10	1.76	0.01	13.94	0.03	12.0	7.16	0.03	10.93	0.04	2.77	0.02
7	49.88	0.07	1.82	0.01	13.99	0.06	12.0	6.90	0.06	11.23	0.07	2.82	0.02
8	49.55	0.07	1.73	0.01	14.11	0.04	12.0	6.98	0.03	10.82	0.04	2.78	0.02
11	49.43	0.10	1.84	0.01	13.87	0.03	12.0	6.80	0.03	10.96	0.03	2.70	0.02
12	49.91	0.07	1.66	0.01	14.04	0.02	12.0	6.88	0.02	10.94	0.02	2.70	0.01
14	49.70		1.82	0.01	14.00	0.03	12.1	6.88	0.02	11.19	0.01	2.68	0.01
15	49.57	0.06	1.62	0.02	14.16	0.03	12.1	6.95	0.02	10.80	0.06	2.74	0.01

a: MnO is ~0.2 wt%, K_2O and P_2O_5 are ~0.1 wt%.
b: FeO profiles are not fitted. The interface FeO concentrations are approximately estimated.

The saturation of Mg- and Ca-rich clinopyroxene may be determined by three major components MgO, CaO and SiO_2. Putirka (1999) used two empirical expressions for diopside equilibrium, one involving $C_0^{MgO} \times C_0^{CaO} \times (C_0^{SiO_2})^2$, and the other one involving essentially $C_0^{CaO} \times (C_0^{SiO_2})^2$. These expressions and $C_0^{MgO} \times C_0^{CaO}$ were tried in modeling the interface melt composition. Available experimental data do not show consistent trends in $C_0^{CaO} \times (C_0^{SiO_2})^2$ versus T and P. At a given P, $C_0^{MgO} \times C_0^{CaO} \times (C_0^{SiO_2})^2$ versus $1/T$ show stronger curvature (i.e. stronger non-linear relation) than $C_0^{MgO} \times C_0^{CaO}$ versus $1/T$. Including SiO_2 in the saturation model hence does not improve the accuracy, but brings in more complexity. Therefore, the clinopyroxene saturation is treated as being determined by $C_0^{MgO} \times C_0^{CaO}$. Note that weight percent is used instead of mole fraction for simplicity. The role of SiO_2 is difficult to pin down based on the available data.

Fig. 4-16 shows the dependence of $C_0^{MgO} \times C_0^{CaO}$ on T and P. $C_0^{MgO} \times C_0^{CaO}$ increases with increasing temperature, and decreases with increasing pressure. $C_0^{MgO} \times C_0^{CaO}$ is modeled as:

$$\ln(C_0^{MgO} \times C_0^{CaO}) = 22.85(\pm 1.82) - 2.10(\pm 0.44)P - \frac{26360(\pm 2565)}{T} + 1.22(\pm 0.43) \times 10^6 \frac{P^2}{T^2}, \quad (4\text{-}8)$$

where C_0 is in wt%, P is in GPa, and T is in K. The multiple linear correlation coefficient r is 0.9907. Two data points from the literature are not used in the regression because they deviate from the trend constrained by the others. Eqn. (4-8) has second-order terms

of T and P and should not be extrapolated beyond the T and P range of the data (Fig. 4-16). Fig. 4-17 shows the prediction by this formula compared to the data. The 2σ errors in predicting C_0^{MgO} and C_0^{CaO} are 1.2 wt% and 1.5 wt%, respectively.

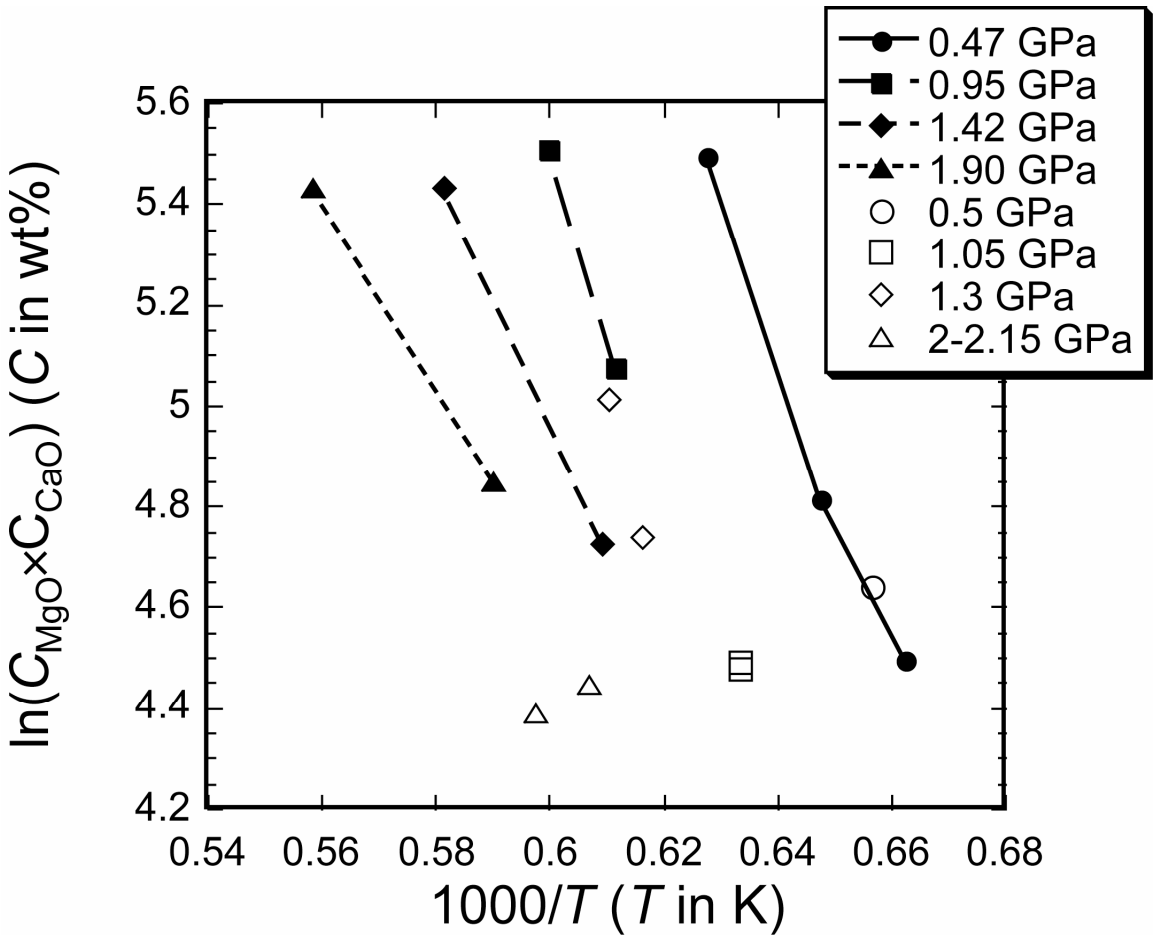

Figure 4-16. $C_0^{\mathrm{MgO}} \times C_0^{\mathrm{CaO}}$ at different P versus 1000/T. Solid symbols are data from this study. Hollow symbols are literature data, including: Scarfe et al. (1980), 1400 °C, 2 GPa, clinopyroxene dissolution in basalt; Brearley and Scarfe (1986), 1250 °C, 0.5 GPa, clinopyroxene dissolution in alkali basalt; Zhang et al. (1989), 1305-1375 °C, 1.05-2.15 GPa, diopside dissolution in andesite; van Orman and Grove (2000), 1350 °C, 1.3 GPa, diopside dissolution in basalt.

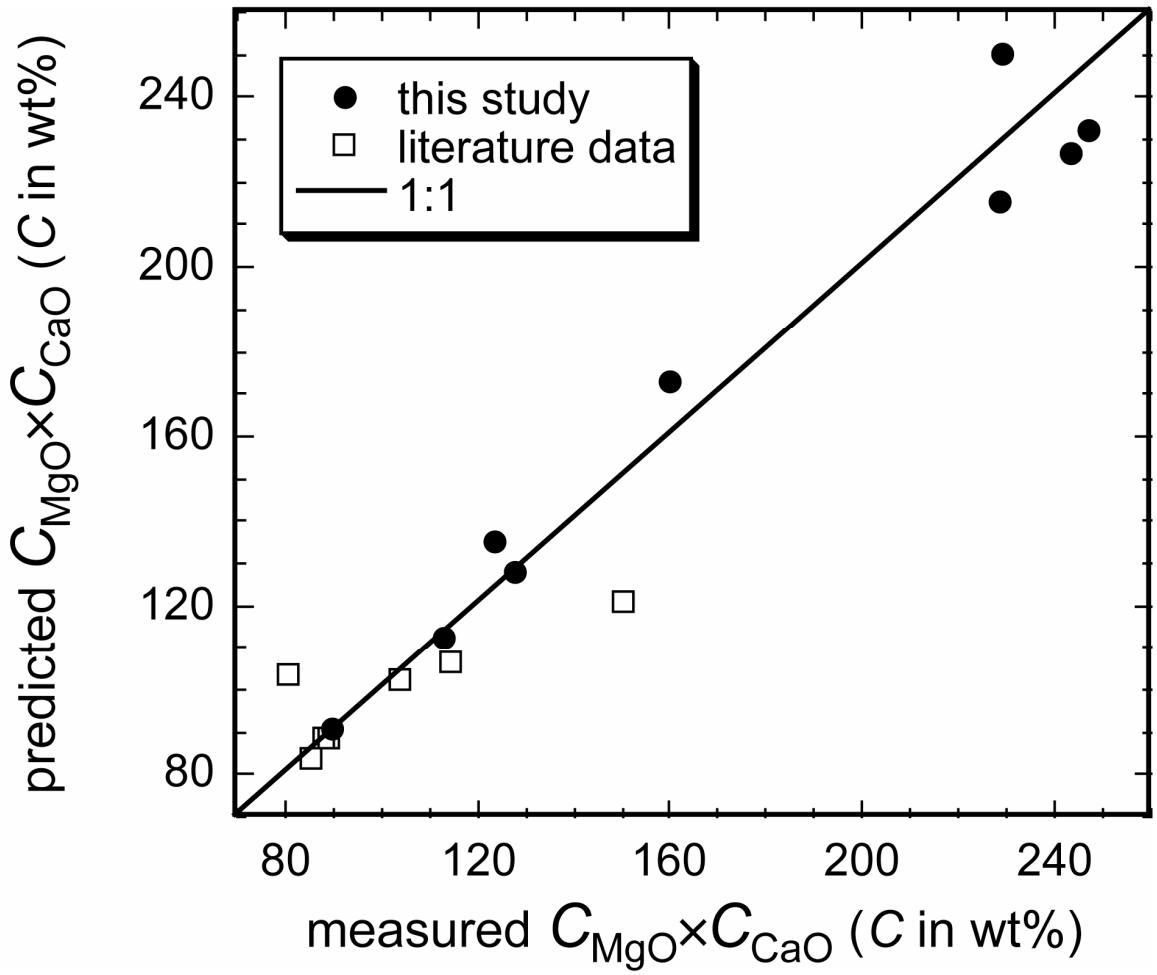

Figure 4-17. Comparison between the prediction by Eqn. 4-8 and the measured values. 1:1 line is shown as reference.

4.5.4. Diffusive Clinopyroxene Dissolution Distance

Diffisive clinopyroxene dissolution distance L can be calculated with Eqn. (4-1). Glass density (ρ_m) is taken as 2.77 g/cc (Tilley, 1922), and clinopyroxene density (ρ_c) is taken as 3.278 g/cc (Thompson et al., 2005). The calculation results are listed in Table 4-2 as L_4. Errors in L_4 are obtained by letting D and C_0 vary within their error bounds. The errors in melt and clinopyroxene densities and density variation along the compositional profiles are ignored. Hence, this error estimation is the lower limit. Because the fitting results are based on compositional profiles in the melt and do not incorporate the directly measured clinopyroxene dissolution distance, L_4 is independent of the direct measurements. The comparison provides crosscheck to our experiments. For all experiments except Exp#7, the dissolution distances calculated by different methods agree with each other. The L_4 for Exp#7 is much larger than L_2 and L_3. The cause for this disagreement is uncertain. One possibility is that the thickness the clinopyroxene disc used in Exp#7 was significantly uneven. The rim may be much thinner than the center. Using the rim as the reference position for the initial clinopyroxene-melt interface may under-estimate the dissolution distance, leading to smaller L_2 and L_3.

4.5.5. Convective Clinopyroxene Dissolution in Basaltic Melt

Following the treatment in Chen and Zhang (2008), the kinetic and dynamic aspect (characterized by the effective boundary layer thickness δ and the diffusivity D) and the thermodynamic aspect (characterized by β, Eqn. 4-2) of convective crystal dissolution are considered separately. The kinetic and dynamic aspects depend strongly on the absolute temperature of the system, but depend only weakly on pressure within the

low pressure range discussed in this study. They depend indirectly on the crystal and melt compositions, because the compositions affect the densities and melt viscosity. The modeled D/δ does not depend on the thermodynamic status of the system, and may be applied to both convective crystal dissolution and growth. The β term, however, depends on temperature and pressure in a relative sense (superheating). It depends directly on the crystal and melt compositions because the compositions control the thermodynamic status. Extrapolation to convective crystal growth requires additional considerations (e.g., the growing crystal composition responses to the melt composition).

To calculate $(D/\delta)_{MgO}$ and $(D/\delta)_{CaO}$, it is necessary to know D_{MgO}, D_{CaO}, melt density, clinopyroxene density and melt viscosity. The melt composition in our calculation is chosen to be the same as in our experiments. Melt density at 1 bar is calculated by the model of Lange and Carmichael (1987) and Ochs and Lange (1999). Melt density up to 2 GPa is calculated by combining the 1 bar density with the Birch-Murnaghan equation of state by Agee (1998) and Ohtani and Maeda (2001). The two Birch-Murnaghan models yield consistent results (<0.1% relative difference). Clinopyroxene density is calculated by the model of Thompson et al. (2006). Melt viscosity is calculated by the model of Hui and Zhang (2007). The clinopyroxene composition is considered in the density model. The melt compositional gradient from the interface melt to the far-field melt is not considered in calculating the melt density and viscosity. Based on these models and our experiment result, $(D/\delta)_{MgO}$ and $(D/\delta)_{CaO}$ are calculated for 1150 to 1450 °C, 1 bar to 2 GPa and clinopyroxene composition from Di80 to Di100 within diopside-hedenbergite binary system. For single clinopyroxene crystal with 1 mm radius, the Re and Pe numbers are 2×10^{-8} to 3×10^{-3}, and 2×10^{3} to

2×10^4, at 1150°C and 1450°C respectively. For a xenolith with 100 mm radius, the Re and Pe numbers are 3×10^{-2} to 3×10^2, and 2×10^9 to 2×10^9, at 1150°C and 1450°C respectively. $(D/\delta)_{MgO}$ and $(D/\delta)_{CaO}$ depend on the diffusivity and melt viscosity, both of which depend strongly on temperature. They depend weakly on melt and crystal densities, which in turn depend on temperature, pressure, melt and crystal compositions. They depend weakly on grain radius. When radius changes from 1 to 100 mm, $(D/\delta)_{MgO}$ and $(D/\delta)_{CaO}$ vary by ~10%. For convenience, the calculation result is re-cast to the following equations:

$$\ln(\frac{D}{\delta})_{MgO} = 6.64(\pm0.01) - \frac{34800(\pm14)}{T} - 0.0760(\pm0.0008)P \\ -0.299(\pm0.008)X_{Di}, \quad \text{(4-9a)}$$

and

$$\ln(\frac{D}{\delta})_{CaO} = 3.87(\pm0.01) - \frac{29340(\pm18)}{T} - 0.0741(\pm0.001)P \\ -0.292(\pm0.010)X_{Di}, \quad \text{(4-9b)}$$

where $(D/\delta)_{MgO}$ and $(D/\delta)_{CaO}$ are in m/s, T in K, P in GPa, and X_{Di} is the mole fraction of diopside in clinopyroxene within diopside-hedenbergite binary system (for pure diopside, $X_{Di} = 1$). Eqn. (4-9a) can reproduce the calculated $\ln(D/\delta)_{MgO}$ values with a 2σ error of 0.008. Eqn. (4-9b) can reproduce the calculated and $\ln(D/\delta)_{CaO}$ values with a 2σ error of 0.01.

Following the error estimation in Chen and Zhang (2008), for $(D/\delta)_{MgO}$ and $(D/\delta)_{CaO}$ in this study, the uncertainty mainly comes from the errors of: (1) 0.09 in $\ln D_{MgO}$ and 0.17 in $\ln D_{CaO}$; and (2) 1.4 in $\ln\eta$ (0.61 $\log\eta$ units in Hui and Zhang, 2007). The errors in melt and olivine densities and the error in the calculation scheme are much smaller than the above errors. To assess the uncertainty in $(D/\delta)_{MgO}$ and $(D/\delta)_{CaO}$, we

allowed D_{MgO}, D_{CaO} and η to vary in their corresponding error bounds. Fig. 18 shows $\ln(D/\delta)_{MgO}$ and $\ln(D/\delta)_{CaO}$ as a functions of temperature and the error bounds resulted from the uncertainties in D_{MgO}, D_{CaO} and η. $\ln(D/\delta)_{MgO}$ varies by ± 0.06 as $\ln(D_{MgO})$ varies by ± 0.09, and ∓ 0.45 as $\ln\eta$ varies by ± 1.4. $\ln(D/\delta)_{CaO}$ varies by ± 0.12 as $\ln(D_{MgO})$ varies by ± 0.17, and ∓ 0.43 as $\ln\eta$ varies by ± 1.4. Assuming the errors in D_{MgO}, D_{CaO} and η are not correlated, the overall uncertainty in $\ln(D/\delta)_{MgO}$ is roughly $\sqrt{0.06^2 + 0.45^2} \approx 0.45$ (a factor of 1.6 in $(D/\delta)_{MgO}$), and $\sqrt{0.12^2 + 0.43^2} \approx 0.45$ for $\ln(D/\delta)_{CaO}$.

D_{MgO}/δ for olivine dissolution in basaltic melt is compared in Fig. 4-18. It is only slightly greater than $(D/\delta)_{MgO}$ and slightly smaller than $(D/\delta)_{CaO}$ for clinopyroxene dissolution in basaltic melt. The small difference is mainly caused by the difference in D_{MgO} (Fig. 4-15). When the model error due to viscosity uncertainty is considered, D/δ for olivine and clinopyroxene dissolution are roughly within error. Further refinement of the viscosity of natural silicate melts can improve the accuracy of convective crystal dissolution models.

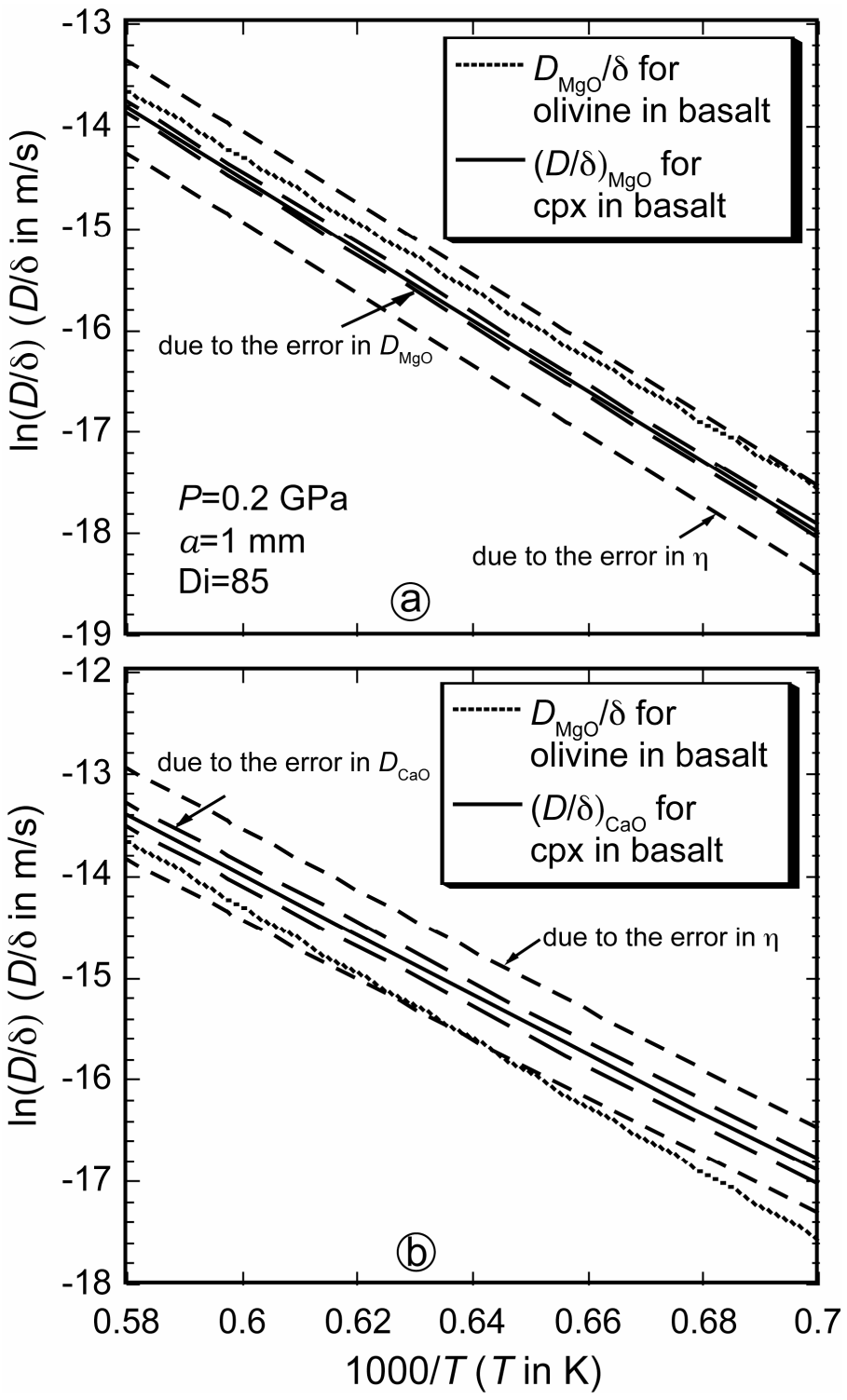

Figure 4-18. $(D/\delta)_{MgO}$ and $(D/\delta)_{CaO}$ for clinopyroxene dissolution in basalt versus temperature. Their error bounds and comparison to D_{MgO}/δ for olivine dissolution in basalt are shown.

The parameter β depends on the degree of under-saturation, which is modeled empirically as in Eqn. (4-8). Other saturation models can be implemented following the scheme in Section 4.2. The error in β comes mainly from that in predicting $C_0^{\mathrm{MgO}} \times C_0^{\mathrm{CaO}}$ (Eqn. 4-8). The relative error of β becomes unbounded as C_0 approaches C_∞ (the system approaches the liquidus temperature of the melt). This results in large relative error (but absolute error stays roughly the same) when we calculate the convective dissolution rate close to the liquidus temperature. An example of calculation is shown in Table 4-6. If the radius of the clinopyroxene crystal is 2 mm, it would take more than 2 days for the clinopyroxene crystal to completely dissolve at 1250°C and 0.5 GPa. Under similar conditions, an olivine crystal with a radius of 2 mm would survive 10 days (Chen and Zhang, 2008). The comparison is discussed in section 4.5.6.

Table 4-6. An example of modeled convective clinopyroxene dissolution rate.

Conditions: 1250 °C, 0.5 GPa, Di90											
	C_c	C_∞	C_0	ρ_m	ρ_c	η	β	D	δ	D/δ	u
	wt%	wt%	wt%	g/cc	g/cc	Pa·s		$\mu m^2/s$	μm	$\mu m/s$	$\mu m/s$
MgO	16.5	7.0	8.5	2.693	3.190	51.2	0.155	7.35	110	0.067	0.0103
CaO	25.5	11.0	12.1				0.068	24.3	160	0.15	

For dissolution in some time interval with temperature (and/or pressure) variation, finite time integration method can be applied to find the remaining size of the crystal. Fig. 4-19 shows the calculated survival time and falling distance of a sinking spherical clinopyroxene crystal in an infinite basalt reservoir at given temperature and 0.2 GPa. For 8 mm radius (maximum grain size in Figure 4-19), the corresponding Re and Pe numbers are 1×10^{-5} to 1, and 1×10^{6} to 9×10^{6}, at 1150°C and 1450°C respectively. The survival time for a clinopyroxene crystal (Di90) of 1 to 8 mm radius varies from about 0.5 to 30 days. The falling distance relative to the magma body varies from negligible up to about three hundred meters. For large clinopyroxene grains, the temperature and pressure may need to be considered as variables because the falling distance becomes very large. The result shown in Fig. 4-19 can be used to estimate the ascent rate of the hosting magma if the extent of dissolution (i.e., the initial grain radius) can be estimated. Suppose 1 mm radius clinopyroxene xenocrysts are observed in an erupted magma with eruption temperature of 1200°C. If the initial crystal radius was 4 mm, the dissolution time would be roughly 10 – 3 = 7 days. The falling distance would be less than 100 m. If the initial crystal radius was 2 mm, the dissolution time would be roughly 6 – 3 = 3 days. The falling distance in this case would be less than 10 m. If the dissolution occurred starting at 5 km depth, the ascent rate would be roughly 0.7-1.7 km/day.

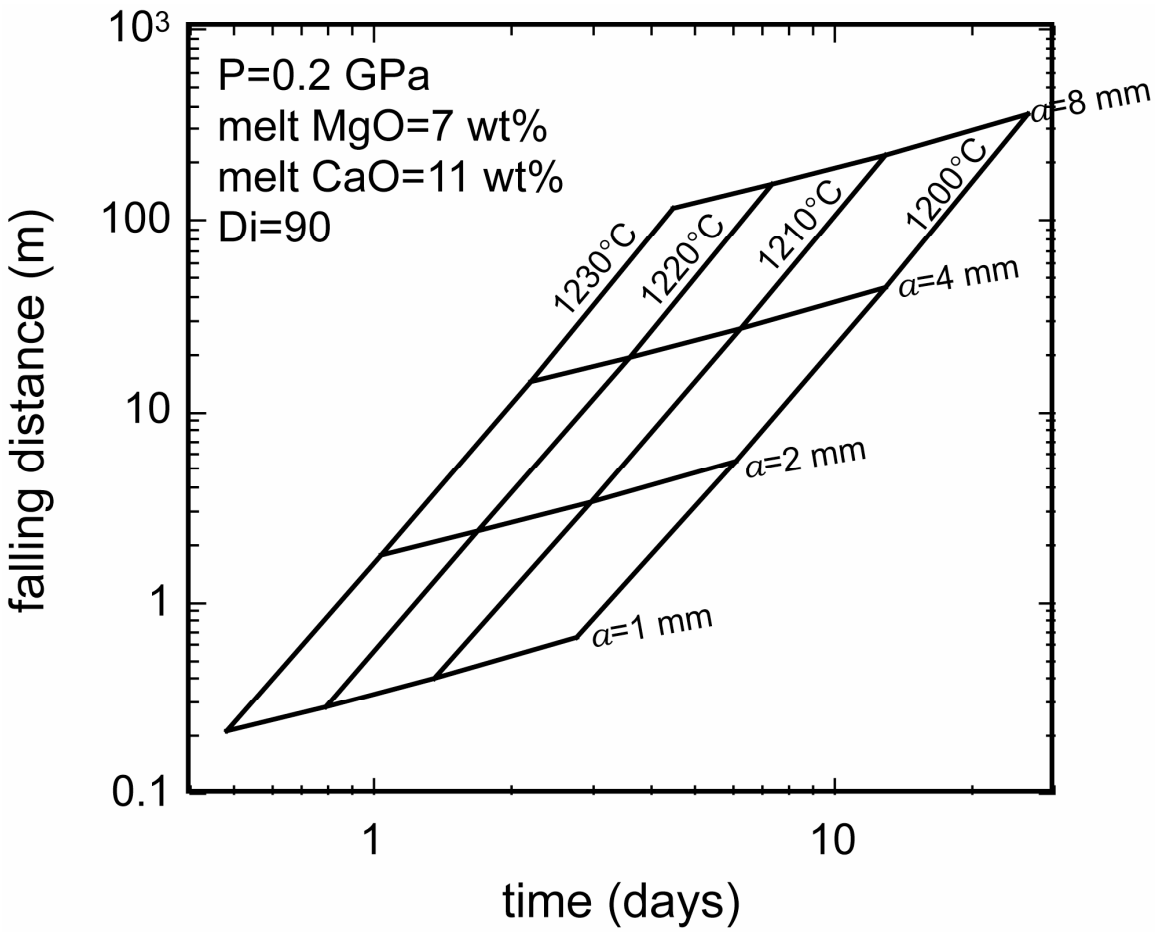

Figure 4-19. Survival time and falling distance for a single clinopyroxene grain falling in an infinite basaltic magma chamber. The liquidus temperature is about 1190 °C.

4.5.6. Convective Clinopyroxene Dissolution vs. Olivine Dissolution in Basaltic Melt

This section discusses the convective dissolution rates for olivine and clinopyroxene as separated xenocrysts. Fig. 4-20 compares the convective dissolution rates for 1 mm radius Fo90 olivine and Di90 clinopyroxene at 0.2 GPa in a basaltic melt. The liquidus *T* is ~1190 °C at 0.2 GPa. Both olivine and clinopyroxene are close to saturation at the liquidus *T*. As the degree of super heating increases, dissolution rate of clinopyroxene increases more rapidly than olivine (Fig. 4-20a). Comparison on the kinetic/dynamic and thermodynamic aspects separately (Figs. 4-20b and 4-20c) shows that the different behavior in response to super heating is due to the difference in thermodynamics of the two minerals, represented by the β terms. The difference in D/δ terms of the two minerals is roughly constant throughout the temperature range and is within the error bounds of the models.

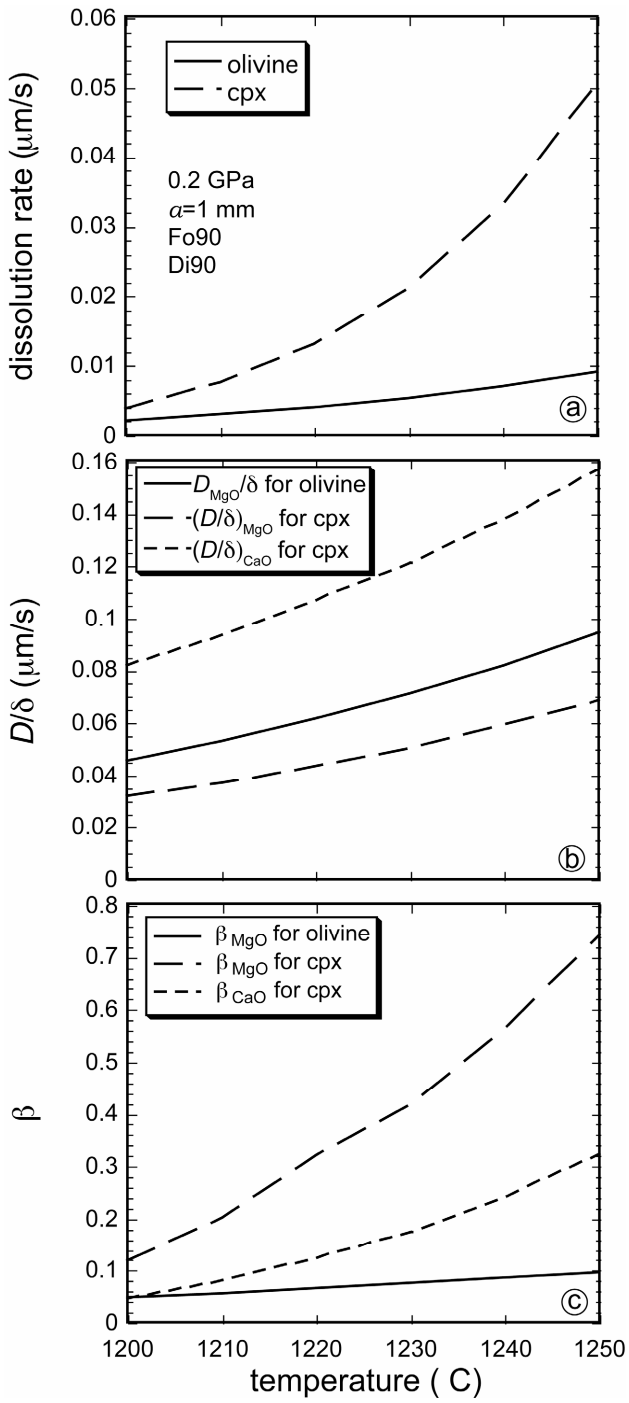

Figure 4-20. Convective dissolution rates of olivine and clinopyroxene. a: Comparison between the modeled convective dissolution rates of olivine and clinopyroxene in basalt. b: Comparison between the corresponding D/δ terms. c: Comparison between the corresponding β terms.

4.5.7. Convective Dissolution Rates for Olivine and Clinopyroxene in a Mantle Xenolith in Basaltic Melt

At a given T and P, olivine saturation in a basalt occurs at a single MgO concentration (Chen and Zhang, 2008), whereas diopside saturation occurs when $C_{\text{cpx}}^{\text{MgO}} \times C_{\text{cpx}}^{\text{CaO}}$ is a constant in our simplified approach. Hence, when CaO is plotted against MgO, olivine saturation curve is roughly a vertical line, and diopside saturation curve is a hyperbola. Fig. 4-21 shows a melt composition regime defined by MgO and CaO concentrations to examine the dissolution or growth regime of olivine and clinopyroxene. At 0.2 GPa and 1200 °C, the interface melt composition of olivine dissolution is determined as (Chen and Zhang 2008):

$$C_{0,\text{ol}}^{\text{MgO}} = \exp(7.82 + 2.66P - \frac{8040}{T} - \frac{4960P}{T}) = 9.216 \text{ wt\%}, \quad \text{(4-10a)}$$

which is shown in Fig. 4-21 as the vertical line AB.

The interface melt composition of clinopyroxene dissolution is constrained by (this study):

$$C_{0,\text{cpx}}^{\text{MgO}} \times C_{0,\text{cpx}}^{\text{CaO}} = \exp(22.85 - 2.10P - \frac{26360}{T} + 1.22 \times 10^6 \frac{P^2}{T^2}) = 95.474, \quad \text{(4-10b)}$$

which is shown in Fig. 4-21 as the curve CD.

Interface melt with the composition defined by point O, where AB and CD intersect, is multiply-saturated with olivine and clinopyroxene (i.e., the interface melts of olivine dissolution and clinopyroxene dissolution have the same composition as defined by O).

The following equation defines a family of linear equations relating $C_{\infty}^{\mathrm{MgO}}$ and $C_{\infty}^{\mathrm{CaO}}$:

$$(\frac{D}{\delta})_{\mathrm{MgO}} \frac{C_{0,\mathrm{cpx}}^{\mathrm{MgO}} - C_{\infty}^{\mathrm{MgO}}}{C_{\mathrm{cpx}}^{\mathrm{MgO}} - C_{0,\mathrm{cpx}}^{\mathrm{MgO}}} = (\frac{D}{\delta})_{\mathrm{CaO}} \frac{C_{0,\mathrm{cpx}}^{\mathrm{CaO}} - C_{\infty}^{\mathrm{CaO}}}{C_{\mathrm{cpx}}^{\mathrm{CaO}} - C_{0,\mathrm{cpx}}^{\mathrm{CaO}}}. \quad (4\text{-}11)$$

Three lines belong to this equation family are shown as dashed lines EF, P_1P_3 and P_4P_6 in Fig. 4-21. The significance of this linear equation family is: when the initial melt composition varies along a line defined by Eqn. 4-11, the interface melt composition for clinopyrxene dissolution does not change. For example, if the initial melt composition changes from P_1 to P_3, the interface melt composition is fixed at S_1^{cpx}. Among the linear equation family, a particular line EF intersects AB and CD at O. Melts with initial compositions falling on EF have the fixed interface melt that is multiply-saturated with olivine and clinopyroxene. Note that the line EF is *T* and *P* dependent, as well as the olivine and clinopyroxene saturation curves (AB and CD).

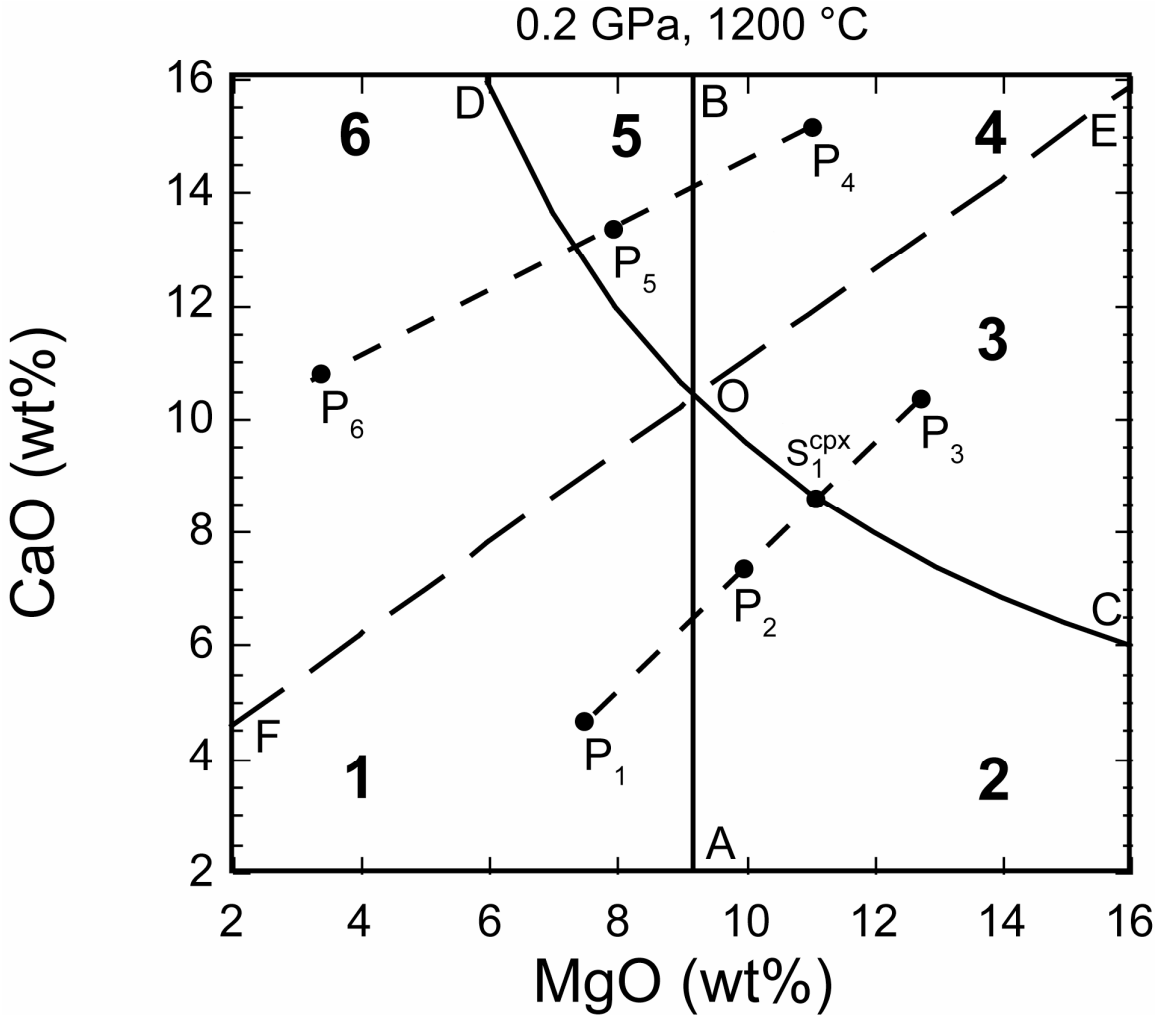

Figure 4-21. MgO-CaO composition regime and olivine and clinopyroxene behavior.

AB, CD and EF divide the MgO-CaO composition regime into six regions, numbered 1 to 6 in Fig. 4-21. Depending on the position of the melt in the MgO-CaO regime, the behavior of olivine and clinopyroxene in the melt is summarized in Table 4-7. For example, suppose the initial melt composition is 10 wt% MgO and 7 wt% CaO (P_2 in Fig. 4-21), the MgO concentration in the interface melt of olivine is ~9.2 wt% (independent of the initial melt composition). Because this interface melt has lower MgO than the initial melt, olivine is over-saturated. The interface melt of clinopyroxene is at S_1^{cpx} (~11 wt% MgO and 8.7 wt% CaO). Because this interface melt has higher $C_{0,\mathrm{cpx}}^{\mathrm{MgO}} \times C_{0,\mathrm{cpx}}^{\mathrm{CaO}}$ than the initial melt, clinopyroxene is under-saturated. Hence, olivine would grow and clinopyroxene dissolve.

The interface melt of clinopyroxene (11 wt% MgO) is olivine over-saturated. Hence, olivine would grow in the interface melt of clinopyroxene. The CaO concentration in the interface melt of olivine is not buffered by olivine dissolution. Assuming the CaO in the interface melt of olivine is not more than in the initial melt based on the profiles in Chen and Zhang (2008), $C_{0,\mathrm{ol}}^{\mathrm{MgO}} \times C_{0,\mathrm{ol}}^{\mathrm{CaO}} \le 9.2 \times 7 = 64.4$, which is lower than the clinopyroxene saturation curve. Hence, clinopyroxene would not grow in the interface melt of olivine.

MgO in the interface melt of clinopyroxene (11 wt%) is higher than that in the interface melt of olivine (9.2 wt%). Therefore, MgO would diffuse along the xenolith surface from clinopyroxene to olivine. Because of this diffusion flux, olivine dissolution rate would decrease (growth rate would increase) and clinopyroxene dissolution rate would increase compared to the dissolution rates of separated olivine and clinopyroxene xenocrysts. To predict dissolution rates under such situations would require new models.

When the initial melt composition falls on EF, the diffusion flux becomes zero and the dissolution rates equal those of separated xenocrysts and can be modeled as in Section 4.5.6.

Table 4-7. Behavior of olivine and clinopyroxene when coexisting in xenoliths.

Initial melt composition region	Initial and interface melt composition relations	Ol dissolve or grow?	Cpx dissolve or grow?	Cpx grow at the ol interface?[a]	Ol grow at the cpx interface?	Surface MgO diffusion direction
1 (P_1)	$C_\infty^{MgO} < C_{0,ol}^{MgO} < C_{0,cpx}^{MgO}$ $C_\infty^{CaO} < C_{0,cpx}^{CaO}$ $C_\infty^{MgO} \times C_\infty^{CaO} < C_{0,cpx}^{MgO} \times C_{0,cpx}^{CaO}$	dissolve	dissolve	no	yes	cpx→ol
AO	$C_\infty^{MgO} = C_{0,ol}^{MgO} < C_{0,cpx}^{MgO}$ $C_\infty^{CaO} < C_{0,cpx}^{CaO}$ $C_\infty^{MgO} \times C_\infty^{CaO} < C_{0,cpx}^{MgO} \times C_{0,cpx}^{CaO}$	at saturation	dissolve	no	yes	cpx→ol
2 (P_2)	$C_{0,ol}^{MgO} < C_\infty^{MgO} < C_{0,cpx}^{MgO}$ $C_\infty^{CaO} < C_{0,cpx}^{CaO}$ $C_\infty^{MgO} \times C_\infty^{CaO} < C_{0,cpx}^{MgO} \times C_{0,cpx}^{CaO}$	grow	dissolve	no	yes	cpx→ol
CO	$C_{0,ol}^{MgO} < C_\infty^{MgO} = C_{0,cpx}^{MgO}$ $C_\infty^{CaO} = C_{0,cpx}^{CaO}$ $C_\infty^{MgO} \times C_\infty^{CaO} = C_{0,cpx}^{MgO} \times C_{0,cpx}^{CaO}$	grow	at saturation	no	yes	cpx→ol
3 (P_3)	$C_{0,ol}^{MgO} < C_{0,cpx}^{MgO} < C_\infty^{MgO}$ $C_{0,cpx}^{CaO} < C_\infty^{CaO}$ $C_{0,cpx}^{MgO} \times C_{0,cpx}^{CaO} < C_\infty^{MgO} \times C_\infty^{CaO}$	grow	grow	uncertain	yes	cpx→ol
EO	$C_{0,ol}^{MgO} = C_{0,cpx}^{MgO} < C_\infty^{MgO}$ $C_{0,cpx}^{CaO} < C_\infty^{CaO}$ $C_{0,cpx}^{MgO} \times C_{0,cpx}^{CaO} < C_\infty^{MgO} \times C_\infty^{CaO}$	grow	grow	uncertain	yes	No flux
4 (P_4)	$C_{0,cpx}^{MgO} < C_{0,ol}^{MgO} < C_\infty^{MgO}$ $C_{0,cpx}^{CaO} < C_\infty^{CaO}$ $C_{0,cpx}^{MgO} \times C_{0,cpx}^{CaO} < C_\infty^{MgO} \times C_\infty^{CaO}$	grow	grow	uncertain	yes	ol→cpx
BO	$C_{0,cpx}^{MgO} < C_{0,ol}^{MgO} = C_\infty^{MgO}$ $C_{0,cpx}^{CaO} < C_\infty^{CaO}$ $C_{0,cpx}^{MgO} \times C_{0,cpx}^{CaO} < C_\infty^{MgO} \times C_\infty^{CaO}$	at saturation	grow	uncertain	no	ol→cpx
5 (P_5)	$C_{0,cpx}^{MgO} < C_\infty^{MgO} < C_{0,ol}^{MgO}$ $C_{0,cpx}^{CaO} < C_\infty^{CaO}$ $C_{0,cpx}^{MgO} \times C_{0,cpx}^{CaO} < C_\infty^{MgO} \times C_\infty^{CaO}$	dissolve	grow	uncertain	no	ol→cpx
DO	$C_{0,cpx}^{MgO} = C_\infty^{MgO} < C_{0,ol}^{MgO}$ $C_{0,cpx}^{CaO} = C_\infty^{CaO}$ $C_{0,cpx}^{MgO} \times C_{0,cpx}^{CaO} = C_\infty^{MgO} \times C_\infty^{CaO}$	dissolve	at saturation	uncertain	no	ol→cpx
6 (P_6)	$C_\infty^{MgO} < C_{0,ol}^{MgO} < C_{0,cpx}^{MgO}$ $C_\infty^{CaO} < C_{0,cpx}^{CaO}$ $C_\infty^{MgO} \times C_\infty^{CaO} < C_{0,cpx}^{MgO} \times C_{0,cpx}^{CaO}$	dissolve	dissolve	uncertain	no	ol→cpx
FO	$C_\infty^{MgO} < C_{0,cpx}^{MgO} = C_{0,ol}^{MgO}$	dissolve	dissolve	no	no	No flux

$C_{\infty}^{CaO} < C_{0,cpx}^{CaO}$
$C_{\infty}^{MgO} \times C_{\infty}^{CaO} < C_{0,cpx}^{MgO} \times C_{0,cpx}^{CaO}$

a: assuming $C_{0,ol}^{CaO} \leq C_{\infty}^{CaO}$

4.5.8. Applications

Given T, P and the initial melt composition, the behavior of xenoliths can be predicted from Fig. 4-21 and Table 4-7. Morgan and Liang (2005) conducted lherzolite reactive dissolution experiments in an alkali basalt and a basaltic andesite at 1 GPa and 1300 °C. They observed dissolution of olivine and clinopyroxene and precipitation of orthopyroxene in the basaltic andesite, and dissolution of clinopyroxene and orthopyroxene and precipitation of olivine in the alkali basalt. In Fig. 4-22, the dissolution of olivine and clinopyroxene in the basaltic andesite is predicted by this model. For the alkali basalt, olivine and clinopyroxene is predicted to dissolve, which does not agree with the experimental result by Morgan and Liang (2005). However, because the alkali basalt composition is close to the multiple-saturation of olivine and clinopyroxene, the prediction can be affected strongly by the errors in the olivine and clinopyroxene saturation models. For the clinopyroxene saturation model, the 2σ errors in predicting C_0^{MgO} and C_0^{CaO} are 1.2 wt% and 1.5 wt%, respectively (section 4.5.3). Hence, within uncertainty the prediction is consistent with the experimental data.

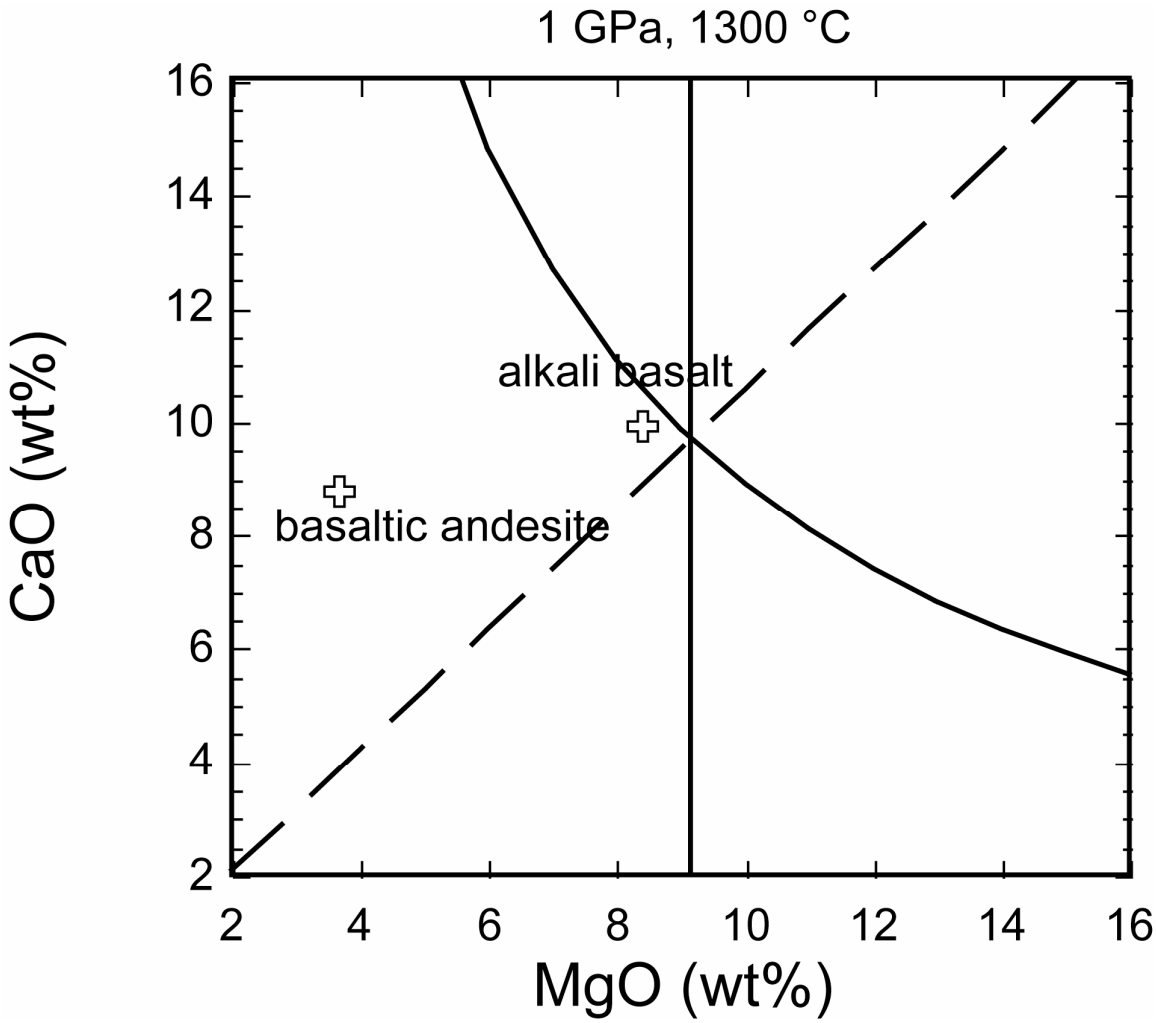

Figure 4-22. Application of the olivine and clinopyroxene dissolution models to the experiments by Morgan and Liang (2005).

Given initial melt composition and reactive textures between xenoliths and melt, constrains on the *P* and *T* conditions may be inferred from Fig. 4-21 and Table 4-7. An example is discussed below. The basalt at Kuandian contains abundant mantle xenolith, mainly spinel lherzolite (e.g. Chen et al. 2007). The basalt has 48.72 wt% SiO_2, 7.92 wt% MgO and 7.51 wt% CaO (Chen et al., 2007). As shown in Fig. 4-23a, olivine, clinopyroxene and orthopyroxene all have reaction textures along their rims in contact with the hosting basalt. Fig. 4-23b shows a closer view at the textures of the olivine and clinopyroxene rims. The reaction for orthopyroxene is not discussed in this study. The olivine has a homogeneous core and a Fe-rich rim. No embayment can be observed along the edge of the core. The composition of the rim changes gradually, with the inner part being less Fe-rich and the outer part being more Fe-rich. No distinct boundary can be observed between the core and the rim. These features suggest that olivine grew after being entrained. The basalt could not be olivine undersaturated because dissolution texture is not observed. The clinopyroxene also has a homogeneous core and a Fe-rich rim. The boundary between the core and the rim, however, is quite distinct. Embayment is frequently seen along the boundary. The rim contains pockets of glass and regions that have similar composition as the core. These features suggest that clinopyroxene was first dissolved after entrainment and then grew. The growth most likely occurred during cooling after eruption, because fast magma upwelling (otherwise mantle xenoliths would have been lost) leads to greater degree of under-saturation but not over-saturation. The regions within the rim that have similar composition as the core may be dissolution remnants. The boundary between the core and the rim is then interpreted as the dissolution front. Fig. 4-23c shows an estimation of the clinopyroxene dissolution

distance. The upper dashed line marks the dissolution front. The initial clinopyroxene boundary is estimated as the lower dashed line extending from the clinopyroxne-olivine boundary (the left most part). The dissolution distance is estimated as ~50 μm. Note that the estimated clinopyroxene boundary is not parallel to the current clinopyroxene boundary.

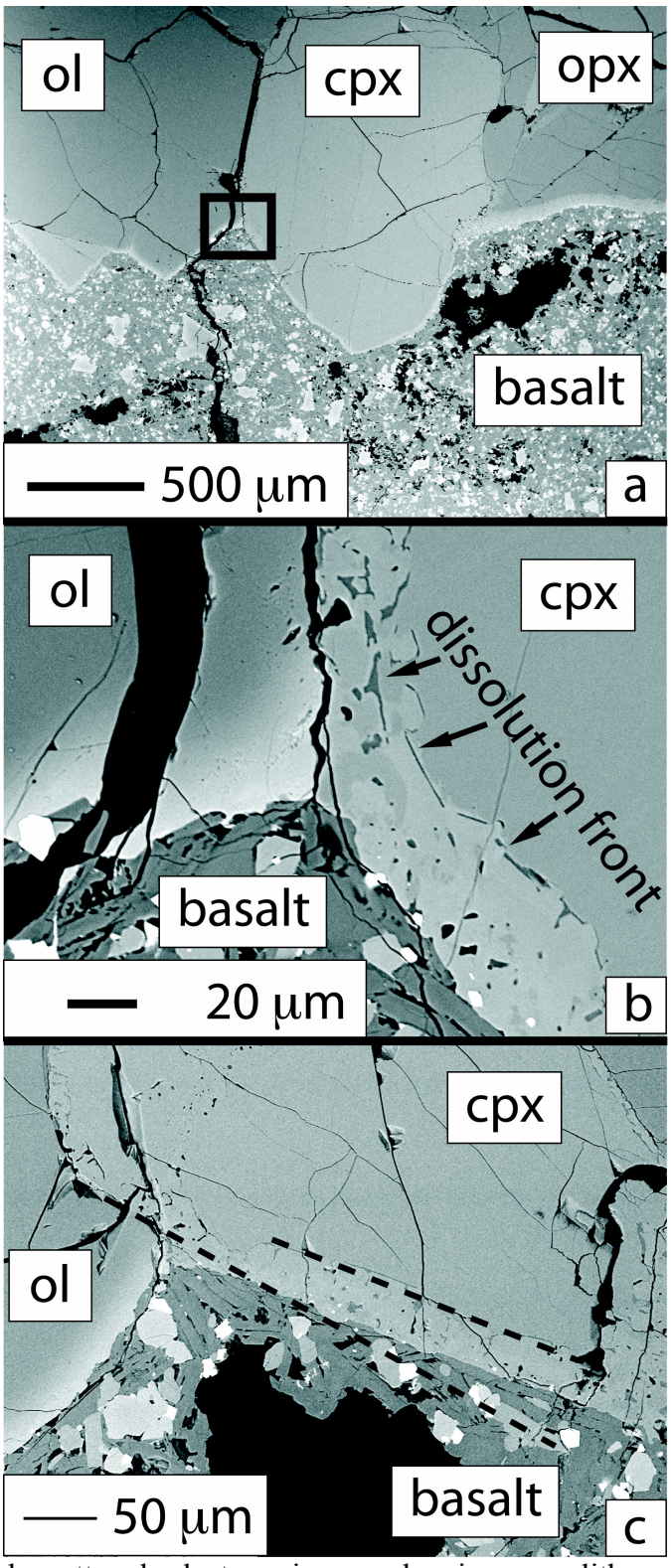

Figure 4-23. Back-scattered electron image showing xenolith reactive textures in Kuandian, Northeast China. a: olivine, clinopyroxene and orthopyroxene show reaction textures along the rims. b: a closer view of the boxed region in a. c: The clinopyroxene dissolution distance is estimated to be ~50 μm.

Because clinopyroxene dissolved and olivine grew after entrainment, the basalt composition must lie to the left of the clinopyroxene saturation curve, and to the right of the olivine saturation curve in the MgO-CaO composition regime (i.e., region 2 in Fig. 4-21).

As in Fig. 4-24a, if the dissolution started at 1.5 GPa, the temperature would be ~1310 °C. At these conditions, the dissolution rate of a single clinopyroxene xenocryst would be 0.0039 μm/s. The dissolution rate of a clinopyroxene crystal in a xenolith would be 0.002 μm/s because it only exposes one side to the melt. This clinopyroxene dissolution rate is a lower limit, because the mass flux along the xenolith surface goes from clinopyroxene to olivine. Furthermore, as the magma rises, the dissolution rate increases. Dissolving 50 μm would require less than ~7.1 hours. The ascent rate would be at least 1.5*30/7.1≅6.3 km/hour.

If the dissolution started at 1 GPa, the temperature would be ~1270 °C (Fig. 4-24b). The dissolution rate would be 0.0018 μm/s. Dissolving 50 μm would require less than ~7.5 hours. The ascent rate would be at least 1*30/7.5≅4.0 km/hour.

If the dissolution started at 0.5 GPa, the temperature would be ~1210 °C, as in Fig. 4-24c. The dissolution rate would be 0.00067 μm/s. Dissolving 50 μm would require less than ~20.6 hours. The ascent rate would be at least 0.5*30/20.6≅0.73 km/hour.

If the dissolution started at 0.2 GPa, the temperature would be ~1163 °C, as in Fig. 4-24d. The dissolution rate is 0.000061 μm/s. Dissolving 50 μm would require less than ~228 hours (9.5 days). The ascent rate would be at least 0.2*30/228≅26 m/hour.

In summary, the residence time varies from a few hours to a few days, and the ascent rate varies from 26 m/hour to ~6.3 km/hour. The residence time was very short,

and only small amount of clinopyroxene was digested. The composition of the hosting basalt could not have been changed significantly by the xenoliths.

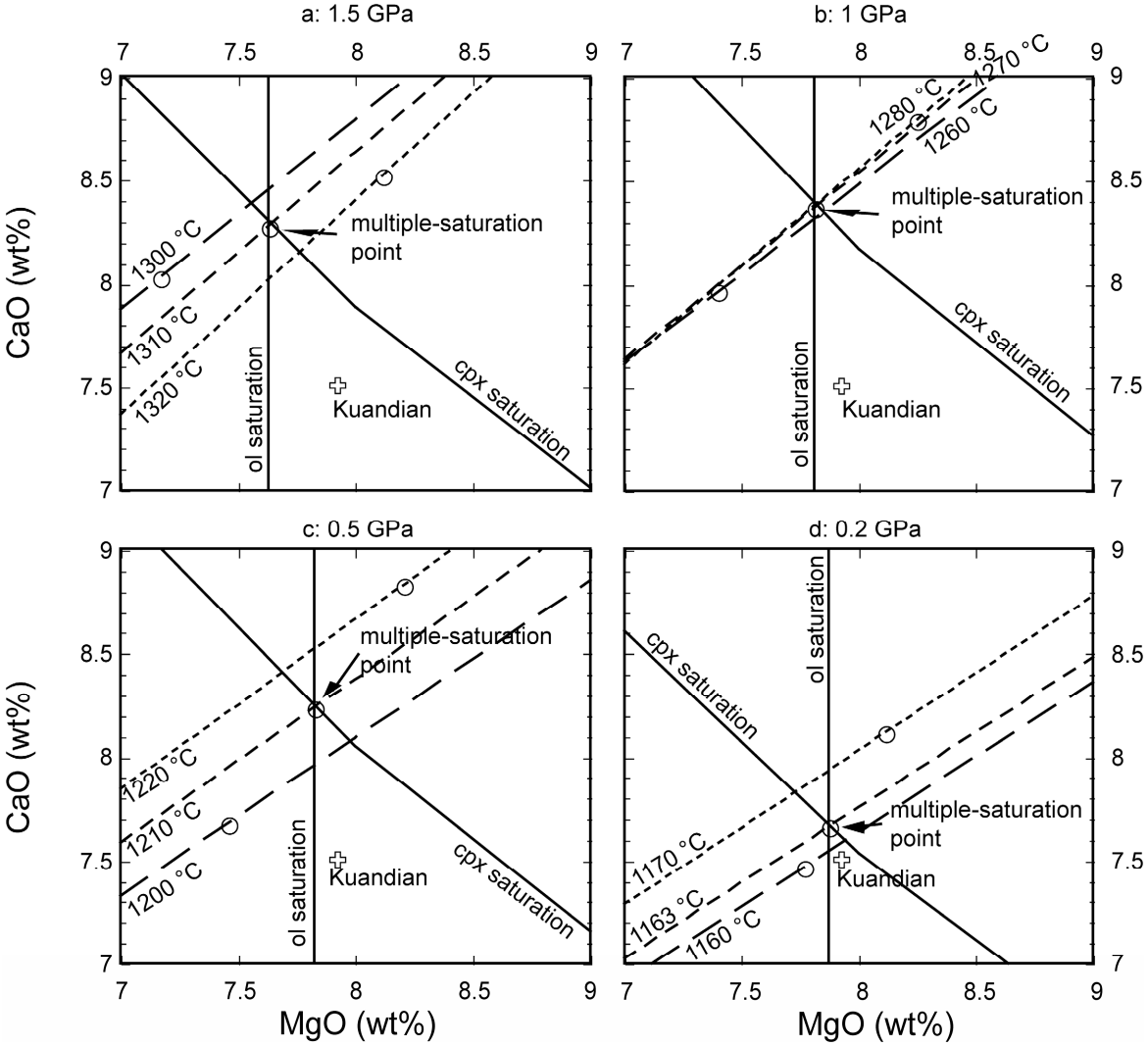

Figure 4-24. Application of the olivine and clinopyroxene dissolution models to the basalt at Kuandian, Northeast China (Chen et al., 2007).

4.6. Conclusions

The diffusivities, D_{MgO} and D_{CaO}, and the interface melt compositions, C_0^{MgO} and C_0^{CaO}, are extracted from the diffusion-controlled clinopyroxene dissolution experiments. D_{MgO} and D_{CaO} show Arrhenian dependence on temperature. The pressure dependence is small and not resolved within 0.47-1.90 GPa. The interface melt is roughly saturated with respect to clinopyroxene. Clinopyroxene saturation is treated as being determined by MgO and CaO. The parameter $C_0^{MgO} \times C_0^{CaO}$ is modeled as a function of temperature and pressure.

The $(D/\delta)_{MgO}$ and $(D/\delta)_{CaO}$ values for Di80-100 clinopyroxene are calculated within 1150-1450 °C and 1 bar-2 GPa and are given as functions of T, P, and X_{Di}. The uncertainty in both $(D/\delta)_{MgO}$ and $(D/\delta)_{CaO}$ is a factor of ~1.6, mainly due to the uncertainties in viscosity. The $(D/\delta)_{MgO}$ and $(D/\delta)_{CaO}$ for clinopyroxene dissolution in basalt is within calculation error to the D_{MgO}/δ for olivine dissolution in basalt (Chen and Zhang, 2008). With increasing degree of super heating, clinopyroxene dissolution rate increases more rapidly than olivine. The different response to superheating is mainly due to the difference in the thermodynamic aspect characterized by the β term.

The crystal dissolution models in this study and Chen and Zhang (2008) are applied to xenolith digestion in the basalts at Kuandian, Northeast China (Chen et al., 2007). Depending on the pressure at which the dissolution of clinopyroxene started, the eruption temperature is estimated to be between 1160 to 1310 °C. The residence time of the xenoliths is within a few hours to a few days. The ascent rate is within 26 m/hour to ~6.3 km/hour. The magma upwelling and eruption occurred very quickly. Only a small

amount of xenolith was digested and the composition of the hosting basalt was not significantly affected.

Acknowledgements

Y. Chen thanks Zhengjiu Xu, Hejiu Hui and Huaiwei Ni, for training and help on piston-cylinder experiment and FTIR measurement. This work is supported by NSF grants EAR-0537598 and EAR-0711050. Electron microprobe work is carried out on a Cameca SX100 instrument at Electron Microbeam Analysis Laboratory of the University of Michigan, which is supported by NSF grant 9911352.

References

Agee C.B. (1998) Crystal-liquid density inversions in terrestrial and lunar magmas. *Phys. Earth Planet. Interiors* **107**: 63-74.

Asimow P.D. and Ghiorso M.S. (1998) Algorithmic modifications extending MELTS to calculate subsolidus phase relations. *Am. Mineral.* **83**, 1127-1131.

Baker D.R. (1990) Chemical interdiffusion of dacite and rhyolite: anhydrous measurements at 1 atm and 10 kbar, application of transition state theory, and diffusion in zoned magma chambers. *Contrib. Mineral. Petrol.* **104**, 407-423.

Boyd, F.R., England, J.L. (1963) Effect of pressure on the melting of diopside, CaMgSi2O6, and albite, NaAlSi3O8, in the range up to 50 kilobars, *Journal of Geophysical Research* 68, 311-323.

Brearley M. and Scarfe C.M. (1986) Dissolution rates of upper mantle minerals in an alkali basalt melt at high pressure: an experimental study and implications for ultramafic xenolith survival. *J. Petrol.* **27**, 1157-1182.

Chen Y., Zhang Y. (2008) Olivine dissolution in basaltic melt. *Geochim. Cosmochim. Acta*. doi 10.1016/j.gca.2008.07.014.

Clift R., Grace J.R. and Weber M.E. (1978) *Bubbles, Drops, and Particles.* Academic Press, New York.

Gavrilenko, P., Keppler, H. (2007) Water solubility in clinopyroxene. *Geochimica et Cosmochimica Acta Suppl. S* 71, A312-A312.

Ghiorso M. S. and Sack R.O. (1995) Chemical mass transfer in magmatic processes. IV. A revised and internally consistent thermodynamic model for the interpolation

and extrapolation of liquid-solid equilibria in magmatic systems at elevated temperatures and pressures. *Contrib. Mineral. Petrol.* **119**, 197-212.

Hui H. and Zhang Y. (2007) Toward a general viscosity equation for natural anhydrous and hydrous silicate melts. *Geochim. Cosmochim. Acta* **71**, 403-416.

Kerr R.C. (1995) Convective crystal dissolution. *Contrib. Mineral. Petrol.* **121**, 237-246.

Putirka, K. (1999) Clinopyroxene + liquid equilibria to 100 kbar and 2450 K. *Contrib. Mineral. Petrol.* **135**, 151-163.

Kress V.C. and Ghiorso M.S. (1995) Multicomponent diffusion in basaltic melts. *Geochim. Cosmochim. Acta* **59**: 313-324.

Kubicki J.D., Muncill C.E. and Lasaga A.C. (1990) Chemical diffusion in melts on the $CaMgSi_2O_6$-$CaAl_2Si_2O_8$ join under high pressures. *Geochim. Cosmochim. Acta* **54**: 2709-2715.

Kuo L.-C. and Kirkpatrick R.J. (1985) Kinetics of crystal dissolution in the system diopside-forsterite-silica. *Am. J. Sci.* **285**: 51-90.

Lange R.A. and Carmichael I.S.E. (1987) Densities of Na_2O-K_2O-CaO-MgO-FeO-Fe_2O_3-TiO_2-SiO_2 liquids: new measurements and derived partial molar properties. *Geochim. Cosmochim. Acta* **51**, 2931-2946.

Martin D., Nokes R. (1988) Crystal settling in a vigorously convecting magma chamber. *Nature* **332**: 534-536.

Morgan Z., Liang Y. and Hess P. (2006) An experimental study of anorthosite dissolution in lunar picritic magmas: implications for crustal assimilation processes. *Geochim. Cosmochim. Acta* **70**, 3477-3491.

Ochs III F.A. and Lange R.A. (1999) The Density of Hydrous Magmatic Liquids. *Science* **283**, 1314-1317.

Ohtani E and Maeda M. (2001) Density of basaltic melt at high pressure and stability of the melt at the base of the lower mantle. *Earth Planet. Sci. Lett.* **193**, 69-75.

Scarfe C.M., Takahashi E., Yoder, H.S.Jr. (1980) Ultramafic nodules, kimberlite, and carbonatite. Carnegie Institution Year Book 79.

Thompson, R.M., Downs, R.T., Redhammer, G.J. (2005) Model pyroxenes III: Volume of *C*2/*c* pyroxene at mantle *P*, *T*, and *x*. *American Mineralogist* 90, 1840-1851.

Tilley C.E. (1922) Density, refractivity, and composition relations of some natural glasses. *Mineral. Mag.* **19**, 275-294.

Turcotte D.L. and Schubert G. (1982) *Geodynamics: Applications of Continuum Physics to Geological Problems.* Wiley & Sons, New York, NY. pp. 450.

Van Orman, J.A., Grove, T.L. (2000) Origin of lunar high-titanium ultramafic glasses: Constratins from phase relations and dissolution kinetics of clinopyroxene-ilmenite cumulates. *Meteoritics & Planetary Science* 35, 783-794.

Williams, D.W., Kennedy, G.C. (1969) Melting cruve of diopside to 50 kilobars, *Journal of Geophysical Research* 74, 4359-4365.

Zhang Y. (2005) Fate of rising CO_2 droplets in seawater. *Environmental Science & Technology* **39**, 7719-7724.

Zhang Y. (2008) *Geochemical Kinetics.* Princeton University Press. Princeton, NJ.

Zhang Y. and Xu Z. (2003) Kinetics of convective crystal dissolution and melting, with applications to methane hydrate dissolution and dissociation in seawater. *Earth Planet. Sci. Lett.* **213**, 133-148.

Zhang Y. and Xu Z. (2008) "Fizzics" of bubble growth in beer and champagne. *Elements* **4**, 47-49.

Zhang Y., Walker D. and Lesher C.E. (1989) Diffusive crystal dissolution. *Contrib. Mineral. Petrol.* **102**, 495-513.

Appendices

Appendix A
Major and Trace Elements Data of Northeast China Cenozoic Basalt

Table 1a. Comparison with standards

Standard	BCR-2					K1919	
	USGS recommended value	StDev (1s)	Kelley et al., 2003	MSU 2005 Average	WSU 2005	Kelley et al., 2003	MSU 2004
XRF							
SiO2 (%)	54.1	0.8		54.13	54.235	50.00	49.48
TiO2	2.26	0.05	2.25	2.25	2.262	2.70	2.75
Al2O3	13.5	0.2		13.34	13.444	13.85	13.79
Fe2O3t	15.3	0.2		15.31	14.705	12.28	12.11
MnO	0.2	0.01		0.20	0.201	0.17	0.17
MgO	3.59	0.05		3.64	3.623	7.01	6.90
CaO	7.12	0.11		7.05	7.224	11.36	11.37
Na2O	3.16	0.11		2.87	3.181	2.36	2.08
K2O	1.79	0.05		1.77	1.792	0.54	0.51
P2O5	0.35	0.02		0.36	0.353	0.28	0.27
Sr (ppm)	346	14	347	317	332.8	398	387
Zr	188	16	206	188	179.8	186	169
Sc	33	2	34.3		33.4		
V	416	14	407		410.7		
Ga	23	2	149		22.0		
Cu	19	2	28.2		18.2		
Zn	127	9	34.7		128.8		
ICP-MS							
Cs (ppm)	1.1	0.1	1.18		1.13		
V	416	14	407	363		304	303
Y	37	2	38.0	37.8	37.52	26.9	26.6
Nb			13.6	11.8	12.16	20.054	18.3
Ba	683	28	674	658	678	135	133
La	25	1	25.7	25.4	25.75	15.056	15.0
Ce	53	2	54.0	49.0	50.87	38.528	36.8
Pr	6.8	0.3	7.02	6.76	6.24	5.583	5.27
Nd	28	2	29.7	29.2	27.26	25.115	24.8
Sm	6.7	0.3	6.75	6.57	6.93	6.195	5.85
Eu	2.0	0.1	2.07	1.94	2.10	2.074	1.96
Gd	6.8	0.3	7.36	6.70	7.06	6.408	5.84
Tb	1.07	0.04	1.13	1.06	1.17	1.004	0.90
Dy			6.79	6.40	7.01	5.483	5.11
Ho	1.33	0.06	1.38	1.31	1.45	1.018	0.92
Er			3.75	3.70	3.76	2.568	2.43
Tm					0.54		
Hf	4.8	0.2	5.27	5.12	4.86	4.772	4.54
Ta			0.864	0.80	0.81	1.4	1.23
Th	6.2	0.7	6.23	6.38	6.11	1.234	1.32

Table 1a. Continued

Standard	BHVO-2				
	USGS recommended value	StDev (1s)	Kelley et al., 2003	MSU 2005 Average	WSU 2005
XRF					
SiO2 (%)	49.9	0.6		49.53	49.782
TiO2	2.73	0.04	2.60	2.70	2.727
Al2O3	13.5	0.2		13.35	13.432
Fe2O3t	13.7	0.2		13.62	13.500
MnO	0.17	0.01		0.17	0.172
MgO	7.23	0.12		7.30	7.233
CaO	11.4	0.2		11.35	11.488
Na2O	2.22	0.08		1.92	2.230
K2O	0.52	0.01		0.50	0.517
P2O5	0.27	0.02		0.27	0.267
Sr (ppm)	389	23	388	367	386.5
Zr	172	11	180	172	165.8
Sc	32	1	30.8		32.9
V	317	11	299		313.1
Ga	21.7	0.9	96.1		18.7
Cu	127	7	131		129.3
Zn	103	6	20.6		99.3
ICP-MS					
Cs (ppm)			0.0965		0.10
V	317	11	299	272	
Y	26	2	26.2	25.8	26.84
Nb	18	2	19.2	16.9	17.69
Ba	130	13	129	129	125
La	15	1	15.0	15.0	15.20
Ce	38	2	36.8	34.8	34.77
Pr			5.29	5.30	4.72
Nd	25.0	1.8	24.2	24.7	22.36
Sm	6.2	0.4	5.92	6.03	6.22
Eu			1.94	2.05	2.18
Gd	6.3	0.2	6.32	5.76	6.46
Tb	0.9		0.950	0.90	1.00
Dy			5.34	5.19	5.64
Ho	1.04	0.04	0.984	0.96	1.07
Er			2.46	2.52	2.54
Tm					0.34
Hf	4.1	0.3	4.45	4.55	4.34
Ta	1.4		1.19	1.11	1.21
Th	1.2	0.3	1.19	1.29	1.24

Table 1b. XRF and ICP-MS analytical results

Volcanic field	Wudalianchi	Wudalianchi	Wudalianchi	Wudalianchi	Wudalianchi
Latitude	48.71627	48.71532	48.73665	48.73665	48.68289
Longitude	126.11974	126.12732	126.15907	126.15907	126.08392
Batch	MSU 05	MSU 05	MSU 05	WSU 05	MSU 05
Sample #	WDLC-LHS-1a	WDLC-LHS-2a	WDLC-HSS-1a	WDLC-HSS-1a	WDLC-BJS-1a
Rock type	Mugearite	Phonotephrite	Phonotephrite	Phonotephrite	Mugearite
XRF					
SiO_2 (%)	51.98	48.47	49.49	49.719	51.75
TiO_2	2.36	2.26	2.16	2.184	2.19
Al_2O_3	13.36	12.58	13.01	13.217	13.40
Fe_2O_3t	8.58	9.75	9.31	9.354	8.77
MnO	0.11	0.14	0.13	0.135	0.12
MgO	7.01	8.19	7.82	7.736	7.34
CaO	5.99	7.84	7.48	7.626	6.63
Na_2O	3.40	3.89	3.59	3.907	3.40
K_2O	5.23	4.60	4.33	4.351	4.42
P_2O_5	1.04	1.20	0.99	0.962	0.83
Total	99.06	98.92	98.31	99.192	98.85
LOI	0.50	0.61	1.26	-0.149	0.77
Sr (ppm)	1383	1579	1380	1486	1182
Zr	405	376	340	327	336
Sc				15.5	
V				138.9	
Ga				21.0	
Cu				32.4	
Zn				117.5	
ICP-MS					
Cs (ppm)				0.74	
V	112	125	128		118
Y	21.2	27.2	24.7	24.50	21.1
Nb	55.5	68.0	57.2	57.46	50.0
Ba	1742	1728	1595	1633	1447
La	79.7	100.6	84.8	88.87	64.8
Ce	143.0	179.0	148.5	157.02	116.7
Pr	17.33	21.51	17.89	16.84	14.30
Nd	64.6	82.4	69.5	65.79	54.7
Sm	10.85	13.82	12.07	12.29	9.44
Eu	3.15	3.84	3.42	3.57	2.69
Gd	9.66	11.80	10.58	9.37	8.53
Tb	1.19	1.47	1.29	1.19	1.08
Dy	4.78	6.10	5.46	5.70	4.62
Ho	0.78	1.00	0.89	0.95	0.77
Er	1.83	2.34	2.12	2.05	1.87
Tm				0.24	
Hf	10.20	9.51	8.60	8.00	8.42
Ta	2.88	3.43	2.90	3.08	2.62
Th	6.50	9.47	7.72	7.46	6.48

Table 1b. Continued

Volcanic field	Wudalianchi	Wudalianchi	Wudalianchi	Wudalianchi	Erkeshan
Latitude	48.73554	48.70907	48.60746	48.66236	48.05589
Longitude	126.00124	126.0461	125.84136	126.26816	126.25974
Batch	MSU 05	MSU 05	MSU 05	MSU 05	MSU 05
Sample #	WDLC-NGL-1a	WDLC-LHS-3a	WDLC-DJS-1a	WDLC-JDB-1a	Ek-1a
Rock type	Shoshonite	Latite	Latite	Mugearite	Shoshonite
XRF					
SiO2 (%)	52.61	53.18	51.78	51.83	50.92
TiO2	2.31	2.36	2.29	2.22	2.52
Al2O3	13.76	13.74	13.67	13.50	13.23
Fe2O3t	8.36	8.09	8.05	8.54	8.53
MnO	0.11	0.11	0.11	0.11	0.11
MgO	6.55	5.88	5.91	6.85	7.01
CaO	5.87	5.19	6.18	5.99	5.79
Na2O	3.14	3.51	2.90	3.35	3.12
K2O	5.14	5.61	5.97	4.66	5.42
P2O5	0.89	1.01	0.90	1.02	1.13
Total	98.74	98.68	97.76	98.07	97.78
LOI	0.87	0.89	1.78	1.52	1.74
Sr (ppm)	1170	1317	1499	1479	1459
Zr	396	534	328	289	486
Sc					
V					
Ga					
Cu					
Zn					
ICP-MS					
Cs (ppm)					
V	117	101	130	114	112
Y	20.0	23.1	18.2	19.9	23.2
Nb	52.5	64.0	51.9	61.7	62.7
Ba	1591	1564	1899	1656	1918
La	66.5	84.8	68.4	74.4	92.6
Ce	120.7	153.4	124.6	133.8	165.3
Pr	14.90	18.24	15.15	16.15	19.85
Nd	57.3	68.0	58.5	61.8	73.6
Sm	10.02	11.35	9.65	10.67	11.97
Eu	2.75	3.18	2.72	3.01	3.30
Gd	8.68	10.20	8.31	9.28	10.63
Tb	1.09	1.26	1.00	1.14	1.29
Dy	4.46	5.21	4.09	4.57	5.12
Ho	0.73	0.85	0.68	0.74	0.85
Er	1.71	2.03	1.64	1.69	2.01
Tm					
Hf	10.15	12.90	8.66	7.31	11.72
Ta	2.83	3.44	2.82	3.12	3.22
Th	6.41	7.57	5.66	6.77	7.13

Table 1b. Continued

Volcanic field	Erkeshan	Jixi	Jixi	Mudanjiang	Mudanjiang
Latitude	48.05589	45.13873	45.14826	44.15004	44.15004
Longitude	126.25974	131.13792	130.90132	129.62636	129.62636
Batch	WSU 05	MSU 05	MSU 05	MSU 05	WSU 05
Sample #	Ek-1a	JX-1a	JX-3a	MDJ-1a	MDJ-1a
Rock type	Phonotephrite	Basalt	Alkali basalt	Alkali basalt	Alkali basalt
XRF					
SiO2 (%)	51.101	50.72	46.09	45.79	46.092
TiO2	2.517	1.49	2.69	2.11	2.141
Al2O3	13.354	15.95	13.71	14.25	14.330
Fe2O3t	8.56	11.32	12.61	12.24	12.240
MnO	0.114	0.14	0.17	0.18	0.183
MgO	6.901	6.88	8.84	8.86	8.789
CaO	5.922	7.93	8.45	8.63	8.754
Na2O	3.403	3.38	2.88	2.71	2.996
K2O	5.436	1.30	1.85	1.60	1.611
P2O5	1.104	0.30	0.59	0.62	0.605
Total	98.414	99.41	97.88	96.99	97.743
LOI		0.47	1.96	2.84	1.999
Sr (ppm)	1549	405	603	649	684
Zr	451	111	238	211	208
Sc	13.0				22.3
V	119.6				202.3
Ga	21.2				20.0
Cu	28.7				53.7
Zn	105.9				112.3
ICP-MS					
Cs (ppm)	0.75				0.60
V		146	189	177	
Y	22.40	21.0	29.6	24.5	25.50
Nb	61.60	20.8	42.5	37.1	37.97
Ba	1952	202	233	331	334
La	94.51	13.9	29.7	30.8	31.54
Ce	168.30	26.0	57.6	60.7	61.57
Pr	17.92	3.70	7.67	8.20	7.37
Nd	68.07	16.2	33.4	34.7	32.16
Sm	12.16	4.08	7.51	7.27	7.68
Eu	3.46	1.46	2.48	2.33	2.48
Gd	8.72	4.26	7.26	6.88	7.07
Tb	1.10	0.68	1.09	0.99	1.04
Dy	5.21	3.93	5.81	5.13	5.54
Ho	0.85	0.74	1.04	0.91	1.01
Er	1.88	1.95	2.70	2.34	2.37
Tm	0.23				0.31
Hf	11.02	2.97	6.04	5.18	4.89
Ta	3.43	1.27	2.70	2.28	2.34
Th	6.65	1.95	3.97	3.85	3.48

Table 1b. Continued

Volcanic field	Mudanjiang	Mudanjiang	Mudanjiang	Mudanjiang	Mudanjiang
Latitude	44.32746	44.34162	44.49536	44.50758	44.50758
Longitude	129.69847	129.5578	129.9227	129.92406	129.92406
Batch	MSU 05	MSU 05	MSU 05	MSU 05	MSU 05
Sample #	MDJ-2a	MDJ-3a	MDJ-4a	MDJ-5a	MDJ-6a
Rock type	Hawaiite	Basanite	Alkali basalt	Basanite	Basanite
XRF					
SiO2 (%)	47.54	44.64	46.06	45.88	44.40
TiO2	1.64	2.37	2.32	2.36	2.40
Al2O3	14.92	13.84	15.08	14.87	14.09
Fe2O3t	11.62	12.07	12.09	12.83	12.94
MnO	0.17	0.17	0.17	0.17	0.18
MgO	8.45	8.75	8.05	8.49	9.28
CaO	8.51	7.37	8.23	7.55	9.13
Na2O	3.90	4.63	3.08	4.05	3.22
K2O	2.19	3.09	1.57	2.45	1.97
P2O5	0.64	1.07	0.59	0.61	0.75
Total	99.58	98.00	97.24	99.26	98.36
LOI	0.19	1.72	2.59	0.55	1.41
Sr (ppm)	689	1168	652	712	773
Zr	203	371	237	244	226
Sc					
V					
Ga					
Cu					
Zn					
ICP-MS					
Cs (ppm)					
V	136	133	152	151	178
Y	23.0	24.0	23.8	21.5	25.9
Nb	61.1	67.7	43.8	49.2	54.6
Ba	638	409	325	352	467
La	44.0	61.6	28.2	32.4	37.1
Ce	74.7	117.2	56.2	62.6	70.9
Pr	8.86	14.87	7.62	8.09	9.20
Nd	34.5	59.0	32.3	33.8	37.9
Sm	6.71	11.46	6.99	7.22	7.77
Eu	2.24	3.50	2.31	2.40	2.53
Gd	6.83	10.00	6.77	6.88	7.57
Tb	0.95	1.32	0.98	0.96	1.07
Dy	4.62	5.85	5.05	4.71	5.46
Ho	0.82	0.90	0.89	0.80	0.95
Er	2.18	2.01	2.18	1.99	2.40
Tm					
Hf	4.81	8.61	5.73	5.93	5.44
Ta	3.55	4.31	2.84	3.18	3.40
Th	8.24	6.81	3.74	4.28	4.73

Table 1b. Continued

Volcanic field	Mudanjiang	Mudanjiang	Jingbohu	Jingbohu	Jingbohu
Latitude	44.57371	44.48109	44.17995	44.17995	44.17995
Longitude	129.53992	129.74329	128.53813	128.53813	128.53813
Batch	MSU 05	MSU 05	MSU 03-04	MSU 03-04	MSU 03-04
Sample #	MDJ-HH-1a	MDJ-7a	JBH-BH-1a	JBH-BH-1g	JBH-BH-1u
Rock type	Basaltic andesite	Basalt	Basanite	Basanite	Basanite
XRF					
SiO2 (%)	54.26	49.42	44.22	44.15	44.29
TiO2	1.78	1.95	1.80	1.79	1.79
Al2O3	15.15	14.01	14.44	14.40	14.37
Fe2O3t	10.41	13.36	11.01	10.98	11.06
MnO	0.13	0.16	0.17	0.17	0.17
MgO	5.13	8.20	9.18	9.08	9.14
CaO	7.29	8.35	8.36	8.33	8.38
Na2O	3.11	2.74	4.72	4.82	4.87
K2O	1.36	1.03	2.81	2.99	2.73
P2O5	0.35	0.30	1.05	1.06	1.06
Total	98.97	99.52	97.76	97.77	97.86
LOI	0.87	0.35			
Sr (ppm)	580	366	978	1024	1002
Zr	128	139	282	280	278
Sc					
V					
Ga					
Cu					
Zn					
ICP-MS					
Cs (ppm)					
V	133	174	145	142	145
Y	17.5	22.3	25.9	25.4	25.8
Nb	16.0	16.2	89.2	86.7	86.7
Ba	537	210	584	646	620
La	16.1	14.1	62.8	68.0	65.8
Ce	33.3	28.7	117.6	117.8	111.5
Pr	4.81	4.26	12.47	13.69	13.20
Nd	22.6	19.5	48.7	51.9	50.7
Sm	5.68	4.81	8.73	8.65	8.78
Eu	1.93	1.63	2.83	2.82	2.73
Gd	5.16	4.84	7.53	8.70	8.72
Tb	0.75	0.75	1.00	1.04	1.04
Dy	3.95	4.41	4.97	5.10	5.27
Ho	0.66	0.82	0.87	0.84	0.86
Er	1.60	2.21	2.03	2.02	2.04
Tm					
Hf	3.52	3.63	5.71	5.69	5.89
Ta	0.96	1.04	4.97	4.50	4.69
Th	2.05	1.72	8.49	9.35	9.39

Table 1b. Continued

Volcanic field	Jingbohu	Jingbohu	Jingbohu	Jingbohu	Jingbohu
Latitude	44.18895	44.19588	44.19588	44.19588	44.0603
Longitude	128.52737	128.52737	128.52737	128.52737	129.01248
Batch	MSU 03-04	MSU 03-04	MSU 03-04	MSU 03-04	MSU 05
Sample #	JBH-BH-1af	JBH-3a	JBH-3c	JBH-3d	JBH-1a
Rock type	Basanite	Basanite	Basanite	Basanite	Hawaiite
XRF					
SiO2 (%)	44.53	44.60	44.05	44.12	46.96
TiO2	1.77	1.80	1.79	1.79	1.53
Al2O3	14.36	14.65	14.42	14.48	14.36
Fe2O3t	11.06	11.07	10.94	11.00	11.57
MnO	0.17	0.17	0.17	0.17	0.17
MgO	9.34	8.89	9.15	9.13	9.18
CaO	8.29	8.35	8.32	8.29	8.63
Na2O	4.65	4.72	4.70	4.76	3.75
K2O	3.20	3.09	2.98	2.87	2.00
P2O5	1.04	1.06	1.06	1.06	0.57
Total	98.41	98.40	97.58	97.67	98.72
LOI					1.06
Sr (ppm)	1000	1019	1012	996	671
Zr	280	287	274	282	183
Sc					
V					
Ga					
Cu					
Zn					
ICP-MS					
Cs (ppm)					
V	140	143	144	138	143
Y	26.0	26.7	24.9	26.5	21.0
Nb	88.5	89.8	87.1	88.7	55.4
Ba	580	583	632	582	572
La	62.2	62.7	65.7	63.8	39.1
Ce	113.1	115.7	112.4	118.9	68.1
Pr	12.00	12.70	13.14	12.72	8.02
Nd	47.6	50.3	49.8	50.0	30.8
Sm	8.43	8.81	8.45	8.79	6.08
Eu	2.68	2.79	2.70	2.80	2.02
Gd	7.54	7.84	8.25	7.94	6.07
Tb	1.05	1.06	1.04	1.05	0.84
Dy	5.05	5.30	5.02	5.06	4.17
Ho	0.88	0.91	0.84	0.89	0.76
Er	2.10	2.20	2.08	2.16	1.96
Tm					
Hf	5.74	5.79	5.60	5.71	4.20
Ta	5.05	5.20	4.47	5.02	2.99
Th	8.74	8.98	9.46	8.77	6.84

Table 1b. Continued

Volcanic field	Jingbohu	Jingbohu	Jingbohu	Jingbohu	Jingbohu
Latitude	44.06722	44.1785	44.1785	44.1785	44.1785
Longitude	128.96124	128.58844	128.58844	128.58844	128.58844
Batch	MSU 05	MSU 05	WSU 05	MSU 05	MSU 05
Sample #	JBH-2a	JBH-3a	JBH-3a	JBH-4a	JBH-5a
Rock type	Hawaiite	Hawaiite	Hawaiite	Hawaiite	Basanite
XRF					
SiO2 (%)	47.69	47.20	47.560	47.60	45.21
TiO2	1.66	1.56	1.576	1.61	1.80
Al2O3	14.88	14.33	14.464	14.65	14.79
Fe2O3t	11.47	11.56	11.496	11.53	11.33
MnO	0.17	0.17	0.173	0.17	0.17
MgO	8.07	9.45	9.431	8.52	8.86
CaO	8.50	8.27	8.399	8.36	8.43
Na2O	4.07	3.64	3.917	3.86	4.38
K2O	2.22	1.95	1.961	2.04	3.14
P2O5	0.64	0.57	0.557	0.58	0.97
Total	99.37	98.70	99.533	98.92	99.08
LOI	0.42	1.09	-0.373	0.87	0.68
Sr (ppm)	644	607	647	609	920
Zr	197	179	174	187	252
Sc			20.7		
V			155.9		
Ga			16.6		
Cu			38.6		
Zn			104.5		
ICP-MS					
Cs (ppm)			0.40		
V	136	134		139	134
Y	23.0	21.4	21.77	22.2	25.9
Nb	59.4	50.7	52.81	54.2	74.1
Ba	628	552	554	576	638
La	41.9	36.3	37.22	38.1	56.6
Ce	71.5	63.0	63.03	65.9	95.4
Pr	8.40	7.49	6.70	7.78	11.25
Nd	33.0	29.1	27.03	30.3	43.6
Sm	6.47	5.87	6.15	6.03	8.12
Eu	2.16	2.00	2.09	2.04	2.57
Gd	6.44	6.02	5.69	6.05	8.04
Tb	0.91	0.83	0.84	0.85	1.09
Dy	4.56	4.20	4.59	4.39	5.31
Ho	0.83	0.75	0.83	0.79	0.92
Er	2.13	1.99	2.01	2.02	2.32
Tm			0.26		
Hf	4.55	4.14	4.02	4.32	5.53
Ta	3.23	2.82	3.08	2.94	4.03
Th	7.41	6.26	6.16	6.63	8.39

Table 1b. Continued

Volcanic field	Jingbohu	Jingbohu	Jingbohu	Jingbohu	Jingbohu
Latitude	44.17481	44.12774	44.08514	44.27037	44.21961
Longitude	28.51468	128.6254	128.6768	128.73703	128.76419
Batch	MSU 05	MSU 05	MSU 05	MSU 05	MSU 05
Sample #	JBH-6a	JBH-7a	JBH-8a	JBH-HMT-1a	JBH-HMT-2a
Rock type	Basanite	Hawaiite	Hawaiite	Phonotephrite	Phonotephrite
XRF					
SiO2 (%)	44.39	46.24	47.34	46.61	47.53
TiO2	1.78	2.77	1.62	1.93	1.87
Al2O3	14.48	14.50	14.58	17.09	16.87
Fe2O3t	11.08	12.43	11.65	11.18	10.82
MnO	0.17	0.17	0.17	0.15	0.15
MgO	8.89	7.89	8.65	4.32	4.42
CaO	8.30	8.56	8.32	5.68	5.69
Na2O	4.81	3.04	3.85	6.23	5.96
K2O	3.31	2.01	2.07	4.54	4.66
P2O5	0.98	0.75	0.57	1.10	1.07
Total	98.19	98.36	98.82	98.83	99.04
LOI	1.54	1.41	0.97	0.92	0.72
Sr (ppm)	960	952	614	1008	972
Zr	264	254	184	395	384
Sc					
V					
Ga					
Cu					
Zn					
ICP-MS					
Cs (ppm)					
V	135	195	136	81	83
Y	25.5	26.3	22.4	20.6	21.0
Nb	78.1	38.2	54.0	103.8	98.7
Ba	671	433	562	630	641
La	60.0	31.4	36.8	61.2	60.8
Ce	103.6	64.5	63.3	107.5	105.9
Pr	12.20	8.85	7.60	13.00	12.85
Nd	47.2	38.6	30.1	50.2	49.7
Sm	8.70	8.25	6.01	9.23	9.02
Eu	2.74	2.57	2.00	2.87	2.80
Gd	8.47	7.51	6.05	8.60	8.61
Tb	1.14	1.04	0.85	1.13	1.11
Dy	5.26	5.41	4.50	4.82	4.85
Ho	0.92	0.95	0.80	0.75	0.76
Er	2.24	2.38	2.09	1.65	1.75
Tm					
Hf	5.91	6.03	4.37	8.88	8.87
Ta	4.41	2.28	3.01	6.42	6.15
Th	8.47	3.32	6.60	11.61	11.79

Table 1b. Continued

Volcanic field	Jingbohu	Jingbohu	Tianchi, Changbaishan	Tianchi, Changbaishan	Tianchi, Changbaishan
Latitude	44.26098	43.96297	42.02558	42.02558	42.02558
Longitude	128.70238	129.35881	128.06656	128.06656	128.06656
Batch	MSU 05	MSU 05	MSU 03-04	MSU 03-04	MSU 03-04
Sample #	JBH-HMT-3a	JBH-10a	CB-1a	CB-1c	CB-1d
Rock type	Phonotephrite	Basanite	Peralkaline rhyolite	Trachyte	Peralkaline trachyte
XRF					
SiO2 (%)	46.76	44.08	67.89	64.23	64.51
TiO2	1.89	1.79	0.32	0.52	0.47
Al2O3	16.93	14.49	11.88	16.20	15.74
Fe2O3t	10.88	11.33	5.33	4.94	4.94
MnO	0.15	0.18	0.12	0.12	0.12
MgO	4.13	10.21	0.00	0.23	0.19
CaO	5.57	9.32	0.45	1.38	1.25
Na2O	6.07	3.35	5.63	5.54	5.63
K2O	4.74	2.61	4.70	5.93	5.76
P2O5	1.09	0.65	0.01	0.09	0.08
Total	98.21	98.01	96.33	99.18	98.69
LOI	1.54	1.79			
Sr (ppm)	1021	678	4	41	31
Zr	394	187	2164	528	654
Sc					
V					
Ga					
Cu					
Zn					
ICP-MS					
Cs (ppm)					
V	78	169	3	4	3
Y	20.7	24.3	119.5	36.6	44.1
Nb	102.3	56.7	270.9	81.2	99.9
Ba	649	587	11	154	90
La	63.0	38.5	179.9	66.4	79.8
Ce	110.6	68.1	367.8	145.0	172.3
Pr	13.36	8.23	37.34	14.59	17.27
Nd	51.4	32.4	141.0	54.3	63.9
Sm	9.38	6.46	26.02	10.02	11.58
Eu	2.89	2.10	0.49	0.90	0.65
Gd	8.80	6.38	24.75	8.84	10.28
Tb	1.14	0.92	3.87	1.30	1.53
Dy	5.11	4.86	22.04	6.72	7.84
Ho	0.81	0.89	4.23	1.23	1.51
Er	1.77	2.35	10.85	3.13	3.84
Tm					
Hf	9.31	4.41	48.81	10.85	13.87
Ta	6.41	3.25	16.12	4.16	5.21
Th	11.90	6.02	40.53	10.55	13.64

Table 1b. Continued

Volcanic field	Tianchi, Changbaishan	Tianchi, Changbaishan	Tianchi, Changbaishan	Tianchi, Changbaishan	Tianchi, Changbaishan
Latitude	42.20831	42.33306	42.05951	42.05573	42.4081
Longitude	128.19586	128.14288	128.25932	128.24887	128.11256
Batch	MSU 05	MSU 05	MSU 05	MSU 05	MSU 05
Sample #	CBS-1b	CBS-6a	CBS-10a	CBS-15a	CBS-19a
Rock type	Hawaiite	Mugearite	Hawaiite	Basaltic andesite	Basalt
XRF					
SiO2 (%)	47.54	49.13	50.46	52.30	48.27
TiO2	2.43	3.38	2.90	1.84	2.42
Al2O3	15.17	15.32	17.16	15.84	14.91
Fe2O3t	11.52	11.73	9.91	10.76	12.60
MnO	0.16	0.15	0.12	0.13	0.17
MgO	8.03	3.97	4.68	6.64	7.22
CaO	7.40	7.48	8.31	8.58	9.29
Na2O	4.37	3.64	3.41	2.94	2.82
K2O	1.37	2.57	1.95	0.53	1.57
P2O5	0.69	0.92	0.60	0.21	0.49
Total	98.68	98.29	99.50	99.77	99.76
LOI	1.05	1.49	0.29	0.11	0.03
Sr (ppm)	1059	690	823	464	616
Zr	337	221	287	102	143
Sc					
V					
Ga					
Cu					
Zn					
ICP-MS					
Cs (ppm)					
V	151	200	211	80	173
Y	27.7	19.2	39.3	13.6	22.9
Nb	50.0	28.3	54.5	18.9	11.5
Ba	520	474	898	362	241
La	43.7	22.2	58.9	20.0	10.1
Ce	81.3	42.8	108.8	33.9	20.5
Pr	10.07	5.42	14.77	4.89	3.06
Nd	41.2	22.4	62.0	20.8	15.7
Sm	7.94	4.64	12.45	4.34	4.65
Eu	2.48	1.46	3.73	1.46	1.84
Gd	7.78	4.61	11.98	4.18	4.81
Tb	1.07	0.66	1.66	0.58	0.77
Dy	5.35	3.57	8.10	2.76	4.46
Ho	0.99	0.67	1.45	0.49	0.81
Er	2.47	1.79	3.41	1.14	2.03
Tm					
Hf	7.33	3.64	8.40	2.93	2.94
Ta	3.25	1.67	3.35	1.15	0.73
Th	5.08	3.46	5.92	2.08	1.20

Table 1b. Continued

Volcanic field	Tianchi, Changbaishan	Tianchi, Changbaishan	Zengfengshan, Changbaishan	Zengfengshan, Changbaishan	Zengfengshan, Changbaishan
Latitude	42.4028	42.46831	42.49938	42.50506	42.463
Longitude	128.10153	128.20244	128.70715	128.7117	128.73503
Batch	MSU 05	MSU 05	MSU 05	MSU 05	MSU 05
Sample #	CBS-21a	CBS-22a	CBS-24a	CBS-25A	CBS-26a
Rock type	Hawaiite	Basaltic andesite	Hawaiite	Basalt	Mugearite
XRF					
SiO2 (%)	48.80	52.44	48.26	47.64	48.76
TiO2	1.35	1.68	2.52	2.12	2.51
Al2O3	14.64	14.05	17.16	15.44	16.95
Fe2O3t	9.23	11.43	11.99	11.78	12.11
MnO	0.15	0.15	0.18	0.14	0.18
MgO	9.41	7.77	4.19	8.06	3.85
CaO	8.77	7.74	6.21	9.82	5.55
Na2O	2.23	2.86	4.72	1.97	4.37
K2O	3.29	0.72	1.73	1.22	2.08
P2O5	0.47	0.24	0.88	0.39	0.86
Total	98.34	99.08	97.84	98.58	97.22
LOI	1.44	0.79	1.95	1.34	2.57
Sr (ppm)	700	343	989	574	887
Zr	178	96	314	168	307
Sc					
V					
Ga					
Cu					
Zn					
ICP-MS					
Cs (ppm)					
V	213	140	91	248	73
Y	22.8	20.9	28.1	22.2	30.9
Nb	37.7	11.0	64.8	29.8	57.8
Ba	740	264	621	298	564
La	33.2	10.8	48.2	20.5	44.3
Ce	61.3	20.9	89.5	42.6	82.6
Pr	7.62	3.03	10.98	5.40	10.62
Nd	31.0	14.4	43.4	22.5	43.5
Sm	6.21	4.12	8.05	5.72	8.25
Eu	2.26	1.49	2.48	1.73	2.68
Gd	6.31	4.41	8.16	4.87	8.31
Tb	0.89	0.71	1.10	0.75	1.16
Dy	4.60	4.15	5.41	4.21	5.92
Ho	0.84	0.75	1.03	0.75	1.12
Er	2.13	1.84	2.57	2.12	2.91
Tm					
Hf	4.94	2.57	6.88	3.77	6.97
Ta	2.23	0.66	4.09	1.66	3.62
Th	4.58	1.27	6.11	2.54	5.52

Table 1b. Continued

Volcanic field	Longgang	Longgang	Longgang	Longgang	Longgang
Latitude	42.33611	42.33611	42.33611	42.33611	42.38813
Longitude	126.41672	126.41672	126.41672	126.41672	126.29681
Batch	MSU 03-04	MSU 03-04	MSU 03-04	MSU 03-04	MSU 05
Sample #	LG-1c	LG-DLW-1w	LG-DLW-1p	LG-DLW-1aa	LG-1a
Rock type	Hawaiite	Phonotephrite	Hawaiite	Mugearite	Hawaiite
XRF					
SiO2 (%)	46.70	48.45	47.18	49.47	48.72
TiO2	2.42	2.18	2.40	2.11	2.28
Al2O3	16.49	17.88	16.22	17.45	16.62
Fe2O3t	11.47	11.27	11.58	11.28	11.85
MnO	0.16	0.17	0.16	0.17	0.17
MgO	6.61	4.70	7.23	4.68	5.66
CaO	7.47	6.02	7.49	6.00	6.95
Na2O	3.64	4.43	3.57	4.20	4.08
K2O	2.36	2.95	2.30	2.98	2.59
P2O5	0.59	0.88	0.57	0.89	0.71
Total	97.91	98.93	98.70	99.23	99.63
LOI					0.12
Sr (ppm)	743	869	744	902	775
Zr	237	291	224	291	257
Sc					
V					
Ga					
Cu					
Zn					
ICP-MS					
Cs (ppm)					
V	139	80	136	77	121
Y	25.9	28.4	24.4	27.9	27.1
Nb	67.3	81.8	64.4	83.1	71.6
Ba	757	954	804	1067	886
La	46.5	60.1	47.8	64.2	53.3
Ce	87.1	110.8	85.6	112.4	92.9
Pr	9.10	11.41	9.88	12.76	10.54
Nd	35.3	44.4	37.6	46.7	39.3
Sm	6.50	7.53	6.63	7.56	7.21
Eu	2.14	2.46	2.22	2.53	2.33
Gd	6.04	6.88	6.54	7.75	7.15
Tb	0.86	0.97	0.87	0.97	0.99
Dy	4.59	4.91	4.57	5.02	4.89
Ho	0.86	0.97	0.83	0.92	0.93
Er	2.27	2.54	2.24	2.59	2.42
Tm					
Hf	5.03	5.91	5.10	6.29	5.82
Ta	3.80	4.65	3.49	4.52	3.82
Th	6.72	8.88	7.35	10.27	8.20

Table 1b. Continued

Volcanic field	Longgang	Longgang	Longgang	Longgang	Longgang
Latitude	42.39497	42.30673	42.49692	42.38114	42.34271
Longitude	126.2915	126.35176	126.48228	126.16321	126.11224
Batch	MSU 05	MSU 05	MSU 05	MSU 05	MSU 05
Sample #	LG-2a	LG-3a	Lg-4a	LG-5b	LG-6a
Rock type	Hawaiite	Basaltic andesite	Hawaiite	Hawaiite	Basalt
XRF					
SiO2 (%)	48.72	53.10	49.03	47.17	50.18
TiO2	2.22	1.63	2.12	2.30	1.65
Al2O3	16.39	14.92	15.99	15.21	14.72
Fe2O3t	11.83	11.04	11.67	12.28	11.97
MnO	0.17	0.15	0.14	0.18	0.16
MgO	5.72	6.97	6.32	8.45	8.91
CaO	6.79	7.99	6.70	6.86	7.99
Na2O	4.11	3.17	3.81	3.55	3.13
K2O	2.57	1.02	2.20	2.13	1.21
P2O5	0.71	0.28	0.63	0.59	0.29
Total	99.23	100.27	98.61	98.72	100.21
LOI	0.51	0.00	1.13	1.04	0.00
Sr (ppm)	764	367	828	694	435
Zr	263	124	300	221	133
Sc					
V					
Ga					
Cu					
Zn					
ICP-MS					
Cs (ppm)					
V	112	140	121	115	140
Y	27.3	21.1	18.1	26.7	18.6
Nb	69.4	19.5	66.5	61.5	25.7
Ba	871	316	765	743	399
La	51.8	17.4	47.0	43.5	19.3
Ce	90.7	33.6	86.8	77.6	36.5
Pr	10.60	4.18	10.45	9.06	4.55
Nd	40.4	17.8	41.7	35.0	18.5
Sm	7.37	4.39	8.23	6.64	4.05
Eu	2.35	1.59	2.64	2.26	1.46
Gd	7.16	4.55	7.33	6.84	4.31
Tb	0.99	0.71	0.94	0.94	0.63
Dy	4.99	3.81	4.09	4.82	3.54
Ho	0.94	0.71	0.65	0.92	0.65
Er	2.50	1.90	1.47	2.51	1.77
Tm					
Hf	5.86	3.15	6.78	5.04	3.29
Ta	3.74	1.06	3.75	3.33	1.47
Th	8.16	2.56	7.32	6.96	2.86

Table 1b. Continued

Volcanic field	Longgang	Longgang	Kuandian	Kuandian	Kuandian
Latitude	42.34271	42.44016	40.73119	40.72339	40.72325
Longitude	126.11224	126.26681	124.75322	124.76103	124.76136
Batch	WSU 05	MSU 05	MSU 03-04	MSU 03-04	MSU 03-04
Sample #	LG-6a	LG-7b	KD-HY-1d	KD-HY-2a	KD-HY-3a
Rock type	Basalt	Hawaiite	Basalt	Hawaiite	Hawaiite
XRF					
SiO2 (%)	50.193	49.61	47.72	47.76	48.72
TiO2	1.638	1.99	2.07	2.02	1.90
Al2O3	14.794	15.91	14.66	14.70	14.82
Fe2O3t	11.631	11.52	11.50	11.44	11.40
MnO	0.164	0.16	0.16	0.16	0.16
MgO	8.787	6.88	9.79	8.13	7.92
CaO	8.071	7.36	7.27	7.53	7.51
Na2O	3.407	3.70	2.69	3.65	3.64
K2O	1.220	1.99	2.08	2.03	1.85
P2O5	0.288	0.55	0.52	0.57	0.56
Total	100.193	99.67	98.46	97.99	98.48
LOI	-0.648	0.11			
Sr (ppm)	462	610	554	695	649
Zr	129	209	219	248	237
Sc	21.2				
V	152.8				
Ga	18.2				
Cu	43.9				
Zn	99.1				
ICP-MS					
Cs (ppm)	0.19				
V		126	153	134	124
Y	18.76	23.8	24.0	22.6	21.7
Nb	25.43	48.1	44.4	55.4	49.0
Ba	412	669	459	415	365
La	20.47	37.4	31.0	35.6	33.0
Ce	37.63	65.7	60.4	65.7	63.3
Pr	4.21	7.91	6.76	7.88	7.73
Nd	17.97	30.1	28.5	32.4	31.0
Sm	4.33	5.89	5.99	6.64	6.48
Eu	1.61	1.95	2.07	2.39	2.13
Gd	4.36	5.97	5.99	6.72	6.08
Tb	0.69	0.83	0.87	0.90	0.83
Dy	3.88	4.55	4.54	4.58	4.30
Ho	0.73	0.81	0.82	0.78	0.73
Er	1.81	2.26	2.02	1.88	1.77
Tm	0.25				
Hf	3.25	4.60	4.71	5.63	5.16
Ta	1.55	2.61	2.59	3.25	2.79
Th	2.75	5.82	4.45	5.68	5.28

Table 1b. Continued

Volcanic field	Kuandian	Kuandian	Kuandian	Kuandian	Kuandian
Latitude	40.72325	40.72194	40.72194	40.67814	40.67814
Longitude	124.76136	124.76117	124.76117	124.75744	124.75744
Batch	MSU 03-04	MSU 03-04	MSU 03-04	MSU 03-04	WSU 05
Sample #	KD-HY-3b	KD-HY-4a	KD-HY-4d	KD-LJ-1a	KD-LJ-1a
Rock type	Hawaiite	Basanite	Basanite	Hawaiite	Mugearite
XRF					
SiO2 (%)	48.62	46.70	46.53	50.06	51.525
TiO2	1.92	2.30	2.31	1.62	1.639
Al2O3	15.03	14.80	15.05	14.63	14.753
Fe2O3t	11.35	12.14	12.06	10.71	10.841
MnO	0.16	0.16	0.16	0.15	0.153
MgO	7.45	7.03	6.90	7.64	7.688
CaO	7.54	6.91	6.82	8.10	8.257
Na2O	3.74	4.38	4.42	3.13	3.618
K2O	1.88	2.74	2.75	1.74	1.828
P2O5	0.56	0.81	0.82	0.43	0.424
Total	98.25	97.97	97.82	98.21	100.726
LOI					
Sr (ppm)	663	855	907	524	555
Zr	245	308	316	142	140
Sc					21.3
V					144.6
Ga					19.9
Cu					49.7
Zn					102.4
ICP-MS					
Cs (ppm)					0.24
V	131	132	130	127	
Y	22.1	24.5	25.2	18.6	18.99
Nb	50.7	74.1	73.6	35.2	33.18
Ba	377	529	529	293	334
La	34.3	47.3	46.6	21.2	22.22
Ce	64.2	91.3	91.4	41.8	40.10
Pr	7.72	9.98	10.21	4.61	4.53
Nd	31.1	41.7	42.7	19.5	19.23
Sm	6.50	8.23	8.42	4.39	4.97
Eu	2.21	2.75	2.82	1.56	1.76
Gd	6.46	7.36	7.76	4.38	4.88
Tb	0.87	1.01	1.04	0.65	0.73
Dy	4.57	4.85	5.16	3.31	4.00
Ho	0.77	0.83	0.87	0.60	0.75
Er	1.98	1.92	2.00	1.56	1.75
Tm					0.23
Hf	5.46	6.64	6.79	3.10	3.30
Ta	3.05	4.50	4.64	1.98	2.00
Th	5.66	6.48	6.66	2.82	3.01

Table 1b. Continued

Volcanic field	Kuandian	Kuandian	Kuandian	Kuandian	Kuandian
Latitude	40.67814	40.68681	40.68681	40.68681	40.71272
Longitude	124.75744	124.78892	124.78892	124.78892	124.63458
Batch	MSU 03-04	MSU 03-04	MSU 03-04	MSU 03-04	MSU 03-04
Sample #	KD-LJ-1b	KD-LJ-1d	KD-LJ-1e	KD-LJ-1h	KD-QY-1a
Rock type	Mugearite	Basalt	Hawaiite	Hawaiite	Hawaiite
XRF					
SiO2 (%)	51.54	50.07	49.86	51.03	48.08
TiO2	1.69	1.56	1.76	1.78	1.95
Al2O3	15.17	14.82	14.73	14.96	14.97
Fe2O3t	10.20	11.18	11.28	11.22	10.96
MnO	0.14	0.15	0.16	0.16	0.16
MgO	7.26	8.05	7.14	7.28	8.20
CaO	8.07	8.12	7.88	7.94	7.92
Na2O	3.50	3.37	3.55	3.77	3.70
K2O	1.90	1.28	1.63	1.73	2.14
P2O5	0.48	0.32	0.41	0.41	0.61
Total	99.95	98.92	98.40	100.28	98.69
LOI					
Sr (ppm)	535	472	517	487	675
Zr	148	156	217	210	233
Sc					
V					
Ga					
Cu					
Zn					
ICP-MS					
Cs (ppm)					
V	131	130	141	138	135
Y	18.7	18.0	22.2	20.6	21.8
Nb	35.5	26.0	42.8	37.8	49.4
Ba	335	262	291	292	458
La	22.7	19.4	26.0	24.2	34.1
Ce	43.0	38.5	52.6	46.0	64.1
Pr	5.12	4.66	5.69	5.48	7.74
Nd	21.8	19.6	24.6	23.1	31.8
Sm	4.82	4.35	5.36	5.07	6.48
Eu	1.73	1.53	1.86	1.81	2.16
Gd	4.84	4.47	5.31	5.38	6.41
Tb	0.69	0.65	0.78	0.75	0.86
Dy	3.69	3.55	4.10	4.02	4.32
Ho	0.66	0.63	0.74	0.70	0.73
Er	1.72	1.62	1.80	1.84	1.85
Tm					
Hf	3.49	3.56	4.62	4.52	4.87
Ta	2.02	1.49	2.57	2.15	2.77
Th	3.50	2.97	4.09	4.11	5.17

Table 1b. Continued

Volcanic field	Kuandian	Kuandian	Kuandian	Kuandian	Datong
Latitude	40.71272	40.71272	40.71219	40.71219	40.02042
Longitude	124.63458	124.63458	124.63478	124.63478	113.66369
Batch	MSU 03-04	MSU 03-04	MSU 03-04	MSU 03-04	MSU 03-04
Sample #	KD-QY-1d	KD-QY-1b	KD-QY-1o	KD-QY-1p	DT-1c
Rock type	Hawaiite	Hawaiite	Hawaiite	Hawaiite	Basaltic andesite
XRF					
SiO2 (%)	48.37	47.85	48.31	48.62	51.78
TiO2	1.96	1.95	1.93	1.91	1.96
Al2O3	15.02	14.38	14.86	14.57	15.22
Fe2O3t	10.96	11.17	10.86	11.15	11.38
MnO	0.16	0.16	0.15	0.16	0.14
MgO	8.02	8.23	8.16	8.11	6.62
CaO	7.88	7.84	7.80	7.76	8.06
Na2O	3.73	3.61	3.79	3.63	3.45
K2O	2.22	2.09	2.27	2.17	1.14
P2O5	0.61	0.61	0.60	0.59	0.40
Total	98.93	97.89	98.73	98.67	100.15
LOI					
Sr (ppm)	683	668	673	658	433
Zr	232	226	232	222	178
Sc					
V					
Ga					
Cu					
Zn					
ICP-MS					
Cs (ppm)					
V	136	147	132	139	144
Y	22.1	22.3	21.5	22.2	25.6
Nb	50.7	53.9	49.6	52.4	28.1
Ba	459	431	471	424	221
La	33.8	33.8	35.1	32.8	19.7
Ce	63.6	67.5	65.7	66.0	40.3
Pr	7.57	7.64	7.73	7.30	4.53
Nd	31.8	32.1	31.3	30.7	20.2
Sm	6.45	6.50	6.37	6.31	4.79
Eu	2.24	2.23	2.19	2.15	1.77
Gd	6.53	6.12	6.42	6.06	5.24
Tb	0.88	0.85	0.85	0.84	0.84
Dy	4.48	4.35	4.19	4.30	4.57
Ho	0.78	0.76	0.79	0.77	0.85
Er	1.95	1.86	1.87	1.89	2.17
Tm					
Hf	4.96	4.96	4.76	4.76	3.99
Ta	2.88	3.20	2.80	3.15	1.63
Th	5.18	4.73	5.27	4.73	2.53

Table 1b. Continued

Volcanic field	Datong	Datong	Datong	Datong	Datong
Latitude	40.00722	40.00722	40.00722	40.00722	40.00722
Longitude	113.80689	113.80689	113.80689	113.80689	113.80689
Batch	MSU 03-04	MSU 03-04	MSU 03-04	WSU 05	MSU 03-04
Sample #	DT-1f	DT-1g	DT-1h	DT-1h	DT-1i
Rock type	Basaltic andesite	Basaltic andesite	Basaltic andesite	Basaltic andesite	Basaltic andesite
XRF					
SiO2 (%)	52.43	52.14	51.80	52.536	52.97
TiO2	2.14	2.15	2.05	2.098	2.41
Al2O3	14.19	14.10	13.56	13.534	14.06
Fe2O3t	11.66	11.87	12.34	12.010	11.95
MnO	0.15	0.15	0.15	0.158	0.15
MgO	7.15	7.26	7.46	7.496	6.23
CaO	8.01	8.03	8.00	8.005	7.87
Na2O	3.19	3.17	2.90	3.376	3.29
K2O	0.87	0.88	0.81	0.867	0.98
P2O5	0.33	0.32	0.30	0.307	0.37
Total	100.12	100.07	99.37	100.387	100.28
LOI				-0.162	
Sr (ppm)	344	342	333	344	340
Zr	192	189	182	176	218
Sc				22.8	
V				168.0	
Ga				21.6	
Cu				52.0	
Zn				110.8	
ICP-MS					
Cs (ppm)				0.15	
V	145	155	152		158
Y	28.4	26.7	27.7	27.62	30.7
Nb	20.6	19.8	21.4	20.15	23.7
Ba	188	189	174	185	210
La	14.7	14.2	13.8	14.65	16.4
Ce	29.4	29.6	30.1	28.69	33.8
Pr	3.77	3.80	3.62	3.55	4.41
Nd	17.9	17.9	17.4	16.69	20.5
Sm	5.09	4.72	4.94	5.22	5.45
Eu	1.82	1.76	1.77	1.86	2.03
Gd	5.52	5.26	5.37	5.99	6.16
Tb	0.89	0.85	0.87	0.98	0.96
Dy	5.25	4.71	5.05	5.66	5.47
Ho	0.95	0.88	0.96	1.07	1.02
Er	2.57	2.44	2.44	2.61	2.76
Tm				0.35	
Hf	4.63	4.15	4.34	4.43	5.10
Ta	1.28	1.23	1.34	1.33	1.45
Th	2.20	2.14	2.02	2.15	2.41

Table 1b. Continued

Volcanic field	Wudi	Wudi	Wudi	Wudi	Wudi
Latitude	38.01006	38.01006	38.01006	38.01006	38.01006
Longitude	117.68049	117.68049	117.68049	117.68049	117.68049
Batch	MSU 05	WSU 05	MSU 05	MSU 05	MSU 05
Sample #	SD-WD-1a	SD-WD-1a	SD-WD-1b	SD-WD-2a	SD-WD-2c
Rock type	Foidite	Basanite	Foidite	Basanite	Basanite
XRF					
SiO2 (%)	39.85	40.067	39.46	39.73	39.86
TiO2	2.71	2.653	2.61	2.82	2.80
Al2O3	9.30	9.507	9.32	10.28	10.45
Fe2O3t	15.70	14.789	15.24	15.40	15.01
MnO	0.22	0.221	0.22	0.22	0.21
MgO	14.72	14.831	14.88	11.82	12.07
CaO	9.45	9.612	9.47	9.64	9.79
Na2O	4.56	4.765	4.48	4.57	4.38
K2O	1.29	1.277	1.26	2.40	2.56
P2O5	0.97	1.001	1.04	1.18	1.28
Total	98.77	98.724	97.98	98.06	98.41
LOI	0.97	0.287	1.79	1.63	1.30
Sr (ppm)	815	860	802	1020	1040
Zr	343	306	335	358	324
Sc		17.7			
V		192.8			
Ga		19.7			
Cu		39.6			
Zn		150.3			
ICP-MS					
Cs (ppm)		0.40			
V	171		161	170	176
Y	31.3	30.14	31.0	33.1	31.2
Nb	104.7	106.51	113.2	119.9	103.7
Ba	164	174	161	506	553
La	65.9	67.33	66.9	68.3	62.8
Ce	111.9	119.21	113.5	115.3	107.8
Pr	14.11	13.17	13.94	14.39	13.28
Nd	58.6	53.99	57.5	58.7	55.0
Sm	11.21	12.15	11.13	11.36	10.85
Eu	3.39	3.90	3.41	3.46	3.37
Gd	10.79	10.74	10.76	11.03	10.51
Tb	1.42	1.46	1.43	1.47	1.40
Dy	6.56	7.12	6.59	7.03	6.53
Ho	1.14	1.19	1.10	1.20	1.11
Er	2.47	2.51	2.39	2.68	2.54
Tm		0.29			
Hf	7.30	7.04	7.41	7.74	7.21
Ta	6.00	6.83	6.41	6.74	6.05
Th	8.72	8.78	9.23	10.00	8.79

Table 1b. Continued

Volcanic field	Changle	Changle	Changle	Changle	Changle
Latitude	36.54181	36.54181	36.54181	36.55603	36.58604
Longitude	118.88348	118.88348	118.88348	118.79591	118.75026
Batch	MSU 05	WSU 05	MSU 05	MSU 05	MSU 05
Sample #	SD-CL-1a	SD-CL-1a	SD-CL-2a	SD-CL-3a	SD-CL-4a
Rock type	Basanite	Basanite	Basanite	Basanite	Alkali basalt
XRF					
SiO2 (%)	41.92	42.128	41.71	42.40	44.00
TiO2	2.65	2.647	2.61	2.36	2.45
Al2O3	12.84	12.881	12.81	13.70	13.25
Fe2O3t	13.27	12.912	13.01	13.17	12.68
MnO	0.19	0.193	0.19	0.21	0.17
MgO	10.90	10.751	10.93	7.44	11.12
CaO	9.75	9.792	9.80	8.08	9.23
Na2O	3.62	3.899	3.57	4.85	2.34
K2O	1.63	1.639	1.77	3.08	1.76
P2O5	0.88	0.847	0.87	1.20	0.49
Total	97.65	97.689	97.27	96.49	97.49
LOI	2.11	1.530	2.50	3.24	2.33
Sr (ppm)	851	911	850	1177	552
Zr	237	229	238	439	167
Sc		20.7			
V		237.2			
Ga		18.4			
Cu		70.2			
Zn		105.2			
ICP-MS					
Cs (ppm)		0.33			
V	216		211	141	198
Y	24.4	24.31	24.3	31.2	20.5
Nb	67.3	68.65	67.1	99.7	39.5
Ba	382	411	374	374	298
La	49.0	51.50	49.8	71.9	24.1
Ce	84.8	91.71	86.2	123.4	44.5
Pr	10.20	9.90	10.44	14.67	5.65
Nd	40.8	39.64	41.8	57.1	23.7
Sm	7.60	8.60	7.78	10.36	5.09
Eu	2.39	2.79	2.47	3.17	1.67
Gd	7.75	7.46	7.76	10.30	5.19
Tb	1.02	1.06	1.04	1.37	0.75
Dy	4.90	5.44	4.93	6.34	3.97
Ho	0.86	0.94	0.86	1.10	0.73
Er	2.04	2.11	2.00	2.60	1.84
Tm		0.26			
Hf	5.28	5.22	5.41	8.91	3.97
Ta	3.99	4.46	4.05	6.20	2.40
Th	5.97	5.96	5.95	10.01	2.97

Table 1b. Continued

Volcanic field	Changle
Latitude	36.58604
Longitude	118.75026
Batch	MSU 05
Sample #	SD-CL-4c
Rock type	Alkali basalt
XRF	
SiO2 (%)	44.46
TiO2	2.48
Al2O3	13.38
Fe2O3t	12.79
MnO	0.17
MgO	11.26
CaO	9.13
Na2O	2.36
K2O	1.80
P2O5	0.50
Total	98.33
LOI	1.49
Sr (ppm)	553
Zr	169
Sc	
V	
Ga	
Cu	
Zn	
ICP-MS	
Cs (ppm)	
V	203
Y	20.7
Nb	40.7
Ba	299
La	24.3
Ce	45.1
Pr	5.72
Nd	24.0
Sm	5.04
Eu	1.69
Gd	5.41
Tb	0.79
Dy	4.01
Ho	0.73
Er	1.79
Tm	
Hf	4.05
Ta	2.46
Th	3.06

Table 1b. Notes:

1) For XRF analysis, samples done by MSU are prepared under oxidizing condition (see Method part in Hannah et al., 2002), Fe is reported as Fe_2O_3; samples at WSU are prepared under reducing condition (see Sample Preparation part in Johnson et al., 1999), Fe is reported as FeO and then calculated to Fe_2O_3.

2) LOI analyzed by WSU is done under oxidizing condition. It includes both loss of volatiles and oxygen gain by FeO and MnO (oxidize to Fe_2O_3 and Mn_2O_3).

3) Sr, Zr, Sc and Ba by WSU are average values of XRF and ICP-MS analysis. The differences between these two methods are <10% for Sr, Zr and Ba, and <20% for Sc.

Appendix B
Composition Profiles of Olivine Dissolution in Basalt

Exp 15

SiO2	TiO2	Al2O3	FeO	MnO	MgO	CaO	Na2O	K2O	P2O5	Total	d (um)
47.73	1.74	12.62	12.59	0.22	10.29	10.97	2.19	0.12	0.18	98.65	3.0
49.24	1.80	12.51	12.04	0.16	9.34	11.09	2.35	0.15	0.19	98.87	4.9
47.21	1.75	12.59	12.60	0.19	10.53	10.88	2.20	0.15	0.13	98.23	5.5
48.99	1.68	11.91	12.17	0.29	11.40	10.56	2.12	0.19	0.10	99.42	5.6
49.45	1.91	12.62	12.53	0.22	8.47	11.44	2.12	0.17	0.12	99.03	6.1
47.83	1.67	12.63	12.41	0.17	10.52	10.94	2.27	0.11	0.12	98.67	8.0
47.44	1.81	12.41	12.43	0.15	10.31	10.96	2.23	0.14	0.16	98.04	10.5
48.52	1.78	12.00	12.91	0.20	9.68	11.14	2.08	0.14	0.11	98.56	10.6
48.63	1.74	11.95	12.89	0.21	10.21	11.04	2.02	0.15	0.08	98.93	10.7
48.74	1.78	11.90	12.87	0.11	9.90	11.18	2.05	0.11	0.06	98.69	11.4
47.82	1.74	12.52	12.64	0.19	10.27	10.96	2.18	0.14	0.13	98.58	13.0
47.71	1.77	12.49	12.56	0.27	10.26	11.05	2.16	0.10	0.10	98.47	14.6
47.28	1.76	12.56	12.45	0.25	10.13	10.87	2.38	0.14	0.08	97.89	15.5
48.54	1.74	12.09	12.76	0.31	10.18	11.06	2.13	0.11	0.24	99.15	15.6
48.44	1.76	12.12	12.76	0.31	10.33	10.98	2.14	0.11	0.21	99.14	16.5
48.60	1.75	11.91	12.64	0.19	10.08	10.94	2.09	0.16	0.16	98.53	16.6
47.95	1.73	12.64	12.45	0.25	10.21	10.90	2.30	0.12	0.17	98.72	18.0
47.38	1.76	12.47	12.54	0.16	10.16	10.82	2.21	0.13	0.12	97.75	20.5
48.63	1.77	12.00	12.61	0.22	10.10	10.72	2.17	0.13	0.13	98.48	20.6
49.14	1.70	11.98	12.61	0.17	10.07	10.66	2.06	0.11	0.21	98.70	21.9
48.60	1.75	12.19	12.55	0.29	10.20	10.83	2.15	0.11	0.03	98.69	22.2
48.14	1.71	12.64	12.68	0.19	10.12	10.75	2.33	0.16	0.11	98.84	22.9
47.82	1.78	12.64	12.66	0.26	10.04	10.86	2.33	0.16	0.20	98.75	24.5
47.52	1.76	12.52	12.53	0.28	10.12	10.70	2.21	0.07	0.13	97.82	25.5
49.03	1.73	12.04	12.41	0.22	9.93	10.83	2.19	0.11	0.12	98.61	25.6
47.90	1.69	12.64	12.34	0.27	10.00	10.77	2.24	0.14	0.16	98.14	27.9
49.10	1.73	12.02	12.59	0.14	10.00	10.87	2.16	0.15	0.10	98.87	28.0
48.10	1.77	12.66	12.41	0.21	9.93	10.84	2.27	0.12	0.20	98.50	29.5
47.51	1.79	12.51	12.40	0.11	9.97	10.83	2.32	0.16	0.10	97.69	30.5
47.84	1.72	12.69	12.46	0.28	9.97	10.85	2.30	0.19	0.18	98.47	32.9
48.19	1.74	12.69	12.37	0.31	9.82	10.94	2.32	0.13	0.12	98.62	34.5
47.44	1.74	12.54	12.39	0.18	9.88	10.86	2.29	0.20	0.06	97.58	35.5
47.85	1.73	12.76	12.45	0.24	9.80	10.85	2.37	0.17	0.17	98.39	37.9
47.79	1.76	12.75	12.49	0.27	9.67	10.91	2.29	0.17	0.21	98.31	39.5
47.41	1.72	12.57	12.28	0.21	9.87	10.84	2.38	0.16	0.09	97.53	40.5
48.17	1.76	12.81	12.36	0.19	9.86	10.71	2.33	0.14	0.13	98.44	42.9
48.09	1.70	12.88	12.38	0.14	9.66	10.75	2.29	0.14	0.05	98.07	44.5
47.67	1.76	12.81	12.34	0.16	9.79	10.87	2.36	0.15	0.15	98.05	45.5
48.14	1.72	12.85	12.44	0.18	9.58	10.86	2.35	0.16	0.19	98.46	47.9
48.02	1.79	12.99	12.37	0.18	9.46	10.91	2.37	0.20	0.17	98.46	49.5
47.99	1.77	12.64	12.16	0.19	9.72	10.81	2.34	0.15	0.06	97.82	50.5
47.88	1.72	12.73	12.17	0.21	9.65	11.02	2.31	0.17	0.18	98.04	52.9
48.03	1.77	13.01	12.28	0.23	9.34	10.94	2.36	0.16	0.19	98.31	54.5
47.88	1.72	12.74	12.20	0.23	9.68	10.83	2.42	0.13	0.17	98.00	55.5

48.09	1.74	13.03	12.06	0.22	9.33	10.86	2.38	0.15	0.12	97.97	59.5
48.40	1.76	13.51	11.85	0.10	8.91	10.88	2.51	0.11	0.19	98.21	90.0
48.40	1.74	13.41	11.93	0.16	8.60	10.85	2.54	0.15	0.14	97.93	97.7
48.85	1.82	13.76	11.66	0.14	8.36	10.76	2.54	0.23	0.15	98.26	126.9
48.49	1.78	13.62	11.74	0.15	8.15	10.86	2.58	0.22	0.10	97.70	135.9
48.74	1.85	13.97	11.60	0.28	7.90	10.78	2.76	0.17	0.13	98.17	164.0
48.91	1.76	13.92	11.66	0.22	7.76	10.95	2.65	0.14	0.13	98.09	174.0
48.79	1.85	14.02	11.56	0.17	7.84	10.93	2.71	0.17	0.21	98.25	201.1
49.06	1.85	13.93	11.72	0.21	7.59	10.83	2.65	0.17	0.17	98.18	212.2
48.80	1.83	13.97	11.70	0.11	7.47	10.85	2.68	0.20	0.12	97.73	238.0
49.14	1.84	13.96	11.61	0.14	7.43	10.89	2.73	0.20	0.19	98.13	250.4
48.66	1.85	13.97	11.52	0.17	7.42	10.87	2.63	0.15	0.21	97.46	275.1
48.79	1.91	13.87	11.60	0.14	7.35	10.86	2.64	0.17	0.19	97.53	288.5
49.01	1.85	13.97	11.73	0.19	7.35	11.00	2.76	0.15	0.11	98.12	312.2
48.61	1.88	13.99	11.72	0.17	7.20	11.14	2.67	0.17	0.13	97.69	326.7
48.98	1.89	14.01	11.80	0.19	7.21	10.94	2.60	0.14	0.14	97.91	349.2
48.79	1.90	13.99	11.83	0.27	7.26	10.95	2.81	0.19	0.16	98.13	365.0
48.83	1.86	13.96	11.77	0.25	7.23	10.94	2.63	0.21	0.10	97.77	386.2
48.80	1.88	13.90	11.74	0.27	7.11	11.01	2.67	0.14	0.13	97.64	403.2
48.48	1.83	13.91	11.74	0.24	7.25	10.86	2.64	0.17	0.21	97.32	404.9
48.76	1.85	13.90	11.86	0.28	7.11	11.03	2.69	0.19	0.17	97.82	423.3
48.46	1.86	13.85	11.85	0.17	7.15	11.08	2.60	0.17	0.17	97.36	439.8
48.78	1.93	13.93	11.88	0.18	7.20	10.94	2.66	0.17	0.13	97.78	441.3
48.71	1.83	13.86	11.86	0.18	7.00	11.08	2.63	0.19	0.20	97.53	460.3
48.61	1.93	13.83	11.75	0.11	7.02	11.00	2.70	0.20	0.12	97.26	474.8
48.61	1.88	13.85	11.89	0.25	7.03	10.98	2.75	0.20	0.16	97.59	479.5
48.75	1.87	13.91	11.86	0.26	7.13	11.12	2.68	0.17	0.15	97.90	497.3
48.36	1.91	13.90	11.87	0.22	6.96	11.04	2.73	0.14	0.20	97.33	509.7
48.89	1.81	13.94	11.91	0.21	7.00	10.99	2.77	0.22	0.21	97.94	517.7
48.80	1.84	13.96	11.94	0.20	7.02	11.11	2.63	0.18	0.20	97.87	534.3
48.59	1.89	13.95	11.98	0.21	6.95	11.19	2.68	0.16	0.17	97.76	544.6
48.67	1.85	13.90	11.89	0.23	6.92	11.10	2.75	0.20	0.11	97.60	555.8
48.69	1.84	13.97	11.93	0.24	7.01	11.16	2.69	0.19	0.23	97.95	571.4
48.46	1.92	13.93	11.89	0.18	6.92	11.23	2.65	0.18	0.17	97.51	579.6
48.74	1.94	13.92	11.91	0.21	6.97	11.23	2.70	0.17	0.22	98.01	594.0
48.54	1.93	14.00	11.96	0.23	6.90	11.10	2.66	0.17	0.25	97.73	608.4
48.15	1.87	13.99	11.91	0.29	6.96	11.01	2.71	0.19	0.16	97.22	614.5
48.48	1.86	13.88	11.89	0.31	6.90	11.19	2.63	0.14	0.14	97.42	632.2
48.50	1.90	13.99	12.03	0.21	6.80	11.12	2.62	0.15	0.10	97.41	645.4
48.32	1.92	14.03	12.04	0.20	6.86	11.14	2.73	0.21	0.27	97.72	649.4
48.43	1.91	13.82	12.04	0.24	6.95	11.03	2.81	0.15	0.28	97.65	670.3
48.69	1.87	13.88	12.12	0.25	6.91	11.28	2.66	0.15	0.11	97.92	682.5
48.55	1.90	13.81	12.08	0.24	6.94	11.18	2.63	0.13	0.26	97.72	684.4
48.60	1.85	13.89	12.16	0.14	6.91	11.05	2.75	0.20	0.21	97.75	708.5
48.34	1.87	13.79	12.13	0.18	6.96	11.13	2.70	0.17	0.14	97.40	719.3
48.62	1.81	13.92	11.99	0.15	6.84	11.26	2.61	0.21	0.20	97.61	719.5
48.64	1.89	13.76	11.86	0.17	7.01	11.16	2.68	0.16	0.17	97.49	746.7
47.97	1.89	13.94	11.92	0.34	7.00	11.29	2.64	0.14	0.22	97.36	754.3
48.60	1.89	13.91	12.07	0.18	6.88	11.15	2.64	0.12	0.14	97.57	756.5

48.45	1.92	13.96	11.96	0.17	6.86	11.13	2.60	0.19	0.12	97.35	784.9
48.36	1.90	13.85	11.89	0.19	6.84	11.02	2.61	0.16	0.12	96.93	789.2
48.51	1.87	13.87	12.11	0.18	6.96	11.22	2.61	0.21	0.17	97.70	793.6
48.52	1.86	13.90	12.11	0.20	6.90	11.10	2.65	0.18	0.10	97.51	823.0
48.67	1.84	13.86	11.96	0.16	6.79	11.00	2.69	0.21	0.22	97.40	824.1
48.34	1.89	13.87	12.05	0.28	6.92	11.14	2.61	0.19	0.24	97.53	830.6
48.29	1.89	13.98	11.86	0.34	6.80	11.10	2.71	0.18	0.18	97.32	859.1
48.64	1.89	13.87	11.96	0.21	6.86	11.15	2.63	0.17	0.18	97.56	861.2
48.32	1.87	13.87	12.06	0.20	6.79	11.23	2.58	0.14	0.14	97.19	867.6
48.77	1.86	13.89	11.81	0.20	6.81	11.12	2.64	0.20	0.13	97.43	894.1
48.49	1.84	13.90	12.06	0.29	6.92	11.20	2.59	0.22	0.10	97.60	899.5
48.57	1.91	13.87	11.97	0.21	6.97	11.18	2.65	0.19	0.15	97.67	904.7
48.59	1.88	13.99	11.78	0.15	6.79	11.23	2.67	0.15	0.24	97.45	928.9
48.59	1.89	13.89	12.00	0.24	6.79	11.31	2.72	0.17	0.20	97.80	937.6
48.61	1.92	13.89	11.80	0.14	6.81	11.29	2.57	0.20	0.19	97.41	941.7
48.65	1.83	14.08	11.81	0.32	6.79	11.14	2.71	0.18	0.19	97.70	963.9
48.52	1.90	13.96	11.89	0.19	6.85	11.17	2.61	0.18	0.21	97.48	975.8
48.42	1.80	13.98	11.99	0.16	6.78	11.21	2.70	0.21	0.13	97.36	978.7
48.70	1.86	13.97	11.63	0.32	6.78	11.03	2.66	0.23	0.11	97.28	998.9
48.44	1.88	13.84	12.16	0.22	6.74	11.11	2.67	0.17	0.21	97.44	1014.0
48.24	1.85	13.85	12.21	0.28	6.92	11.32	2.59	0.20	0.19	97.65	1052.2

Exp 16

SiO2	TiO2	Al2O3	FeO	MnO	MgO	CaO	Na2O	K2O	P2O5	Total	d (um)
48.52	1.82	12.72	12.85	0.36	9.22	11.41	2.03	0.14	0.18	99.24	2.8
48.48	1.83	12.13	12.99	0.27	9.31	11.37	2.06	0.09	0.09	98.62	3.4
46.83	1.74	12.46	12.90	0.25	11.06	10.54	2.21	0.12	0.25	98.36	5.0
46.71	1.72	12.39	13.03	0.27	11.02	10.71	2.23	0.14	0.12	98.32	5.8
49.07	1.87	12.24	12.32	0.26	9.04	11.17	2.27	0.10	0.24	98.57	6.2
48.41	1.76	11.94	13.15	0.29	10.66	10.86	2.10	0.11	0.15	99.42	8.0
47.90	1.70	11.98	13.11	0.29	10.49	10.97	1.94	0.12	0.18	98.68	8.8
46.93	1.74	12.39	13.06	0.23	10.85	10.78	2.25	0.11	0.10	98.44	10.0
47.03	1.72	12.15	13.13	0.27	10.82	10.74	2.15	0.09	0.14	98.23	10.8
48.39	1.74	11.89	12.97	0.25	10.17	11.00	1.99	0.12	0.19	98.69	11.2
46.70	1.71	12.68	12.38	0.25	10.72	10.69	2.39	0.09	0.14	97.75	12.1
48.25	1.69	12.02	13.07	0.26	10.63	10.76	2.09	0.13	0.21	99.10	13.2
48.19	1.71	12.02	13.03	0.26	10.67	10.76	2.06	0.12	0.12	98.94	14.1
47.10	1.75	12.29	12.89	0.21	10.84	10.80	2.22	0.10	0.10	98.29	15.0
47.14	1.75	12.43	13.06	0.23	10.75	10.61	2.17	0.09	0.21	98.44	15.8
48.42	1.76	11.89	13.08	0.19	10.47	10.82	2.02	0.12	0.19	98.96	16.2
47.22	1.76	12.70	12.64	0.15	10.52	10.73	2.33	0.13	0.15	98.31	17.1
48.25	1.70	12.07	13.02	0.16	10.56	10.80	2.10	0.14	0.21	99.00	18.4
48.13	1.70	12.03	12.89	0.22	10.60	10.77	2.15	0.14	0.17	98.77	19.4
47.28	1.75	12.19	12.90	0.22	10.58	10.77	2.16	0.13	0.12	98.08	20.0
47.41	1.72	12.37	13.00	0.17	10.70	10.60	2.21	0.14	0.15	98.46	20.8
48.36	1.70	11.81	12.97	0.27	10.25	10.80	2.01	0.12	0.19	98.49	21.2
47.92	1.72	12.61	12.64	0.14	10.46	10.60	2.27	0.15	0.22	98.73	22.1
48.46	1.69	12.23	12.87	0.21	10.62	10.65	2.12	0.16	0.13	99.12	23.6
48.19	1.71	12.27	12.84	0.29	10.66	10.67	2.10	0.11	0.15	98.98	24.8
47.49	1.70	12.39	12.87	0.19	10.50	10.66	2.23	0.11	0.16	98.29	25.0
47.45	1.77	12.14	12.92	0.29	10.56	10.78	2.10	0.11	0.15	98.27	25.8
48.65	1.69	11.46	12.81	0.25	9.84	10.81	1.91	0.15	0.14	97.73	26.2
47.97	1.75	12.59	12.65	0.20	10.35	10.69	2.29	0.09	0.14	98.71	27.1
48.18	1.80	12.22	12.88	0.25	10.58	10.68	2.14	0.09	0.14	98.96	28.8
47.62	1.70	12.34	12.83	0.30	10.52	10.73	2.18	0.19	0.08	98.49	30.0
48.21	1.69	12.08	12.65	0.25	10.60	10.77	2.14	0.10	0.21	98.70	30.1
47.39	1.77	12.32	12.93	0.37	10.43	10.71	2.22	0.10	0.10	98.35	30.8
48.01	1.74	12.74	12.44	0.11	10.24	10.86	2.31	0.14	0.21	98.78	32.1
48.26	1.74	12.25	12.72	0.37	10.38	10.74	2.14	0.12	0.15	98.86	34.0
47.63	1.76	12.35	12.89	0.28	10.44	10.77	2.27	0.12	0.09	98.58	35.0
48.38	1.74	12.25	12.62	0.24	10.42	10.74	2.17	0.13	0.13	98.81	35.4
47.72	1.73	12.25	12.95	0.17	10.41	10.73	2.18	0.14	0.23	98.52	35.8
48.05	1.74	12.68	12.36	0.26	10.09	10.67	2.28	0.14	0.14	98.41	37.1
48.67	1.73	12.25	12.69	0.14	10.38	10.78	2.12	0.17	0.13	99.06	39.2
47.48	1.75	12.40	12.98	0.22	10.34	10.83	2.23	0.11	0.16	98.51	40.0
47.78	1.84	12.45	12.92	0.22	10.27	10.75	2.26	0.14	0.14	98.76	40.8
48.30	1.75	12.37	12.72	0.28	10.34	10.56	2.19	0.13	0.14	98.78	40.8
47.88	1.73	12.86	12.40	0.29	10.08	10.81	2.27	0.10	0.12	98.55	42.1
48.26	1.76	12.38	12.74	0.17	10.36	10.72	2.13	0.10	0.15	98.76	44.4
47.55	1.76	12.44	12.73	0.30	10.34	10.76	2.20	0.11	0.15	98.34	45.0
47.79	1.73	12.59	12.91	0.21	10.23	10.65	2.26	0.12	0.19	98.68	45.8

48.70	1.72	12.23	12.59	0.19	10.45	10.84	2.20	0.13	0.14	99.18	46.1
48.17	1.74	12.82	12.25	0.22	9.98	10.70	2.32	0.16	0.06	98.40	47.1
48.30	1.71	12.29	12.76	0.21	10.32	10.74	2.16	0.11	0.10	98.71	49.6
47.24	1.76	12.40	12.67	0.16	10.28	10.77	2.25	0.15	0.18	97.85	50.0
47.54	1.73	12.36	12.80	0.21	10.24	10.79	2.18	0.12	0.09	98.05	50.8
48.58	1.67	12.34	12.63	0.25	10.25	10.77	2.13	0.13	0.11	98.85	51.4
48.28	1.74	12.80	12.26	0.20	10.04	10.71	2.37	0.16	0.25	98.79	52.1
48.46	1.72	12.49	12.53	0.21	10.20	10.73	2.06	0.10	0.17	98.66	54.8
47.47	1.74	12.41	12.73	0.21	10.16	10.77	2.24	0.13	0.15	98.03	55.0
47.54	1.75	12.44	12.68	0.20	10.19	10.79	2.17	0.12	0.12	97.99	55.8
48.89	1.67	12.36	12.54	0.25	10.12	10.78	2.20	0.12	0.15	99.08	56.8
48.38	1.72	12.86	12.14	0.17	9.78	10.68	2.33	0.17	0.18	98.39	57.1
48.52	1.74	12.49	12.42	0.16	10.10	10.79	2.22	0.10	0.11	98.64	60.0
48.30	1.72	13.02	12.38	0.24	9.85	10.81	2.31	0.10	0.16	98.87	62.1
48.78	1.72	12.24	12.63	0.29	9.98	10.83	2.26	0.16	0.16	99.05	65.2
48.95	1.71	12.28	12.53	0.23	9.82	10.81	2.19	0.17	0.06	98.74	70.4
47.78	1.73	12.62	12.33	0.11	9.64	10.85	2.31	0.16	0.17	97.70	98.0
48.15	1.72	12.98	12.36	0.18	9.67	10.83	2.38	0.10	0.03	98.40	98.6
48.31	1.71	13.18	12.01	0.18	9.15	10.75	2.46	0.17	0.05	97.96	140.9
48.29	1.70	13.19	12.22	0.30	9.24	10.80	2.40	0.14	0.10	98.36	141.3
48.68	1.74	13.35	12.05	0.23	8.79	10.72	2.60	0.15	0.21	98.52	183.8
48.53	1.79	13.56	11.96	0.21	8.68	10.68	2.55	0.17	0.10	98.25	184.1
48.77	1.79	13.72	11.68	0.22	8.31	10.65	2.59	0.19	0.14	98.05	226.8
48.59	1.77	13.66	11.83	0.20	8.32	10.76	2.56	0.19	0.07	97.93	226.8
48.51	1.78	13.70	11.77	0.10	7.99	10.64	2.63	0.23	0.21	97.56	269.6
48.87	1.79	13.75	11.70	0.21	8.01	10.75	2.63	0.20	0.12	98.02	269.7
49.23	1.81	14.02	11.54	0.12	7.90	10.77	2.60	0.20	0.10	98.28	276.8
48.69	1.82	13.79	11.69	0.28	7.78	10.80	2.82	0.16	0.22	98.03	312.4
48.93	1.78	13.76	11.67	0.17	7.77	10.83	2.67	0.16	0.19	97.92	312.7
49.36	1.89	14.01	11.57	0.23	7.69	10.88	2.71	0.17	0.18	98.70	319.7
48.46	1.80	14.02	11.73	0.05	7.41	10.98	2.65	0.18	0.22	97.48	355.1
48.65	1.83	13.94	11.70	0.18	7.59	10.78	2.70	0.17	0.20	97.72	355.7
48.94	1.86	13.98	11.64	0.16	7.40	10.73	2.73	0.16	0.18	97.78	362.6
48.83	1.92	13.99	11.70	0.16	7.30	10.85	2.68	0.18	0.16	97.77	397.9
49.01	1.90	13.97	11.73	0.16	7.41	10.73	2.67	0.18	0.17	97.93	398.6
49.07	1.90	14.06	11.71	0.20	7.28	10.96	2.65	0.19	0.23	98.25	405.5
48.85	1.91	13.93	12.00	0.15	7.32	10.77	2.70	0.20	0.14	97.96	440.6
48.72	1.89	13.90	11.78	0.23	7.29	10.80	2.73	0.16	0.12	97.62	441.6
49.30	1.89	14.20	11.65	0.16	7.20	11.02	2.64	0.16	0.26	98.48	448.5
48.71	1.89	13.96	11.96	0.21	7.22	10.97	2.60	0.16	0.18	97.86	483.4
48.79	1.87	13.82	11.66	0.23	7.23	10.84	2.72	0.16	0.18	97.49	484.6
49.07	1.86	14.19	11.66	0.23	7.10	10.95	2.63	0.17	0.12	97.96	491.4
48.72	1.81	13.89	12.00	0.19	7.11	11.09	2.68	0.19	0.16	97.84	526.1
48.84	1.88	14.05	11.85	0.25	7.17	10.90	2.62	0.19	0.15	97.90	527.4
49.24	1.91	14.18	11.46	0.16	7.04	11.25	2.64	0.21	0.29	98.37	534.3
48.51	1.87	13.93	12.19	0.08	6.99	11.06	2.65	0.18	0.27	97.73	568.9
48.79	1.89	13.82	11.91	0.27	6.97	11.00	2.67	0.20	0.13	97.66	570.4
49.14	1.81	14.51	11.55	0.16	6.87	11.09	2.78	0.20	0.13	98.24	577.3
48.66	1.83	13.95	12.14	0.16	6.94	11.17	2.66	0.18	0.29	97.97	611.7

48.63	1.84	13.92	11.93	0.17	6.96	11.03	2.64	0.18	0.17	97.45	613.4
48.82	1.85	13.87	12.03	0.28	7.06	11.17	2.62	0.16	0.13	97.98	654.4
48.60	1.86	13.92	11.97	0.22	7.07	11.05	2.67	0.18	0.14	97.67	656.3
48.70	1.90	13.97	11.91	0.15	6.82	11.13	2.63	0.19	0.07	97.46	697.2
48.60	1.86	13.78	12.02	0.23	6.87	11.04	2.69	0.17	0.12	97.38	699.3
48.50	1.86	13.87	12.11	0.22	6.95	11.00	2.62	0.14	0.16	97.42	739.9
48.68	1.96	13.85	12.02	0.10	6.92	11.22	2.60	0.18	0.17	97.69	742.2
48.42	1.92	13.64	12.10	0.25	6.94	11.16	2.58	0.15	0.19	97.35	782.7
48.46	1.87	13.87	11.97	0.20	6.94	11.18	2.61	0.19	0.10	97.39	785.2
48.49	1.89	13.81	12.00	0.14	6.82	11.11	2.59	0.18	0.22	97.24	828.2
48.50	1.87	13.97	11.91	0.28	6.87	11.11	2.57	0.14	0.13	97.35	868.2
48.64	1.86	13.82	12.21	0.20	6.92	11.16	2.66	0.16	0.21	97.84	871.0
48.66	1.84	13.79	12.30	0.17	6.86	11.04	2.60	0.12	0.18	97.56	911.0
48.54	1.85	13.97	12.04	0.15	6.87	11.17	2.63	0.14	0.13	97.48	914.0
48.40	1.86	13.89	11.91	0.23	6.80	11.08	2.71	0.16	0.14	97.16	953.7
48.58	1.89	13.80	11.78	0.25	6.90	11.03	2.74	0.16	0.09	97.23	957.0
48.49	1.88	13.83	12.19	0.16	6.89	11.11	2.61	0.24	0.10	97.49	996.5
48.62	1.88	13.80	11.98	0.07	6.79	11.01	2.71	0.16	0.23	97.25	999.9
48.72	1.83	13.96	12.06	0.18	6.82	11.06	2.68	0.18	0.10	97.60	1039.2
48.69	1.88	13.97	12.01	0.13	6.87	11.00	2.63	0.16	0.08	97.43	1042.9
49.22	1.90	14.17	11.81	0.20	6.83	11.12	2.68	0.21	0.23	98.35	1049.5
48.28	1.84	13.82	11.85	0.25	6.80	11.10	2.70	0.16	0.26	97.06	1082.0
48.42	1.90	13.92	12.03	0.26	6.89	11.19	2.71	0.15	0.16	97.63	1085.9
49.27	1.88	14.13	11.84	0.14	6.70	11.15	2.67	0.17	0.19	98.14	1092.4
48.63	1.87	13.92	11.98	0.19	6.94	11.25	2.73	0.16	0.17	97.84	1124.8
48.58	1.88	13.96	11.85	0.22	6.80	11.16	2.58	0.18	0.04	97.25	1128.8
49.48	1.89	14.04	11.74	0.27	6.70	11.17	2.73	0.16	0.15	98.32	1135.4
48.89	1.88	14.01	11.82	0.23	6.85	11.16	2.60	0.19	0.09	97.71	1167.5
48.94	1.86	13.87	11.73	0.25	6.89	11.11	2.66	0.18	0.21	97.69	1171.7
49.30	1.89	14.04	11.66	0.19	6.74	11.05	2.77	0.16	0.10	97.91	1178.3
48.99	1.84	13.85	11.81	0.20	6.83	11.08	2.62	0.20	0.12	97.54	1210.3
48.97	1.81	13.84	11.88	0.20	6.80	11.12	2.60	0.15	0.16	97.54	1214.7
49.51	1.89	14.09	11.85	0.12	6.75	11.00	2.66	0.16	0.18	98.22	1221.2
49.29	1.87	13.82	11.76	0.33	6.81	11.12	2.57	0.20	0.12	97.88	1253.0
49.14	1.87	13.74	11.86	0.27	6.73	11.05	2.63	0.17	0.18	97.63	1257.6
49.64	1.85	14.06	11.69	0.22	6.78	10.97	2.60	0.16	0.15	98.11	1264.2

Exp 18

SiO2	TiO2	Al2O3	FeO	MnO	MgO	CaO	Na2O	K2O	P2O5	Total	d (um)
48.43	1.83	11.97	13.10	0.23	9.49	11.38	2.14	0.14	0.19	98.90	5.2
48.37	1.74	11.92	12.99	0.13	9.88	11.29	2.07	0.10	0.17	98.67	8.0
48.46	1.77	12.03	13.07	0.18	9.87	11.28	2.15	0.13	0.07	99.01	9.2
47.79	1.74	12.04	13.03	0.29	10.35	10.89	2.06	0.12	0.10	98.39	10.2
48.52	1.70	12.06	13.03	0.19	10.47	10.96	2.18	0.10	0.11	99.30	13.0
48.38	1.78	12.11	13.06	0.22	10.34	11.04	2.17	0.15	0.08	99.31	14.2
48.15	1.76	12.16	12.84	0.24	10.59	11.00	2.13	0.12	0.13	99.12	15.2
48.38	1.72	12.14	13.04	0.23	10.52	10.83	2.17	0.11	0.20	99.36	18.0
48.45	1.73	12.14	12.87	0.28	10.62	10.84	2.13	0.14	0.11	99.28	19.2
48.17	1.74	12.11	12.85	0.22	10.60	10.89	2.15	0.10	0.11	98.94	20.2
48.47	1.74	12.22	12.80	0.25	10.56	10.83	2.25	0.12	0.08	99.34	23.0
48.48	1.72	12.18	12.93	0.11	10.44	10.94	2.17	0.13	0.22	99.29	24.2
48.42	1.75	12.25	12.88	0.28	10.47	10.94	2.22	0.15	0.18	99.53	25.1
48.34	1.72	12.11	13.01	0.29	10.53	10.76	2.18	0.11	0.14	99.19	28.0
47.96	1.73	12.22	13.00	0.23	10.56	10.92	2.25	0.12	0.12	99.12	29.2
48.10	1.73	12.27	12.91	0.17	10.36	10.92	2.19	0.12	0.12	98.88	30.1
48.59	1.70	12.15	12.95	0.20	10.47	10.97	2.25	0.12	0.16	99.55	33.0
48.07	1.80	12.06	13.03	0.18	10.38	10.96	2.17	0.15	0.15	98.94	34.2
48.20	1.75	12.18	12.87	0.17	10.45	10.78	2.24	0.14	0.19	98.98	35.1
48.50	1.78	12.33	12.89	0.19	10.51	10.90	2.24	0.11	0.16	99.60	38.0
48.45	1.73	12.25	12.81	0.40	10.49	10.85	2.30	0.10	0.08	99.48	39.2
47.98	1.77	12.31	12.97	0.26	10.41	10.89	2.19	0.13	0.16	99.07	40.1
48.46	1.74	12.29	12.86	0.27	10.35	10.80	2.21	0.12	0.11	99.20	42.9
48.34	1.76	12.45	12.71	0.27	10.39	10.97	2.16	0.14	0.13	99.30	44.1
48.31	1.75	12.30	12.88	0.18	10.34	10.81	2.28	0.13	0.15	99.13	45.1
48.59	1.72	12.19	12.91	0.19	10.44	10.82	2.16	0.13	0.16	99.29	47.9
48.35	1.76	12.40	12.84	0.27	10.36	10.67	2.23	0.15	0.11	99.14	49.1
48.12	1.75	12.31	12.82	0.26	10.42	10.88	2.27	0.12	0.05	99.00	55.4
48.49	1.77	12.39	12.70	0.23	10.31	10.78	2.23	0.16	0.18	99.25	57.8
48.27	1.82	12.36	12.62	0.16	10.28	10.86	2.25	0.17	0.20	98.99	59.4
48.53	1.73	12.43	12.84	0.19	10.25	10.85	2.20	0.15	0.14	99.29	65.7
48.23	1.72	12.42	12.71	0.22	10.41	10.93	2.32	0.14	0.14	99.23	67.6
47.88	1.77	12.18	12.64	0.19	10.13	10.94	2.29	0.17	0.10	98.29	69.7
48.21	1.69	12.42	12.64	0.27	10.24	10.82	2.26	0.11	0.11	98.77	76.0
48.65	1.70	12.50	12.70	0.21	10.15	10.89	2.27	0.14	0.12	99.31	77.5
48.53	1.77	12.38	12.81	0.26	10.24	11.00	2.25	0.09	0.23	99.55	80.0
48.33	1.77	12.44	12.69	0.14	9.98	10.84	2.27	0.11	0.18	98.73	86.3
48.41	1.77	12.50	12.54	0.16	10.05	10.94	2.34	0.11	0.10	98.92	87.2
48.65	1.72	12.64	12.66	0.11	10.09	10.87	2.27	0.12	0.21	99.34	90.1
48.66	1.76	12.72	12.39	0.17	10.10	10.78	2.41	0.15	0.11	99.24	90.5
48.64	1.75	12.60	12.46	0.17	9.94	10.80	2.29	0.12	0.11	98.89	96.7
48.74	1.72	12.44	12.64	0.34	9.94	10.84	2.25	0.11	0.16	99.17	97.1
48.54	1.74	12.67	12.56	0.24	10.25	11.05	2.35	0.13	0.16	99.70	100.4
48.63	1.71	12.80	12.45	0.13	9.94	10.70	2.36	0.12	0.17	99.01	106.3
48.78	1.81	12.58	12.55	0.22	10.04	10.81	2.36	0.11	0.10	99.35	106.9
48.62	1.79	12.58	12.66	0.11	9.96	10.87	2.33	0.11	0.14	99.16	106.9
48.71	1.74	12.69	12.52	0.29	9.96	10.91	2.29	0.08	0.13	99.32	110.7

48.80	1.71	12.77	12.51	0.16	9.89	10.91	2.34	0.16	0.11	99.34	116.8
48.51	1.72	12.64	12.49	0.25	9.84	10.97	2.32	0.15	0.09	98.98	117.2
48.65	1.71	12.70	12.59	0.18	9.78	10.86	2.32	0.14	0.06	98.99	121.0
49.08	1.74	12.76	12.50	0.19	9.65	10.82	2.40	0.17	0.13	99.45	121.4
48.61	1.79	12.80	12.59	0.22	9.86	10.91	2.43	0.13	0.08	99.42	127.6
48.84	1.75	12.92	12.48	0.28	9.58	10.81	2.43	0.15	0.21	99.45	136.5
48.69	1.73	12.90	12.30	0.17	9.68	10.87	2.31	0.11	0.06	98.84	137.9
48.64	1.70	12.78	12.29	0.21	9.56	10.80	2.36	0.14	0.22	98.69	142.0
49.11	1.76	12.88	12.18	0.21	9.36	10.77	2.42	0.13	0.16	98.98	152.3
48.76	1.73	12.99	12.27	0.20	9.41	10.92	2.47	0.13	0.13	99.00	166.6
49.09	1.76	13.02	12.20	0.21	9.44	10.70	2.39	0.13	0.10	99.04	172.0
49.03	1.78	13.26	12.10	0.16	9.18	10.79	2.55	0.14	0.08	99.07	183.2
49.05	1.73	13.30	12.12	0.24	9.11	10.86	2.49	0.09	0.08	99.06	196.7
49.31	1.74	13.21	12.10	0.26	9.00	10.78	2.56	0.19	0.15	99.29	202.0
49.42	1.75	13.26	11.93	0.25	9.10	10.92	2.52	0.13	0.22	99.50	214.0
49.09	1.72	13.41	12.10	0.11	8.98	10.93	2.50	0.16	0.24	99.24	226.8
49.19	1.76	13.40	11.75	0.23	9.00	10.80	2.57	0.16	0.17	99.03	232.1
49.14	1.82	13.47	11.86	0.13	8.99	10.85	2.44	0.16	0.21	99.07	244.8
49.40	1.75	13.50	11.87	0.24	8.81	10.86	2.56	0.17	0.11	99.26	257.0
49.07	1.78	13.33	11.78	0.20	8.65	10.90	2.56	0.19	0.15	98.61	262.1
49.48	1.74	13.58	11.81	0.18	8.59	10.62	2.59	0.16	0.17	98.90	275.8
49.07	1.72	13.51	11.86	0.08	8.62	10.86	2.67	0.16	0.13	98.68	287.1
49.61	1.81	13.59	11.75	0.24	8.47	10.69	2.67	0.14	0.07	99.04	292.1
49.58	1.75	13.79	11.76	0.28	8.54	10.86	2.63	0.17	0.16	99.51	306.6
49.41	1.82	13.65	11.76	0.24	8.41	10.80	2.56	0.17	0.17	98.95	317.2
49.58	1.78	13.78	11.55	0.26	8.29	10.73	2.71	0.14	0.22	99.02	322.1
49.72	1.73	13.67	11.62	0.13	8.19	10.75	2.66	0.18	0.12	98.76	337.5
49.14	1.77	13.84	11.71	0.21	8.16	10.87	2.59	0.16	0.13	98.58	347.4
49.75	1.76	13.80	11.60	0.20	8.20	10.76	2.66	0.20	0.16	99.07	352.2
49.78	1.80	13.80	11.58	0.19	8.20	10.81	2.70	0.18	0.18	99.22	368.3
49.31	1.83	13.97	11.64	0.23	8.11	10.95	2.67	0.15	0.18	99.03	377.6
49.85	1.79	13.93	11.54	0.22	7.96	10.79	2.78	0.16	0.07	99.08	382.2
49.71	1.79	13.78	11.42	0.12	8.05	10.82	2.67	0.16	0.14	98.66	399.3
49.20	1.85	14.00	11.68	0.21	8.03	10.84	2.70	0.17	0.22	98.89	407.7
50.09	1.85	13.90	11.47	0.19	7.98	10.70	2.75	0.19	0.17	99.30	412.2
49.84	1.82	13.85	11.67	0.17	7.86	10.83	2.74	0.16	0.15	99.10	430.1
49.48	1.79	14.00	11.70	0.24	7.83	10.86	2.76	0.14	0.23	99.01	437.8
50.03	1.79	13.92	11.39	0.24	7.73	10.81	2.80	0.19	0.07	98.96	442.3
49.98	1.82	14.08	11.52	0.20	7.76	10.80	2.73	0.14	0.11	99.13	461.0
49.54	1.83	13.96	11.63	0.23	7.83	11.03	2.78	0.18	0.16	99.18	468.0
49.76	1.81	13.90	11.38	0.10	7.75	10.78	2.68	0.22	0.13	98.51	472.3
49.59	1.81	14.19	11.41	0.18	7.69	10.90	2.76	0.19	0.15	98.86	491.8
49.77	1.81	14.14	11.67	0.07	7.83	10.86	2.80	0.16	0.21	99.32	498.1
50.13	1.88	14.05	11.47	0.16	7.60	10.81	2.79	0.18	0.21	99.25	502.3
49.68	1.80	13.96	11.43	0.16	7.49	10.85	2.80	0.19	0.08	98.43	522.8
49.30	1.83	14.09	11.61	0.29	7.46	10.89	2.77	0.14	0.08	98.47	528.2
49.88	1.83	14.14	11.49	0.18	7.44	10.84	2.84	0.20	0.17	99.02	532.3
49.91	1.85	14.06	11.53	0.34	7.53	10.81	2.77	0.18	0.06	99.04	553.6
49.81	1.85	14.32	11.64	0.17	7.51	10.87	2.75	0.18	0.17	99.24	558.3

49.98	1.87	14.10	11.43	0.17	7.41	10.83	2.72	0.17	0.09	98.76	562.4
49.74	1.86	14.02	11.64	0.20	7.42	10.85	2.71	0.17	0.10	98.69	584.5
49.63	1.82	14.07	11.65	0.15	7.41	11.01	2.75	0.16	0.18	98.82	588.5
49.63	1.88	14.19	11.55	0.26	7.23	10.83	2.83	0.17	0.20	98.76	592.4
49.90	1.91	14.19	11.64	0.25	7.35	10.98	2.82	0.16	0.14	99.33	615.3
49.38	1.85	14.25	11.73	0.18	7.30	10.93	2.82	0.15	0.09	98.66	618.6
50.33	1.80	13.98	11.61	0.23	7.21	10.79	2.86	0.21	0.12	99.14	622.4
49.62	1.85	13.95	11.59	0.11	7.30	11.04	2.79	0.17	0.14	98.53	646.3
49.47	1.89	14.37	11.51	0.26	7.37	11.02	2.76	0.19	0.13	98.98	648.7
50.01	1.82	13.93	11.42	0.23	7.27	10.82	2.80	0.18	0.14	98.62	652.5
49.56	1.87	13.97	11.66	0.08	7.24	11.08	2.79	0.16	0.19	98.59	677.1
49.77	1.90	14.28	11.45	0.20	7.21	11.07	2.74	0.18	0.10	98.90	678.8
50.05	1.84	14.08	11.46	0.17	7.18	11.02	2.78	0.24	0.18	98.99	682.6
49.60	1.94	14.22	11.67	0.21	7.07	10.94	2.88	0.18	0.15	98.84	708.0
49.76	1.85	14.28	11.58	0.17	7.20	11.05	2.73	0.17	0.17	98.96	709.0
49.98	1.92	14.10	11.55	0.15	7.16	11.01	2.76	0.18	0.15	98.95	712.6
49.65	1.86	14.06	11.64	0.23	7.15	11.09	2.80	0.20	0.14	98.81	738.8
49.72	1.87	14.16	11.59	0.18	7.19	11.10	2.82	0.20	0.05	98.87	739.1
49.96	1.85	14.19	11.73	0.25	7.08	10.85	2.82	0.15	0.13	99.01	742.6
49.71	1.87	14.41	11.43	0.07	7.10	11.10	2.79	0.14	0.14	98.77	769.2
49.63	1.90	14.11	11.64	0.24	7.08	11.01	2.85	0.19	0.16	98.81	769.8
50.10	1.87	14.12	11.66	0.18	7.01	10.97	2.82	0.14	0.21	99.07	772.7
49.37	1.86	14.52	11.53	0.12	7.04	11.14	2.78	0.17	0.12	98.66	799.4
49.51	1.90	14.12	11.62	0.21	7.05	11.03	2.73	0.16	0.15	98.47	800.6
50.16	1.88	14.01	11.68	0.19	7.01	11.04	2.79	0.16	0.18	99.10	802.7
49.49	1.81	14.47	11.56	0.12	6.99	11.06	2.83	0.16	0.13	98.62	829.5
49.38	1.87	14.08	11.68	0.19	7.04	11.03	2.85	0.17	0.22	98.50	831.5
49.96	1.92	14.05	11.71	0.24	7.05	11.03	2.71	0.18	0.08	98.92	832.7
49.42	1.80	14.61	11.54	0.17	6.95	11.09	2.84	0.16	0.16	98.72	859.6
49.29	1.92	14.12	11.75	0.20	7.13	11.18	2.76	0.15	0.17	98.67	862.3
50.08	1.87	14.09	11.78	0.17	6.95	11.13	2.84	0.19	0.20	99.29	862.7
49.68	1.76	14.76	11.60	0.24	6.81	11.17	2.81	0.16	0.09	99.08	889.7
49.96	1.88	13.97	11.77	0.17	7.02	11.09	2.79	0.16	0.20	99.00	892.8
49.27	1.88	14.18	11.82	0.15	6.92	11.10	2.78	0.17	0.13	98.40	893.3
49.47	1.85	14.78	11.36	0.18	6.84	11.03	2.84	0.20	0.20	98.74	919.9
49.81	1.92	14.09	11.87	0.20	6.92	10.95	2.74	0.12	0.19	98.79	922.8
49.06	1.89	14.17	11.60	0.17	6.91	11.09	2.80	0.10	0.20	98.00	924.1
49.73	1.78	14.87	11.51	0.22	6.72	11.19	2.90	0.14	0.09	99.14	950.0
49.95	1.87	14.10	11.58	0.21	6.96	11.08	2.80	0.14	0.17	98.85	952.8
49.22	1.89	14.33	11.69	0.21	6.86	11.06	2.83	0.16	0.14	98.39	955.0
50.08	1.87	14.08	11.90	0.24	6.84	11.08	2.91	0.19	0.17	99.34	982.8
49.15	1.82	14.18	11.57	0.30	6.92	11.23	2.86	0.19	0.21	98.42	985.8
50.01	1.88	13.97	11.89	0.20	6.97	11.04	2.84	0.17	0.20	99.17	1012.9
49.41	1.82	14.53	11.58	0.20	6.79	11.11	2.72	0.13	0.18	98.46	1016.8
50.07	1.91	14.03	11.99	0.23	6.90	11.10	2.79	0.16	0.20	99.38	1042.9
49.15	1.88	14.46	11.58	0.22	6.84	11.15	2.78	0.18	0.21	98.44	1047.6
49.98	1.89	13.98	11.62	0.19	6.70	11.07	2.77	0.19	0.14	98.53	1072.9
49.93	1.86	14.02	11.76	0.28	6.78	11.15	2.83	0.15	0.11	98.87	1102.9
50.27	1.84	14.00	11.81	0.11	6.86	11.16	2.86	0.17	0.20	99.27	1133.0

50.07	1.91	13.97	11.87	0.16	6.87	11.22	2.80	0.20	0.20	99.25	1163.0
50.24	1.86	14.05	11.81	0.20	6.92	11.05	2.74	0.19	0.10	99.16	1193.0
49.90	1.84	14.02	11.89	0.21	6.84	11.08	2.71	0.19	0.13	98.79	1223.1
49.93	1.80	14.03	11.87	0.18	6.88	10.96	2.75	0.19	0.17	98.74	1253.1
50.07	1.88	13.91	11.88	0.24	6.81	11.18	2.79	0.18	0.12	99.06	1283.1

Exp 20

SiO2	TiO2	Al2O3	FeO	MnO	MgO	CaO	Na2O	K2O	P2O5	Total	d (um)
49.01	1.80	12.53	12.46	0.25	8.27	11.20	2.32	0.12	0.13	98.09	3.1
48.69	1.83	12.73	12.52	0.18	8.51	11.27	2.38	0.18	0.11	98.40	3.6
47.89	1.75	12.30	13.26	0.18	9.66	11.32	2.15	0.17	0.13	98.81	7.1
48.08	1.76	12.13	13.08	0.24	9.55	11.29	2.19	0.12	0.19	98.62	8.5
47.86	1.77	12.26	13.10	0.22	9.76	11.00	2.19	0.13	0.16	98.45	9.6
48.32	1.73	12.24	13.12	0.25	9.91	10.95	2.24	0.11	0.13	98.99	12.2
48.44	1.76	12.39	12.86	0.20	9.78	10.95	2.21	0.16	0.05	98.80	13.8
48.03	1.71	12.45	12.82	0.28	9.77	10.88	2.22	0.14	0.17	98.45	15.6
48.38	1.82	12.42	12.79	0.23	9.70	10.80	2.32	0.11	0.16	98.71	17.4
48.14	1.76	12.27	12.68	0.23	9.45	10.81	2.29	0.13	0.15	97.90	19.1
48.38	1.71	12.41	12.93	0.21	9.66	10.85	2.35	0.16	0.20	98.86	21.6
48.11	1.72	12.40	12.66	0.19	9.60	10.90	2.25	0.13	0.11	98.08	22.5
47.92	1.76	13.01	12.43	0.18	9.88	10.78	2.38	0.19	0.02	98.56	23.9
48.43	1.75	12.48	12.76	0.26	9.60	10.76	2.28	0.13	0.10	98.53	24.5
47.94	1.78	13.27	12.19	0.25	9.55	10.92	2.42	0.17	0.19	98.68	26.0
47.81	1.80	12.64	12.61	0.20	9.54	10.95	2.39	0.12	0.21	98.27	27.6
48.24	1.78	12.53	12.72	0.27	9.55	10.71	2.30	0.13	0.16	98.37	27.6
48.35	1.75	12.88	12.41	0.30	9.47	10.77	2.34	0.18	0.08	98.53	29.4
48.55	1.69	12.55	12.59	0.16	9.44	10.85	2.32	0.14	0.11	98.39	29.8
48.44	1.71	13.07	12.28	0.25	9.21	10.74	2.43	0.14	0.13	98.39	31.7
48.60	1.71	12.60	12.61	0.28	9.46	10.87	2.38	0.16	0.17	98.83	32.7
48.45	1.76	12.69	12.53	0.30	9.43	10.76	2.43	0.16	0.11	98.61	33.5
48.19	1.72	13.56	12.11	0.23	9.15	10.79	2.65	0.14	0.17	98.71	33.7
48.43	1.75	13.13	12.33	0.15	9.32	10.97	2.45	0.15	0.14	98.82	34.9
48.67	1.75	12.67	12.39	0.17	9.34	10.86	2.28	0.20	0.12	98.44	35.1
47.91	1.68	13.35	12.11	0.17	9.41	10.71	2.53	0.18	0.10	98.14	35.5
48.84	1.78	13.15	12.24	0.19	8.94	10.73	2.45	0.12	0.14	98.58	37.2
48.74	1.70	12.75	12.39	0.31	9.23	10.85	2.43	0.15	0.10	98.65	37.8
48.47	1.75	12.92	12.52	0.28	9.20	10.75	2.42	0.14	0.20	98.64	39.5
48.44	1.80	13.04	12.29	0.26	9.20	10.83	2.41	0.11	0.17	98.54	40.4
48.90	1.75	12.73	12.42	0.29	9.22	10.81	2.34	0.21	0.13	98.78	40.5
49.28	1.74	12.80	12.34	0.37	8.99	10.79	2.40	0.11	0.22	99.03	42.9
48.38	1.76	13.26	12.11	0.20	8.82	10.85	2.49	0.21	0.15	98.22	42.9
48.47	1.75	13.01	12.36	0.30	9.13	10.80	2.41	0.15	0.21	98.59	45.5
49.78	1.74	12.57	12.27	0.29	8.67	10.96	2.30	0.17	0.17	98.91	45.8
49.03	1.76	13.07	12.02	0.24	8.99	10.85	2.49	0.19	0.14	98.77	45.9
48.32	1.74	13.68	12.04	0.19	8.79	10.72	2.61	0.16	0.13	98.37	47.2
48.62	1.85	13.57	12.10	0.22	8.83	10.85	2.51	0.15	0.17	98.86	48.6
48.42	1.76	13.19	12.05	0.24	8.90	10.85	2.49	0.18	0.19	98.25	51.4
49.03	1.73	12.86	12.20	0.29	8.78	10.86	2.37	0.14	0.25	98.51	51.5
48.81	1.77	13.51	11.97	0.25	8.73	10.86	2.52	0.15	0.21	98.78	54.2
49.50	1.78	13.27	11.89	0.29	8.63	10.74	2.43	0.22	0.15	98.89	56.9
48.86	1.75	13.36	11.91	0.16	8.44	10.78	2.57	0.14	0.15	98.11	59.9
49.16	1.75	13.57	11.86	0.18	8.43	10.76	2.64	0.18	0.13	98.66	65.6
49.06	1.78	13.72	11.80	0.21	8.37	10.68	2.69	0.16	0.17	98.64	65.7
49.11	1.77	13.73	11.88	0.29	8.31	10.77	2.62	0.22	0.13	98.82	67.4
49.27	1.85	13.54	11.83	0.21	8.16	10.71	2.58	0.19	0.16	98.49	71.2

49.45	1.82	13.52	11.75	0.12	8.08	10.79	2.58	0.16	0.21	98.47	76.9
49.08	1.80	13.85	11.91	0.19	7.96	10.88	2.70	0.18	0.19	98.74	78.5
49.22	1.79	13.88	11.78	0.23	7.89	10.77	2.73	0.16	0.09	98.53	97.7
49.16	1.80	14.00	11.85	0.27	7.82	10.72	2.76	0.19	0.12	98.69	99.4
49.05	1.83	14.05	11.85	0.26	7.69	10.75	2.74	0.22	0.13	98.57	109.8
49.15	1.84	14.14	11.62	0.23	7.47	11.00	2.81	0.17	0.24	98.67	129.7
49.01	1.85	13.90	11.81	0.19	7.42	10.84	2.79	0.19	0.14	98.15	131.3
49.11	1.88	13.91	11.73	0.22	7.45	10.90	2.76	0.14	0.16	98.26	141.0
49.02	1.80	13.89	11.77	0.21	7.26	10.91	2.70	0.18	0.16	97.88	161.7
49.11	1.83	14.15	11.82	0.25	7.08	11.06	2.70	0.15	0.14	98.30	163.3
49.28	1.89	13.87	11.83	0.26	7.09	10.93	2.76	0.19	0.20	98.30	172.2
49.30	1.86	13.91	11.87	0.26	7.02	10.92	2.82	0.18	0.09	98.22	193.7
49.47	1.86	13.97	11.85	0.29	7.11	10.98	2.67	0.19	0.05	98.44	195.2
49.12	1.90	13.85	11.79	0.13	7.05	11.00	2.75	0.19	0.17	97.94	203.5
49.18	1.89	13.99	12.01	0.13	6.89	11.04	2.72	0.17	0.10	98.11	225.7
49.25	1.86	14.09	12.14	0.21	7.02	11.07	2.84	0.20	0.08	98.75	227.2
49.20	1.81	14.11	11.95	0.26	6.99	11.04	2.76	0.19	0.09	98.39	234.8
49.27	1.85	13.94	12.06	0.25	6.91	11.19	2.77	0.21	0.20	98.64	257.7
49.38	1.91	14.04	12.37	0.22	6.95	11.03	2.80	0.24	0.11	99.05	259.1
48.99	1.84	14.12	12.07	0.29	6.91	11.14	2.74	0.15	0.12	98.36	266.1
49.30	1.84	13.94	12.09	0.19	6.86	11.10	2.73	0.14	0.14	98.32	289.6
49.39	1.81	13.89	12.14	0.23	6.86	11.15	2.82	0.18	0.18	98.64	291.1
49.06	1.82	14.05	11.88	0.27	6.83	11.25	2.73	0.18	0.06	98.13	297.4
49.07	1.86	13.92	12.11	0.18	6.99	11.17	2.66	0.16	0.20	98.31	321.6
49.22	1.83	13.82	12.03	0.26	6.79	11.16	2.72	0.19	0.18	98.20	323.0
49.11	1.89	13.98	12.00	0.12	6.91	11.15	2.66	0.14	0.23	98.18	328.6
48.83	1.81	14.04	12.05	0.24	6.85	11.11	2.86	0.19	0.16	98.15	353.6
49.08	1.90	13.86	12.11	0.32	6.90	11.16	2.71	0.15	0.15	98.34	355.0
49.24	1.93	13.84	12.05	0.23	6.79	11.25	2.79	0.18	0.11	98.40	359.9
48.69	1.85	14.00	12.13	0.27	6.95	11.19	2.71	0.16	0.14	98.09	385.6
49.32	1.84	13.87	12.14	0.15	6.77	11.16	2.76	0.21	0.19	98.40	386.9
49.19	1.84	14.07	12.16	0.24	6.91	11.16	2.75	0.14	0.17	98.62	391.1
48.82	1.88	13.92	12.14	0.26	6.87	11.04	2.72	0.19	0.17	97.99	417.6
49.07	1.81	13.90	12.11	0.18	6.80	11.11	2.80	0.19	0.14	98.11	418.9
49.41	1.86	13.88	12.04	0.28	6.91	11.06	2.76	0.17	0.14	98.50	422.4
48.83	1.91	13.83	12.11	0.19	6.85	11.18	2.69	0.17	0.13	97.89	449.6
49.44	1.93	13.92	12.15	0.19	6.84	11.06	2.75	0.19	0.07	98.54	450.8
48.98	1.89	14.02	12.08	0.17	6.86	11.21	2.71	0.18	0.19	98.29	453.7
48.94	1.84	13.98	12.13	0.32	6.76	11.16	2.76	0.19	0.17	98.24	481.6
49.06	1.87	13.93	12.23	0.16	6.91	11.16	2.75	0.19	0.14	98.39	482.8
48.89	1.84	13.97	12.17	0.16	6.89	11.14	2.72	0.21	0.24	98.25	485.0
48.88	1.85	14.00	12.10	0.25	6.91	11.21	2.80	0.17	0.12	98.28	513.6
49.21	1.87	14.03	12.17	0.19	6.80	11.13	2.72	0.21	0.24	98.55	514.7
48.79	1.93	14.04	12.12	0.31	6.86	11.16	2.70	0.14	0.10	98.15	516.2
48.71	1.91	13.97	12.11	0.29	6.92	11.16	2.72	0.16	0.14	98.09	545.5
49.42	1.91	13.85	12.14	0.23	6.84	11.06	2.72	0.18	0.24	98.57	546.7
49.16	1.82	14.00	12.04	0.18	6.84	11.21	2.73	0.17	0.23	98.37	547.5
48.96	1.87	14.06	12.21	0.23	6.83	11.16	2.77	0.19	0.19	98.46	577.5
49.49	1.87	13.98	12.03	0.22	6.80	11.15	2.71	0.20	0.16	98.59	578.6

48.87	1.87	14.03	12.11	0.17	6.86	11.10	2.70	0.16	0.16	98.01	578.8
48.93	1.84	14.02	12.03	0.15	6.80	11.23	2.73	0.22	0.17	98.10	609.5
48.97	1.90	14.05	12.21	0.25	6.79	11.06	2.70	0.13	0.17	98.24	610.1
49.33	1.86	13.83	12.14	0.09	6.79	11.15	2.71	0.18	0.09	98.18	610.6
49.09	1.83	14.01	12.30	0.22	6.91	11.05	2.70	0.17	0.13	98.41	641.3
48.79	1.91	14.07	12.31	0.16	6.88	11.11	2.71	0.17	0.08	98.19	641.5
49.29	1.84	14.01	12.04	0.29	6.72	11.07	2.74	0.18	0.11	98.30	642.5
49.01	1.89	13.97	12.11	0.19	6.95	11.12	2.77	0.21	0.20	98.41	672.5
48.91	1.87	14.04	11.98	0.25	6.70	11.01	2.69	0.18	0.08	97.70	673.5
49.52	1.88	14.04	12.19	0.23	6.88	11.14	2.66	0.21	0.24	99.01	674.5
48.67	1.89	13.92	12.13	0.23	6.84	11.23	2.73	0.15	0.21	98.00	703.8
48.75	1.84	13.90	12.16	0.10	6.80	11.21	2.68	0.23	0.19	97.85	705.5
48.97	1.88	14.05	11.98	0.23	6.75	11.18	2.78	0.23	0.15	98.19	706.4
48.78	1.88	13.89	12.16	0.24	6.84	11.21	2.77	0.17	0.09	98.01	735.1
49.02	1.90	13.88	12.11	0.20	6.89	11.14	2.76	0.17	0.07	98.14	737.5
49.19	1.80	13.86	12.05	0.24	6.93	11.17	2.78	0.18	0.13	98.31	738.4
49.00	1.86	13.84	12.16	0.16	6.80	11.19	2.69	0.17	0.25	98.10	766.4
48.90	1.86	13.95	12.04	0.21	6.79	11.06	2.70	0.16	0.13	97.81	769.5
48.88	1.87	14.02	11.79	0.25	6.82	11.11	2.79	0.19	0.28	98.00	770.3
49.27	1.83	13.86	12.15	0.24	6.84	11.14	2.75	0.18	0.16	98.42	797.7
48.78	1.83	13.98	12.07	0.24	6.94	11.16	2.73	0.16	0.17	98.05	801.4
49.66	1.86	13.90	11.75	0.21	6.71	11.04	2.82	0.20	0.13	98.29	802.3
49.01	1.89	13.88	12.26	0.12	6.84	11.11	2.60	0.15	0.18	98.05	829.0
48.90	1.93	13.94	11.97	0.23	6.78	11.15	2.68	0.17	0.19	97.91	833.4
49.17	1.85	13.92	12.07	0.15	6.87	11.18	2.78	0.16	0.19	98.35	834.2
48.95	1.89	13.98	12.14	0.26	6.84	11.14	2.73	0.15	0.15	98.23	860.2
48.75	1.85	14.06	12.09	0.18	6.91	11.26	2.81	0.18	0.17	98.26	865.4
48.91	1.84	13.96	12.11	0.19	7.01	11.18	2.73	0.17	0.25	98.36	866.2
49.10	1.85	13.96	12.31	0.20	6.90	11.10	2.61	0.19	0.13	98.35	891.4
48.71	1.88	13.93	12.08	0.13	6.77	11.16	2.69	0.19	0.14	97.68	897.4
49.46	1.90	13.94	12.15	0.31	6.85	11.03	2.70	0.17	0.29	98.79	898.1
48.69	1.83	13.82	12.17	0.14	6.86	11.23	2.68	0.21	0.23	97.84	922.7
48.76	1.90	14.00	12.33	0.18	6.79	11.20	2.73	0.19	0.13	98.20	929.4
48.79	1.89	13.86	12.16	0.22	6.85	11.11	2.65	0.17	0.22	97.91	930.1
49.09	1.88	13.86	12.17	0.19	6.87	11.13	2.75	0.21	0.17	98.33	954.0
49.13	1.87	13.94	12.11	0.27	6.87	11.21	2.65	0.17	0.11	98.31	961.4
49.37	1.90	13.87	12.20	0.19	6.88	11.17	2.75	0.12	0.08	98.52	962.0
48.70	1.85	13.85	12.21	0.25	6.90	11.18	2.69	0.18	0.17	97.98	985.3
48.94	1.86	14.01	12.19	0.19	6.86	11.24	2.80	0.18	0.14	98.40	993.4
49.62	1.87	13.88	12.33	0.28	6.79	11.18	2.71	0.19	0.21	99.06	994.0
48.71	1.87	13.89	12.25	0.25	6.89	11.13	2.66	0.17	0.19	98.00	1016.5
48.71	1.88	13.86	12.19	0.30	6.92	11.15	2.68	0.16	0.05	97.92	1025.4
49.53	1.85	13.78	12.19	0.22	6.78	11.15	2.68	0.20	0.15	98.52	1025.9
49.20	1.83	13.94	12.28	0.24	6.91	11.29	2.60	0.18	0.12	98.58	1047.8
49.13	1.87	13.87	12.24	0.20	6.89	11.20	2.73	0.19	0.26	98.58	1057.3
49.18	1.87	13.88	12.13	0.28	6.82	11.24	2.70	0.17	0.12	98.37	1057.9
49.00	1.85	13.97	12.34	0.23	6.90	11.19	2.68	0.13	0.06	98.34	1079.1
48.98	1.85	13.96	12.23	0.19	6.75	11.27	2.64	0.20	0.18	98.26	1089.3
49.09	1.88	13.85	12.15	0.18	6.83	11.22	2.61	0.17	0.14	98.12	1089.8

49.38	1.88	13.93	12.08	0.21	6.84	11.33	2.64	0.21	0.15	98.65	1110.4
49.15	1.90	13.95	12.26	0.19	6.89	11.21	2.74	0.15	0.27	98.70	1121.3
48.97	1.86	13.97	12.23	0.13	6.84	11.13	2.67	0.19	0.18	98.16	1121.8
49.02	1.91	13.96	12.08	0.33	7.01	11.19	2.66	0.18	0.08	98.40	1141.7
48.97	1.93	14.07	11.99	0.27	6.85	11.32	2.62	0.13	0.17	98.30	1153.3
49.30	1.90	14.08	12.17	0.29	6.92	11.11	2.64	0.16	0.17	98.72	1153.7
49.70	1.85	13.93	11.98	0.21	6.89	11.22	2.67	0.17	0.25	98.87	1172.9
49.05	1.84	13.88	12.07	0.12	6.88	11.10	2.60	0.17	0.15	97.85	1185.3
49.37	1.87	13.92	12.19	0.23	6.97	11.14	2.67	0.17	0.18	98.70	1185.7
49.54	1.91	13.95	11.91	0.16	6.87	11.11	2.65	0.18	0.11	98.41	1204.1
49.32	1.88	14.10	11.84	0.21	6.74	11.18	2.65	0.16	0.20	98.28	1217.3
49.43	1.89	13.90	11.77	0.14	6.79	11.16	2.60	0.19	0.18	98.04	1217.6
49.95	1.90	13.98	11.63	0.25	6.75	11.10	2.71	0.15	0.12	98.52	1235.4
49.86	1.92	13.92	11.47	0.18	6.74	10.93	2.70	0.19	0.16	98.07	1249.3
49.62	1.86	14.06	11.50	0.21	6.66	11.00	2.77	0.24	0.07	98.00	1249.6
50.76	1.89	13.39	11.17	0.28	6.27	11.06	2.59	0.21	0.27	97.88	1266.7
51.38	1.83	13.36	11.13	0.22	6.25	11.05	2.73	0.21	0.13	98.28	1281.3
51.03	1.81	13.68	11.16	0.25	6.27	11.02	2.66	0.21	0.15	98.24	1281.5

Exp 21

SiO2	TiO2	Al2O3	FeO	MnO	MgO	CaO	Na2O	K2O	P2O5	Total	d (um)
48.68	1.77	12.28	12.40	0.20	10.50	10.66	2.43	0.12	0.18	99.21	0.2
48.31	1.47	11.06	12.72	0.25	15.17	9.08	2.10	0.15	0.21	100.53	0.5
48.57	1.78	11.95	13.23	0.16	9.95	11.24	1.95	0.10	0.17	99.08	5.6
47.84	1.78	11.84	13.45	0.23	10.53	10.94	2.12	0.11	0.08	98.91	5.7
47.85	1.78	11.83	13.64	0.24	10.22	11.05	2.02	0.14	0.09	98.86	5.9
46.12	1.64	11.35	12.82	0.20	10.38	10.30	2.01	0.11	0.05	94.99	11.2
47.86	1.68	11.81	13.41	0.22	10.98	10.68	2.07	0.14	0.12	98.97	11.3
48.20	1.66	11.82	13.36	0.20	10.92	10.83	2.03	0.12	0.11	99.24	11.7
47.98	1.70	11.99	13.36	0.26	10.89	10.62	2.11	0.13	0.11	99.14	16.4
47.94	1.73	11.96	13.21	0.27	11.02	10.80	2.16	0.14	0.14	99.36	16.8
48.17	1.69	11.82	13.29	0.26	10.91	10.67	2.10	0.14	0.18	99.24	17.9
47.95	1.71	12.01	13.22	0.34	10.88	10.54	2.15	0.12	0.18	99.10	21.8
48.05	1.71	12.05	13.21	0.26	10.86	10.65	2.13	0.13	0.13	99.17	22.4
48.19	1.74	12.08	13.26	0.25	11.00	10.74	2.07	0.13	0.20	99.66	24.0
48.16	1.73	11.99	13.28	0.23	10.87	10.55	2.16	0.15	0.16	99.27	27.1
47.91	1.70	12.24	12.84	0.28	10.86	10.61	2.18	0.15	0.21	98.97	27.9
48.09	1.74	11.94	13.13	0.17	10.74	10.68	2.18	0.11	0.12	98.88	30.1
48.14	1.70	12.22	12.99	0.18	10.85	10.57	2.23	0.13	0.15	99.14	32.4
48.04	1.71	12.18	13.01	0.21	10.87	10.62	2.20	0.11	0.15	99.08	33.5
47.86	1.69	12.21	13.03	0.27	10.82	10.66	2.25	0.08	0.09	98.97	36.2
48.12	1.76	12.14	13.05	0.25	10.76	10.60	2.24	0.13	0.15	99.18	37.8
47.68	1.75	12.37	12.74	0.22	10.75	10.67	2.27	0.14	0.07	98.65	38.3
48.34	1.71	12.25	13.00	0.18	10.69	10.55	2.18	0.16	0.14	99.19	39.1
47.88	1.76	12.35	12.93	0.23	10.68	10.57	2.16	0.12	0.17	98.85	40.2
47.54	1.71	12.42	12.87	0.24	10.63	10.64	2.32	0.13	0.08	98.58	41.8
48.33	1.72	12.29	13.02	0.19	10.62	10.55	2.25	0.15	0.11	99.24	42.3
48.77	1.77	12.21	12.96	0.22	10.58	10.66	2.11	0.11	0.18	99.57	43.1
48.60	1.69	12.21	12.90	0.26	10.45	10.59	2.24	0.15	0.18	99.25	44.6
48.56	1.71	12.26	12.84	0.27	10.54	10.62	2.22	0.13	0.12	99.29	48.4
48.77	1.70	12.87	12.56	0.17	10.04	10.64	2.33	0.14	0.12	99.35	68.2
47.65	1.70	12.73	12.79	0.22	10.10	10.58	2.36	0.17	0.15	98.45	70.2
48.31	1.74	12.81	12.43	0.25	9.85	10.70	2.33	0.13	0.11	98.64	71.7
48.74	1.69	13.17	12.14	0.13	9.29	10.76	2.57	0.18	0.17	98.84	98.1
48.76	1.70	13.12	12.43	0.18	9.58	10.58	2.47	0.18	0.20	99.19	100.1
48.26	1.75	13.20	12.27	0.25	9.30	10.66	2.42	0.16	0.15	98.43	101.7
49.38	1.73	13.52	11.95	0.12	8.72	10.68	2.61	0.15	0.18	99.02	127.9
48.55	1.70	13.33	12.29	0.23	9.05	10.80	2.52	0.14	0.25	98.86	130.1
48.83	1.72	13.54	11.82	0.25	8.87	10.43	2.53	0.16	0.16	98.29	131.6
48.99	1.80	13.90	11.88	0.18	8.39	10.55	2.58	0.19	0.12	98.57	157.8
48.93	1.75	13.77	11.89	0.21	8.43	10.71	2.64	0.18	0.11	98.61	160.0
48.93	1.78	13.75	11.80	0.17	8.40	10.61	2.67	0.19	0.15	98.45	161.6
49.90	1.85	14.08	11.56	0.16	7.80	10.67	2.75	0.20	0.09	99.06	187.7
49.39	1.82	13.81	11.88	0.22	8.29	10.60	2.62	0.19	0.19	99.00	190.0
49.25	1.84	13.94	11.70	0.21	8.08	10.62	2.73	0.18	0.12	98.66	191.5
50.06	1.80	13.98	11.95	0.19	7.78	10.67	2.66	0.24	0.09	99.41	217.6
49.07	1.78	13.88	11.90	0.14	7.96	10.65	2.73	0.21	0.21	98.52	219.9
49.24	1.82	13.95	11.77	0.15	7.85	10.69	2.72	0.20	0.31	98.70	221.5

49.56	1.84	14.12	11.69	0.15	7.56	10.77	2.71	0.22	0.22	98.84	247.5
49.22	1.84	13.97	11.83	0.24	7.62	10.68	2.75	0.19	0.08	98.43	249.9
49.53	1.89	14.18	11.78	0.08	7.63	10.69	2.69	0.20	0.15	98.80	251.4
49.49	1.88	14.06	11.80	0.19	7.47	10.79	2.75	0.24	0.09	98.76	277.3
49.04	1.87	14.16	11.87	0.19	7.48	10.75	2.81	0.23	0.06	98.47	279.8
49.38	1.87	14.02	11.84	0.17	7.49	10.78	2.71	0.17	0.12	98.55	281.4
49.61	1.83	14.03	11.81	0.12	7.38	10.91	2.71	0.21	0.19	98.79	307.2
49.34	1.84	13.91	11.96	0.18	7.39	10.84	2.80	0.20	0.23	98.68	309.8
49.23	1.85	14.10	11.87	0.25	7.23	10.87	2.65	0.17	0.20	98.43	311.3
49.41	1.86	14.00	12.14	0.29	7.32	11.03	2.75	0.19	0.17	99.13	337.1
49.25	1.90	14.04	12.09	0.16	7.24	10.99	2.77	0.20	0.15	98.77	339.7
49.21	1.86	14.10	12.02	0.21	7.26	10.96	2.77	0.21	0.18	98.78	341.3
49.58	1.87	13.97	12.10	0.29	7.14	10.96	2.78	0.18	0.12	98.99	367.0
49.24	1.83	13.91	12.00	0.26	7.18	10.88	2.76	0.14	0.10	98.30	369.7
49.22	1.88	13.98	11.97	0.26	7.11	11.02	2.76	0.18	0.19	98.55	371.2
49.60	1.88	14.01	12.09	0.17	7.00	10.98	2.72	0.15	0.28	98.88	396.8
49.09	1.89	13.90	12.06	0.24	7.16	10.95	2.72	0.18	0.17	98.34	399.6
49.36	1.87	14.23	11.90	0.18	7.08	10.92	2.78	0.19	0.17	98.67	401.2
49.67	1.81	14.02	12.23	0.23	7.03	11.06	2.65	0.17	0.14	99.00	426.7
49.30	1.85	14.11	12.27	0.25	7.10	11.11	2.80	0.15	0.18	99.11	429.6
49.06	1.87	14.09	11.97	0.24	7.06	11.10	2.76	0.17	0.24	98.56	431.1
49.21	1.88	14.05	12.23	0.17	7.03	11.08	2.72	0.15	0.21	98.73	456.6
49.44	1.84	13.87	12.21	0.21	7.02	11.10	2.67	0.19	0.18	98.74	459.5
48.89	1.87	14.17	12.10	0.18	6.94	11.02	2.77	0.17	0.14	98.26	461.1
49.44	1.84	14.15	12.35	0.27	7.12	11.08	2.71	0.21	0.13	99.30	486.5
48.79	1.85	14.09	12.14	0.12	6.97	11.13	2.83	0.16	0.08	98.16	489.5
49.25	1.97	14.17	12.25	0.16	7.02	11.05	2.68	0.18	0.19	98.90	491.0
49.10	1.87	13.98	12.21	0.31	7.01	10.94	2.76	0.19	0.23	98.58	543.7
49.68	1.88	14.14	12.19	0.19	6.99	11.14	2.64	0.17	0.21	99.22	545.8
49.08	1.86	13.90	12.20	0.20	6.88	11.15	2.67	0.15	0.18	98.25	546.4
49.08	1.82	14.19	12.24	0.25	7.07	11.10	2.61	0.21	0.31	98.87	596.3
48.98	1.84	13.94	12.29	0.29	6.90	11.17	2.67	0.21	0.21	98.47	603.3
49.76	1.91	14.02	12.46	0.23	6.95	11.12	2.74	0.18	0.16	99.51	605.3
49.03	1.83	14.17	12.15	0.19	6.95	11.09	2.62	0.19	0.19	98.41	648.9
48.59	1.86	13.89	12.32	0.30	6.97	11.21	2.76	0.22	0.14	98.25	660.2
49.78	1.88	14.02	12.19	0.21	6.98	11.11	2.69	0.18	0.20	99.23	664.7
49.47	1.87	14.00	12.07	0.17	6.95	11.17	2.65	0.20	0.12	98.66	701.6
48.70	1.94	13.94	12.45	0.21	6.84	11.09	2.67	0.23	0.13	98.19	717.1
49.59	1.84	14.11	12.30	0.19	7.00	11.05	2.63	0.17	0.22	99.11	724.1
49.65	1.85	13.92	12.27	0.24	6.94	11.12	2.67	0.21	0.16	99.03	754.2
49.47	1.87	13.86	12.35	0.24	6.84	11.10	2.74	0.17	0.19	98.84	774.0
49.39	1.87	14.08	12.34	0.15	7.00	11.03	2.72	0.16	0.15	98.89	783.5
49.71	1.87	14.07	12.13	0.25	6.95	11.15	2.64	0.18	0.18	99.13	806.8
49.20	1.85	13.98	12.20	0.15	6.83	11.22	2.68	0.19	0.18	98.48	830.9
49.72	1.88	13.99	12.31	0.20	7.01	11.09	2.79	0.19	0.22	99.39	842.9
49.48	1.85	13.89	12.19	0.24	6.89	11.06	2.62	0.22	0.11	98.56	859.4
48.92	1.82	13.99	12.35	0.23	6.88	11.20	2.71	0.19	0.14	98.45	887.8
49.83	1.87	13.88	12.34	0.31	6.98	11.15	2.70	0.17	0.23	99.45	902.3
49.02	1.85	14.05	12.07	0.16	6.92	11.16	2.74	0.17	0.16	98.30	912.0

49.12	1.93	13.91	12.25	0.25	6.85	11.16	2.68	0.20	0.13	98.48	944.7
49.74	1.86	14.07	12.34	0.17	6.99	11.14	2.72	0.19	0.15	99.37	961.6
49.15	1.86	14.18	12.13	0.21	6.91	11.09	2.68	0.20	0.12	98.54	964.7
49.20	1.83	13.94	12.25	0.21	6.82	11.06	2.71	0.19	0.15	98.36	1001.6
49.45	1.96	14.09	12.05	0.23	6.96	11.07	2.65	0.17	0.18	98.80	1017.3
49.65	1.84	14.10	12.21	0.11	7.03	11.11	2.62	0.20	0.12	98.99	1021.1
49.06	1.91	14.07	12.21	0.21	6.94	11.16	2.71	0.19	0.21	98.66	1058.5
49.11	1.95	14.02	12.07	0.30	7.00	11.03	2.76	0.17	0.21	98.62	1070.0
49.82	1.91	13.96	12.11	0.16	7.00	11.22	2.67	0.18	0.09	99.11	1080.5
49.42	1.90	13.88	12.19	0.20	6.92	11.16	2.72	0.18	0.14	98.70	1115.4
50.00	1.89	14.15	12.14	0.17	6.85	11.02	2.70	0.18	0.15	99.25	1122.6
49.77	1.92	14.10	12.21	0.23	7.00	11.07	2.65	0.21	0.17	99.32	1139.9
49.26	1.88	13.88	12.08	0.28	6.81	11.19	2.69	0.19	0.19	98.46	1172.3
49.53	1.87	14.11	11.98	0.10	6.82	11.01	2.73	0.19	0.21	98.54	1175.2
49.56	1.82	14.24	11.98	0.24	6.95	11.15	2.61	0.17	0.26	98.98	1199.3
49.77	1.88	14.00	11.90	0.18	6.79	10.96	2.77	0.20	0.15	98.60	1227.8
50.03	1.88	13.99	11.93	0.27	6.84	11.13	2.66	0.22	0.18	99.12	1229.3
50.37	1.88	14.11	11.88	0.20	6.90	10.91	2.70	0.20	0.17	99.34	1258.7
50.32	1.87	13.88	11.74	0.17	6.71	11.00	2.70	0.19	0.18	98.75	1286.2
50.63	1.82	14.14	11.49	0.19	6.81	10.85	2.75	0.15	0.18	99.02	1318.1

Exp 22

SiO2	TiO2	Al2O3	FeO	MnO	MgO	CaO	Na2O	K2O	P2O5	Total	d (um)
48.46	1.84	13.04	12.12	0.15	9.13	10.85	2.39	0.21	0.22	98.40	2.7
48.36	1.78	13.32	12.36	0.24	8.45	10.87	2.39	0.19	0.15	98.10	7.5
48.31	1.74	13.21	12.42	0.19	8.56	11.02	2.39	0.17	0.20	98.20	7.7
48.66	1.73	13.37	12.26	0.15	8.38	10.72	2.47	0.21	0.16	98.13	9.3
48.62	1.76	13.77	11.52	0.21	7.96	10.51	2.58	0.22	0.22	97.38	13.7
49.07	1.74	13.81	11.97	0.26	8.24	10.92	2.51	0.16	0.16	98.85	14.1
49.41	1.79	13.79	11.68	0.19	7.68	10.70	2.59	0.17	0.23	98.22	16.0
49.36	1.82	14.27	11.66	0.28	7.65	10.76	2.69	0.23	0.19	98.91	19.9
49.09	1.77	14.18	11.70	0.19	7.68	10.80	2.70	0.18	0.15	98.45	20.4
49.42	1.77	14.26	11.68	0.28	7.25	10.73	2.70	0.22	0.22	98.52	26.2
49.35	1.90	14.23	11.76	0.23	7.32	10.75	2.66	0.17	0.09	98.46	26.7
49.03	1.86	14.26	11.71	0.11	7.27	10.80	2.78	0.17	0.10	98.09	26.8
49.27	1.86	14.26	11.60	0.24	6.98	10.90	2.71	0.22	0.21	98.24	32.4
49.15	1.83	14.39	11.80	0.32	7.05	10.88	2.72	0.16	0.13	98.42	33.1
49.41	1.90	14.13	11.81	0.26	7.01	10.96	2.68	0.19	0.20	98.55	33.6
49.41	1.78	14.33	11.89	0.18	6.91	10.91	2.75	0.20	0.20	98.54	38.7
49.39	1.82	14.31	11.96	0.23	6.91	10.93	2.71	0.19	0.10	98.55	39.5
49.68	1.84	14.26	11.94	0.19	6.99	10.87	2.70	0.14	0.14	98.76	40.6
49.48	1.86	14.38	11.95	0.20	6.97	11.02	2.75	0.18	0.15	98.95	44.9
49.23	1.89	14.24	11.95	0.19	6.89	11.08	2.75	0.14	0.15	98.51	45.9
48.89	1.86	14.18	11.90	0.11	6.78	11.06	2.68	0.15	0.19	97.81	47.6
49.32	1.89	14.32	11.74	0.20	6.80	10.86	2.70	0.18	0.16	98.18	51.1
49.25	1.96	14.25	12.11	0.13	6.90	11.05	2.74	0.20	0.14	98.72	52.2
49.27	1.87	14.14	11.80	0.20	6.73	11.07	2.60	0.21	0.19	98.08	54.5
49.40	1.89	14.23	11.82	0.19	6.77	11.01	2.64	0.23	0.20	98.38	57.4
49.12	1.89	14.22	12.10	0.13	6.73	11.03	2.66	0.22	0.17	98.28	58.6
49.18	1.89	14.23	11.97	0.19	6.72	11.04	2.74	0.19	0.22	98.36	61.5
49.49	1.85	14.29	11.95	0.20	6.74	11.07	2.84	0.22	0.14	98.79	63.6
49.28	1.87	14.21	12.02	0.31	6.76	11.18	2.68	0.18	0.13	98.62	64.9
49.18	1.90	14.30	11.97	0.22	6.83	10.95	2.66	0.17	0.19	98.37	68.4
49.41	1.83	14.24	11.97	0.19	6.82	10.94	2.68	0.23	0.22	98.52	69.8
49.29	1.81	14.21	12.18	0.26	6.74	11.14	2.71	0.20	0.21	98.75	71.3
49.34	1.87	14.14	11.83	0.20	6.67	10.98	2.75	0.19	0.20	98.17	75.4
49.52	1.88	14.36	11.90	0.18	6.68	11.11	2.66	0.20	0.05	98.55	76.1
49.59	1.85	14.19	12.03	0.26	6.80	11.16	2.76	0.21	0.19	99.04	77.6
49.00	1.88	14.22	11.92	0.20	6.68	11.06	2.65	0.13	0.11	97.84	82.3
49.64	1.83	14.39	11.88	0.22	6.71	11.11	2.69	0.23	0.15	98.84	82.3
49.81	1.83	14.12	11.96	0.13	6.70	11.04	2.66	0.20	0.18	98.62	84.0
49.70	1.84	14.13	11.92	0.17	6.69	10.99	2.65	0.21	0.19	98.49	88.5
49.44	1.90	14.25	11.87	0.16	6.67	11.04	2.62	0.22	0.15	98.31	89.3
49.41	1.93	14.25	11.93	0.18	6.81	10.98	2.70	0.21	0.17	98.56	94.8
49.04	1.90	14.14	11.91	0.28	6.67	11.02	2.61	0.19	0.18	97.95	96.3
49.60	1.85	14.36	11.77	0.13	6.71	11.09	2.74	0.19	0.14	98.59	101.0
49.09	1.88	14.21	12.07	0.20	6.73	11.01	2.67	0.18	0.19	98.23	103.2
49.17	1.88	14.25	11.83	0.24	6.62	11.02	2.74	0.18	0.22	98.13	110.2
48.98	1.88	14.30	11.95	0.20	6.76	11.18	2.69	0.17	0.12	98.22	114.0
48.70	1.86	14.38	12.08	0.25	6.88	11.06	2.64	0.22	0.17	98.22	114.0

49.45	1.90	14.23	11.94	0.21	6.70	11.03	2.74	0.18	0.19	98.57	117.1
49.09	1.86	14.17	11.92	0.16	6.77	11.07	2.64	0.20	0.23	98.11	124.1
49.08	1.87	14.38	11.87	0.17	6.86	11.16	2.72	0.19	0.16	98.45	154.0
49.47	1.86	14.28	11.82	0.19	6.71	11.19	2.65	0.19	0.19	98.54	157.8
49.28	1.82	14.38	12.04	0.25	6.82	11.22	2.68	0.16	0.16	98.82	164.0
49.53	1.89	14.12	11.91	0.30	6.69	10.97	2.70	0.22	0.22	98.56	201.5
48.99	1.83	14.16	11.88	0.21	6.69	11.11	2.64	0.19	0.16	97.85	204.5
49.49	1.88	14.13	11.96	0.23	6.71	11.16	2.66	0.17	0.19	98.59	245.3
49.25	1.84	14.14	11.89	0.18	6.73	11.09	2.64	0.19	0.11	98.06	255.0
49.59	1.81	14.25	12.06	0.18	6.72	11.17	2.67	0.17	0.19	98.81	264.0
49.74	1.88	14.00	11.87	0.21	6.66	11.06	2.68	0.17	0.13	98.39	289.0
49.06	1.94	14.15	11.85	0.25	6.67	11.11	2.64	0.21	0.15	98.03	305.5
49.55	1.89	14.18	11.80	0.21	6.68	11.12	2.71	0.26	0.23	98.62	314.0
48.83	1.90	14.24	12.02	0.27	6.76	11.05	2.64	0.19	0.15	98.04	336.0
49.56	1.84	14.17	12.14	0.24	6.72	11.06	2.69	0.16	0.17	98.74	356.0
48.96	1.85	14.10	12.03	0.19	6.73	11.15	2.66	0.17	0.13	97.97	452.7
48.98	1.87	14.30	12.09	0.26	6.65	11.06	2.75	0.21	0.24	98.43	569.3
48.61	1.89	14.09	11.84	0.15	6.65	11.13	2.64	0.19	0.09	97.27	686.0
49.16	1.91	14.18	11.95	0.15	6.70	10.97	2.64	0.19	0.17	98.01	802.7
49.26	1.91	14.13	11.90	0.26	6.62	11.20	2.66	0.19	0.14	98.25	919.3
49.08	1.88	14.15	11.99	0.18	6.75	11.15	2.65	0.19	0.14	98.15	1036.0
49.60	1.91	14.04	11.90	0.20	6.75	11.04	2.72	0.19	0.16	98.52	1152.7
49.22	1.92	14.15	11.98	0.13	6.71	11.02	2.75	0.17	0.18	98.24	1269.3
49.99	1.89	13.82	11.77	0.17	6.69	11.14	2.66	0.21	0.13	98.46	1386.0

Exp 23

SiO2	TiO2	Al2O3	FeO	MnO	MgO	CaO	Na2O	K2O	P2O5	Total	d (um)
48.18	1.78	11.39	12.78	0.17	11.45	10.95	2.06	0.10	0.15	99.00	1.3
47.49	1.72	10.79	13.43	0.23	12.60	10.90	1.88	0.08	0.18	99.33	2.3
47.00	1.62	10.33	13.63	0.27	14.05	10.40	1.77	0.10	0.15	99.30	5.9
47.34	1.59	10.40	13.72	0.18	13.97	10.41	1.77	0.10	0.14	99.62	7.7
46.78	1.51	10.39	13.76	0.27	14.07	10.36	1.80	0.12	0.22	99.27	9.0
47.01	1.54	10.41	13.53	0.18	14.50	10.19	1.69	0.07	0.12	99.24	12.6
47.33	1.54	10.12	13.42	0.27	14.33	10.11	1.70	0.06	0.16	99.03	14.0
46.74	1.49	10.54	13.31	0.26	14.48	9.98	1.79	0.07	0.06	98.72	15.7
47.17	1.58	10.40	13.16	0.33	14.66	10.10	1.83	0.10	0.16	99.49	20.3
47.15	1.59	10.65	13.29	0.26	14.32	9.97	1.92	0.08	0.16	99.38	22.5
47.25	1.58	10.58	13.28	0.20	14.46	10.01	1.87	0.10	0.15	99.47	25.9
47.03	1.56	10.49	13.19	0.28	14.14	10.12	1.76	0.09	0.15	98.79	26.7
47.60	1.59	10.81	13.07	0.11	13.99	9.87	1.84	0.10	0.16	99.14	29.2
46.85	1.53	10.75	13.24	0.23	14.24	9.98	1.82	0.08	0.21	98.93	32.6
47.35	1.57	10.56	12.93	0.27	13.98	9.93	1.78	0.11	0.06	98.53	33.0
47.79	1.58	11.02	12.84	0.18	13.76	9.86	1.96	0.10	0.15	99.23	35.9
47.14	1.60	10.83	13.16	0.22	14.05	9.93	1.89	0.12	0.20	99.14	39.3
47.93	1.61	11.33	12.64	0.13	13.54	9.92	1.94	0.14	0.12	99.28	42.6
47.06	1.55	11.06	12.88	0.26	13.68	10.00	1.94	0.13	0.19	98.74	44.3
47.30	1.54	10.99	13.02	0.23	13.81	10.04	1.92	0.11	0.12	99.09	45.9
47.69	1.61	11.13	12.78	0.22	13.45	9.88	1.95	0.11	0.12	98.93	52.6
48.37	1.59	11.30	12.79	0.23	13.28	10.10	1.98	0.13	0.17	99.94	56.3
47.71	1.63	11.31	12.63	0.27	13.39	10.07	2.02	0.12	0.16	99.29	59.3
47.98	1.64	11.49	12.53	0.24	13.04	10.14	1.98	0.10	0.19	99.33	65.9
48.65	1.60	11.47	12.42	0.26	12.76	10.10	1.99	0.13	0.19	99.58	72.6
48.07	1.63	11.79	12.53	0.20	12.66	10.04	2.10	0.13	0.16	99.31	77.1
47.53	1.57	12.05	12.44	0.30	12.50	10.13	2.15	0.12	0.21	98.98	82.1
47.84	1.61	12.17	12.14	0.16	12.34	10.37	2.19	0.15	0.19	99.16	87.2
48.42	1.61	12.76	11.95	0.15	11.11	10.21	2.31	0.14	0.12	98.79	127.1
49.22	1.66	12.99	11.64	0.17	10.55	10.18	2.46	0.17	0.15	99.18	132.1
48.82	1.69	13.26	11.46	0.19	10.55	10.23	2.43	0.16	0.13	98.92	137.2
49.09	1.72	13.74	11.54	0.25	9.52	10.20	2.50	0.13	0.16	98.85	177.1
49.59	1.76	13.88	11.41	0.31	9.13	10.28	2.59	0.17	0.09	99.19	182.0
49.89	1.74	13.90	11.22	0.24	8.96	10.32	2.70	0.15	0.20	99.32	187.2
49.80	1.77	13.92	11.33	0.13	8.50	10.41	2.73	0.21	0.13	98.92	227.1
49.58	1.87	14.16	11.38	0.24	8.25	10.51	2.87	0.23	0.14	99.24	232.0
50.04	1.85	14.25	11.46	0.15	8.12	10.53	2.74	0.18	0.26	99.59	237.2
49.75	1.81	14.23	11.52	0.22	7.83	10.63	2.77	0.21	0.14	99.09	277.1
49.62	1.87	14.11	11.75	0.12	7.60	10.61	2.78	0.16	0.12	98.73	282.0
49.63	1.82	14.15	11.39	0.22	7.49	10.71	2.78	0.20	0.15	98.54	287.2
49.80	1.85	14.15	11.85	0.16	7.35	10.68	2.81	0.18	0.15	98.98	327.1
49.44	1.86	14.17	11.79	0.26	7.40	10.70	2.78	0.16	0.17	98.74	332.0
49.62	1.91	14.20	11.78	0.18	7.43	10.80	2.73	0.17	0.12	98.95	337.1
49.85	1.87	14.16	12.01	0.18	7.15	10.83	2.68	0.18	0.18	99.07	377.1
49.95	1.89	14.28	12.10	0.23	6.98	10.93	2.62	0.18	0.07	99.22	382.0
49.83	1.90	14.18	12.07	0.27	7.15	10.96	2.73	0.15	0.14	99.38	387.1
49.76	1.88	14.16	11.99	0.23	7.06	10.97	2.70	0.19	0.20	99.14	427.1

49.09	1.86	14.24	12.07	0.29	7.03	11.01	2.70	0.15	0.07	98.50	431.9
49.47	1.93	14.15	11.86	0.20	7.02	11.00	2.69	0.15	0.12	98.58	437.1
49.37	1.96	14.16	12.30	0.06	7.05	11.08	2.58	0.16	0.21	98.91	477.1
49.62	1.93	14.11	12.01	0.18	6.81	11.10	2.79	0.21	0.25	99.03	481.9
49.64	1.87	14.07	11.97	0.28	7.07	11.08	2.66	0.16	0.19	98.98	487.1
49.35	1.88	14.26	12.19	0.22	6.79	11.07	2.67	0.17	0.18	98.78	527.1
49.93	1.85	14.16	12.13	0.27	6.83	11.06	2.74	0.19	0.11	99.25	531.9
49.91	1.86	14.13	12.06	0.21	6.94	11.11	2.73	0.20	0.14	99.29	537.0
49.61	1.88	14.17	12.23	0.22	6.95	11.01	2.70	0.16	0.22	99.14	577.1
49.48	1.88	14.02	12.22	0.29	6.83	11.08	2.72	0.20	0.22	98.95	581.9
49.66	1.82	14.15	12.03	0.22	6.87	11.03	2.67	0.17	0.22	98.83	587.0
49.71	1.90	14.12	12.12	0.21	6.88	11.07	2.69	0.14	0.04	98.88	627.1
49.38	1.91	14.09	12.28	0.18	6.81	11.14	2.78	0.17	0.22	98.95	631.9
49.58	1.88	14.10	12.20	0.19	6.97	11.15	2.78	0.15	0.14	99.13	637.0
49.32	1.87	14.25	12.18	0.30	6.82	11.13	2.63	0.13	0.34	98.96	677.1
49.67	1.89	14.13	12.03	0.21	6.93	11.07	2.74	0.18	0.30	99.14	681.8
49.77	1.90	14.24	12.05	0.23	6.91	11.11	2.62	0.15	0.19	99.17	687.0
49.32	1.84	14.18	12.24	0.21	6.85	11.30	2.62	0.19	0.22	98.96	727.1
49.35	1.87	14.12	12.20	0.25	6.81	11.04	2.68	0.18	0.22	98.72	731.8
49.63	1.86	14.26	12.02	0.19	6.86	11.08	2.70	0.14	0.18	98.92	737.0
49.17	1.87	14.20	12.14	0.13	6.86	10.99	2.74	0.20	0.09	98.39	777.1
49.59	1.87	14.05	12.17	0.18	6.79	11.09	2.61	0.18	0.07	98.59	781.8
49.53	1.88	14.10	12.15	0.20	6.85	11.10	2.72	0.17	0.35	99.05	786.9
49.34	1.87	14.01	12.21	0.18	6.80	11.18	2.79	0.20	0.12	98.70	831.8
50.15	1.85	14.16	12.11	0.30	6.99	10.94	2.60	0.13	0.22	99.44	836.9
49.74	1.85	14.14	12.26	0.20	6.80	11.17	2.64	0.19	0.24	99.23	911.1
49.78	1.84	14.08	12.08	0.26	6.84	11.13	2.76	0.15	0.24	99.16	954.7
49.53	1.83	14.16	12.20	0.28	6.88	11.05	2.63	0.17	0.16	98.87	959.4
49.30	1.80	14.16	12.03	0.30	6.86	11.14	2.71	0.15	0.17	98.62	1045.0
49.65	1.88	14.08	11.90	0.23	6.80	11.05	2.65	0.23	0.17	98.63	1077.7
49.59	1.89	14.24	12.18	0.16	6.85	11.01	2.62	0.20	0.22	98.96	1081.8
49.51	1.86	14.07	12.00	0.24	6.89	11.15	2.68	0.18	0.20	98.77	1179.0
50.01	1.93	14.06	12.00	0.25	6.85	11.11	2.61	0.18	0.22	99.22	1200.6
49.69	1.83	14.11	11.93	0.23	6.96	11.21	2.73	0.16	0.16	99.00	1204.3

Exp 24

SiO2	TiO2	Al2O3	FeO	MnO	MgO	CaO	Na2O	K2O	P2O5	Total	d (um)
48.04	1.76	11.36	13.19	0.23	11.41	10.83	1.92	0.07	0.12	98.93	1.0
47.58	1.67	10.94	13.21	0.25	12.29	10.67	1.86	0.12	0.13	98.71	4.2
47.60	1.59	11.08	13.22	0.27	12.81	10.34	1.82	0.10	0.14	98.96	4.8
47.15	1.61	11.12	13.21	0.14	12.79	10.10	1.86	0.09	0.20	98.26	7.6
47.65	1.61	11.43	12.95	0.27	12.79	10.21	1.91	0.12	0.14	99.06	11.2
47.59	1.56	11.36	12.86	0.27	12.81	10.15	2.03	0.15	0.12	98.89	11.4
47.72	1.56	11.61	12.54	0.19	12.49	10.22	2.02	0.10	0.08	98.53	14.2
48.23	1.63	12.33	12.25	0.27	12.15	10.07	2.23	0.15	0.10	99.41	18.0
48.16	1.62	12.19	12.24	0.25	12.11	10.14	2.03	0.15	0.15	99.03	18.3
48.56	1.64	12.37	11.97	0.30	11.71	10.05	2.26	0.17	0.15	99.16	20.7
48.62	1.66	13.00	11.53	0.25	10.95	10.04	2.31	0.10	0.16	98.60	24.6
48.60	1.62	12.95	11.73	0.21	10.96	10.06	2.37	0.14	0.17	98.80	25.4
49.02	1.66	13.03	11.42	0.24	10.77	10.11	2.42	0.14	0.19	99.00	27.3
49.43	1.64	13.41	11.27	0.20	10.18	10.11	2.56	0.19	0.16	99.14	31.1
49.50	1.67	13.65	11.34	0.19	9.68	10.03	2.48	0.19	0.12	98.85	32.5
49.46	1.68	13.68	11.24	0.19	9.66	10.18	2.56	0.16	0.20	99.01	33.8
49.94	1.74	14.04	10.95	0.20	9.25	10.14	2.65	0.16	0.18	99.25	37.7
49.67	1.76	14.03	11.15	0.14	8.97	10.19	2.75	0.14	0.17	98.96	39.5
49.29	1.75	14.00	11.02	0.19	8.93	10.28	2.71	0.17	0.19	98.51	40.4
50.18	1.82	14.00	11.06	0.21	8.64	10.27	2.78	0.19	0.21	99.35	44.3
49.91	1.82	14.09	11.22	0.26	8.35	10.36	2.66	0.16	0.19	99.01	46.6
49.77	1.84	14.16	11.43	0.31	8.38	10.45	2.71	0.18	0.14	99.36	46.9
50.55	1.83	14.18	11.39	0.19	8.09	10.59	2.81	0.21	0.13	99.97	50.9
49.57	1.84	14.17	11.21	0.13	7.96	10.50	2.77	0.17	0.16	98.48	53.5
49.94	1.84	14.11	11.30	0.21	7.80	10.60	2.76	0.17	0.15	98.87	53.7
49.82	1.77	14.18	11.10	0.21	7.92	10.50	2.81	0.13	0.16	98.59	56.0
50.47	1.82	14.06	11.27	0.16	7.69	10.51	2.74	0.18	0.18	99.08	57.5
49.54	1.88	14.17	11.58	0.18	7.55	10.75	2.76	0.21	0.19	98.80	58.0
49.68	1.89	14.31	11.50	0.22	7.69	10.82	2.79	0.20	0.22	99.32	60.0
49.78	1.88	14.06	11.68	0.24	7.45	10.71	2.80	0.19	0.23	99.04	60.7
50.20	1.82	14.28	11.23	0.14	7.86	10.64	2.76	0.16	0.16	99.25	62.0
49.25	1.86	14.21	11.64	0.22	7.30	10.77	2.81	0.22	0.19	98.46	64.1
49.89	1.84	14.32	11.65	0.26	7.23	10.72	2.76	0.20	0.17	99.04	66.6
49.96	1.89	14.25	11.70	0.24	7.19	10.86	2.85	0.21	0.14	99.28	67.8
50.16	1.84	14.14	11.36	0.30	7.52	10.60	2.74	0.17	0.15	98.97	68.0
49.62	1.92	14.20	11.75	0.20	7.12	10.87	2.77	0.21	0.23	98.89	73.2
50.02	1.88	14.28	11.83	0.21	7.02	10.82	2.71	0.17	0.22	99.13	74.9
49.85	1.88	14.13	11.78	0.13	7.08	10.91	2.76	0.20	0.15	98.87	79.7
50.06	1.83	14.14	11.86	0.15	6.95	11.06	2.75	0.22	0.18	99.21	82.0
49.04	1.81	14.32	12.05	0.22	6.96	10.98	2.75	0.20	0.14	98.46	82.6
49.81	1.85	14.32	12.04	0.25	6.83	11.05	2.71	0.16	0.12	99.13	83.0
50.10	1.92	14.17	11.86	0.10	6.96	10.98	2.69	0.17	0.12	99.07	86.3
50.40	1.86	14.21	11.90	0.22	6.93	10.94	2.63	0.16	0.15	99.41	89.0
49.91	1.91	14.11	11.90	0.30	6.82	10.91	2.70	0.16	0.17	98.87	92.8
49.97	1.83	14.06	11.85	0.21	6.92	10.93	2.70	0.15	0.13	98.76	99.4
50.05	1.88	14.12	11.94	0.22	6.82	10.94	2.70	0.12	0.26	99.05	105.9
49.88	1.90	14.29	12.06	0.18	6.93	11.18	2.69	0.15	0.16	99.42	108.0

49.80	1.86	14.22	12.03	0.16	6.81	11.00	2.79	0.21	0.12	98.99	133.0
49.89	1.88	13.99	11.91	0.23	6.64	11.13	2.59	0.15	0.15	98.55	158.0
49.45	1.91	14.21	12.02	0.18	6.84	11.17	2.71	0.19	0.23	98.89	186.9
49.35	1.89	14.29	12.04	0.24	6.93	11.00	2.65	0.19	0.19	98.77	199.3
49.93	1.82	14.08	12.10	0.30	6.84	11.14	2.66	0.20	0.12	99.19	309.8
49.53	1.91	14.17	12.07	0.24	6.77	11.07	2.68	0.16	0.10	98.70	315.8
49.63	1.85	14.10	11.93	0.22	6.88	11.23	2.71	0.14	0.20	98.91	432.5
49.78	1.83	14.16	11.95	0.25	6.74	11.09	2.80	0.16	0.14	98.88	432.6
49.54	1.87	14.05	11.95	0.24	6.69	11.08	2.76	0.18	0.13	98.50	549.2
49.89	1.95	14.01	11.83	0.20	6.81	11.20	2.67	0.14	0.22	98.92	555.3
49.47	1.88	14.13	12.06	0.26	6.79	11.04	2.70	0.17	0.14	98.62	665.7
50.05	1.92	14.04	12.11	0.21	6.95	11.19	2.69	0.18	0.25	99.58	678.2
50.02	1.87	14.01	11.92	0.30	6.87	11.16	2.63	0.17	0.24	99.17	782.4
49.59	1.92	14.16	11.96	0.17	6.95	11.20	2.70	0.19	0.09	98.92	801.0
50.16	1.82	14.25	12.07	0.24	6.88	11.06	2.61	0.19	0.17	99.43	899.1
49.54	1.91	14.04	11.86	0.15	6.71	11.25	2.72	0.16	0.15	98.47	923.8
49.86	1.88	14.15	12.01	0.26	6.79	11.24	2.72	0.20	0.14	99.24	1015.6
49.59	1.92	14.03	12.11	0.21	6.73	11.09	2.75	0.16	0.17	98.75	1046.7

Exp 25

SiO2	TiO2	Al2O3	FeO	MnO	MgO	CaO	Na2O	K2O	P2O5	Total	d (um)
47.73	1.72	10.86	13.60	0.30	12.27	10.82	1.81	0.10	0.19	99.41	0.3
48.63	1.77	11.27	13.22	0.27	11.72	10.86	1.94	0.09	0.17	99.93	1.2
46.95	1.55	10.07	13.84	0.32	14.04	10.28	1.77	0.08	0.07	98.97	6.4
47.33	1.58	10.07	14.02	0.25	13.95	10.20	1.73	0.07	0.17	99.37	6.5
47.86	1.62	10.34	13.68	0.26	13.92	10.17	1.67	0.07	0.08	99.66	6.8
47.28	1.52	10.02	13.77	0.18	14.55	9.87	1.76	0.07	0.09	99.10	12.7
46.97	1.57	10.00	13.54	0.18	14.67	10.05	1.70	0.10	0.07	98.84	13.2
47.86	1.55	10.35	13.23	0.29	14.66	9.82	1.77	0.11	0.13	99.76	18.0
47.39	1.52	10.19	13.49	0.20	14.63	9.89	1.79	0.10	0.15	99.35	18.9
47.12	1.52	10.36	13.25	0.27	14.59	9.73	1.81	0.10	0.09	98.84	20.0
47.89	1.51	10.51	13.12	0.24	14.48	9.69	1.81	0.10	0.15	99.49	23.6
47.39	1.52	10.39	13.11	0.20	14.34	9.75	1.76	0.10	0.13	98.69	25.1
47.38	1.54	10.60	13.16	0.17	14.39	9.86	1.89	0.08	0.01	99.07	26.9
47.69	1.58	10.69	13.13	0.24	14.04	9.83	1.84	0.11	0.09	99.23	33.7
47.39	1.59	11.17	12.87	0.24	13.72	9.94	1.96	0.11	0.19	99.18	37.6
47.87	1.59	11.67	12.37	0.26	12.68	9.89	2.19	0.11	0.11	98.72	55.3
48.31	1.59	11.86	12.31	0.23	12.39	9.96	2.14	0.10	0.11	99.01	61.0
48.43	1.57	12.11	12.34	0.18	11.92	10.14	2.16	0.12	0.09	99.05	67.6
48.95	1.63	12.89	11.84	0.19	10.81	10.10	2.44	0.15	0.09	99.08	85.3
49.30	1.68	13.11	11.56	0.21	10.36	10.07	2.47	0.17	0.10	99.03	91.0
48.73	1.68	12.97	11.62	0.10	10.57	10.10	2.43	0.17	0.09	98.46	97.6
49.47	1.74	13.56	11.36	0.16	9.58	10.15	2.59	0.17	0.17	98.94	115.3
49.69	1.78	13.74	11.31	0.24	8.76	10.39	2.66	0.18	0.11	98.84	121.0
49.47	1.70	13.59	11.46	0.21	9.17	10.25	2.63	0.15	0.09	98.71	127.6
49.75	1.85	13.94	11.37	0.20	8.41	10.40	2.79	0.18	0.13	99.02	145.2
49.62	1.87	14.08	11.47	0.13	7.80	10.67	2.72	0.24	0.12	98.73	150.9
49.59	1.79	13.89	11.52	0.16	8.23	10.38	2.70	0.23	0.24	98.73	157.6
49.87	1.85	14.03	11.49	0.22	7.76	10.50	2.76	0.19	0.16	98.83	175.2
49.91	1.85	14.11	11.77	0.18	7.44	10.56	2.68	0.20	0.14	98.83	180.9
49.78	1.91	13.95	11.52	0.15	7.69	10.59	2.66	0.20	0.09	98.56	187.5
49.55	1.87	14.00	11.69	0.26	7.44	10.68	2.82	0.20	0.19	98.70	205.2
49.48	1.88	14.14	11.84	0.23	7.14	10.82	2.70	0.21	0.09	98.52	210.9
49.58	1.88	14.03	11.82	0.31	7.28	10.86	2.70	0.19	0.19	98.84	217.5
49.65	1.85	14.05	11.96	0.13	7.25	10.81	2.83	0.19	0.19	98.91	235.2
49.81	1.88	14.17	12.15	0.19	7.03	10.90	2.77	0.19	0.23	99.33	240.9
49.40	1.84	14.11	12.06	0.26	7.21	10.88	2.74	0.18	0.22	98.88	247.5
49.36	1.88	14.00	12.20	0.28	7.07	10.91	2.84	0.15	0.15	98.83	265.2
49.91	1.87	14.10	12.30	0.17	6.86	11.10	2.74	0.18	0.23	99.47	270.9
49.34	1.93	14.00	12.31	0.25	6.93	10.94	2.71	0.18	0.15	98.74	277.5
49.60	1.86	13.97	12.06	0.14	6.94	11.01	2.78	0.13	0.29	98.77	295.2
49.83	1.91	14.09	12.25	0.18	6.91	11.02	2.72	0.17	0.20	99.29	300.9
49.63	1.89	13.94	12.23	0.28	6.80	11.00	2.68	0.18	0.10	98.72	307.5
49.76	1.83	13.98	12.16	0.18	6.76	11.08	2.75	0.15	0.16	98.81	325.2
49.58	1.86	14.22	12.33	0.18	6.91	11.23	2.77	0.15	0.14	99.37	330.9
49.42	1.89	13.90	12.13	0.26	6.81	11.11	2.70	0.18	0.16	98.55	337.5
49.46	1.91	14.05	12.20	0.26	6.82	11.10	2.79	0.17	0.25	99.01	355.2
49.58	1.91	13.95	12.32	0.22	6.83	11.26	2.76	0.18	0.20	99.21	360.9

49.49	1.85	13.83	12.30	0.12	6.88	11.10	2.66	0.15	0.19	98.58	367.5
49.15	1.91	13.91	12.19	0.21	6.73	11.12	2.70	0.15	0.21	98.28	385.2
49.56	1.89	14.10	12.26	0.27	6.75	11.05	2.63	0.14	0.23	98.87	390.9
49.61	1.91	13.98	12.24	0.18	6.73	11.11	2.67	0.14	0.19	98.75	397.5
49.49	1.91	14.10	12.20	0.20	6.81	11.17	2.74	0.17	0.22	98.99	415.2
49.89	1.86	14.03	12.29	0.20	6.75	11.04	2.72	0.19	0.22	99.17	420.9
49.11	1.89	14.00	12.34	0.18	6.69	11.30	2.70	0.20	0.19	98.59	427.5
49.25	1.87	13.90	12.30	0.15	6.69	11.13	2.73	0.18	0.12	98.31	445.2
49.55	1.92	14.01	12.40	0.13	6.82	11.16	2.76	0.13	0.17	99.05	450.9
49.42	1.87	14.05	12.37	0.38	6.76	11.30	2.70	0.14	0.12	99.12	457.5
49.39	1.85	14.01	12.32	0.17	6.84	11.12	2.75	0.16	0.10	98.70	475.1
49.45	1.85	13.99	12.23	0.27	6.76	11.16	2.71	0.15	0.12	98.68	480.9
49.36	1.87	14.10	12.42	0.17	6.80	11.13	2.76	0.15	0.15	98.90	487.5
49.35	1.93	14.03	12.15	0.24	6.77	11.13	2.68	0.16	0.13	98.57	542.0
49.46	1.87	14.07	12.33	0.14	6.77	11.16	2.71	0.14	0.20	98.85	547.4
49.51	1.91	13.97	12.28	0.19	6.75	11.13	2.65	0.20	0.16	98.75	553.6
49.66	1.90	14.00	12.23	0.21	6.77	11.07	2.77	0.11	0.17	98.89	609.0
49.60	1.83	14.11	12.03	0.13	6.70	11.09	2.70	0.21	0.21	98.61	614.1
49.27	1.87	13.91	12.43	0.29	6.72	11.13	2.67	0.16	0.20	98.65	619.8
49.66	1.90	14.13	11.98	0.09	6.70	11.24	2.71	0.13	0.12	98.66	675.9
49.36	1.93	14.12	12.33	0.24	6.70	11.15	2.73	0.13	0.12	98.79	680.7
49.48	1.87	14.01	12.40	0.13	6.71	11.18	2.68	0.19	0.17	98.81	686.0
49.64	1.86	13.99	11.87	0.22	6.77	11.15	2.66	0.20	0.13	98.48	742.8
49.69	1.90	14.06	12.31	0.20	6.69	11.28	2.63	0.14	0.09	98.98	747.4
49.30	1.86	13.97	12.37	0.19	6.81	11.12	2.66	0.15	0.12	98.56	752.3
49.60	1.82	13.96	12.00	0.14	6.70	11.08	2.80	0.16	0.22	98.46	809.7
49.85	1.88	13.95	12.24	0.12	6.68	11.16	2.59	0.18	0.21	98.85	814.0
48.94	1.84	13.92	12.35	0.26	6.74	11.19	2.71	0.17	0.15	98.26	818.5
49.36	1.87	13.98	12.11	0.26	6.68	11.11	2.69	0.16	0.12	98.34	876.6
50.00	1.87	13.96	12.20	0.18	6.77	11.20	2.74	0.19	0.13	99.23	880.6
49.36	1.88	13.79	12.04	0.27	6.67	11.29	2.68	0.15	0.19	98.31	884.6
49.46	1.87	13.96	12.24	0.20	6.75	11.10	2.63	0.16	0.13	98.50	943.5
49.75	1.88	13.87	12.27	0.18	6.71	11.08	2.71	0.18	0.12	98.75	947.2
49.17	1.88	13.96	12.38	0.09	6.75	11.32	2.79	0.17	0.17	98.68	950.8
49.31	1.87	13.96	12.23	0.20	6.64	11.15	2.74	0.17	0.12	98.40	1010.4
49.52	1.87	13.93	12.28	0.15	6.71	11.11	2.76	0.13	0.18	98.63	1013.8
49.43	1.91	13.96	12.33	0.23	6.75	11.14	2.69	0.15	0.19	98.77	1017.0
49.19	1.88	13.72	12.46	0.19	6.68	11.13	2.65	0.16	0.19	98.25	1077.4
49.76	1.93	13.91	12.33	0.16	6.81	11.07	2.68	0.19	0.18	99.00	1080.5
49.21	1.89	13.87	12.42	0.27	6.57	11.17	2.65	0.14	0.25	98.44	1083.2
49.54	1.92	13.78	12.46	0.20	6.83	11.03	2.66	0.20	0.16	98.77	1144.3
49.53	1.87	13.93	12.52	0.30	6.70	11.16	2.71	0.13	0.11	98.94	1147.1
49.43	1.95	13.84	12.44	0.16	6.74	11.24	2.70	0.17	0.11	98.77	1149.4
49.18	1.86	13.90	12.21	0.20	6.70	11.14	2.76	0.17	0.12	98.23	1211.1
49.97	1.88	14.10	12.39	0.15	6.84	11.13	2.68	0.14	0.09	99.36	1213.8
49.19	1.91	13.98	12.41	0.17	6.72	11.08	2.61	0.14	0.09	98.30	1215.6
49.53	1.90	13.80	12.21	0.17	6.79	11.34	2.60	0.18	0.23	98.75	1278.0
49.91	1.88	14.04	12.22	0.18	6.81	11.02	2.67	0.18	0.18	99.09	1280.3
49.40	1.93	13.84	12.16	0.24	6.74	11.32	2.57	0.14	0.14	98.47	1281.8

Exp 26

SiO2	TiO2	Al2O3	FeO	MnO	MgO	CaO	Na2O	K2O	P2O5	Total	d (um)
47.94	1.68	10.52	13.47	0.25	12.81	10.73	1.82	0.10	0.07	99.38	3.5
47.39	1.68	10.21	13.70	0.17	13.55	10.50	1.80	0.10	0.05	99.16	5.1
47.67	1.63	10.19	13.82	0.25	13.96	10.41	1.76	0.10	0.11	99.90	8.3
47.54	1.56	9.86	13.60	0.22	14.56	10.06	1.74	0.11	0.10	99.35	9.5
47.38	1.58	10.04	13.81	0.25	14.73	9.99	1.71	0.07	0.11	99.66	11.9
47.66	1.54	9.83	13.74	0.21	14.99	10.11	1.70	0.09	0.09	99.95	14.6
47.79	1.53	10.03	13.67	0.23	14.98	9.89	1.75	0.08	0.09	100.03	15.5
47.22	1.51	10.07	13.69	0.32	15.05	9.91	1.75	0.10	0.04	99.65	18.7
47.38	1.50	9.97	13.49	0.48	15.42	9.77	1.75	0.06	0.04	99.86	20.9
48.18	1.56	9.96	13.14	0.23	15.10	9.87	1.76	0.10	0.09	99.98	21.5
46.82	1.59	10.47	13.49	0.16	15.25	9.83	1.85	0.14	0.13	99.73	23.9
47.31	1.59	10.10	13.47	0.21	14.87	9.73	1.74	0.05	0.09	99.17	25.6
46.81	1.62	10.36	13.37	0.28	15.08	9.74	1.84	0.11	0.04	99.23	25.8
47.78	1.50	9.99	13.26	0.06	15.38	9.85	1.75	0.09	0.11	99.76	27.3
47.94	1.54	10.04	13.40	0.25	14.83	9.76	1.71	0.07	0.14	99.69	32.4
47.64	1.53	10.08	13.24	0.24	14.95	9.84	1.83	0.07	0.10	99.50	33.6
46.83	1.56	10.58	13.11	0.27	14.61	9.78	1.87	0.13	0.16	98.90	35.8
46.90	1.54	10.56	13.24	0.28	14.60	9.88	1.83	0.09	0.16	99.09	41.1
46.62	1.52	10.51	13.15	0.24	14.83	9.83	1.91	0.13	0.13	98.86	43.6
47.11	1.49	10.75	13.01	0.27	14.64	9.80	1.92	0.08	0.04	99.10	45.8
47.23	1.56	10.75	13.03	0.28	14.20	9.92	1.95	0.10	0.05	99.07	45.8
47.22	1.57	11.08	13.10	0.30	13.84	9.98	1.99	0.08	0.12	99.27	55.8
47.36	1.58	10.75	13.13	0.25	14.25	9.90	1.97	0.09	0.16	99.43	58.5
47.59	1.61	11.03	12.84	0.21	13.30	10.03	1.92	0.13	0.16	98.81	65.8
47.52	1.61	11.18	12.66	0.22	13.50	9.90	2.01	0.11	0.09	98.79	73.6
47.65	1.57	11.14	12.92	0.24	13.57	9.98	1.99	0.15	0.14	99.34	75.8
47.29	1.52	10.94	12.99	0.19	13.72	9.77	2.01	0.12	0.08	98.61	75.8
47.59	1.55	11.24	12.81	0.30	13.25	10.02	2.03	0.11	0.12	99.00	93.1
47.52	1.56	11.43	12.58	0.27	13.00	10.02	2.10	0.10	0.14	98.73	103.6
47.58	1.57	11.58	12.57	0.22	13.02	10.09	2.13	0.12	0.18	99.06	105.8
47.58	1.58	11.59	12.53	0.22	13.01	10.06	2.09	0.10	0.12	98.87	110.5
47.68	1.59	11.74	12.41	0.19	12.52	10.01	2.22	0.11	0.07	98.54	127.8
47.93	1.64	11.99	12.41	0.15	12.32	10.16	2.19	0.11	0.16	99.06	133.6
47.92	1.61	12.08	12.36	0.22	12.40	10.10	2.26	0.11	0.14	99.20	135.8
47.89	1.59	11.86	12.31	0.25	12.18	10.11	2.25	0.10	0.12	98.64	145.1
48.20	1.65	12.23	12.17	0.21	11.86	10.11	2.22	0.11	0.07	98.82	162.5
48.17	1.62	12.39	12.13	0.28	11.80	9.98	2.34	0.16	0.20	99.05	163.6
48.19	1.62	12.37	12.15	0.20	11.71	9.96	2.32	0.14	0.12	98.77	165.8
48.67	1.69	12.37	12.06	0.30	11.36	10.14	2.32	0.19	0.15	99.25	168.3
48.46	1.62	12.69	11.77	0.15	11.12	10.06	2.37	0.18	0.15	98.54	193.6
48.43	1.62	12.76	12.08	0.19	11.21	10.01	2.37	0.10	0.18	98.94	195.8
48.67	1.65	13.11	11.68	0.19	10.57	10.19	2.52	0.11	0.16	98.85	223.6
48.59	1.66	13.11	11.54	0.10	10.60	10.19	2.49	0.17	0.20	98.63	225.8
49.12	1.66	13.35	11.69	0.19	10.49	10.16	2.47	0.16	0.21	99.51	230.9
48.73	1.68	13.32	11.57	0.20	9.93	10.14	2.57	0.20	0.08	98.41	253.6
49.11	1.69	13.28	11.55	0.18	10.04	10.31	2.49	0.15	0.15	98.94	255.8
49.40	1.66	13.47	11.34	0.24	9.93	10.09	2.64	0.17	0.06	99.00	260.9

48.96	1.74	13.60	11.30	0.16	9.48	10.23	2.67	0.14	0.16	98.44	283.6
49.22	1.70	13.61	11.35	0.18	9.55	10.32	2.63	0.20	0.06	98.81	285.8
49.79	1.76	13.82	11.61	0.22	9.52	10.13	2.70	0.19	0.22	99.96	290.9
49.45	1.72	13.80	11.26	0.17	9.01	10.36	2.72	0.17	0.15	98.80	313.6
49.58	1.73	13.74	11.29	0.17	9.18	10.36	2.70	0.20	0.16	99.13	315.8
49.89	1.76	14.00	11.25	0.21	9.03	10.32	2.74	0.19	0.21	99.60	320.9
49.59	1.80	13.90	11.36	0.18	8.57	10.38	2.77	0.20	0.06	98.82	343.6
49.40	1.81	13.97	11.40	0.26	8.82	10.30	2.82	0.20	0.16	99.13	345.8
49.99	1.76	14.02	11.27	0.13	8.73	10.18	2.81	0.23	0.14	99.25	350.9
49.46	1.76	14.19	11.25	0.22	8.38	10.55	2.79	0.21	0.14	98.95	373.6
49.67	1.75	14.06	11.39	0.24	8.50	10.20	2.80	0.15	0.14	98.88	375.8
50.12	1.81	14.12	11.31	0.30	8.30	10.40	2.86	0.17	0.13	99.52	380.8
49.17	1.83	14.04	11.31	0.26	7.97	10.48	2.75	0.19	0.17	98.15	403.6
49.64	1.79	14.03	11.30	0.15	8.13	10.59	2.74	0.20	0.13	98.70	405.8
50.08	1.86	14.14	11.33	0.19	8.18	10.46	2.96	0.21	0.12	99.53	410.8
49.28	1.86	14.20	11.20	0.26	7.65	10.56	2.78	0.22	0.16	98.16	433.6
49.68	1.92	14.01	11.40	0.14	7.83	10.46	2.78	0.17	0.18	98.57	435.8
50.10	1.92	14.17	11.31	0.23	7.84	10.55	2.84	0.16	0.13	99.24	440.8
49.13	1.91	14.01	11.55	0.13	7.59	10.61	2.73	0.18	0.10	97.94	463.6
49.85	1.88	14.01	11.43	0.11	7.70	10.54	2.80	0.14	0.06	98.53	465.8
50.14	1.87	14.36	11.63	0.14	7.56	10.61	2.88	0.17	0.19	99.56	470.8
49.25	1.80	14.11	11.38	0.24	7.36	10.54	2.74	0.18	0.22	97.82	493.6
49.69	1.89	14.18	11.69	0.19	7.60	10.64	2.88	0.17	0.19	99.10	495.8
50.24	1.91	14.19	11.51	0.13	7.51	10.72	2.90	0.16	0.15	99.42	500.8
50.02	1.90	14.27	11.67	0.13	7.36	10.69	2.84	0.19	0.16	99.21	530.8
49.72	1.87	14.21	11.73	0.14	7.42	10.82	2.87	0.16	0.14	99.07	551.6
50.13	1.92	14.25	11.63	0.16	7.28	10.81	2.84	0.17	0.15	99.33	560.8
50.12	1.95	14.27	11.75	0.20	7.22	10.78	2.84	0.17	0.22	99.51	590.8
49.22	1.85	13.98	11.70	0.21	7.01	10.82	2.81	0.19	0.13	97.92	605.5
49.37	1.88	14.13	11.87	0.22	7.09	10.86	2.71	0.19	0.16	98.46	607.4
50.19	1.87	14.33	11.83	0.25	7.09	10.94	2.81	0.16	0.16	99.62	620.8
49.83	1.87	14.21	11.98	0.20	6.91	10.82	2.84	0.14	0.12	98.91	650.7
49.01	1.88	14.06	11.98	0.22	6.85	10.86	2.82	0.13	0.22	98.04	661.4
49.25	1.85	14.03	12.00	0.22	7.08	10.93	2.74	0.18	0.13	98.41	663.2
49.74	1.87	14.15	11.98	0.12	6.99	10.89	2.84	0.17	0.16	98.90	680.7
49.12	1.87	14.02	11.94	0.24	6.79	11.01	2.78	0.20	0.19	98.17	717.3
49.65	1.85	14.11	12.00	0.18	6.85	10.94	2.79	0.18	0.12	98.67	718.9
49.83	1.92	14.31	11.98	0.16	6.99	10.87	2.79	0.19	0.19	99.22	722.7
50.25	1.82	14.26	12.13	0.17	6.97	11.06	2.79	0.16	0.19	99.78	764.7
48.79	1.90	14.02	12.04	0.21	6.75	11.04	2.83	0.17	0.22	97.98	773.2
49.62	1.90	14.17	12.08	0.20	6.89	11.12	2.83	0.17	0.19	99.16	774.7
49.81	1.85	14.30	12.02	0.20	6.90	10.94	2.79	0.15	0.15	99.11	806.7
48.31	1.85	13.82	11.92	0.23	6.56	11.00	2.75	0.17	0.15	96.76	829.2
49.38	1.90	14.19	12.16	0.16	6.81	11.13	2.76	0.20	0.16	98.85	830.5
49.85	1.87	14.19	12.09	0.18	6.95	11.13	2.76	0.19	0.20	99.41	848.7
48.99	1.92	13.89	12.10	0.14	6.64	11.35	2.87	0.14	0.12	98.16	885.1
49.69	1.87	14.05	12.14	0.13	6.78	11.17	2.67	0.15	0.08	98.71	886.3
49.71	1.89	14.20	12.02	0.29	6.88	11.02	2.88	0.18	0.14	99.21	890.7
50.13	1.90	14.21	12.29	0.24	6.85	11.08	2.85	0.17	0.19	99.90	932.6

49.25	1.96	13.95	12.14	0.28	6.73	11.09	2.71	0.17	0.09	98.34	941.0
50.20	1.85	14.25	12.02	0.15	6.68	10.95	2.83	0.18	0.15	99.25	974.6
49.04	1.93	13.94	12.08	0.24	6.67	11.11	2.75	0.20	0.15	98.11	997.0
49.70	1.90	14.15	12.17	0.20	6.72	11.13	2.92	0.19	0.22	99.30	997.9
50.50	1.85	14.29	12.22	0.38	6.69	11.05	2.75	0.16	0.21	100.12	1016.6
49.21	1.94	13.94	12.11	0.20	6.64	11.20	2.75	0.19	0.15	98.33	1052.9
50.25	1.87	14.32	12.07	0.13	6.76	10.97	2.80	0.15	0.13	99.45	1058.6
50.15	1.85	14.22	12.10	0.26	6.77	11.03	2.81	0.17	0.11	99.47	1100.6
49.17	1.89	13.93	12.15	0.25	6.64	11.21	2.79	0.19	0.10	98.32	1108.8
49.71	1.89	14.07	12.25	0.11	6.70	11.20	2.78	0.20	0.17	99.07	1109.4
50.35	1.85	14.11	12.14	0.19	6.69	11.09	2.78	0.18	0.09	99.45	1142.6
49.42	1.92	13.96	11.95	0.24	6.58	11.12	2.80	0.19	0.12	98.28	1164.7
49.83	1.89	14.14	12.17	0.26	6.76	11.10	2.68	0.17	0.11	99.10	1165.2
50.72	1.88	14.21	11.95	0.26	6.68	11.09	2.75	0.16	0.18	99.88	1184.6
49.22	1.83	13.92	12.00	0.21	6.47	11.19	2.74	0.17	0.12	97.89	1220.7
49.82	1.86	14.04	12.12	0.29	6.76	11.11	2.75	0.12	0.21	99.07	1221.0
50.31	1.87	14.21	11.93	0.24	6.81	11.13	2.84	0.16	0.14	99.64	1226.5
50.14	1.92	13.55	12.07	0.19	6.46	11.25	2.66	0.22	0.21	98.66	1276.6
50.46	1.83	13.99	12.06	0.23	6.67	11.07	2.63	0.15	0.17	99.26	1276.8

Exp 29

SiO2	TiO2	Al2O3	FeO	MnO	MgO	CaO	Na2O	K2O	P2O5	Total	d (um)
47.19	1.63	10.15	13.17	0.23	13.88	10.25	1.70	0.06	0.18	98.44	5.8
47.04	1.66	10.17	13.44	0.23	13.43	10.58	1.68	0.07	0.13	98.44	6.4
46.99	1.62	10.22	13.12	0.30	13.64	10.33	1.78	0.06	0.08	98.14	8.4
46.07	1.49	9.76	13.16	0.21	14.57	9.83	1.62	0.10	0.12	96.92	11.8
46.96	1.55	9.97	13.48	0.12	14.73	10.20	1.73	0.07	0.11	98.92	12.5
46.64	1.50	9.94	13.23	0.24	14.89	9.86	1.68	0.08	0.12	98.18	14.3
46.95	1.53	10.07	13.00	0.24	15.02	9.75	1.77	0.07	0.17	98.55	17.8
46.41	1.52	10.16	13.22	0.32	14.92	9.72	1.73	0.10	0.12	98.21	18.6
46.73	1.50	9.96	13.20	0.13	15.26	9.74	1.75	0.07	0.11	98.44	20.3
46.97	1.54	10.09	12.79	0.22	15.09	9.62	1.86	0.07	0.08	98.32	23.8
46.70	1.52	10.33	13.13	0.25	14.96	9.78	1.82	0.10	0.11	98.71	24.6
46.83	1.50	10.19	12.83	0.23	15.16	9.67	1.69	0.09	0.12	98.30	26.2
47.07	1.55	10.33	12.60	0.19	14.99	9.64	1.90	0.10	0.19	98.56	29.8
46.91	1.50	10.55	12.92	0.32	14.83	9.76	1.83	0.11	0.12	98.84	30.7
46.83	1.55	10.56	13.00	0.19	15.02	9.57	1.83	0.10	0.14	98.77	32.1
46.99	1.55	10.47	12.58	0.21	14.73	9.70	1.89	0.12	0.17	98.42	35.7
47.07	1.55	10.63	12.75	0.27	14.69	9.86	1.84	0.06	0.15	98.86	36.8
47.17	1.55	10.66	12.74	0.17	14.61	9.74	1.87	0.09	0.12	98.71	38.0
47.04	1.50	10.72	12.56	0.21	14.44	9.77	2.03	0.14	0.09	98.50	41.7
47.48	1.53	10.90	12.74	0.31	14.24	9.67	1.94	0.11	0.09	99.00	42.8
47.62	1.56	11.22	12.17	0.15	13.62	9.77	2.03	0.11	0.22	98.46	43.5
47.19	1.55	10.91	12.35	0.21	14.35	9.78	1.91	0.11	0.15	98.50	43.9
47.50	1.54	10.89	12.43	0.26	14.26	9.73	1.89	0.15	0.13	98.77	47.7
47.64	1.54	11.03	12.46	0.31	14.03	9.78	2.00	0.07	0.09	98.93	48.9
47.33	1.56	11.09	12.51	0.19	13.86	9.84	1.89	0.11	0.11	98.48	49.8
47.66	1.54	11.07	12.11	0.17	13.85	9.80	2.03	0.10	0.15	98.46	53.7
47.24	1.49	11.18	12.36	0.24	13.68	9.82	2.07	0.06	0.15	98.29	55.0
47.67	1.57	11.31	12.26	0.22	13.46	9.82	1.95	0.12	0.02	98.38	55.8
47.82	1.55	11.77	11.97	0.27	13.05	9.87	2.16	0.16	0.21	98.82	59.0
47.62	1.51	11.42	12.08	0.14	13.62	9.76	2.00	0.12	0.12	98.39	59.7
47.57	1.56	11.46	12.29	0.33	13.35	9.91	2.01	0.12	0.14	98.72	61.0
47.72	1.54	11.47	12.14	0.16	13.07	9.92	2.12	0.11	0.12	98.37	61.7
47.67	1.61	11.68	12.10	0.24	13.26	10.01	2.15	0.10	0.09	98.89	63.3
48.28	1.55	11.61	11.86	0.29	13.13	9.77	2.11	0.18	0.12	98.89	65.7
47.83	1.57	11.70	11.99	0.13	13.18	9.90	2.07	0.11	0.12	98.59	67.1
48.20	1.61	11.69	11.91	0.24	12.64	9.92	2.11	0.14	0.16	98.62	67.6
48.17	1.55	11.79	12.09	0.14	12.84	10.10	2.06	0.15	0.18	99.08	73.2
48.27	1.55	12.19	11.58	0.24	12.33	10.18	2.23	0.13	0.12	98.82	74.4
48.17	1.52	12.04	11.90	0.19	12.70	9.97	2.20	0.18	0.23	99.11	79.2
47.85	1.59	12.15	11.84	0.22	11.98	10.08	2.24	0.11	0.12	98.18	79.8
48.21	1.58	12.14	11.79	0.24	12.20	9.90	2.09	0.15	0.14	98.44	85.2
48.44	1.59	12.63	11.60	0.28	11.71	9.94	2.37	0.13	0.09	98.77	89.9
48.49	1.55	12.75	11.43	0.21	11.03	10.16	2.38	0.14	0.12	98.26	96.3
48.63	1.60	13.20	11.25	0.16	11.10	10.08	2.50	0.14	0.13	98.80	96.4
48.79	1.68	13.48	11.34	0.35	10.53	10.26	2.49	0.22	0.23	99.37	105.4
49.05	1.72	13.45	11.22	0.23	10.13	10.17	2.67	0.18	0.15	98.98	111.8
49.22	1.68	13.17	11.32	0.16	10.23	10.09	2.54	0.18	0.22	98.80	112.8

49.21	1.67	13.61	11.19	0.22	9.79	10.41	2.52	0.15	0.12	98.89	120.8
49.07	1.78	13.67	11.01	0.18	9.59	10.12	2.67	0.17	0.18	98.42	127.0
49.45	1.75	13.49	11.21	0.16	9.43	10.27	2.56	0.16	0.15	98.63	129.3
49.13	1.76	13.75	11.20	0.18	9.10	10.45	2.64	0.15	0.20	98.54	136.3
49.48	1.78	13.88	11.12	0.24	8.93	10.32	2.69	0.18	0.16	98.79	142.4
49.64	1.75	13.87	11.09	0.28	8.75	10.28	2.60	0.23	0.19	98.66	145.8
49.42	1.78	14.02	11.21	0.26	8.75	10.50	2.79	0.22	0.26	99.22	151.7
49.74	1.88	13.91	10.95	0.19	8.62	10.42	2.73	0.21	0.27	98.91	157.8
49.49	1.82	13.95	11.16	0.27	8.44	10.33	2.70	0.21	0.12	98.49	162.3
49.62	1.81	14.04	11.01	0.16	8.26	10.47	2.75	0.21	0.16	98.48	167.2
49.63	1.82	14.03	10.96	0.15	8.19	10.45	2.85	0.19	0.22	98.47	173.0
49.65	1.76	13.99	11.32	0.29	7.97	10.52	2.71	0.22	0.17	98.60	178.8
49.76	1.84	13.97	11.30	0.29	8.04	10.33	2.76	0.21	0.16	98.65	182.7
49.88	1.81	14.09	11.15	0.21	7.92	10.43	2.83	0.17	0.21	98.68	188.4
49.78	1.86	14.02	11.46	0.20	7.94	10.61	2.66	0.23	0.12	98.87	195.3
49.40	1.83	14.07	11.38	0.26	7.87	10.72	2.90	0.17	0.21	98.80	198.1
49.70	1.85	14.14	11.27	0.20	7.64	10.68	2.86	0.20	0.19	98.73	203.7
49.53	1.88	14.09	11.47	0.09	7.53	10.71	2.69	0.17	0.08	98.25	211.8
49.76	1.84	14.00	11.40	0.24	7.68	10.85	2.75	0.23	0.12	98.85	213.6
49.54	1.88	13.94	11.34	0.21	7.58	10.72	2.83	0.23	0.18	98.45	219.0
49.76	1.90	14.06	11.49	0.25	7.40	10.77	2.72	0.23	0.28	98.86	228.3
49.85	1.86	14.13	11.46	0.23	7.46	10.70	2.76	0.18	0.20	98.83	229.1
49.53	1.90	14.12	11.46	0.23	7.36	10.72	2.74	0.17	0.27	98.48	234.4
49.26	1.82	14.15	11.69	0.22	7.29	10.90	2.78	0.21	0.17	98.48	243.4
50.11	1.79	14.16	11.40	0.23	7.33	10.79	2.80	0.19	0.16	98.96	244.5
49.70	1.86	14.08	11.69	0.20	7.25	10.91	2.64	0.19	0.20	98.71	244.8
49.33	1.83	14.09	11.72	0.13	7.26	10.93	2.83	0.19	0.16	98.48	246.5
49.56	1.87	14.00	11.62	0.20	7.22	10.82	2.77	0.21	0.08	98.36	249.7
49.52	1.83	14.06	11.30	0.30	7.20	11.03	2.71	0.19	0.22	98.35	255.4
49.67	1.82	13.93	11.70	0.23	7.22	10.85	2.74	0.18	0.21	98.55	261.3
50.09	1.78	13.99	11.45	0.24	7.09	10.87	2.72	0.22	0.09	98.54	265.0
49.75	1.88	14.12	11.71	0.15	7.17	10.87	2.64	0.18	0.18	98.64	277.8
49.27	1.83	13.86	11.94	0.29	6.99	10.97	2.77	0.19	0.19	98.29	285.3
49.71	1.83	13.88	11.60	0.21	7.07	10.88	2.67	0.16	0.15	98.15	288.6
50.15	1.79	14.03	11.69	0.22	7.13	10.91	2.64	0.21	0.21	98.97	294.3
49.80	1.93	13.96	11.60	0.28	6.97	11.03	2.76	0.16	0.30	98.79	296.4
49.56	1.91	14.10	11.83	0.16	7.05	11.03	2.66	0.16	0.15	98.62	327.2
49.66	1.83	14.01	11.69	0.25	6.95	11.16	2.78	0.16	0.18	98.66	330.8
49.55	1.87	14.03	11.63	0.26	6.91	11.01	2.76	0.15	0.15	98.33	337.4
49.24	1.85	13.84	12.06	0.27	6.97	11.13	2.71	0.19	0.20	98.47	369.1
49.52	1.88	14.08	11.86	0.21	6.87	11.04	2.79	0.16	0.10	98.52	372.9
49.83	1.87	14.06	11.59	0.19	6.90	11.15	2.75	0.19	0.10	98.62	378.5
49.41	1.87	13.97	12.04	0.15	6.90	11.09	2.75	0.16	0.21	98.54	411.0
49.64	1.94	13.95	11.94	0.10	6.87	11.17	2.69	0.15	0.15	98.59	415.1
49.52	1.90	13.99	11.80	0.17	6.81	11.01	2.66	0.17	0.19	98.23	419.5
49.48	1.86	13.96	12.21	0.26	6.90	11.15	2.82	0.19	0.11	98.93	452.9
49.52	1.88	14.01	12.03	0.22	6.93	11.02	2.68	0.21	0.17	98.68	457.3
49.98	1.91	14.06	11.86	0.23	6.88	11.30	2.64	0.19	0.13	99.18	460.5
49.30	1.89	14.03	12.03	0.20	6.84	11.22	2.78	0.19	0.09	98.57	494.9

49.56	1.85	14.01	11.94	0.28	6.77	11.08	2.77	0.15	0.22	98.64	499.4
49.46	1.92	13.97	11.83	0.13	6.90	11.13	2.74	0.16	0.15	98.40	501.6
49.56	1.81	13.98	12.11	0.19	6.92	11.12	2.64	0.19	0.10	98.62	536.7
49.55	1.83	14.06	11.82	0.23	6.89	11.15	2.74	0.18	0.32	98.77	541.6
49.42	1.89	13.84	12.00	0.33	6.80	11.02	2.70	0.21	0.20	98.41	542.6
49.71	1.88	14.10	11.83	0.22	6.83	11.14	2.66	0.17	0.13	98.66	578.7
49.69	1.76	13.97	11.95	0.28	6.88	10.98	2.67	0.17	0.13	98.48	583.6
49.55	1.91	13.92	12.06	0.22	6.84	11.10	2.76	0.16	0.19	98.71	583.7
49.72	1.88	13.97	12.08	0.17	6.88	11.02	2.72	0.19	0.22	98.85	620.5
49.57	1.82	14.04	12.13	0.22	6.87	10.95	2.81	0.19	0.27	98.87	624.6
49.67	1.91	14.00	11.89	0.18	6.79	11.13	2.71	0.20	0.13	98.61	625.9
49.96	1.81	14.00	11.97	0.25	6.78	11.00	2.68	0.17	0.15	98.76	662.5
49.47	1.87	13.99	11.89	0.20	6.70	11.13	2.70	0.20	0.12	98.27	665.7
50.00	1.84	14.07	11.91	0.17	6.80	11.15	2.68	0.15	0.09	98.87	668.0
49.72	1.84	14.08	11.98	0.20	6.79	11.19	2.63	0.19	0.22	98.83	704.3
49.23	1.89	13.75	12.01	0.26	6.85	11.22	2.64	0.15	0.13	98.11	706.7
49.43	1.89	14.00	12.00	0.18	6.87	11.19	2.80	0.18	0.24	98.77	710.2
49.89	1.82	14.01	11.91	0.25	6.80	11.03	2.77	0.19	0.22	98.89	746.3
49.55	1.87	13.99	12.07	0.22	6.84	11.13	2.72	0.19	0.13	98.70	747.7
49.31	1.87	14.00	12.14	0.25	6.82	11.06	2.72	0.20	0.25	98.59	752.3
49.59	1.79	14.07	11.92	0.23	6.91	11.09	2.71	0.16	0.13	98.59	788.2
49.32	1.88	13.87	12.22	0.28	6.88	11.21	2.68	0.16	0.19	98.69	788.8
49.57	1.88	14.18	12.00	0.25	6.78	11.12	2.69	0.20	0.22	98.88	794.5
49.62	1.84	13.93	12.00	0.21	6.80	11.25	2.72	0.17	0.20	98.73	829.9
49.67	1.85	13.95	11.87	0.26	6.83	11.05	2.72	0.20	0.22	98.61	830.1
49.38	1.85	13.99	11.93	0.29	6.83	11.29	2.73	0.16	0.12	98.56	836.6
49.51	1.84	14.12	12.07	0.12	6.76	11.07	2.70	0.18	0.11	98.46	870.9
49.73	1.84	14.04	12.01	0.15	6.88	11.18	2.69	0.18	0.13	98.82	872.0
49.36	1.85	14.02	11.92	0.27	6.86	11.25	2.65	0.16	0.22	98.55	878.8
49.60	1.87	13.95	12.08	0.18	6.80	11.05	2.68	0.16	0.22	98.58	911.9
49.48	1.91	13.96	12.03	0.19	6.90	11.20	2.68	0.20	0.16	98.69	913.9
49.60	1.86	14.19	11.92	0.26	6.89	11.15	2.61	0.17	0.08	98.73	921.0
49.26	1.88	13.86	12.07	0.15	6.78	11.13	2.64	0.19	0.09	98.05	952.9
49.47	1.85	13.87	12.12	0.21	6.83	11.04	2.78	0.19	0.22	98.57	955.8
49.57	1.82	13.92	11.94	0.26	6.81	11.13	2.68	0.21	0.24	98.57	963.2
49.45	1.84	13.94	12.00	0.14	6.83	11.13	2.63	0.18	0.22	98.36	994.0
49.72	1.81	14.02	11.90	0.13	6.85	11.13	2.66	0.19	0.11	98.51	997.8
50.00	1.84	14.13	11.92	0.24	6.91	11.03	2.72	0.13	0.10	99.02	1005.3
49.62	1.79	13.90	12.15	0.18	6.81	11.13	2.67	0.14	0.12	98.50	1035.0
49.82	1.88	14.10	11.96	0.23	6.99	11.07	2.75	0.17	0.16	99.13	1039.6
49.84	1.83	13.93	12.09	0.29	6.88	11.13	2.70	0.18	0.18	99.06	1047.5
49.68	1.88	14.10	12.13	0.17	6.91	11.23	2.62	0.16	0.12	98.99	1076.0
49.71	1.86	14.21	11.95	0.23	6.84	11.16	2.69	0.18	0.18	99.00	1081.6
49.52	1.85	13.99	11.98	0.17	6.88	11.05	2.65	0.20	0.22	98.51	1089.6
49.40	1.93	13.99	12.01	0.19	6.91	11.14	2.60	0.19	0.16	98.52	1117.0
49.17	1.83	13.96	11.91	0.22	6.87	10.97	2.68	0.17	0.13	97.91	1123.4
49.67	1.86	14.06	11.87	0.22	6.85	11.00	2.67	0.19	0.12	98.51	1131.8
49.71	1.94	14.01	11.85	0.26	6.87	11.17	2.66	0.17	0.12	98.76	1158.1
49.87	1.92	13.98	11.82	0.19	6.79	11.18	2.66	0.17	0.24	98.81	1165.4

49.44	1.92	14.01	11.92	0.25	6.81	11.06	2.67	0.20	0.18	98.44	1173.9
49.90	1.88	14.03	11.62	0.22	6.85	11.17	2.66	0.19	0.15	98.65	1199.1
49.65	1.95	13.94	11.80	0.23	6.83	10.92	2.73	0.19	0.22	98.45	1207.2
49.96	1.87	14.04	11.68	0.23	6.73	11.04	2.73	0.21	0.20	98.69	1216.1

Exp 33

SiO2	TiO2	Al2O3	FeO	MnO	MgO	CaO	Na2O	K2O	P2O5	Total	d (um)
46.70	1.65	10.64	13.84	0.29	13.01	10.83	1.85	0.07	0.03	98.91	6.6
47.54	1.73	10.79	13.55	0.18	12.60	10.98	1.82	0.11	0.08	99.38	7.3
46.97	1.66	10.12	13.89	0.24	13.52	10.63	1.78	0.08	0.13	99.01	10.4
46.85	1.65	9.99	13.76	0.26	14.27	10.45	1.79	0.09	0.13	99.24	13.4
46.71	1.64	9.98	13.76	0.21	14.51	10.17	1.71	0.11	0.19	98.98	16.8
47.08	1.63	10.00	13.66	0.20	14.76	10.09	1.77	0.08	0.13	99.39	19.5
46.77	1.59	10.11	13.73	0.25	14.81	10.11	1.82	0.09	0.11	99.39	23.3
46.78	1.50	10.12	13.74	0.29	14.85	10.10	1.78	0.10	0.14	99.38	25.0
47.60	1.55	10.04	13.62	0.22	14.81	10.01	1.80	0.09	0.09	99.82	25.6
47.56	1.57	10.20	13.52	0.29	14.78	10.03	1.82	0.06	0.14	99.96	29.7
47.41	1.58	10.15	13.76	0.25	14.83	9.97	1.79	0.10	0.21	100.03	31.1
47.61	1.58	10.07	13.53	0.26	14.74	10.02	1.74	0.10	0.03	99.68	33.1
47.37	1.51	10.37	13.48	0.23	14.74	9.90	1.77	0.09	0.19	99.63	33.6
47.39	1.54	10.18	13.53	0.24	14.73	10.00	1.82	0.08	0.14	99.63	36.2
47.47	1.56	10.26	13.47	0.32	14.70	9.90	1.81	0.14	0.16	99.80	37.2
48.76	1.54	10.27	13.31	0.24	14.67	9.98	1.80	0.09	0.14	100.78	37.6
46.97	1.63	10.14	13.86	0.25	14.81	10.01	1.80	0.05	0.16	99.67	39.0
46.70	1.51	10.36	13.50	0.19	14.77	9.89	1.87	0.10	0.15	99.05	40.0
48.46	1.60	10.41	13.33	0.23	14.48	10.01	1.85	0.08	0.03	100.48	43.3
49.11	1.59	10.11	13.31	0.23	14.53	9.98	1.87	0.09	0.14	100.97	43.7
46.47	1.61	10.34	13.60	0.28	14.73	10.02	1.85	0.11	0.18	99.18	44.9
47.90	1.53	10.47	13.19	0.23	14.75	10.08	1.89	0.08	0.10	100.20	46.3
46.55	1.50	10.65	13.19	0.27	14.62	9.94	1.98	0.13	0.13	98.97	48.7
50.01	1.54	10.24	13.40	0.17	14.58	10.16	1.90	0.08	0.13	102.20	49.4
46.85	1.53	10.24	13.45	0.27	14.59	10.00	1.80	0.10	0.20	99.02	49.8
47.22	1.56	10.41	13.45	0.24	14.55	9.97	1.81	0.13	0.14	99.47	50.8
47.12	1.56	10.50	13.29	0.16	14.54	9.91	1.92	0.11	0.18	99.28	52.7
47.38	1.58	10.71	13.41	0.31	14.56	10.07	1.86	0.06	0.12	100.04	55.1
47.67	1.58	10.36	13.32	0.19	14.49	9.99	1.87	0.10	0.14	99.70	55.9
46.63	1.54	10.41	13.53	0.15	14.51	10.09	1.84	0.09	0.12	98.92	56.8
48.08	1.52	10.53	13.26	0.32	14.42	9.97	1.94	0.12	0.07	100.24	59.1
47.33	1.53	10.73	13.25	0.28	14.26	10.01	1.93	0.13	0.12	99.57	61.6
47.02	1.60	10.24	13.35	0.24	14.27	10.10	1.88	0.07	0.13	98.89	62.0
46.40	1.55	10.40	13.52	0.23	14.56	9.94	1.84	0.10	0.03	98.57	62.6
47.90	1.55	10.62	13.07	0.24	14.29	10.02	1.92	0.11	0.13	99.83	65.4
47.52	1.54	10.78	13.46	0.22	14.18	10.10	1.96	0.14	0.09	100.00	68.1
47.93	1.53	10.38	13.39	0.24	14.19	10.01	1.86	0.11	0.17	99.82	68.5
47.36	1.58	10.95	13.23	0.27	14.08	10.11	1.92	0.09	0.20	99.78	74.5
47.47	1.54	10.86	12.93	0.32	13.92	9.78	1.99	0.12	0.12	99.05	77.7
47.25	1.61	10.81	13.14	0.20	13.94	10.13	1.95	0.11	0.18	99.31	81.0
47.77	1.61	10.94	13.11	0.19	13.95	10.05	1.90	0.10	0.08	99.71	82.6
47.29	1.59	11.05	13.15	0.24	13.93	9.92	1.90	0.10	0.17	99.33	87.4
47.83	1.53	10.96	13.15	0.28	13.61	10.22	1.92	0.09	0.13	99.72	93.9
47.61	1.63	11.14	12.90	0.38	13.56	10.13	1.98	0.13	0.14	99.59	94.8
48.66	1.53	11.08	13.11	0.17	13.78	10.16	1.95	0.09	0.18	100.69	100.4
48.29	1.61	11.26	13.07	0.25	13.35	10.17	2.06	0.06	0.12	100.24	107.1
47.65	1.61	11.23	12.96	0.22	13.70	10.17	2.07	0.10	0.03	99.73	114.2

47.67	1.57	11.13	12.76	0.29	13.38	9.94	2.11	0.09	0.16	99.10	114.8
47.26	1.60	11.18	12.94	0.21	13.32	10.17	2.02	0.12	0.19	99.01	119.3
46.88	1.62	11.30	12.78	0.17	13.07	10.27	2.02	0.12	0.14	98.36	131.5
48.01	1.59	11.40	12.69	0.21	12.87	10.12	1.98	0.08	0.15	99.09	143.8
48.44	1.59	11.74	12.67	0.25	12.97	10.14	2.13	0.18	0.11	100.21	149.1
48.23	1.64	11.78	12.54	0.19	12.97	10.21	2.18	0.09	0.13	99.94	150.5
47.50	1.70	11.41	12.68	0.21	12.50	10.29	2.12	0.14	0.19	98.72	156.0
48.33	1.68	11.69	12.61	0.28	12.38	10.29	2.08	0.12	0.20	99.66	168.3
48.88	1.66	11.74	12.42	0.24	12.33	10.28	2.14	0.09	0.04	99.83	180.5
48.17	1.54	12.03	12.47	0.13	12.29	10.29	2.18	0.16	0.15	99.39	183.3
48.69	1.65	12.08	12.33	0.22	12.28	10.10	2.26	0.13	0.14	99.88	186.9
47.92	1.59	11.86	12.42	0.20	12.10	10.06	2.24	0.18	0.15	98.73	197.2
48.93	1.53	12.38	12.32	0.21	11.78	10.23	2.25	0.16	0.37	100.15	217.5
50.18	1.63	12.59	12.07	0.18	11.47	10.15	2.25	0.18	0.07	100.77	223.3
48.83	1.65	12.38	12.20	0.23	11.63	10.25	2.26	0.15	0.06	99.62	227.8
49.39	1.59	12.84	11.95	0.14	11.24	10.32	2.42	0.16	0.15	100.19	251.7
49.32	1.67	12.57	12.11	0.30	11.18	10.24	2.31	0.15	0.10	99.95	258.2
49.20	1.65	12.94	11.73	0.20	10.78	10.27	2.48	0.13	0.17	99.54	259.7
50.80	1.66	13.27	11.89	0.25	10.66	10.31	2.52	0.19	0.15	101.69	286.0
49.07	1.68	12.80	12.12	0.24	10.63	10.23	2.39	0.12	0.15	99.42	288.7
49.46	1.63	13.48	11.64	0.28	10.32	10.32	2.62	0.17	0.12	100.04	296.1
49.61	1.67	13.11	11.69	0.26	10.26	10.38	2.52	0.20	0.12	99.82	319.2
50.18	1.66	13.33	11.63	0.26	10.14	10.36	2.56	0.15	0.15	100.44	320.2
50.32	1.63	13.69	11.46	0.17	9.79	10.25	2.62	0.18	0.16	100.27	332.5
49.85	1.66	13.30	11.61	0.26	9.86	10.41	2.66	0.13	0.22	99.96	349.7
50.19	1.71	13.61	11.44	0.19	9.60	10.31	2.66	0.22	0.14	100.05	354.5
49.43	1.70	13.93	11.19	0.15	9.34	10.40	2.77	0.21	0.15	99.27	368.9
49.83	1.65	13.46	11.59	0.14	9.46	10.35	2.56	0.16	0.10	99.30	380.1
49.98	1.70	13.90	11.37	0.26	9.04	10.45	2.70	0.17	0.24	99.81	388.6
50.24	1.77	13.94	11.24	0.27	8.91	10.47	2.76	0.19	0.21	100.00	405.3
49.12	1.72	13.78	11.49	0.17	9.04	10.32	2.65	0.18	0.14	98.60	410.7
49.86	1.81	13.97	11.39	0.11	8.78	10.34	2.80	0.19	0.21	99.45	422.9
50.66	1.71	13.90	11.59	0.19	8.87	10.50	2.78	0.19	0.14	100.51	441.1
50.74	1.81	14.03	11.17	0.16	8.61	10.38	2.80	0.19	0.20	100.08	441.7
50.82	1.80	14.11	11.32	0.12	8.36	10.45	2.73	0.21	0.17	100.09	457.1
50.87	1.82	13.77	11.30	0.16	8.40	10.67	2.69	0.15	0.17	100.00	471.7
50.35	1.88	14.21	11.37	0.29	8.24	10.38	2.91	0.17	0.15	99.94	478.0
49.97	1.78	14.14	11.39	0.22	8.27	10.58	2.89	0.16	0.25	99.64	491.4
50.55	1.82	13.94	11.41	0.23	8.17	10.60	2.82	0.14	0.21	99.89	502.1
50.06	1.83	14.06	11.11	0.31	8.09	10.65	2.78	0.26	0.10	99.23	514.4
49.93	1.88	14.24	11.60	0.21	7.98	10.59	2.81	0.21	0.21	99.66	525.6
49.79	1.82	14.12	11.31	0.15	8.06	10.53	2.79	0.16	0.19	98.92	532.6
52.20	1.89	14.25	11.36	0.23	7.84	10.64	2.83	0.20	0.19	101.62	550.8
50.42	1.83	14.22	11.49	0.20	7.76	10.60	2.75	0.18	0.22	99.68	559.8
50.15	1.83	14.12	11.39	0.24	7.86	10.59	2.81	0.22	0.15	99.34	563.1
51.07	1.85	14.34	11.43	0.16	7.62	10.90	2.88	0.19	0.09	100.53	587.2
51.65	1.86	14.11	11.67	0.23	7.72	10.62	2.72	0.21	0.21	100.99	593.6
50.40	1.81	14.34	11.50	0.21	7.74	10.79	2.78	0.24	0.15	99.96	594.0
50.99	1.90	14.40	11.43	0.27	7.56	10.69	2.84	0.19	0.26	100.52	623.6

51.78	1.83	14.17	11.64	0.27	7.61	10.65	2.76	0.15	0.25	101.11	624.0
50.29	1.95	14.10	11.64	0.32	7.54	10.71	2.78	0.16	0.12	99.59	628.3
50.27	1.85	13.99	11.67	0.16	7.40	10.95	2.87	0.18	0.20	99.52	654.6
50.24	1.90	14.18	11.55	0.15	7.42	10.68	2.99	0.20	0.14	99.44	660.0
50.53	1.93	14.09	11.82	0.23	7.29	10.96	2.84	0.15	0.23	100.07	662.5
49.29	1.84	14.09	11.74	0.20	7.47	10.84	2.73	0.19	0.14	98.52	685.0
50.47	1.90	14.14	11.59	0.22	7.35	10.87	2.87	0.23	0.19	99.83	696.4
50.67	1.91	14.16	11.70	0.26	7.39	10.88	2.80	0.20	0.12	100.09	696.8
50.18	1.90	13.97	11.75	0.17	7.15	10.74	2.76	0.17	0.12	98.91	715.5
50.25	1.89	14.18	11.94	0.22	7.27	10.94	2.77	0.12	0.15	99.74	730.9
50.84	1.84	14.39	11.66	0.20	7.13	10.83	2.86	0.18	0.19	100.12	732.8
49.98	1.77	14.16	11.68	0.22	7.28	10.78	2.80	0.20	0.20	99.09	746.0
50.17	1.91	14.33	11.92	0.19	7.11	10.85	2.78	0.19	0.20	99.65	765.2
50.35	1.90	14.29	11.69	0.15	7.14	10.82	2.90	0.18	0.21	99.62	769.2
50.12	1.89	14.05	11.87	0.26	7.14	10.82	2.81	0.19	0.13	99.29	776.5
50.29	1.82	14.19	11.90	0.31	7.17	10.96	2.81	0.17	0.09	99.71	799.4
50.55	1.85	14.19	11.74	0.20	7.18	10.98	2.91	0.16	0.09	99.86	805.6
49.86	1.82	13.96	11.67	0.19	7.09	10.90	2.77	0.20	0.20	98.65	807.0
49.70	1.93	14.09	11.91	0.24	7.12	10.96	2.80	0.15	0.17	99.08	833.7
50.39	1.85	13.99	11.78	0.22	7.06	10.93	2.85	0.18	0.20	99.44	837.5
50.53	1.84	14.18	11.83	0.13	6.97	10.89	2.86	0.14	0.16	99.52	841.9
50.10	1.91	14.08	11.85	0.22	7.04	10.97	2.78	0.13	0.20	99.27	867.9
49.78	1.88	14.13	11.79	0.24	7.04	10.93	2.75	0.19	0.22	98.95	867.9
50.45	1.86	14.15	11.72	0.17	7.01	10.90	2.87	0.19	0.20	99.51	878.4
49.98	1.87	13.99	11.75	0.25	6.94	11.03	2.76	0.18	0.25	98.99	898.5
49.82	1.89	14.02	11.98	0.21	7.10	11.17	2.76	0.20	0.20	99.35	902.1
50.87	1.87	14.27	11.65	0.10	6.91	10.98	2.93	0.24	0.15	99.97	914.7
50.65	1.90	14.02	11.90	0.24	6.90	10.97	2.68	0.19	0.19	99.64	928.9
50.41	1.90	14.06	11.84	0.21	6.84	11.16	2.96	0.15	0.20	99.74	936.3
50.97	1.82	14.08	11.81	0.28	6.81	11.06	2.87	0.16	0.10	99.95	951.2
50.34	1.83	14.12	11.89	0.18	6.83	11.00	2.78	0.13	0.28	99.37	959.4
49.95	1.82	14.00	11.84	0.23	6.86	11.05	2.93	0.18	0.26	99.09	970.6
50.70	1.93	14.23	11.75	0.12	6.90	10.90	2.96	0.20	0.18	99.87	987.5
51.18	1.95	14.03	11.72	0.26	6.75	11.10	2.76	0.19	0.07	99.99	990.0
50.28	1.86	14.17	11.99	0.19	6.97	10.99	2.74	0.16	0.10	99.45	1004.8
51.04	1.86	14.12	11.92	0.16	6.82	11.00	2.84	0.16	0.16	100.08	1020.4
51.01	1.85	14.20	11.57	0.19	6.90	10.94	2.89	0.20	0.15	99.90	1024.0
50.49	1.87	13.98	11.88	0.18	6.89	11.11	2.78	0.18	0.18	99.54	1039.0
50.58	1.89	14.19	11.71	0.11	6.77	10.92	2.91	0.19	0.15	99.41	1060.3
50.53	1.89	14.01	11.85	0.23	6.81	11.15	2.69	0.17	0.30	99.64	1073.2
51.48	1.86	14.19	11.55	0.16	6.81	10.97	2.79	0.18	0.17	100.16	1096.8

Exp 34

SiO2	TiO2	Al2O3	FeO	MnO	MgO	CaO	Na2O	K2O	P2O5	Total	d (um)
47.17	1.41	9.85	12.80	0.22	17.94	9.17	1.80	0.11	0.10	100.56	6.4
46.15	1.31	8.43	13.87	0.33	19.77	9.11	1.47	0.10	0.05	100.59	23.5
46.32	1.29	8.30	13.80	0.25	20.94	8.57	1.44	0.10	0.15	101.16	40.6
46.23	1.21	8.58	13.38	0.24	20.67	8.49	1.46	0.06	0.08	100.40	57.8
46.64	1.29	9.06	12.95	0.22	19.71	8.61	1.58	0.06	0.18	100.29	92.0
46.78	1.33	9.40	12.93	0.18	19.09	8.75	1.59	0.08	0.11	100.24	109.1
46.33	1.27	8.50	13.22	0.29	19.94	8.47	1.55	0.07	0.09	99.72	56.2
46.20	1.30	8.43	13.09	0.31	19.85	8.45	1.46	0.07	0.06	99.22	60.8
46.00	1.30	8.54	13.17	0.26	19.48	8.53	1.52	0.07	0.08	98.93	61.6
46.57	1.33	8.38	13.01	0.17	19.73	8.58	1.47	0.08	0.19	99.50	65.9
46.16	1.38	8.54	13.09	0.26	19.65	8.47	1.56	0.08	0.17	99.36	66.9
45.89	1.33	8.28	13.03	0.25	19.49	8.42	1.41	0.04	0.17	98.30	67.5
46.63	1.32	8.48	13.06	0.23	19.64	8.56	1.50	0.07	0.06	99.54	71.0
46.13	1.33	8.79	13.25	0.22	19.57	8.53	1.55	0.07	0.08	99.51	72.3
46.62	1.29	8.54	12.77	0.21	19.73	8.50	1.51	0.05	0.12	99.34	72.8
46.21	1.33	8.60	13.28	0.26	19.63	8.59	1.53	0.09	0.13	99.64	76.1
46.42	1.33	8.83	13.01	0.19	19.29	8.64	1.45	0.06	0.05	99.26	77.7
46.50	1.36	8.69	12.94	0.22	19.58	8.51	1.51	0.08	0.10	99.50	78.0
46.37	1.37	8.80	13.12	0.30	19.57	8.56	1.47	0.07	0.11	99.74	81.3
46.26	1.32	8.85	12.99	0.24	19.17	8.64	1.61	0.08	0.07	99.23	83.0
46.77	1.37	8.65	12.91	0.21	19.33	8.55	1.52	0.06	0.12	99.48	83.3
46.28	1.31	8.74	13.00	0.22	19.30	8.49	1.68	0.03	0.11	99.16	86.4
46.08	1.36	9.03	12.95	0.22	19.06	8.60	1.56	0.09	0.11	99.06	88.3
46.94	1.39	8.79	13.00	0.15	19.36	8.65	1.50	0.07	0.13	99.99	88.5
46.58	1.35	8.72	12.98	0.18	19.16	8.61	1.53	0.06	0.12	99.29	91.5
46.47	1.39	9.03	12.93	0.30	18.96	8.66	1.55	0.07	0.10	99.46	93.7
46.76	1.31	8.99	12.85	0.11	19.07	8.58	1.52	0.05	0.10	99.34	96.6
46.51	1.38	9.22	12.94	0.27	18.76	8.67	1.55	0.09	0.13	99.51	99.1
46.69	1.31	9.02	12.98	0.26	18.90	8.60	1.61	0.07	0.15	99.59	101.7
46.64	1.36	9.04	12.68	0.25	18.76	8.74	1.76	0.09	0.06	99.36	104.3
46.54	1.35	9.25	12.88	0.23	18.65	8.78	1.75	0.05	0.16	99.64	104.4
46.69	1.42	9.44	12.78	0.22	18.33	8.81	1.55	0.07	0.14	99.46	109.2
46.82	1.37	9.12	12.77	0.19	18.79	8.64	1.59	0.08	0.09	99.46	109.5
46.50	1.43	9.30	12.87	0.20	18.31	8.78	1.66	0.06	0.12	99.22	109.8
46.48	1.37	9.11	12.75	0.24	18.40	8.78	1.59	0.11	0.09	98.92	114.8
46.60	1.42	9.52	12.89	0.20	18.25	8.76	1.76	0.07	0.13	99.61	115.2
47.20	1.41	9.63	12.54	0.12	17.97	8.82	1.63	0.08	0.10	99.50	119.2
46.94	1.39	9.34	12.52	0.21	18.24	8.72	1.66	0.04	0.07	99.13	119.9
46.47	1.36	9.54	12.63	0.25	18.03	8.82	1.64	0.08	0.15	98.96	120.5
47.19	1.42	9.30	12.61	0.22	18.08	8.79	1.71	0.06	0.19	99.57	125.2
46.80	1.33	9.67	12.80	0.23	18.02	8.78	1.74	0.10	0.08	99.54	125.9
47.08	1.38	9.76	12.59	0.16	17.74	8.97	1.61	0.09	0.11	99.48	129.2
47.16	1.36	9.29	12.48	0.25	17.89	8.79	1.64	0.11	0.09	99.05	130.4
46.77	1.38	9.68	12.64	0.23	17.68	9.06	1.77	0.08	0.12	99.41	131.3
47.09	1.35	9.71	12.61	0.19	17.40	8.93	1.67	0.08	0.12	99.14	136.6
47.09	1.45	9.99	12.43	0.25	17.24	8.97	1.80	0.09	0.12	99.41	139.2
46.78	1.43	9.88	12.49	0.34	17.35	9.00	1.66	0.04	0.21	99.18	142.0

46.79	1.38	10.04	12.22	0.17	17.26	8.81	1.82	0.11	0.12	98.71	146.0
47.10	1.42	10.19	12.35	0.26	16.99	8.94	1.84	0.11	0.14	99.34	149.1
46.82	1.40	10.63	12.44	0.20	16.65	9.02	1.84	0.10	0.11	99.19	156.6
47.35	1.36	10.36	12.36	0.27	16.73	9.00	1.92	0.11	0.09	99.54	159.1
47.29	1.43	10.39	12.04	0.19	16.71	9.04	1.79	0.12	0.13	99.13	161.0
47.23	1.38	10.61	12.32	0.20	16.32	8.88	1.73	0.13	0.10	98.89	166.6
47.41	1.47	10.70	12.21	0.29	16.23	9.13	1.81	0.08	0.15	99.47	169.1
47.85	1.47	10.76	12.04	0.17	15.99	9.19	1.98	0.11	0.13	99.68	175.9
47.25	1.42	10.96	12.15	0.28	15.89	9.07	1.88	0.13	0.16	99.19	176.6
47.49	1.43	10.71	12.23	0.27	15.96	9.32	1.95	0.11	0.14	99.60	179.1
47.47	1.42	11.03	11.94	0.22	15.63	9.25	1.90	0.10	0.23	99.20	186.5
48.26	1.46	10.99	12.10	0.20	15.66	9.13	1.96	0.09	0.17	100.02	189.1
47.71	1.47	10.99	11.95	0.27	15.55	9.15	1.93	0.16	0.23	99.41	190.9
47.69	1.44	11.38	11.88	0.25	15.43	9.15	2.06	0.17	0.18	99.63	196.5
47.78	1.48	11.11	11.97	0.23	15.29	9.42	1.95	0.12	0.08	99.41	199.1
47.77	1.46	11.37	11.90	0.19	15.03	9.23	1.77	0.11	0.17	98.98	205.9
47.75	1.43	11.44	11.90	0.23	14.91	9.26	2.18	0.15	0.08	99.33	206.5
47.76	1.48	11.42	11.96	0.28	14.73	9.31	1.86	0.11	0.12	99.03	209.1
47.90	1.46	11.78	11.82	0.23	14.55	9.31	2.12	0.14	0.19	99.47	216.5
47.92	1.55	11.57	11.81	0.23	14.48	9.44	2.04	0.14	0.18	99.35	219.1
47.92	1.55	11.50	11.68	0.23	14.29	9.27	1.99	0.14	0.23	98.80	220.9
48.08	1.45	11.72	11.64	0.21	14.27	9.38	2.07	0.14	0.18	99.13	226.5
48.38	1.47	11.75	11.68	0.20	14.23	9.48	1.94	0.16	0.03	99.33	229.1
48.33	1.54	11.84	11.50	0.23	13.85	9.42	2.04	0.19	0.14	99.07	235.9
48.55	1.49	12.01	11.60	0.17	13.82	9.33	2.37	0.11	0.08	99.53	236.5
49.05	1.53	11.95	11.66	0.18	13.92	9.56	2.13	0.11	0.18	100.26	239.1
48.69	1.46	12.09	11.61	0.23	13.51	9.42	2.36	0.14	0.19	99.70	246.5
48.93	1.51	12.25	11.69	0.17	13.41	9.59	2.19	0.14	0.14	100.01	249.1
48.50	1.52	12.16	11.30	0.23	13.30	9.47	2.21	0.16	0.07	98.92	250.9
48.53	1.56	12.30	11.42	0.17	13.05	9.42	2.21	0.17	0.13	98.96	256.5
49.42	1.60	12.21	11.49	0.27	12.98	9.65	2.34	0.12	0.20	100.27	259.1
48.71	1.60	12.54	11.30	0.32	12.72	9.49	2.34	0.13	0.16	99.31	265.8
48.80	1.52	12.53	11.37	0.13	12.82	9.58	2.18	0.14	0.15	99.22	266.5
49.17	1.56	12.48	11.51	0.16	12.81	9.63	2.37	0.16	0.16	100.02	269.0
48.99	1.52	12.83	11.28	0.23	12.36	9.62	2.29	0.15	0.12	99.38	276.4
49.27	1.58	12.65	11.44	0.25	12.33	9.61	2.34	0.18	0.16	99.82	279.0
49.06	1.59	12.69	11.19	0.13	12.26	9.74	2.36	0.15	0.14	99.30	280.8
49.44	1.57	12.86	11.19	0.17	12.00	9.63	2.39	0.15	0.08	99.47	286.4
49.43	1.64	12.89	11.37	0.26	12.17	9.69	2.50	0.17	0.13	100.24	289.0
49.09	1.57	12.95	11.10	0.18	11.82	9.63	2.44	0.16	0.16	99.09	295.8
49.15	1.54	12.96	11.09	0.17	11.75	9.64	2.49	0.16	0.23	99.18	296.4
49.15	1.62	12.94	11.15	0.21	11.68	9.74	2.43	0.14	0.18	99.23	299.0
49.49	1.61	13.14	10.96	0.18	11.46	9.66	2.47	0.18	0.15	99.30	306.4
49.26	1.61	13.21	10.93	0.19	11.21	9.66	2.48	0.17	0.07	98.79	310.8
50.14	1.58	13.24	11.00	0.21	11.19	9.79	2.38	0.15	0.08	99.75	316.4
49.61	1.71	13.42	10.95	0.19	10.68	9.74	2.55	0.19	0.13	99.16	325.8
49.48	1.66	13.42	11.06	0.21	10.89	9.65	2.67	0.17	0.19	99.39	326.4
49.82	1.66	13.44	10.89	0.27	10.60	9.85	2.65	0.14	0.20	99.53	336.4
49.64	1.71	13.61	10.88	0.21	10.34	9.86	2.92	0.19	0.20	99.57	340.7

49.73	1.67	13.56	10.90	0.27	10.30	9.83	2.45	0.17	0.16	99.03	346.4
49.99	1.71	13.51	10.92	0.15	10.10	9.94	2.57	0.23	0.14	99.26	353.0
49.72	1.68	13.69	10.81	0.26	9.77	9.95	2.66	0.20	0.16	98.89	355.7
50.20	1.75	13.87	10.91	0.29	9.59	10.05	2.64	0.21	0.19	99.70	370.7
49.91	1.74	13.85	10.78	0.30	9.21	10.09	2.76	0.19	0.21	99.04	385.7
50.10	1.73	13.99	10.90	0.19	9.05	9.89	2.64	0.19	0.12	98.79	400.2
50.10	1.84	13.94	10.97	0.11	8.88	10.08	2.86	0.18	0.15	99.10	400.7
50.02	1.77	13.85	11.05	0.24	9.00	10.23	2.77	0.19	0.12	99.24	406.9
50.03	1.79	13.97	10.90	0.25	8.65	10.19	2.80	0.18	0.14	98.89	415.7
49.94	1.84	14.15	11.19	0.13	8.49	10.15	2.80	0.21	0.22	99.12	430.6
50.15	1.81	14.13	11.05	0.16	8.34	10.17	2.69	0.19	0.19	98.87	454.1
50.30	1.82	14.24	11.13	0.19	8.09	10.34	2.75	0.13	0.26	99.22	460.9
50.01	1.84	14.16	11.25	0.16	7.87	10.46	2.89	0.14	0.20	98.96	479.9
50.35	1.83	14.01	11.53	0.21	7.78	10.38	2.83	0.21	0.12	99.25	508.0
49.90	1.90	14.18	11.40	0.12	7.78	10.59	2.87	0.19	0.18	99.10	514.8
50.23	1.85	14.13	11.48	0.18	7.54	10.69	2.81	0.18	0.19	99.27	529.0
49.96	1.91	14.06	11.75	0.28	7.33	10.63	2.74	0.21	0.14	98.99	561.9
49.89	1.96	14.13	11.70	0.26	7.44	10.69	2.66	0.21	0.24	99.15	568.8
49.87	1.86	14.19	11.60	0.19	7.31	10.77	2.81	0.16	0.23	98.98	578.3
49.74	1.81	14.22	11.81	0.14	7.12	10.84	2.82	0.21	0.12	98.84	615.7
50.07	1.92	14.10	11.87	0.12	7.20	10.88	2.74	0.17	0.25	99.32	622.8
50.14	1.89	14.13	11.75	0.13	7.11	11.01	2.69	0.17	0.18	99.19	627.5
49.95	1.86	13.92	12.06	0.16	7.00	10.89	2.79	0.18	0.11	98.91	669.7
49.85	1.87	14.08	12.07	0.21	7.15	11.04	2.65	0.20	0.18	99.29	676.6
49.97	1.87	14.02	11.84	0.15	7.17	10.91	2.66	0.17	0.22	98.98	676.7
50.21	1.86	14.08	12.18	0.29	7.06	10.92	2.81	0.18	0.15	99.75	723.5
49.72	1.90	14.10	11.98	0.23	6.93	11.03	2.74	0.17	0.16	98.95	725.9
50.15	1.86	14.12	11.94	0.22	7.02	10.98	2.64	0.18	0.16	99.28	730.7
49.96	1.87	14.15	12.00	0.22	6.89	10.99	2.69	0.15	0.11	99.04	775.0
50.14	1.81	14.01	12.11	0.29	6.93	10.85	2.72	0.16	0.18	99.21	777.4
50.00	1.90	14.07	12.06	0.25	6.90	11.05	2.76	0.17	0.20	99.35	784.6
50.05	1.83	14.03	11.90	0.23	7.01	11.05	2.61	0.20	0.07	98.98	824.3
49.87	1.81	13.98	12.24	0.26	6.92	10.93	2.68	0.18	0.17	99.04	831.3
50.32	1.90	14.08	12.19	0.23	6.89	11.08	2.69	0.18	0.13	99.68	838.6
49.80	1.82	14.06	12.09	0.20	6.95	11.11	2.72	0.20	0.09	99.04	873.5
50.00	1.82	14.00	12.13	0.14	6.88	11.03	2.71	0.20	0.21	99.13	885.2
50.11	1.96	14.10	12.05	0.25	6.90	11.00	2.64	0.20	0.13	99.33	892.5
50.03	1.86	14.05	12.03	0.14	6.91	11.12	2.72	0.14	0.21	99.20	922.7
49.87	1.74	14.07	12.21	0.24	6.82	10.92	2.73	0.15	0.20	98.97	939.0
50.15	1.91	14.10	12.03	0.18	7.04	11.01	2.70	0.14	0.17	99.42	946.5
49.68	1.83	14.10	12.14	0.25	7.01	11.13	2.44	0.16	0.26	98.99	971.9
50.07	1.85	14.04	12.16	0.25	6.92	10.89	2.73	0.20	0.22	99.33	993.0
49.81	1.85	13.99	11.98	0.22	6.90	11.08	2.59	0.15	0.23	98.80	1000.5
50.05	1.89	14.07	12.10	0.20	6.91	10.95	2.52	0.18	0.14	99.03	1021.1
49.81	1.89	14.15	11.97	0.24	6.91	11.09	2.68	0.17	0.19	99.08	1046.8
50.20	1.85	14.09	12.08	0.26	6.88	10.97	2.74	0.20	0.16	99.44	1054.4
49.62	1.84	14.07	12.14	0.16	6.98	10.98	2.76	0.18	0.23	98.96	1070.3
50.15	1.76	14.12	12.03	0.18	6.84	11.05	2.68	0.17	0.18	99.17	1100.8
50.06	1.88	14.15	11.98	0.27	6.86	11.10	2.60	0.17	0.28	99.35	1108.4

49.80	1.89	13.97	12.01	0.28	6.84	11.05	2.64	0.19	0.18	98.84	1119.5
50.48	1.86	14.10	12.11	0.26	6.93	11.04	2.74	0.21	0.15	99.89	1154.6
50.17	1.90	14.12	11.87	0.14	6.90	11.09	2.94	0.22	0.17	99.52	1162.3
50.08	1.93	13.97	11.94	0.20	6.77	11.05	2.76	0.19	0.12	99.01	1168.7
50.27	1.80	14.02	11.85	0.22	6.84	11.01	2.71	0.19	0.14	99.05	1208.5
50.44	1.85	14.03	11.85	0.21	7.01	11.17	2.76	0.21	0.18	99.70	1216.3
50.08	1.84	14.14	11.88	0.17	6.82	11.04	2.71	0.19	0.17	99.05	1217.9
50.40	1.76	14.01	11.81	0.18	6.82	11.00	2.71	0.17	0.22	99.07	1262.4
50.21	1.84	14.07	11.81	0.22	6.90	11.03	2.90	0.15	0.19	99.30	1267.1
50.66	1.88	13.96	11.77	0.17	6.78	11.08	2.61	0.15	0.09	99.14	1270.2
50.56	1.77	14.05	11.90	0.25	6.90	10.94	2.53	0.18	0.14	99.22	1316.3
50.44	1.81	14.05	11.71	0.21	6.82	11.02	2.73	0.16	0.12	99.06	1316.3
50.65	1.82	13.92	11.77	0.21	6.65	11.03	2.64	0.19	0.22	99.10	1324.2

Exp 35

SiO2	TiO2	Al2O3	FeO	MnO	MgO	CaO	Na2O	K2O	P2O5	Total	d (um)
47.72	1.64	10.00	13.55	0.23	13.74	10.55	1.84	0.08	0.14	99.49	4.9
47.30	1.59	9.98	13.73	0.21	14.55	10.47	1.72	0.05	0.13	99.73	5.3
47.37	1.55	9.49	13.78	0.24	15.10	10.36	1.59	0.10	0.12	99.72	8.3
47.29	1.48	9.37	13.97	0.30	15.69	9.82	1.63	0.05	0.07	99.65	9.9
47.19	1.46	9.37	13.70	0.20	16.12	9.80	1.53	0.08	0.20	99.65	10.8
46.87	1.45	9.47	13.65	0.21	16.52	9.52	1.48	0.08	0.19	99.43	14.5
47.05	1.42	9.40	13.60	0.27	16.64	9.45	1.63	0.04	0.12	99.63	14.9
46.63	1.47	9.51	13.48	0.24	16.63	9.45	1.65	0.05	0.15	99.25	16.3
46.72	1.40	10.32	12.81	0.27	16.40	9.23	1.73	0.11	0.11	99.10	19.2
46.97	1.40	9.72	13.09	0.25	16.65	9.32	1.72	0.08	0.10	99.30	19.9
46.85	1.38	10.22	12.99	0.15	16.44	9.28	1.74	0.11	0.17	99.34	20.6
47.02	1.39	9.96	12.99	0.27	16.38	9.41	1.69	0.12	0.09	99.31	21.8
47.74	1.43	10.36	12.56	0.19	15.90	9.30	1.96	0.14	0.07	99.64	27.3
47.19	1.43	10.79	12.49	0.20	15.95	9.39	1.79	0.12	0.16	99.49	28.7
47.63	1.46	11.33	12.18	0.24	14.92	9.46	1.96	0.12	0.07	99.36	33.1
48.20	1.48	11.43	11.93	0.33	14.91	9.35	1.98	0.16	0.13	99.90	33.8
47.92	1.53	12.28	11.82	0.17	13.69	9.59	2.03	0.12	0.14	99.28	41.5
48.54	1.52	12.21	11.66	0.18	13.15	9.61	2.22	0.13	0.17	99.39	47.0
48.23	1.55	12.48	11.45	0.19	13.01	9.59	2.31	0.15	0.18	99.14	47.1
48.53	1.57	12.97	11.40	0.16	11.99	9.70	2.29	0.13	0.18	98.91	54.3
49.94	1.61	13.24	10.96	0.21	11.21	9.74	2.38	0.15	0.14	99.57	60.4
49.98	1.55	13.22	11.25	0.19	11.28	9.79	2.57	0.13	0.15	100.10	60.9
49.38	1.68	13.36	11.08	0.27	10.58	10.05	2.61	0.17	0.16	99.33	67.1
49.91	1.67	13.70	11.09	0.20	10.35	9.94	2.70	0.21	0.17	99.94	72.3
50.22	1.72	13.85	11.04	0.23	9.95	9.94	2.70	0.20	0.12	99.95	73.6
50.22	1.73	13.82	11.04	0.21	9.63	10.09	2.50	0.23	0.16	99.62	80.0
49.71	1.72	13.96	11.08	0.20	9.15	10.17	2.82	0.21	0.26	99.29	86.2
49.94	1.76	14.11	10.87	0.16	8.98	10.13	2.83	0.22	0.07	99.06	86.8
49.62	1.78	14.04	11.40	0.22	8.80	10.40	2.67	0.23	0.11	99.25	92.8
49.82	1.84	14.10	11.18	0.25	8.15	10.23	2.76	0.23	0.16	98.71	100.0
50.10	1.82	14.07	11.28	0.23	8.35	10.36	2.58	0.18	0.22	99.18	100.1
49.84	1.89	14.02	11.74	0.37	7.90	10.62	2.69	0.17	0.00	99.24	105.7
50.60	1.82	14.05	11.43	0.23	7.90	10.30	2.91	0.20	0.21	99.65	113.3
49.67	1.92	14.11	11.43	0.27	7.79	10.53	2.73	0.22	0.21	98.87	114.0
49.42	1.85	14.00	11.61	0.18	7.70	10.74	2.61	0.20	0.15	98.45	118.5
50.63	1.80	14.21	11.63	0.24	7.71	10.72	2.65	0.17	0.12	99.87	126.6
50.44	1.84	14.17	11.72	0.15	7.56	10.71	2.70	0.21	0.15	99.64	127.8
50.02	1.88	14.10	11.90	0.22	7.36	10.84	2.69	0.17	0.22	99.40	131.2
50.11	1.81	14.05	11.89	0.10	7.35	10.67	2.73	0.17	0.11	99.00	139.8
50.00	1.92	14.19	12.03	0.27	7.33	10.98	2.73	0.18	0.06	99.69	144.1
49.93	1.84	14.13	12.01	0.22	7.30	10.79	2.69	0.21	0.17	99.27	153.1
50.06	1.83	14.11	12.03	0.22	7.25	10.87	2.63	0.22	0.26	99.48	155.5
50.08	1.92	14.12	11.92	0.19	7.16	10.99	2.60	0.23	0.16	99.37	156.9
50.33	1.84	14.01	12.12	0.21	7.15	11.02	2.82	0.17	0.16	99.83	166.4
49.81	1.89	14.00	12.10	0.16	7.06	10.95	2.81	0.22	0.15	99.15	169.4
50.05	1.84	14.16	12.01	0.14	7.17	11.05	2.66	0.17	0.17	99.41	169.8
50.28	1.91	13.98	12.11	0.16	7.04	10.89	2.70	0.17	0.07	99.30	179.5

49.74	1.86	14.17	12.09	0.28	7.03	11.08	2.53	0.21	0.13	99.11	182.6
49.93	1.87	14.12	12.02	0.16	7.04	10.93	2.55	0.20	0.19	99.00	183.3
50.10	1.81	14.14	12.22	0.26	7.02	11.04	2.78	0.21	0.11	99.69	192.8
49.47	1.87	14.16	12.10	0.25	7.08	11.17	2.76	0.14	0.12	99.13	195.4
49.93	1.84	14.01	12.00	0.17	7.09	10.92	2.73	0.18	0.12	98.98	197.2
50.12	1.92	14.04	12.13	0.08	6.90	11.16	2.75	0.16	0.15	99.41	206.0
49.54	1.85	14.06	12.15	0.24	7.10	11.07	2.63	0.18	0.25	99.08	208.2
49.84	1.83	14.16	12.44	0.33	6.95	11.04	2.73	0.18	0.12	99.61	211.0
50.03	1.84	14.14	12.09	0.16	6.77	11.16	2.68	0.17	0.16	99.20	219.3
50.34	1.85	14.01	12.15	0.27	7.00	11.02	2.92	0.18	0.12	99.85	221.0
50.09	1.80	14.13	12.22	0.25	7.02	11.06	2.60	0.20	0.13	99.49	224.9
49.83	1.87	14.09	12.22	0.27	6.90	11.03	2.69	0.19	0.12	99.21	232.6
49.64	1.89	14.02	12.27	0.22	6.90	11.17	2.68	0.15	0.20	99.14	233.9
49.84	1.84	13.95	12.18	0.23	6.87	11.07	2.72	0.17	0.22	99.07	238.8
50.18	1.83	14.06	12.22	0.22	6.83	11.15	2.69	0.16	0.16	99.49	245.7
50.26	1.80	14.07	11.98	0.21	6.88	11.09	2.64	0.16	0.24	99.32	246.7
50.28	1.85	14.07	12.06	0.17	6.94	11.13	2.71	0.14	0.17	99.52	252.7
50.85	1.87	14.07	12.16	0.21	6.83	11.03	2.64	0.20	0.21	100.04	259.0
49.82	1.82	13.96	12.16	0.27	6.98	11.19	2.60	0.20	0.16	99.14	259.6
50.66	1.77	14.14	11.95	0.23	6.99	11.16	2.87	0.18	0.09	100.03	272.4
49.75	1.79	13.97	12.02	0.19	7.01	11.08	2.68	0.22	0.23	98.93	309.8
49.70	1.88	14.10	12.18	0.19	7.01	10.88	2.79	0.21	0.14	99.08	321.6
49.71	1.82	14.15	12.17	0.19	6.95	11.16	2.54	0.17	0.16	99.04	325.3
50.07	1.83	14.18	12.02	0.19	6.96	11.06	2.79	0.17	0.21	99.47	338.1
49.93	1.92	13.96	12.16	0.27	6.94	11.18	2.66	0.15	0.25	99.41	340.7
50.58	1.86	14.05	12.01	0.19	6.91	11.03	2.66	0.23	0.15	99.65	354.6
50.18	1.79	14.01	12.19	0.23	6.92	11.12	2.66	0.20	0.09	99.40	356.2
50.56	1.85	13.96	11.92	0.24	6.84	11.09	2.58	0.19	0.21	99.45	371.7
49.81	1.83	14.24	12.22	0.19	7.08	10.94	2.69	0.19	0.22	99.40	372.9
49.48	1.86	14.08	11.93	0.29	7.03	11.15	2.77	0.19	0.13	98.89	378.2
49.20	1.85	13.97	12.05	0.18	6.93	11.02	2.79	0.17	0.19	98.37	383.8
49.83	1.86	14.04	12.13	0.25	7.01	11.00	2.70	0.16	0.25	99.22	397.0
49.70	1.84	13.95	12.25	0.19	6.95	11.08	2.71	0.22	0.17	99.04	413.0
49.63	1.84	13.83	12.09	0.20	6.96	11.22	2.61	0.21	0.16	98.74	415.7
49.95	1.88	14.05	12.35	0.25	6.98	11.06	2.66	0.21	0.13	99.53	425.9
50.09	1.83	14.05	12.11	0.17	6.86	10.99	2.68	0.20	0.15	99.11	434.4
49.79	1.87	14.01	11.93	0.14	6.86	11.02	2.72	0.19	0.15	98.66	450.6
49.97	1.80	14.03	12.25	0.26	6.97	11.05	2.65	0.18	0.07	99.23	452.9
50.84	1.89	13.96	12.14	0.18	6.75	11.06	2.69	0.21	0.17	99.89	453.1
50.25	1.84	14.09	12.24	0.16	6.91	11.04	2.75	0.21	0.12	99.59	467.9
49.70	1.90	14.05	12.30	0.22	6.79	11.03	2.63	0.18	0.30	99.11	487.7
50.09	1.86	14.16	12.31	0.18	6.89	11.12	2.54	0.17	0.09	99.42	493.0
50.02	1.84	14.09	12.21	0.24	6.86	10.96	2.80	0.14	0.25	99.43	509.9
49.47	1.81	13.99	12.26	0.24	6.74	11.07	2.73	0.17	0.22	98.70	524.9
50.32	1.81	13.96	12.37	0.22	6.90	10.96	2.62	0.19	0.11	99.45	532.9
50.03	1.83	13.93	12.32	0.16	6.94	11.01	2.64	0.18	0.12	99.15	552.0
49.60	1.81	13.94	12.28	0.24	6.87	11.10	2.65	0.17	0.14	98.80	562.0
50.15	1.85	14.02	12.35	0.29	6.91	11.09	2.65	0.18	0.24	99.73	572.9
50.42	1.82	14.08	12.44	0.29	6.98	10.90	2.67	0.16	0.12	99.88	594.0

50.29	1.84	14.02	12.27	0.18	6.94	11.05	2.66	0.18	0.20	99.62	599.2
49.22	1.83	13.93	12.27	0.23	6.81	10.97	2.80	0.20	0.17	98.43	612.9
50.31	1.82	13.91	12.26	0.21	7.07	11.01	2.81	0.18	0.14	99.73	636.1
49.68	1.81	14.02	12.33	0.16	6.83	11.11	2.86	0.15	0.24	99.17	636.4
50.34	1.82	14.16	12.26	0.25	6.90	11.10	2.76	0.22	0.12	99.93	652.9
50.18	1.84	13.99	12.16	0.25	6.85	11.09	2.72	0.17	0.18	99.42	673.6
50.14	1.83	13.95	11.99	0.22	6.83	10.95	2.75	0.17	0.14	98.97	678.1
49.93	1.89	14.05	12.28	0.25	6.88	11.15	2.65	0.18	0.12	99.39	692.9
50.29	1.86	14.14	12.00	0.30	6.82	11.11	2.73	0.18	0.21	99.63	710.7
50.02	1.86	14.02	12.06	0.23	6.73	10.99	2.69	0.19	0.18	98.98	720.2
49.67	1.84	14.09	12.18	0.19	6.92	11.12	2.73	0.18	0.19	99.10	732.9
49.85	1.88	13.87	12.17	0.25	6.82	11.06	2.77	0.19	0.12	98.96	747.9
50.39	1.83	14.07	12.18	0.27	6.87	10.97	2.84	0.17	0.20	99.77	762.2
50.32	1.84	14.14	12.26	0.31	6.89	10.99	2.69	0.18	0.10	99.71	772.9
50.23	1.80	14.04	12.06	0.23	6.71	11.06	2.75	0.18	0.21	99.27	785.0
50.40	1.83	14.03	11.92	0.29	6.84	11.10	2.63	0.13	0.23	99.39	804.4
50.27	1.87	14.12	12.21	0.24	6.87	11.08	2.84	0.18	0.16	99.83	812.9
49.67	1.86	14.07	12.18	0.25	6.88	11.06	2.65	0.18	0.21	98.99	822.2
50.04	1.84	14.04	12.26	0.22	6.78	10.96	2.87	0.19	0.16	99.36	846.4
50.38	1.83	14.00	12.27	0.19	6.92	11.06	2.44	0.17	0.14	99.39	852.9
49.99	1.83	14.05	12.10	0.21	6.91	11.00	2.64	0.23	0.18	99.14	859.3
49.98	1.86	13.97	12.12	0.18	6.94	11.02	2.86	0.16	0.16	99.24	888.5
50.24	1.91	14.12	12.24	0.26	6.91	11.08	2.69	0.18	0.14	99.75	892.9
50.26	1.84	13.90	12.24	0.27	6.84	10.96	2.66	0.18	0.16	99.29	896.5
49.68	1.89	14.06	12.17	0.21	6.76	11.21	2.71	0.20	0.11	98.99	930.5
50.10	1.79	14.16	12.18	0.28	6.83	10.98	2.69	0.17	0.19	99.38	932.9
50.37	1.84	13.84	12.15	0.26	6.91	11.07	2.71	0.18	0.12	99.46	933.6
50.35	1.79	14.09	12.20	0.18	6.92	11.11	2.76	0.18	0.17	99.75	970.8
50.60	1.84	14.02	12.16	0.13	6.88	10.98	2.72	0.20	0.18	99.70	972.5
50.01	1.79	14.21	12.19	0.20	6.84	11.03	2.77	0.17	0.17	99.39	972.9
49.97	1.85	14.06	12.07	0.20	7.02	11.04	2.73	0.24	0.10	99.27	1008.0
50.78	1.77	14.15	12.17	0.21	6.95	11.13	2.77	0.19	0.12	100.23	1012.9
50.23	1.79	14.00	12.20	0.27	6.78	11.00	2.64	0.16	0.13	99.18	1014.6
49.75	1.82	13.97	12.06	0.21	7.09	11.17	2.78	0.19	0.13	99.17	1045.2
49.92	1.80	13.98	12.27	0.30	6.88	11.08	2.62	0.17	0.16	99.17	1052.9
50.04	1.88	14.06	12.21	0.11	6.81	11.00	2.53	0.22	0.14	98.99	1056.6
50.62	1.82	14.06	11.98	0.20	6.99	11.14	2.59	0.17	0.13	99.69	1082.3
50.17	1.85	14.05	12.20	0.27	6.91	11.11	2.65	0.13	0.17	99.51	1092.9
49.79	1.90	13.98	12.08	0.15	6.84	10.99	2.76	0.21	0.20	98.89	1098.7
50.05	1.83	14.11	12.08	0.27	6.84	11.27	2.73	0.17	0.11	99.47	1119.5
50.56	1.83	14.08	12.09	0.21	6.94	11.06	2.75	0.17	0.13	99.82	1132.9
50.31	1.84	13.87	12.13	0.19	6.84	10.96	2.55	0.21	0.13	99.03	1140.7
50.38	1.87	14.07	11.93	0.26	6.85	11.11	2.75	0.18	0.16	99.57	1156.6
50.60	1.79	14.08	12.09	0.20	6.87	11.05	2.58	0.15	0.16	99.57	1182.8

Exp 37

SiO2	TiO2	Al2O3	FeO	MnO	MgO	CaO	Na2O	K2O	P2O5	Total	d (um)
46.26	1.27	9.25	13.03	0.21	20.87	8.35	1.62	0.05	0.14	101.06	2.6
45.57	1.28	8.27	13.90	0.29	21.12	8.55	1.44	0.07	0.13	100.62	20.0
45.69	1.19	7.99	13.72	0.21	21.74	8.52	1.39	0.06	0.08	100.58	37.3
46.48	1.25	8.15	13.43	0.25	20.83	8.71	1.42	0.08	0.09	100.69	54.6
45.70	1.26	8.56	13.11	0.22	20.96	8.38	1.43	0.08	0.13	99.82	72.0
43.76	1.29	8.57	12.96	0.21	20.28	8.34	1.65	0.09	0.06	97.20	72.6
44.84	1.27	8.36	13.00	0.25	20.08	8.21	1.31	0.08	0.12	97.50	73.0
44.65	1.32	8.15	12.85	0.23	20.48	8.33	1.49	0.03	0.15	97.67	73.6
45.20	1.32	8.42	12.93	0.21	20.14	8.33	1.54	0.08	0.14	98.31	78.6
44.80	1.27	8.34	13.16	0.25	20.26	8.18	1.49	0.10	0.14	97.98	79.1
45.29	1.27	8.52	13.14	0.29	19.96	8.29	1.56	0.06	0.17	98.55	84.2
45.10	1.26	8.30	13.07	0.27	20.34	8.42	1.49	0.03	0.10	98.38	84.5
43.89	1.21	8.61	12.69	0.24	20.06	8.42	1.60	0.09	0.09	96.89	84.6
46.20	1.23	8.45	13.11	0.28	20.81	8.36	1.48	0.07	0.11	100.07	89.3
45.63	1.30	8.53	13.00	0.18	19.80	8.41	1.53	0.07	0.07	98.53	89.9
45.26	1.25	8.32	12.98	0.37	20.14	8.39	1.60	0.07	0.12	98.49	90.0
45.86	1.27	8.34	12.97	0.23	20.10	8.48	1.51	0.07	0.15	98.98	95.4
45.66	1.29	8.60	12.95	0.23	19.95	8.37	1.44	0.09	0.02	98.60	95.5
44.36	1.29	8.82	12.77	0.25	19.78	8.27	1.41	0.06	0.07	97.09	96.6
44.11	1.30	8.97	12.72	0.13	19.97	8.44	1.46	0.09	0.07	97.25	100.5
44.84	1.32	8.42	12.88	0.25	20.07	8.30	1.59	0.07	0.08	97.83	100.9
45.71	1.31	8.66	12.85	0.18	19.75	8.46	1.51	0.09	0.08	98.59	101.1
45.80	1.29	8.60	12.80	0.18	19.66	8.48	1.66	0.05	0.08	98.60	106.3
45.10	1.26	8.70	12.88	0.16	19.53	8.43	1.50	0.07	0.07	97.70	106.7
44.06	1.31	8.85	12.72	0.34	19.62	8.51	1.52	0.09	0.16	97.18	108.6
44.42	1.31	9.18	12.84	0.26	19.45	8.62	1.61	0.08	0.10	97.87	111.6
45.76	1.28	8.52	12.71	0.17	19.77	8.38	1.51	0.10	0.11	98.31	111.8
45.55	1.31	8.84	12.84	0.26	19.36	8.48	1.52	0.10	0.05	98.32	112.4
44.61	1.32	9.05	12.87	0.16	19.39	8.43	1.52	0.12	0.09	97.57	112.5
45.59	1.34	8.59	12.80	0.19	19.42	8.58	1.53	0.07	0.16	98.28	117.2
46.34	1.34	8.85	12.79	0.23	19.07	8.46	1.54	0.06	0.18	98.86	118.0
44.33	1.31	9.05	12.57	0.27	19.31	8.43	1.70	0.06	0.13	97.17	120.6
46.01	1.33	9.00	12.71	0.27	18.84	8.62	1.57	0.05	0.03	98.44	121.9
44.16	1.35	9.33	12.67	0.26	18.85	8.67	1.71	0.07	0.02	97.10	123.6
45.58	1.32	9.00	12.62	0.22	19.13	8.56	1.65	0.09	0.11	98.27	124.5
45.54	1.28	9.09	12.63	0.18	18.51	8.76	1.58	0.07	0.14	97.78	127.8
45.61	1.32	9.17	12.73	0.35	19.12	8.64	1.66	0.09	0.14	98.82	132.6
45.19	1.34	9.54	12.71	0.14	18.70	8.62	1.68	0.10	0.12	98.14	135.6
45.52	1.42	9.30	12.47	0.23	18.79	8.63	1.71	0.10	0.09	98.24	136.5
45.32	1.31	9.44	12.48	0.30	18.89	8.60	1.77	0.08	0.09	98.27	144.6
44.76	1.32	9.70	12.64	0.20	18.30	8.68	1.62	0.05	0.15	97.41	147.5
45.10	1.31	9.22	12.62	0.23	18.59	8.61	1.73	0.08	0.12	97.61	148.5
45.22	1.35	9.42	12.49	0.24	18.37	8.50	1.79	0.08	0.05	97.51	156.6
45.13	1.37	9.77	12.38	0.20	18.18	8.63	1.60	0.09	0.11	97.45	159.5
45.40	1.31	9.51	12.50	0.20	18.39	8.72	1.78	0.13	0.15	98.09	160.5
44.57	1.37	9.61	12.48	0.20	18.28	8.74	1.73	0.06	0.08	97.12	168.6
44.42	1.33	9.79	12.60	0.27	18.14	8.80	1.72	0.08	0.08	97.23	172.5

45.28	1.38	9.77	12.47	0.26	17.90	8.85	1.75	0.09	0.10	97.85	180.6
45.26	1.36	9.95	12.40	0.09	17.75	8.82	1.84	0.07	0.04	97.57	183.5
45.70	1.39	9.88	12.54	0.26	17.83	8.76	1.79	0.10	0.27	98.51	184.5
47.09	1.41	9.76	12.09	0.27	17.70	8.62	1.79	0.09	0.14	98.97	192.6
45.96	1.36	10.02	12.30	0.24	17.35	8.83	1.66	0.08	0.15	97.94	195.5
44.82	1.37	9.95	12.11	0.18	17.61	8.68	1.76	0.11	0.07	96.65	196.5
45.72	1.42	10.02	12.38	0.19	17.45	8.81	2.03	0.11	0.16	98.28	204.6
46.24	1.38	10.19	12.21	0.25	17.08	8.90	1.71	0.10	0.12	98.18	207.5
45.71	1.41	10.18	12.28	0.24	17.34	8.90	2.04	0.09	0.08	98.25	208.5
46.11	1.39	10.11	12.18	0.22	17.18	8.88	1.93	0.08	0.14	98.21	216.6
46.09	1.41	10.39	12.17	0.18	16.75	8.90	1.84	0.12	0.17	98.02	219.5
46.61	1.38	10.22	12.21	0.16	16.88	8.98	1.83	0.08	0.14	98.48	220.5
46.46	1.39	10.33	12.05	0.14	16.87	8.94	1.98	0.11	0.10	98.37	228.6
46.03	1.41	10.57	11.94	0.20	16.61	9.03	1.95	0.11	0.11	97.95	231.5
45.53	1.35	10.40	12.27	0.16	16.64	8.95	1.91	0.09	0.13	97.45	232.5
45.38	1.39	10.63	11.92	0.13	16.52	8.93	2.11	0.11	0.08	97.20	240.6
45.98	1.45	10.76	11.80	0.11	16.39	9.09	1.92	0.09	0.06	97.64	243.5
45.86	1.42	10.53	12.06	0.24	16.58	9.01	1.95	0.11	0.13	97.89	244.5
45.65	1.42	11.02	11.77	0.25	16.02	9.06	1.92	0.13	0.17	97.41	255.5
45.85	1.49	10.78	11.90	0.16	16.27	9.02	1.96	0.11	0.14	97.66	256.5
46.74	1.39	10.94	11.88	0.22	15.88	9.03	2.14	0.14	0.12	98.47	264.6
46.48	1.42	10.98	11.89	0.25	15.86	9.11	2.15	0.15	0.22	98.51	267.5
47.13	1.47	10.86	11.96	0.13	15.70	9.16	1.91	0.11	0.14	98.57	268.5
46.55	1.41	11.01	11.96	0.19	15.54	9.05	2.02	0.13	0.13	97.98	276.6
47.14	1.39	11.10	12.01	0.28	15.46	9.14	1.91	0.07	0.11	98.61	279.5
46.84	1.45	11.03	11.86	0.18	15.58	9.03	1.98	0.10	0.25	98.28	280.5
46.57	1.48	11.17	11.59	0.14	15.11	9.24	2.07	0.11	0.16	97.63	288.6
46.55	1.43	11.35	11.76	0.23	15.27	9.13	2.07	0.09	0.10	97.98	291.5
45.87	1.45	11.28	11.81	0.27	15.18	8.98	1.98	0.16	0.14	97.10	292.5
47.06	1.47	11.33	11.69	0.21	15.05	9.28	2.25	0.08	0.12	98.54	300.6
46.12	1.41	11.58	11.71	0.23	14.93	9.10	1.97	0.17	0.06	97.29	303.5
46.19	1.45	11.42	11.89	0.19	15.06	9.26	2.16	0.12	0.13	97.86	304.5
46.88	1.46	11.54	11.53	0.23	14.85	9.27	2.11	0.15	0.19	98.21	312.6
46.75	1.44	11.64	11.58	0.16	14.70	9.42	2.18	0.12	0.15	98.13	315.5
46.79	1.52	11.50	11.50	0.17	14.64	9.27	2.15	0.12	0.15	97.80	316.5
47.26	1.46	11.71	11.34	0.30	14.45	9.24	2.09	0.14	0.17	98.16	324.6
47.48	1.46	11.66	11.44	0.18	14.29	9.23	2.10	0.10	0.17	98.11	327.5
46.11	1.48	11.73	11.54	0.18	14.37	9.24	2.28	0.13	0.22	97.28	328.5
47.21	1.48	11.81	11.33	0.26	14.16	9.32	2.25	0.07	0.13	98.01	336.6
46.66	1.41	12.10	11.65	0.23	14.00	9.35	2.28	0.17	0.14	97.98	339.5
46.77	1.46	11.82	11.30	0.14	14.14	9.33	2.21	0.13	0.13	97.42	340.5
46.96	1.47	12.08	11.52	0.18	13.86	9.33	2.25	0.15	0.17	97.98	348.6
47.56	1.50	12.16	11.39	0.24	13.88	9.45	2.30	0.15	0.06	98.68	351.5
47.61	1.52	12.04	11.43	0.25	13.99	9.20	2.30	0.14	0.23	98.71	352.5
47.39	1.52	12.13	11.20	0.24	13.61	9.35	2.25	0.14	0.12	97.93	360.6
47.92	1.48	12.24	11.24	0.21	13.49	9.38	2.14	0.14	0.10	98.33	363.5
47.44	1.49	12.15	11.38	0.26	13.56	9.24	2.27	0.13	0.18	98.08	364.5
48.39	1.49	12.25	11.17	0.15	13.24	9.35	2.40	0.14	0.19	98.78	372.6
47.54	1.46	12.30	11.25	0.18	13.14	9.35	2.33	0.16	0.12	97.82	375.5

47.39	1.57	12.27	11.03	0.26	13.53	9.39	2.29	0.11	0.21	98.04	376.5
47.94	1.51	12.43	11.13	0.27	12.95	9.28	2.23	0.13	0.14	98.01	384.6
47.70	1.48	12.58	11.09	0.18	13.14	9.43	2.25	0.19	0.24	98.26	387.5
48.19	1.54	12.38	11.10	0.17	13.12	9.41	2.39	0.13	0.20	98.64	388.4
47.37	1.55	12.68	11.03	0.22	12.80	9.42	2.35	0.17	0.17	97.76	396.6
47.83	1.51	12.65	11.20	0.21	12.66	9.45	2.48	0.15	0.08	98.22	399.5
46.58	1.51	12.50	11.20	0.24	12.86	9.47	2.32	0.14	0.18	96.98	400.4
48.74	1.58	12.67	10.96	0.16	12.32	9.43	2.50	0.14	0.24	98.73	408.6
48.73	1.47	12.81	11.04	0.22	12.48	9.45	2.45	0.17	0.18	98.98	411.5
48.49	1.58	12.54	11.12	0.22	12.38	9.50	2.35	0.14	0.15	98.47	412.4
47.80	1.55	12.98	10.96	0.18	12.16	9.54	2.43	0.20	0.11	97.91	420.6
47.00	1.54	12.95	11.06	0.23	12.19	9.44	2.52	0.13	0.16	97.21	423.5
48.06	1.66	12.83	10.93	0.18	12.19	9.52	2.46	0.14	0.15	98.11	424.4
47.48	1.57	12.96	10.88	0.31	11.91	9.55	2.38	0.14	0.19	97.35	432.6
48.43	1.63	12.86	10.92	0.17	11.82	9.51	2.50	0.18	0.11	98.12	435.5
48.82	1.62	12.80	10.94	0.20	11.91	9.55	2.35	0.16	0.12	98.46	436.4
48.48	1.62	13.15	10.94	0.21	11.66	9.69	2.58	0.19	0.17	98.65	447.5
47.75	1.60	13.01	10.97	0.17	11.67	9.63	2.38	0.19	0.28	97.65	448.4
48.55	1.58	13.12	10.89	0.15	11.40	9.47	2.60	0.18	0.25	98.17	459.5
48.19	1.56	13.04	10.77	0.25	11.54	9.67	2.73	0.16	0.20	98.10	460.4
48.26	1.59	13.24	10.90	0.16	11.22	9.55	2.60	0.17	0.06	97.73	461.9
48.59	1.61	13.29	10.98	0.21	11.15	9.54	2.73	0.17	0.10	98.36	471.5
48.27	1.60	13.32	10.92	0.22	10.96	9.72	2.54	0.20	0.25	98.00	490.5
48.01	1.62	13.49	10.76	0.23	10.67	9.69	2.72	0.20	0.21	97.61	491.3
48.79	1.66	13.41	10.65	0.21	10.49	9.82	2.66	0.18	0.12	98.00	501.3
49.17	1.68	13.60	10.82	0.18	10.35	9.69	2.73	0.20	0.11	98.52	520.6
47.97	1.65	13.62	10.75	0.21	10.18	9.82	2.68	0.20	0.17	97.23	520.7
48.77	1.66	13.82	10.57	0.23	10.08	9.71	2.63	0.18	0.13	97.77	531.1
49.24	1.68	13.80	10.68	0.20	9.75	9.91	2.90	0.22	0.10	98.47	550.2
48.91	1.74	13.75	10.82	0.23	9.87	9.82	3.03	0.20	0.10	98.47	550.7
48.64	1.75	13.86	10.76	0.20	9.57	9.86	2.76	0.17	0.19	97.74	560.9
49.49	1.73	13.78	10.82	0.21	9.41	9.94	2.83	0.20	0.17	98.57	579.6
49.19	1.78	13.80	10.66	0.21	9.42	9.91	2.77	0.20	0.27	98.22	580.8
48.49	1.76	14.00	10.84	0.19	9.20	9.96	2.86	0.17	0.24	97.71	590.7
48.14	1.78	13.99	10.91	0.20	9.03	10.08	3.12	0.20	0.18	97.62	609.0
48.78	1.75	13.84	10.93	0.22	9.04	9.96	2.64	0.18	0.17	97.50	610.9
48.91	1.82	14.06	10.81	0.14	8.86	10.04	2.93	0.18	0.05	97.78	620.5
48.90	1.81	13.97	10.77	0.14	8.69	10.08	2.72	0.18	0.14	97.39	638.4
48.27	1.75	14.07	10.89	0.26	8.75	9.98	2.74	0.16	0.14	97.01	641.0
47.99	1.80	13.96	11.00	0.25	8.65	10.30	2.89	0.18	0.12	97.14	650.3
48.30	1.84	13.94	10.92	0.23	8.64	10.18	2.97	0.19	0.24	97.44	671.1
48.59	1.81	14.20	11.13	0.18	8.33	10.17	2.99	0.19	0.07	97.64	680.1
49.18	1.83	14.26	11.00	0.18	8.25	10.08	3.08	0.16	0.19	98.20	697.2
49.01	1.87	14.14	11.04	0.23	8.16	10.41	2.89	0.18	0.19	98.12	709.8
49.47	1.79	14.20	11.35	0.18	8.09	10.20	2.77	0.20	0.16	98.41	726.6
49.11	1.83	14.14	11.16	0.11	7.86	10.36	2.77	0.22	0.13	97.70	739.6
49.13	1.76	14.29	11.16	0.14	8.04	10.20	2.77	0.19	0.14	97.81	756.1
49.22	1.84	14.27	11.20	0.19	7.90	10.33	2.88	0.18	0.21	98.22	761.4
49.42	1.83	14.17	11.32	0.11	7.69	10.40	2.94	0.21	0.08	98.16	769.4

48.89	1.83	14.23	11.09	0.21	7.79	10.49	2.93	0.16	0.16	97.77	785.5
48.88	1.83	14.25	11.33	0.13	7.73	10.39	2.87	0.19	0.26	97.84	791.5
48.94	1.83	14.18	11.39	0.26	7.67	10.48	2.83	0.20	0.07	97.86	799.2
48.68	1.85	14.17	11.40	0.25	7.47	10.60	2.75	0.16	0.25	97.59	814.9
48.54	1.87	14.11	11.27	0.15	7.58	10.55	2.83	0.17	0.20	97.26	821.6
48.52	1.86	14.11	11.61	0.19	7.48	10.65	2.84	0.17	0.18	97.60	829.0
48.75	1.85	14.18	11.52	0.17	7.52	10.60	2.96	0.15	0.19	97.90	844.3
49.44	1.77	14.19	11.43	0.25	7.64	10.41	2.90	0.18	0.10	98.31	851.7
48.39	1.88	14.24	11.68	0.25	7.50	10.59	2.91	0.17	0.30	97.89	858.8
48.50	1.83	14.32	11.52	0.20	7.45	10.54	2.87	0.18	0.20	97.62	873.7
49.18	1.85	14.11	11.62	0.24	7.39	10.65	2.72	0.19	0.19	98.12	881.8
48.68	1.84	13.97	11.57	0.30	7.39	10.70	2.88	0.21	0.21	97.75	888.5
48.41	1.81	14.19	11.41	0.22	7.46	10.56	2.96	0.14	0.10	97.25	903.1
49.57	1.84	14.12	11.66	0.25	7.22	10.62	2.83	0.18	0.23	98.51	912.0
49.13	1.82	14.18	11.60	0.21	7.15	10.79	2.84	0.15	0.15	98.02	918.3
48.24	1.85	14.21	11.49	0.22	7.34	10.63	2.83	0.18	0.17	97.14	932.5
48.46	1.87	14.16	11.62	0.25	7.19	10.60	2.96	0.18	0.15	97.43	942.1
48.83	1.82	14.06	11.73	0.05	7.27	10.72	2.79	0.21	0.13	97.61	948.1
48.85	1.81	14.14	11.56	0.15	7.23	10.78	2.75	0.20	0.18	97.65	961.9
47.97	1.91	14.09	11.72	0.24	7.28	10.75	2.82	0.17	0.18	97.14	977.9
48.72	1.89	14.16	11.53	0.20	7.11	10.70	2.76	0.20	0.17	97.43	991.4
49.09	1.83	14.12	11.62	0.19	7.17	10.73	2.79	0.18	0.12	97.83	1002.2
49.26	1.87	14.18	11.83	0.24	7.08	10.92	2.90	0.17	0.16	98.60	1007.7
49.67	1.83	14.13	11.65	0.17	7.09	10.82	2.89	0.19	0.18	98.61	1020.8
49.33	1.91	14.10	11.73	0.28	6.99	10.89	2.74	0.17	0.24	98.38	1032.3
48.09	1.85	14.16	11.84	0.16	7.05	10.87	2.90	0.17	0.07	97.16	1037.5
48.44	1.81	14.23	11.67	0.22	7.00	10.74	2.81	0.11	0.16	97.18	1050.2
48.89	1.87	14.11	11.85	0.29	7.02	10.89	2.88	0.15	0.27	98.21	1062.4
49.02	1.82	14.24	11.65	0.09	6.96	10.88	2.96	0.14	0.17	97.92	1067.3
48.60	1.78	14.18	11.71	0.27	7.03	10.84	2.94	0.18	0.15	97.68	1079.6
49.28	1.88	13.92	11.70	0.20	7.07	10.82	2.91	0.16	0.12	98.05	1092.5
48.84	1.77	14.09	11.73	0.26	6.96	10.87	2.92	0.20	0.24	97.88	1097.1
49.19	1.90	14.02	11.75	0.24	6.97	10.71	2.92	0.20	0.14	98.03	1109.0
50.12	1.85	13.92	11.85	0.07	7.00	10.82	2.85	0.16	0.17	98.81	1122.6
47.99	1.85	14.18	11.58	0.15	7.09	10.81	2.86	0.17	0.24	96.90	1138.3
48.60	1.83	14.10	11.68	0.16	6.97	10.94	2.90	0.19	0.09	97.46	1152.7
49.04	1.79	14.09	11.81	0.24	6.93	10.96	2.92	0.20	0.14	98.11	1156.6
50.05	1.80	14.02	11.68	0.24	7.00	10.72	2.86	0.21	0.17	98.75	1167.7
49.22	1.82	14.00	11.75	0.25	6.96	10.94	2.77	0.17	0.30	98.18	1182.8
49.08	1.87	14.09	11.77	0.14	6.91	10.91	2.80	0.22	0.20	97.99	1186.4
48.83	1.82	14.14	11.49	0.16	6.91	10.82	2.82	0.16	0.10	97.25	1197.2
49.72	1.83	13.85	11.84	0.21	6.81	10.95	2.67	0.15	0.17	98.19	1212.9
49.21	1.81	13.95	11.64	0.28	6.88	10.86	2.71	0.18	0.21	97.72	1226.6
49.25	1.83	13.97	11.90	0.18	6.90	10.94	2.80	0.17	0.16	98.11	1243.0
49.40	1.83	13.96	11.70	0.22	6.92	10.87	2.83	0.16	0.23	98.11	1246.0
50.11	1.80	14.02	11.64	0.26	6.81	10.81	2.86	0.18	0.18	98.66	1256.0
48.70	1.77	14.06	11.66	0.19	6.79	10.99	2.87	0.19	0.18	97.40	1273.1
49.14	1.82	14.09	11.73	0.21	6.83	10.91	2.82	0.18	0.14	97.86	1275.8
49.67	1.85	13.92	11.41	0.27	6.71	10.87	2.86	0.18	0.27	98.02	1285.4

49.13	1.78	13.92	11.63	0.22	6.75	10.93	2.82	0.16	0.21	97.55	1303.2

Exp 38

SiO2	TiO2	Al2O3	FeO	MnO	MgO	CaO	Na2O	K2O	P2O5	Total	d (um)
45.92	1.26	8.41	14.24	0.32	21.02	8.48	1.42	0.09	0.12	101.28	5.8
44.74	0.98	6.81	14.27	0.25	26.13	6.26	1.22	0.11	0.08	100.84	9.9
44.16	0.95	6.21	14.04	0.24	28.17	5.63	1.15	0.06	0.07	100.67	23.4
45.70	1.16	7.58	13.77	0.24	22.96	7.58	1.42	0.01	0.09	100.50	30.3
45.33	1.33	8.42	13.92	0.26	18.89	8.69	1.20	0.07	0.08	98.19	36.1
44.98	1.02	7.31	13.07	0.17	26.12	5.81	1.39	0.09	0.20	100.16	41.0
45.30	1.33	8.74	13.45	0.27	18.96	8.59	1.38	0.08	0.10	98.18	41.1
44.94	1.37	8.78	13.48	0.23	18.86	8.77	1.42	0.11	0.11	98.06	43.6
45.48	1.35	8.74	13.30	0.21	18.98	8.70	1.48	0.09	0.13	98.46	46.1
44.57	1.35	8.93	13.21	0.28	18.63	8.72	1.47	0.08	0.07	97.30	49.0
46.83	1.31	8.97	12.83	0.24	19.29	8.83	1.53	0.06	0.15	100.04	50.6
45.87	1.29	8.99	12.99	0.25	18.73	8.70	1.49	0.10	0.13	98.51	51.0
45.44	1.38	9.13	13.18	0.15	18.55	8.84	1.46	0.07	0.11	98.30	54.4
45.72	1.33	9.19	13.06	0.25	18.39	8.75	1.44	0.09	0.10	98.31	56.0
45.23	1.39	9.50	13.05	0.22	18.27	8.76	1.54	0.07	0.13	98.15	56.5
45.33	1.14	8.69	12.50	0.18	18.47	8.35	1.47	0.07	0.19	96.39	58.5
46.04	1.37	9.36	12.90	0.20	17.88	8.90	1.53	0.10	0.09	98.35	59.8
45.13	1.45	9.82	12.75	0.21	17.54	8.92	1.68	0.06	0.16	97.73	66.5
44.84	1.40	9.68	13.14	0.26	17.70	8.99	1.71	0.08	0.15	97.93	67.0
46.06	1.44	10.26	12.68	0.16	17.12	9.16	1.75	0.12	0.10	98.85	76.5
46.50	1.45	9.88	12.85	0.31	17.02	9.10	1.67	0.09	0.12	98.99	77.0
44.85	1.48	10.57	12.53	0.23	16.14	9.15	1.71	0.08	0.08	96.81	86.5
45.88	1.44	10.28	12.97	0.17	16.27	9.34	1.69	0.11	0.10	98.24	87.1
45.98	1.51	10.90	12.44	0.19	15.49	9.28	1.81	0.07	0.16	97.81	96.3
45.25	1.49	10.40	12.68	0.24	15.63	9.36	1.83	0.13	0.17	97.18	97.1
46.13	1.47	11.16	12.43	0.30	15.08	9.41	1.93	0.10	0.08	98.09	106.3
45.92	1.53	10.76	12.60	0.20	15.07	9.61	1.87	0.11	0.08	97.76	107.1
46.84	1.59	11.14	12.48	0.19	14.37	9.56	1.85	0.13	0.15	98.29	117.1
46.70	1.51	11.89	12.16	0.19	14.01	9.67	2.12	0.15	0.12	98.52	126.3
47.13	1.56	11.45	12.48	0.22	13.77	9.72	1.90	0.12	0.19	98.53	127.1
46.52	1.55	12.03	12.03	0.19	13.38	9.72	2.08	0.17	0.09	97.74	136.3
47.17	1.59	11.78	12.45	0.24	13.27	9.83	2.08	0.15	0.17	98.73	137.1
47.59	1.57	12.35	11.95	0.24	12.79	9.68	2.27	0.19	0.16	98.77	146.3
47.23	1.56	12.22	12.31	0.19	12.75	9.92	2.08	0.12	0.16	98.54	147.2
48.15	1.60	12.69	11.79	0.16	12.21	9.84	2.28	0.21	0.13	99.05	156.3
47.59	1.65	12.42	11.89	0.19	12.05	10.09	2.28	0.16	0.14	98.47	157.2
48.32	1.69	12.87	11.69	0.17	11.58	9.89	2.39	0.19	0.13	98.94	166.2
48.11	1.68	12.64	11.91	0.21	11.65	10.10	2.25	0.16	0.14	98.85	167.2
48.56	1.65	13.04	11.54	0.15	11.13	10.05	2.49	0.19	0.18	98.97	176.2
48.19	1.67	12.98	11.66	0.20	10.99	10.22	2.36	0.13	0.18	98.58	177.2
47.42	1.69	13.40	11.55	0.13	10.64	9.98	2.57	0.21	0.16	97.74	186.2
47.93	1.68	13.11	11.63	0.22	10.51	10.08	2.35	0.17	0.14	97.81	187.3
47.77	1.68	13.54	11.55	0.19	10.21	10.05	2.41	0.16	0.16	97.71	196.2
48.50	1.75	13.26	11.71	0.19	10.01	10.13	2.30	0.16	0.07	98.10	197.3
48.06	1.70	13.75	11.55	0.21	9.86	10.04	2.67	0.20	0.20	98.23	206.2
48.27	1.72	13.60	11.75	0.18	9.66	10.21	2.42	0.18	0.14	98.13	207.3
49.14	1.67	13.84	11.38	0.17	9.59	10.03	2.59	0.18	0.16	98.73	216.1

49.08	1.80	13.59	11.61	0.18	9.40	10.22	2.51	0.21	0.14	98.72	217.4
48.39	1.79	13.89	11.64	0.21	9.06	10.12	2.56	0.17	0.15	97.98	226.0
49.02	1.75	13.77	11.59	0.30	8.92	10.30	2.73	0.14	0.27	98.78	227.3
49.04	1.80	13.98	11.27	0.27	8.87	10.18	2.54	0.16	0.08	98.17	236.0
49.31	1.79	13.85	11.57	0.19	8.55	10.26	2.57	0.18	0.10	98.36	237.3
49.63	1.81	13.95	11.51	0.21	8.59	10.33	2.76	0.22	0.15	99.16	246.0
47.29	1.82	13.98	11.56	0.28	8.44	10.36	2.77	0.17	0.13	96.80	247.4
48.31	1.84	14.20	11.47	0.17	8.31	10.37	2.64	0.18	0.09	97.58	256.0
48.29	1.80	13.95	11.64	0.19	8.14	10.56	2.53	0.19	0.12	97.40	257.4
49.03	1.81	14.14	11.59	0.14	8.30	10.41	2.77	0.21	0.15	98.54	266.0
49.32	1.90	14.19	11.70	0.24	7.91	10.56	2.74	0.19	0.08	98.83	267.4
49.64	1.85	14.01	11.65	0.18	7.92	10.56	2.71	0.21	0.11	98.84	276.0
48.26	1.90	14.23	11.76	0.14	7.73	10.63	2.67	0.20	0.24	97.74	277.5
49.28	1.85	14.15	11.66	0.20	7.74	10.48	2.88	0.20	0.16	98.60	285.9
49.43	1.89	14.05	11.93	0.26	7.72	10.62	2.62	0.25	0.15	98.90	287.5
48.93	1.85	14.10	11.79	0.14	7.67	10.44	2.59	0.21	0.22	97.94	295.9
49.29	1.87	14.13	11.95	0.26	7.67	10.70	2.76	0.18	0.18	98.99	297.5
49.23	1.89	14.09	11.82	0.17	7.58	10.74	2.69	0.20	0.14	98.54	305.9
49.45	1.88	14.05	12.05	0.22	7.37	10.68	2.76	0.19	0.14	98.80	307.6
48.89	1.84	13.98	12.10	0.26	7.21	10.85	2.75	0.20	0.13	98.20	317.6
48.65	1.89	14.12	12.19	0.21	7.18	10.85	2.56	0.21	0.15	98.00	349.3
49.38	1.93	14.13	12.23	0.22	7.05	10.94	2.70	0.19	0.19	98.95	360.7
49.34	1.85	14.22	12.18	0.25	6.96	10.87	2.80	0.21	0.25	98.93	392.9
49.26	1.89	14.22	12.50	0.20	7.04	11.03	2.73	0.21	0.11	99.20	403.9
47.89	1.83	14.34	12.42	0.20	6.98	11.02	2.81	0.15	0.06	97.69	436.4
48.88	1.88	14.01	12.38	0.29	6.79	10.92	2.60	0.20	0.13	98.09	447.1
47.78	1.86	14.00	12.37	0.26	6.74	11.07	2.46	0.19	0.22	96.94	479.8
49.02	1.94	14.13	12.19	0.21	6.83	11.00	2.70	0.17	0.21	98.40	490.3
48.43	1.83	14.15	12.42	0.21	6.91	11.05	2.71	0.19	0.11	98.01	523.3
49.07	1.88	14.19	12.43	0.25	6.77	11.02	2.63	0.18	0.20	98.62	533.5
48.97	1.82	14.12	12.49	0.15	6.86	11.02	2.68	0.17	0.12	98.40	566.7
47.84	1.87	14.20	12.54	0.22	6.79	11.05	2.54	0.18	0.13	97.37	576.6
48.79	1.88	14.03	12.20	0.21	6.76	11.05	2.69	0.18	0.01	97.79	610.2
49.05	1.86	14.18	12.42	0.28	6.77	11.03	2.64	0.17	0.19	98.58	619.8
48.28	1.86	14.16	12.47	0.24	6.84	10.95	2.64	0.20	0.16	97.79	653.7
48.02	1.89	14.08	12.48	0.26	6.83	11.09	2.81	0.23	0.16	97.85	663.0
49.05	1.89	14.10	12.33	0.23	6.80	10.99	2.58	0.19	0.16	98.32	697.2
48.01	1.94	14.19	12.26	0.32	6.82	10.99	2.69	0.16	0.13	97.51	706.1
48.90	1.80	14.01	12.30	0.32	6.78	11.03	2.79	0.19	0.21	98.33	740.7
48.89	1.90	14.19	12.44	0.26	6.77	11.09	2.63	0.17	0.22	98.54	749.4
48.58	1.88	14.09	12.39	0.26	6.84	10.90	2.70	0.16	0.16	97.95	784.2
47.55	1.82	14.12	12.32	0.18	6.76	11.10	2.68	0.21	0.20	96.93	792.6
48.42	1.87	14.12	12.49	0.14	6.75	11.15	2.66	0.19	0.14	97.92	827.6
48.06	1.90	14.22	12.21	0.25	6.80	11.12	2.52	0.17	0.19	97.45	835.7
49.09	1.86	14.16	12.39	0.19	6.83	11.04	2.56	0.17	0.23	98.52	871.1
48.50	1.88	14.11	12.28	0.17	6.80	10.89	2.58	0.20	0.16	97.56	878.9
48.60	1.84	14.10	12.30	0.27	6.70	11.03	2.57	0.19	0.14	97.73	914.5
48.23	1.89	14.00	12.44	0.18	6.73	11.14	2.60	0.22	0.13	97.55	922.1
48.70	1.84	14.09	12.38	0.19	6.86	11.16	2.66	0.19	0.16	98.22	958.1

49.37	1.91	14.06	12.34	0.21	6.81	11.17	2.55	0.20	0.19	98.81	965.2
48.94	1.80	14.11	12.49	0.19	6.82	11.08	2.68	0.18	0.22	98.50	1001.6
49.06	1.85	14.18	12.44	0.24	6.85	11.07	2.53	0.20	0.22	98.64	1008.5
48.73	1.81	14.12	12.23	0.24	6.85	11.14	2.78	0.18	0.14	98.20	1045.0
48.64	1.93	14.05	12.32	0.29	6.84	11.09	2.44	0.17	0.26	98.02	1051.6
49.06	1.92	14.16	12.50	0.25	6.76	11.07	2.51	0.18	0.18	98.59	1088.5
49.17	1.92	14.02	12.56	0.26	6.92	11.12	2.46	0.17	0.09	98.68	1094.8
48.31	1.88	14.15	12.41	0.27	6.83	11.10	2.53	0.17	0.22	97.88	1132.0
48.59	1.92	14.04	12.47	0.21	6.80	11.08	2.56	0.18	0.19	98.03	1138.0
48.06	1.92	14.11	12.43	0.27	6.94	11.19	2.60	0.14	0.14	97.78	1175.4
48.16	1.87	14.00	12.53	0.22	6.91	11.08	2.56	0.16	0.17	97.66	1181.1
48.46	1.86	14.21	12.33	0.19	6.92	11.18	2.52	0.20	0.21	98.07	1219.0
48.22	1.91	14.07	12.43	0.20	6.81	11.04	2.49	0.19	0.23	97.59	1224.4
48.53	1.88	14.10	12.10	0.23	6.80	11.20	2.35	0.19	0.12	97.51	1262.4
49.02	1.92	14.15	12.23	0.18	6.82	11.10	2.52	0.20	0.10	98.23	1267.5

Exp 39

SiO2	TiO2	Al2O3	FeO	MnO	MgO	CaO	Na2O	K2O	P2O5	Total	d (um)
48.81	1.86	11.92	12.50	0.22	9.93	11.07	2.14	0.13	0.14	98.72	0.6
48.50	1.77	11.37	12.73	0.25	10.69	11.21	2.06	0.09	0.20	98.86	0.9
48.48	1.83	11.85	12.77	0.23	10.59	11.15	2.03	0.14	0.15	99.22	2.9
47.77	1.70	11.11	13.24	0.20	12.28	10.56	1.86	0.13	0.19	99.02	6.2
47.88	1.65	10.64	13.15	0.27	12.48	10.55	1.90	0.12	0.08	98.73	6.4
47.64	1.61	11.01	13.44	0.25	12.50	10.54	1.92	0.11	0.17	99.19	8.6
48.11	1.59	10.63	13.13	0.19	12.96	10.49	1.92	0.12	0.19	99.34	11.9
47.57	1.64	11.00	13.22	0.25	12.62	10.30	2.00	0.13	0.09	98.82	14.3
47.65	1.68	11.15	12.82	0.25	12.68	10.26	1.98	0.11	0.17	98.75	17.5
47.65	1.59	10.81	12.96	0.28	13.00	10.25	1.97	0.13	0.09	98.73	17.5
47.43	1.74	11.26	13.02	0.27	12.61	10.26	1.97	0.12	0.15	98.83	20.1
47.89	1.65	11.12	12.86	0.24	12.59	10.17	2.02	0.14	0.18	98.85	23.1
48.04	1.63	10.92	12.62	0.27	12.89	10.29	2.02	0.14	0.09	98.92	23.1
47.97	1.65	11.35	13.08	0.27	12.53	10.28	1.99	0.14	0.12	99.37	25.8
47.79	1.60	11.09	12.61	0.13	12.66	10.31	2.00	0.14	0.14	98.48	28.6
48.20	1.68	11.45	12.83	0.15	12.56	10.23	2.03	0.13	0.14	99.39	28.7
47.99	1.64	11.43	12.82	0.31	12.43	10.17	2.01	0.17	0.07	99.03	31.5
48.12	1.62	11.62	12.51	0.23	12.46	10.25	2.17	0.09	0.18	99.25	32.5
48.48	1.61	10.99	12.58	0.23	12.39	10.13	1.98	0.14	0.16	98.69	34.2
48.35	1.70	11.52	12.86	0.20	12.43	10.20	2.01	0.09	0.14	99.50	34.4
48.27	1.62	11.61	12.68	0.25	12.28	10.45	2.00	0.13	0.16	99.44	37.2
48.55	1.68	11.73	12.56	0.16	12.22	10.37	2.14	0.13	0.20	99.75	37.6
48.32	1.63	11.56	12.71	0.27	12.36	10.13	2.09	0.17	0.21	99.44	40.0
48.31	1.58	11.70	12.34	0.15	11.97	10.27	2.17	0.13	0.26	98.87	42.2
47.68	1.67	11.73	12.67	0.33	12.00	10.36	2.10	0.15	0.13	98.81	42.7
48.18	1.68	11.90	12.36	0.12	11.60	10.31	2.16	0.16	0.12	98.58	47.8
47.88	1.64	12.05	12.34	0.23	11.63	10.24	2.19	0.15	0.19	98.54	51.8
48.13	1.66	12.08	12.45	0.22	11.56	10.24	2.22	0.16	0.14	98.86	53.0
48.33	1.65	12.09	12.28	0.18	11.54	10.39	2.26	0.13	0.15	98.99	58.0
48.63	1.52	11.96	12.07	0.24	11.38	10.32	2.22	0.14	0.14	98.62	61.5
48.37	1.66	12.54	12.47	0.32	11.30	10.26	2.20	0.18	0.14	99.44	63.3
48.40	1.65	12.41	12.19	0.23	11.37	10.37	2.29	0.12	0.17	99.20	68.1
48.55	1.64	12.30	11.99	0.19	11.15	10.50	2.28	0.15	0.17	98.92	71.2
48.44	1.68	12.41	12.32	0.16	11.13	10.47	2.32	0.15	0.10	99.17	73.5
48.75	1.61	12.55	12.00	0.20	10.83	10.26	2.34	0.13	0.09	98.75	78.3
48.70	1.67	12.65	11.94	0.15	10.65	10.18	2.33	0.13	0.15	98.53	80.8
48.60	1.67	12.73	12.17	0.23	10.77	10.44	2.36	0.19	0.29	99.43	83.7
48.93	1.67	12.74	11.91	0.20	10.61	10.37	2.36	0.15	0.09	99.03	88.5
48.70	1.63	12.62	11.81	0.23	10.55	10.37	2.33	0.12	0.19	98.56	90.5
48.87	1.65	12.82	11.98	0.18	10.22	10.42	2.40	0.19	0.20	98.93	94.0
49.08	1.65	12.97	11.92	0.17	10.30	10.37	2.42	0.17	0.18	99.22	98.7
49.24	1.68	12.86	11.76	0.20	10.31	10.41	2.37	0.23	0.22	99.29	100.2
48.92	1.66	13.03	11.95	0.15	10.00	10.43	2.38	0.16	0.23	98.91	104.3
49.08	1.66	13.20	11.67	0.17	9.96	10.40	2.42	0.22	0.21	98.99	108.9
49.20	1.72	13.28	11.54	0.19	9.93	10.31	2.47	0.18	0.23	99.04	109.7
49.33	1.73	13.57	11.79	0.16	9.71	10.42	2.57	0.19	0.14	99.62	118.1
49.16	1.67	13.16	11.81	0.21	9.64	10.43	2.49	0.18	0.29	99.03	119.1

49.11	1.63	13.13	11.72	0.26	9.74	10.48	2.47	0.17	0.21	98.92	119.4
49.64	1.75	13.70	11.75	0.22	9.47	10.41	2.67	0.17	0.16	99.93	127.9
49.54	1.68	13.41	11.43	0.21	9.46	10.41	2.53	0.18	0.22	99.07	129.1
49.41	1.71	13.39	11.53	0.22	9.41	10.67	2.52	0.20	0.14	99.19	129.3
49.17	1.74	13.49	11.33	0.18	9.21	10.47	2.55	0.17	0.20	98.53	138.7
49.48	1.75	13.62	11.68	0.10	9.05	10.64	2.58	0.23	0.17	99.29	138.9
49.73	1.72	13.78	11.55	0.19	8.91	10.46	2.67	0.22	0.16	99.36	148.2
49.65	1.78	13.51	11.30	0.23	8.96	10.46	2.55	0.22	0.15	98.82	148.4
49.60	1.76	13.51	11.54	0.20	8.78	10.51	2.62	0.19	0.14	98.84	158.1
49.61	1.75	13.82	11.62	0.26	8.62	10.71	2.63	0.17	0.19	99.38	159.7
50.03	1.72	13.81	11.29	0.16	8.60	10.54	2.70	0.20	0.19	99.23	162.8
49.89	1.80	13.78	11.44	0.22	8.70	10.56	2.64	0.21	0.17	99.41	167.7
49.51	1.75	13.71	11.47	0.18	8.45	10.66	2.69	0.21	0.17	98.81	168.5
49.69	1.83	13.94	11.48	0.20	8.25	10.65	2.72	0.21	0.19	99.15	180.5
49.68	1.76	13.85	11.43	0.18	8.23	10.70	2.72	0.25	0.16	98.96	182.8
49.72	1.78	13.93	11.55	0.27	8.17	10.60	2.69	0.19	0.22	99.11	188.8
49.69	1.82	14.00	11.60	0.21	7.92	10.79	2.59	0.17	0.22	98.99	201.2
49.65	1.77	14.08	11.42	0.31	7.98	10.55	2.75	0.17	0.15	98.82	202.7
49.61	1.77	13.90	11.71	0.21	8.01	10.77	2.61	0.22	0.25	99.04	209.0
49.73	1.81	13.93	11.55	0.25	7.64	10.76	2.77	0.22	0.24	98.89	222.0
49.98	1.82	13.87	11.39	0.23	7.70	10.72	2.68	0.21	0.18	98.78	222.7
49.85	1.75	14.07	11.66	0.17	7.84	10.82	2.77	0.16	0.21	99.28	229.3
49.86	1.77	14.02	11.38	0.23	7.54	10.66	2.74	0.17	0.12	98.49	242.7
49.85	1.76	14.09	11.86	0.18	7.66	10.90	2.71	0.18	0.10	99.30	242.8
49.73	1.80	14.04	11.89	0.26	7.64	10.81	2.72	0.18	0.26	99.33	249.6
49.81	1.82	13.84	11.54	0.24	7.48	10.88	2.77	0.14	0.18	98.70	262.7
49.69	1.81	13.91	11.82	0.24	7.39	10.79	2.68	0.21	0.31	98.84	263.6
49.62	1.84	14.10	11.66	0.14	7.48	10.99	2.83	0.21	0.18	99.04	269.9
49.85	1.81	13.99	11.57	0.22	7.37	10.95	2.69	0.18	0.24	98.86	282.7
49.80	1.83	13.97	11.91	0.27	7.41	10.96	2.65	0.17	0.25	99.22	284.4
49.96	1.84	14.03	11.94	0.23	7.39	10.92	2.76	0.18	0.19	99.44	290.1
49.66	1.85	14.19	11.95	0.18	7.29	11.09	2.72	0.21	0.24	99.37	298.3
49.91	1.79	14.03	11.72	0.16	7.23	10.91	2.72	0.18	0.22	98.86	302.6
49.63	1.86	13.97	11.88	0.29	7.25	11.19	2.73	0.18	0.23	99.19	303.3
49.34	1.85	13.96	11.90	0.19	7.26	11.00	2.68	0.20	0.22	98.59	305.1
49.80	1.81	13.81	11.77	0.26	7.26	11.06	2.63	0.22	0.20	98.80	310.4
49.84	1.84	14.07	12.19	0.18	7.16	10.98	2.70	0.21	0.14	99.31	315.8
49.59	1.81	13.84	12.11	0.17	7.17	11.01	2.63	0.17	0.20	98.69	318.7
50.49	1.82	13.69	11.66	0.20	7.11	11.03	2.57	0.21	0.15	98.94	322.6
49.61	1.87	13.98	11.84	0.22	7.16	10.88	2.75	0.18	0.18	98.68	323.2
50.13	1.84	13.88	11.71	0.15	7.07	10.99	2.65	0.16	0.21	98.77	325.9
49.58	1.81	13.72	11.90	0.19	7.01	11.19	2.73	0.21	0.18	98.51	335.4
49.82	1.79	13.89	11.99	0.22	6.94	11.08	2.60	0.22	0.23	98.77	339.1
49.82	1.88	14.02	11.94	0.25	7.13	11.12	2.67	0.16	0.19	99.17	343.1
49.77	1.81	14.03	12.10	0.32	7.05	11.06	2.72	0.18	0.09	99.12	355.2
49.70	1.79	13.92	12.09	0.26	6.98	11.10	2.61	0.21	0.15	98.81	359.5
49.74	1.80	14.13	12.04	0.18	7.12	11.05	2.64	0.18	0.23	99.10	363.0
49.74	1.82	14.03	12.07	0.14	7.09	11.11	2.69	0.16	0.35	99.20	374.9
49.53	1.79	13.99	12.06	0.22	7.07	11.14	2.73	0.19	0.14	98.84	379.8

49.86	1.75	14.15	11.97	0.23	7.08	11.11	2.66	0.14	0.20	99.14	382.9
49.59	1.82	13.88	11.95	0.25	6.97	11.09	2.70	0.19	0.27	98.72	394.6
49.63	1.84	14.01	12.04	0.19	7.03	11.02	2.80	0.18	0.11	98.83	400.2
49.61	1.74	14.05	11.74	0.22	7.19	10.95	2.73	0.22	0.18	98.62	402.9
49.95	1.85	13.91	12.11	0.15	7.00	11.08	2.75	0.17	0.25	99.20	414.2
49.43	1.85	13.96	12.02	0.20	7.07	11.13	2.66	0.16	0.12	98.58	420.6
49.89	1.81	13.96	11.98	0.25	7.07	11.18	2.69	0.17	0.13	99.13	422.8
49.65	1.79	13.84	12.07	0.17	6.99	11.12	2.68	0.21	0.22	98.74	434.0
49.61	1.85	14.14	11.95	0.19	6.97	11.12	2.65	0.18	0.18	98.85	441.0
49.89	1.78	14.08	12.02	0.20	7.13	11.11	2.71	0.13	0.24	99.28	442.7
49.78	1.78	13.94	12.02	0.22	7.01	11.16	2.77	0.21	0.11	98.98	453.7
49.75	1.82	13.88	12.04	0.17	7.06	11.12	2.67	0.15	0.12	98.79	461.4
49.72	1.77	13.91	11.79	0.25	7.03	11.18	2.70	0.26	0.27	98.87	462.6
49.56	1.79	13.82	12.11	0.22	7.09	11.26	2.63	0.17	0.15	98.79	473.4
49.75	1.81	13.89	11.87	0.17	6.97	10.93	2.73	0.16	0.12	98.40	481.7
49.81	1.84	14.00	11.84	0.27	7.03	11.02	2.71	0.20	0.13	98.83	482.5
49.77	1.81	14.02	12.08	0.26	6.96	11.10	2.77	0.12	0.16	99.03	493.1
49.69	1.75	13.87	12.03	0.25	7.02	11.11	2.57	0.19	0.27	98.76	502.1
49.74	1.81	13.89	11.82	0.20	7.03	11.17	2.72	0.18	0.09	98.66	502.5
49.51	1.80	13.89	12.14	0.21	6.95	11.02	2.57	0.20	0.17	98.44	512.8
49.86	1.76	14.01	11.88	0.27	7.04	11.16	2.64	0.17	0.14	98.92	522.4
49.74	1.85	13.82	11.97	0.26	6.92	11.06	2.68	0.16	0.25	98.70	532.5
49.89	1.74	14.08	11.94	0.25	6.99	11.15	2.70	0.18	0.18	99.11	542.2
49.69	1.75	13.95	11.76	0.15	6.92	11.13	2.65	0.20	0.31	98.51	562.2
49.91	1.84	13.92	11.81	0.18	6.95	11.08	2.64	0.17	0.18	98.67	582.1
49.94	1.78	13.94	12.02	0.23	7.00	11.13	2.70	0.15	0.19	99.08	602.1
49.72	1.82	14.06	12.16	0.24	7.13	11.16	2.66	0.17	0.22	99.35	607.0
49.84	1.82	13.89	12.21	0.22	7.05	11.06	2.67	0.20	0.24	99.19	626.0
50.05	1.76	14.05	12.07	0.15	7.03	11.09	2.72	0.16	0.16	99.24	637.2
49.89	1.76	13.98	12.00	0.23	7.10	11.25	2.66	0.13	0.24	99.24	644.9
49.67	1.82	13.87	12.15	0.15	6.97	11.11	2.65	0.22	0.20	98.82	657.8
49.67	1.81	13.92	12.03	0.15	7.01	11.20	2.65	0.22	0.12	98.77	663.9
49.76	1.78	13.94	11.92	0.23	7.01	11.15	2.71	0.15	0.09	98.75	678.4
49.59	1.80	14.03	12.06	0.16	7.04	11.22	2.71	0.18	0.21	99.00	682.9
49.50	1.77	13.88	12.03	0.20	6.92	11.13	2.70	0.20	0.18	98.51	699.1
49.76	1.85	13.99	12.06	0.24	6.94	11.01	2.75	0.17	0.23	99.00	701.9
49.63	1.84	13.96	12.11	0.22	6.98	11.21	2.69	0.18	0.20	99.02	719.6
49.64	1.85	13.90	11.93	0.20	7.02	11.10	2.68	0.18	0.19	98.70	720.9
50.39	1.87	14.19	11.70	0.21	7.14	11.26	2.78	0.19	0.15	99.88	733.1
49.86	1.78	14.00	12.09	0.24	6.96	11.20	2.68	0.22	0.18	99.21	739.8
49.54	1.81	13.83	12.06	0.19	6.99	10.98	2.69	0.18	0.17	98.45	740.2
49.71	1.84	13.97	11.75	0.23	7.01	11.01	2.74	0.21	0.13	98.59	753.6
49.96	1.84	13.78	11.94	0.28	6.91	11.16	2.64	0.25	0.15	98.90	758.8
49.80	1.80	13.90	12.02	0.21	7.05	11.13	2.67	0.22	0.13	98.93	760.8
50.14	1.76	14.04	11.72	0.14	6.98	11.05	2.64	0.21	0.11	98.77	774.1
49.92	1.80	13.95	12.11	0.18	7.04	11.14	2.77	0.20	0.16	99.27	781.5
49.78	1.79	14.00	11.69	0.27	6.97	11.06	2.69	0.20	0.12	98.56	794.6
50.21	1.75	13.76	11.91	0.21	6.98	11.05	2.63	0.24	0.24	98.97	802.1
50.09	1.82	14.14	11.84	0.09	6.99	11.17	2.74	0.17	0.18	99.22	815.1

49.53	1.81	14.00	12.34	0.25	7.17	11.21	2.75	0.19	0.14	99.39	828.2
49.87	1.77	13.94	11.75	0.26	6.92	11.23	2.69	0.16	0.18	98.77	835.5
50.08	1.75	13.88	11.66	0.23	6.89	11.16	2.60	0.20	0.30	98.74	856.0
49.54	1.81	13.96	11.91	0.27	6.97	11.03	2.62	0.17	0.21	98.49	865.4
49.56	1.81	13.91	12.03	0.23	6.91	11.18	2.82	0.14	0.18	98.77	867.1
49.92	1.82	14.20	11.87	0.17	7.19	11.24	2.74	0.15	0.25	99.55	885.3
49.74	1.71	13.95	11.99	0.24	6.93	11.10	2.70	0.18	0.16	98.70	904.6
49.51	1.76	13.88	12.08	0.29	6.94	11.18	2.66	0.20	0.15	98.64	906.1
49.73	1.83	13.94	11.78	0.17	6.98	11.10	2.68	0.18	0.25	98.65	925.3
49.67	1.81	13.98	12.11	0.32	7.06	11.14	2.70	0.19	0.07	99.04	944.0
49.69	1.83	13.86	12.06	0.18	7.04	11.28	2.62	0.19	0.28	99.02	945.0
49.71	1.77	13.91	11.84	0.22	6.84	11.11	2.66	0.21	0.18	98.45	965.2
49.29	1.81	13.97	12.09	0.19	7.06	11.05	2.70	0.18	0.22	98.56	983.2
49.39	1.75	13.79	12.17	0.30	7.03	11.10	2.71	0.22	0.16	98.62	984.0
49.65	1.77	13.99	11.90	0.23	6.98	11.21	2.69	0.15	0.22	98.79	1005.2
49.62	1.74	13.97	11.90	0.20	6.99	11.18	2.71	0.22	0.08	98.59	1022.5
49.71	1.79	13.79	12.23	0.21	6.95	11.29	2.64	0.17	0.23	99.02	1023.0
49.52	1.84	13.89	11.94	0.23	7.06	11.02	2.68	0.13	0.21	98.51	1045.1
49.83	1.77	13.96	12.31	0.21	7.05	11.13	2.60	0.17	0.14	99.16	1061.8
49.76	1.77	13.78	12.06	0.19	6.88	11.31	2.66	0.20	0.18	98.79	1061.9
49.61	1.80	13.86	12.03	0.20	7.02	10.99	2.60	0.19	0.18	98.49	1085.1
49.64	1.79	13.89	12.18	0.24	6.98	11.14	2.65	0.16	0.16	98.83	1100.9
49.93	1.77	13.90	11.97	0.28	6.95	11.15	2.64	0.21	0.20	98.99	1101.1
49.84	1.82	14.00	11.97	0.18	6.95	11.17	2.71	0.24	0.16	99.03	1125.1
49.48	1.81	13.77	12.06	0.22	6.95	11.22	2.67	0.15	0.13	98.46	1139.8
50.06	1.81	13.92	12.05	0.23	6.96	11.01	2.69	0.21	0.20	99.13	1140.4
49.88	1.78	13.97	12.06	0.17	6.95	11.09	2.67	0.21	0.20	98.98	1165.0
49.53	1.83	13.92	12.12	0.20	6.92	11.22	2.69	0.17	0.25	98.86	1178.8
49.88	1.74	13.97	12.00	0.19	7.00	11.05	2.68	0.21	0.19	98.90	1179.7
49.91	1.83	13.89	12.02	0.18	7.02	11.06	2.70	0.16	0.16	98.93	1205.0
49.48	1.75	13.90	12.09	0.18	7.06	11.06	2.73	0.15	0.15	98.55	1217.8
49.84	1.79	13.97	11.82	0.20	7.00	11.05	2.64	0.18	0.06	98.55	1219.0
49.98	1.81	14.13	11.99	0.14	7.01	11.21	2.64	0.21	0.23	99.35	1231.9
49.68	1.85	14.11	11.96	0.22	6.94	11.08	2.70	0.21	0.12	98.84	1244.9
49.67	1.80	13.98	12.21	0.23	6.95	11.23	2.69	0.18	0.21	99.15	1256.7
49.66	1.86	13.98	11.97	0.22	7.01	11.01	2.61	0.14	0.18	98.64	1274.3
49.60	1.81	14.03	11.86	0.22	7.02	11.12	2.66	0.17	0.23	98.72	1284.9
49.77	1.82	13.92	12.04	0.18	7.03	11.07	2.67	0.16	0.22	98.87	1295.7
49.99	1.83	13.93	11.64	0.24	6.88	11.13	2.69	0.18	0.20	98.71	1316.8
50.05	1.77	13.84	11.89	0.26	7.00	11.07	2.48	0.18	0.22	98.76	1324.8
49.88	1.80	13.84	11.84	0.24	6.83	11.05	2.62	0.18	0.24	98.51	1334.6
49.46	1.85	14.07	11.95	0.20	7.09	11.07	2.57	0.20	0.23	98.68	1341.2
49.29	1.83	14.01	12.02	0.19	6.95	11.00	2.68	0.18	0.31	98.44	1349.6
49.89	1.81	13.94	12.02	0.25	6.97	11.06	2.68	0.20	0.14	98.94	1375.9
49.45	1.76	13.89	12.04	0.16	7.03	11.24	2.62	0.16	0.14	98.50	1387.2
50.01	1.83	14.07	11.94	0.20	7.01	11.07	2.76	0.19	0.14	99.21	1410.4
49.99	1.84	13.92	12.05	0.25	7.01	11.14	2.61	0.19	0.25	99.23	1424.6
49.99	1.79	14.13	11.92	0.25	7.11	11.24	2.70	0.21	0.24	99.58	1439.4
50.27	1.81	13.92	11.92	0.26	6.89	11.03	2.67	0.17	0.32	99.25	1445.1

49.85	1.82	14.12	11.95	0.26	7.03	11.04	2.66	0.22	-0.02	98.94	1462.2
49.68	1.80	13.98	11.74	0.16	6.97	11.20	2.74	0.19	0.25	98.71	1477.1
49.78	1.80	13.94	11.86	0.15	7.01	11.13	2.58	0.16	0.27	98.69	1499.8
50.10	1.77	13.83	11.85	0.29	6.90	11.03	2.68	0.19	0.19	98.85	1514.6
49.99	1.77	14.07	11.75	0.19	7.05	11.16	2.72	0.21	0.22	99.13	1537.3
50.53	1.79	13.73	11.58	0.21	6.88	11.15	2.71	0.17	0.34	99.07	1552.3
50.00	1.79	13.99	11.53	0.25	6.99	11.14	2.66	0.18	0.12	98.65	1574.8
50.23	1.81	13.67	11.66	0.11	6.74	11.06	2.51	0.19	0.23	98.21	1612.3

Exp 40

SiO2	TiO2	Al2O3	FeO	MnO	MgO	CaO	Na2O	K2O	P2O5	Total	d (um)
48.61	1.85	12.40	11.90	0.23	9.85	11.01	2.28	0.12	0.11	98.35	0.8
48.58	1.83	12.33	12.19	0.35	10.00	10.98	2.31	0.14	0.11	98.82	1.4
47.82	1.68	10.98	13.19	0.22	12.48	10.63	1.83	0.13	0.06	99.03	6.0
48.76	1.86	12.28	12.27	0.26	9.94	11.13	2.31	0.09	0.10	99.00	6.0
47.54	1.67	10.97	13.33	0.27	12.44	10.67	2.00	0.08	0.12	99.09	6.8
47.75	1.71	11.04	13.24	0.26	12.31	10.65	1.98	0.10	0.15	99.19	11.6
47.44	1.58	10.70	13.39	0.25	13.38	10.16	1.89	0.08	0.04	98.91	12.1
47.48	1.60	10.92	13.15	0.29	13.46	10.13	1.95	0.16	0.12	99.26	16.3
47.41	1.55	10.93	13.17	0.24	13.09	10.36	1.97	0.10	0.07	98.90	17.0
47.84	1.57	10.82	13.22	0.25	13.48	10.14	1.96	0.09	0.09	99.46	17.5
47.32	1.53	10.90	12.95	0.28	13.31	10.10	1.95	0.14	0.02	98.49	21.5
47.39	1.57	10.82	13.27	0.30	13.37	10.00	1.90	0.10	0.08	98.80	22.4
47.81	1.61	10.88	13.14	0.18	13.35	10.05	2.00	0.10	0.11	99.22	22.9
47.44	1.57	11.08	12.99	0.27	13.28	10.05	1.93	0.13	0.03	98.76	26.7
47.43	1.56	10.85	13.04	0.22	13.37	10.12	2.01	0.10	0.13	98.82	27.9
47.57	1.62	11.09	12.95	0.19	13.39	9.98	1.98	0.08	0.21	99.04	31.9
47.81	1.58	11.03	12.97	0.17	13.49	10.01	2.03	0.14	0.11	99.33	33.4
47.80	1.56	11.22	12.73	0.18	13.19	10.10	1.97	0.12	0.05	98.91	37.1
47.88	1.56	11.07	12.94	0.15	13.19	10.09	2.05	0.13	0.02	99.08	38.8
47.77	1.61	11.01	13.09	0.27	13.24	10.06	1.96	0.10	0.08	99.21	38.8
47.75	1.61	11.11	12.88	0.22	13.15	10.19	2.02	0.10	-0.01	99.03	39.8
47.87	1.60	11.27	12.87	0.21	13.05	10.12	1.97	0.15	0.15	99.25	42.2
47.77	1.55	11.27	12.74	0.22	12.89	10.11	2.02	0.16	0.19	98.91	47.4
47.98	1.61	11.28	12.89	0.25	13.00	10.21	2.05	0.15	0.04	99.46	49.0
47.55	1.55	10.99	12.62	0.25	12.83	10.08	2.02	0.12	0.15	98.15	49.5
48.06	1.56	11.35	12.63	0.29	12.78	10.00	2.03	0.11	0.15	98.96	52.6
47.95	1.60	11.41	12.82	0.17	12.74	10.12	2.04	0.10	0.06	99.00	59.2
47.92	1.64	11.58	12.77	0.19	12.82	10.10	2.06	0.10	0.12	99.30	59.4
48.13	1.58	11.51	12.76	0.27	12.58	10.18	2.09	0.13	0.15	99.39	69.2
48.12	1.62	11.50	12.69	0.30	12.76	9.96	2.07	0.08	0.15	99.24	69.4
48.09	1.61	11.61	12.69	0.19	12.64	10.15	2.14	0.11	0.16	99.39	78.9
48.18	1.57	11.54	12.85	0.23	12.71	10.06	2.12	0.14	0.14	99.53	79.6
48.00	1.59	11.63	12.60	0.17	12.28	10.01	2.10	0.18	0.11	98.66	88.7
48.32	1.61	11.74	12.51	0.18	12.40	10.19	2.20	0.15	0.11	99.40	89.8
48.52	1.61	11.88	12.49	0.24	12.20	10.17	2.15	0.16	0.19	99.61	97.2
48.25	1.54	11.93	12.67	0.29	12.14	10.23	2.18	0.14	0.18	99.54	98.5
48.38	1.60	11.76	12.57	0.28	12.18	10.28	2.12	0.13	0.01	99.31	100.0
48.49	1.62	11.99	12.36	0.21	11.91	10.17	2.20	0.13	0.18	99.25	107.1
48.34	1.56	11.94	12.36	0.14	11.96	10.19	2.13	0.14	0.16	98.93	108.2
48.38	1.58	11.91	12.46	0.20	11.95	10.13	2.12	0.12	0.13	98.98	110.2
48.18	1.62	12.04	12.34	0.22	11.89	10.32	2.22	0.17	0.18	99.19	116.9
48.45	1.60	11.99	12.41	0.17	11.81	10.29	2.25	0.15	0.10	99.21	118.1
48.59	1.61	12.03	12.59	0.25	11.79	10.09	2.27	0.16	-0.01	99.38	120.5
48.57	1.61	12.53	12.16	0.24	11.76	10.13	2.33	0.17	0.15	99.64	121.2
48.37	1.59	12.24	12.36	0.22	11.63	10.21	2.26	0.16	0.17	99.20	126.9
48.73	1.55	12.29	12.43	0.31	11.77	10.02	2.20	0.14	0.15	99.59	127.9
48.44	1.63	12.13	12.58	0.23	11.63	10.24	2.25	0.15	0.15	99.44	130.6

48.89	1.66	12.37	12.22	0.25	11.39	10.24	2.30	0.15	0.11	99.59	131.4
48.48	1.63	12.27	12.36	0.15	11.56	10.31	2.28	0.13	0.07	99.23	136.8
48.60	1.63	12.16	12.31	0.30	11.55	10.20	2.30	0.18	0.11	99.33	137.6
48.68	1.57	12.18	12.34	0.34	11.58	10.30	2.29	0.17	0.11	99.57	140.9
48.93	1.62	12.57	12.24	0.26	11.21	10.34	2.41	0.16	0.14	99.86	141.7
48.73	1.61	12.42	12.18	0.28	11.44	10.23	2.32	0.15	0.11	99.45	146.7
48.72	1.71	12.57	12.31	0.26	11.15	10.22	2.41	0.15	0.14	99.64	146.7
48.73	1.63	12.59	12.17	0.23	11.16	10.30	2.31	0.16	0.15	99.42	151.9
48.71	1.64	12.52	12.10	0.26	11.19	10.25	2.35	0.12	0.07	99.21	156.6
48.99	1.68	12.67	12.13	0.21	10.81	10.37	2.34	0.18	0.11	99.48	156.7
49.00	1.65	12.67	11.97	0.11	10.83	10.32	2.48	0.15	0.12	99.29	162.1
48.84	1.66	12.75	11.96	0.20	11.07	10.30	2.30	0.11	0.08	99.25	166.5
48.78	1.61	12.81	11.98	0.23	10.89	10.29	2.32	0.11	0.15	99.16	166.7
48.98	1.65	12.78	11.99	0.21	10.72	10.28	2.37	0.15	0.08	99.21	172.4
48.74	1.65	12.71	12.05	0.23	10.90	10.25	2.34	0.19	0.11	99.17	176.4
49.02	1.64	12.72	11.97	0.19	10.65	10.30	2.46	0.18	0.11	99.23	176.6
49.03	1.67	13.06	11.96	0.22	10.51	10.37	2.39	0.17	0.03	99.40	182.6
48.72	1.68	12.69	12.12	0.22	10.79	10.38	2.42	0.15	0.15	99.33	186.3
49.41	1.63	12.82	11.78	0.23	10.71	10.28	2.46	0.18	0.14	99.64	186.6
49.24	1.66	12.98	11.84	0.22	10.42	10.40	2.46	0.17	0.14	99.52	192.9
48.97	1.69	12.94	11.93	0.25	10.55	10.27	2.39	0.16	0.08	99.24	196.2
49.36	1.60	13.18	11.80	0.18	10.42	10.41	2.41	0.21	0.14	99.71	196.5
49.13	1.64	13.03	11.61	0.22	10.26	10.25	2.47	0.15	0.10	98.85	203.1
49.12	1.67	12.96	12.02	0.19	10.41	10.31	2.38	0.19	0.05	99.30	206.2
49.41	1.67	13.17	11.85	0.18	10.24	10.35	2.50	0.18	0.08	99.62	206.5
49.29	1.63	13.19	11.83	0.28	10.01	10.31	2.48	0.16	0.08	99.24	213.4
49.19	1.71	12.99	12.00	0.25	10.34	10.44	2.51	0.16	0.08	99.66	216.0
49.29	1.65	13.07	11.92	0.16	10.12	10.37	2.47	0.19	0.06	99.30	216.4
49.28	1.65	13.16	11.74	0.16	9.96	10.25	2.41	0.20	0.18	98.99	223.6
49.15	1.68	13.13	11.76	0.19	10.22	10.37	2.44	0.15	0.12	99.19	226.0
49.18	1.60	13.30	11.84	0.17	9.87	10.33	2.50	0.23	0.17	99.18	226.4
49.59	1.68	13.25	11.69	0.26	9.78	10.41	2.56	0.18	0.10	99.49	233.8
49.06	1.69	13.07	11.69	0.19	10.08	10.39	2.44	0.16	0.15	98.92	235.8
49.33	1.71	13.33	11.61	0.24	9.70	10.42	2.57	0.14	0.12	99.18	236.4
49.57	1.63	13.46	11.71	0.24	9.69	10.35	2.52	0.16	0.11	99.44	244.0
49.15	1.70	13.33	11.79	0.24	9.85	10.44	2.55	0.18	0.08	99.28	245.8
49.51	1.62	13.45	11.58	0.26	9.71	10.31	2.57	0.18	0.10	99.28	246.3
49.26	1.69	13.28	11.45	0.17	9.49	10.50	2.54	0.16	0.08	98.62	254.3
49.20	1.69	13.40	11.59	0.15	9.56	10.42	2.51	0.20	0.14	98.85	256.3
49.26	1.69	13.92	11.56	0.26	9.42	10.37	2.73	0.22	0.18	99.61	260.8
49.75	1.66	13.52	11.62	0.11	9.36	10.26	2.52	0.21	0.08	99.10	264.5
49.62	1.73	13.34	11.62	0.17	9.62	10.47	2.60	0.17	0.15	99.48	265.6
49.36	1.68	13.57	11.65	0.25	9.32	10.30	2.59	0.17	0.12	99.02	266.2
49.48	1.65	13.65	11.55	0.26	9.27	10.31	2.63	0.17	0.14	99.13	267.9
49.80	1.74	13.83	11.62	0.22	9.18	10.35	2.64	0.20	0.20	99.78	272.2
49.59	1.79	13.27	11.66	0.12	9.57	10.58	2.56	0.21	0.05	99.40	275.4
49.91	1.68	13.80	11.47	0.23	9.02	10.46	2.70	0.18	0.14	99.58	275.8
49.35	1.73	13.57	11.51	0.22	9.09	10.41	2.63	0.23	0.05	98.78	276.2
49.65	1.66	13.61	11.51	0.22	9.13	10.39	2.63	0.18	0.11	99.08	283.6

49.90	1.65	13.70	11.57	0.17	8.89	10.63	2.67	0.19	0.12	99.48	287.9
49.79	1.75	13.91	11.33	0.20	8.86	10.42	2.70	0.23	0.12	99.32	290.8
49.57	1.76	13.65	11.35	0.21	9.01	10.45	2.56	0.19	0.06	98.80	299.5
49.80	1.67	13.84	11.43	0.09	8.78	10.53	2.64	0.21	0.12	99.11	303.6
49.94	1.77	13.67	11.51	0.18	8.80	10.50	2.72	0.16	0.08	99.33	305.8
49.78	1.73	13.86	11.45	0.23	8.81	10.41	2.68	0.19	0.08	99.21	315.2
49.70	1.73	13.81	11.39	0.23	8.54	10.45	2.63	0.18	0.16	98.81	319.3
49.92	1.72	13.81	11.43	0.22	8.53	10.47	2.79	0.17	0.14	99.19	320.8
49.68	1.73	13.85	11.51	0.17	8.68	10.59	2.70	0.18	0.10	99.19	331.0
49.76	1.68	14.07	11.44	0.14	8.51	10.51	2.65	0.22	0.12	99.08	335.0
49.94	1.74	13.87	11.29	0.18	8.58	10.50	2.67	0.22	0.12	99.10	335.9
50.03	1.72	13.83	11.56	0.17	8.53	10.57	2.69	0.17	0.10	99.36	346.7
50.05	1.75	13.76	11.38	0.27	8.32	10.45	2.73	0.23	0.17	99.09	350.7
49.97	1.73	13.96	11.45	0.17	8.37	10.51	2.68	0.22	0.07	99.12	350.8
49.73	1.75	13.78	11.45	0.20	8.35	10.60	2.77	0.25	0.13	99.00	362.6
50.18	1.76	14.04	11.51	0.22	8.20	10.58	2.77	0.21	0.18	99.63	365.8
50.01	1.71	13.91	11.48	0.22	8.20	10.55	2.70	0.18	0.15	99.11	366.5
49.66	1.77	13.83	11.50	0.25	8.22	10.62	2.75	0.18	0.21	98.99	378.4
49.78	1.82	13.98	11.54	0.23	8.03	10.50	2.73	0.17	0.16	98.93	380.9
49.75	1.80	13.88	11.48	0.32	8.19	10.65	2.71	0.19	0.12	99.10	382.2
49.79	1.75	13.95	11.63	0.16	8.10	10.64	2.70	0.16	0.06	98.94	394.1
50.05	1.82	13.97	11.43	0.26	8.06	10.65	2.75	0.14	0.20	99.32	395.8
49.87	1.72	14.11	11.57	0.25	7.90	10.62	2.76	0.15	0.16	99.10	397.9
50.00	1.78	13.98	11.52	0.21	8.20	10.61	2.68	0.17	0.18	99.33	410.0
50.10	1.83	14.12	11.60	0.22	7.95	10.63	2.76	0.18	0.19	99.57	410.8
49.94	1.80	13.86	11.55	0.21	8.00	10.65	2.72	0.17	0.17	99.07	413.6
50.11	1.80	13.99	11.60	0.14	7.98	10.63	2.72	0.17	0.18	99.32	425.7
49.92	1.77	14.07	11.57	0.21	7.81	10.79	2.74	0.25	0.12	99.24	425.9
50.15	1.81	14.14	11.51	0.24	7.73	10.50	2.68	0.21	0.01	98.96	429.3
49.89	1.82	14.05	11.68	0.22	7.85	10.66	2.75	0.20	0.10	99.22	440.9
50.10	1.86	14.02	11.66	0.24	7.91	10.64	2.75	0.21	0.12	99.51	441.5
49.89	1.73	14.04	11.55	0.23	7.78	10.80	2.81	0.24	0.19	99.26	445.0
49.78	1.81	13.90	11.57	0.22	7.63	10.87	2.75	0.19	0.09	98.80	455.4
49.95	1.87	14.15	11.49	0.15	7.67	10.81	2.79	0.18	0.13	99.20	455.8
49.85	1.81	14.14	11.62	0.23	7.63	10.75	2.72	0.22	0.18	99.14	455.9
50.05	1.77	13.90	11.59	0.23	7.80	10.69	2.78	0.19	0.09	99.09	457.3
50.02	1.83	13.98	11.61	0.12	7.62	10.60	2.74	0.22	0.26	98.98	460.7
49.87	1.84	14.15	11.66	0.22	7.55	10.80	2.71	0.18	0.09	99.06	465.9
49.84	1.82	14.07	11.71	0.14	7.69	10.85	2.79	0.20	0.09	99.21	469.1
49.84	1.76	14.18	11.64	0.22	7.44	10.70	2.69	0.21	0.12	98.79	471.8
50.04	1.79	14.11	11.66	0.23	7.77	10.66	2.72	0.18	0.10	99.25	473.1
50.19	1.84	13.94	11.71	0.24	7.51	10.85	2.75	0.16	0.13	99.32	476.5
49.88	1.85	14.01	11.77	0.13	7.53	10.82	2.78	0.20	0.19	99.17	482.8
49.63	1.84	14.03	11.66	0.27	7.58	10.94	2.79	0.22	0.02	98.95	483.1
50.00	1.80	14.03	11.89	0.21	7.57	10.89	2.73	0.18	0.19	99.50	487.8
49.73	1.78	14.09	11.69	0.22	7.46	10.81	2.72	0.16	0.20	98.86	496.3
50.17	1.85	13.97	11.67	0.21	7.46	10.94	2.72	0.19	0.04	99.22	496.4
49.78	1.85	14.02	11.77	0.28	7.46	10.88	2.72	0.14	0.17	99.06	496.8
50.02	1.80	13.91	11.60	0.28	7.57	10.78	2.76	0.21	0.18	99.11	500.3

50.21	1.80	14.03	11.64	0.28	7.41	10.93	2.74	0.19	0.13	99.36	503.7
50.11	1.89	13.98	11.83	0.28	7.49	10.90	2.76	0.17	0.06	99.48	517.4
49.80	1.78	14.03	11.66	0.24	7.39	10.97	2.78	0.16	0.16	98.96	526.3
49.73	1.80	14.03	11.69	0.23	7.25	10.85	2.74	0.15	0.14	98.62	526.4
50.04	1.76	13.95	11.87	0.19	7.31	10.83	2.75	0.18	0.15	99.02	555.8
49.90	1.82	13.92	11.90	0.13	7.28	10.92	2.71	0.18	0.18	98.96	556.5
49.82	1.81	13.88	11.83	0.19	7.28	10.89	2.72	0.19	0.11	98.71	562.2
50.24	1.72	14.07	11.79	0.27	7.31	10.85	2.74	0.20	0.12	99.30	585.2
49.81	1.78	14.12	11.84	0.21	7.16	11.01	2.80	0.18	0.07	98.97	586.7
49.87	1.79	14.08	11.79	0.31	7.32	10.88	2.69	0.20	0.09	99.01	592.6
49.74	1.76	13.87	11.95	0.15	7.21	10.87	2.71	0.19	0.11	98.56	614.6
49.84	1.75	13.99	11.89	0.17	7.21	10.98	2.75	0.16	0.19	98.94	616.7
50.07	1.83	13.98	11.84	0.29	7.16	10.94	2.73	0.20	0.14	99.19	623.0
49.83	1.75	14.05	11.87	0.18	7.23	10.80	2.72	0.18	0.21	98.81	644.1
49.88	1.76	13.97	11.88	0.32	7.20	10.89	2.71	0.14	0.17	98.92	646.9
49.68	1.83	14.08	11.86	0.14	7.24	10.91	2.72	0.19	0.21	98.86	653.4
49.77	1.81	13.90	11.88	0.20	7.25	11.00	2.73	0.18	0.11	98.82	673.6
50.05	1.77	14.04	11.97	0.27	7.09	10.88	2.75	0.21	0.08	99.12	677.0
49.96	1.84	14.01	11.95	0.23	7.22	10.96	2.72	0.22	0.21	99.31	683.9
49.91	1.71	13.97	12.03	0.25	7.19	11.01	2.77	0.20	0.12	99.15	703.0
49.85	1.86	13.99	12.03	0.13	7.09	11.04	2.81	0.16	0.18	99.14	707.0
50.08	1.77	14.00	11.98	0.17	7.08	10.96	2.72	0.22	0.14	99.12	714.2
50.00	1.80	13.94	12.00	0.23	7.05	11.09	2.80	0.19	0.11	99.21	732.5
49.74	1.77	14.00	11.97	0.24	7.11	11.01	2.74	0.21	0.11	98.90	737.2
50.26	1.79	14.12	12.03	0.23	7.08	10.96	2.71	0.20	0.16	99.53	744.7
50.20	1.82	13.99	11.94	0.24	7.16	10.93	2.68	0.19	0.22	99.38	762.0
49.71	1.83	14.08	11.97	0.19	7.02	11.12	2.74	0.16	0.06	98.85	767.3
50.05	1.77	13.98	12.03	0.17	7.20	10.92	2.71	0.16	0.19	99.17	775.1
49.98	1.83	13.94	12.01	0.22	7.22	11.09	2.69	0.17	0.08	99.23	791.4
49.78	1.75	13.90	12.01	0.15	7.06	11.07	2.75	0.16	0.08	98.72	797.4
49.94	1.85	14.06	11.91	0.15	6.99	11.11	2.66	0.16	0.16	99.00	805.5
49.89	1.81	14.00	11.99	0.27	7.04	10.99	2.71	0.17	0.11	98.96	820.8
49.93	1.80	14.10	11.99	0.21	7.04	11.01	2.73	0.16	0.11	99.07	827.5
49.89	1.85	14.09	12.09	0.18	7.09	11.04	2.76	0.18	0.10	99.26	835.9
49.75	1.83	13.91	12.15	0.26	7.04	11.06	2.69	0.21	0.11	99.01	850.3
49.78	1.81	14.04	12.12	0.20	7.07	11.11	2.70	0.23	0.13	99.18	857.6
50.03	1.83	14.04	11.98	0.20	7.10	11.04	2.62	0.21	0.18	99.23	866.4
49.93	1.85	14.02	12.02	0.18	7.05	10.94	2.74	0.16	0.11	98.99	879.7
50.07	1.80	14.11	11.93	0.22	7.07	11.06	2.74	0.19	0.11	99.30	887.7
49.83	1.80	13.93	11.92	0.20	7.14	11.12	2.71	0.20	0.03	98.89	896.7
49.75	1.90	13.98	12.02	0.21	7.00	11.19	2.69	0.20	0.21	99.14	909.2
49.65	1.79	13.94	12.08	0.20	6.98	11.16	2.70	0.18	0.10	98.77	917.8
49.79	1.85	13.97	12.03	0.21	7.06	11.12	2.73	0.16	0.23	99.14	927.2
49.84	1.88	14.01	12.05	0.21	7.12	10.98	2.67	0.20	0.08	99.02	938.7
49.83	1.84	14.02	11.93	0.23	7.06	11.05	2.68	0.20	0.15	98.99	948.0
49.79	1.77	13.93	12.10	0.29	7.03	11.16	2.68	0.16	0.09	99.00	957.6
49.69	1.88	14.01	12.03	0.20	7.10	11.16	2.72	0.19	0.13	99.10	968.2
49.96	1.83	14.07	12.04	0.28	7.15	11.06	2.71	0.20	0.06	99.35	978.0
49.54	1.78	14.04	11.95	0.25	7.04	11.17	2.68	0.16	0.10	98.70	988.0

49.91	1.84	14.02	11.94	0.20	7.00	11.08	2.75	0.15	0.20	99.07	997.6
49.70	1.71	13.98	12.01	0.24	7.07	11.11	2.66	0.18	0.13	98.80	1008.2
49.95	1.79	13.98	11.98	0.15	7.08	11.01	2.76	0.20	0.18	99.08	1018.4
49.68	1.81	14.00	12.08	0.19	6.98	11.11	2.62	0.20	0.16	98.82	1027.0
49.93	1.78	13.88	11.99	0.23	7.16	11.17	2.75	0.15	0.16	99.21	1038.3
49.89	1.79	13.95	11.80	0.21	6.96	11.01	2.70	0.19	0.16	98.66	1048.9
50.05	1.87	14.01	12.25	0.20	6.92	10.92	2.71	0.19	0.21	99.33	1056.5
49.89	1.81	14.11	12.06	0.25	7.02	11.10	2.66	0.16	0.16	99.20	1068.3
49.98	1.77	13.95	11.98	0.20	7.05	11.07	2.72	0.16	0.26	99.14	1079.2
49.87	1.82	14.03	11.95	0.20	7.04	11.04	2.70	0.15	0.20	98.98	1085.9
49.96	1.83	13.92	11.99	0.15	7.03	11.08	2.63	0.20	0.18	98.95	1098.5
49.87	1.84	14.03	11.98	0.21	7.08	10.94	2.73	0.22	0.13	99.01	1109.7
49.80	1.85	14.12	11.99	0.31	7.12	11.09	2.67	0.18	0.16	99.29	1115.4
49.80	1.82	14.01	11.97	0.22	7.04	11.05	2.70	0.21	0.10	98.92	1128.6
49.75	1.80	14.01	12.03	0.19	7.12	11.07	2.68	0.15	0.06	98.86	1140.1
49.71	1.93	14.06	11.96	0.11	7.06	11.16	2.72	0.16	0.19	99.06	1144.9
49.77	1.78	13.97	11.95	0.27	6.97	11.12	2.68	0.24	0.23	98.97	1158.7
49.99	1.83	13.94	11.98	0.17	6.98	11.16	2.67	0.21	0.18	99.08	1170.5
49.70	1.86	13.78	11.86	0.27	6.99	11.04	2.71	0.20	0.16	98.57	1174.3
49.64	1.75	13.85	11.93	0.21	7.07	11.07	2.75	0.16	0.15	98.57	1188.8
50.02	1.74	13.98	12.00	0.25	7.03	11.02	2.68	0.17	0.20	99.09	1200.9
49.73	1.86	13.85	12.09	0.22	6.96	11.14	2.64	0.21	0.21	98.89	1203.8
49.66	1.85	13.75	11.92	0.18	6.98	11.17	2.71	0.19	0.24	98.65	1218.9
49.70	1.82	14.02	11.91	0.16	7.04	11.01	2.73	0.20	0.16	98.75	1231.3
49.80	1.79	14.01	11.91	0.18	7.06	11.08	2.70	0.16	0.18	98.87	1233.2
49.78	1.76	14.06	12.04	0.29	7.01	11.06	2.67	0.19	0.12	98.99	1249.0
49.85	1.83	13.85	12.01	0.12	7.01	11.09	2.72	0.17	0.14	98.80	1261.7
49.70	1.80	13.87	11.95	0.27	7.00	11.09	2.78	0.18	0.18	98.80	1262.6
49.90	1.81	13.91	11.97	0.18	6.94	11.22	2.69	0.18	0.11	98.92	1279.1
49.99	1.83	13.89	12.03	0.23	7.03	11.17	2.67	0.14	0.20	99.18	1292.1
49.80	1.73	13.86	12.04	0.19	7.00	11.12	2.68	0.19	0.23	98.82	1292.2
49.86	1.79	14.00	11.93	0.20	6.98	11.13	2.62	0.20	0.11	98.81	1309.3
50.01	1.84	13.96	11.82	0.25	6.95	11.02	2.70	0.13	0.15	98.82	1321.6
49.95	1.80	13.94	11.87	0.28	7.02	10.90	2.73	0.21	0.03	98.74	1322.6
49.68	1.80	13.87	11.79	0.23	6.96	11.10	2.71	0.21	0.07	98.40	1339.3
49.95	1.79	14.09	12.05	0.09	6.97	11.20	2.63	0.21	0.20	99.17	1353.0
50.02	1.86	14.06	11.87	0.17	6.97	11.06	2.79	0.21	0.17	99.16	1383.5
49.96	1.82	14.03	11.84	0.22	6.94	11.07	2.75	0.17	0.15	98.95	1413.8

Exp 41

SiO2	TiO2	Al2O3	FeO	MnO	MgO	CaO	Na2O	K2O	P2O5	Total	d (um)
47.93	1.65	11.40	13.36	0.22	11.44	10.78	1.93	0.12	0.13	98.95	4.8
47.97	1.73	11.44	13.40	0.23	11.25	10.87	2.01	0.12	0.06	99.07	5.3
47.84	1.69	11.26	13.54	0.23	11.45	10.81	1.96	0.09	0.08	98.94	7.5
47.65	1.63	11.14	13.32	0.25	12.40	10.40	1.93	0.15	0.06	98.92	10.0
47.42	1.66	11.06	13.42	0.29	12.24	10.58	1.82	0.10	0.08	98.66	10.4
47.85	1.62	11.04	13.36	0.26	12.35	10.50	1.90	0.13	0.06	99.07	12.7
47.72	1.57	11.17	13.24	0.23	12.77	10.21	1.88	0.11	0.14	99.04	15.3
47.55	1.62	11.08	13.41	0.21	12.86	10.29	1.94	0.12	0.08	99.15	15.6
47.84	1.61	11.60	13.30	0.26	13.08	10.18	2.06	0.12	0.05	100.11	16.4
47.64	1.60	11.03	13.26	0.16	12.68	10.10	1.90	0.11	0.06	98.53	17.9
47.55	1.54	11.13	13.29	0.24	12.97	10.13	1.83	0.11	0.08	98.87	20.7
47.86	1.55	11.15	13.13	0.27	12.61	10.30	1.94	0.13	0.07	99.01	23.1
48.14	1.53	11.63	13.14	0.25	12.90	10.11	2.05	0.13	0.09	99.96	23.2
47.85	1.59	11.21	13.10	0.17	12.68	10.15	2.05	0.13	0.07	99.00	25.8
47.65	1.61	11.21	13.21	0.15	12.77	10.14	1.94	0.12	0.05	98.85	25.9
47.69	1.58	11.62	13.13	0.17	12.64	10.26	2.05	0.13	0.14	99.41	26.4
47.79	1.63	11.29	13.05	0.18	12.76	10.15	2.10	0.11	0.06	99.11	31.0
47.80	1.59	11.16	13.18	0.25	12.66	10.18	1.99	0.13	0.08	99.01	31.0
47.84	1.54	11.72	13.04	0.24	12.43	10.02	2.07	0.15	0.18	99.22	33.2
48.28	1.61	11.74	12.92	0.29	12.61	10.29	2.07	0.17	0.12	100.09	34.4
47.93	1.57	11.37	12.76	0.23	12.58	10.16	1.98	0.17	0.17	98.91	36.3
47.73	1.56	11.65	13.00	0.13	12.19	10.07	2.12	0.12	0.05	98.62	36.4
47.78	1.55	11.85	12.74	0.21	12.31	10.17	2.05	0.13	0.15	98.93	40.1
47.85	1.62	11.76	12.87	0.22	12.27	10.33	2.15	0.15	0.02	99.24	43.1
47.91	1.58	11.68	12.60	0.34	12.19	10.18	2.04	0.09	0.08	98.67	45.7
47.76	1.60	11.71	12.89	0.22	12.24	10.18	2.13	0.15	0.08	98.95	46.3
48.11	1.59	11.95	12.77	0.15	11.93	10.18	2.07	0.13	0.08	98.96	51.4
47.72	1.59	11.91	12.90	0.26	12.11	10.24	2.12	0.16	0.11	99.10	53.1
47.97	1.60	11.95	12.87	0.18	11.90	10.30	2.19	0.13	0.08	99.15	56.3
48.38	1.57	11.92	12.78	0.29	11.67	10.11	2.19	0.11	0.09	99.11	63.1
48.01	1.62	11.95	12.80	0.23	11.77	10.26	2.15	0.12	0.05	98.96	66.3
48.45	1.64	12.25	12.84	0.29	12.09	10.24	2.21	0.20	0.11	100.31	70.1
48.19	1.62	12.33	12.64	0.18	11.50	10.21	2.26	0.19	0.17	99.28	73.0
48.25	1.59	12.20	12.70	0.18	11.64	10.19	2.23	0.18	0.14	99.30	76.3
48.11	1.53	12.30	12.60	0.18	11.44	10.28	2.15	0.11	0.07	98.77	80.1
48.58	1.60	12.21	12.60	0.15	11.37	10.32	2.19	0.12	0.14	99.28	83.0
48.26	1.56	12.37	12.60	0.28	11.37	10.18	2.20	0.14	0.10	99.06	86.3
48.30	1.61	12.36	12.44	0.19	11.24	10.30	2.27	0.10	0.18	98.98	90.0
48.63	1.60	12.37	12.48	0.17	11.18	10.31	2.29	0.15	0.10	99.28	92.9
48.30	1.59	12.44	12.57	0.22	11.10	10.37	2.24	0.11	0.20	99.13	96.3
48.37	1.64	12.55	12.25	0.16	11.17	10.27	2.17	0.15	0.10	98.82	100.0
48.47	1.63	12.59	12.32	0.16	10.90	10.33	2.25	0.18	0.11	98.93	102.9
48.51	1.55	12.50	12.19	0.14	10.87	10.31	2.29	0.15	0.12	98.62	106.2
48.65	1.62	12.73	12.26	0.23	10.84	10.35	2.29	0.15	0.11	99.22	109.9
48.56	1.59	12.67	12.21	0.22	10.69	10.33	2.28	0.17	0.07	98.77	112.9
48.52	1.61	12.67	12.15	0.15	10.64	10.37	2.41	0.14	0.19	98.84	116.2
48.58	1.61	12.83	12.05	0.16	10.52	10.46	2.29	0.17	0.06	98.72	119.9

48.67	1.66	12.81	12.11	0.28	10.54	10.30	2.35	0.11	0.07	98.89	122.8
48.58	1.52	12.89	12.20	0.21	10.44	10.37	2.28	0.16	0.05	98.72	126.2
48.65	1.63	12.88	12.08	0.23	10.42	10.35	2.35	0.15	0.15	98.88	129.9
48.86	1.59	12.89	12.14	0.17	10.29	10.33	2.42	0.16	0.11	98.96	132.8
48.89	1.63	12.90	12.15	0.21	10.37	10.16	2.39	0.16	0.08	98.93	136.2
48.92	1.62	13.08	12.01	0.31	10.18	10.44	2.36	0.20	0.02	99.14	139.8
49.16	1.59	12.98	12.16	0.19	10.26	10.34	2.41	0.17	0.13	99.40	142.8
48.72	1.59	13.03	11.98	0.16	10.07	10.33	2.42	0.16	0.08	98.53	146.2
48.99	1.60	13.31	12.11	0.16	9.99	10.39	2.36	0.15	0.15	99.20	149.8
48.98	1.65	13.28	11.92	0.14	9.82	10.48	2.40	0.19	0.11	98.97	152.7
48.83	1.63	13.23	12.10	0.19	9.89	10.48	2.42	0.18	0.05	99.00	156.1
49.18	1.61	13.32	11.87	0.26	9.79	10.44	2.42	0.17	0.12	99.15	159.8
49.16	1.67	13.28	12.08	0.26	9.85	10.42	2.41	0.19	0.05	99.37	162.7
49.09	1.63	13.21	11.91	0.15	9.54	10.40	2.54	0.20	0.12	98.80	166.1
49.04	1.66	13.30	11.83	0.23	9.63	10.49	2.50	0.20	0.05	98.92	169.7
49.30	1.64	13.34	12.00	0.18	9.71	10.54	2.45	0.19	0.08	99.42	172.7
49.16	1.54	13.39	12.04	0.16	9.68	10.45	2.49	0.21	0.13	99.24	176.1
49.21	1.68	13.49	11.77	0.20	9.36	10.47	2.49	0.19	0.02	98.88	179.7
49.26	1.67	13.26	11.75	0.23	9.36	10.52	2.52	0.18	0.20	98.94	182.6
49.09	1.64	13.57	11.96	0.15	9.40	10.43	2.51	0.17	0.09	99.01	186.1
49.32	1.68	13.67	11.74	0.15	9.19	10.49	2.45	0.19	0.05	98.92	189.6
49.38	1.63	13.47	11.83	0.25	9.20	10.41	2.53	0.16	0.19	99.05	192.6
49.18	1.66	13.58	11.85	0.15	9.29	10.49	2.55	0.19	0.12	99.06	196.1
49.57	1.66	13.65	11.48	0.25	9.01	10.40	2.53	0.19	0.11	98.84	199.6
49.54	1.68	13.59	11.66	0.22	9.05	10.51	2.50	0.21	0.10	99.05	202.5
49.30	1.70	13.61	11.76	0.26	9.01	10.39	2.61	0.25	0.08	98.97	206.1
49.49	1.69	13.65	11.73	0.15	8.87	10.42	2.56	0.19	0.08	98.81	209.6
49.53	1.69	13.68	11.74	0.23	8.93	10.65	2.64	0.20	0.05	99.34	212.5
49.56	1.69	13.66	11.62	0.12	8.98	10.50	2.57	0.22	0.11	99.04	216.0
49.44	1.63	13.70	11.60	0.30	8.78	10.60	2.56	0.21	0.15	98.97	219.5
49.73	1.77	13.78	11.67	0.17	8.80	10.33	2.68	0.19	0.11	99.22	222.5
49.39	1.67	13.81	11.69	0.28	8.65	10.60	2.52	0.21	0.06	98.88	229.5
49.43	1.71	13.89	11.35	0.27	8.49	10.54	2.71	0.20	0.15	98.73	239.4
49.60	1.77	13.75	11.58	0.18	8.42	10.53	2.68	0.22	0.05	98.78	247.7
49.65	1.69	13.92	11.66	0.34	8.36	10.52	2.65	0.22	0.11	99.11	249.4
49.70	1.67	13.75	11.59	0.15	8.44	10.68	2.64	0.20	0.15	98.98	253.9
49.51	1.67	14.03	11.62	0.27	8.27	10.55	2.65	0.21	0.09	98.87	259.4
49.42	1.78	14.12	11.53	0.16	8.13	10.81	2.64	0.18	0.09	98.85	269.3
49.53	1.72	14.04	11.64	0.20	8.06	10.67	2.71	0.23	0.08	98.88	279.3
49.53	1.77	13.98	11.51	0.14	8.10	10.63	2.69	0.21	0.12	98.68	285.3
50.03	1.79	14.12	11.61	0.27	7.81	10.70	2.73	0.19	0.18	99.40	298.6
49.82	1.75	14.14	11.70	0.23	7.80	10.79	2.81	0.17	0.05	99.25	310.9
49.67	1.79	13.98	11.68	0.20	7.84	10.76	2.81	0.17	0.19	99.07	316.7
49.64	1.78	14.31	11.56	0.15	7.60	10.88	2.71	0.18	0.22	99.02	327.9
49.80	1.78	14.04	11.89	0.22	7.58	10.65	2.72	0.23	0.19	99.10	342.6
49.86	1.78	14.02	11.80	0.23	7.58	10.79	2.63	0.19	0.05	98.93	348.1
49.90	1.82	14.17	11.78	0.13	7.47	10.91	2.63	0.20	0.08	99.11	357.2
49.71	1.73	14.09	11.72	0.32	7.34	10.83	2.73	0.19	0.10	98.75	374.2
49.72	1.82	14.08	11.92	0.21	7.46	10.86	2.68	0.20	0.15	99.08	379.5

49.73	1.81	14.01	11.86	0.31	7.25	10.91	2.71	0.22	0.15	98.97	386.5
49.78	1.88	14.12	11.77	0.31	7.25	10.92	2.70	0.27	0.14	99.12	405.8
49.69	1.79	13.97	11.96	0.20	7.21	10.66	2.69	0.18	0.11	98.47	410.9
49.84	1.91	14.18	11.91	0.22	7.25	10.97	2.64	0.22	0.12	99.24	415.8
49.65	1.81	14.17	11.94	0.21	7.16	11.03	2.67	0.17	0.11	98.91	437.5
49.74	1.78	14.08	11.79	0.22	7.11	11.05	2.71	0.18	0.17	98.82	442.3
49.82	1.89	14.22	12.04	0.27	7.19	11.01	2.64	0.19	0.13	99.40	445.1
49.71	1.86	14.06	12.05	0.23	7.06	10.96	2.76	0.17	0.12	98.97	469.1
49.88	1.80	14.13	11.95	0.17	7.02	11.04	2.82	0.17	0.19	99.14	473.7
49.60	1.81	14.25	11.94	0.22	7.07	10.93	2.71	0.14	0.12	98.78	474.5
49.63	1.82	14.15	12.00	0.20	7.10	11.19	2.80	0.16	0.10	99.16	500.7
49.64	1.81	14.11	12.01	0.22	6.98	11.13	2.67	0.17	0.12	98.86	503.8
49.66	1.74	14.00	12.12	0.22	6.97	11.14	2.74	0.17	0.19	98.94	505.1
49.51	1.82	14.02	12.08	0.08	6.95	11.09	2.71	0.20	0.09	98.56	532.4
49.82	1.86	14.07	12.05	0.17	6.86	11.07	2.73	0.16	0.15	98.94	533.1
49.80	1.86	14.13	12.05	0.21	6.88	11.10	2.69	0.21	0.06	98.98	536.5
49.77	1.83	14.03	12.16	0.16	7.00	11.01	2.73	0.19	0.15	99.02	562.4
49.55	1.81	14.15	12.24	0.20	6.90	11.17	2.73	0.21	0.11	99.07	564.0
49.55	1.79	14.01	11.99	0.26	6.95	11.13	2.61	0.18	0.12	98.58	567.9
49.72	1.81	14.05	12.16	0.23	6.93	11.11	2.69	0.13	0.16	98.99	591.7
49.81	1.81	14.06	12.23	0.21	6.84	11.18	2.70	0.21	0.07	99.13	595.6
49.94	1.84	14.13	12.07	0.16	6.96	11.13	2.67	0.20	0.08	99.17	599.3
49.90	1.85	14.13	12.21	0.22	6.92	11.12	2.68	0.23	0.08	99.34	621.0
49.53	1.85	14.24	12.14	0.22	6.88	11.10	2.69	0.18	0.12	98.93	627.3
49.57	1.86	14.21	12.10	0.21	6.91	11.20	2.69	0.17	0.06	98.97	630.7
49.68	1.81	14.13	12.35	0.18	6.80	11.01	2.72	0.17	0.15	99.01	650.3
49.78	1.87	14.08	12.06	0.15	6.89	11.19	2.67	0.21	0.15	99.05	658.9
49.70	1.87	14.01	12.11	0.21	6.83	11.18	2.65	0.20	0.07	98.82	662.1
49.75	1.75	14.02	12.24	0.30	6.92	11.14	2.65	0.18	0.11	99.05	679.6
49.90	1.84	14.02	12.04	0.23	6.85	11.28	2.68	0.19	0.10	99.13	690.5
49.55	1.89	13.94	12.22	0.30	6.89	11.22	2.69	0.17	0.17	99.04	693.5
49.51	1.83	14.04	12.28	0.27	6.91	11.21	2.69	0.15	0.02	98.90	708.9
49.90	1.82	14.25	12.16	0.16	6.87	11.12	2.77	0.19	0.03	99.28	722.2
49.57	1.85	14.16	12.31	0.16	6.80	11.10	2.70	0.19	0.09	98.90	724.9
49.84	1.86	14.06	12.03	0.18	6.82	11.10	2.72	0.16	0.08	98.85	738.2
49.70	1.81	14.17	12.29	0.21	6.84	11.14	2.71	0.15	0.06	99.07	753.8
49.57	1.84	13.95	12.27	0.25	6.92	11.12	2.73	0.19	0.21	99.05	756.3
49.73	1.80	14.17	12.24	0.21	6.85	11.23	2.67	0.18	0.13	99.19	767.5
49.22	1.82	14.00	12.32	0.15	6.83	11.24	2.73	0.16	0.18	98.65	785.4
49.91	1.83	14.00	12.39	0.20	6.82	11.22	2.73	0.19	0.09	99.39	787.7
49.61	1.83	13.97	12.13	0.20	6.87	11.26	2.60	0.20	0.08	98.75	796.8
49.80	1.87	14.11	12.14	0.23	6.91	11.15	2.63	0.16	0.07	99.05	817.1
49.75	1.84	14.00	12.16	0.24	6.88	11.27	2.66	0.19	0.12	99.10	819.2
49.87	1.84	14.14	12.23	0.13	6.73	11.19	2.66	0.24	0.21	99.24	826.1
49.79	1.80	14.17	12.37	0.13	6.71	11.29	2.73	0.22	0.05	99.26	848.7
49.75	1.82	14.06	12.41	0.20	6.90	11.35	2.68	0.22	0.17	99.56	850.6
49.74	1.80	14.15	12.18	0.23	6.87	11.18	2.66	0.14	0.14	99.07	855.4
49.35	1.81	14.28	12.23	0.23	6.87	11.16	2.64	0.19	0.12	98.85	880.3
49.86	1.89	14.12	12.18	0.18	6.88	11.25	2.68	0.14	0.10	99.28	882.0

49.65	1.83	14.11	12.25	0.18	6.78	11.08	2.62	0.19	0.13	98.83	884.7
49.79	1.89	13.97	12.27	0.26	6.85	11.24	2.65	0.17	0.12	99.22	912.0
49.67	1.81	14.03	12.13	0.22	6.78	11.05	2.60	0.17	0.09	98.55	913.4
49.54	1.86	14.06	12.24	0.23	6.82	11.19	2.62	0.17	0.15	98.88	914.0
49.64	1.79	13.92	12.31	0.18	6.80	11.25	2.64	0.16	0.06	98.75	943.3
49.87	1.82	14.05	12.28	0.14	6.89	11.25	2.65	0.20	0.17	99.32	943.6
49.81	1.76	13.93	12.26	0.18	6.89	11.25	2.64	0.19	0.13	99.04	944.8
49.81	1.83	14.01	12.13	0.21	6.69	11.13	2.72	0.20	0.18	98.90	972.6
49.73	1.84	13.98	12.28	0.27	6.79	11.25	2.61	0.21	0.15	99.12	975.2
49.67	1.75	13.95	12.19	0.23	6.72	11.15	2.64	0.21	0.17	98.69	976.2
49.68	1.86	13.99	12.21	0.22	6.78	11.28	2.60	0.15	0.05	98.80	1001.9
49.74	1.86	14.21	12.25	0.24	6.90	11.13	2.63	0.20	0.12	99.27	1006.9
49.68	1.80	13.89	12.22	0.21	6.83	11.35	2.58	0.19	0.11	98.86	1007.6
49.64	1.80	14.01	12.28	0.25	6.79	11.27	2.63	0.22	0.15	99.05	1031.2
49.65	1.85	13.91	12.26	0.24	6.79	11.20	2.68	0.19	0.17	98.94	1038.5
49.63	1.89	13.92	12.33	0.20	6.83	11.09	2.64	0.18	0.24	98.95	1039.0
49.82	1.86	14.01	12.20	0.10	6.71	11.22	2.61	0.20	0.08	98.79	1060.5
49.68	1.80	14.07	12.04	0.21	6.77	11.17	2.60	0.17	0.14	98.64	1070.1
49.77	1.89	14.11	12.32	0.24	6.83	11.22	2.63	0.16	0.08	99.26	1070.4
50.01	1.83	14.06	12.32	0.25	6.77	11.14	2.62	0.19	0.05	99.24	1089.8
49.78	1.88	14.09	12.22	0.17	6.78	11.29	2.72	0.19	0.12	99.25	1101.8
49.80	1.85	14.06	12.22	0.22	6.82	11.17	2.68	0.18	0.06	99.07	1101.8
50.00	1.79	14.04	12.19	0.21	6.75	11.12	2.62	0.18	0.14	99.03	1133.2
49.87	1.84	14.15	12.05	0.21	6.72	11.32	2.61	0.23	0.08	99.07	1133.4
49.62	1.89	14.00	12.09	0.18	6.87	10.92	2.71	0.14	0.17	98.59	1244.2
49.31	1.75	14.24	12.40	0.18	6.89	11.10	2.71	0.21	0.15	98.95	1255.0
49.65	1.89	14.01	12.41	0.28	6.83	11.15	2.65	0.22	0.22	99.30	1262.1
49.59	1.86	14.04	12.07	0.24	6.87	11.09	2.75	0.18	0.12	98.81	1284.3
49.70	1.85	14.05	12.11	0.17	6.81	11.21	2.59	0.23	0.09	98.81	1296.1
49.73	1.82	14.09	12.25	0.19	6.81	11.05	2.55	0.21	0.13	98.82	1300.8
50.09	1.85	14.12	12.11	0.26	6.88	11.19	2.62	0.15	0.19	99.46	1324.4
49.90	1.86	14.01	12.30	0.23	6.78	11.33	2.66	0.23	0.10	99.39	1337.2
49.65	1.79	14.09	12.13	0.22	6.79	11.06	2.64	0.20	0.13	98.69	1339.6
49.86	1.85	14.06	12.13	0.24	6.91	11.14	2.63	0.19	0.17	99.18	1364.5
49.89	1.79	14.03	12.17	0.19	6.82	11.23	2.66	0.16	0.18	99.13	1378.3
49.97	1.81	14.20	12.03	0.18	6.78	11.19	2.64	0.21	0.19	99.21	1378.4
50.00	1.82	14.03	11.97	0.22	6.78	11.23	2.66	0.18	0.17	99.05	1404.6
49.89	1.82	14.19	12.04	0.22	6.79	11.19	2.65	0.15	0.11	99.06	1417.2
49.70	1.85	14.21	12.20	0.29	6.85	11.23	2.64	0.19	0.15	99.30	1419.4
49.96	1.89	14.17	12.06	0.21	6.84	11.22	2.67	0.15	0.14	99.30	1444.7
49.74	1.86	13.95	12.04	0.22	6.82	11.24	2.58	0.21	0.13	98.80	1460.5
50.13	1.87	14.11	11.93	0.21	6.86	11.08	2.65	0.17	0.02	99.03	1484.9
49.99	1.82	13.96	11.94	0.20	6.80	11.08	2.64	0.18	0.10	98.72	1525.0
50.27	1.89	13.87	12.03	0.22	6.76	11.15	2.63	0.17	0.13	99.11	1565.1

Exp 43

SiO2	TiO2	Al2O3	FeO	MnO	MgO	CaO	Na2O	K2O	P2O5	Total	d (um)
47.46	1.67	10.93	12.49	0.25	14.28	10.13	1.98	0.07	0.04	99.28	4.9
47.52	1.58	10.61	12.39	0.27	14.56	10.28	1.94	0.11	0.07	99.32	5.4
47.02	1.55	9.85	13.30	0.22	16.60	9.19	1.87	0.11	0.07	99.78	6.5
47.21	1.49	9.81	13.38	0.22	15.60	9.84	1.76	0.06	0.18	99.55	9.5
46.91	1.54	9.43	13.21	0.16	16.16	9.91	1.70	0.08	0.12	99.21	10.3
46.44	1.41	8.87	13.37	0.24	19.09	8.66	1.67	0.09	0.00	99.83	10.5
47.08	1.37	8.65	13.70	0.27	16.90	9.86	1.42	0.04	0.11	99.40	11.7
46.68	1.43	8.82	13.47	0.24	17.99	9.40	1.58	0.07	0.12	99.80	15.6
46.77	1.37	8.71	13.21	0.16	18.69	9.17	1.53	0.05	0.03	99.69	15.7
46.79	1.29	8.60	13.63	0.28	18.51	8.89	1.33	0.07	0.08	99.46	17.0
46.83	1.28	8.66	13.47	0.32	19.26	8.81	1.42	0.08	0.15	100.27	20.7
46.40	1.34	8.46	13.72	0.22	18.42	9.05	1.40	0.07	0.05	99.13	21.0
46.31	1.26	8.56	13.19	0.19	19.17	8.56	1.51	0.05	0.02	98.82	22.2
46.68	1.29	8.70	13.14	0.19	19.78	8.61	1.49	0.08	-0.01	99.94	25.9
46.23	1.33	8.71	13.23	0.27	19.02	8.66	1.44	0.13	0.03	99.04	26.4
46.38	1.28	8.75	13.63	0.25	19.39	8.87	1.56	0.09	0.12	100.30	26.5
46.26	1.26	8.55	13.26	0.24	19.29	8.56	1.49	0.06	0.12	99.10	27.5
46.49	1.34	8.66	13.05	0.17	19.50	8.50	1.48	0.06	0.05	99.30	31.0
46.14	1.36	8.67	13.24	0.24	19.35	8.53	1.52	0.08	0.06	99.19	31.8
46.38	1.27	8.67	13.13	0.18	19.53	8.66	1.52	0.14	0.06	99.55	32.7
46.28	1.31	8.80	13.03	0.16	19.56	8.67	1.57	0.08	0.05	99.53	36.0
46.39	1.40	8.82	13.12	0.20	19.17	8.55	1.52	0.05	0.05	99.26	37.2
46.34	1.30	8.63	12.96	0.23	19.37	8.63	1.53	0.07	0.06	99.13	38.0
46.40	1.34	8.81	13.08	0.21	19.28	8.63	1.50	0.11	0.07	99.42	41.2
46.48	1.33	8.85	13.13	0.26	19.22	8.60	1.55	0.07	0.08	99.57	42.6
46.52	1.29	8.81	13.08	0.21	19.19	8.56	1.54	0.07	0.05	99.33	43.2
46.77	1.22	8.83	13.17	0.22	19.25	8.51	1.47	0.08	0.02	99.53	43.4
46.29	1.25	8.74	12.79	0.32	19.20	8.69	1.55	0.11	0.07	99.01	46.3
46.29	1.35	8.88	13.11	0.23	18.89	8.60	1.59	0.09	0.07	99.09	47.9
46.49	1.32	8.97	12.93	0.27	18.90	8.62	1.53	0.07	0.15	99.25	48.5
46.31	1.33	8.90	12.93	0.19	19.15	8.73	1.63	0.08	0.05	99.29	51.4
46.73	1.30	9.05	12.88	0.17	18.93	8.69	1.55	0.09	0.08	99.47	53.7
46.68	1.33	8.97	12.78	0.24	19.06	8.72	1.66	0.12	0.11	99.66	56.5
46.66	1.38	9.10	12.87	0.19	18.74	8.68	1.57	0.05	0.07	99.31	58.7
46.95	1.34	9.03	12.86	0.17	18.67	8.69	1.59	0.06	0.04	99.40	59.0
47.03	1.27	9.19	12.93	0.28	19.00	8.54	1.63	0.05	0.10	100.01	60.4
46.60	1.31	9.05	12.69	0.21	18.96	8.67	1.56	0.08	0.08	99.23	61.7
46.73	1.37	9.23	12.79	0.24	18.52	8.64	1.53	0.10	0.18	99.32	64.1
46.64	1.33	9.19	12.69	0.18	18.69	8.58	1.60	0.08	0.07	99.05	66.7
46.34	1.41	9.68	12.75	0.28	18.09	8.96	1.66	0.10	0.08	99.35	74.1
46.34	1.32	9.70	12.36	0.20	17.94	8.82	1.76	0.08	0.05	98.56	78.8
46.07	1.40	9.69	12.73	0.12	17.88	8.79	1.67	0.12	0.11	98.57	80.8
46.47	1.39	9.89	12.53	0.21	17.57	8.98	1.77	0.12	0.03	98.96	89.5
46.71	1.37	10.05	12.29	0.11	17.47	8.91	1.82	0.09	0.12	98.94	94.3
46.31	1.41	9.94	12.55	0.21	17.60	9.00	1.71	0.12	0.11	98.94	95.9
46.70	1.37	10.23	12.43	0.11	17.25	9.10	1.77	0.09	0.11	99.16	104.8
47.24	1.33	10.26	12.16	0.25	17.01	8.91	1.88	0.13	0.03	99.21	109.8

46.72	1.42	10.24	12.55	0.26	17.01	9.01	1.84	0.12	0.14	99.30	111.1
46.75	1.44	10.58	12.39	0.25	16.85	9.20	1.96	0.11	0.13	99.65	120.2
47.05	1.38	10.61	12.09	0.24	16.53	9.16	1.91	0.14	0.18	99.28	125.3
46.74	1.43	10.58	12.48	0.27	16.68	9.16	1.92	0.11	0.02	99.38	126.3
47.24	1.40	10.76	12.33	0.27	16.42	9.09	1.90	0.14	0.10	99.63	135.5
47.35	1.35	11.00	11.97	0.19	15.93	9.22	1.96	0.11	0.09	99.15	140.7
47.16	1.43	10.66	12.10	0.21	16.13	9.17	1.91	0.10	0.07	98.94	141.5
47.27	1.50	11.02	12.24	0.14	15.92	9.38	1.94	0.09	0.09	99.59	150.9
47.45	1.41	11.07	11.83	0.16	15.36	9.48	1.96	0.11	0.17	99.00	156.2
46.96	1.38	10.87	12.05	0.15	15.75	9.36	2.01	0.12	0.08	98.73	156.6
47.34	1.52	11.21	12.00	0.20	15.45	9.37	2.01	0.14	0.12	99.35	166.2
47.68	1.41	11.58	11.75	0.20	14.97	9.35	2.02	0.10	0.07	99.12	171.7
47.24	1.45	11.19	11.92	0.20	15.26	9.30	1.94	0.12	0.08	98.68	171.8
47.37	1.47	11.47	11.79	0.26	15.05	9.53	2.06	0.16	0.08	99.24	181.6
47.45	1.48	11.41	11.84	0.07	14.61	9.34	1.98	0.13	0.02	98.32	187.0
47.87	1.43	11.62	11.66	0.24	14.53	9.46	2.15	0.16	0.18	99.30	187.1
47.64	1.49	11.64	11.91	0.25	14.39	9.55	2.12	0.14	0.11	99.21	196.9
47.62	1.45	11.74	11.71	0.17	14.34	9.53	2.13	0.11	0.09	98.90	202.2
47.91	1.47	12.03	11.59	0.14	14.00	9.67	2.21	0.13	0.17	99.32	202.6
47.55	1.53	11.96	11.69	0.13	13.96	9.50	2.14	0.14	0.07	98.64	212.3
47.93	1.45	11.94	11.53	0.16	13.93	9.54	2.04	0.13	0.09	98.74	217.3
48.24	1.51	12.16	11.62	0.21	13.51	9.61	2.28	0.15	0.11	99.39	218.1
48.01	1.54	12.20	11.67	0.25	13.52	9.52	2.14	0.14	0.07	99.06	227.6
48.13	1.52	12.12	11.61	0.23	13.40	9.59	2.26	0.17	0.13	99.15	232.5
48.44	1.54	12.33	11.39	0.23	13.00	9.61	2.29	0.18	0.09	99.09	233.6
48.19	1.54	12.41	11.64	0.21	12.94	9.77	2.33	0.16	0.11	99.27	243.0
48.47	1.51	12.48	11.32	0.14	12.86	9.65	2.32	0.18	0.10	99.04	247.7
48.61	1.48	12.76	11.38	0.18	12.47	9.71	2.33	0.13	0.09	99.13	249.0
48.47	1.52	12.63	11.43	0.26	12.60	9.72	2.34	0.18	0.11	99.25	258.3
48.05	1.46	12.47	11.43	0.15	12.49	9.81	2.43	0.15	0.08	98.51	262.9
48.64	1.56	12.67	11.31	0.20	12.13	9.87	2.37	0.17	0.07	98.99	264.5
48.42	1.54	12.77	11.28	0.18	12.09	9.77	2.36	0.15	0.15	98.73	273.7
48.48	1.52	12.81	11.29	0.20	12.14	9.75	2.39	0.15	0.14	98.86	278.0
48.65	1.57	12.99	11.24	0.27	11.85	9.91	2.48	0.14	0.13	99.24	280.0
48.59	1.62	12.88	11.26	0.10	11.66	9.97	2.37	0.19	0.16	98.80	289.0
48.54	1.55	13.06	11.25	0.14	11.60	9.80	2.42	0.18	0.08	98.61	293.2
49.01	1.61	13.14	11.14	0.15	11.39	9.80	2.48	0.16	0.10	98.97	295.4
48.73	1.67	13.18	11.24	0.22	11.16	9.94	2.51	0.17	0.13	98.95	304.4
49.01	1.52	13.02	11.26	0.14	11.30	9.87	2.49	0.15	0.12	98.88	308.4
49.05	1.59	13.28	11.14	0.24	10.90	10.00	2.58	0.16	0.19	99.11	310.9
48.99	1.62	13.28	11.11	0.20	10.90	10.07	2.55	0.19	0.15	99.05	319.7
48.94	1.58	13.39	11.05	0.17	10.89	9.95	2.63	0.19	0.06	98.85	323.6
49.08	1.66	13.55	10.96	0.16	10.48	10.01	2.64	0.19	0.09	98.82	326.4
49.00	1.70	13.49	11.16	0.19	10.50	9.98	2.65	0.17	0.06	98.91	335.1
49.41	1.59	13.27	11.11	0.23	10.50	9.97	2.58	0.17	0.10	98.93	338.7
49.16	1.65	13.55	10.90	0.21	10.10	10.02	2.56	0.22	0.15	98.49	341.9
49.48	1.69	13.64	11.11	0.24	10.19	10.27	2.64	0.18	0.11	99.56	350.4
49.23	1.64	13.51	11.05	0.15	10.08	10.11	2.63	0.21	0.15	98.75	353.9
49.68	1.71	13.69	10.96	0.18	10.05	10.23	2.75	0.17	0.18	99.59	357.3

49.18	1.69	13.60	11.09	0.28	9.71	10.25	2.75	0.22	0.18	98.95	365.8
49.43	1.63	13.59	11.00	0.29	9.81	10.19	2.65	0.21	0.08	98.89	369.1
49.75	1.72	13.70	11.07	0.20	9.54	10.30	2.74	0.20	0.15	99.37	372.8
49.41	1.71	13.66	11.01	0.13	9.45	10.27	2.66	0.20	0.11	98.61	381.1
49.55	1.69	13.87	11.12	0.17	9.62	10.17	2.65	0.21	0.06	99.10	384.3
49.33	1.79	13.91	11.01	0.17	9.30	10.41	2.74	0.23	0.15	99.04	388.3
49.63	1.74	13.71	11.01	0.16	9.24	10.35	2.71	0.19	0.04	98.78	396.5
49.44	1.71	13.69	10.92	0.17	9.25	10.33	2.76	0.17	0.00	98.45	399.4
49.81	1.81	13.91	11.03	0.09	8.99	10.39	2.81	0.21	0.14	99.16	403.7
49.70	1.74	13.93	11.13	0.27	9.01	10.32	2.65	0.19	0.13	99.06	411.8
49.98	1.72	13.80	11.18	0.19	9.08	10.32	2.68	0.22	0.08	99.25	414.6
49.84	1.79	13.91	11.20	0.26	8.66	10.59	2.67	0.21	0.14	99.28	419.2
50.50	1.75	14.06	11.13	0.20	8.57	10.44	2.74	0.18	0.09	99.65	434.7
49.54	1.74	13.97	11.26	0.23	8.45	10.62	2.80	0.21	0.13	98.95	437.4
49.44	1.75	14.11	11.06	0.17	8.40	10.60	2.78	0.22	0.15	98.67	439.8
49.52	1.72	13.99	11.18	0.24	8.23	10.51	2.83	0.22	0.18	98.63	460.4
49.51	1.73	14.01	11.40	0.23	8.07	10.50	2.79	0.18	0.13	98.54	469.8
49.68	1.78	14.10	11.25	0.18	8.17	10.62	2.79	0.21	0.14	98.91	471.6
49.41	1.76	14.14	11.40	0.17	7.96	10.70	2.81	0.21	0.10	98.66	492.3
49.84	1.73	14.10	11.51	0.29	7.85	10.70	2.83	0.18	0.10	99.13	502.1
49.92	1.77	14.11	11.42	0.13	7.87	10.72	2.78	0.26	0.09	99.05	503.3
49.86	1.79	14.20	11.57	0.24	7.75	10.74	2.77	0.19	0.14	99.26	524.1
49.55	1.79	14.15	11.73	0.18	7.65	10.84	2.81	0.21	0.13	99.05	534.4
49.83	1.81	14.06	11.57	0.21	7.70	10.76	2.65	0.21	0.15	98.95	535.1
49.87	1.76	14.11	11.77	0.19	7.53	10.91	2.77	0.21	0.11	99.20	556.0
49.46	1.75	14.16	11.84	0.15	7.56	10.89	2.76	0.19	0.08	98.84	566.8
49.75	1.82	13.99	11.52	0.19	7.63	10.91	2.72	0.19	0.14	98.86	566.9
49.63	1.77	14.04	11.83	0.25	7.33	10.90	2.82	0.17	0.11	98.84	587.8
49.10	1.80	14.09	11.73	0.23	7.44	10.91	2.68	0.20	0.17	98.35	598.7
49.48	1.72	14.01	11.77	0.31	7.31	10.93	2.79	0.23	0.11	98.66	599.1
49.91	1.78	14.17	12.00	0.20	7.36	11.23	2.73	0.18	0.15	99.73	617.4
49.45	1.77	14.03	12.00	0.18	7.31	11.01	2.72	0.19	0.05	98.73	619.6
49.35	1.81	13.97	11.72	0.17	7.31	10.90	2.69	0.21	0.08	98.20	630.4
49.42	1.84	14.10	12.05	0.22	7.32	11.00	2.76	0.17	0.11	98.98	631.4
49.66	1.74	14.15	11.92	0.17	7.28	10.99	2.64	0.18	0.11	98.85	651.5
49.63	1.78	14.23	12.08	0.16	7.27	11.19	2.70	0.12	0.14	99.28	652.4
49.16	1.75	13.95	12.04	0.17	7.26	11.11	2.83	0.17	0.10	98.53	653.5
49.20	1.80	13.91	11.78	0.21	7.34	11.00	2.74	0.14	0.14	98.27	662.2
49.28	1.81	13.87	12.20	0.16	7.24	11.05	2.75	0.20	0.21	98.77	663.8
49.37	1.74	14.08	12.09	0.23	7.16	11.22	2.77	0.20	0.14	99.00	679.2
49.62	1.78	14.06	12.09	0.17	7.19	11.08	2.75	0.17	0.17	99.07	683.3
49.95	1.71	14.03	11.71	0.16	7.22	11.05	2.71	0.18	0.11	98.81	694.0
49.66	1.76	13.95	12.17	0.19	7.20	11.08	2.75	0.19	0.14	99.09	696.1
49.24	1.73	13.92	12.02	0.21	7.15	11.19	2.70	0.15	0.11	98.42	712.8
49.22	1.79	14.03	11.95	0.07	7.15	11.12	2.74	0.16	0.10	98.32	714.4
49.70	1.76	13.99	11.97	0.22	7.14	11.00	2.76	0.18	0.16	98.87	715.2
49.27	1.77	14.00	11.92	0.25	7.14	11.11	2.75	0.18	0.17	98.56	741.0
50.03	1.79	13.82	12.00	0.27	6.97	11.10	2.64	0.19	0.15	98.97	747.0
49.31	1.76	13.93	12.09	0.23	7.17	11.03	2.73	0.20	0.13	98.59	772.0

49.55	1.80	13.99	11.83	0.18	7.05	11.13	2.75	0.18	0.08	98.54	776.4
49.46	1.75	14.06	12.27	0.24	7.25	11.25	2.71	0.15	0.20	99.33	802.8
49.31	1.73	14.01	11.92	0.18	7.03	11.07	2.64	0.18	0.15	98.21	831.2
49.59	1.76	14.05	11.96	0.24	7.07	11.17	2.67	0.20	0.04	98.75	838.4
49.53	1.71	13.92	12.21	0.21	7.16	11.24	2.71	0.16	0.12	98.96	864.5
49.24	1.71	13.92	12.15	0.15	6.99	11.15	2.67	0.18	0.19	98.34	890.5
49.27	1.79	14.07	12.06	0.18	7.15	11.16	2.77	0.20	0.17	98.83	900.4
49.25	1.77	14.07	12.17	0.25	7.09	11.19	2.69	0.18	0.08	98.73	926.3
49.40	1.72	14.04	12.14	0.25	7.07	11.08	2.77	0.18	0.14	98.79	949.7
49.65	1.75	14.19	12.10	0.19	7.08	11.12	2.69	0.17	0.14	99.08	962.4
49.54	1.77	14.02	12.00	0.19	7.06	11.03	2.64	0.12	0.22	98.59	988.2
49.16	1.81	14.02	12.09	0.17	7.16	11.20	2.74	0.25	0.19	98.79	1008.9
49.28	1.82	13.93	12.04	0.25	7.03	11.16	2.73	0.22	0.12	98.59	1024.4
49.87	1.77	14.03	11.98	0.23	7.15	11.13	2.72	0.20	0.02	99.09	1050.0
49.35	1.76	13.99	12.05	0.18	7.06	11.08	2.70	0.16	0.14	98.47	1068.1
49.40	1.71	13.97	12.02	0.21	7.04	10.92	2.75	0.19	0.11	98.32	1086.4
49.69	1.81	14.08	12.03	0.24	7.13	11.12	2.75	0.21	0.08	99.14	1111.8
49.58	1.78	14.03	12.08	0.16	7.07	11.22	2.80	0.18	0.06	98.95	1127.4
49.47	1.86	13.99	11.84	0.28	7.12	11.11	2.68	0.18	0.14	98.66	1148.4
49.46	1.80	14.13	12.05	0.16	7.06	11.18	2.71	0.21	0.17	98.93	1173.6
49.67	1.80	14.01	11.91	0.25	7.10	11.11	2.74	0.19	0.14	98.91	1186.6
49.93	1.75	13.97	12.02	0.28	7.03	10.91	2.83	0.15	0.14	98.99	1210.4
49.61	1.67	14.02	11.89	0.21	7.03	10.98	2.69	0.24	0.15	98.49	1235.3
49.66	1.76	14.06	11.91	0.22	7.03	11.17	2.71	0.18	0.08	98.77	1245.8
49.74	1.69	13.94	12.02	0.16	7.14	11.21	2.66	0.18	0.11	98.85	1272.4
50.34	1.77	13.95	11.64	0.25	7.01	11.00	2.72	0.20	0.07	98.94	1297.1
49.84	1.80	14.20	11.99	0.28	7.05	11.04	2.70	0.20	0.18	99.28	1305.1
49.30	1.77	14.05	11.90	0.18	7.06	11.12	2.69	0.15	0.11	98.33	1334.4
49.59	1.72	14.03	12.10	0.24	7.00	11.21	2.66	0.23	0.08	98.87	1396.4

Exp 44

SiO2	TiO2	Al2O3	FeO	MnO	MgO	CaO	Na2O	K2O	P2O5	Total	d (um)
48.51	1.70	11.86	13.01	0.36	11.73	11.44	1.64	0.10	0.15	100.49	2.6
48.62	1.76	11.96	13.06	0.23	11.48	11.83	1.63	0.08	0.10	100.75	7.9
48.53	1.69	12.27	12.22	0.26	12.48	11.26	1.41	0.09	0.11	100.31	20.7
48.78	1.73	12.44	12.37	0.18	11.81	11.10	1.55	0.10	0.11	100.18	25.8
48.91	1.68	12.68	12.51	0.19	11.08	11.20	1.70	0.12	0.03	100.10	26.3
48.96	1.72	12.69	12.97	0.20	9.98	10.62	1.93	0.19	0.04	99.29	28.7
48.20	1.73	12.54	12.25	0.31	11.57	11.30	1.47	0.09	0.10	99.56	30.9
49.39	1.73	12.79	12.36	0.15	10.35	10.86	1.66	0.20	0.15	99.63	34.0
49.49	1.59	12.99	12.26	0.29	10.79	10.87	2.17	0.13	0.20	100.78	34.6
49.17	1.72	12.88	12.44	0.23	10.71	11.01	1.67	0.14	0.17	100.13	36.1
49.11	1.77	12.87	12.71	0.33	9.99	10.82	1.85	0.12	0.15	99.73	36.7
49.52	1.74	12.99	12.55	0.15	10.34	10.69	1.93	0.19	0.16	100.25	39.2
49.20	1.73	13.12	12.66	0.30	9.98	10.68	1.68	0.16	0.18	99.67	41.2
49.43	1.76	12.86	12.49	0.26	10.01	10.77	1.76	0.13	0.08	99.55	44.4
49.49	1.74	13.19	12.70	0.26	9.92	10.78	1.94	0.12	0.12	100.26	46.3
49.05	1.81	12.92	12.67	0.21	9.88	10.97	1.77	0.15	0.23	99.67	47.2
49.33	1.78	13.13	12.31	0.15	9.97	10.81	1.77	0.14	0.13	99.52	49.6
49.22	1.81	13.08	12.68	0.19	9.91	10.69	1.76	0.14	0.21	99.68	51.4
49.37	1.63	13.40	12.35	0.19	9.69	10.56	2.37	0.18	0.20	99.93	51.4
49.23	1.81	13.00	12.74	0.26	10.10	10.99	1.62	0.12	0.07	99.94	52.4
50.16	1.72	13.24	12.43	0.21	9.76	10.76	1.76	0.12	0.12	100.29	54.8
49.49	1.79	13.29	12.56	0.22	9.60	10.85	1.71	0.13	0.09	99.71	56.5
49.38	1.78	13.30	12.44	0.21	9.60	10.92	1.77	0.17	0.15	99.72	57.6
50.08	1.69	13.27	12.19	0.12	9.38	10.73	1.90	0.18	0.12	99.66	60.0
50.15	1.76	13.23	12.42	0.30	9.45	10.69	1.72	0.15	0.14	100.02	61.6
50.09	1.77	13.41	12.47	0.18	9.58	10.81	1.66	0.15	0.20	100.31	62.8
49.44	1.72	12.90	11.99	0.16	9.40	10.59	2.40	0.15	0.16	98.92	65.3
49.22	1.78	12.98	11.98	0.23	9.46	10.60	2.36	0.16	0.08	98.83	66.8
49.35	1.74	13.07	12.20	0.21	9.36	10.62	2.38	0.17	0.13	99.22	68.0
49.86	1.60	13.55	12.05	0.22	9.40	10.46	2.53	0.14	0.14	99.95	68.3
49.62	1.68	13.25	12.16	0.26	9.45	10.65	2.37	0.17	0.14	99.75	70.5
49.37	1.71	13.10	12.26	0.26	9.25	10.70	2.45	0.17	0.05	99.31	71.9
49.51	1.76	13.26	12.15	0.13	9.34	10.76	2.42	0.18	0.23	99.74	73.3
49.78	1.72	13.25	12.12	0.18	9.32	10.68	2.50	0.18	0.15	99.87	75.7
49.34	1.74	13.19	12.18	0.21	9.24	10.74	2.39	0.17	0.13	99.33	77.0
49.16	1.73	13.24	11.99	0.18	9.08	10.74	2.49	0.13	0.05	98.79	78.5
49.33	1.71	13.32	12.14	0.11	9.24	10.58	2.52	0.15	0.13	99.22	80.9
49.12	1.70	13.32	12.13	0.19	9.16	10.91	2.41	0.18	0.16	99.28	83.7
49.27	1.68	13.48	11.89	0.24	9.18	10.66	2.57	0.20	0.10	99.25	86.1
49.47	1.76	13.35	12.20	0.32	9.07	10.78	2.49	0.13	0.13	99.70	88.9
49.51	1.68	13.27	11.94	0.17	9.00	10.52	2.54	0.19	0.16	98.97	91.3
49.52	1.74	13.44	11.98	0.13	9.00	10.75	2.56	0.16	0.08	99.36	94.1
49.35	1.75	13.52	11.81	0.24	8.91	10.62	2.59	0.20	0.15	99.12	96.6
49.42	1.80	13.64	12.03	0.25	8.85	10.66	2.57	0.16	0.15	99.54	99.3
49.63	1.68	13.75	11.93	0.21	8.94	10.68	2.55	0.18	0.17	99.72	101.8
49.33	1.73	13.46	11.85	0.17	8.81	10.63	2.52	0.17	0.16	98.82	104.6
49.75	1.72	13.51	11.90	0.17	8.81	10.75	2.58	0.17	0.05	99.41	107.0

49.41	1.77	13.58	11.80	0.07	8.73	10.77	2.54	0.19	0.09	98.94	109.8
49.59	1.73	13.66	11.90	0.20	8.74	10.77	2.67	0.19	0.22	99.67	115.0
49.77	1.74	13.78	11.74	0.24	8.55	10.72	2.61	0.19	0.11	99.46	124.8
49.56	1.70	13.62	11.72	0.15	8.48	10.69	2.64	0.19	0.10	98.83	130.0
49.44	1.72	13.75	11.80	0.18	8.42	10.78	2.65	0.16	0.07	98.94	134.4
49.59	1.81	13.73	11.81	0.24	8.23	10.71	2.67	0.21	0.17	99.15	140.7
49.83	1.80	13.71	11.88	0.16	8.28	10.72	2.64	0.17	0.09	99.27	145.7
49.52	1.74	13.68	11.82	0.24	8.27	10.86	2.73	0.21	0.11	99.18	149.3
49.71	1.81	13.86	11.69	0.27	8.04	10.76	2.63	0.20	0.13	99.09	156.7
49.88	1.72	13.72	11.68	0.16	8.01	10.81	2.64	0.18	0.16	98.95	161.3
49.58	1.78	13.73	11.81	0.18	8.08	10.89	2.67	0.20	0.18	99.10	164.1
49.59	1.74	13.80	11.82	0.21	7.92	10.71	2.74	0.20	0.14	98.87	172.6
50.16	1.73	13.94	11.86	0.20	7.90	10.88	2.70	0.19	0.05	99.61	177.0
49.67	1.82	13.94	11.87	0.24	7.99	11.03	2.70	0.16	0.14	99.54	179.0
50.04	1.81	13.90	11.76	0.24	7.75	10.79	2.65	0.19	0.13	99.25	188.5
49.85	1.77	13.98	11.75	0.21	7.77	10.74	2.70	0.24	0.14	99.14	192.7
49.79	1.80	13.90	11.76	0.26	7.73	10.83	2.66	0.21	0.15	99.08	193.9
49.72	1.82	13.72	11.81	0.24	7.74	10.95	2.70	0.18	0.14	99.02	204.5
50.00	1.80	13.94	11.75	0.14	7.64	10.96	2.60	0.15	0.16	99.14	208.3
49.76	1.81	14.11	11.88	0.18	7.74	10.90	2.73	0.17	0.10	99.36	208.7
49.74	1.86	13.95	11.71	0.16	7.56	10.78	2.67	0.20	0.13	98.77	220.4
49.85	1.85	13.83	11.94	0.21	7.51	11.15	2.75	0.14	0.14	99.36	223.6
49.78	1.85	13.87	11.90	0.25	7.57	10.84	2.78	0.23	0.13	99.20	224.0
49.77	1.79	13.90	11.68	0.16	7.40	10.94	2.70	0.15	0.13	98.62	236.3
49.93	1.83	13.88	11.84	0.15	7.38	11.03	2.66	0.16	0.16	99.04	238.5
49.65	1.83	13.92	11.84	0.14	7.37	11.00	2.71	0.20	0.19	98.84	239.7
49.93	1.86	14.14	11.69	0.22	7.48	11.05	2.61	0.19	0.11	99.26	252.3
49.94	1.83	13.99	11.97	0.25	7.40	11.02	2.78	0.19	0.09	99.45	253.3
50.11	1.86	14.17	11.85	0.13	7.39	11.02	2.71	0.21	0.05	99.51	255.3
49.75	1.85	13.91	11.84	0.19	7.31	11.16	2.71	0.16	0.07	98.93	268.2
49.68	1.83	14.03	11.94	0.17	7.45	10.94	2.78	0.17	0.16	99.16	268.2
49.95	1.82	13.90	11.87	0.19	7.29	11.02	2.76	0.14	0.11	99.06	271.0
50.04	1.85	14.00	11.92	0.19	7.20	10.97	2.72	0.19	0.10	99.19	284.1
49.49	1.82	14.03	11.81	0.22	7.20	11.06	2.75	0.21	0.14	98.72	286.7
49.57	1.84	14.01	12.16	0.22	7.24	11.01	2.77	0.17	0.14	99.14	297.9
49.82	1.80	14.07	11.81	0.10	7.12	11.00	2.77	0.21	0.18	98.88	300.1
49.84	1.89	14.04	12.01	0.19	7.25	11.06	2.71	0.17	0.21	99.37	302.3
49.89	1.89	13.96	11.87	0.16	7.25	11.09	2.71	0.21	0.10	99.12	312.8
50.03	1.87	14.02	11.78	0.15	7.21	10.94	2.83	0.21	0.17	99.20	316.0
49.72	1.81	13.97	12.17	0.20	7.22	10.97	2.76	0.18	0.13	99.13	318.0
49.98	1.91	14.05	12.27	0.26	7.17	11.20	2.63	0.18	0.09	99.75	318.8
50.09	1.86	14.24	12.06	0.14	7.16	11.14	2.73	0.17	0.14	99.73	321.1
49.98	1.84	14.01	11.98	0.18	7.13	11.10	2.73	0.19	0.11	99.25	327.7
50.09	1.90	13.94	12.02	0.20	7.14	11.17	2.74	0.17	0.20	99.56	331.9
49.83	1.87	14.12	12.08	0.20	7.12	11.18	2.72	0.18	0.06	99.36	332.9
49.99	1.84	14.22	12.21	0.24	7.11	11.22	2.76	0.20	0.14	99.94	333.4
49.70	1.83	14.02	12.07	0.22	7.12	11.11	2.71	0.19	0.17	99.14	333.7
50.04	1.89	14.09	12.25	0.25	7.09	11.35	2.76	0.17	0.12	100.00	338.6
49.71	1.85	14.12	12.05	0.26	7.11	11.35	2.73	0.18	0.13	99.49	342.5

49.90	1.76	14.00	11.95	0.11	7.02	11.20	2.68	0.20	0.11	98.94	347.9
49.90	1.83	14.08	11.92	0.25	7.02	11.06	2.70	0.18	0.19	99.12	349.3
49.85	1.85	14.00	12.02	0.24	7.15	11.24	2.71	0.18	0.14	99.37	349.5
49.92	1.86	13.89	11.92	0.18	7.19	11.26	2.64	0.13	0.16	99.14	357.4
49.56	1.86	14.05	12.13	0.29	7.12	11.27	2.66	0.21	0.10	99.24	360.3
49.52	1.84	14.13	12.04	0.17	7.12	11.14	2.73	0.23	0.24	99.16	361.5
49.72	1.87	14.04	11.88	0.22	6.99	11.22	2.78	0.16	0.16	99.04	363.8
49.67	1.80	13.94	12.03	0.24	6.94	11.27	2.68	0.23	0.15	98.94	364.4
49.51	1.91	14.09	12.13	0.28	7.13	11.13	2.71	0.19	0.10	99.18	365.0
49.69	1.88	13.94	12.18	0.25	7.00	11.15	2.73	0.13	0.16	99.09	377.8
49.71	1.83	13.95	12.05	0.29	7.11	11.19	2.70	0.25	0.11	99.18	377.9
49.60	1.87	14.00	12.13	0.16	7.04	11.22	2.66	0.22	0.17	99.05	390.1
49.77	1.87	14.10	12.07	0.24	7.12	11.21	2.69	0.15	0.13	99.34	395.4
49.84	1.89	13.95	12.19	0.20	7.22	11.18	2.68	0.20	0.14	99.49	401.8
49.56	1.86	13.88	12.06	0.10	7.06	11.41	2.64	0.17	0.19	98.93	406.3
49.79	1.91	14.05	12.26	0.25	7.03	11.37	2.78	0.20	0.11	99.73	417.1
49.62	1.89	14.08	12.22	0.18	7.04	11.35	2.71	0.14	0.16	99.39	418.7
49.98	1.80	13.94	12.17	0.23	6.99	11.25	2.65	0.18	0.09	99.28	426.4
49.70	1.87	14.02	11.96	0.28	7.06	11.28	2.69	0.17	0.08	99.10	434.7
49.73	1.93	13.84	12.22	0.19	7.12	11.21	2.65	0.19	0.12	99.20	443.3
49.72	1.89	13.86	12.22	0.22	7.07	11.26	2.71	0.17	0.13	99.24	447.3
49.77	1.82	13.91	12.29	0.23	6.88	11.28	2.68	0.19	0.05	99.09	456.3
49.66	1.85	13.94	12.03	0.17	7.03	11.18	2.61	0.21	0.13	98.82	457.4
49.85	1.86	13.92	12.16	0.27	7.03	11.27	2.64	0.21	0.09	99.29	463.1
49.38	1.87	13.96	12.32	0.22	7.05	11.15	2.68	0.14	0.10	98.86	475.9
49.64	1.87	13.89	12.25	0.33	7.16	11.26	2.68	0.20	0.19	99.49	484.8
49.96	1.86	13.83	12.18	0.15	7.02	11.20	2.72	0.17	0.16	99.24	488.4
49.72	1.85	13.79	12.25	0.26	6.97	11.19	2.64	0.12	0.13	98.93	495.6
49.43	1.88	13.89	12.20	0.20	7.06	11.21	2.67	0.20	0.15	98.88	586.0
49.73	1.87	13.87	12.15	0.23	7.04	11.18	2.67	0.19	0.19	99.10	626.2
49.70	1.90	13.79	12.12	0.25	7.10	11.20	2.61	0.22	0.16	99.04	666.5
49.66	1.83	13.96	12.12	0.22	6.99	11.32	2.68	0.16	0.10	99.04	706.7
49.61	1.81	13.76	12.15	0.14	6.95	11.13	2.65	0.17	0.13	98.49	727.0
49.64	1.84	13.94	12.16	0.27	7.03	11.13	2.61	0.22	0.22	99.06	747.0
49.36	1.86	13.93	12.08	0.27	6.89	11.16	2.73	0.18	0.19	98.65	753.0
49.54	1.89	13.94	12.01	0.18	7.09	11.29	2.68	0.21	0.18	99.00	765.0
49.39	1.92	13.88	12.17	0.19	7.10	11.19	2.62	0.17	0.10	98.72	807.3
49.81	1.90	14.01	12.28	0.11	7.05	11.37	2.78	0.19	0.11	99.59	831.3
49.43	1.83	14.04	12.15	0.23	7.04	11.32	2.69	0.16	0.15	99.04	841.3
49.98	1.93	13.89	12.27	0.20	6.94	11.18	2.69	0.15	0.10	99.32	887.7
49.63	1.91	13.99	12.27	0.24	7.01	11.47	2.67	0.15	0.20	99.54	909.7
49.86	1.82	13.92	12.18	0.21	7.12	11.27	2.71	0.15	0.09	99.32	917.7
49.59	1.84	13.87	12.24	0.13	6.91	11.30	2.68	0.19	0.22	98.97	968.0
49.90	1.88	13.93	12.02	0.19	6.99	11.33	2.67	0.17	0.10	99.19	988.0
49.98	1.84	13.91	12.13	0.23	7.11	11.28	2.69	0.17	0.11	99.46	994.0
49.52	1.95	13.84	12.16	0.19	7.09	11.24	2.76	0.15	0.23	99.13	994.0
49.38	1.83	13.95	12.08	0.25	7.01	11.28	2.77	0.19	0.16	98.90	1023.0
49.49	1.82	14.01	12.15	0.25	7.06	11.09	2.73	0.19	0.13	98.91	1025.0
49.90	1.92	13.87	12.29	0.18	7.06	11.28	2.70	0.22	0.05	99.47	1096.5

49.86	1.97	13.98	12.01	0.18	7.11	11.30	2.75	0.18	0.09	99.43	1131.5
49.74	1.88	14.10	12.24	0.23	6.96	11.03	2.75	0.16	0.23	99.32	1148.0
49.47	1.95	13.87	12.17	0.13	7.04	11.13	2.75	0.14	0.17	98.80	1211.0
49.41	1.86	13.90	12.22	0.22	7.12	11.06	2.66	0.15	0.08	98.68	1223.0
49.52	1.87	13.96	12.25	0.24	7.03	11.25	2.72	0.22	0.18	99.23	1240.0
49.86	1.87	14.03	12.18	0.18	7.09	11.15	2.72	0.22	0.05	99.36	1271.0
49.76	1.90	13.80	12.17	0.18	7.08	11.14	2.78	0.15	0.08	99.03	1291.0
50.27	1.93	14.01	12.08	0.19	6.95	11.19	2.73	0.21	0.15	99.70	1571.0
49.98	1.92	13.86	12.19	0.24	6.99	11.23	2.72	0.22	0.09	99.43	1574.0
50.00	1.93	13.85	12.08	0.34	6.83	11.27	2.64	0.13	0.13	99.19	1597.0

Exp 45

SiO2	TiO2	Al2O3	FeO	MnO	MgO	CaO	Na2O	K2O	P2O5	Total	d (um)
49.01	1.81	11.75	12.30	0.21	11.13	11.08	2.13	0.13	0.12	99.66	1.0
47.85	1.36	11.03	12.79	0.12	15.20	9.18	2.26	0.17	0.12	100.08	3.2
48.42	1.65	11.52	12.32	0.16	11.46	10.81	1.97	0.10	0.11	98.53	5.0
48.72	1.80	11.37	12.42	0.19	11.61	10.92	2.11	0.08	0.01	99.22	5.3
47.41	1.63	10.65	12.92	0.21	13.77	9.95	1.81	0.08	0.11	98.52	6.1
47.83	1.49	10.77	12.96	0.19	14.18	9.95	1.82	0.10	0.05	99.33	10.3
47.55	1.61	10.56	13.02	0.29	14.77	9.92	1.87	0.08	0.14	99.80	11.2
47.78	1.49	10.57	12.76	0.19	14.72	9.71	1.84	0.10	0.15	99.29	15.6
47.67	1.47	10.58	13.05	0.24	14.64	9.72	1.85	0.11	0.10	99.44	15.9
47.63	1.57	10.57	13.01	0.10	14.91	9.66	1.85	0.13	0.12	99.54	16.4
47.51	1.50	10.60	12.59	0.21	14.84	9.46	1.89	0.09	0.11	98.81	21.0
47.81	1.51	10.60	12.91	0.24	14.85	9.64	1.86	0.10	0.12	99.63	21.2
47.66	1.62	10.64	12.83	0.24	14.76	9.58	1.96	0.13	0.18	99.60	21.5
47.83	1.51	10.78	12.43	0.23	14.75	9.58	1.92	0.09	0.15	99.28	26.3
47.69	1.52	10.73	12.78	0.19	14.65	9.55	1.93	0.13	0.06	99.23	26.5
47.53	1.65	10.63	12.76	0.19	14.88	9.64	1.96	0.12	0.22	99.59	26.6
47.56	1.47	10.77	12.49	0.18	14.74	9.57	1.95	0.06	0.12	98.89	31.6
47.99	1.58	10.87	12.78	0.25	14.77	9.75	1.89	0.11	0.09	100.08	31.7
47.69	1.47	10.81	12.46	0.29	14.63	9.53	1.89	0.13	0.12	99.01	31.8
48.17	1.48	11.17	12.76	0.23	14.85	9.48	1.93	0.10	0.13	100.29	36.1
47.54	1.65	10.94	12.62	0.20	14.57	9.75	1.99	0.11	0.12	99.49	36.8
47.80	1.52	10.94	12.43	0.15	14.48	9.61	1.92	0.12	0.12	99.08	37.0
47.61	1.51	10.84	12.62	0.16	14.65	9.58	1.98	0.06	0.11	99.12	37.1
47.58	1.64	10.94	12.60	0.17	14.42	9.74	1.95	0.10	0.15	99.28	41.9
47.69	1.53	11.01	12.42	0.11	14.49	9.71	2.02	0.09	0.12	99.20	42.3
47.64	1.50	10.85	12.52	0.13	14.37	9.58	1.89	0.15	0.14	98.76	42.4
47.60	1.63	11.02	12.52	0.14	14.29	9.75	1.92	0.14	0.18	99.19	47.0
47.77	1.55	11.19	12.31	0.21	14.26	9.72	1.95	0.11	0.12	99.19	47.6
47.89	1.50	11.19	12.61	0.27	14.23	9.71	1.96	0.14	0.12	99.59	47.7
47.90	1.61	11.22	12.68	0.18	14.18	9.72	2.13	0.09	0.14	99.85	52.1
48.50	1.42	11.36	12.70	0.30	14.32	9.66	2.16	0.11	0.15	100.68	52.6
47.75	1.48	11.08	12.57	0.27	13.93	9.77	1.97	0.15	0.19	99.16	53.0
47.67	1.55	11.25	12.31	0.19	14.22	9.77	1.97	0.13	0.16	99.23	53.0
47.84	1.63	11.28	12.48	0.21	13.96	9.90	2.03	0.09	0.15	99.56	57.2
47.76	1.49	11.40	12.53	0.21	13.84	9.68	2.12	0.13	0.07	99.22	58.3
47.83	1.56	11.27	12.36	0.21	14.08	9.78	2.08	0.13	0.18	99.47	58.3
47.93	1.67	11.32	12.50	0.28	13.73	9.78	1.99	0.12	0.21	99.51	62.4
48.08	1.50	11.45	12.42	0.23	13.62	9.79	2.06	0.10	0.08	99.33	63.6
47.89	1.58	11.45	12.29	0.15	13.92	9.83	2.02	0.13	0.15	99.40	63.6
48.05	1.65	11.38	12.34	0.28	13.66	9.90	2.05	0.08	0.12	99.52	67.5
47.77	1.50	11.52	12.47	0.19	13.53	9.89	2.11	0.14	0.08	99.19	68.8
47.97	1.56	11.56	12.18	0.28	13.71	9.77	2.07	0.13	0.17	99.40	69.0
48.06	1.45	11.62	12.43	0.21	13.51	9.42	2.22	0.14	0.19	99.26	69.1
47.96	1.70	11.49	12.31	0.12	13.57	9.85	2.10	0.17	0.15	99.41	72.5
48.20	1.56	11.64	12.32	0.14	13.55	9.81	2.13	0.12	0.15	99.59	74.1
47.96	1.67	11.52	12.31	0.21	13.52	9.97	2.10	0.12	0.15	99.52	77.6
47.98	1.53	11.69	12.38	0.21	13.53	9.75	2.15	0.11	0.07	99.39	79.4

47.99	1.55	11.79	12.14	0.19	13.49	9.77	2.08	0.11	0.10	99.20	79.6
48.14	1.63	11.69	12.17	0.16	13.19	9.92	2.16	0.16	0.19	99.42	82.7
48.49	1.56	11.76	12.24	0.24	13.14	9.82	2.19	0.15	0.12	99.71	84.7
47.94	1.59	11.85	12.09	0.17	13.20	9.83	2.14	0.11	0.18	99.09	85.0
48.23	1.43	11.83	12.23	0.23	13.31	9.68	2.12	0.15	0.15	99.35	85.6
48.28	1.64	11.76	12.37	0.25	13.00	9.85	2.20	0.14	0.12	99.61	87.8
48.39	1.53	11.82	12.22	0.20	13.01	9.84	2.25	0.16	0.07	99.47	90.0
48.07	1.58	11.90	11.97	0.21	13.04	9.93	2.11	0.13	0.21	99.13	90.3
48.14	1.70	11.76	12.24	0.24	12.91	9.99	2.18	0.15	0.17	99.46	92.9
48.12	1.59	11.99	12.00	0.20	12.74	9.80	2.20	0.15	0.16	98.95	95.3
48.55	1.60	11.97	11.95	0.26	12.89	9.82	2.16	0.17	0.14	99.51	95.6
48.60	1.64	11.90	12.20	0.22	12.85	10.08	2.14	0.14	0.08	99.86	98.0
48.34	1.49	11.97	12.13	0.21	12.61	9.86	2.16	0.14	0.08	98.97	100.6
48.37	1.59	12.15	11.95	0.15	12.58	10.00	2.03	0.15	0.11	99.06	101.0
48.67	1.41	12.17	11.99	0.13	12.65	9.69	2.20	0.11	0.27	99.28	102.1
48.11	1.66	12.00	12.06	0.28	12.65	9.97	2.07	0.14	0.15	99.08	103.1
48.38	1.62	12.16	11.90	0.11	12.55	10.06	2.25	0.16	0.10	99.29	105.9
48.36	1.55	12.20	12.09	0.14	12.58	9.82	2.15	0.12	0.15	99.15	106.3
48.59	1.64	12.08	12.09	0.22	12.58	10.01	2.26	0.15	0.06	99.67	108.3
48.46	1.50	12.14	12.03	0.23	12.39	9.93	2.24	0.18	0.05	99.14	111.2
48.50	1.58	12.19	11.80	0.24	12.39	10.09	2.27	0.17	0.17	99.39	111.6
48.34	1.63	12.21	12.17	0.17	12.40	10.05	2.23	0.17	0.08	99.45	113.4
48.39	1.48	12.18	11.86	0.20	12.14	10.00	2.32	0.15	0.18	98.89	116.5
48.48	1.56	12.40	11.78	0.20	12.19	9.93	2.23	0.18	0.15	99.09	117.0
48.52	1.61	12.16	12.11	0.25	12.31	10.01	2.26	0.17	0.12	99.51	118.5
48.75	1.50	12.41	11.86	0.17	12.29	9.69	2.28	0.16	0.17	99.27	118.6
48.42	1.59	12.41	11.87	0.23	12.12	10.04	2.30	0.14	0.15	99.27	121.8
48.52	1.61	12.37	12.02	0.18	12.28	10.10	2.25	0.14	0.19	99.66	122.3
48.46	1.67	12.24	12.11	0.32	12.10	10.09	2.23	0.14	0.11	99.46	123.6
48.59	1.60	12.54	11.89	0.26	11.85	10.12	2.22	0.15	0.10	99.31	127.1
48.69	1.61	12.57	11.75	0.10	11.92	9.97	2.28	0.19	0.12	99.19	127.6
48.51	1.71	12.29	11.95	0.25	11.94	10.15	2.28	0.14	0.12	99.35	128.7
48.43	1.54	12.42	11.75	0.27	11.83	10.15	2.34	0.14	0.13	99.00	132.4
48.70	1.59	12.50	11.63	0.29	11.75	9.98	2.25	0.16	0.09	98.93	133.0
48.92	1.47	12.61	11.85	0.14	11.86	9.77	2.29	0.18	0.15	99.25	135.1
48.82	1.60	12.54	11.79	0.16	11.49	10.12	2.33	0.15	0.18	99.18	137.7
48.81	1.63	12.64	11.74	0.18	11.62	10.09	2.27	0.15	0.11	99.23	138.3
49.05	1.64	12.78	11.83	0.19	11.18	10.25	2.33	0.19	0.11	99.56	147.6
48.97	1.64	13.03	11.44	0.22	11.17	10.14	2.39	0.19	0.14	99.32	148.1
49.07	1.46	12.97	11.66	0.32	11.61	9.86	2.37	0.16	0.18	99.65	151.6
48.92	1.68	12.84	11.61	0.14	10.90	10.23	2.45	0.17	0.11	99.04	157.6
48.85	1.65	13.14	11.37	0.21	11.04	10.25	2.51	0.16	0.16	99.35	158.4
48.72	1.64	13.05	11.66	0.15	10.79	10.22	2.40	0.20	0.19	99.02	167.7
48.94	1.69	13.26	11.37	0.13	10.69	10.22	2.51	0.19	0.19	99.18	168.7
49.26	1.65	13.09	11.63	0.29	10.58	10.37	2.43	0.15	0.13	99.57	172.4
49.05	1.65	13.24	11.64	0.18	10.36	10.31	2.55	0.19	0.17	99.34	177.7
49.06	1.67	13.29	11.42	0.19	10.32	10.24	2.43	0.17	0.11	98.89	178.9
49.09	1.67	13.21	11.50	0.23	10.31	10.42	2.47	0.15	0.20	99.25	182.2
49.40	1.61	13.32	11.60	0.08	10.14	10.16	2.53	0.21	0.15	99.21	187.8

49.25	1.71	13.35	11.38	0.16	10.05	10.32	2.48	0.17	0.10	98.97	189.2
49.15	1.71	13.33	11.44	0.20	10.03	10.39	2.44	0.20	0.13	99.01	192.0
49.28	1.67	13.34	11.36	0.16	10.00	10.29	2.45	0.19	0.08	98.83	197.8
49.12	1.71	13.39	11.42	0.18	9.89	10.39	2.49	0.18	0.04	98.80	199.5
49.18	1.73	13.37	11.50	0.17	9.99	10.46	2.54	0.14	0.27	99.34	201.8
49.46	1.63	13.47	11.36	0.12	9.66	10.40	2.56	0.19	0.19	99.02	207.9
49.31	1.66	13.62	11.40	0.22	9.53	10.40	2.63	0.17	0.15	99.08	209.8
49.24	1.73	13.46	11.30	0.24	9.74	10.41	2.60	0.20	0.15	99.07	211.5
49.47	1.68	13.57	11.61	0.13	9.62	10.49	2.60	0.18	0.03	99.37	217.9
49.59	1.72	13.49	11.49	0.20	9.55	10.48	2.63	0.18	0.16	99.49	221.3
49.50	1.69	13.61	11.33	0.11	9.35	10.52	2.58	0.21	0.22	99.11	228.0
49.35	1.74	13.54	11.40	0.21	9.23	10.56	2.66	0.20	0.20	99.09	231.1
49.58	1.68	13.60	11.46	0.13	9.28	10.46	2.54	0.16	0.23	99.11	238.0
49.49	1.74	13.63	11.38	0.24	9.17	10.45	2.62	0.19	0.16	99.06	240.9
49.77	1.79	13.74	11.51	0.12	8.93	10.49	2.70	0.18	0.19	99.43	248.1
49.61	1.82	13.78	11.40	0.14	9.03	10.59	2.69	0.20	0.16	99.43	250.7
49.73	1.70	13.69	11.44	0.23	8.86	10.35	2.64	0.24	0.15	99.03	258.1
49.45	1.82	13.73	11.50	0.15	8.70	10.51	2.64	0.17	0.16	98.83	260.5
49.71	1.75	13.75	11.52	0.13	8.62	10.57	2.70	0.16	0.17	99.08	268.2
49.72	1.79	13.82	11.35	0.22	8.61	10.48	2.67	0.23	0.22	99.11	270.3
49.93	1.75	13.81	11.45	0.17	8.46	10.70	2.79	0.16	0.12	99.34	278.2
49.59	1.85	13.90	11.45	0.29	8.51	10.79	2.63	0.18	0.12	99.32	280.1
49.73	1.76	13.95	11.46	0.19	8.49	10.59	2.69	0.17	0.14	99.18	288.3
49.73	1.80	13.82	11.45	0.26	8.39	10.56	2.68	0.21	0.20	99.08	289.9
50.09	1.79	13.87	11.42	0.21	8.20	10.69	2.69	0.16	0.12	99.24	298.3
49.88	1.81	13.99	11.47	0.20	8.27	10.79	2.83	0.18	0.18	99.61	299.7
49.81	1.79	13.76	11.49	0.15	8.21	10.60	2.64	0.16	0.19	98.80	308.4
49.85	1.85	13.89	11.53	0.23	8.20	10.65	2.71	0.20	0.12	99.23	309.5
50.17	1.77	13.93	11.43	0.30	8.11	10.80	2.75	0.17	0.21	99.62	318.4
49.87	1.83	13.94	11.46	0.25	8.07	10.72	2.76	0.13	0.12	99.14	319.3
50.11	1.81	14.08	11.46	0.18	7.98	10.95	2.64	0.18	0.16	99.56	328.5
49.71	1.78	13.99	11.60	0.21	7.92	10.78	2.66	0.15	0.23	99.04	329.1
49.95	1.83	13.91	11.42	0.24	7.84	10.87	2.67	0.19	0.21	99.13	338.4
49.60	1.90	13.83	11.51	0.25	7.79	11.01	2.81	0.18	0.09	98.97	338.9
49.26	1.87	13.93	11.61	0.24	7.75	10.89	2.70	0.18	0.22	98.65	348.7
49.68	1.81	13.95	11.57	0.18	7.67	11.01	2.71	0.20	0.08	98.87	352.7
49.65	1.81	13.89	11.53	0.19	7.66	10.86	2.75	0.15	0.15	98.65	353.2
49.94	1.82	14.03	11.68	0.21	7.51	10.95	2.73	0.21	0.19	99.27	366.1
49.60	1.84	14.05	11.67	0.19	7.54	11.00	2.73	0.17	0.25	99.04	372.3
49.77	1.77	13.91	11.64	0.20	7.48	11.07	2.73	0.14	0.27	98.98	372.8
49.69	1.90	13.91	11.68	0.17	7.47	10.90	2.69	0.18	0.12	98.71	385.0
49.59	1.85	13.97	11.82	0.27	7.45	10.93	2.75	0.20	0.17	98.99	392.0
49.54	1.83	14.01	11.89	0.28	7.43	11.04	2.77	0.20	0.15	99.13	392.5
49.80	1.86	14.06	11.83	0.20	7.40	10.93	2.74	0.17	0.21	99.21	404.0
49.87	1.85	14.00	11.76	0.22	7.29	10.90	2.70	0.19	0.11	98.89	411.6
49.43	1.88	13.96	11.71	0.14	7.39	10.99	2.73	0.19	0.14	98.56	412.2
49.93	1.88	14.00	11.92	0.22	7.34	10.98	2.66	0.18	0.22	99.32	423.0
49.87	1.85	13.89	11.78	0.20	7.34	11.03	2.75	0.23	0.21	99.16	431.2
49.92	1.84	13.99	12.02	0.14	7.28	11.04	2.74	0.16	0.12	99.24	431.7

49.86	1.88	13.93	11.84	0.19	7.25	10.90	2.69	0.15	0.15	98.85	442.0
49.79	1.83	14.06	12.09	0.17	7.33	11.03	2.80	0.21	0.18	99.49	450.9
49.66	1.83	13.95	12.00	0.21	7.15	11.06	2.77	0.20	0.09	98.92	451.4
49.64	1.89	13.88	11.96	0.26	7.28	11.02	2.72	0.19	0.13	98.97	461.0
49.86	1.83	13.94	12.02	0.17	7.16	10.99	2.73	0.17	0.19	99.05	470.6
49.40	1.78	13.91	11.88	0.19	7.23	11.21	2.72	0.23	0.23	98.76	471.1
49.71	1.87	13.84	11.92	0.25	7.17	11.24	2.72	0.21	0.10	99.03	480.0
49.87	1.80	13.76	12.08	0.18	7.20	11.11	2.70	0.19	0.12	99.01	490.2
49.77	1.82	14.00	11.93	0.31	7.16	11.03	2.69	0.17	0.12	99.01	490.7
49.57	1.90	13.88	12.04	0.19	7.24	11.23	2.66	0.17	0.18	99.03	499.0
50.16	1.85	13.93	12.01	0.20	7.00	11.11	2.73	0.19	0.12	99.32	509.9
49.69	1.84	14.06	12.05	0.25	7.07	10.95	2.70	0.19	0.12	98.91	510.4
50.00	1.82	13.88	12.02	0.21	7.00	11.05	2.64	0.21	0.15	98.96	518.0
49.75	1.80	13.95	11.95	0.25	7.02	11.14	2.69	0.17	0.11	98.82	614.7
49.96	1.81	14.01	12.01	0.23	6.97	11.19	2.75	0.15	0.24	99.30	620.8
49.53	1.79	13.74	12.02	0.31	7.09	11.19	2.82	0.19	0.14	98.80	626.9
49.34	1.78	13.86	12.23	0.11	7.11	11.16	2.71	0.19	0.11	98.57	655.1
49.69	1.77	14.01	12.12	0.23	7.15	11.15	2.72	0.16	0.13	99.12	660.9
49.36	1.81	13.96	11.94	0.22	7.09	11.17	2.65	0.16	0.06	98.41	665.5
49.69	1.74	13.93	12.20	0.30	7.09	11.12	2.66	0.19	0.14	99.06	701.1
49.58	1.76	13.96	12.27	0.25	7.08	11.15	2.74	0.20	0.13	99.12	704.1
49.43	1.79	13.75	12.09	0.25	7.07	11.10	2.67	0.22	0.11	98.48	735.7
49.80	1.71	13.91	12.17	0.32	7.05	11.06	2.67	0.15	0.08	98.92	741.3
49.55	1.80	13.90	12.10	0.21	7.08	11.26	2.68	0.15	0.20	98.93	742.8
49.65	1.83	13.82	12.19	0.19	7.01	11.08	2.74	0.14	0.14	98.78	776.1
49.64	1.82	13.88	12.04	0.13	7.07	11.04	2.73	0.17	0.08	98.59	781.4
49.90	1.75	13.97	12.04	0.13	7.13	10.96	2.70	0.15	0.18	98.91	781.4
49.99	1.79	13.83	12.23	0.20	7.05	11.02	2.66	0.17	0.22	99.14	816.4
49.47	1.71	13.93	12.22	0.10	7.18	11.09	2.75	0.14	0.21	98.80	820.1
49.72	1.86	13.95	12.09	0.23	7.04	10.98	2.73	0.15	0.18	98.92	821.5
49.60	1.67	13.87	12.28	0.15	7.10	11.07	2.72	0.18	0.16	98.78	873.1
49.49	1.83	13.87	12.32	0.20	7.14	11.06	2.70	0.16	0.19	98.96	886.4
49.71	1.73	13.79	12.03	0.16	7.04	11.16	2.74	0.17	0.10	98.62	899.4
49.75	1.70	13.84	12.12	0.22	7.00	10.99	2.64	0.16	0.09	98.49	914.4
49.78	1.75	14.02	12.06	0.14	6.91	11.05	2.69	0.19	0.17	98.75	929.9
49.92	1.77	13.82	11.98	0.25	7.01	11.09	2.75	0.15	0.13	98.86	955.7
50.06	1.71	13.87	12.14	0.21	7.01	11.15	2.60	0.22	0.22	99.19	956.9
49.85	1.73	13.98	12.21	0.22	7.12	11.20	2.72	0.18	0.10	99.32	1066.4
49.44	1.69	13.86	12.14	0.16	7.00	11.00	2.78	0.18	0.21	98.44	1076.4
49.75	1.71	13.96	12.21	0.15	7.07	11.03	2.77	0.19	0.26	99.09	1083.8
49.72	1.70	13.97	12.05	0.27	7.06	11.10	2.70	0.17	0.19	98.92	1172.4
49.57	1.73	13.89	12.16	0.24	7.10	11.10	2.80	0.21	0.24	99.02	1175.9
49.58	1.80	13.71	12.17	0.14	7.06	11.03	2.72	0.19	0.14	98.53	1187.3
49.77	1.71	13.86	12.08	0.13	7.06	11.06	2.67	0.18	0.14	98.66	1275.6
49.65	1.86	14.01	12.04	0.24	7.08	11.19	2.69	0.18	0.24	99.19	1278.4
49.75	1.76	13.84	12.25	0.25	7.04	11.22	2.71	0.21	0.24	99.26	1290.7
49.69	1.73	13.85	12.09	0.23	6.95	11.05	2.73	0.19	0.15	98.65	1375.2
49.59	1.71	14.07	12.09	0.26	7.11	11.15	2.70	0.19	0.20	99.08	1384.3
49.56	1.72	13.88	12.14	0.25	7.04	11.14	2.63	0.22	0.11	98.67	1394.2

49.66	1.77	13.89	12.13	0.15	7.02	11.15	2.65	0.14	0.22	98.79	1474.8
49.72	1.74	14.02	11.96	0.18	7.03	11.18	2.63	0.18	0.18	98.82	1490.3
49.63	1.77	13.96	12.07	0.29	7.04	11.22	2.73	0.18	0.18	99.07	1497.6
49.95	1.81	13.82	11.98	0.25	6.99	11.06	2.67	0.19	0.19	98.90	1574.5
49.99	1.77	13.70	11.97	0.21	6.94	11.04	2.70	0.17	0.21	98.70	1596.2
49.90	1.77	13.81	11.83	0.19	7.03	11.15	2.56	0.17	0.27	98.68	1601.1

Exp 46

SiO2	TiO2	Al2O3	FeO	MnO	MgO	CaO	Na2O	K2O	P2O5	Total	d (um)
48.84	1.71	11.92	11.95	0.18	10.71	10.74	2.25	0.10	0.16	98.56	5.9
48.37	1.67	11.80	12.36	0.15	11.02	10.89	2.04	0.10	0.11	98.51	7.5
47.70	1.58	10.93	12.55	0.26	12.51	10.42	2.06	0.12	0.12	98.24	7.6
48.44	1.45	11.02	13.02	0.21	13.87	10.11	1.77	0.08	0.16	100.14	8.0
47.33	1.54	10.74	12.68	0.26	14.77	9.38	1.94	0.14	0.10	98.86	10.4
47.14	1.49	10.50	13.09	0.25	13.83	10.06	1.87	0.09	0.06	98.37	11.6
47.42	1.51	10.52	13.02	0.20	14.06	10.00	1.85	0.08	0.14	98.79	12.8
47.24	1.52	10.46	13.04	0.19	14.22	9.83	1.85	0.07	0.10	98.52	12.9
47.32	1.49	10.43	13.00	0.31	14.49	9.68	1.96	0.09	0.06	98.81	18.2
47.36	1.49	10.42	12.88	0.30	14.62	9.54	1.90	0.09	0.04	98.63	18.2
47.31	1.50	10.47	12.83	0.27	14.75	9.60	1.87	0.11	0.15	98.85	23.4
47.32	1.44	10.56	12.90	0.18	14.73	9.64	1.87	0.11	0.17	98.89	23.6
47.30	1.45	10.94	12.83	0.21	14.84	9.43	2.00	0.14	0.14	99.28	24.9
47.46	1.45	10.96	12.76	0.21	14.69	9.73	2.05	0.12	0.05	99.47	28.4
47.26	1.46	10.63	12.75	0.31	14.66	9.57	1.99	0.11	0.13	98.86	28.6
47.19	1.43	10.50	12.86	0.14	14.83	9.44	1.91	0.13	0.10	98.53	28.9
47.61	1.46	10.51	12.69	0.21	14.63	9.61	1.93	0.11	0.10	98.85	33.9
47.34	1.45	10.59	12.89	0.17	14.77	9.52	1.99	0.11	0.10	98.92	34.3
47.43	1.48	10.95	12.66	0.12	14.55	9.72	1.99	0.12	0.15	99.16	37.3
48.43	1.36	11.02	12.87	0.17	15.00	9.59	1.84	0.11	0.06	100.45	38.2
47.16	1.46	10.51	12.73	0.16	14.57	9.52	2.01	0.08	0.07	98.25	39.2
47.54	1.46	10.93	12.58	0.18	14.52	9.73	2.03	0.10	0.11	99.18	39.5
47.38	1.52	10.63	12.75	0.23	14.79	9.58	2.03	0.07	0.14	99.11	39.6
47.50	1.46	10.64	12.70	0.18	14.43	9.39	1.96	0.14	0.14	98.52	44.4
47.34	1.48	10.95	12.46	0.25	14.20	9.58	2.01	0.13	0.09	98.49	46.0
47.18	1.46	10.72	12.67	0.20	14.35	9.55	1.91	0.13	0.11	98.27	49.7
47.50	1.41	11.03	12.62	0.21	14.30	9.55	2.06	0.11	0.10	98.89	54.0
47.33	1.41	11.09	12.47	0.29	14.10	9.66	2.00	0.10	0.09	98.54	54.6
47.34	1.45	10.91	12.46	0.09	13.92	9.69	2.06	0.12	0.02	98.06	63.8
47.62	1.47	11.14	12.53	0.17	14.14	9.63	2.08	0.15	0.19	99.13	68.6
47.34	1.49	11.25	12.42	0.19	13.92	9.87	2.13	0.11	0.05	98.75	71.8
47.94	1.40	11.24	12.82	0.25	14.45	9.67	1.95	0.08	0.06	99.85	73.4
47.35	1.49	11.46	12.39	0.19	13.79	9.73	2.20	0.16	0.06	98.81	81.4
47.47	1.40	11.24	12.47	0.28	13.86	9.68	2.12	0.09	0.11	98.72	83.1
47.65	1.53	11.35	12.35	0.19	13.42	9.64	2.08	0.14	0.06	98.41	89.1
48.22	1.40	11.32	12.83	0.28	14.29	9.70	1.92	0.08	0.28	100.32	90.9
47.75	1.49	11.44	12.53	0.14	13.64	9.76	2.14	0.11	0.15	99.15	97.7
47.40	1.50	11.48	12.35	0.14	13.45	9.67	2.13	0.12	0.07	98.31	99.0
47.65	1.45	11.62	12.33	0.23	13.29	9.74	2.23	0.10	0.13	98.73	106.4
48.19	1.45	11.60	12.67	0.09	13.84	9.83	2.04	0.17	0.22	100.08	108.6
47.96	1.49	11.56	12.44	0.24	13.44	9.71	2.15	0.14	0.15	99.27	112.3
47.52	1.50	11.73	12.30	0.17	13.02	9.87	2.22	0.13	0.13	98.58	116.8
47.70	1.47	11.62	12.19	0.19	12.91	9.93	2.15	0.14	0.12	98.40	123.6
47.87	1.52	11.78	12.26	0.21	13.26	9.79	2.19	0.15	0.15	99.17	126.7
47.67	1.51	11.85	12.22	0.27	12.72	9.83	2.25	0.15	0.08	98.53	134.4
47.78	1.51	11.99	12.09	0.18	12.78	9.81	2.18	0.12	0.16	98.60	140.9
47.95	1.45	11.79	12.25	0.24	12.81	9.89	2.13	0.15	0.09	98.75	141.3

48.47	1.47	11.83	12.29	0.15	13.08	9.73	2.24	0.11	0.15	99.51	143.7
47.67	1.48	11.97	11.92	0.26	12.55	9.88	2.32	0.13	0.10	98.29	152.2
47.97	1.48	11.89	12.13	0.13	12.66	9.81	2.24	0.15	0.08	98.54	155.9
48.10	1.54	12.11	12.10	0.20	12.38	9.91	2.26	0.12	0.23	98.96	158.1
48.12	1.45	11.95	12.06	0.25	12.79	9.67	2.20	0.16	0.16	98.81	161.4
47.91	1.51	12.27	12.04	0.22	12.29	9.97	2.24	0.14	0.09	98.68	169.8
48.01	1.54	12.17	12.02	0.17	12.31	9.81	2.27	0.12	0.10	98.50	170.5
48.00	1.52	12.25	12.05	0.23	12.19	9.98	2.27	0.17	0.17	98.84	175.4
48.27	1.44	12.17	12.50	0.12	12.59	9.72	2.21	0.15	0.08	99.26	178.9
47.99	1.49	12.38	12.03	0.13	12.10	9.93	2.36	0.13	0.14	98.67	184.9
48.38	1.51	12.46	11.81	0.16	11.78	9.90	2.26	0.16	0.16	98.57	187.4
47.98	1.49	12.31	11.89	0.22	11.95	10.02	2.36	0.18	0.09	98.50	192.8
48.14	1.51	12.55	11.99	0.15	11.86	10.14	2.36	0.21	0.15	99.05	199.5
48.08	1.56	12.29	11.81	0.33	11.61	9.93	2.32	0.18	0.16	98.27	205.2
48.32	1.54	12.56	11.79	0.30	11.72	9.97	2.37	0.16	0.09	98.82	210.0
48.06	1.49	12.50	11.63	0.08	11.68	9.88	2.27	0.18	0.13	97.89	211.8
48.42	1.54	12.67	11.94	0.23	11.47	10.01	2.27	0.15	0.11	98.81	222.8
48.21	1.49	12.58	11.82	0.13	11.48	10.01	2.43	0.16	0.10	98.41	225.7
48.34	1.54	12.67	11.81	0.16	11.47	9.97	2.39	0.15	0.20	98.68	227.3
48.20	1.57	12.64	11.85	0.13	11.00	10.09	2.39	0.18	0.16	98.20	239.7
48.23	1.58	12.71	11.64	0.19	11.18	10.04	2.41	0.19	0.17	98.33	240.5
48.16	1.56	12.77	11.64	0.19	11.17	10.11	2.41	0.17	0.11	98.27	244.6
48.75	1.59	12.88	11.65	0.20	10.98	10.24	2.42	0.12	0.16	98.98	253.7
48.58	1.51	12.83	11.76	0.21	10.89	10.10	2.44	0.18	0.08	98.57	258.2
48.37	1.53	12.97	11.57	0.15	10.77	10.12	2.41	0.16	0.15	98.19	261.8
48.45	1.59	13.09	11.74	0.30	10.76	10.22	2.42	0.13	0.13	98.82	267.7
48.62	1.53	12.94	11.59	0.17	10.67	10.31	2.43	0.16	0.09	98.51	275.8
48.59	1.57	12.89	11.70	0.14	10.61	10.26	2.51	0.15	0.16	98.59	279.1
48.86	1.56	13.23	11.63	0.21	10.62	10.18	2.59	0.19	0.12	99.18	281.7
48.55	1.60	13.18	11.65	0.15	10.31	10.27	2.53	0.17	0.06	98.48	293.6
48.72	1.62	13.15	11.54	0.18	10.32	10.28	2.50	0.19	0.18	98.68	295.6
48.68	1.56	13.12	11.52	0.16	10.39	10.20	2.46	0.21	0.19	98.49	296.3
48.83	1.59	13.25	11.68	0.26	10.19	10.23	2.66	0.20	0.11	98.99	309.6
48.91	1.57	13.28	11.58	0.18	10.16	10.33	2.55	0.15	0.13	98.83	311.2
48.53	1.60	13.31	11.39	0.20	10.16	10.27	2.53	0.22	0.09	98.28	313.6
48.80	1.64	13.25	11.59	0.19	9.89	10.25	2.68	0.18	0.12	98.59	323.6
48.83	1.58	13.36	11.33	0.23	9.88	10.22	2.65	0.18	0.21	98.46	328.9
49.04	1.66	13.45	11.57	0.15	10.02	10.28	2.61	0.15	0.09	99.01	330.9
49.13	1.61	13.46	11.61	0.20	9.82	10.28	2.62	0.19	0.08	98.99	337.6
49.02	1.70	13.44	11.59	0.23	9.76	10.35	2.45	0.20	0.15	98.89	348.1
48.68	1.60	13.37	11.43	0.26	9.42	10.42	2.59	0.16	0.10	98.01	359.0
49.11	1.75	13.84	11.45	0.13	9.56	10.50	2.71	0.17	0.06	99.27	363.1
48.98	1.65	13.49	11.47	0.16	9.53	10.39	2.65	0.18	0.08	98.57	364.2
48.90	1.67	13.40	11.39	0.21	9.55	10.48	2.51	0.21	0.13	98.44	365.4
49.29	1.73	13.73	11.35	0.10	9.40	10.57	2.72	0.19	0.10	99.18	371.5
49.04	1.68	13.75	11.39	0.25	9.23	10.39	2.74	0.18	0.08	98.71	383.1
49.23	1.74	13.56	11.46	0.09	9.05	10.38	2.72	0.20	0.06	98.48	388.3
48.94	1.73	13.70	11.29	0.19	9.06	10.56	2.74	0.17	0.14	98.52	396.0
49.44	1.70	13.72	11.34	0.26	8.96	10.43	2.71	0.19	0.07	98.81	407.3

49.35	1.74	13.83	11.46	0.22	8.82	10.56	2.71	0.17	0.10	98.96	413.6
49.13	1.76	13.74	11.31	0.26	8.81	10.65	2.65	0.20	0.14	98.63	420.4
49.21	1.72	13.75	11.67	0.19	8.63	10.64	2.68	0.19	0.12	98.79	431.3
49.42	1.78	13.83	11.37	0.14	8.67	10.51	2.77	0.20	0.09	98.76	438.8
49.42	1.75	13.77	11.46	0.17	8.64	10.64	2.74	0.21	0.20	98.99	444.9
49.32	1.69	13.93	11.35	0.19	8.56	10.43	2.71	0.18	0.18	98.53	455.5
49.17	1.75	13.85	11.36	0.21	8.45	10.62	2.75	0.16	0.09	98.40	469.5
49.46	1.65	13.90	11.58	0.23	8.37	10.51	2.74	0.17	0.14	98.76	479.6
49.51	1.81	13.83	11.48	0.19	8.21	10.62	2.78	0.18	0.11	98.74	489.1
49.31	1.86	13.88	11.47	0.21	8.30	10.65	2.73	0.19	0.04	98.62	494.0
49.50	1.72	13.88	11.61	0.12	8.22	10.55	2.77	0.20	0.06	98.62	503.7
49.36	1.85	13.95	11.49	0.28	8.06	10.79	2.80	0.19	0.11	98.89	514.3
49.16	1.73	13.96	11.57	0.17	8.13	10.72	2.78	0.17	0.16	98.55	515.2
49.54	1.80	14.04	11.44	0.24	8.16	10.81	2.77	0.19	0.13	99.12	518.4
49.44	1.85	14.25	11.64	0.21	8.05	10.87	2.77	0.18	0.14	99.39	526.5
49.34	1.67	13.83	11.51	0.19	7.98	10.72	2.78	0.18	0.15	98.33	527.8
49.45	1.83	14.09	11.63	0.07	7.99	10.86	2.81	0.23	0.13	99.10	534.5
49.39	1.80	13.95	11.68	0.09	7.98	10.67	2.70	0.17	0.15	98.57	539.5
49.36	1.79	14.07	11.48	0.20	8.04	10.74	2.83	0.18	0.12	98.81	542.9
49.46	1.76	14.08	11.57	0.15	7.77	10.84	2.77	0.15	0.18	98.73	552.4
49.29	1.88	13.97	11.60	0.15	7.82	10.94	2.73	0.18	0.10	98.65	565.0
49.36	1.85	14.08	11.54	0.18	7.73	11.00	2.77	0.23	0.22	98.94	575.0
49.30	1.76	13.91	11.58	0.20	7.77	10.85	2.75	0.18	0.06	98.36	589.7
49.33	1.88	13.98	11.63	0.20	7.65	10.83	2.76	0.23	0.13	98.61	603.6
49.29	1.85	13.92	11.78	0.16	7.62	10.87	2.78	0.19	0.17	98.62	615.3
49.07	1.90	13.95	11.73	0.24	7.44	10.98	2.73	0.16	0.09	98.28	642.2
49.24	1.85	13.73	11.86	0.21	7.55	10.94	2.76	0.19	0.19	98.50	655.8
49.73	1.75	13.98	11.88	0.21	7.45	10.75	2.74	0.20	0.10	98.78	664.2
49.36	1.85	13.93	11.74	0.23	7.50	10.99	2.81	0.19	0.05	98.65	680.8
49.23	1.87	14.01	11.91	0.23	7.38	11.01	2.78	0.15	0.16	98.72	696.2
49.41	1.72	13.87	11.97	0.16	7.32	10.87	2.75	0.13	0.18	98.38	701.6
49.07	1.88	13.78	12.08	0.20	7.17	11.11	2.72	0.18	0.14	98.33	712.6
49.32	1.89	14.00	11.93	0.29	7.33	10.94	2.82	0.19	0.16	98.88	736.7
49.35	1.89	14.05	12.04	0.20	7.34	11.20	2.80	0.20	0.20	99.27	740.5
49.43	1.85	14.12	12.08	0.13	7.34	11.02	2.78	0.24	0.17	99.15	741.1
49.26	1.86	13.91	11.93	0.20	7.33	11.08	2.77	0.14	0.13	98.60	758.0
49.12	1.93	13.95	11.91	0.21	7.35	11.25	2.81	0.20	0.10	98.83	777.1
49.08	1.75	14.05	12.00	0.20	7.24	10.91	2.74	0.17	0.10	98.23	794.1
49.29	1.90	13.89	11.86	0.26	7.28	11.03	2.81	0.16	0.18	98.66	796.6
49.48	1.73	13.98	11.85	0.18	7.28	10.88	2.69	0.16	0.14	98.36	827.0
49.23	1.82	13.94	11.80	0.19	7.21	11.11	2.84	0.17	0.15	98.46	840.4
49.14	1.82	13.92	11.98	0.19	7.05	11.00	2.82	0.20	0.12	98.23	841.2
49.42	1.79	14.02	11.86	0.11	7.24	11.08	2.82	0.19	0.07	98.61	860.0
49.47	1.74	14.03	11.92	0.22	7.24	11.08	2.84	0.20	0.17	98.90	883.0
49.21	1.79	13.98	12.00	0.19	7.14	11.09	2.75	0.19	0.20	98.54	939.7
49.19	1.83	13.97	12.02	0.19	7.05	11.18	2.77	0.21	0.23	98.64	941.9
49.22	1.76	13.96	12.16	0.20	7.15	11.02	2.76	0.13	0.16	98.52	976.5
49.00	1.80	13.85	12.09	0.18	7.09	11.15	2.72	0.18	0.18	98.24	1039.0
48.82	1.81	13.77	12.03	0.19	7.04	11.24	2.82	0.18	0.16	98.05	1042.5

49.52	1.75	14.05	12.10	0.22	7.13	11.09	2.77	0.16	0.17	98.96	1070.0
49.06	1.85	14.04	12.09	0.15	7.17	11.16	2.68	0.16	0.15	98.52	1143.2
49.31	1.75	14.11	12.05	0.28	7.22	10.94	2.73	0.19	0.09	98.66	1163.5
49.30	1.80	13.93	12.08	0.18	7.08	11.12	2.73	0.19	0.09	98.48	1237.7
49.20	1.87	14.03	11.98	0.28	7.23	11.20	2.73	0.17	0.09	98.78	1243.8
49.05	1.81	13.89	11.89	0.16	7.14	11.02	2.71	0.18	0.09	97.95	1257.1
49.26	1.82	14.01	12.10	0.20	7.06	11.04	2.72	0.16	0.14	98.51	1337.0
49.37	1.85	13.78	11.93	0.18	7.07	11.24	2.65	0.16	0.16	98.38	1344.5
49.59	1.76	13.98	11.89	0.19	7.15	11.03	2.67	0.19	0.13	98.57	1350.6

Appendix C
Fittings to Composition Profiles of Olivine Dissolution in Basalt

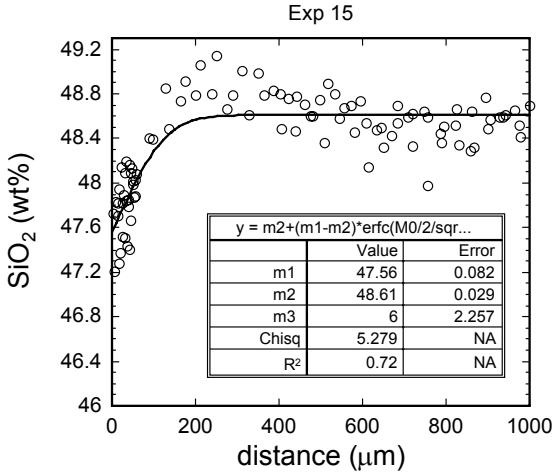

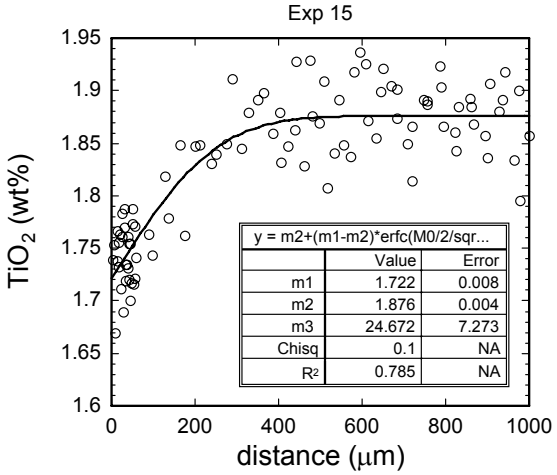

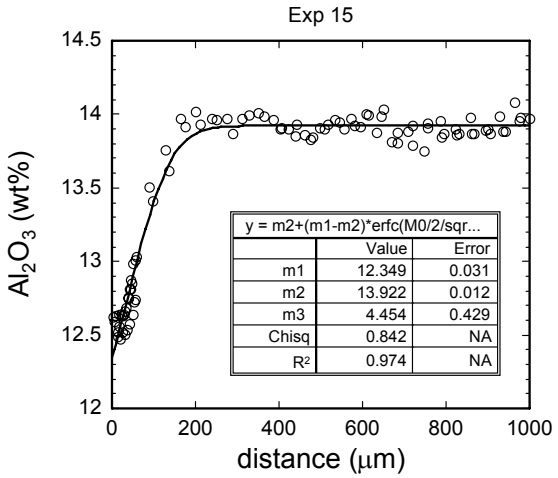

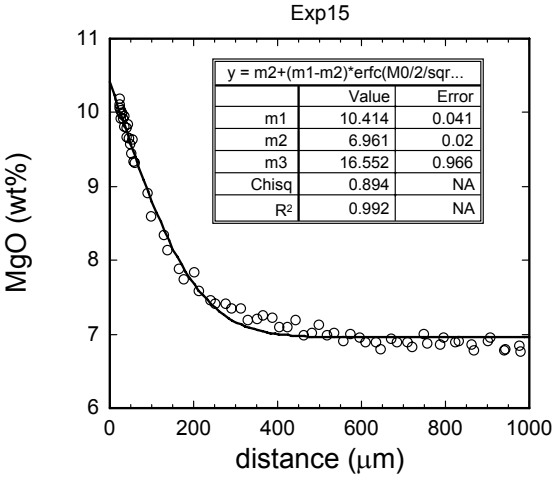

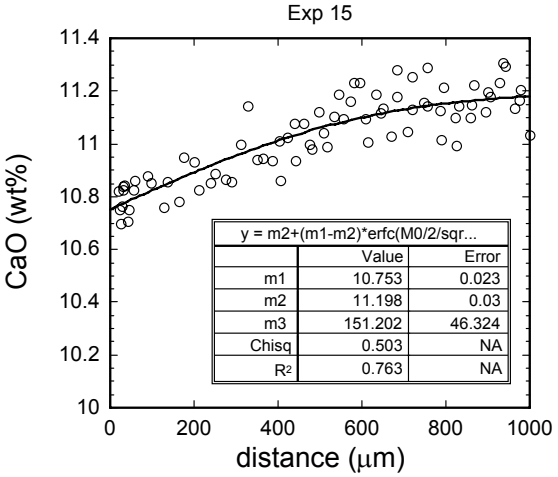

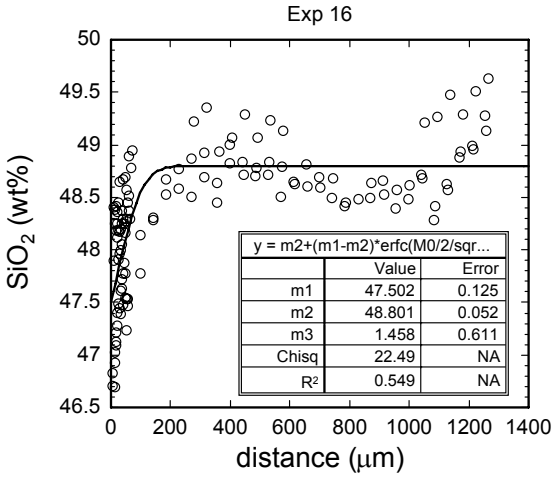
Exp 16
SiO2 (wt%)
distance (μm)
y = m2+(m1-m2)*erfc(M0/2/sqr...
Value Error
m1 47.502 0.125
m2 48.801 0.052
m3 1.458 0.611
Chisq 22.49 NA
R² 0.549 NA

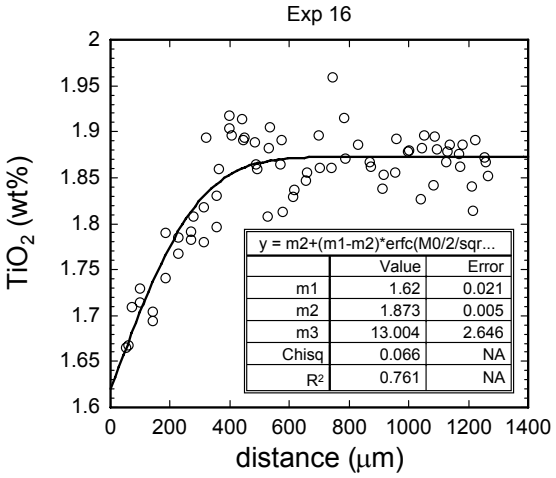
Exp 16
TiO2 (wt%)
distance (μm)
y = m2+(m1-m2)*erfc(M0/2/sqr...
Value Error
m1 1.62 0.021
m2 1.873 0.005
m3 13.004 2.646
Chisq 0.066 NA
R² 0.761 NA

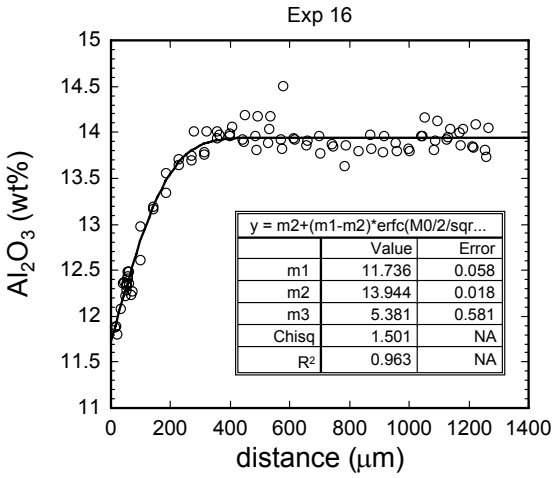
Exp 16
Al2O3 (wt%)
distance (μm)
y = m2+(m1-m2)*erfc(M0/2/sqr...
Value Error
m1 11.736 0.058
m2 13.944 0.018
m3 5.381 0.581
Chisq 1.501 NA
R² 0.963 NA

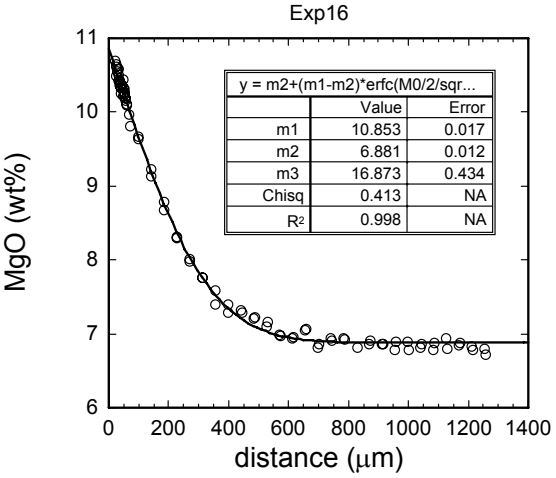
Exp16
MgO (wt%)
distance (μm)
y = m2+(m1-m2)*erfc(M0/2/sqr...
Value Error
m1 10.853 0.017
m2 6.881 0.012
m3 16.873 0.434
Chisq 0.413 NA
R² 0.998 NA

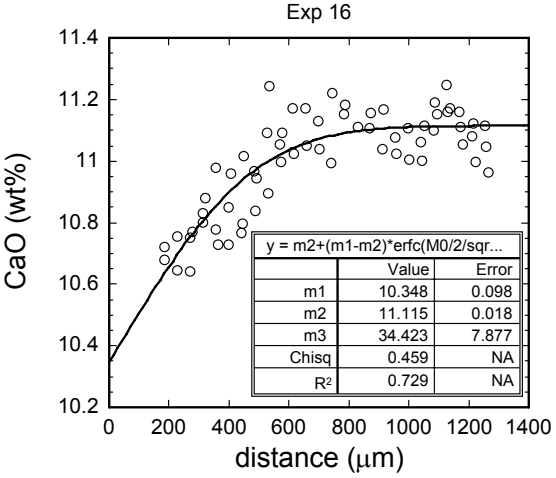
Exp 16
CaO (wt%)
distance (μm)
y = m2+(m1-m2)*erfc(M0/2/sqr...
Value Error
m1 10.348 0.098
m2 11.115 0.018
m3 34.423 7.877
Chisq 0.459 NA
R² 0.729 NA

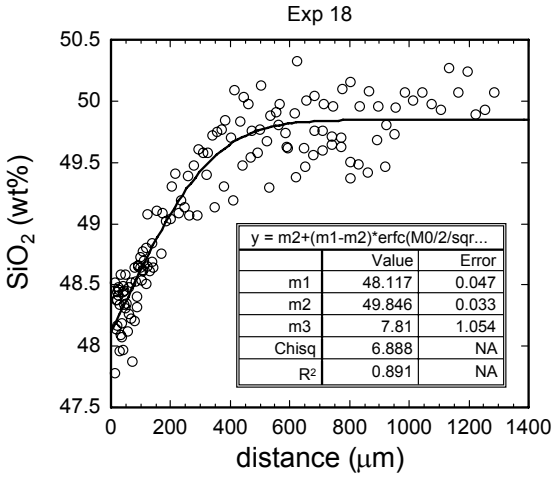
Exp 18
SiO2 (wt%)
distance (μm)
y = m2+(m1-m2)*erfc(M0/2/sqr...
Value Error
m1 48.117 0.047
m2 49.846 0.033
m3 7.81 1.054
Chisq 6.888 NA
R² 0.891 NA

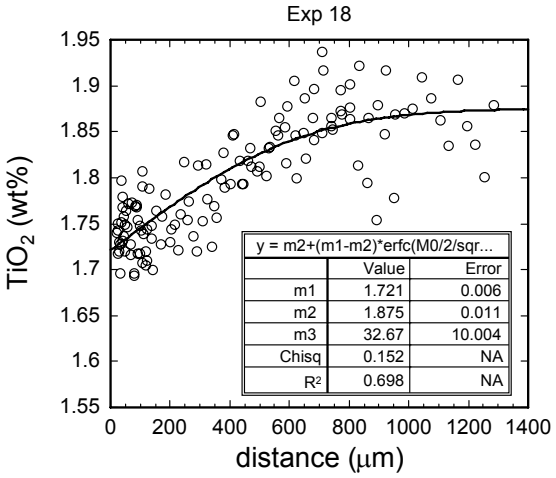
Exp 18
TiO2 (wt%)
distance (μm)
y = m2+(m1-m2)*erfc(M0/2/sqr...
Value Error
m1 1.721 0.006
m2 1.875 0.011
m3 32.67 10.004
Chisq 0.152 NA
R² 0.698 NA

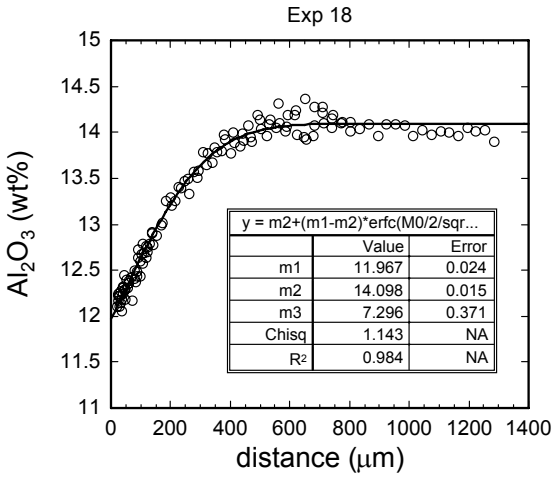
Exp 18
Al2O3 (wt%)
distance (μm)
y = m2+(m1-m2)*erfc(M0/2/sqr...
Value Error
m1 11.967 0.024
m2 14.098 0.015
m3 7.296 0.371
Chisq 1.143 NA
R² 0.984 NA

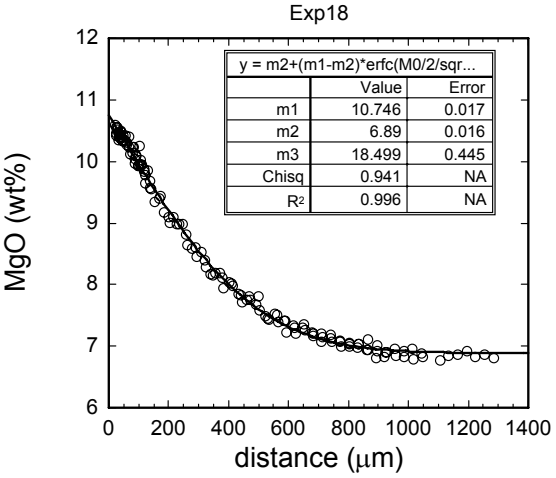
Exp18
MgO (wt%)
distance (μm)
y = m2+(m1-m2)*erfc(M0/2/sqr...
Value Error
m1 10.746 0.017
m2 6.89 0.016
m3 18.499 0.445
Chisq 0.941 NA
R² 0.996 NA

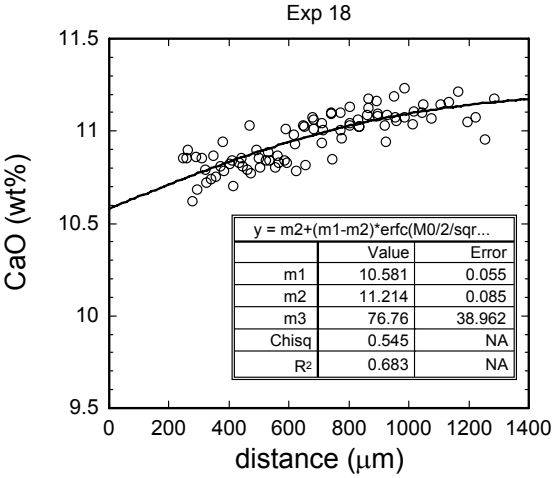
Exp 18
CaO (wt%)
distance (μm)
y = m2+(m1-m2)*erfc(M0/2/sqr...
Value Error
m1 10.581 0.055
m2 11.214 0.085
m3 76.76 38.962
Chisq 0.545 NA
R² 0.683 NA

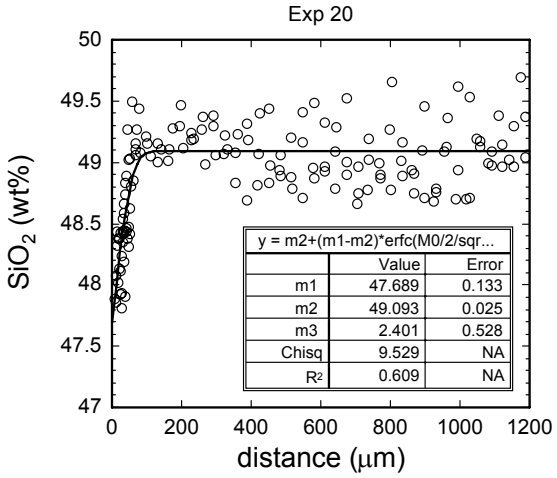
Exp 20
SiO2 (wt%)
distance (μm)
y = m2+(m1-m2)*erfc(M0/2/sqr...
Value Error
m1 47.689 0.133
m2 49.093 0.025
m3 2.401 0.528
Chisq 9.529 NA
R² 0.609 NA

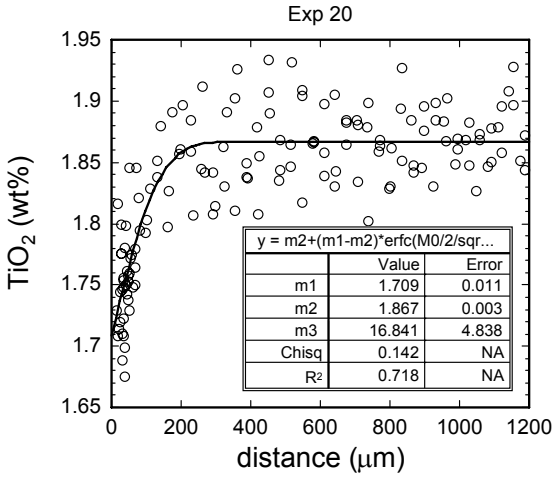
Exp 20
TiO2 (wt%)
distance (μm)
y = m2+(m1-m2)*erfc(M0/2/sqr...
Value Error
m1 1.709 0.011
m2 1.867 0.003
m3 16.841 4.838
Chisq 0.142 NA
R² 0.718 NA

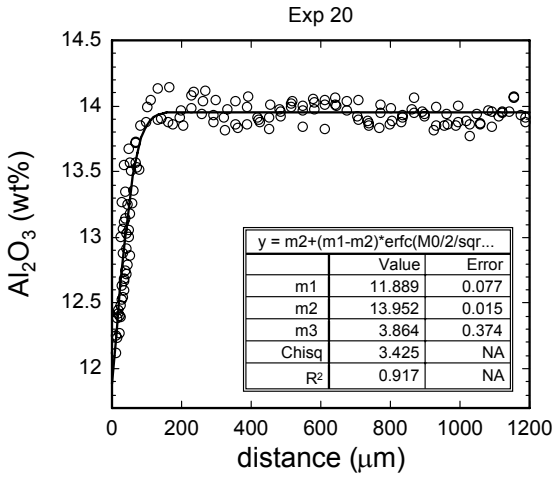
Exp 20
Al2O3 (wt%)
distance (μm)
y = m2+(m1-m2)*erfc(M0/2/sqr...
Value Error
m1 11.889 0.077
m2 13.952 0.015
m3 3.864 0.374
Chisq 3.425 NA
R² 0.917 NA

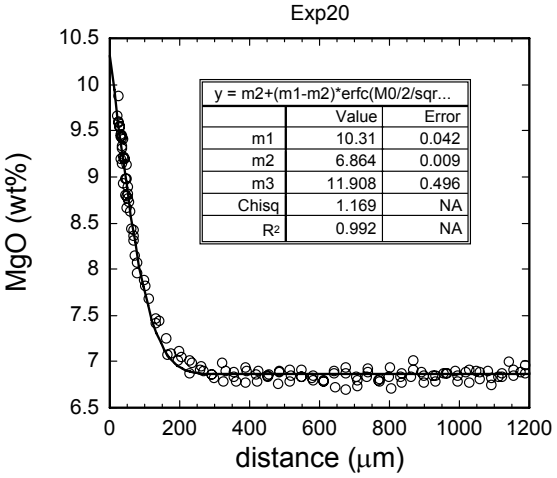
Exp20
MgO (wt%)
distance (μm)
y = m2+(m1-m2)*erfc(M0/2/sqr...
Value Error
m1 10.31 0.042
m2 6.864 0.009
m3 11.908 0.496
Chisq 1.169 NA
R² 0.992 NA

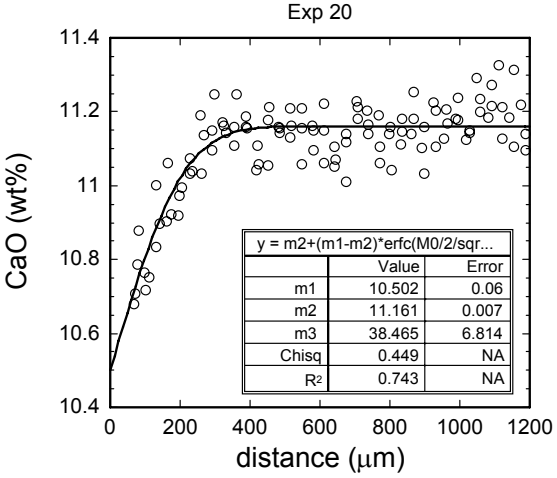
Exp 20
CaO (wt%)
distance (μm)
y = m2+(m1-m2)*erfc(M0/2/sqr...
Value Error
m1 10.502 0.06
m2 11.161 0.007
m3 38.465 6.814
Chisq 0.449 NA
R² 0.743 NA

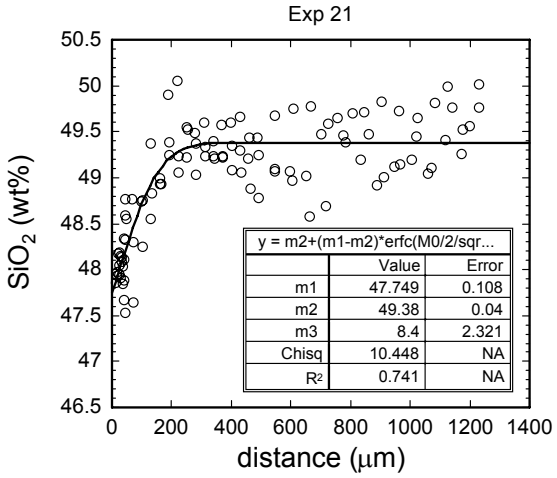
Exp 21
SiO2 (wt%)
distance (μm)
y = m2+(m1-m2)*erfc(M0/2/sqr...
Value Error
m1 47.749 0.108
m2 49.38 0.04
m3 8.4 2.321
Chisq 10.448 NA
R² 0.741 NA

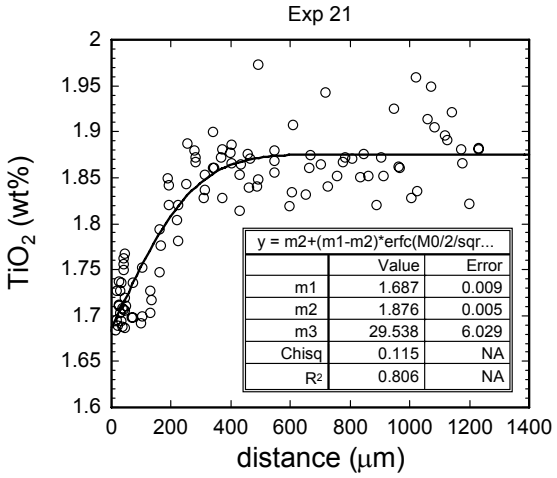
Exp 21
TiO2 (wt%)
distance (μm)
y = m2+(m1-m2)*erfc(M0/2/sqr...
Value Error
m1 1.687 0.009
m2 1.876 0.005
m3 29.538 6.029
Chisq 0.115 NA
R² 0.806 NA

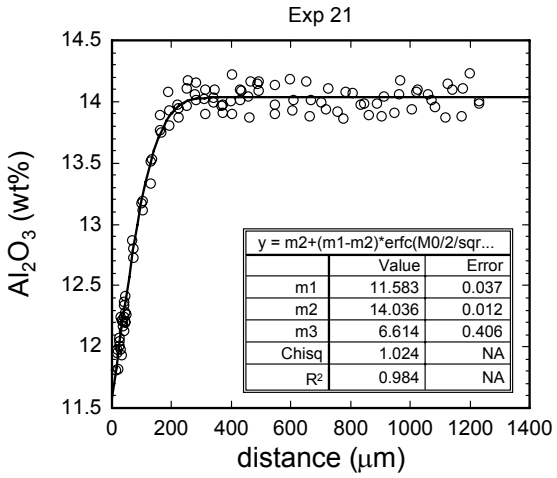
Exp 21
Al2O3 (wt%)
distance (μm)
y = m2+(m1-m2)*erfc(M0/2/sqr...
Value Error
m1 11.583 0.037
m2 14.036 0.012
m3 6.614 0.406
Chisq 1.024 NA
R² 0.984 NA

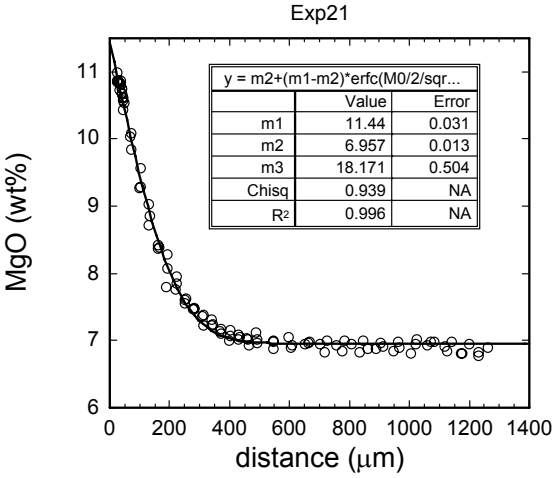
Exp21
MgO (wt%)
distance (μm)
y = m2+(m1-m2)*erfc(M0/2/sqr...
Value Error
m1 11.44 0.031
m2 6.957 0.013
m3 18.171 0.504
Chisq 0.939 NA
R² 0.996 NA

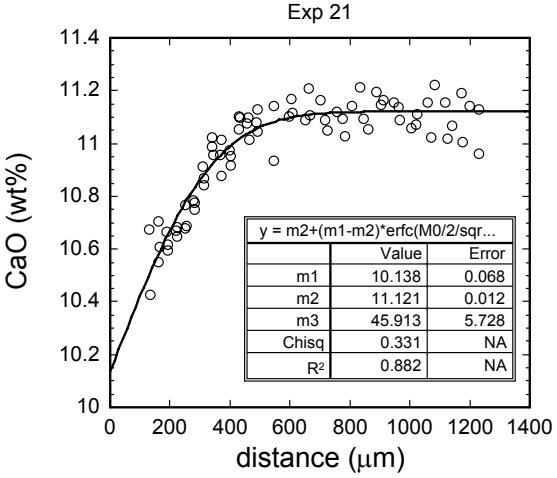
Exp 21
CaO (wt%)
distance (μm)
y = m2+(m1-m2)*erfc(M0/2/sqr...
Value Error
m1 10.138 0.068
m2 11.121 0.012
m3 45.913 5.728
Chisq 0.331 NA
R² 0.882 NA

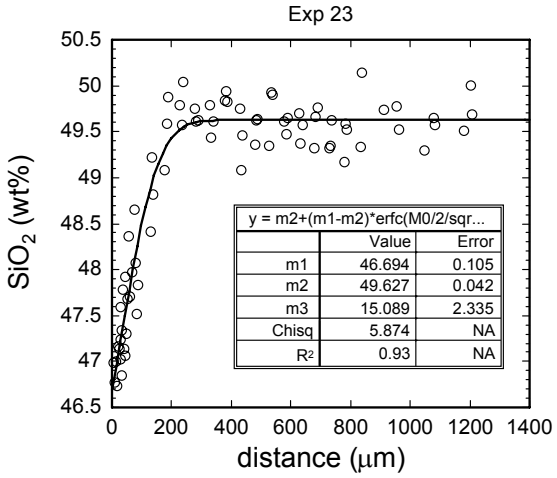
Exp 23
SiO2 (wt%)
distance (μm)
y = m2+(m1-m2)*erfc(M0/2/sqr...
Value Error
m1 46.694 0.105
m2 49.627 0.042
m3 15.089 2.335
Chisq 5.874 NA
R² 0.93 NA

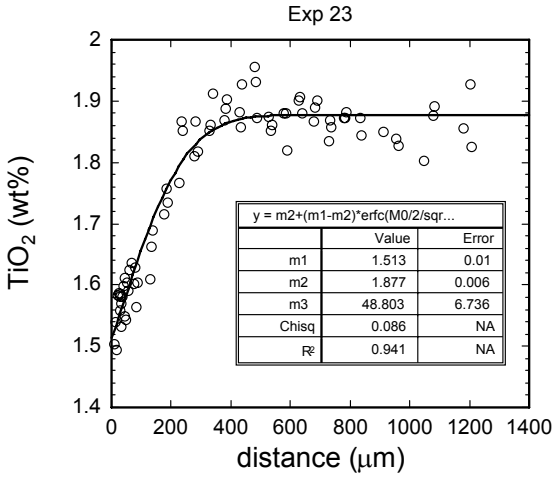
Exp 23
TiO2 (wt%)
distance (μm)
y = m2+(m1-m2)*erfc(M0/2/sqr...
Value Error
m1 1.513 0.01
m2 1.877 0.006
m3 48.803 6.736
Chisq 0.086 NA
R² 0.941 NA

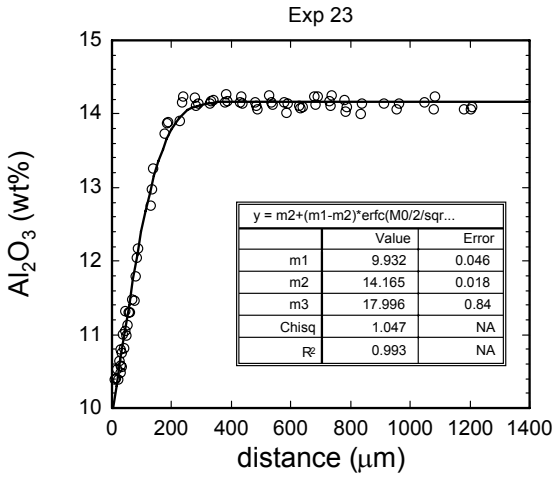
Exp 23
Al2O3 (wt%)
distance (μm)
y = m2+(m1-m2)*erfc(M0/2/sqr...
Value Error
m1 9.932 0.046
m2 14.165 0.018
m3 17.996 0.84
Chisq 1.047 NA
R² 0.993 NA

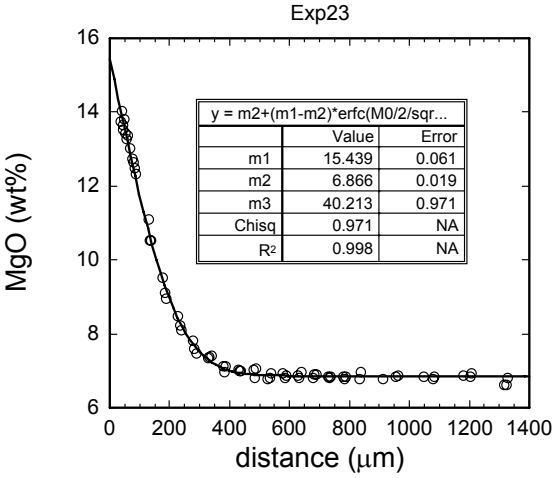
Exp23
MgO (wt%)
distance (μm)
y = m2+(m1-m2)*erfc(M0/2/sqr...
Value Error
m1 15.439 0.061
m2 6.866 0.019
m3 40.213 0.971
Chisq 0.971 NA
R² 0.998 NA

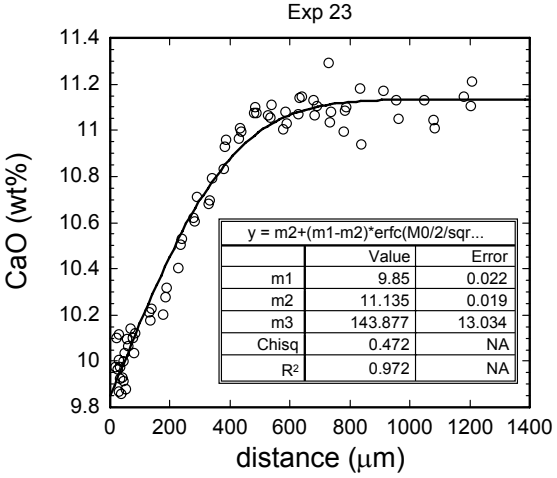
Exp 23
CaO (wt%)
distance (μm)
y = m2+(m1-m2)*erfc(M0/2/sqr...
Value Error
m1 9.85 0.022
m2 11.135 0.019
m3 143.877 13.034
Chisq 0.472 NA
R² 0.972 NA

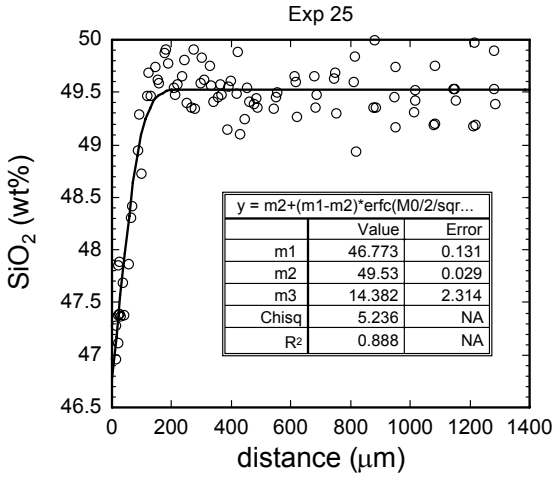
Exp 25
SiO2 (wt%)
distance (μm)
y = m2+(m1-m2)*erfc(M0/2/sqr...
Value Error
m1 46.773 0.131
m2 49.53 0.029
m3 14.382 2.314
Chisq 5.236 NA
R² 0.888 NA

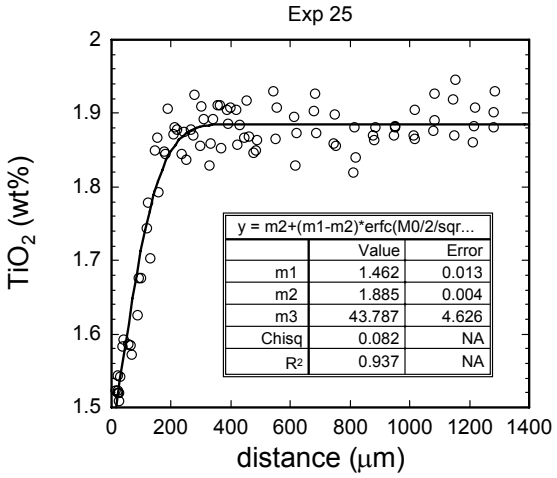
Exp 25
TiO2 (wt%)
distance (μm)
y = m2+(m1-m2)*erfc(M0/2/sqr...
Value Error
m1 1.462 0.013
m2 1.885 0.004
m3 43.787 4.626
Chisq 0.082 NA
R² 0.937 NA

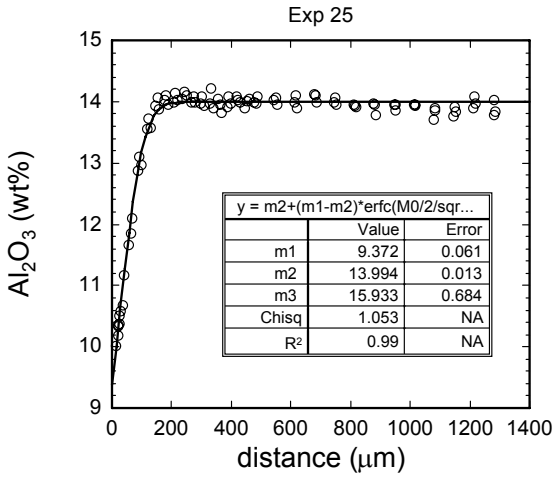
Exp 25
Al2O3 (wt%)
distance (μm)
y = m2+(m1-m2)*erfc(M0/2/sqr...
Value Error
m1 9.372 0.061
m2 13.994 0.013
m3 15.933 0.684
Chisq 1.053 NA
R² 0.99 NA

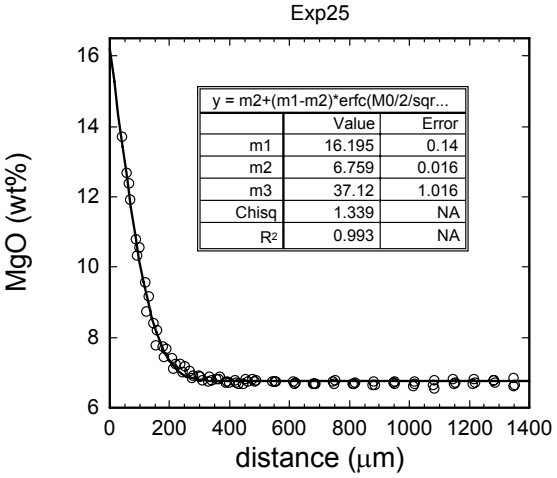
Exp25
MgO (wt%)
distance (μm)
y = m2+(m1-m2)*erfc(M0/2/sqr...
Value Error
m1 16.195 0.14
m2 6.759 0.016
m3 37.12 1.016
Chisq 1.339 NA
R² 0.993 NA

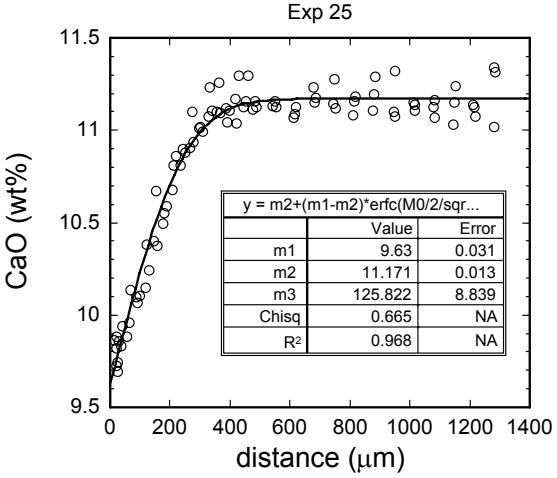
Exp 25
CaO (wt%)
distance (μm)
y = m2+(m1-m2)*erfc(M0/2/sqr...
Value Error
m1 9.63 0.031
m2 11.171 0.013
m3 125.822 8.839
Chisq 0.665 NA
R² 0.968 NA

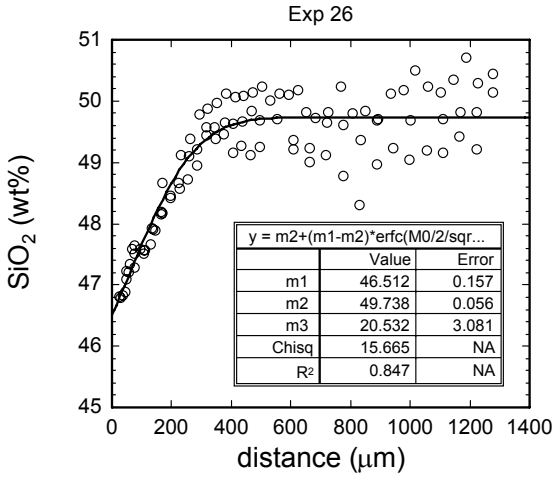
Exp 26
SiO2 (wt%)
distance (μm)
y = m2+(m1-m2)*erfc(M0/2/sqr...
Value Error
m1 46.512 0.157
m2 49.738 0.056
m3 20.532 3.081
Chisq 15.665 NA
R² 0.847 NA

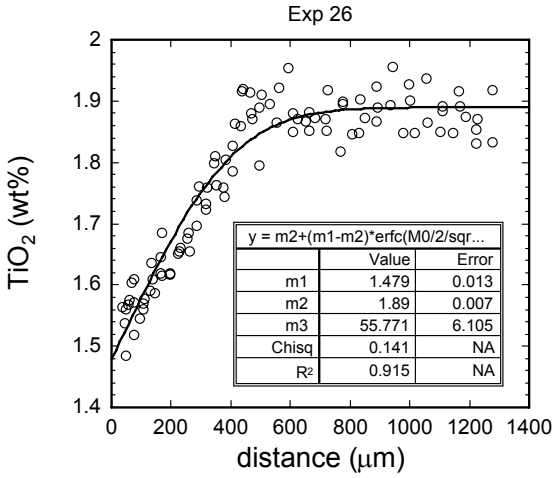
Exp 26
TiO2 (wt%)
distance (μm)
y = m2+(m1-m2)*erfc(M0/2/sqr...
Value Error
m1 1.479 0.013
m2 1.89 0.007
m3 55.771 6.105
Chisq 0.141 NA
R² 0.915 NA

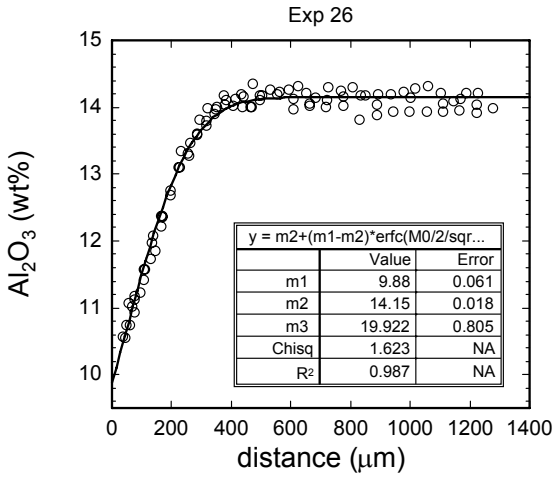
Exp 26
Al2O3 (wt%)
distance (μm)
y = m2+(m1-m2)*erfc(M0/2/sqr...
Value Error
m1 9.88 0.061
m2 14.15 0.018
m3 19.922 0.805
Chisq 1.623 NA
R² 0.987 NA

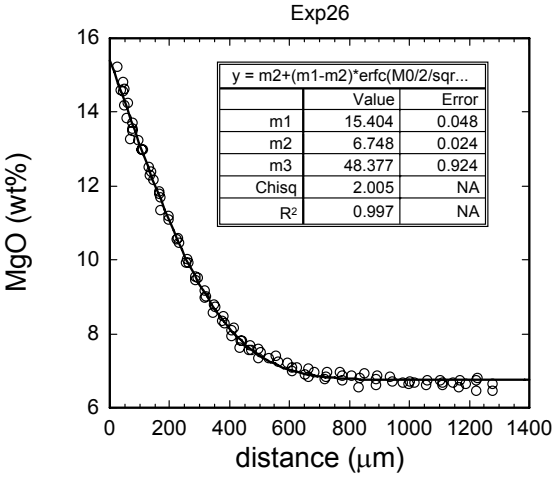
Exp26
MgO (wt%)
distance (μm)
y = m2+(m1-m2)*erfc(M0/2/sqr...
Value Error
m1 15.404 0.048
m2 6.748 0.024
m3 48.377 0.924
Chisq 2.005 NA
R² 0.997 NA

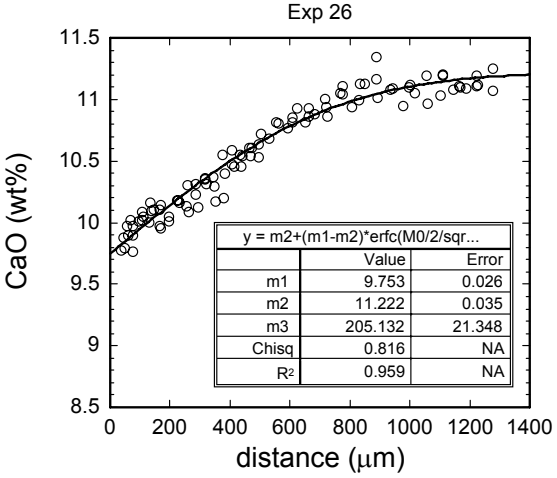
Exp 26
CaO (wt%)
distance (μm)
y = m2+(m1-m2)*erfc(M0/2/sqr...
Value Error
m1 9.753 0.026
m2 11.222 0.035
m3 205.132 21.348
Chisq 0.816 NA
R² 0.959 NA

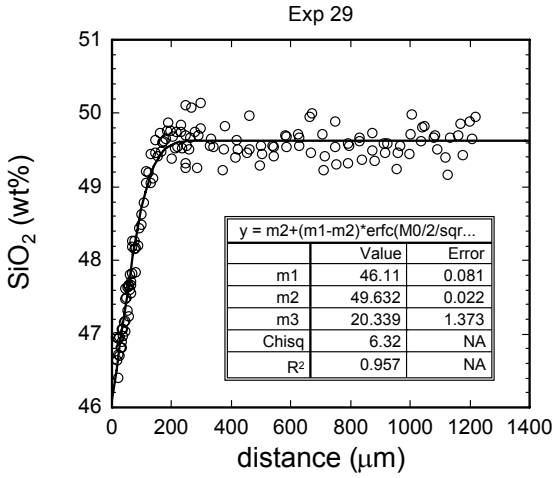
Exp 29
SiO2 (wt%)
distance (μm)
y = m2+(m1-m2)*erfc(M0/2/sqr...
Value Error
m1 46.11 0.081
m2 49.632 0.022
m3 20.339 1.373
Chisq 6.32 NA
R² 0.957 NA

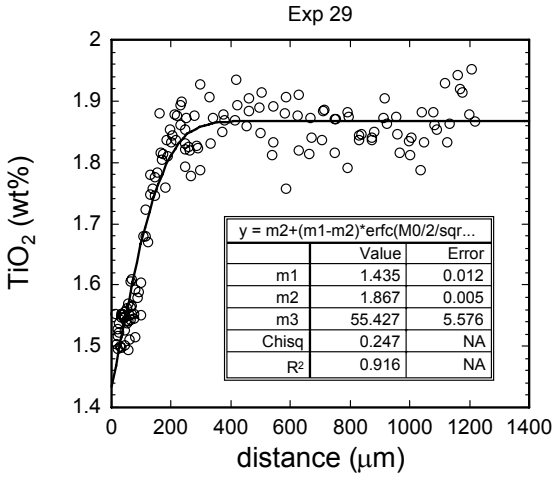
Exp 29
TiO2 (wt%)
distance (μm)
y = m2+(m1-m2)*erfc(M0/2/sqr...
Value Error
m1 1.435 0.012
m2 1.867 0.005
m3 55.427 5.576
Chisq 0.247 NA
R² 0.916 NA

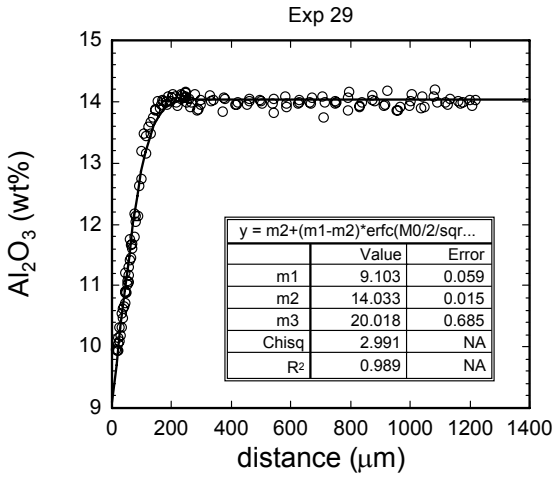
Exp 29
Al2O3 (wt%)
distance (μm)
y = m2+(m1-m2)*erfc(M0/2/sqr...
Value Error
m1 9.103 0.059
m2 14.033 0.015
m3 20.018 0.685
Chisq 2.991 NA
R² 0.989 NA

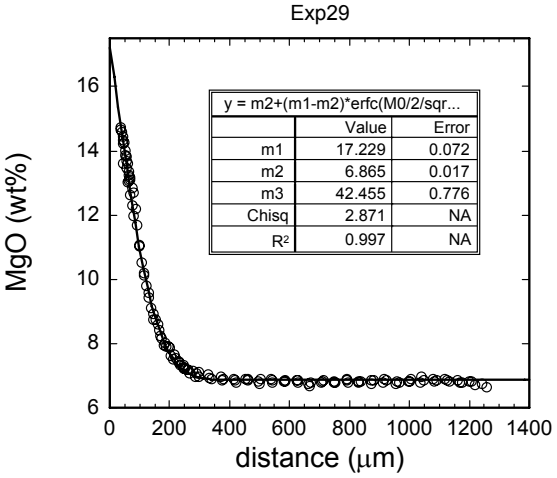
Exp29
MgO (wt%)
distance (μm)
y = m2+(m1-m2)*erfc(M0/2/sqr...
Value Error
m1 17.229 0.072
m2 6.865 0.017
m3 42.455 0.776
Chisq 2.871 NA
R² 0.997 NA

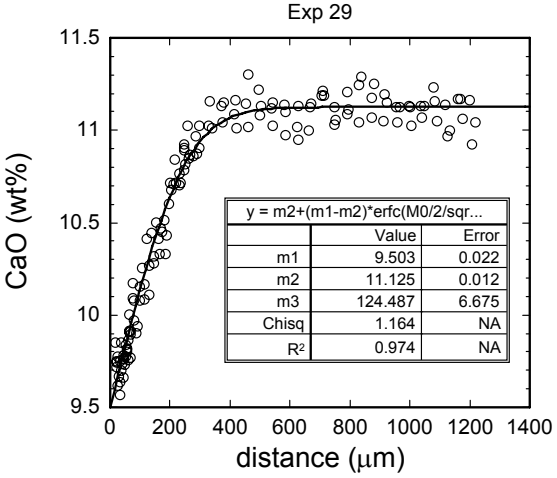
Exp 29
CaO (wt%)
distance (μm)
y = m2+(m1-m2)*erfc(M0/2/sqr...
Value Error
m1 9.503 0.022
m2 11.125 0.012
m3 124.487 6.675
Chisq 1.164 NA
R² 0.974 NA

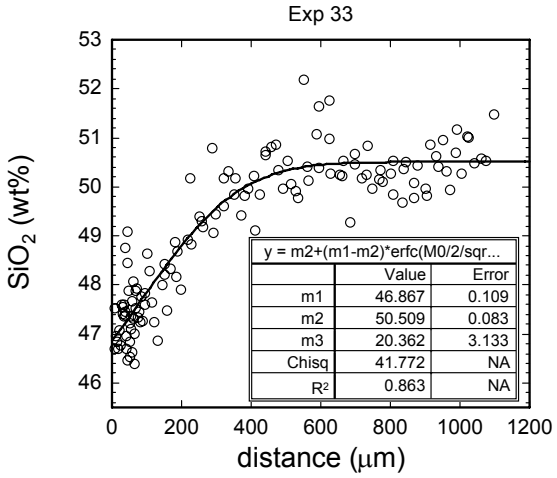
Exp 33
SiO2 (wt%)
distance (μm)
y = m2+(m1-m2)*erfc(M0/2/sqr...
Value Error
m1 46.867 0.109
m2 50.509 0.083
m3 20.362 3.133
Chisq 41.772 NA
R² 0.863 NA

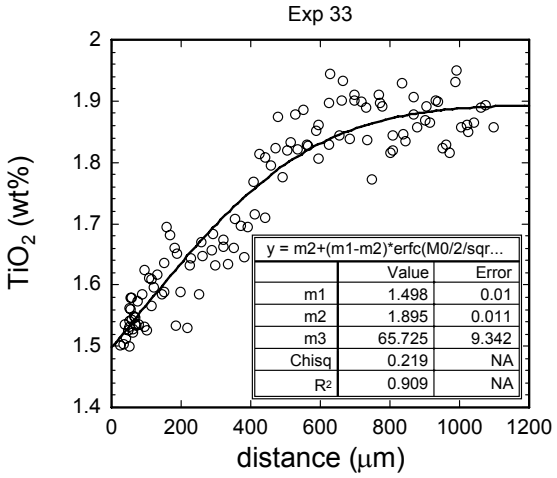
Exp 33
TiO2 (wt%)
distance (μm)
y = m2+(m1-m2)*erfc(M0/2/sqr...
Value Error
m1 1.498 0.01
m2 1.895 0.011
m3 65.725 9.342
Chisq 0.219 NA
R² 0.909 NA

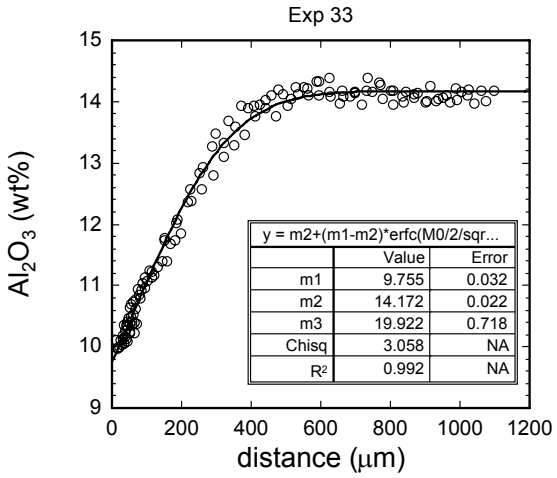
Exp 33
Al2O3 (wt%)
distance (μm)
y = m2+(m1-m2)*erfc(M0/2/sqr...
Value Error
m1 9.755 0.032
m2 14.172 0.022
m3 19.922 0.718
Chisq 3.058 NA
R² 0.992 NA

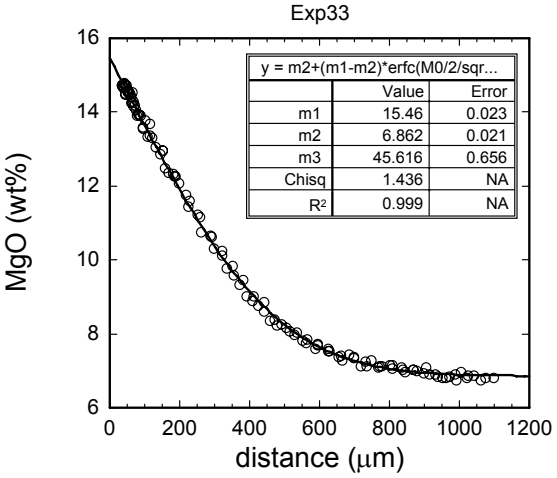
Exp33
MgO (wt%)
distance (μm)
y = m2+(m1-m2)*erfc(M0/2/sqr...
Value Error
m1 15.46 0.023
m2 6.862 0.021
m3 45.616 0.656
Chisq 1.436 NA
R² 0.999 NA

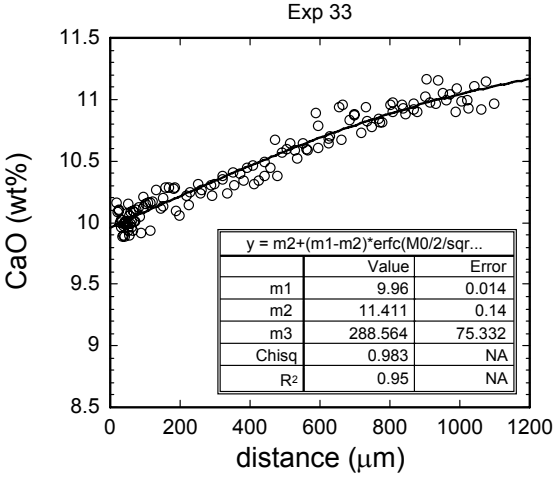
Exp 33
CaO (wt%)
distance (μm)
y = m2+(m1-m2)*erfc(M0/2/sqr...
Value Error
m1 9.96 0.014
m2 11.411 0.14
m3 288.564 75.332
Chisq 0.983 NA
R² 0.95 NA

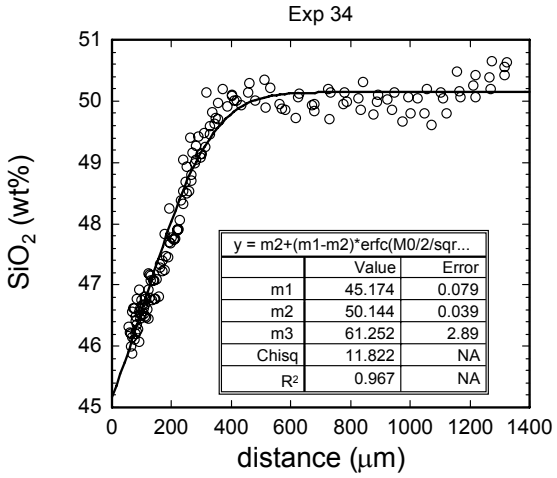
Exp 34
SiO2 (wt%)
distance (μm)
y = m2+(m1-m2)*erfc(M0/2/sqr...
Value Error
m1 45.174 0.079
m2 50.144 0.039
m3 61.252 2.89
Chisq 11.822 NA
R² 0.967 NA

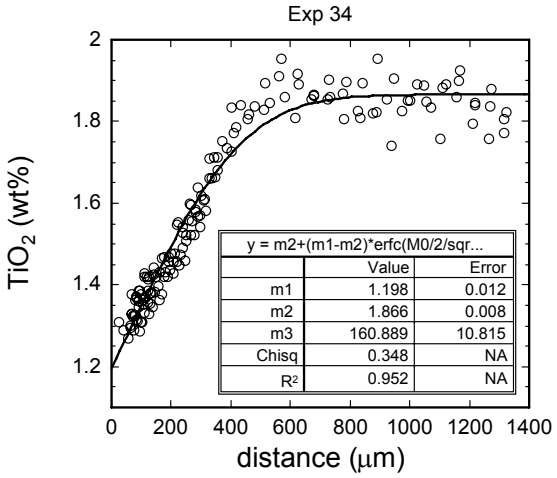
Exp 34
TiO2 (wt%)
distance (μm)
y = m2+(m1-m2)*erfc(M0/2/sqr...
Value Error
m1 1.198 0.012
m2 1.866 0.008
m3 160.889 10.815
Chisq 0.348 NA
R² 0.952 NA

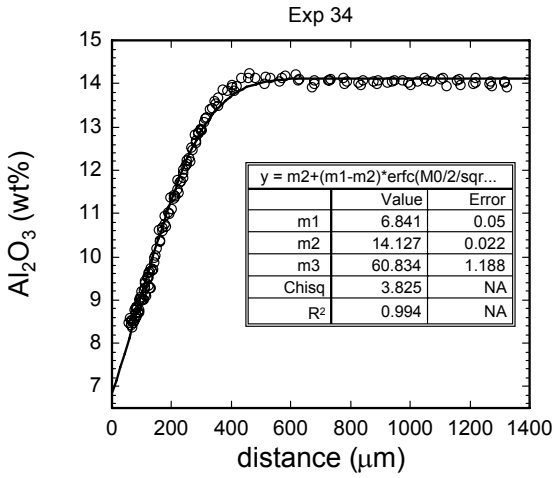
Exp 34
Al2O3 (wt%)
distance (μm)
y = m2+(m1-m2)*erfc(M0/2/sqr...
Value Error
m1 6.841 0.05
m2 14.127 0.022
m3 60.834 1.188
Chisq 3.825 NA
R² 0.994 NA

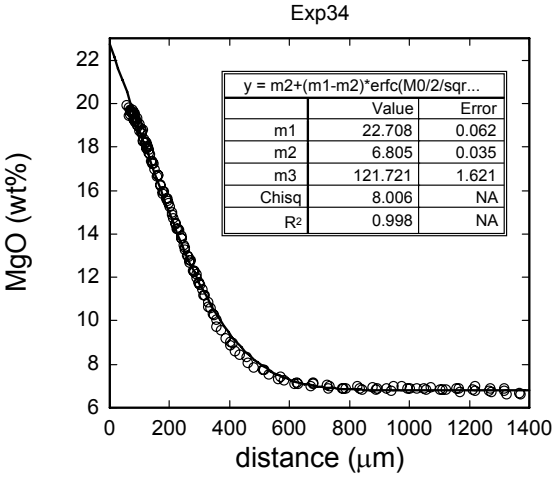
Exp34
MgO (wt%)
distance (μm)
y = m2+(m1-m2)*erfc(M0/2/sqr...
Value Error
m1 22.708 0.062
m2 6.805 0.035
m3 121.721 1.621
Chisq 8.006 NA
R² 0.998 NA

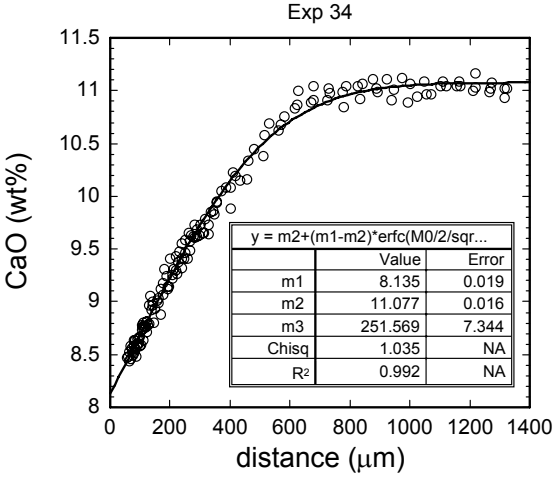
Exp 34
CaO (wt%)
distance (μm)
y = m2+(m1-m2)*erfc(M0/2/sqr...
Value Error
m1 8.135 0.019
m2 11.077 0.016
m3 251.569 7.344
Chisq 1.035 NA
R² 0.992 NA

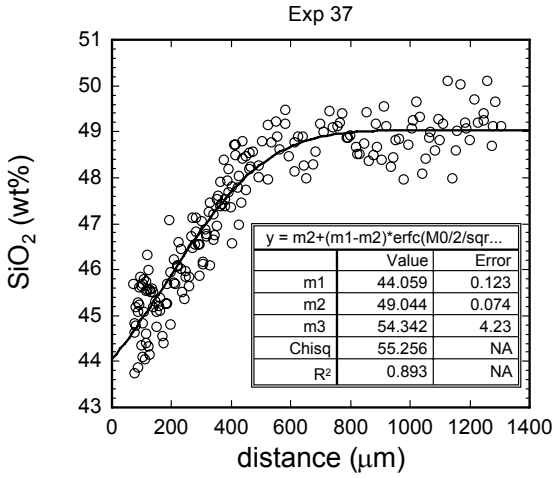
Exp 37
SiO2 (wt%)
distance (μm)
y = m2+(m1-m2)*erfc(M0/2/sqr...
Value Error
m1 44.059 0.123
m2 49.044 0.074
m3 54.342 4.23
Chisq 55.256 NA
R² 0.893 NA

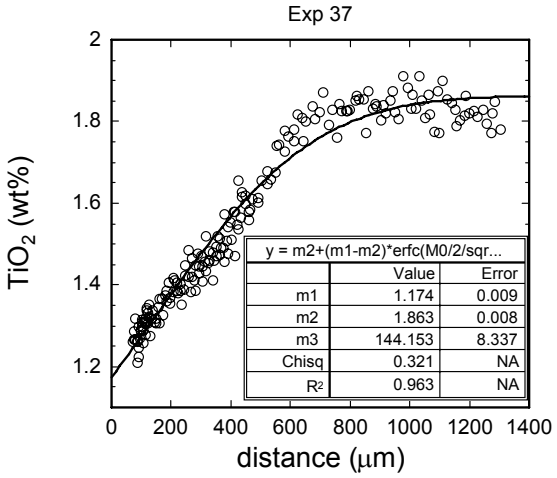
Exp 37
TiO2 (wt%)
distance (μm)
y = m2+(m1-m2)*erfc(M0/2/sqr...
Value Error
m1 1.174 0.009
m2 1.863 0.008
m3 144.153 8.337
Chisq 0.321 NA
R² 0.963 NA

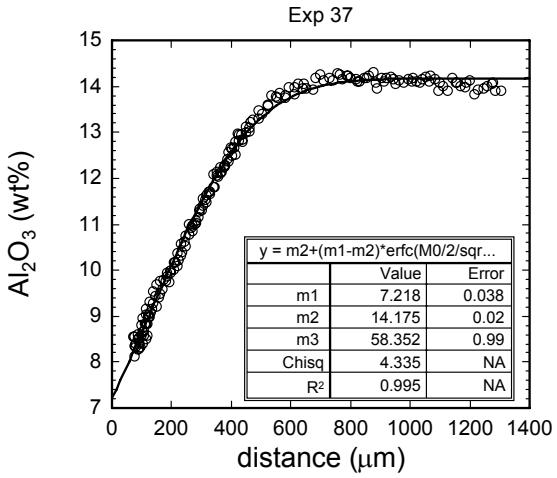
Exp 37
Al2O3 (wt%)
distance (μm)
y = m2+(m1-m2)*erfc(M0/2/sqr...
Value Error
m1 7.218 0.038
m2 14.175 0.02
m3 58.352 0.99
Chisq 4.335 NA
R² 0.995 NA

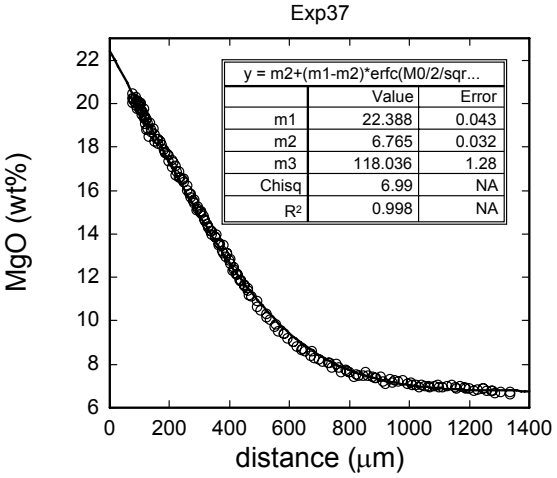
Exp37
MgO (wt%)
distance (μm)
y = m2+(m1-m2)*erfc(M0/2/sqr...
Value Error
m1 22.388 0.043
m2 6.765 0.032
m3 118.036 1.28
Chisq 6.99 NA
R² 0.998 NA

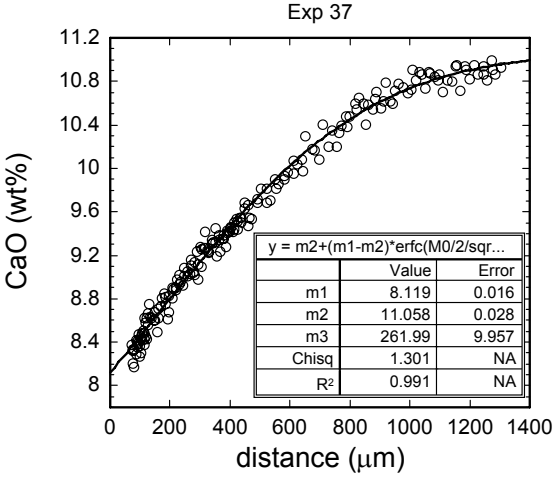
Exp 37
CaO (wt%)
distance (μm)
y = m2+(m1-m2)*erfc(M0/2/sqr...
Value Error
m1 8.119 0.016
m2 11.058 0.028
m3 261.99 9.957
Chisq 1.301 NA
R² 0.991 NA

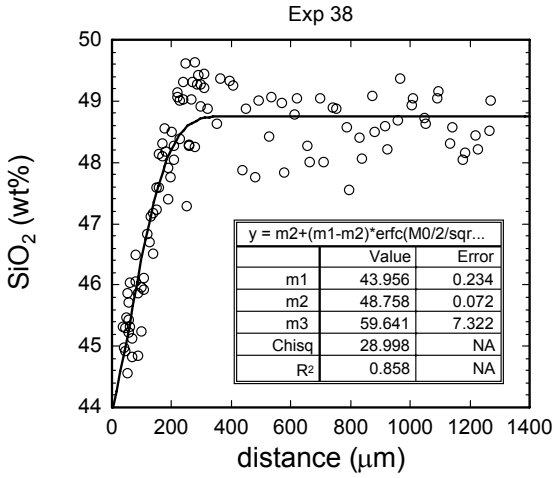
Exp 38
SiO2 (wt%)
distance (μm)
y = m2+(m1-m2)*erfc(M0/2/sqr...
Value Error
m1 43.956 0.234
m2 48.758 0.072
m3 59.641 7.322
Chisq 28.998 NA
R² 0.858 NA

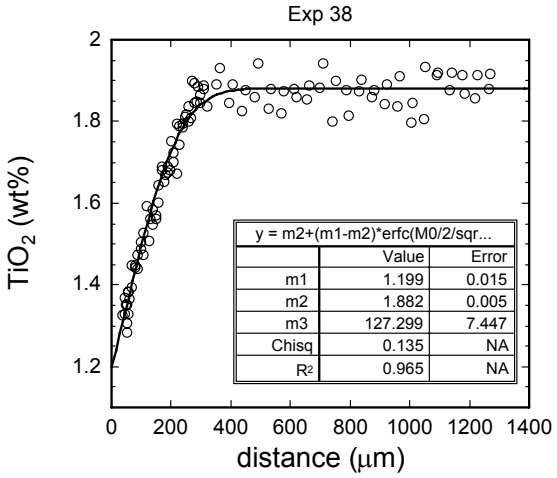
Exp 38
TiO2 (wt%)
distance (μm)
y = m2+(m1-m2)*erfc(M0/2/sqr...
Value Error
m1 1.199 0.015
m2 1.882 0.005
m3 127.299 7.447
Chisq 0.135 NA
R² 0.965 NA

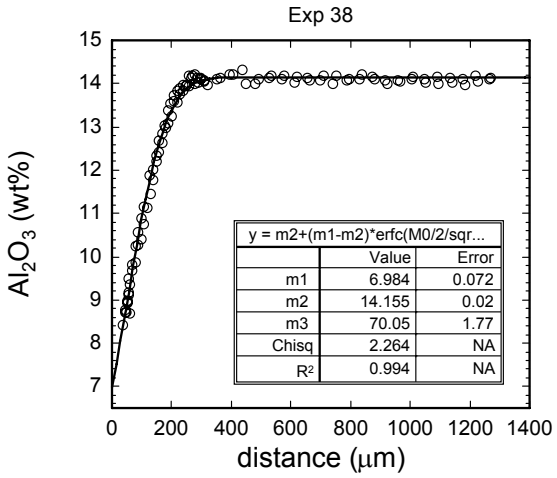
Exp 38
Al2O3 (wt%)
distance (μm)
y = m2+(m1-m2)*erfc(M0/2/sqr...
Value Error
m1 6.984 0.072
m2 14.155 0.02
m3 70.05 1.77
Chisq 2.264 NA
R² 0.994 NA

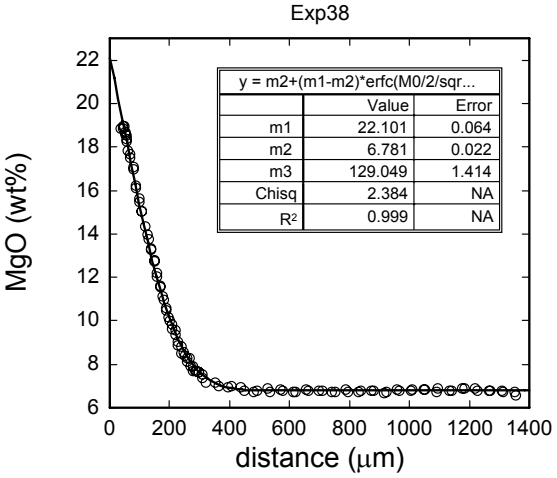
Exp38
MgO (wt%)
distance (μm)
y = m2+(m1-m2)*erfc(M0/2/sqr...
Value Error
m1 22.101 0.064
m2 6.781 0.022
m3 129.049 1.414
Chisq 2.384 NA
R² 0.999 NA

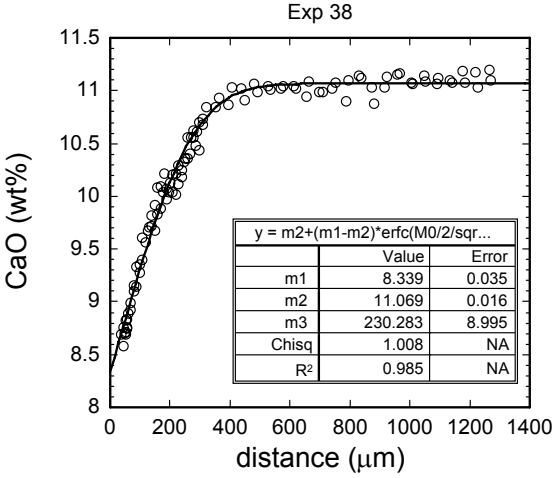
Exp 38
CaO (wt%)
distance (μm)
y = m2+(m1-m2)*erfc(M0/2/sqr...
Value Error
m1 8.339 0.035
m2 11.069 0.016
m3 230.283 8.995
Chisq 1.008 NA
R² 0.985 NA

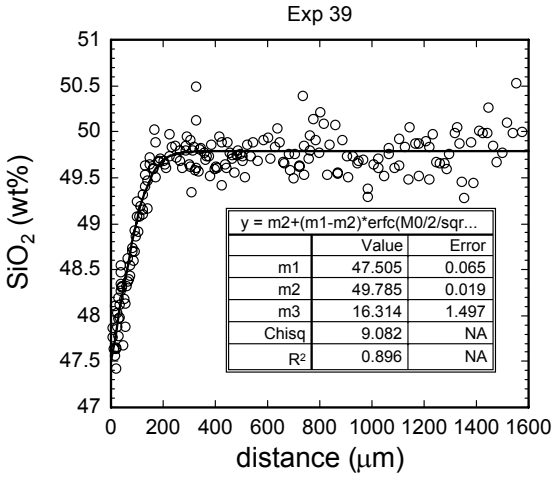
Exp 39
SiO2 (wt%)
distance (μm)
y = m2+(m1-m2)*erfc(M0/2/sqr...
Value Error
m1 47.505 0.065
m2 49.785 0.019
m3 16.314 1.497
Chisq 9.082 NA
R² 0.896 NA

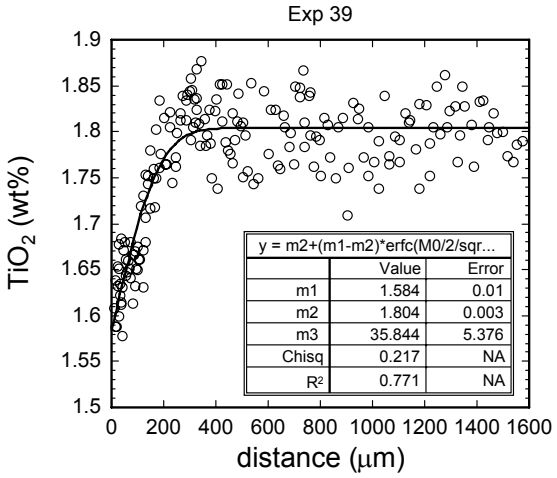
Exp 39
TiO2 (wt%)
distance (μm)
y = m2+(m1-m2)*erfc(M0/2/sqr...
Value Error
m1 1.584 0.01
m2 1.804 0.003
m3 35.844 5.376
Chisq 0.217 NA
R² 0.771 NA

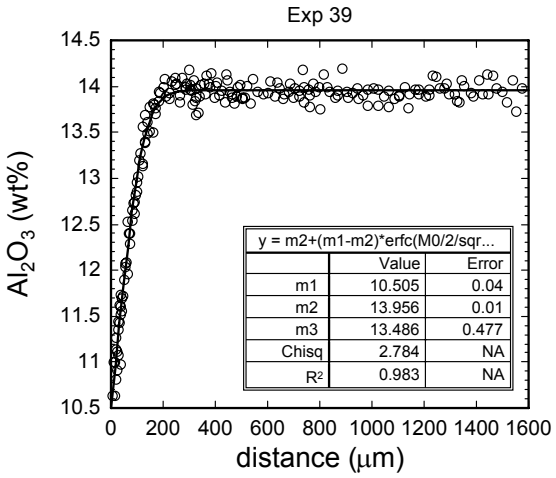
Exp 39
Al2O3 (wt%)
distance (μm)
y = m2+(m1-m2)*erfc(M0/2/sqr...
Value Error
m1 10.505 0.04
m2 13.956 0.01
m3 13.486 0.477
Chisq 2.784 NA
R² 0.983 NA

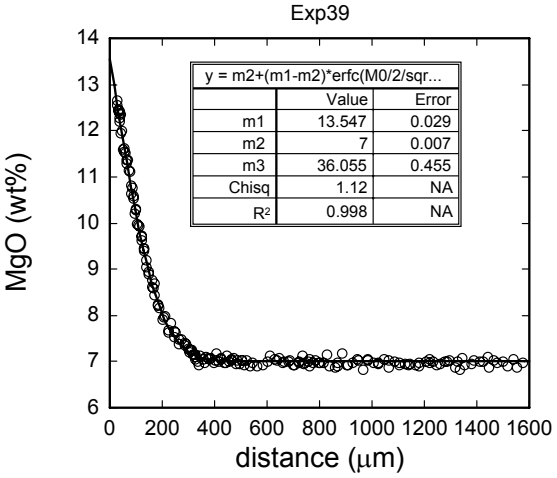
Exp39
MgO (wt%)
distance (μm)
y = m2+(m1-m2)*erfc(M0/2/sqr...
Value Error
m1 13.547 0.029
m2 7 0.007
m3 36.055 0.455
Chisq 1.12 NA
R² 0.998 NA

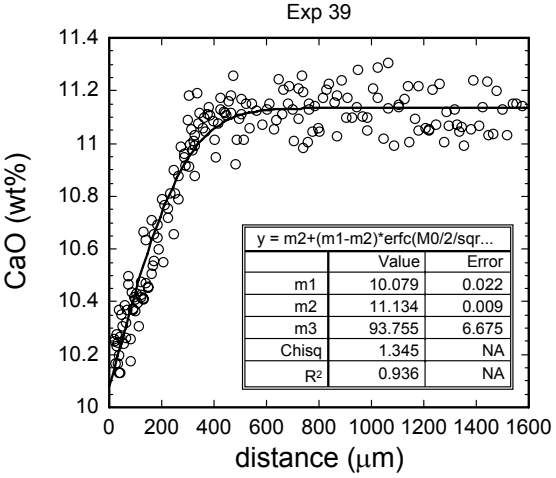
Exp 39
CaO (wt%)
distance (μm)
y = m2+(m1-m2)*erfc(M0/2/sqr...
Value Error
m1 10.079 0.022
m2 11.134 0.009
m3 93.755 6.675
Chisq 1.345 NA
R² 0.936 NA

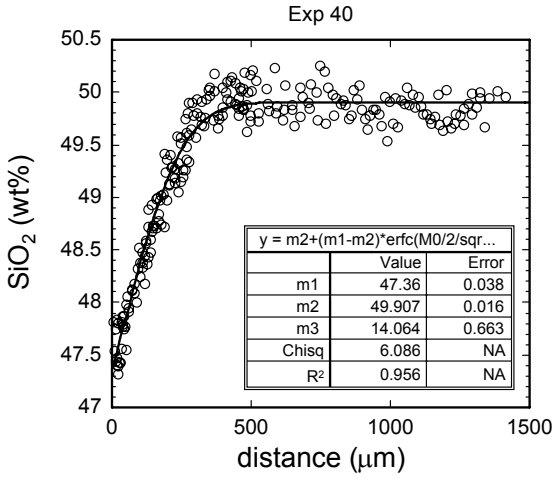
Exp 40
SiO2 (wt%)
distance (μm)
y = m2+(m1-m2)*erfc(M0/2/sqr...
Value Error
m1 47.36 0.038
m2 49.907 0.016
m3 14.064 0.663
Chisq 6.086 NA
R² 0.956 NA

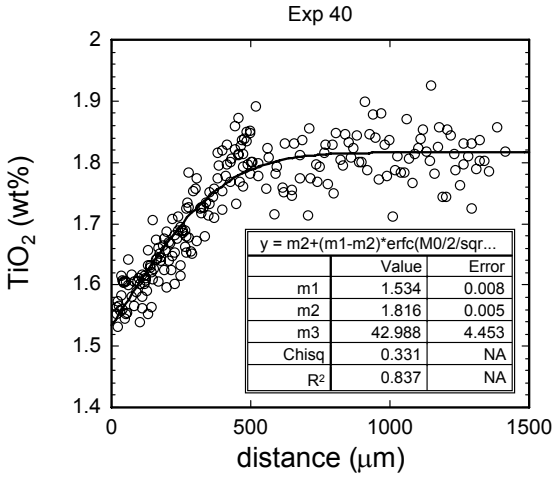
Exp 40
TiO2 (wt%)
distance (μm)
y = m2+(m1-m2)*erfc(M0/2/sqr...
Value Error
m1 1.534 0.008
m2 1.816 0.005
m3 42.988 4.453
Chisq 0.331 NA
R² 0.837 NA

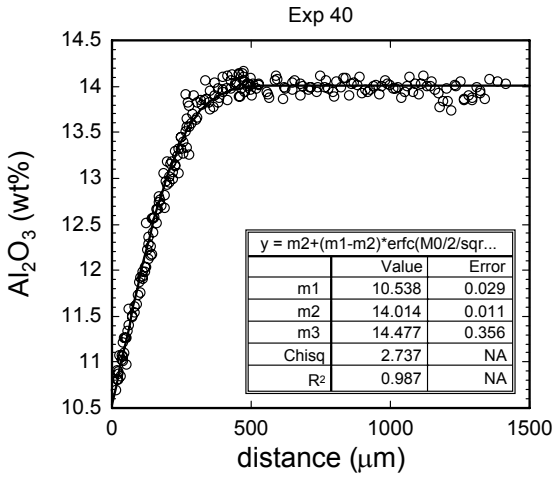
Exp 40
Al2O3 (wt%)
distance (μm)
y = m2+(m1-m2)*erfc(M0/2/sqr...
Value Error
m1 10.538 0.029
m2 14.014 0.011
m3 14.477 0.356
Chisq 2.737 NA
R² 0.987 NA

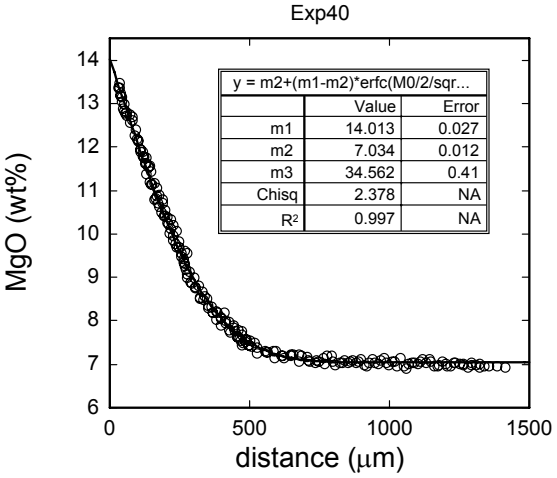
Exp40
MgO (wt%)
distance (μm)
y = m2+(m1-m2)*erfc(M0/2/sqr...
Value Error
m1 14.013 0.027
m2 7.034 0.012
m3 34.562 0.41
Chisq 2.378 NA
R² 0.997 NA

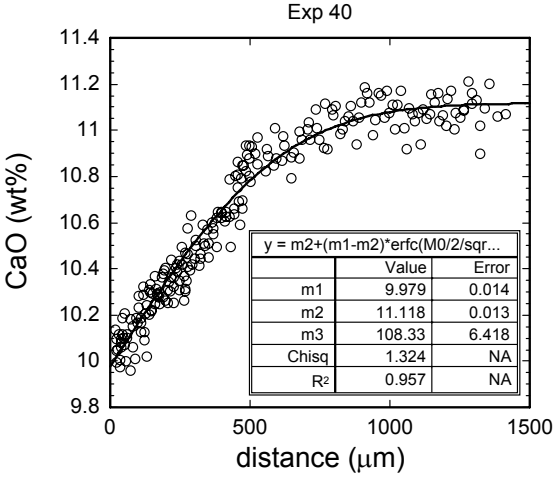
Exp 40
CaO (wt%)
distance (μm)
y = m2+(m1-m2)*erfc(M0/2/sqr...
Value Error
m1 9.979 0.014
m2 11.118 0.013
m3 108.33 6.418
Chisq 1.324 NA
R² 0.957 NA

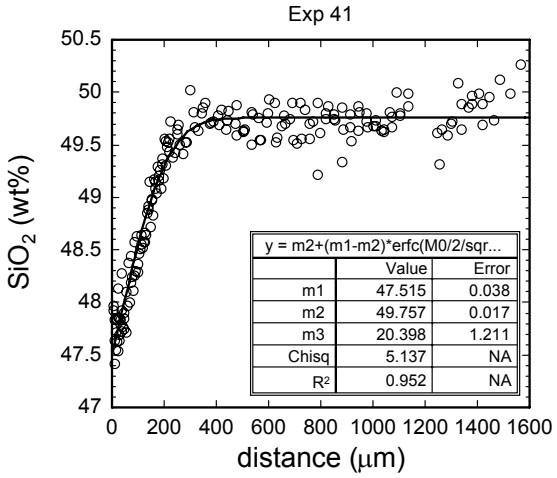
Exp 41
SiO2 (wt%)
distance (μm)
y = m2+(m1-m2)*erfc(M0/2/sqr...
Value Error
m1 47.515 0.038
m2 49.757 0.017
m3 20.398 1.211
Chisq 5.137 NA
R² 0.952 NA

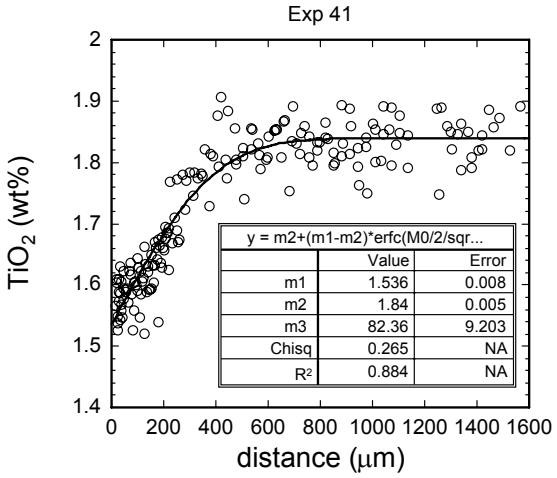
Exp 41
TiO2 (wt%)
distance (μm)
y = m2+(m1-m2)*erfc(M0/2/sqr...
Value Error
m1 1.536 0.008
m2 1.84 0.005
m3 82.36 9.203
Chisq 0.265 NA
R² 0.884 NA

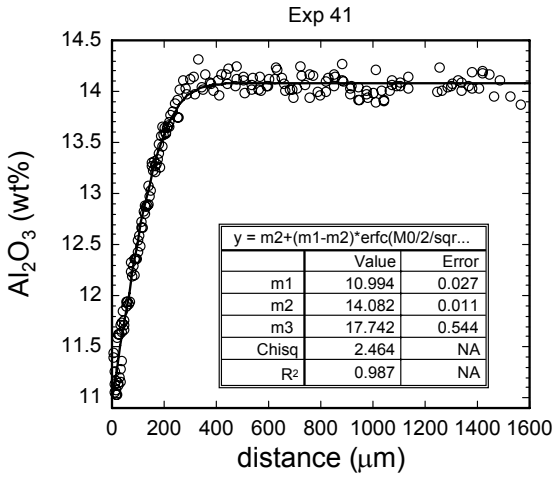
Exp 41
Al2O3 (wt%)
distance (μm)
y = m2+(m1-m2)*erfc(M0/2/sqr...
Value Error
m1 10.994 0.027
m2 14.082 0.011
m3 17.742 0.544
Chisq 2.464 NA
R² 0.987 NA

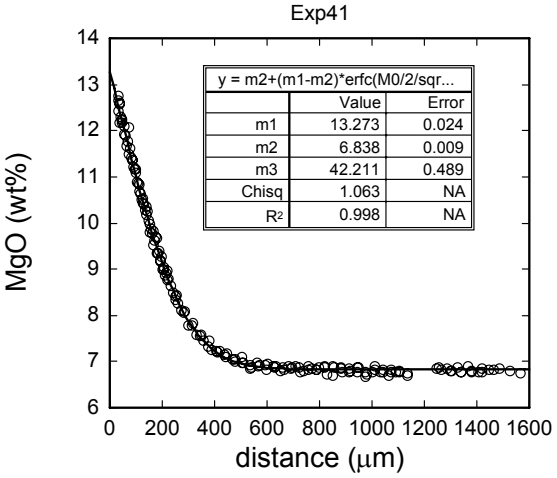
Exp41
MgO (wt%)
distance (μm)
y = m2+(m1-m2)*erfc(M0/2/sqr...
Value Error
m1 13.273 0.024
m2 6.838 0.009
m3 42.211 0.489
Chisq 1.063 NA
R² 0.998 NA

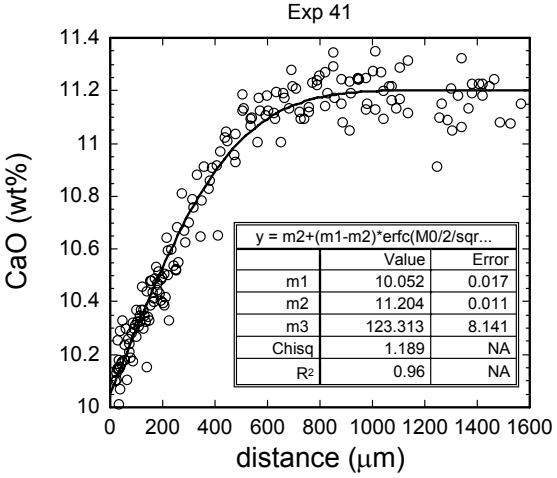
Exp 41
CaO (wt%)
distance (μm)
y = m2+(m1-m2)*erfc(M0/2/sqr...
Value Error
m1 10.052 0.017
m2 11.204 0.011
m3 123.313 8.141
Chisq 1.189 NA
R² 0.96 NA

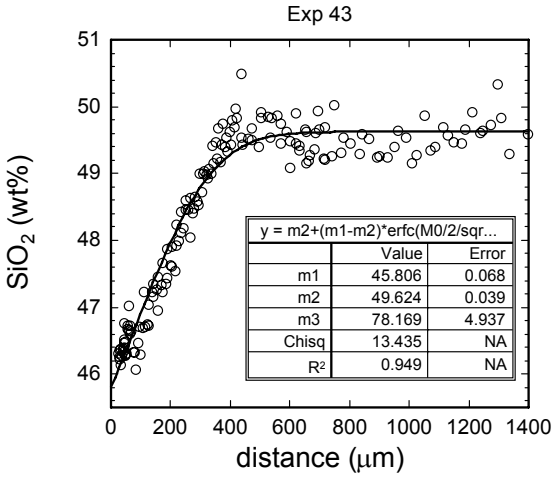
Exp 43
SiO2 (wt%)
distance (μm)
y = m2+(m1-m2)*erfc(M0/2/sqr...
Value Error
m1 45.806 0.068
m2 49.624 0.039
m3 78.169 4.937
Chisq 13.435 NA
R² 0.949 NA

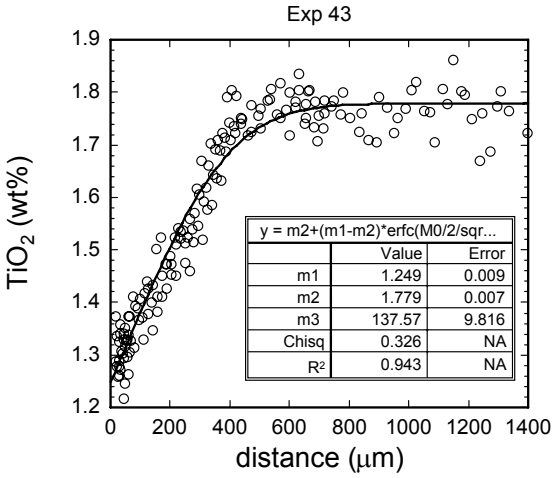
Exp 43
TiO2 (wt%)
distance (μm)
y = m2+(m1-m2)*erfc(M0/2/sqr...
Value Error
m1 1.249 0.009
m2 1.779 0.007
m3 137.57 9.816
Chisq 0.326 NA
R² 0.943 NA

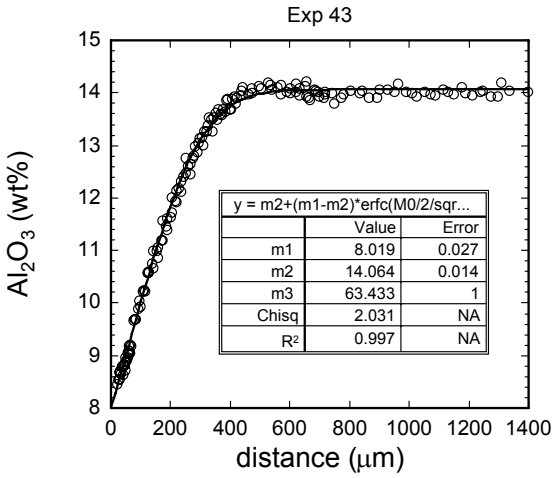
Exp 43
Al2O3 (wt%)
distance (μm)
y = m2+(m1-m2)*erfc(M0/2/sqr...
Value Error
m1 8.019 0.027
m2 14.064 0.014
m3 63.433 1
Chisq 2.031 NA
R² 0.997 NA

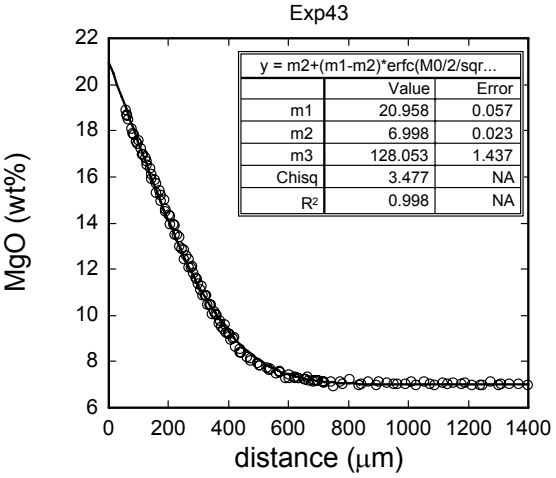
Exp43
MgO (wt%)
distance (μm)
y = m2+(m1-m2)*erfc(M0/2/sqr...
Value Error
m1 20.958 0.057
m2 6.998 0.023
m3 128.053 1.437
Chisq 3.477 NA
R² 0.998 NA

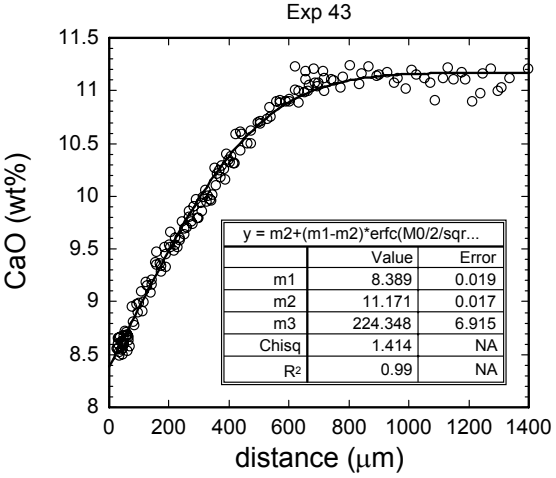
Exp 43
CaO (wt%)
distance (μm)
y = m2+(m1-m2)*erfc(M0/2/sqr...
Value Error
m1 8.389 0.019
m2 11.171 0.017
m3 224.348 6.915
Chisq 1.414 NA
R² 0.99 NA

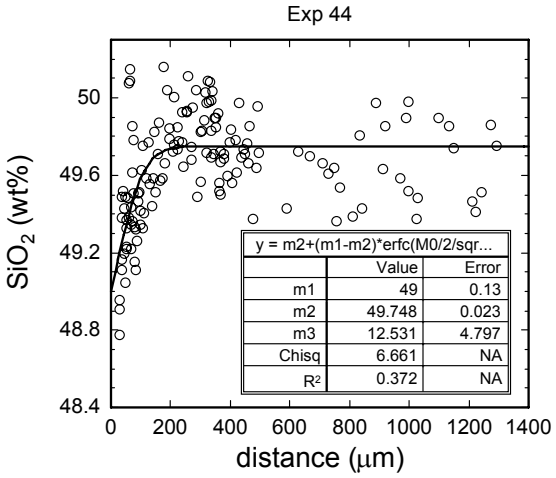
Exp 44
SiO2 (wt%)
distance (μm)
y = m2+(m1-m2)*erfc(M0/2/sqr...
Value Error
m1 49 0.13
m2 49.748 0.023
m3 12.531 4.797
Chisq 6.661 NA
R² 0.372 NA

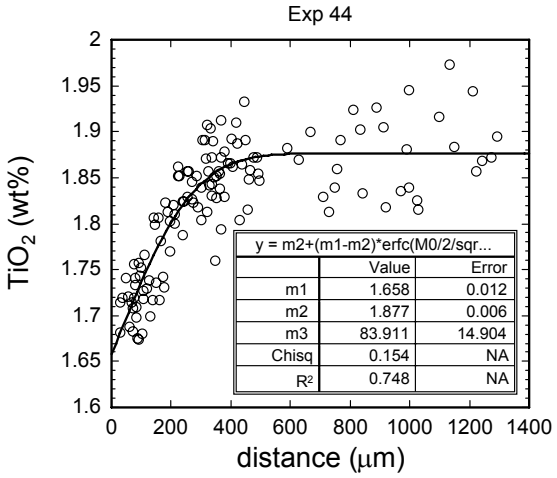
Exp 44
TiO2 (wt%)
distance (μm)
y = m2+(m1-m2)*erfc(M0/2/sqr...
Value Error
m1 1.658 0.012
m2 1.877 0.006
m3 83.911 14.904
Chisq 0.154 NA
R² 0.748 NA

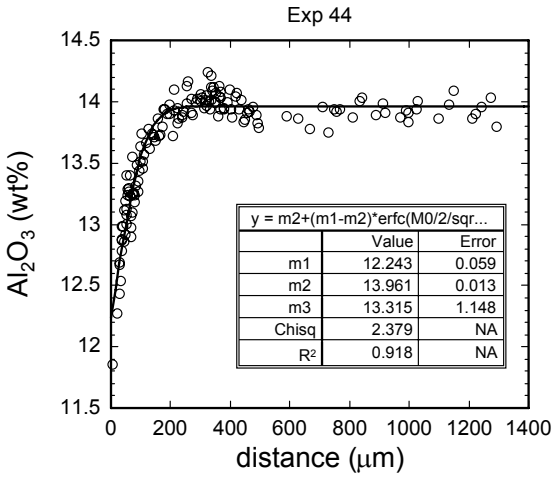
Exp 44
Al2O3 (wt%)
distance (μm)
y = m2+(m1-m2)*erfc(M0/2/sqr...
Value Error
m1 12.243 0.059
m2 13.961 0.013
m3 13.315 1.148
Chisq 2.379 NA
R² 0.918 NA

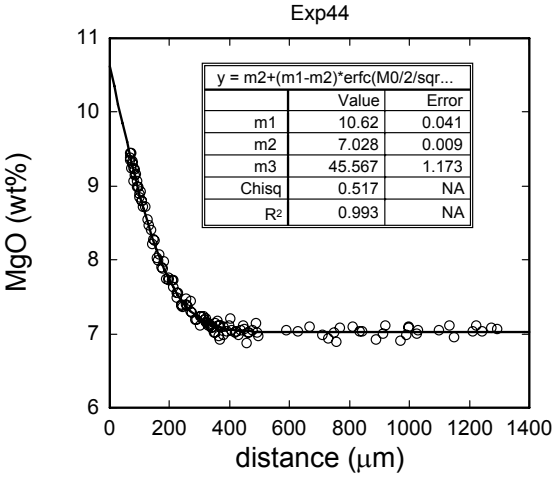
Exp44
MgO (wt%)
distance (μm)
y = m2+(m1-m2)*erfc(M0/2/sqr...
Value Error
m1 10.62 0.041
m2 7.028 0.009
m3 45.567 1.173
Chisq 0.517 NA
R² 0.993 NA

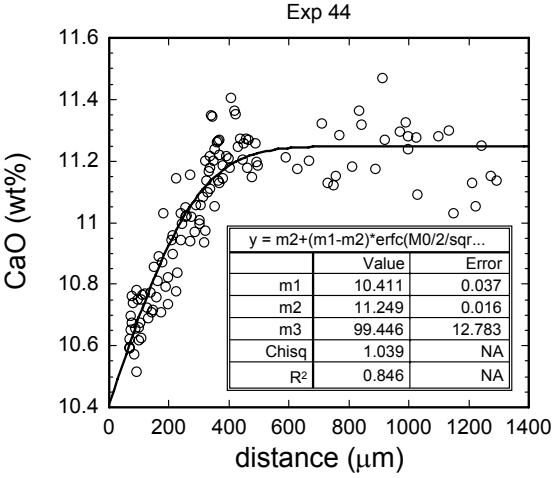
Exp 44
CaO (wt%)
distance (μm)
y = m2+(m1-m2)*erfc(M0/2/sqr...
Value Error
m1 10.411 0.037
m2 11.249 0.016
m3 99.446 12.783
Chisq 1.039 NA
R² 0.846 NA

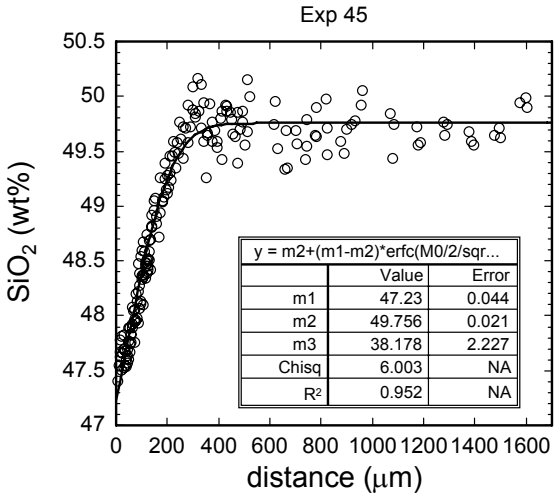
Exp 45
SiO2 (wt%)
distance (μm)
y = m2+(m1-m2)*erfc(M0/2/sqr...
Value Error
m1 47.23 0.044
m2 49.756 0.021
m3 38.178 2.227
Chisq 6.003 NA
R² 0.952 NA

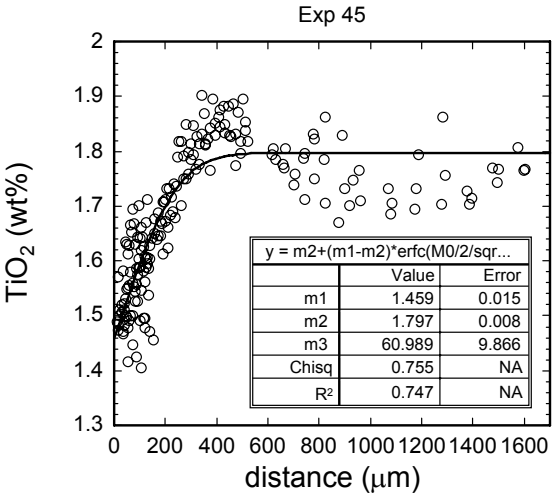
Exp 45
TiO2 (wt%)
distance (μm)
y = m2+(m1-m2)*erfc(M0/2/sqr...
Value Error
m1 1.459 0.015
m2 1.797 0.008
m3 60.989 9.866
Chisq 0.755 NA
R² 0.747 NA

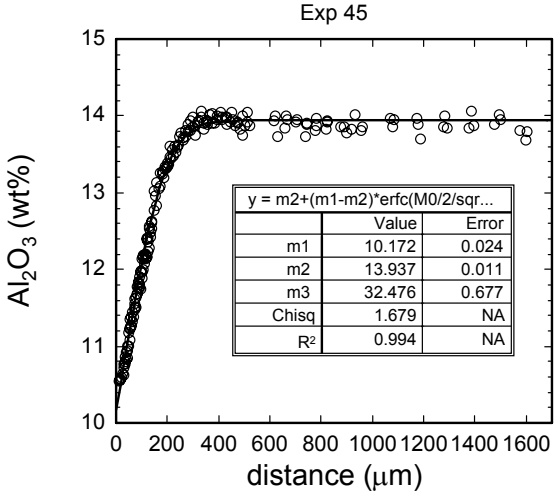
Exp 45
Al2O3 (wt%)
distance (μm)
y = m2+(m1-m2)*erfc(M0/2/sqr...
Value Error
m1 10.172 0.024
m2 13.937 0.011
m3 32.476 0.677
Chisq 1.679 NA
R² 0.994 NA

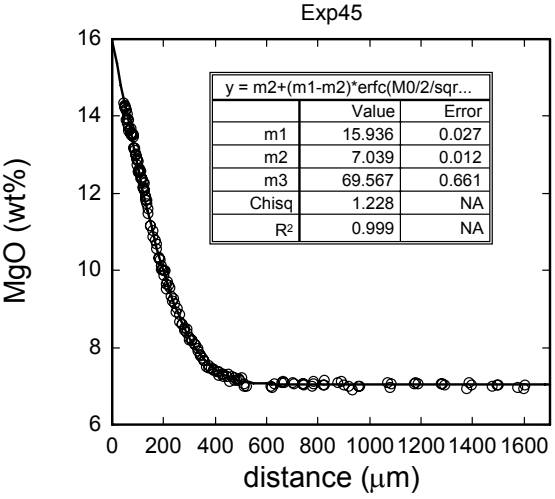
Exp45
MgO (wt%)
distance (μm)
y = m2+(m1-m2)*erfc(M0/2/sqr...
Value Error
m1 15.936 0.027
m2 7.039 0.012
m3 69.567 0.661
Chisq 1.228 NA
R² 0.999 NA

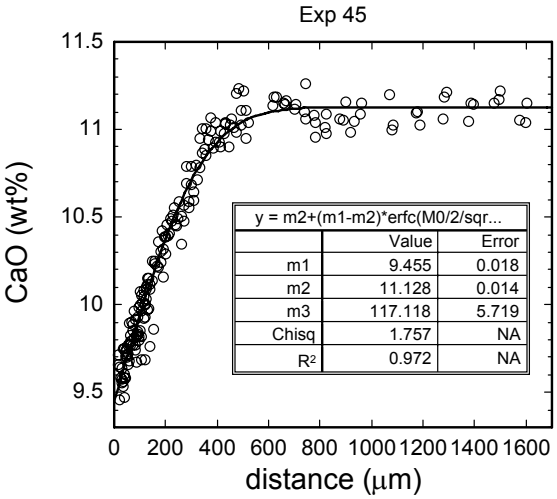
Exp 45
CaO (wt%)
distance (μm)
y = m2+(m1-m2)*erfc(M0/2/sqr...
Value Error
m1 9.455 0.018
m2 11.128 0.014
m3 117.118 5.719
Chisq 1.757 NA
R² 0.972 NA

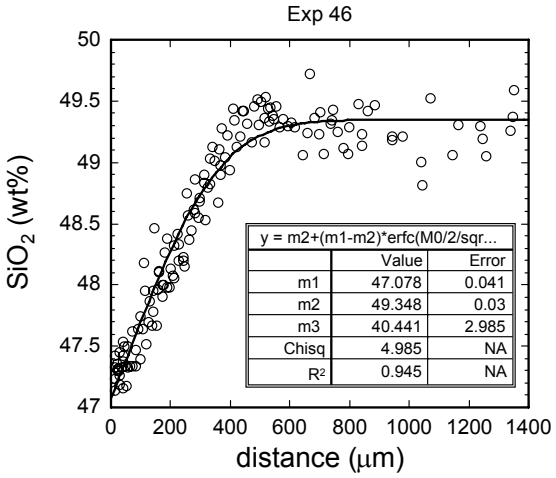
Exp 46
SiO2 (wt%)
distance (μm)
y = m2+(m1-m2)*erfc(M0/2/sqr...
Value Error
m1 47.078 0.041
m2 49.348 0.03
m3 40.441 2.985
Chisq 4.985 NA
R² 0.945 NA

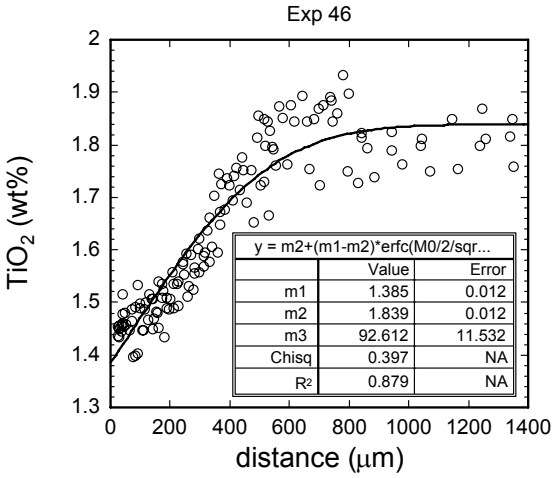
Exp 46
TiO2 (wt%)
distance (μm)
y = m2+(m1-m2)*erfc(M0/2/sqr...
Value Error
m1 1.385 0.012
m2 1.839 0.012
m3 92.612 11.532
Chisq 0.397 NA
R² 0.879 NA

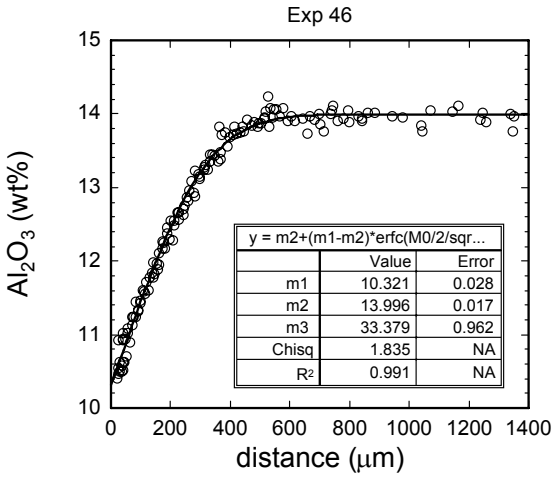
Exp 46
Al2O3 (wt%)
distance (μm)
y = m2+(m1-m2)*erfc(M0/2/sqr...
Value Error
m1 10.321 0.028
m2 13.996 0.017
m3 33.379 0.962
Chisq 1.835 NA
R² 0.991 NA

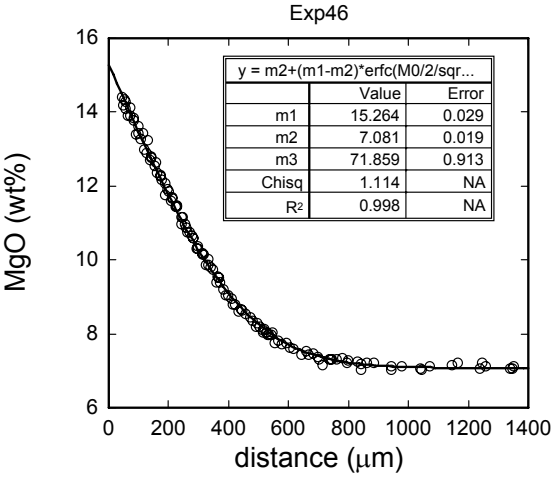
Exp46
MgO (wt%)
distance (μm)
y = m2+(m1-m2)*erfc(M0/2/sqr...
Value Error
m1 15.264 0.029
m2 7.081 0.019
m3 71.859 0.913
Chisq 1.114 NA
R² 0.998 NA

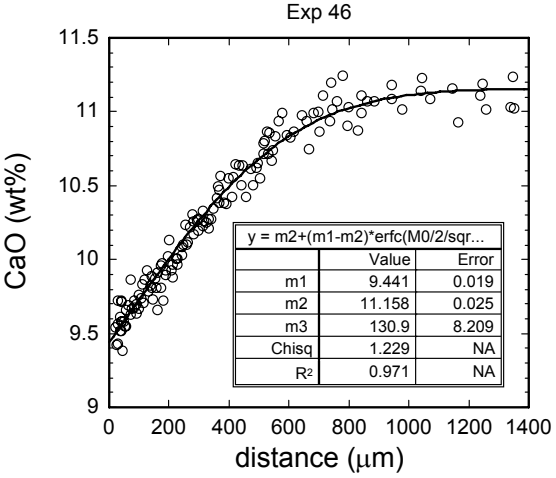
Exp 46
CaO (wt%)
distance (μm)
y = m2+(m1-m2)*erfc(M0/2/sqr...
Value Error
m1 9.441 0.019
m2 11.158 0.025
m3 130.9 8.209
Chisq 1.229 NA
R² 0.971 NA

Appendix D
Composition Profiles of Clinopyroxene Dissolution in Basalt

Exp 1

SiO2	TiO2	Al2O3	FeO	MnO	MgO	CaO	Na2O	K2O	P2O5	Total	d (um)
50.69	1.43	10.01	11.62	0.22	9.32	13.03	2.14	0.12	0.08	98.66	8.0
50.67	1.39	9.94	11.61	0.21	9.37	13.10	2.18	0.13	0.11	98.70	15.4
50.90	1.44	10.26	11.42	0.23	9.27	13.02	2.21	0.14	0.12	99.01	22.2
50.71	1.42	10.20	11.42	0.23	9.12	13.05	2.17	0.13	0.09	98.54	28.6
50.73	1.49	10.51	11.37	0.19	9.12	12.98	2.29	0.13	0.12	98.93	36.3
50.90	1.42	10.55	11.55	0.22	9.11	12.97	2.22	0.12	0.12	99.17	41.8
50.84	1.43	10.84	11.33	0.21	9.00	12.90	2.30	0.13	0.12	99.09	50.5
50.76	1.44	10.85	11.43	0.20	8.87	12.90	2.22	0.13	0.13	98.93	55.0
50.83	1.48	11.17	11.35	0.26	8.83	12.83	2.27	0.12	0.16	99.30	64.7
50.54	1.47	11.09	11.31	0.21	8.70	12.91	2.21	0.14	0.14	98.70	68.2
50.61	1.50	11.39	11.30	0.19	8.66	12.78	2.33	0.14	0.14	99.03	78.8
50.69	1.54	11.33	11.34	0.23	8.51	12.76	2.28	0.15	0.16	99.00	81.4
51.00	1.53	11.63	11.21	0.20	8.50	12.75	2.31	0.14	0.13	99.39	93.0
50.02	1.53	12.01	11.16	0.19	8.42	12.65	2.38	0.14	0.16	98.66	99.2
49.63	1.59	12.48	11.20	0.22	8.26	12.56	2.44	0.14	0.17	98.69	112.7
50.13	1.62	12.91	11.14	0.21	7.95	12.45	2.52	0.15	0.18	99.25	153.5
49.89	1.68	13.15	11.16	0.21	7.85	12.37	2.51	0.15	0.17	99.12	166.8
49.75	1.69	13.48	11.14	0.24	7.63	12.25	2.57	0.16	0.20	99.12	207.8
49.71	1.70	13.65	11.16	0.22	7.62	12.18	2.61	0.16	0.18	99.19	220.9
49.85	1.74	13.74	11.19	0.21	7.38	12.01	2.66	0.16	0.18	99.13	262.1
49.91	1.78	13.88	11.23	0.18	7.37	11.97	2.60	0.16	0.15	99.22	274.9
50.18	1.83	13.96	11.28	0.21	7.24	11.88	2.65	0.17	0.17	99.56	316.4
49.97	1.78	13.96	11.30	0.19	7.21	11.81	2.67	0.18	0.20	99.26	329.0
49.97	1.79	14.01	11.41	0.22	7.10	11.75	2.75	0.17	0.17	99.34	370.7
50.14	1.76	14.08	11.40	0.20	7.16	11.68	2.70	0.17	0.17	99.47	383.1
49.82	1.86	14.01	11.57	0.19	7.09	11.62	2.72	0.18	0.19	99.24	424.9
49.55	1.83	14.03	11.52	0.20	7.06	11.57	2.69	0.19	0.19	98.83	437.2
49.68	1.77	14.07	11.69	0.22	6.99	11.54	2.70	0.17	0.18	99.00	479.2
49.88	1.81	14.06	11.65	0.21	6.99	11.47	2.77	0.18	0.15	99.16	491.3
49.95	1.85	13.98	11.84	0.20	6.97	11.45	2.76	0.19	0.18	99.36	533.5
49.73	1.85	14.06	11.85	0.19	6.96	11.41	2.80	0.17	0.17	99.19	545.4
49.71	1.83	13.96	11.97	0.23	6.96	11.35	2.79	0.18	0.19	99.17	587.7
49.96	1.81	14.08	11.88	0.23	6.96	11.31	2.80	0.17	0.18	99.37	599.4
49.87	1.82	14.02	11.96	0.19	6.94	11.29	2.79	0.18	0.16	99.21	642.0
49.62	1.81	14.03	11.95	0.24	6.94	11.33	2.73	0.18	0.17	98.99	653.5
49.87	1.81	14.01	11.99	0.24	6.89	11.24	2.70	0.17	0.17	99.09	696.3
49.77	1.83	14.05	11.96	0.23	6.92	11.23	2.79	0.19	0.22	99.19	707.6
50.20	1.79	14.06	12.09	0.24	6.90	11.22	2.76	0.18	0.19	99.63	750.6
49.77	1.83	14.00	12.07	0.22	6.93	11.22	2.79	0.19	0.18	99.20	761.7
49.91	1.81	14.00	12.09	0.24	6.94	11.26	2.75	0.17	0.20	99.36	804.9
49.68	1.85	14.00	12.12	0.23	6.93	11.24	2.76	0.16	0.19	99.15	815.8
50.04	1.79	14.06	12.09	0.21	6.91	11.18	2.75	0.18	0.19	99.38	859.2
49.69	1.79	13.95	12.14	0.24	6.91	11.19	2.77	0.17	0.18	99.02	869.9
49.79	1.83	14.00	12.15	0.19	6.85	11.19	2.86	0.18	0.15	99.17	913.5

50.00	1.82	14.06	12.08	0.22	6.94	11.16	2.74	0.17	0.21	99.41	923.9
49.68	1.82	14.01	12.16	0.22	6.88	11.20	2.75	0.18	0.17	99.07	967.8
49.83	1.82	14.03	12.09	0.24	6.90	11.15	2.76	0.18	0.20	99.19	978.0
49.94	1.84	14.01	12.14	0.24	6.89	11.18	2.76	0.17	0.19	99.35	1022.1
49.85	1.84	13.97	12.15	0.21	6.90	11.16	2.75	0.16	0.18	99.17	1032.1
49.77	1.81	13.94	12.12	0.21	6.87	11.17	2.75	0.17	0.21	99.01	1076.3
49.79	1.83	14.07	12.15	0.23	6.92	11.16	2.79	0.17	0.16	99.28	1086.2
50.24	1.83	14.06	12.08	0.24	6.89	11.14	2.77	0.17	0.20	99.63	1130.6
49.87	1.83	14.10	12.11	0.21	6.89	11.11	2.77	0.18	0.17	99.26	1140.3
49.77	1.84	14.05	12.09	0.21	6.84	11.16	2.74	0.18	0.16	99.02	1184.9

Exp 5

SiO2	TiO2	Al2O3	FeO	MnO	MgO	CaO	Na2O	K2O	P2O5	Total	d (um)
52.25	1.37	9.15	12.32	0.18	7.97	13.56	2.31	0.15	0.11	99.37	2.6
51.57	1.35	8.28	11.26	0.21	10.05	15.11	1.88	0.12	0.08	99.89	2.9
52.47	1.27	9.00	13.16	0.19	7.30	12.76	2.44	0.15	0.12	98.86	5.6
52.28	1.19	8.21	13.44	0.24	8.01	13.32	2.27	0.12	0.11	99.19	8.0
51.52	1.12	7.03	10.99	0.32	11.22	15.81	1.53	0.08	0.08	99.70	8.7
52.18	1.14	8.19	11.82	0.19	9.40	14.21	1.86	0.09	0.13	99.19	10.9
52.67	1.19	8.42	12.50	0.21	8.26	13.02	2.40	0.15	0.10	98.90	13.5
51.44	1.11	7.40	10.63	0.14	11.16	15.06	1.55	0.11	0.09	98.70	14.4
52.35	1.17	8.34	12.09	0.26	9.43	13.93	1.93	0.16	0.07	99.72	16.2
51.79	1.14	8.25	10.85	0.27	9.63	14.45	1.82	0.10	0.08	98.38	18.9
52.27	1.07	7.97	9.67	0.12	11.22	14.79	1.63	0.07	0.12	98.93	20.1
52.02	1.19	8.11	11.20	0.20	10.64	14.87	1.56	0.07	0.07	99.94	21.5
52.13	1.18	8.01	10.27	0.12	10.88	15.01	1.53	0.10	0.14	99.36	24.4
51.90	1.14	7.94	9.41	0.24	11.90	15.57	1.39	0.08	0.12	99.68	25.8
51.82	1.20	8.15	10.96	0.21	10.46	14.74	1.52	0.10	0.03	99.18	26.8
51.99	1.22	8.10	10.65	0.24	10.78	14.90	1.40	0.10	0.07	99.45	29.8
51.98	1.18	8.06	10.02	0.17	11.09	15.02	1.46	0.12	0.12	99.22	31.6
52.12	1.22	8.57	10.62	0.28	10.64	14.72	1.56	0.04	0.05	99.81	32.1
51.88	1.24	8.44	10.44	0.22	10.53	14.82	1.49	0.11	0.16	99.32	35.3
52.09	1.22	8.24	10.11	0.22	10.91	14.97	1.48	0.06	0.15	99.43	37.3
52.37	1.28	8.89	10.47	0.22	10.25	14.57	1.58	0.10	0.06	99.79	37.4
52.37	1.21	8.52	10.50	0.24	10.46	14.66	1.41	0.09	0.13	99.57	40.7
52.45	1.25	8.99	10.40	0.17	10.35	14.43	1.49	0.13	0.07	99.73	42.7
51.65	1.19	8.53	9.74	0.10	10.92	15.05	1.34	0.08	0.11	98.70	43.0
52.23	1.23	8.72	10.01	0.28	10.57	14.74	1.45	0.09	0.13	99.44	46.2
52.45	1.31	9.01	10.19	0.16	10.13	14.39	1.53	0.09	0.08	99.34	48.0
52.40	1.23	8.71	9.94	0.23	10.72	14.70	1.46	0.07	0.15	99.60	48.7
52.28	1.25	8.83	9.92	0.18	10.15	14.27	1.49	0.09	0.10	98.55	51.6
51.71	1.22	8.51	9.98	0.25	10.01	14.33	1.71	0.12	0.16	97.99	54.5
51.62	1.20	8.90	10.11	0.18	10.05	14.49	1.93	0.13	0.16	98.77	57.1
51.68	1.27	8.95	10.08	0.18	10.12	14.34	1.98	0.10	0.06	98.76	60.2
51.94	1.27	9.26	10.30	0.18	9.98	14.14	2.02	0.12	0.12	99.31	62.1
51.59	1.28	9.36	10.66	0.16	10.15	14.00	2.09	0.13	0.08	99.51	66.1
51.32	1.31	9.12	10.45	0.15	10.17	14.30	1.95	0.11	0.06	98.95	66.3
51.66	1.28	9.47	10.22	0.23	10.04	14.04	1.99	0.12	0.10	99.15	68.6
51.43	1.31	9.45	10.65	0.25	10.06	13.84	2.04	0.12	0.04	99.19	71.7
51.49	1.34	9.26	10.23	0.19	10.09	14.08	2.03	0.12	0.01	98.84	71.8
51.58	1.32	9.69	10.70	0.21	9.97	13.90	2.05	0.13	0.19	99.73	77.2
51.48	1.34	9.42	10.49	0.19	10.27	14.18	2.04	0.12	0.13	99.66	77.3
51.34	1.31	9.86	10.64	0.28	9.92	13.87	2.01	0.11	0.08	99.43	81.7
51.54	1.34	9.61	10.40	0.18	9.87	14.05	2.04	0.12	0.15	99.29	82.7
51.20	1.36	9.79	10.59	0.21	9.84	13.81	2.08	0.11	0.11	99.10	82.8
51.41	1.35	9.86	10.66	0.13	9.91	13.99	2.15	0.09	0.12	99.65	86.9
51.29	1.37	10.01	10.75	0.07	9.81	13.71	2.09	0.09	0.13	99.31	88.4
50.83	1.35	10.07	10.40	0.23	9.74	13.97	2.10	0.10	0.11	98.90	92.0
51.28	1.39	10.18	10.81	0.15	9.70	13.79	2.15	0.10	0.19	99.73	94.0
50.86	1.38	10.24	10.44	0.18	9.94	13.96	2.13	0.18	0.07	99.36	97.3

51.40	1.37	10.27	10.62	0.12	9.77	13.70	2.15	0.15	0.07	99.62	99.6
50.52	1.35	10.37	10.41	0.16	9.55	13.91	2.06	0.13	0.16	98.61	101.5
51.07	1.33	10.40	10.44	0.14	9.60	13.87	2.22	0.14	0.20	99.41	102.5
51.38	1.41	10.48	10.58	0.24	9.56	13.60	2.10	0.11	0.13	99.60	105.2
50.69	1.39	10.45	10.46	0.15	9.57	13.78	2.10	0.12	0.08	98.77	106.7
51.24	1.39	10.46	10.48	0.30	9.68	13.69	2.11	0.09	0.16	99.61	107.7
51.07	1.41	10.56	10.79	0.19	9.56	13.48	2.13	0.16	0.17	99.51	110.7
50.84	1.46	10.56	10.40	0.22	9.45	13.71	2.16	0.14	0.14	99.06	112.0
50.85	1.41	10.71	10.59	0.24	9.63	13.76	2.16	0.16	0.18	99.66	112.9
51.31	1.42	10.68	10.56	0.12	9.45	13.68	2.15	0.13	0.13	99.62	116.3
50.85	1.39	10.52	10.24	0.19	9.69	13.84	2.16	0.11	0.10	99.10	117.2
50.85	1.38	10.62	10.48	0.20	9.53	13.81	2.05	0.18	0.15	99.25	118.1
51.31	1.51	10.99	10.52	0.22	9.34	13.56	2.20	0.14	0.08	99.87	121.9
50.56	1.45	10.70	10.31	0.11	9.57	13.76	2.17	0.14	0.13	98.90	122.4
50.67	1.41	10.80	10.58	0.18	9.27	13.73	2.16	0.11	0.22	99.13	123.3
51.34	1.40	10.97	10.63	0.20	9.28	13.41	2.19	0.15	0.14	99.70	127.5
50.48	1.45	11.03	10.36	0.22	9.29	13.64	2.15	0.15	0.14	98.91	127.6
50.55	1.40	10.90	10.38	0.15	9.26	13.80	2.27	0.16	0.15	99.02	128.5
49.76	1.54	11.93	10.75	0.22	9.23	13.39	2.29	0.12	0.12	99.35	132.8
50.48	1.48	11.00	10.31	0.22	9.08	13.61	2.17	0.14	0.10	98.59	132.9
50.64	1.44	11.09	10.45	0.29	9.31	13.51	2.19	0.17	0.07	99.16	133.8
50.68	1.50	11.17	10.45	0.20	9.20	13.64	2.21	0.13	0.14	99.33	138.0
50.61	1.50	11.22	10.48	0.16	8.99	13.61	2.18	0.13	0.05	98.92	139.0
50.72	1.53	11.27	10.36	0.21	9.21	13.58	2.25	0.14	0.13	99.40	143.2
50.98	1.52	11.34	10.33	0.26	8.99	13.60	2.19	0.15	0.25	99.61	144.2
49.48	1.60	12.08	10.71	0.17	9.03	13.21	2.30	0.13	0.16	98.87	147.8
50.87	1.50	11.27	10.40	0.12	9.08	13.57	2.28	0.14	0.25	99.48	149.4
49.52	1.59	12.06	10.32	0.22	8.91	13.10	2.44	0.14	0.20	98.49	156.5
50.29	1.59	12.32	10.65	0.17	8.66	13.18	2.31	0.12	0.18	99.46	162.7
49.61	1.57	12.34	10.63	0.18	8.81	13.23	2.39	0.15	0.11	99.02	163.7
49.54	1.65	12.57	10.66	0.18	8.57	13.02	2.30	0.16	0.25	98.89	171.4
49.60	1.62	12.58	10.75	0.15	8.70	12.99	2.37	0.16	0.14	99.05	177.7
49.65	1.55	12.59	10.38	0.24	8.55	13.06	2.48	0.18	0.10	98.79	178.6
49.79	1.64	12.67	10.54	0.16	8.57	13.07	2.39	0.17	0.26	99.26	186.4
50.10	1.72	12.90	10.82	0.21	8.36	13.04	2.39	0.13	0.22	99.88	192.6
50.10	1.63	12.69	10.48	0.15	8.52	12.90	2.44	0.15	0.07	99.11	193.6
49.63	1.61	12.93	10.57	0.17	8.27	12.96	2.42	0.14	0.22	98.91	201.4
49.65	1.71	13.10	10.74	0.15	8.39	12.73	2.45	0.16	0.14	99.22	207.6
49.72	1.65	13.00	10.67	0.33	8.39	12.88	2.40	0.19	0.27	99.50	208.5
49.63	1.68	13.08	10.49	0.25	8.25	12.77	2.45	0.16	0.26	99.01	216.2
49.67	1.75	13.34	10.84	0.15	8.24	12.63	2.51	0.16	0.11	99.40	222.5
49.51	1.73	13.11	10.66	0.21	8.41	12.87	2.49	0.21	0.16	99.36	223.5
49.44	1.71	13.32	10.58	0.18	8.16	12.75	2.49	0.17	0.18	98.97	231.2
49.87	1.76	13.49	11.00	0.26	8.13	12.46	2.50	0.13	0.10	99.69	237.4
49.57	1.74	13.45	10.83	0.21	8.16	12.79	2.48	0.19	0.17	99.59	238.4
49.71	1.69	13.46	10.63	0.22	8.09	12.76	2.45	0.20	0.18	99.37	246.2
49.87	1.74	13.48	10.80	0.19	7.82	12.58	2.47	0.18	0.05	99.18	252.4
49.56	1.74	13.48	10.74	0.26	8.09	12.67	2.47	0.18	0.14	99.32	253.3
49.70	1.80	13.49	10.81	0.18	7.98	12.51	2.52	0.16	0.19	99.34	261.1

49.27	1.78	13.69	10.99	0.18	8.07	12.42	2.43	0.17	0.14	99.14	267.3
49.81	1.78	13.59	10.76	0.15	7.89	12.62	2.47	0.17	0.09	99.33	268.2
49.58	1.80	13.60	10.65	0.18	7.82	12.35	2.46	0.17	0.18	98.79	276.1
50.00	1.78	13.74	10.95	0.24	7.97	12.32	2.56	0.16	0.23	99.95	282.3
49.72	1.81	13.57	11.00	0.17	7.79	12.37	2.54	0.18	0.23	99.37	283.2
49.40	1.80	13.68	10.70	0.13	7.63	12.39	2.49	0.18	0.25	98.64	291.0
49.81	1.80	13.80	11.08	0.13	7.86	12.21	2.54	0.15	0.13	99.51	297.2
50.09	1.83	13.89	10.74	0.18	7.58	12.39	2.47	0.12	0.19	99.49	298.1
49.50	1.79	13.88	10.73	0.23	7.80	12.37	2.53	0.16	0.21	99.19	306.0
49.47	1.79	13.89	11.04	0.19	7.54	12.11	2.57	0.20	0.11	98.90	312.2
49.65	1.87	13.89	10.95	0.29	7.80	12.44	2.61	0.15	0.24	99.90	313.1
49.48	1.78	13.89	10.88	0.16	7.69	12.15	2.59	0.19	0.24	99.05	320.9
49.52	1.86	13.96	11.09	0.13	7.86	12.21	2.58	0.14	0.23	99.57	327.0
49.34	1.85	13.88	10.99	0.15	7.60	12.29	2.65	0.17	0.10	99.00	328.1
49.61	1.89	13.99	10.87	0.23	7.65	12.16	2.56	0.18	0.18	99.31	335.8
49.63	1.80	14.09	11.02	0.19	7.48	12.03	2.60	0.14	0.17	99.14	342.0
49.70	1.85	14.02	11.17	0.13	7.58	12.26	2.62	0.15	0.13	99.61	342.9
49.94	1.88	13.88	11.01	0.18	7.62	12.16	2.58	0.15	0.15	99.54	350.8
49.60	1.83	14.12	11.42	0.19	7.57	11.93	2.57	0.17	0.21	99.62	356.9
49.29	1.84	14.03	11.08	0.17	7.55	12.18	2.57	0.21	0.12	99.04	357.9
49.32	1.83	13.96	10.97	0.20	7.28	11.94	2.63	0.16	0.17	98.46	365.8
50.16	1.81	13.98	11.20	0.15	7.28	11.89	2.63	0.20	0.27	99.57	371.9
49.58	1.94	14.01	11.26	0.16	7.57	11.94	2.62	0.18	0.20	99.45	372.8
49.48	1.83	13.85	11.06	0.22	7.50	11.98	2.66	0.17	0.22	98.96	380.7
49.37	1.80	14.15	11.24	0.20	7.50	11.98	2.70	0.20	0.18	99.32	386.9
49.78	1.86	14.19	11.25	0.20	7.52	12.08	2.60	0.17	0.17	99.82	387.8
49.24	1.84	13.91	11.12	0.15	7.57	11.87	2.67	0.17	0.15	98.68	395.7
49.52	1.83	14.10	11.43	0.16	7.46	11.86	2.79	0.18	0.22	99.55	401.8
49.47	1.82	14.00	11.31	0.11	7.41	11.87	2.59	0.20	0.15	98.93	402.7
49.40	1.89	13.94	11.09	0.26	7.22	11.90	2.70	0.17	0.18	98.75	410.6
49.29	1.87	13.97	11.33	0.21	7.45	11.90	2.69	0.15	0.20	99.05	416.7
49.29	1.88	14.18	11.19	0.28	7.31	11.85	2.69	0.17	0.18	99.00	417.7
49.29	1.85	13.97	11.28	0.27	7.25	11.83	2.66	0.16	0.20	98.76	425.5
49.31	1.84	14.15	11.37	0.14	7.46	11.76	2.64	0.20	0.24	99.11	431.6
49.43	1.84	14.10	11.30	0.16	7.56	11.94	2.64	0.20	0.18	99.35	432.6
49.50	1.89	14.19	11.22	0.32	7.38	11.74	2.61	0.20	0.23	99.28	440.5
49.35	1.88	14.29	11.34	0.12	7.28	11.91	2.71	0.19	0.20	99.27	447.5
49.43	1.87	14.19	11.29	0.22	7.33	11.72	2.73	0.21	0.06	99.06	468.6
49.49	1.93	14.25	11.43	0.22	7.33	11.68	2.74	0.16	0.13	99.36	474.2
49.27	1.91	14.23	11.47	0.15	7.30	11.66	2.74	0.21	0.26	99.21	482.4
50.25	1.89	14.13	11.63	0.24	7.20	11.51	2.70	0.15	0.13	99.82	505.4
49.10	1.87	14.14	11.45	0.24	7.23	11.68	2.76	0.17	0.29	98.92	507.9
49.36	1.89	14.14	11.61	0.19	7.28	11.52	2.71	0.23	0.12	99.03	517.3
49.46	1.93	14.12	11.40	0.18	7.23	11.48	2.72	0.17	0.16	98.84	541.6
49.35	1.93	14.01	11.66	0.14	7.17	11.53	2.72	0.13	0.20	98.84	542.3
49.74	1.92	14.07	11.66	0.24	7.28	11.53	2.69	0.18	0.08	99.39	552.1
49.30	1.90	14.11	11.68	0.31	7.27	11.49	2.76	0.15	0.19	99.16	575.4
49.44	1.85	14.08	11.78	0.17	7.27	11.48	2.74	0.21	0.20	99.23	579.2
49.97	1.89	14.10	11.70	0.15	7.11	11.38	2.64	0.18	0.12	99.24	587.0

49.35	1.87	14.06	11.75	0.21	7.02	11.32	2.69	0.20	0.11	98.56	609.0
49.58	1.89	14.15	11.91	0.22	7.18	11.31	2.77	0.19	0.19	99.39	616.1
49.35	1.91	14.15	11.85	0.20	7.24	11.52	2.78	0.16	0.28	99.44	621.8
49.30	1.93	14.08	11.72	0.20	7.21	11.42	2.76	0.21	0.31	99.14	642.8
49.78	1.84	14.24	11.78	0.20	7.10	11.50	2.82	0.19	0.30	99.75	653.0
49.63	1.90	14.20	11.93	0.24	7.19	11.41	2.63	0.16	0.15	99.43	656.6
49.40	1.92	14.22	12.10	0.18	7.19	11.36	2.80	0.21	0.25	99.63	676.5
49.25	1.97	14.15	12.00	0.21	7.18	11.29	2.75	0.17	0.18	99.15	689.8
49.42	1.82	14.18	11.74	0.12	7.27	11.41	2.77	0.19	0.19	99.11	691.5
49.14	1.87	14.18	11.83	0.15	7.15	11.37	2.75	0.20	0.16	98.80	710.2
49.49	1.89	14.25	11.80	0.21	7.13	11.27	2.80	0.16	0.20	99.19	726.3
49.45	1.88	14.11	12.04	0.19	7.24	11.30	2.77	0.16	0.12	99.26	726.7
49.28	1.92	14.08	11.91	0.26	7.26	11.38	2.73	0.20	0.14	99.16	743.9
49.54	1.88	14.18	12.03	0.28	7.14	11.29	2.73	0.16	0.13	99.36	761.2
49.25	1.87	14.22	11.86	0.17	7.16	11.36	2.74	0.16	0.15	98.92	763.7
49.05	1.95	14.00	11.88	0.32	7.06	11.40	2.67	0.17	0.21	98.71	777.6
49.70	1.92	14.09	11.89	0.25	7.06	11.28	2.79	0.15	0.07	99.21	796.1
49.31	1.89	14.06	11.94	0.24	7.16	11.20	2.74	0.20	0.22	98.95	800.5
49.70	1.82	14.20	11.94	0.17	7.04	11.24	2.79	0.18	0.20	99.29	811.3
49.97	1.99	14.05	12.10	0.26	7.05	11.35	2.83	0.17	0.13	99.90	830.9
49.34	1.88	14.17	11.91	0.17	7.30	11.39	2.81	0.15	0.19	99.30	837.4
49.25	1.86	14.10	11.98	0.29	7.10	11.24	2.82	0.20	0.20	99.03	845.1
49.58	1.92	14.08	11.90	0.18	6.93	11.34	2.71	0.21	0.11	98.94	865.8
50.11	1.91	14.11	12.00	0.06	6.95	11.24	2.79	0.15	0.08	99.39	874.3
49.12	1.89	14.01	11.75	0.22	7.13	11.16	2.71	0.18	0.19	98.35	878.7
49.56	1.83	14.23	11.86	0.21	7.00	11.29	2.82	0.19	0.07	99.06	900.6
49.28	1.94	14.22	12.02	0.19	7.14	11.12	2.81	0.19	0.18	99.09	911.2
49.52	1.93	14.23	11.96	0.17	7.09	11.21	2.80	0.15	0.08	99.13	912.5
49.37	1.85	14.20	12.04	0.32	7.12	11.05	2.80	0.19	0.18	99.12	935.5
49.34	1.88	14.05	11.92	0.22	7.07	11.10	2.69	0.24	0.28	98.79	946.2
49.54	1.87	14.19	11.99	0.23	7.14	11.09	2.81	0.16	0.09	99.12	948.1
49.32	1.92	14.09	11.93	0.25	7.23	11.21	2.77	0.21	0.12	99.05	970.4
49.51	1.94	14.05	12.08	0.27	7.12	11.14	2.73	0.14	0.20	99.19	979.9
49.43	1.87	14.22	12.05	0.22	7.14	11.22	2.71	0.17	0.19	99.22	984.9
49.59	1.83	13.98	11.91	0.26	7.11	11.31	2.73	0.21	0.07	99.00	1005.2
49.55	1.88	14.32	12.07	0.25	6.96	11.25	2.81	0.20	0.15	99.44	1013.6
49.40	1.93	14.15	12.03	0.19	7.14	11.12	2.83	0.20	0.17	99.13	1021.9
49.59	1.86	14.24	12.03	0.21	7.14	11.18	2.78	0.13	0.09	99.24	1040.1
49.42	1.86	14.16	12.10	0.21	6.99	11.26	2.75	0.21	0.23	99.18	1047.4
49.65	1.91	14.16	12.08	0.28	7.19	11.18	2.78	0.18	0.24	99.64	1058.7
49.42	1.92	14.19	11.95	0.21	7.37	11.17	2.76	0.15	0.23	99.37	1075.0
49.14	1.94	14.15	12.03	0.19	6.91	11.27	2.69	0.18	0.10	98.61	1081.0
50.05	1.94	14.15	12.08	0.20	7.00	11.30	2.78	0.15	0.15	99.79	1095.6
49.55	1.85	14.15	11.92	0.22	7.14	11.14	2.86	0.20	0.14	99.15	1109.8
49.31	1.92	14.09	12.11	0.26	7.27	11.11	2.76	0.17	0.11	99.10	1114.8
49.59	1.88	14.21	12.10	0.24	7.06	11.17	2.81	0.15	0.14	99.35	1132.5
49.58	1.93	14.11	12.02	0.23	6.94	11.21	2.77	0.23	0.12	99.14	1144.7
49.65	1.94	13.98	12.05	0.19	7.09	11.14	2.85	0.17	0.23	99.29	1148.4
49.57	1.86	13.98	11.89	0.22	7.04	11.25	2.73	0.12	0.08	98.73	1169.4

49.18	1.84	14.20	12.01	0.21	7.02	11.28	2.83	0.13	0.12	98.82	1179.5
49.40	1.85	14.15	11.95	0.22	6.96	11.19	2.70	0.21	0.24	98.89	1182.2
49.27	1.89	14.07	12.03	0.15	7.15	11.17	2.74	0.17	0.21	98.83	1206.3
49.49	1.92	14.11	11.98	0.16	7.14	11.25	2.75	0.16	0.28	99.22	1214.3
49.69	1.88	14.02	12.08	0.18	7.05	11.17	2.72	0.16	0.22	99.16	1215.9
49.98	1.93	14.08	11.98	0.19	7.08	11.12	2.79	0.19	0.12	99.45	1243.2
49.62	1.85	14.22	11.99	0.16	7.16	11.25	2.73	0.17	0.16	99.31	1249.2
49.46	1.92	14.05	12.01	0.19	6.97	11.23	2.81	0.16	0.07	98.85	1249.6
49.67	1.87	14.12	11.98	0.14	7.08	11.15	2.80	0.20	0.12	99.12	1280.0
49.53	1.85	14.10	11.94	0.22	6.97	11.12	2.78	0.18	0.23	98.91	1283.3
49.60	1.97	14.11	12.07	0.14	7.22	11.13	2.69	0.14	0.14	99.21	1284.0
49.83	1.92	14.02	12.03	0.15	7.07	11.16	2.76	0.21	0.32	99.46	1317.0
49.26	1.88	14.09	12.08	0.18	7.01	11.20	2.77	0.15	0.17	98.79	1317.1
49.42	1.86	14.23	11.98	0.15	7.12	11.17	2.70	0.19	0.23	99.05	1318.9
49.68	1.86	14.03	11.85	0.18	6.95	11.17	2.86	0.17	0.24	98.99	1350.7
49.77	1.92	13.87	11.89	0.20	7.02	11.18	2.72	0.19	0.18	98.94	1353.8
49.51	1.83	14.18	11.95	0.24	7.08	11.31	2.72	0.17	0.09	99.08	1353.8
49.57	1.90	13.97	12.05	0.19	6.96	11.24	2.78	0.17	0.18	99.02	1384.5
49.82	1.89	14.00	11.91	0.32	7.05	11.03	2.78	0.22	0.12	99.14	1388.6
49.46	1.86	14.16	12.04	0.24	7.08	11.19	2.81	0.16	0.18	99.17	1390.7
49.78	1.84	13.89	12.00	0.22	6.91	11.11	2.59	0.13	0.17	98.63	1418.2
49.94	1.89	14.18	11.88	0.22	7.07	11.16	2.74	0.23	0.22	99.52	1423.5
49.74	1.88	14.06	11.90	0.21	7.01	11.21	2.71	0.22	0.13	99.08	1427.6
49.57	1.87	13.92	11.98	0.17	7.00	11.28	2.65	0.17	0.20	98.81	1458.3
49.94	1.85	14.03	12.16	0.16	7.06	11.17	2.79	0.21	0.28	99.64	1464.5
50.18	1.90	14.10	12.01	0.20	7.05	11.29	2.77	0.19	0.22	99.90	1501.4

Exp 6

SiO2	TiO2	Al2O3	FeO	MnO	MgO	CaO	Na2O	K2O	P2O5	Total	d (um)
53.37	0.84	5.93	9.40	0.21	11.73	16.79	1.83	0.10	0.15	100.35	14.2
52.77	0.77	5.71	8.63	0.14	12.96	16.95	1.54	0.08	0.08	99.64	29.8
52.59	0.78	5.76	8.65	0.09	12.79	16.88	1.63	0.07	0.04	99.27	34.3
51.68	0.76	5.65	8.25	0.17	12.42	16.71	1.57	0.08	-0.05	97.22	34.9
52.50	0.82	5.87	8.39	0.11	13.22	17.10	1.55	0.07	0.08	99.71	51.6
52.51	0.83	6.00	8.73	0.18	12.27	16.95	1.60	0.07	0.12	99.27	55.5
51.94	0.81	5.98	8.71	0.19	12.47	16.80	1.62	0.09	0.14	98.74	57.6
52.23	0.87	6.33	8.27	0.14	12.79	16.71	1.50	0.05	-0.01	98.87	73.3
52.23	0.86	6.20	8.61	0.15	12.45	16.83	1.55	0.13	0.09	99.10	76.2
53.20	0.83	6.43	8.74	0.18	12.15	16.46	1.70	0.08	0.05	99.81	80.8
52.61	0.84	6.63	8.53	0.08	12.25	16.67	1.66	0.06	0.06	99.38	95.1
52.41	0.87	6.35	8.47	0.13	12.58	16.89	1.65	0.08	0.11	99.54	96.9
52.55	0.85	6.59	8.67	0.16	12.32	16.63	1.57	0.10	0.10	99.54	104.1
51.32	0.87	6.95	8.57	0.10	12.10	16.61	1.63	0.09	0.01	98.25	116.8
51.79	0.91	6.76	8.48	0.15	12.22	16.60	1.62	0.08	0.02	98.63	117.6
51.75	0.96	6.80	8.79	0.13	12.27	16.54	1.64	0.09	-0.02	98.94	127.3
51.50	0.97	7.05	8.62	0.27	11.93	16.53	1.63	0.12	0.10	98.72	138.3
52.06	0.98	7.27	8.96	0.13	11.87	16.21	1.60	0.08	0.09	99.26	138.6
52.18	0.98	7.34	8.86	0.12	11.84	16.06	1.67	0.06	0.14	99.23	150.6
51.31	0.99	7.34	8.72	0.24	11.82	16.55	1.72	0.11	0.14	98.96	159.0
50.92	0.96	7.96	8.79	0.25	11.21	15.78	1.67	0.12	0.19	97.86	160.3
52.02	1.02	7.77	8.97	0.16	11.61	15.94	1.77	0.09	0.11	99.43	173.8
51.78	1.05	7.92	8.88	0.21	11.38	16.20	1.71	0.09	0.15	99.37	179.7
52.98	1.05	8.14	8.84	0.16	11.20	15.74	1.72	0.06	0.06	99.94	182.1
52.43	1.05	8.11	9.04	0.22	11.24	15.63	1.82	0.09	0.15	99.78	197.1
52.13	1.11	8.21	9.05	0.26	10.92	15.75	1.78	0.12	0.08	99.39	200.3
52.32	1.10	8.71	8.71	0.17	10.98	15.75	1.78	0.09	0.11	99.71	216.8
52.10	1.10	8.51	8.86	0.27	10.76	15.61	1.74	0.14	0.10	99.19	221.0
52.57	1.16	8.78	8.79	0.14	10.91	15.70	1.81	0.09	0.09	100.03	221.8
50.90	1.16	8.79	9.24	0.13	10.88	15.16	1.86	0.09	0.15	98.34	222.8
52.26	1.14	8.69	8.94	0.13	10.79	15.24	1.82	0.18	0.08	99.25	224.9
52.38	1.14	8.80	8.71	0.12	10.89	15.44	1.77	0.10	0.20	99.54	226.8
52.36	1.14	8.80	9.03	0.24	10.75	15.41	1.78	0.11	0.12	99.73	230.3
50.83	1.15	9.10	9.19	0.23	10.72	15.31	1.84	0.14	0.16	98.68	234.1
50.82	1.23	8.99	9.14	0.25	10.83	15.28	1.82	0.10	0.07	98.52	234.8
51.93	1.16	8.86	9.05	0.21	10.71	15.33	1.86	0.13	0.12	99.36	235.6
50.43	1.19	9.31	9.12	0.23	10.73	15.11	1.89	0.12	0.18	98.30	245.1
51.12	1.22	9.18	9.24	0.22	10.67	15.25	1.87	0.08	0.09	98.94	246.8
50.68	1.26	9.49	9.27	0.21	10.50	15.03	1.92	0.10	0.13	98.59	256.0
50.79	1.25	9.62	9.29	0.26	10.58	15.10	1.99	0.15	0.09	99.10	258.2
50.40	1.21	9.49	9.20	0.18	10.68	15.07	1.89	0.11	0.15	98.38	258.8
50.74	1.21	9.64	9.30	0.17	10.32	14.98	1.97	0.11	0.18	98.60	266.9
50.53	1.21	9.63	9.20	0.15	10.40	15.19	1.97	0.10	0.18	98.54	268.2
50.63	1.20	9.44	9.33	0.18	10.50	15.00	1.93	0.12	0.11	98.43	270.8
50.68	1.24	9.68	9.25	0.18	10.39	15.02	1.92	0.11	0.12	98.59	277.8
50.53	1.23	9.87	9.27	0.25	10.29	14.98	1.99	0.16	0.08	98.65	278.3
50.85	1.29	9.74	9.29	0.23	10.39	14.91	2.00	0.12	0.09	98.92	282.8

50.50	1.28	9.95	9.30	0.12	10.23	14.95	2.01	0.09	0.02	98.44	288.4
51.01	1.22	9.93	9.27	0.19	10.27	14.78	2.02	0.12	0.12	98.94	288.8
50.78	1.28	9.84	9.46	0.12	10.34	14.92	1.97	0.13	0.17	99.01	294.8
50.82	1.28	10.09	9.30	0.23	10.22	14.87	1.94	0.09	0.16	99.00	298.5
50.57	1.26	10.01	9.31	0.16	10.07	14.83	2.02	0.13	0.12	98.48	299.7
50.44	1.29	9.91	9.29	0.21	10.19	14.70	2.00	0.12	0.14	98.30	306.8
50.43	1.33	10.35	9.35	0.10	9.97	14.78	1.99	0.13	0.09	98.52	308.5
50.66	1.30	10.28	9.46	0.16	10.11	14.70	2.02	0.11	0.13	98.92	310.6
50.78	1.32	10.37	9.49	0.23	9.80	14.76	2.08	0.14	0.12	99.08	318.6
50.98	1.32	10.10	9.39	0.21	9.98	14.51	2.02	0.14	0.24	98.88	318.8
50.77	1.36	10.44	9.44	0.14	10.04	14.64	2.00	0.09	0.05	98.96	321.6
50.33	1.32	10.61	9.56	0.23	10.05	14.63	2.10	0.10	0.16	99.08	328.7
50.75	1.34	10.33	9.31	0.17	9.96	14.53	1.97	0.13	0.17	98.67	330.8
50.41	1.33	10.54	9.36	0.26	9.90	14.52	2.08	0.13	0.11	98.62	332.5
50.31	1.33	10.53	9.46	0.09	9.71	14.38	2.12	0.10	0.25	98.29	338.7
50.60	1.37	10.58	9.52	0.20	9.78	14.46	2.12	0.14	0.11	98.87	342.8
50.53	1.30	10.69	9.55	0.17	9.86	14.48	2.04	0.15	0.20	98.97	343.4
50.55	1.37	10.71	9.49	0.13	9.79	14.41	2.08	0.13	0.12	98.78	348.8
50.35	1.36	10.77	9.53	0.18	9.71	14.33	2.12	0.14	0.13	98.61	354.3
50.35	1.34	10.63	9.59	0.22	9.74	14.37	2.10	0.13	0.28	98.73	354.8
50.62	1.34	10.80	9.52	0.13	9.62	14.52	2.05	0.16	0.09	98.86	358.9
50.62	1.33	10.95	9.55	0.15	9.56	14.29	2.15	0.14	0.12	98.86	365.3
50.75	1.39	10.98	9.59	0.17	9.67	14.14	2.10	0.11	0.14	99.03	366.8
50.46	1.40	10.93	9.54	0.19	9.43	14.33	2.14	0.10	0.08	98.58	369.0
50.65	1.41	11.16	9.64	0.21	9.55	14.34	2.06	0.14	0.05	99.19	376.2
51.05	1.41	11.10	9.58	0.27	9.52	14.16	2.08	0.17	0.15	99.49	378.8
50.98	1.39	11.14	9.57	0.11	9.52	14.23	2.17	0.13	0.19	99.43	379.0
51.06	1.39	11.16	9.64	0.18	9.56	14.11	2.03	0.15	0.13	99.39	389.1
49.91	1.50	11.52	9.77	0.20	9.39	13.96	2.21	0.17	0.17	98.81	397.6
49.82	1.46	11.56	9.74	0.17	9.26	14.01	2.19	0.12	0.10	98.43	407.9
49.88	1.47	11.58	9.70	0.21	9.25	13.93	2.18	0.18	0.18	98.55	411.9
50.11	1.44	11.66	9.73	0.19	9.19	13.63	2.16	0.18	0.11	98.41	418.3
50.03	1.50	11.68	9.72	0.14	9.17	13.90	2.17	0.13	0.11	98.56	422.6
50.06	1.50	11.93	9.80	0.20	9.21	13.73	2.20	0.12	0.19	98.93	428.6
49.81	1.50	11.86	9.70	0.14	9.10	13.92	2.21	0.18	0.20	98.63	433.2
49.81	1.50	12.12	9.91	0.18	8.92	13.85	2.26	0.13	0.16	98.84	439.0
49.82	1.50	11.94	9.90	0.15	9.10	13.69	2.22	0.21	0.05	98.57	443.9
49.73	1.58	12.12	9.84	0.14	9.06	13.61	2.17	0.14	0.09	98.48	449.3
49.60	1.60	12.38	9.64	0.12	8.95	13.67	2.23	0.19	0.18	98.53	453.1
49.77	1.51	11.99	9.90	0.18	8.84	13.79	2.22	0.13	0.11	98.44	454.5
49.82	1.52	12.17	9.90	0.23	8.80	13.64	2.27	0.16	0.15	98.65	459.7
49.54	1.55	12.43	9.66	0.20	8.90	13.63	2.26	0.09	0.14	98.40	463.1
50.16	1.50	12.14	9.84	0.19	8.94	13.75	2.33	0.13	0.14	99.11	465.2
50.15	1.60	12.32	9.93	0.20	8.78	13.70	2.29	0.14	0.17	99.28	470.1
49.75	1.58	12.46	9.73	0.21	8.99	13.65	2.32	0.14	0.15	98.97	473.2
50.11	1.58	12.19	9.92	0.18	8.80	13.67	2.22	0.13	0.16	98.96	475.8
49.69	1.58	12.49	10.01	0.25	8.79	13.50	2.25	0.18	0.18	98.92	480.4
49.62	1.59	12.63	9.92	0.18	8.74	13.44	2.29	0.15	0.12	98.68	483.3
49.54	1.51	12.27	9.99	0.14	8.69	13.38	2.19	0.14	0.10	97.94	486.4

49.91	1.58	12.37	9.87	0.11	8.59	13.24	2.31	0.19	0.08	98.23	490.8
49.88	1.60	12.68	9.81	0.09	8.64	13.55	2.30	0.18	0.12	98.86	493.4
49.64	1.55	12.32	9.87	0.15	8.67	13.39	2.34	0.18	0.20	98.30	497.1
50.15	1.63	12.60	10.03	0.27	8.61	13.29	2.30	0.16	0.18	99.23	501.1
50.40	1.60	12.78	9.80	0.21	8.66	13.57	2.30	0.16	0.20	99.66	503.4
50.03	1.56	12.42	9.96	0.12	8.58	13.32	2.34	0.15	0.20	98.67	507.7
50.03	1.58	12.68	10.09	0.14	8.50	13.25	2.31	0.18	0.05	98.80	511.5
50.29	1.67	12.80	9.89	0.13	8.48	13.37	2.34	0.11	0.16	99.23	513.5
50.14	1.56	12.46	10.17	0.25	8.49	13.45	2.33	0.22	0.20	99.27	518.4
50.11	1.60	12.84	10.24	0.12	8.43	13.31	2.32	0.18	0.11	99.24	521.8
49.98	1.67	12.88	10.05	0.15	8.47	13.34	2.36	0.15	0.19	99.24	523.6
49.55	1.66	12.52	10.03	0.23	8.43	13.21	2.27	0.15	0.19	98.23	529.0
50.15	1.63	12.89	10.32	0.21	8.35	13.09	2.22	0.17	0.23	99.26	532.2
49.90	1.69	12.97	10.13	0.17	8.42	13.18	2.41	0.14	0.17	99.17	533.6
50.53	1.53	12.81	10.09	0.16	8.44	13.16	2.34	0.15	0.13	99.34	539.7
50.00	1.65	13.15	9.98	0.26	8.43	13.09	2.43	0.12	0.14	99.23	543.7
49.06	1.66	12.88	10.42	0.08	8.34	12.93	2.35	0.11	0.14	97.95	544.5
49.56	1.67	12.72	10.23	0.23	8.43	13.20	2.42	0.16	0.10	98.72	550.3
49.88	1.69	13.08	10.19	0.19	8.33	13.16	2.33	0.18	0.31	99.33	553.8
49.19	1.66	13.03	10.40	0.19	8.25	12.93	2.35	0.18	0.13	98.32	557.5
49.20	1.64	13.09	10.31	0.21	8.17	13.00	2.36	0.19	0.20	98.37	558.5
49.54	1.69	13.18	10.18	0.19	8.22	12.95	2.45	0.15	0.20	98.73	563.9
49.38	1.68	13.06	10.30	0.18	8.17	12.90	2.46	0.21	0.16	98.48	572.5
49.23	1.71	13.24	10.42	0.22	8.17	12.73	2.35	0.19	0.22	98.47	573.7
50.65	1.62	13.32	10.22	0.17	8.13	12.90	2.37	0.13	0.26	99.76	573.9
50.54	1.64	13.46	10.25	0.24	8.07	12.88	2.42	0.18	0.19	99.87	584.0
49.31	1.71	13.08	10.43	0.14	8.17	12.90	2.42	0.17	0.19	98.51	586.5
49.28	1.68	13.44	10.50	0.17	8.08	12.69	2.43	0.17	0.18	98.61	590.0
49.31	1.74	13.48	10.54	0.14	8.04	12.67	2.49	0.21	0.17	98.78	594.5
49.24	1.68	13.30	10.42	0.18	8.03	12.69	2.43	0.17	0.13	98.27	600.5
49.30	1.69	13.28	10.52	0.19	7.99	12.64	2.47	0.20	0.17	98.45	606.2
49.40	1.74	13.53	10.55	0.10	7.87	12.59	2.50	0.18	0.23	98.69	611.9
49.75	1.71	13.28	10.36	0.23	7.93	12.64	2.52	0.15	0.15	98.71	614.5
49.04	1.71	13.36	10.59	0.27	7.86	12.57	2.42	0.14	0.13	98.08	622.4
49.74	1.75	13.42	10.48	0.22	7.84	12.66	2.50	0.15	0.24	99.00	628.5
49.74	1.79	13.66	10.65	0.17	7.99	12.48	2.51	0.23	0.13	99.34	629.2
49.46	1.67	13.60	10.69	0.16	7.92	12.40	2.59	0.18	0.14	98.81	638.6
49.45	1.69	13.40	10.71	0.12	7.92	12.54	2.53	0.15	0.16	98.67	642.5
49.74	1.78	13.71	10.72	0.15	7.89	12.36	2.57	0.17	0.17	99.25	646.5
49.02	1.72	13.61	10.69	0.16	7.68	12.16	2.55	0.17	0.23	97.98	652.0
49.28	1.71	13.41	10.72	0.13	7.80	12.22	2.57	0.19	0.25	98.26	654.9
49.82	1.71	13.36	10.60	0.21	7.80	12.39	2.51	0.21	0.22	98.83	656.5
49.07	1.73	13.65	10.58	0.25	7.76	12.44	2.58	0.20	0.21	98.47	663.9
49.38	1.68	13.53	10.82	0.28	7.66	12.27	2.57	0.19	0.11	98.49	671.1
49.22	1.78	13.72	10.91	0.16	7.72	12.13	2.64	0.20	0.23	98.72	678.5
49.62	1.76	13.95	10.69	0.23	7.65	12.32	2.63	0.15	0.17	99.17	681.2
50.37	1.73	13.64	10.99	0.18	7.75	12.33	2.58	0.21	0.18	99.97	687.3
50.10	1.74	13.91	10.84	0.20	7.64	12.14	2.62	0.20	0.14	99.54	698.5
49.27	1.70	13.83	11.04	0.27	7.58	12.05	2.67	0.21	0.11	98.73	705.0

49.21	1.78	13.82	10.97	0.18	7.56	12.03	2.56	0.18	0.18	98.46	715.9
49.32	1.77	13.76	11.17	0.22	7.43	12.13	2.62	0.19	0.12	98.74	717.8
49.11	1.81	13.99	11.15	0.31	7.52	11.83	2.75	0.23	0.21	98.91	725.9
49.02	1.76	13.83	11.09	0.18	7.52	11.91	2.64	0.17	0.15	98.28	731.5
50.33	1.76	13.94	10.99	0.17	7.49	11.98	2.65	0.17	0.15	99.63	733.2
49.16	1.75	13.83	11.11	0.17	7.56	11.83	2.68	0.17	0.19	98.45	742.4
49.38	1.73	13.91	11.19	0.21	7.51	11.64	2.64	0.20	0.18	98.59	750.7
49.36	1.69	13.87	11.20	0.23	7.38	11.90	2.67	0.18	0.18	98.66	758.0
49.49	1.82	13.96	11.16	0.24	7.43	11.85	2.71	0.22	0.22	99.10	767.0
49.11	1.74	13.99	11.41	0.29	7.36	11.68	2.71	0.20	0.26	98.75	775.4
49.26	1.73	13.93	11.30	0.16	7.46	11.66	2.71	0.21	0.30	98.72	784.5
49.06	1.80	13.86	11.22	0.22	7.40	11.66	2.56	0.23	0.11	98.10	791.6
49.08	1.76	14.00	11.32	0.19	7.31	11.65	2.71	0.23	0.18	98.42	800.1
49.21	1.82	13.77	11.34	0.13	7.35	11.71	2.62	0.15	0.08	98.19	811.0
49.22	1.78	13.88	11.42	0.17	7.43	11.71	2.66	0.20	0.18	98.65	816.2
49.07	1.77	13.87	11.35	0.14	7.16	11.53	2.59	0.18	0.21	97.87	824.8
49.45	1.73	13.89	11.35	0.25	7.36	11.58	2.74	0.20	0.10	98.64	837.5
49.13	1.78	13.89	11.49	0.21	7.38	11.57	2.72	0.17	0.15	98.49	840.8
49.02	1.76	13.98	11.64	0.18	7.27	11.47	2.74	0.22	0.15	98.42	849.6
49.20	1.76	13.98	11.31	0.22	7.14	11.50	2.74	0.22	0.22	98.29	864.0
49.23	1.82	13.90	11.44	0.18	7.33	11.57	2.62	0.16	0.15	98.38	865.4
49.45	1.78	13.95	11.53	0.20	7.23	11.41	2.76	0.17	0.21	98.68	874.3
49.04	1.77	13.96	11.49	0.24	7.22	11.55	2.77	0.21	0.17	98.42	890.0
49.68	1.77	13.93	11.49	0.19	7.34	11.42	2.73	0.21	0.22	98.98	890.5
48.90	1.74	14.07	11.73	0.09	7.18	11.47	2.77	0.19	0.18	98.31	899.0
49.01	1.76	14.01	11.56	0.25	7.25	11.47	2.70	0.18	0.23	98.41	914.6
49.01	1.79	13.85	11.56	0.20	7.05	11.23	2.80	0.24	0.20	97.92	923.7
50.11	1.78	13.99	11.58	0.27	7.19	11.24	2.73	0.11	0.21	99.21	939.2
49.34	1.76	13.88	11.83	0.16	7.15	11.26	2.69	0.23	0.16	98.46	948.5
49.87	1.76	13.91	11.86	0.19	7.12	11.17	2.76	0.23	0.14	99.00	973.2
49.03	1.67	13.95	11.58	0.23	7.25	11.31	2.75	0.16	0.14	98.06	1009.1
49.38	1.76	13.91	11.59	0.18	7.21	11.23	2.67	0.19	0.15	98.27	1010.7
48.80	1.68	13.90	11.76	0.24	7.11	11.13	2.78	0.19	0.18	97.76	1038.5
49.10	1.73	13.99	11.74	0.18	7.32	11.34	2.72	0.15	0.25	98.52	1048.9
49.68	1.77	14.07	11.85	0.22	7.19	11.25	2.80	0.22	0.24	99.29	1049.2
49.29	1.77	13.92	11.98	0.23	7.14	11.22	2.67	0.19	0.18	98.60	1069.5
49.02	1.81	13.91	11.96	0.19	7.18	11.31	2.78	0.21	0.24	98.62	1087.7
49.61	1.70	13.76	11.75	0.30	7.18	11.18	2.75	0.15	0.19	98.57	1088.7
48.79	1.80	13.93	11.88	0.19	7.16	11.11	2.68	0.18	0.19	97.89	1100.6
49.53	1.80	13.92	11.76	0.25	7.27	11.21	2.84	0.17	0.18	98.92	1126.2
49.25	1.73	13.93	11.92	0.15	7.14	11.08	2.72	0.20	0.20	98.31	1128.4
48.89	1.71	13.92	11.93	0.19	7.11	11.25	2.79	0.18	0.13	98.09	1131.6
48.75	1.68	13.76	12.05	0.18	7.10	11.00	2.79	0.17	0.20	97.67	1162.7
49.13	1.72	13.89	11.77	0.23	7.18	11.07	2.84	0.23	0.19	98.25	1164.7
48.77	1.71	13.86	11.64	0.27	7.22	11.06	2.76	0.15	0.17	97.61	1168.2
48.93	1.67	13.88	12.10	0.16	7.18	11.04	2.80	0.17	0.16	98.08	1193.8
49.39	1.81	13.94	11.88	0.25	7.20	11.06	2.77	0.18	0.25	98.75	1203.2
49.30	1.80	13.92	11.87	0.18	7.12	11.12	2.78	0.21	0.17	98.48	1208.0
49.15	1.78	13.80	11.86	0.24	7.24	11.14	2.75	0.23	0.13	98.31	1224.8

49.48	1.72	13.88	11.99	0.23	7.26	11.12	2.80	0.20	0.19	98.86	1241.7
49.13	1.77	13.71	11.89	0.34	7.28	11.02	2.78	0.19	0.19	98.29	1247.8
49.01	1.73	13.91	12.06	0.22	7.06	10.98	2.74	0.19	0.21	98.10	1255.9
49.04	1.79	13.87	11.93	0.21	7.13	11.02	2.74	0.21	0.17	98.11	1280.2
49.06	1.73	13.82	12.06	0.24	7.06	10.92	2.72	0.17	0.12	97.89	1287.0
49.18	1.78	13.92	11.90	0.27	7.26	10.94	2.72	0.20	0.14	98.31	1287.6
49.16	1.72	13.84	12.08	0.14	7.08	10.97	2.77	0.18	0.15	98.07	1318.0
49.13	1.67	13.83	12.01	0.17	7.21	11.01	2.71	0.17	0.22	98.13	1318.7
49.23	1.77	13.84	12.09	0.17	7.25	11.06	2.75	0.17	0.13	98.45	1327.4
49.26	1.71	13.85	12.13	0.18	7.11	10.91	2.81	0.19	0.14	98.29	1349.1
49.47	1.72	13.91	12.08	0.25	7.15	10.98	2.81	0.21	0.17	98.74	1357.2
48.94	1.77	13.75	12.07	0.16	7.28	11.02	2.74	0.21	0.13	98.07	1367.2
49.35	1.73	13.83	11.94	0.12	7.21	10.89	2.83	0.17	0.12	98.18	1380.1
48.88	1.75	13.89	12.12	0.16	7.26	11.07	2.75	0.17	0.25	98.28	1395.7
49.10	1.73	13.97	12.07	0.24	7.24	11.09	2.69	0.18	0.18	98.49	1406.9
49.14	1.69	13.77	12.07	0.18	7.12	10.88	2.77	0.15	0.18	97.95	1411.2
49.26	1.72	13.76	12.06	0.18	7.16	11.01	2.75	0.18	0.17	98.24	1434.2
49.17	1.68	13.75	12.04	0.20	7.18	10.97	2.71	0.18	0.20	98.09	1442.3
48.78	1.72	13.75	12.19	0.23	7.21	10.96	2.66	0.20	0.16	97.86	1446.7
48.95	1.76	13.83	11.92	0.23	7.21	11.05	2.67	0.21	0.29	98.10	1472.7
49.46	1.72	13.78	12.04	0.16	7.21	10.85	2.77	0.15	0.21	98.34	1473.3
49.30	1.75	13.76	12.11	0.25	7.31	11.08	2.70	0.16	0.21	98.62	1486.5
49.45	1.73	13.60	12.21	0.18	7.14	11.06	2.62	0.16	0.14	98.30	1511.2

Exp 7

SiO2	TiO2	Al2O3	FeO	MnO	MgO	CaO	Na2O	K2O	P2O5	Total	d (um)
52.68	0.72	4.41	8.84	0.18	13.57	17.42	1.39	0.06	0.04	99.30	24.5
52.83	0.72	4.53	8.69	0.17	13.51	17.50	1.32	0.06	0.04	99.38	26.9
52.41	0.78	5.06	8.86	0.17	13.15	17.31	1.49	0.06	0.05	99.34	47.9
52.90	0.79	5.23	8.80	0.20	13.22	17.15	1.51	0.06	0.05	99.89	53.4
52.50	0.88	5.83	9.05	0.22	12.57	16.97	1.59	0.07	0.06	99.74	71.4
52.56	0.88	5.95	9.01	0.19	12.04	16.59	1.67	0.07	0.06	99.03	79.8
51.87	1.02	7.84	8.83	0.16	11.49	16.09	1.77	0.08	0.10	99.23	95.5
51.58	1.07	8.23	8.90	0.12	11.12	15.92	1.80	0.10	0.09	98.94	110.7
51.68	1.12	8.79	8.86	0.17	10.85	15.74	1.88	0.08	0.11	99.27	125.9
51.14	1.19	9.00	9.13	0.18	10.54	15.37	1.96	0.10	0.08	98.67	136.1
51.64	1.20	9.26	8.98	0.19	10.51	15.56	1.89	0.11	0.14	99.48	141.0
51.94	1.19	9.64	8.96	0.18	10.10	15.39	1.88	0.11	0.12	99.51	156.2
50.67	1.31	9.88	9.11	0.19	9.99	15.19	2.00	0.11	0.14	98.59	157.4
50.64	1.35	10.50	9.26	0.20	9.63	14.82	2.01	0.12	0.14	98.67	179.6
50.34	1.43	11.52	9.22	0.19	9.20	14.50	2.13	0.13	0.16	98.82	200.2
50.53	1.48	11.78	9.45	0.20	8.95	14.30	2.20	0.14	0.18	99.19	223.2
50.38	1.57	12.34	9.37	0.18	8.55	14.11	2.28	0.15	0.19	99.11	243.1
50.09	1.55	12.66	9.62	0.19	8.43	13.79	2.32	0.15	0.20	98.99	266.7
50.16	1.65	13.07	9.69	0.17	8.13	13.63	2.32	0.15	0.19	99.15	285.9
50.06	1.65	13.24	9.91	0.19	7.97	13.38	2.43	0.16	0.20	99.17	310.3
49.88	1.74	13.44	9.89	0.21	7.75	13.23	2.56	0.16	0.17	99.03	328.7
49.92	1.72	13.60	10.04	0.20	7.68	12.98	2.60	0.17	0.18	99.10	353.9
50.07	1.76	13.87	10.23	0.19	7.49	12.88	2.60	0.17	0.20	99.47	371.6
49.80	1.76	13.83	10.40	0.19	7.37	12.61	2.58	0.19	0.19	98.92	397.5
49.96	1.76	13.92	10.50	0.21	7.28	12.57	2.61	0.18	0.19	99.17	414.3
49.77	1.82	13.98	10.65	0.21	7.18	12.30	2.69	0.18	0.19	98.97	441.1
49.91	1.78	13.94	10.69	0.21	7.17	12.29	2.74	0.18	0.19	99.11	457.1
49.91	1.84	14.01	10.93	0.18	7.09	12.10	2.69	0.16	0.19	99.10	484.6
49.78	1.80	14.03	11.01	0.21	7.02	12.07	2.69	0.18	0.17	98.96	500.0
49.86	1.79	14.01	11.21	0.20	6.96	11.90	2.72	0.17	0.18	99.01	528.1
49.94	1.83	13.98	11.17	0.22	6.94	11.87	2.73	0.18	0.16	99.02	542.8
49.77	1.83	14.02	11.38	0.19	6.93	11.71	2.76	0.18	0.14	98.91	571.7
50.01	1.81	13.99	11.43	0.22	6.92	11.72	2.82	0.20	0.19	99.29	585.6
49.58	1.82	14.09	11.55	0.24	6.89	11.57	2.78	0.17	0.20	98.89	615.3
49.62	1.81	13.96	11.58	0.22	6.85	11.61	2.77	0.18	0.15	98.76	628.5
49.84	1.85	14.01	11.58	0.22	6.87	11.49	2.74	0.17	0.20	98.95	658.9
50.10	1.84	13.94	11.60	0.19	6.81	11.43	2.72	0.17	0.20	98.99	671.3
49.88	1.86	14.10	11.71	0.20	6.90	11.40	2.80	0.19	0.17	99.20	702.5
49.99	1.83	13.96	11.81	0.24	6.86	11.39	2.81	0.19	0.19	99.26	714.0
49.75	1.83	14.07	11.79	0.20	6.85	11.34	2.86	0.18	0.17	99.03	746.0
49.90	1.85	14.08	11.89	0.23	6.89	11.36	2.81	0.18	0.15	99.33	756.9
49.79	1.83	13.99	11.89	0.24	6.84	11.27	2.85	0.18	0.18	99.06	789.5
49.71	1.78	13.94	11.89	0.20	6.79	11.28	2.81	0.17	0.20	98.77	799.7
49.83	1.81	14.04	11.85	0.18	6.85	11.25	2.85	0.17	0.15	98.97	833.1
49.75	1.82	13.98	11.97	0.21	6.82	11.25	2.78	0.16	0.18	98.91	842.5
49.77	1.84	14.01	11.95	0.23	6.87	11.21	2.83	0.16	0.18	99.03	876.7
50.07	1.86	14.00	11.89	0.24	6.81	11.22	2.82	0.17	0.19	99.26	885.4

49.77	1.79	14.05	12.00	0.23	6.82	11.18	2.86	0.16	0.15	99.01	920.3
49.92	1.84	14.06	11.97	0.25	6.82	11.16	2.81	0.18	0.17	99.18	963.9
49.97	1.82	13.97	12.08	0.26	6.82	11.18	2.85	0.19	0.18	99.33	970.9
50.05	1.82	14.02	11.94	0.20	6.84	11.11	2.85	0.18	0.21	99.23	1007.4
49.86	1.82	14.05	11.96	0.23	6.79	11.14	2.87	0.17	0.20	99.09	1013.8
50.06	1.82	14.07	11.85	0.21	6.79	11.13	2.80	0.19	0.18	99.09	1050.9
49.78	1.83	14.12	11.91	0.20	6.76	11.12	2.79	0.18	0.22	98.90	1056.6
49.98	1.77	14.07	11.82	0.19	6.80	11.12	2.93	0.19	0.19	99.06	1094.5
49.84	1.81	14.09	11.85	0.20	6.74	11.11	2.85	0.19	0.18	98.85	1099.4

Exp 8

SiO2	TiO2	Al2O3	FeO	MnO	MgO	CaO	Na2O	K2O	P2O5	Total	d (um)
53.54	0.72	5.27	9.40	0.19	11.50	15.86	1.78	0.09	0.01	98.36	16.9
53.63	0.68	4.93	8.34	0.11	12.92	16.95	1.47	0.09	0.10	99.21	28.4
53.33	0.70	4.88	8.42	0.23	12.48	16.59	1.60	0.12	-0.03	98.31	41.8
52.62	0.70	4.95	7.98	0.22	13.21	16.98	1.35	0.09	0.03	98.11	66.8
52.81	0.75	5.72	8.24	0.20	12.69	16.67	1.52	0.08	0.03	98.70	91.7
52.82	0.81	6.21	8.56	0.18	12.31	16.41	1.54	0.08	0.05	98.98	116.6
52.57	0.86	6.79	8.66	0.16	11.87	16.01	1.62	0.06	0.02	98.63	141.5
51.99	0.95	7.47	8.68	0.11	11.58	15.66	1.68	0.09	0.13	98.35	166.4
52.32	1.01	8.40	8.55	0.15	10.70	15.32	1.60	0.10	0.17	98.32	189.3
52.39	1.02	8.40	8.69	0.21	10.87	15.29	1.76	0.09	0.10	98.82	199.8
52.25	1.04	8.86	8.69	0.19	10.88	15.35	1.79	0.07	0.10	99.20	210.2
52.14	1.10	9.07	8.66	0.17	10.74	15.30	1.75	0.11	0.04	99.09	220.5
51.66	1.17	9.19	8.67	0.15	10.43	15.17	1.83	0.10	0.15	98.50	230.9
52.33	1.07	9.59	8.55	0.19	10.39	14.84	1.78	0.13	0.02	98.86	236.7
51.49	1.17	9.51	8.67	0.18	10.38	15.09	1.90	0.08	0.12	98.58	241.3
52.31	1.16	9.69	8.69	0.13	10.34	14.94	1.82	0.12	0.10	99.28	245.4
51.64	1.21	9.64	8.73	0.12	10.18	14.89	1.87	0.11	0.07	98.46	251.7
51.93	1.16	10.05	8.56	0.20	10.13	14.87	1.95	0.14	0.13	99.11	254.1
51.43	1.21	10.02	8.76	0.13	10.12	14.71	1.93	0.09	0.10	98.49	262.1
51.59	1.19	10.26	8.59	0.12	10.03	14.78	1.88	0.10	0.17	98.71	262.8
51.15	1.22	10.59	8.74	0.16	9.89	14.72	1.93	0.10	0.06	98.55	271.5
50.43	1.26	10.35	8.80	0.13	9.86	14.75	1.87	0.09	0.16	97.68	272.5
51.26	1.29	10.81	8.70	0.12	9.80	14.62	2.03	0.11	0.17	98.90	280.2
51.46	1.24	10.49	8.99	0.20	9.85	14.68	1.94	0.16	0.23	99.22	282.9
51.28	1.29	11.10	8.80	0.09	9.61	14.53	2.02	0.07	0.17	98.96	288.9
51.28	1.28	10.71	9.00	0.14	9.75	14.55	1.99	0.15	0.17	99.01	293.3
51.17	1.36	11.34	8.90	0.21	9.45	14.53	2.09	0.10	0.17	99.32	297.5
50.90	1.32	10.85	9.07	0.18	9.58	14.47	2.06	0.10	0.13	98.64	303.6
50.79	1.28	11.40	8.79	0.17	9.47	14.17	2.08	0.15	0.04	98.34	306.2
50.77	1.34	11.24	9.10	0.22	9.50	14.37	2.07	0.13	0.16	98.91	314.1
50.56	1.36	11.73	8.89	0.16	9.12	14.03	2.11	0.14	0.10	98.18	314.9
50.37	1.32	11.26	9.16	0.13	9.44	14.13	2.10	0.14	0.13	98.17	324.5
50.53	1.44	12.07	9.13	0.18	8.99	14.02	2.16	0.16	0.13	98.81	332.3
50.50	1.44	12.46	9.19	0.19	8.96	13.83	2.17	0.13	0.12	98.99	341.0
50.08	1.42	12.50	9.03	0.19	8.75	13.88	2.22	0.17	0.22	98.45	349.7
51.30	1.45	12.64	9.17	0.17	8.64	13.51	2.18	0.17	0.21	99.44	351.9
50.62	1.46	12.90	9.35	0.18	8.56	13.59	2.20	0.15	0.14	99.15	366.2
49.96	1.52	13.05	9.42	0.15	8.35	13.32	2.28	0.16	0.23	98.43	380.6
50.56	1.48	13.01	9.53	0.19	8.28	13.28	2.21	0.14	0.13	98.81	386.2
49.73	1.57	13.27	9.51	0.22	8.18	13.18	2.37	0.17	0.20	98.39	394.9
49.65	1.50	12.97	9.53	0.29	8.21	13.26	2.28	0.15	0.15	98.00	398.7
50.02	1.60	13.55	9.50	0.18	8.20	13.09	2.42	0.13	0.15	98.82	409.3
50.14	1.55	13.11	9.64	0.20	8.22	13.17	2.34	0.15	0.16	98.68	411.1
50.22	1.54	13.12	9.94	0.19	8.16	12.82	2.28	0.18	0.15	98.59	414.8
49.81	1.54	13.19	9.71	0.22	8.11	13.09	2.43	0.18	0.09	98.36	423.4
49.85	1.53	13.22	9.99	0.18	7.87	12.88	2.41	0.17	0.30	98.39	435.1
50.06	1.57	13.49	9.70	0.20	8.03	13.00	2.33	0.21	0.11	98.69	435.8

49.84	1.62	13.60	9.86	0.17	8.06	12.84	2.43	0.17	0.21	98.80	448.2
49.86	1.53	13.62	9.48	0.20	7.75	12.86	2.23	0.19	0.13	97.85	454.0
49.93	1.66	13.43	10.03	0.19	7.98	12.74	2.35	0.19	0.08	98.58	455.3
49.70	1.60	13.83	9.94	0.21	8.02	12.79	2.48	0.17	0.21	98.94	460.6
50.06	1.57	13.61	9.69	0.24	7.79	12.82	2.32	0.12	0.22	98.45	474.2
49.76	1.60	13.40	10.15	0.25	7.75	12.44	2.42	0.15	0.06	97.98	475.5
50.02	1.61	13.59	9.76	0.21	7.75	12.62	2.43	0.14	0.25	98.38	494.5
49.21	1.62	13.70	10.21	0.22	7.66	12.46	2.44	0.17	0.16	97.85	495.7
50.15	1.60	13.67	9.97	0.13	7.76	12.52	2.52	0.17	0.19	98.68	514.7
49.76	1.59	13.67	10.44	0.16	7.53	12.27	2.59	0.19	0.23	98.43	516.0
49.96	1.66	13.91	10.12	0.21	7.59	12.42	2.56	0.20	0.14	98.78	535.1
49.64	1.70	13.71	10.56	0.26	7.58	12.11	2.52	0.20	0.04	98.30	536.2
49.69	1.68	13.98	10.21	0.23	7.59	12.33	2.50	0.17	0.27	98.66	555.3
49.59	1.74	13.86	10.67	0.19	7.36	11.95	2.58	0.16	0.30	98.40	556.4
49.79	1.66	13.93	10.32	0.28	7.49	12.15	2.49	0.17	0.08	98.36	575.6
49.92	1.73	13.89	10.70	0.19	7.35	11.98	2.56	0.22	0.22	98.76	576.7
49.77	1.66	14.01	10.54	0.16	7.28	12.05	2.61	0.21	0.14	98.41	595.9
49.28	1.64	14.06	10.84	0.20	7.35	11.78	2.64	0.22	0.17	98.17	596.9
49.73	1.63	14.03	10.51	0.18	7.25	11.84	2.58	0.17	0.13	98.04	616.2
49.81	1.68	13.98	10.75	0.26	7.36	11.54	2.64	0.17	0.18	98.36	617.1
49.85	1.65	14.06	10.66	0.18	7.34	11.84	2.60	0.20	0.09	98.48	636.4
49.88	1.69	13.97	11.02	0.15	7.24	11.62	2.64	0.19	0.14	98.53	637.4
49.89	1.75	14.12	10.78	0.19	7.17	11.89	2.65	0.17	0.15	98.77	656.8
49.72	1.74	14.02	11.10	0.27	7.16	11.52	2.64	0.22	0.19	98.59	657.6
49.43	1.73	14.08	10.86	0.25	7.21	11.57	2.70	0.19	0.30	98.32	677.0
49.75	1.78	13.94	11.14	0.18	7.14	11.47	2.71	0.22	0.23	98.54	677.8
49.76	1.70	14.22	11.09	0.17	7.05	11.69	2.63	0.18	0.17	98.65	697.3
49.84	1.72	14.09	11.33	0.24	7.00	11.33	2.68	0.20	0.23	98.65	698.1
49.77	1.71	14.20	11.04	0.14	7.02	11.55	2.60	0.19	0.27	98.50	717.6
49.72	1.72	14.13	11.26	0.27	7.06	11.29	2.67	0.18	0.24	98.54	718.3
49.77	1.73	14.09	11.27	0.20	7.13	11.42	2.81	0.19	0.21	98.80	737.9
49.31	1.68	14.04	11.31	0.22	7.06	11.29	2.74	0.22	0.21	98.06	738.5
49.74	1.73	14.26	11.21	0.26	7.07	11.46	2.72	0.25	0.19	98.90	758.2
49.80	1.68	14.08	11.42	0.21	7.08	11.27	2.71	0.17	0.18	98.59	758.7
49.60	1.70	14.19	11.27	0.27	7.02	11.43	2.68	0.20	0.19	98.54	778.4
49.57	1.73	14.18	11.67	0.16	6.98	11.16	2.68	0.23	0.18	98.54	779.0
49.92	1.73	14.14	11.33	0.24	7.08	11.20	2.66	0.19	0.22	98.71	798.8
49.45	1.66	14.08	11.61	0.16	7.00	11.19	2.67	0.20	0.15	98.17	799.2
49.26	1.78	14.07	11.44	0.09	6.96	11.25	2.80	0.17	0.24	98.06	819.0
49.88	1.75	13.93	11.59	0.18	7.08	11.08	2.75	0.16	0.24	98.64	819.4
49.44	1.81	14.12	11.48	0.21	6.95	11.20	2.79	0.26	0.18	98.42	839.3
49.20	1.72	14.14	11.61	0.20	7.05	10.97	2.73	0.18	0.34	98.14	839.6
49.42	1.72	13.99	11.67	0.27	6.97	10.99	2.70	0.19	0.22	98.14	859.8
49.71	1.81	14.12	11.55	0.22	7.06	11.17	2.78	0.16	0.14	98.70	878.3
49.47	1.70	14.02	11.72	0.16	6.95	10.95	2.73	0.23	0.24	98.14	880.0
49.41	1.66	13.97	11.83	0.22	6.93	10.99	2.75	0.18	0.19	98.13	900.3
49.54	1.80	14.02	11.79	0.15	6.92	11.10	2.72	0.14	0.16	98.33	917.4
49.57	1.75	13.95	11.92	0.23	7.00	10.93	2.75	0.19	0.16	98.45	920.5
49.83	1.76	14.22	11.89	0.23	6.85	10.98	2.79	0.22	0.16	98.92	940.7

49.47	1.74	14.10	11.77	0.22	6.89	11.08	2.82	0.19	0.19	98.46	956.3
49.68	1.77	14.17	11.94	0.24	6.93	10.85	2.79	0.15	0.22	98.74	961.0
49.62	1.73	14.06	11.92	0.26	6.90	10.96	2.72	0.22	0.18	98.56	981.2
49.74	1.70	14.04	11.84	0.22	6.91	10.93	2.82	0.21	0.07	98.48	995.4
49.33	1.71	14.17	12.07	0.11	6.94	10.74	2.73	0.16	0.19	98.15	1031.4
49.65	1.76	14.26	11.82	0.22	7.00	11.00	2.82	0.21	0.14	98.88	1034.4
49.61	1.74	14.13	12.01	0.20	6.98	10.85	2.79	0.17	0.19	98.65	1073.4
49.53	1.75	14.01	12.03	0.19	6.94	10.89	2.81	0.13	0.19	98.46	1081.5
49.49	1.78	14.09	11.90	0.27	6.99	10.73	2.86	0.20	0.16	98.46	1112.5
49.79	1.74	14.02	11.91	0.14	6.90	10.87	2.77	0.19	0.12	98.45	1131.7
49.46	1.77	14.08	11.99	0.23	6.87	10.83	2.78	0.19	0.16	98.36	1151.5
49.73	1.73	14.06	12.00	0.23	6.90	10.70	2.73	0.18	0.25	98.51	1181.9
49.31	1.75	14.07	12.05	0.18	6.98	10.91	2.83	0.23	0.17	98.48	1190.5
49.28	1.73	14.02	12.00	0.14	6.92	10.76	2.79	0.20	0.13	97.96	1229.5
49.39	1.77	14.03	12.03	0.23	6.93	10.78	2.85	0.20	0.17	98.37	1232.0
49.80	1.75	14.22	12.24	0.18	6.90	10.81	2.73	0.18	0.19	98.98	1268.6
49.55	1.67	14.28	12.02	0.22	6.88	10.64	2.75	0.19	0.21	98.41	1282.2
49.36	1.78	14.10	12.11	0.19	6.82	10.74	2.82	0.20	0.19	98.31	1307.5
49.60	1.75	14.03	12.05	0.23	6.88	10.72	2.82	0.19	0.14	98.39	1332.4
49.89	1.77	14.20	12.16	0.22	7.01	10.91	2.82	0.18	0.12	99.28	1346.6
49.47	1.68	14.21	12.01	0.16	6.87	10.90	2.74	0.24	0.23	98.51	1382.5
49.35	1.77	14.16	11.92	0.27	6.90	10.85	2.76	0.16	0.24	98.39	1385.6
49.36	1.77	14.11	11.95	0.13	6.88	10.75	2.74	0.20	0.16	98.04	1424.6
49.26	1.68	14.14	12.08	0.19	6.88	10.72	2.78	0.18	0.27	98.17	1432.7
49.03	1.69	14.13	12.15	0.14	6.94	10.92	2.81	0.18	0.29	98.28	1463.6
49.10	1.71	14.05	12.18	0.22	7.04	10.89	2.78	0.14	0.20	98.30	1482.9
49.47	1.67	14.14	12.06	0.16	7.04	10.66	2.77	0.18	0.17	98.30	1502.7
49.59	1.76	14.30	12.08	0.15	7.00	10.71	2.86	0.16	0.22	98.82	1541.7
49.78	1.76	14.21	12.18	0.21	7.08	10.77	2.76	0.16	0.15	99.05	1580.7

Exp 11

SiO2	TiO2	Al2O3	FeO	MnO	MgO	CaO	Na2O	K2O	P2O5	Total	d (um)
51.75	1.46	10.48	11.04	0.10	8.53	13.40	2.28	0.13	0.04	99.22	8.2
51.75	1.39	10.44	11.05	0.20	8.38	13.28	2.29	0.14	0.04	98.97	9.4
51.23	1.38	10.09	11.07	0.10	9.09	13.48	2.12	0.14	0.11	98.81	11.6
51.67	1.42	10.39	10.78	0.15	8.80	13.38	2.22	0.12	0.09	99.02	21.0
51.54	1.38	10.29	10.36	0.19	9.13	13.48	2.12	0.12	0.08	98.67	23.2
51.55	1.36	10.43	10.56	0.11	9.30	13.66	2.01	0.15	0.07	99.20	24.4
51.74	1.43	10.45	10.59	0.14	9.00	13.34	2.12	0.11	0.12	99.02	33.7
51.48	1.41	10.57	10.53	0.15	9.21	13.56	2.09	0.10	0.13	99.23	36.9
51.48	1.36	10.64	11.09	0.15	8.87	13.37	2.20	0.13	0.10	99.39	37.1
51.90	1.40	10.75	10.93	0.10	8.94	13.36	2.17	0.14	0.18	99.87	46.4
51.30	1.46	10.64	10.81	0.15	8.92	13.32	2.12	0.14	0.11	98.97	49.9
51.70	1.46	10.83	10.56	0.18	9.05	13.28	2.24	0.14	0.09	99.52	50.7
51.37	1.45	10.87	10.71	0.19	8.99	13.47	2.12	0.15	0.12	99.44	59.2
51.01	1.45	10.79	10.69	0.15	9.03	13.37	2.12	0.13	0.10	98.86	62.7
51.67	1.43	11.00	10.74	0.20	8.94	13.29	2.15	0.15	0.14	99.72	64.5
51.34	1.49	11.14	10.92	0.17	8.92	13.42	2.17	0.13	0.19	99.87	72.0
51.52	1.50	11.02	10.83	0.13	8.76	13.37	2.16	0.12	0.16	99.57	75.5
51.07	1.52	11.17	10.65	0.12	8.81	13.22	2.13	0.10	0.13	98.92	78.3
51.24	1.50	11.40	10.78	0.20	8.72	13.29	2.18	0.12	0.10	99.53	84.6
50.21	1.49	11.04	10.84	0.11	8.57	12.93	2.24	0.16	0.17	97.76	88.2
50.94	1.49	11.39	10.71	0.18	8.65	13.16	2.13	0.14	0.16	98.95	92.0
50.68	1.57	11.51	10.76	0.15	8.66	13.12	2.20	0.13	0.10	98.87	97.4
50.63	1.54	11.38	10.92	0.12	8.69	13.10	2.18	0.14	0.10	98.80	101.0
50.39	1.52	11.45	10.70	0.14	8.45	12.91	2.29	0.09	0.12	98.05	101.1
50.35	1.53	11.62	10.84	0.20	8.48	12.96	2.22	0.12	0.16	98.48	105.8
50.46	1.51	11.71	10.79	0.14	8.47	13.03	2.15	0.13	0.03	98.42	110.2
50.36	1.51	11.50	10.73	0.14	8.42	12.96	2.29	0.11	0.12	98.14	110.6
50.35	1.52	11.63	10.74	0.11	8.49	12.90	2.05	0.18	0.07	98.05	113.8
50.25	1.54	11.46	10.74	0.15	8.60	12.89	2.24	0.12	0.05	98.04	113.8
50.56	1.58	12.01	10.75	0.13	8.40	12.76	2.19	0.19	0.13	98.71	119.6
50.47	1.53	11.66	10.83	0.16	8.47	12.76	2.30	0.16	0.14	98.47	120.2
50.27	1.52	11.75	10.73	0.13	8.55	12.83	2.28	0.18	0.08	98.33	123.3
50.48	1.52	11.56	10.85	0.14	8.43	12.78	2.26	0.13	0.13	98.27	124.3
50.71	1.48	11.70	10.79	0.13	8.37	12.79	2.24	0.15	0.19	98.55	129.7
49.97	1.51	11.93	10.79	0.22	8.28	12.65	2.30	0.13	0.14	97.93	133.7
50.02	1.52	11.64	10.80	0.17	8.42	12.79	2.27	0.19	0.10	97.91	135.0
49.52	1.53	11.85	10.65	0.17	8.28	12.65	2.33	0.18	0.09	97.25	139.3
50.86	1.57	11.88	10.75	0.16	8.21	12.68	2.31	0.14	0.16	98.72	144.1
50.36	1.58	11.99	10.67	0.14	8.37	12.81	2.38	0.12	0.16	98.59	145.7
50.46	1.54	12.06	10.90	0.18	8.26	12.72	2.33	0.16	0.16	98.78	148.8
50.72	1.62	12.05	10.86	0.23	8.21	12.69	2.33	0.12	0.16	98.99	158.4
50.26	1.60	12.70	10.76	0.24	8.29	12.46	2.44	0.13	0.16	99.05	164.9
49.94	1.58	12.04	10.76	0.22	8.25	12.63	2.35	0.13	0.12	98.02	166.9
49.80	1.62	12.15	10.84	0.18	8.10	12.54	2.32	0.16	0.25	97.97	167.9
49.72	1.62	12.24	10.89	0.15	8.09	12.56	2.35	0.13	0.15	97.90	177.5
49.71	1.65	12.14	10.80	0.11	8.18	12.56	2.38	0.15	0.14	97.81	177.6
50.75	1.60	12.66	10.72	0.19	8.16	12.37	2.40	0.17	0.16	99.18	185.7

50.03	1.57	12.25	10.83	0.23	8.15	12.56	2.31	0.13	0.18	98.23	188.2
50.93	1.60	12.50	11.10	0.12	7.96	12.25	2.33	0.17	0.14	99.08	192.5
50.24	1.65	12.52	10.81	0.11	7.90	12.28	2.37	0.21	0.11	98.21	196.2
50.35	1.60	12.29	10.86	0.20	8.03	12.46	2.45	0.15	0.10	98.50	198.9
50.20	1.59	12.55	10.94	0.18	7.83	12.36	2.35	0.18	0.20	98.38	206.1
49.62	1.66	12.70	10.76	0.16	7.90	12.20	2.42	0.16	0.07	97.65	206.6
50.00	1.67	12.76	10.97	0.14	7.73	12.27	2.41	0.16	0.09	98.20	219.7
50.55	1.67	12.72	10.81	0.10	7.62	12.39	2.41	0.18	0.14	98.58	224.0
50.35	1.70	12.87	10.94	0.15	7.78	12.23	2.40	0.18	0.13	98.71	224.9
49.96	1.60	12.87	11.07	0.24	7.86	12.30	2.39	0.16	0.14	98.58	233.3
49.87	1.68	12.82	10.66	0.16	7.60	12.29	2.38	0.11	0.15	97.74	238.3
49.82	1.66	12.75	11.02	0.20	7.54	12.15	2.49	0.17	0.16	97.95	241.1
49.96	1.62	13.06	10.96	0.25	7.67	12.16	2.52	0.15	0.18	98.52	243.8
49.86	1.64	12.92	10.99	0.21	7.70	12.00	2.37	0.19	0.18	98.05	246.8
49.00	1.69	12.96	10.90	0.17	7.54	12.10	2.51	0.17	0.17	97.22	252.4
49.92	1.67	12.95	11.01	0.17	7.65	12.20	2.48	0.16	0.19	98.40	257.2
49.75	1.69	13.10	10.83	0.16	7.49	11.91	2.46	0.18	0.18	97.74	258.2
50.82	1.66	13.25	11.14	0.27	7.37	12.06	2.38	0.18	0.10	99.22	259.0
49.80	1.64	13.12	10.95	0.23	7.83	12.10	2.45	0.14	0.13	98.38	260.4
51.00	1.61	13.07	11.08	0.21	7.42	12.03	2.44	0.14	0.16	99.15	262.4
49.86	1.66	13.41	11.01	0.14	7.52	11.89	2.49	0.13	0.14	98.26	272.7
49.53	1.70	13.00	11.24	0.19	7.68	12.01	2.57	0.13	0.07	98.12	273.4
49.77	1.69	13.18	11.16	0.19	7.49	11.84	2.42	0.17	0.09	98.00	280.5
49.62	1.61	13.12	11.19	0.22	7.41	11.97	2.45	0.16	0.15	97.90	283.9
49.53	1.67	13.40	10.95	0.15	7.48	12.00	2.50	0.17	0.16	98.00	287.1
50.14	1.62	13.62	11.05	0.13	7.43	11.87	2.42	0.18	0.09	98.55	299.3
49.66	1.70	13.38	11.22	0.22	7.43	11.93	2.54	0.19	0.11	98.37	302.0
50.10	1.68	13.33	11.13	0.10	7.37	11.81	2.52	0.15	0.12	98.31	305.5
49.72	1.69	13.17	11.10	0.17	7.42	11.84	2.49	0.19	0.10	97.90	321.0
49.65	1.72	13.53	11.14	0.11	7.35	11.73	2.52	0.16	0.13	98.03	323.6
49.87	1.70	13.49	11.20	0.20	7.30	11.61	2.57	0.14	0.13	98.21	327.1
49.55	1.66	13.23	11.24	0.19	7.48	11.81	2.62	0.14	0.11	98.02	342.6
49.50	1.74	13.47	11.08	0.23	7.23	11.70	2.57	0.16	0.19	97.89	345.2
49.46	1.61	13.59	11.27	0.15	7.18	11.57	2.63	0.18	0.25	97.88	348.7
49.62	1.72	13.48	11.29	0.27	7.36	11.65	2.50	0.14	0.08	98.10	364.4
49.37	1.78	13.50	11.46	0.14	7.27	11.53	2.51	0.18	0.18	97.91	366.7
49.75	1.70	13.56	11.37	0.17	7.32	11.56	2.57	0.18	0.07	98.25	370.2
49.72	1.69	13.55	11.24	0.13	7.31	11.64	2.46	0.20	0.13	98.08	386.0
49.59	1.77	13.80	11.34	0.14	7.21	11.44	2.65	0.16	0.14	98.22	388.3
49.53	1.74	13.66	11.45	0.16	7.30	11.63	2.59	0.22	0.11	98.39	391.8
49.49	1.68	13.60	11.38	0.19	7.18	11.62	2.58	0.21	0.13	98.07	407.7
49.85	1.74	13.81	11.55	0.14	6.96	11.30	2.57	0.15	0.13	98.20	419.3
50.29	1.78	13.89	11.43	0.24	7.14	11.39	2.66	0.17	0.11	99.10	422.3
49.28	1.65	13.85	11.26	0.16	7.24	11.57	2.62	0.18	0.18	97.98	429.3
50.12	1.80	13.67	11.36	0.23	7.06	11.53	2.58	0.15	0.15	98.63	432.3
49.85	1.72	13.75	11.45	0.22	7.14	11.47	2.67	0.15	0.12	98.54	452.8
49.21	1.81	14.07	11.46	0.13	6.98	11.19	2.69	0.18	0.19	97.92	453.2
49.39	1.85	13.79	11.52	0.12	7.00	11.29	2.63	0.20	0.12	97.91	453.8
50.05	1.84	13.88	11.46	0.06	6.92	11.37	2.63	0.16	0.19	98.54	496.2

49.34	1.78	13.65	11.36	0.17	6.95	11.24	2.64	0.18	0.16	97.47	496.9
49.66	1.78	13.68	11.53	0.07	7.02	11.37	2.65	0.19	0.10	98.06	497.5
49.22	1.79	13.77	11.52	0.17	6.99	11.22	2.65	0.15	0.19	97.67	536.7
48.95	1.73	13.99	11.71	0.17	7.08	11.21	2.68	0.22	0.14	97.88	541.5
49.05	1.78	13.82	11.66	0.25	7.07	11.41	2.67	0.18	0.18	98.08	546.8
50.39	1.84	13.84	11.71	0.16	6.90	11.27	2.72	0.14	0.14	99.10	569.1
50.29	1.84	14.06	11.77	0.17	6.88	11.06	2.64	0.22	0.16	99.09	571.4
49.57	1.77	13.81	11.65	0.18	6.73	11.06	2.58	0.20	0.16	97.71	593.5
49.30	1.84	13.82	11.75	0.15	6.86	11.31	2.61	0.14	0.16	97.95	605.5
49.58	1.81	13.92	11.65	0.23	6.80	10.97	2.75	0.21	0.11	98.03	609.1
49.49	1.78	13.77	11.73	0.17	6.84	11.06	2.65	0.16	0.16	97.79	635.4
49.49	1.81	13.82	11.82	0.17	6.87	11.07	2.62	0.18	0.19	98.02	641.9
49.51	1.85	13.80	11.90	0.15	6.84	11.13	2.65	0.19	0.19	98.20	646.9
49.13	1.84	13.79	11.85	0.21	6.72	11.23	2.74	0.17	0.16	97.84	677.3
49.33	1.83	13.90	11.91	0.15	6.76	10.93	2.73	0.18	0.10	97.82	678.2
49.43	1.84	13.87	11.80	0.22	6.83	10.97	2.71	0.19	0.11	97.96	684.7
48.94	1.82	13.97	11.82	0.13	6.84	11.00	2.68	0.21	0.19	97.61	714.6
49.29	1.80	13.78	11.84	0.16	6.81	11.10	2.74	0.21	0.17	97.90	719.2
48.87	1.82	13.90	11.95	0.11	6.81	11.01	2.74	0.21	0.22	97.64	722.5
49.04	1.79	13.91	11.84	0.17	6.86	11.00	2.77	0.19	0.13	97.71	761.1
49.10	1.82	13.74	12.02	0.18	6.72	10.91	2.67	0.15	0.19	97.51	783.1
50.26	1.80	13.80	11.94	0.13	6.67	11.14	2.69	0.19	0.16	98.79	791.6
49.36	1.80	13.82	11.88	0.22	6.84	11.09	2.68	0.19	0.17	98.05	800.0
49.70	1.86	13.92	11.98	0.15	6.91	10.95	2.73	0.20	0.10	98.51	852.6
49.27	1.83	13.82	12.03	0.16	6.72	10.89	2.68	0.21	0.09	97.70	863.5
49.52	1.81	13.74	12.03	0.14	6.76	10.90	2.72	0.16	0.18	97.95	867.4
49.48	1.84	13.83	12.02	0.19	6.75	10.96	2.70	0.16	0.18	98.12	922.1
49.19	1.80	13.86	11.90	0.22	6.71	11.08	2.67	0.19	0.09	97.69	934.8
49.53	1.84	14.04	12.13	0.12	6.85	10.98	2.71	0.16	0.13	98.49	935.4
49.44	1.83	13.88	12.20	0.21	6.81	10.96	2.61	0.21	0.08	98.23	991.6
49.44	1.84	13.76	11.97	0.20	6.83	10.88	2.74	0.18	0.22	98.06	1002.2
49.24	1.84	13.91	12.04	0.21	6.75	10.91	2.70	0.19	0.16	97.93	1007.2
49.39	1.87	13.84	11.95	0.18	6.69	10.86	2.73	0.18	0.16	97.84	1061.1
49.32	1.82	13.86	12.00	0.23	6.72	10.89	2.72	0.13	0.08	97.78	1069.6
49.37	1.88	13.87	12.15	0.09	6.83	10.94	2.72	0.20	0.19	98.21	1079.0
49.20	1.91	13.89	11.87	0.17	6.77	10.86	2.75	0.21	0.19	97.80	1130.6
49.50	1.88	13.98	12.01	0.20	6.68	11.06	2.74	0.20	0.10	98.36	1137.0
49.13	1.87	13.76	11.94	0.19	6.83	10.83	2.71	0.17	0.08	97.51	1150.9
49.31	1.84	13.79	12.17	0.11	6.76	10.97	2.64	0.23	0.13	97.95	1200.2
49.21	1.86	13.77	12.09	0.18	6.74	10.95	2.63	0.19	0.19	97.80	1204.4
49.49	1.83	13.81	12.01	0.15	6.73	10.99	2.60	0.19	0.16	97.95	1222.7
48.98	1.81	13.88	11.98	0.23	6.80	10.85	2.79	0.21	0.23	97.77	1269.6
49.27	1.84	13.93	12.01	0.16	6.81	10.88	2.71	0.16	0.21	97.96	1271.8
49.29	1.85	13.86	11.99	0.21	6.82	10.92	2.64	0.21	0.13	97.91	1294.6
49.30	1.84	13.87	12.01	0.22	6.73	10.91	2.73	0.16	0.16	97.92	1339.2
49.25	1.77	13.85	11.97	0.18	6.78	10.86	2.75	0.15	0.12	97.69	1339.2
49.41	1.88	14.02	12.02	0.16	6.83	11.05	2.74	0.20	0.18	98.49	1366.4
49.71	1.85	13.89	12.08	0.21	6.80	11.01	2.73	0.22	0.10	98.58	1406.6
49.01	1.83	13.95	11.96	0.12	6.77	10.90	2.71	0.18	0.19	97.60	1474.0

Exp 12

SiO2	TiO2	Al2O3	FeO	MnO	MgO	CaO	Na2O	K2O	P2O5	Total	d (um)
51.00	1.38	10.68	11.54	0.11	9.04	12.86	2.10	0.14	0.19	99.04	13.0
50.48	1.42	11.06	11.15	0.19	8.77	13.00	1.86	0.16	0.10	98.19	19.5
50.72	1.50	11.21	11.23	0.19	8.97	13.05	2.08	0.16	0.06	99.17	20.3
52.08	1.39	11.30	10.12	0.16	8.73	12.77	2.41	0.19	0.10	99.24	25.0
50.75	1.47	11.54	11.08	0.22	8.61	12.63	2.36	0.11	0.13	98.89	31.5
50.35	1.46	11.74	11.20	0.22	8.72	12.76	2.30	0.15	0.13	99.02	33.6
51.34	1.44	11.49	11.03	0.26	8.37	12.65	2.35	0.18	0.09	99.19	37.0
50.62	1.47	11.50	11.27	0.16	8.56	12.75	2.23	0.14	0.17	98.87	49.0
50.95	1.44	11.94	10.92	0.16	8.29	12.51	2.31	0.15	0.14	98.78	73.1
50.79	1.48	12.15	10.94	0.29	8.27	12.42	2.41	0.13	0.19	99.08	80.7
50.36	1.53	12.17	10.84	0.15	8.21	12.22	2.35	0.17	0.16	98.17	88.4
51.21	1.48	12.14	11.08	0.11	8.16	12.54	2.39	0.16	0.16	99.41	98.5
51.16	1.52	11.92	10.91	0.13	8.14	12.34	2.29	0.13	0.07	98.60	102.6
50.88	1.49	12.15	10.98	0.18	8.04	12.44	2.30	0.15	0.17	98.78	105.4
50.65	1.49	12.25	10.89	0.14	8.13	12.39	2.34	0.17	0.22	98.67	109.1
50.44	1.53	12.43	10.99	0.15	7.99	12.45	2.43	0.23	0.07	98.72	112.2
50.56	1.49	12.20	11.03	0.27	8.14	12.44	2.38	0.17	0.20	98.88	115.6
50.49	1.47	12.45	10.90	0.21	8.02	12.36	2.41	0.17	0.16	98.62	119.0
50.03	1.50	12.27	11.10	0.17	7.97	12.31	2.42	0.15	0.12	98.03	122.1
50.50	1.47	12.54	11.08	0.23	7.96	12.25	2.42	0.17	0.18	98.79	125.8
50.75	1.54	12.53	10.87	0.13	7.96	12.24	2.39	0.16	0.10	98.66	128.6
50.92	1.46	12.69	10.86	0.09	7.94	12.22	2.48	0.17	0.15	98.98	129.7
50.18	1.46	12.58	11.11	0.21	7.90	12.41	2.36	0.17	0.21	98.59	132.6
50.07	1.46	12.48	10.88	0.28	7.94	12.28	2.45	0.17	0.17	98.17	135.1
50.46	1.53	12.77	10.99	0.21	7.85	12.30	2.42	0.14	0.17	98.84	142.6
50.55	1.50	12.79	10.79	0.19	7.77	12.16	2.47	0.15	0.23	98.59	142.9
49.94	1.52	12.96	11.19	0.19	7.67	12.18	2.45	0.15	0.19	98.45	156.2
50.02	1.56	12.79	10.77	0.17	7.76	12.03	2.53	0.16	0.12	97.91	156.8
49.99	1.56	13.01	10.90	0.19	7.64	12.11	2.44	0.17	0.24	98.25	171.0
50.85	1.61	13.33	10.92	0.16	7.52	11.95	2.52	0.17	0.19	99.22	180.7
50.12	1.58	13.27	10.96	0.16	7.34	11.91	2.45	0.14	0.14	98.08	197.3
50.04	1.63	13.57	11.08	0.24	7.40	11.91	2.49	0.19	0.23	98.79	214.0
50.45	1.58	13.41	11.14	0.14	7.39	11.79	2.38	0.18	0.22	98.67	225.5
50.36	1.68	13.60	11.04	0.25	7.41	11.87	2.54	0.19	0.18	99.09	230.8
50.50	1.57	13.47	11.19	0.24	7.35	11.89	2.49	0.16	0.18	99.03	237.1
50.32	1.60	13.56	11.06	0.27	7.40	11.76	2.54	0.16	0.08	98.75	240.9
50.16	1.61	13.74	11.12	0.23	7.37	11.76	2.60	0.17	0.13	98.89	247.5
50.37	1.64	13.73	11.13	0.15	7.35	11.91	2.51	0.16	0.15	99.09	253.1
50.12	1.61	13.77	11.11	0.19	7.35	11.85	2.51	0.19	0.20	98.88	256.4
50.26	1.72	13.93	10.96	0.19	7.23	11.68	2.51	0.17	0.13	98.79	264.1
50.45	1.64	13.55	11.15	0.30	7.33	11.67	2.52	0.12	0.20	98.92	269.0
50.26	1.63	13.69	11.12	0.25	7.39	11.66	2.49	0.17	0.21	98.86	271.9
49.73	1.69	14.02	11.24	0.19	7.34	11.70	2.58	0.21	0.21	98.89	280.8
49.99	1.63	13.74	11.26	0.19	7.37	11.74	2.67	0.18	0.26	99.01	285.0
50.12	1.64	13.74	11.22	0.19	7.25	11.66	2.65	0.17	0.15	98.78	287.4
49.87	1.62	13.93	11.36	0.12	7.30	11.66	2.55	0.19	0.25	98.85	301.0
49.92	1.71	13.97	11.29	0.14	7.26	11.64	2.68	0.17	0.19	98.96	302.9

50.40	1.63	13.81	11.07	0.27	7.05	11.58	2.60	0.16	0.16	98.74	335.2
50.24	1.68	14.08	11.41	0.16	7.04	11.43	2.69	0.21	0.12	99.07	351.1
50.25	1.65	13.87	11.30	0.13	7.07	11.47	2.58	0.20	0.10	98.61	353.3
50.07	1.61	14.05	11.28	0.21	7.06	11.52	2.71	0.18	0.17	98.87	366.9
50.27	1.66	13.99	11.28	0.20	7.12	11.51	2.61	0.15	0.19	98.99	371.4
50.32	1.64	14.02	11.55	0.22	7.05	11.36	2.71	0.23	0.10	99.21	382.7
50.08	1.66	14.04	11.42	0.20	6.90	11.39	2.67	0.22	0.23	98.80	389.5
49.89	1.70	13.88	11.27	0.13	7.09	11.51	2.61	0.17	0.26	98.51	391.7
50.24	1.70	14.17	11.60	0.11	7.16	11.45	2.72	0.22	0.17	99.52	398.5
49.34	1.71	13.99	11.69	0.09	7.10	11.42	2.57	0.17	0.23	98.30	407.7
49.99	1.64	13.89	11.41	0.19	7.02	11.50	2.66	0.21	0.14	98.67	409.6
49.57	1.72	14.12	11.60	0.19	6.93	11.40	2.70	0.18	0.16	98.56	414.3
49.85	1.67	14.16	11.46	0.22	6.97	11.30	2.67	0.17	0.18	98.64	425.8
50.19	1.71	13.92	11.42	0.13	7.05	11.33	2.66	0.19	0.17	98.77	427.6
49.62	1.71	14.14	11.57	0.18	7.05	11.22	2.63	0.20	0.10	98.41	443.9
49.59	1.74	14.03	11.39	0.20	7.00	11.33	2.66	0.18	0.13	98.24	445.6
49.73	1.61	14.13	11.42	0.13	7.00	11.35	2.59	0.20	0.29	98.44	463.6
50.46	1.67	14.08	11.56	0.31	7.02	11.18	2.67	0.18	0.14	99.27	469.6
50.01	1.69	14.11	11.79	0.21	6.89	11.24	2.65	0.22	0.21	99.01	480.1
49.64	1.70	13.94	11.63	0.16	7.01	11.23	2.68	0.18	0.15	98.32	481.5
50.13	1.59	14.01	11.71	0.21	6.99	11.05	2.67	0.18	0.12	98.66	490.5
50.51	1.67	14.09	11.69	0.23	6.98	11.26	2.68	0.18	0.21	99.50	493.6
49.83	1.72	14.09	11.79	0.18	6.94	11.15	2.65	0.21	0.17	98.72	501.0
49.94	1.63	14.02	11.77	0.19	6.94	11.13	2.68	0.20	0.17	98.67	503.2
49.99	1.68	14.17	11.91	0.17	6.99	11.15	2.73	0.21	0.12	99.11	511.5
50.20	1.68	14.10	11.75	0.13	7.04	11.15	2.66	0.18	0.20	99.08	512.9
49.69	1.67	14.15	11.86	0.20	7.03	11.09	2.66	0.19	0.16	98.69	522.0
50.16	1.63	14.09	11.74	0.21	6.90	11.08	2.71	0.20	0.29	99.01	522.5
50.33	1.65	13.94	11.63	0.14	6.94	11.15	2.63	0.23	0.16	98.81	527.5
49.98	1.68	14.03	11.64	0.24	6.97	11.18	2.70	0.14	0.20	98.77	532.1
50.18	1.65	13.96	11.71	0.22	6.94	11.18	2.67	0.20	0.27	98.98	537.1
49.69	1.70	14.19	11.79	0.21	6.90	11.12	2.74	0.24	0.10	98.69	541.8
49.94	1.66	13.96	11.74	0.19	6.93	11.32	2.63	0.19	0.14	98.70	546.8
49.93	1.65	14.04	11.66	0.19	6.93	11.15	2.74	0.19	0.22	98.70	556.4
49.96	1.70	14.06	11.62	0.30	6.93	11.21	2.73	0.18	0.20	98.89	566.0
49.67	1.67	13.95	11.76	0.15	6.92	11.12	2.77	0.19	0.13	98.33	575.7
49.62	1.67	13.96	11.96	0.25	6.90	10.97	2.65	0.20	0.19	98.36	582.7
50.08	1.58	13.97	11.76	0.17	6.93	11.17	2.65	0.18	0.15	98.62	582.9
49.99	1.61	13.99	11.84	0.23	6.90	11.11	2.67	0.16	0.29	98.79	595.8
49.92	1.72	14.08	11.73	0.14	6.88	11.07	2.72	0.18	0.09	98.54	602.6
50.13	1.64	14.09	11.77	0.18	6.84	10.88	2.76	0.17	0.27	98.73	605.1
49.93	1.68	14.03	11.96	0.21	6.94	11.12	2.69	0.20	0.16	98.90	615.9
49.80	1.66	14.10	11.84	0.28	6.92	11.09	2.57	0.15	0.15	98.55	622.3
49.95	1.63	14.11	11.90	0.29	6.93	11.12	2.73	0.20	0.15	99.01	627.4
49.84	1.65	14.09	11.83	0.20	7.05	11.09	2.72	0.14	0.23	98.84	636.2
49.28	1.65	14.17	11.93	0.21	6.93	10.96	2.72	0.16	0.24	98.25	642.0
50.17	1.64	13.92	11.98	0.24	6.87	11.03	2.78	0.20	0.21	99.05	652.2
49.35	1.71	14.14	11.90	0.24	6.93	10.99	2.74	0.17	0.17	98.34	656.4
49.60	1.66	13.79	12.12	0.20	6.86	11.02	2.56	0.19	0.18	98.17	659.8

50.16	1.65	14.14	11.85	0.20	6.92	11.03	2.80	0.16	0.24	99.14	679.3
50.20	1.71	14.14	11.92	0.18	6.94	10.89	2.62	0.16	0.21	98.97	682.2
50.13	1.63	14.13	11.90	0.27	6.88	11.08	2.68	0.21	0.12	99.01	704.6
50.35	1.57	14.06	11.79	0.20	6.88	10.83	2.67	0.21	0.11	98.67	706.5
50.24	1.61	13.87	11.87	0.21	6.85	11.05	2.66	0.13	0.21	98.71	707.5
49.96	1.63	14.08	11.91	0.22	6.76	10.96	2.67	0.19	0.15	98.51	726.9
49.95	1.64	13.83	11.85	0.23	6.83	10.93	2.76	0.18	0.14	98.34	727.5
50.23	1.66	14.14	12.01	0.17	6.87	10.89	2.73	0.17	0.16	99.03	733.6
49.76	1.63	14.11	11.96	0.19	6.82	11.04	2.68	0.22	0.23	98.64	747.4
49.29	1.67	14.01	11.96	0.22	6.90	10.91	2.70	0.21	0.11	97.98	749.3
49.39	1.59	14.18	12.03	0.21	6.87	10.84	2.71	0.22	0.24	98.29	760.8
49.94	1.59	14.02	12.01	0.17	6.87	11.05	2.78	0.23	0.16	98.82	767.4
50.19	1.64	13.98	11.96	0.25	6.88	10.98	2.71	0.17	0.26	99.03	801.7
50.17	1.64	13.99	11.94	0.23	6.92	10.88	2.78	0.15	0.11	98.81	823.5
50.16	1.71	13.93	11.92	0.17	6.76	11.14	2.75	0.17	0.23	98.94	824.8
50.12	1.60	13.89	12.09	0.24	6.71	10.90	2.72	0.19	0.10	98.56	830.8
50.35	1.65	14.06	11.92	0.18	6.91	10.81	2.69	0.21	0.13	98.91	852.7
49.79	1.67	14.11	11.98	0.23	6.85	11.06	2.66	0.18	0.21	98.74	855.4
50.21	1.63	14.05	12.08	0.19	6.90	11.05	2.71	0.19	0.19	99.19	859.9
50.02	1.66	14.05	11.96	0.26	6.90	11.01	2.80	0.22	0.10	98.98	882.1
49.93	1.65	14.02	11.92	0.23	6.77	11.04	2.70	0.19	0.18	98.62	886.1
50.22	1.65	14.06	12.02	0.22	6.90	10.93	2.71	0.25	0.19	99.15	889.1
50.09	1.65	13.95	12.02	0.35	6.83	10.95	2.70	0.21	0.13	98.88	911.3
49.88	1.66	14.11	11.81	0.20	6.81	10.93	2.77	0.17	0.15	98.50	916.8
50.03	1.69	13.98	12.08	0.22	6.78	10.99	2.57	0.20	0.19	98.72	918.1
49.80	1.62	14.12	12.00	0.18	6.88	10.81	2.69	0.21	0.23	98.55	940.7
49.54	1.61	13.88	12.17	0.21	6.79	10.84	2.63	0.17	0.19	98.01	947.3
49.45	1.65	14.08	12.22	0.16	6.87	11.01	2.63	0.18	0.21	98.46	947.5
49.95	1.56	14.06	11.99	0.18	6.79	10.91	2.62	0.22	0.31	98.60	969.9
49.46	1.66	13.78	12.19	0.20	6.85	11.00	2.70	0.21	0.19	98.25	976.3
49.81	1.61	14.07	12.05	0.26	6.83	10.93	2.72	0.17	0.19	98.63	978.1
50.11	1.57	13.89	12.00	0.20	6.85	10.92	2.64	0.18	0.24	98.61	999.3
49.93	1.65	13.91	11.86	0.17	6.78	10.96	2.70	0.14	0.27	98.37	1005.4
49.82	1.67	13.89	11.88	0.29	6.80	10.88	2.63	0.16	0.26	98.28	1008.8
50.25	1.64	14.18	11.98	0.18	6.87	10.92	2.73	0.19	0.21	99.14	1028.6
50.08	1.66	13.87	12.10	0.28	6.92	10.93	2.70	0.19	0.17	98.90	1034.5
50.14	1.65	14.08	11.96	0.24	6.89	10.98	2.64	0.20	0.14	98.91	1039.4
49.94	1.67	14.11	12.05	0.22	6.86	10.88	2.66	0.15	0.10	98.64	1063.6
49.99	1.68	14.04	11.91	0.14	6.94	10.96	2.77	0.20	0.15	98.76	1070.1
49.75	1.67	13.98	11.99	0.18	6.86	10.90	2.69	0.17	0.19	98.38	1087.3
49.40	1.67	13.97	12.34	0.21	6.90	11.02	2.65	0.19	0.24	98.59	1092.7
49.75	1.69	13.97	11.97	0.26	6.83	10.83	2.60	0.20	0.10	98.19	1100.7
49.76	1.62	14.13	11.86	0.14	6.92	10.99	2.65	0.20	0.18	98.47	1116.5
50.14	1.74	14.10	11.95	0.12	6.87	10.90	2.72	0.18	0.21	98.93	1121.8
49.77	1.66	13.92	11.91	0.21	6.86	11.03	2.72	0.19	0.17	98.45	1131.5
49.80	1.67	13.95	12.00	0.17	6.89	10.93	2.76	0.19	0.29	98.65	1145.9
49.98	1.65	13.99	12.10	0.18	6.91	10.99	2.73	0.18	0.12	98.84	1150.9
49.37	1.68	14.04	12.17	0.23	6.76	10.98	2.71	0.11	0.14	98.17	1162.2
49.67	1.62	14.08	11.99	0.26	6.93	11.01	2.74	0.17	0.10	98.56	1175.1

49.52	1.67	14.03	12.25	0.25	6.88	10.85	2.75	0.21	0.10	98.53	1180.0
49.82	1.67	14.09	11.93	0.15	6.87	10.96	2.67	0.14	0.29	98.58	1192.8
49.51	1.65	14.08	11.98	0.22	6.92	11.01	2.69	0.18	0.18	98.41	1204.5
49.69	1.69	14.01	12.01	0.17	6.99	10.96	2.84	0.20	0.18	98.74	1223.5
50.10	1.76	14.05	12.12	0.11	6.87	11.05	2.74	0.16	0.18	99.14	1277.4
50.09	1.73	14.09	12.09	0.27	6.95	10.99	2.69	0.17	0.14	99.20	1278.4
50.11	1.72	14.17	12.00	0.20	7.00	10.98	2.66	0.21	0.18	99.23	1300.3
49.70	1.75	13.99	12.01	0.23	6.84	10.97	2.66	0.20	0.13	98.48	1333.9
49.99	1.79	14.12	11.93	0.25	6.87	11.00	2.76	0.15	0.13	98.98	1336.5
49.32	1.69	13.89	12.03	0.17	6.78	10.95	2.79	0.20	0.16	97.99	1354.8
49.93	1.75	14.15	12.04	0.27	7.03	11.03	2.71	0.13	0.15	99.18	1389.4
50.02	1.76	14.26	11.91	0.28	6.84	11.13	2.80	0.21	0.13	99.33	1395.6
49.82	1.69	14.04	11.88	0.23	6.88	10.90	2.76	0.19	0.18	98.56	1409.3
49.82	1.75	13.93	11.97	0.19	6.89	11.08	2.71	0.17	0.17	98.67	1444.9
49.10	1.70	13.91	12.08	0.13	6.86	11.13	2.69	0.18	0.15	97.92	1454.7
49.76	1.74	14.08	11.94	0.28	6.94	11.04	2.68	0.17	0.29	98.92	1463.8
49.66	1.73	13.98	12.11	0.32	6.89	11.01	2.74	0.19	0.21	98.83	1500.4
49.81	1.79	14.22	12.01	0.28	7.01	11.10	2.76	0.13	0.23	99.33	1513.8
49.71	1.73	13.92	11.96	0.25	6.97	11.01	2.83	0.16	0.13	98.66	1518.3

Exp 14

SiO2	TiO2	Al2O3	FeO	MnO	MgO	CaO	Na2O	K2O	P2O5	Total	d (um)
50.48	1.67	12.37	11.84	0.20	7.75	11.68	2.53	0.17	0.11	98.79	0.7
50.38	1.69	12.66	11.93	0.18	7.60	11.67	2.54	0.16	0.16	98.95	12.2
50.03	1.66	12.53	11.94	0.21	7.74	11.72	2.52	0.15	0.14	98.65	12.4
50.14	1.67	12.68	11.96	0.21	7.69	11.71	2.56	0.16	0.17	98.94	24.0
50.13	1.69	12.76	11.89	0.21	7.55	11.71	2.55	0.16	0.16	98.79	26.2
49.90	1.69	12.79	11.88	0.23	7.60	11.64	2.54	0.16	0.15	98.59	35.7
49.99	1.68	12.97	11.82	0.22	7.54	11.68	2.56	0.17	0.14	98.77	40.2
50.96	1.70	12.71	11.83	0.21	7.37	11.65	2.54	0.17	0.17	99.30	45.5
50.33	1.72	12.84	11.95	0.21	7.40	11.66	2.55	0.17	0.15	98.99	56.5
50.24	1.70	13.03	11.95	0.26	7.37	11.59	2.62	0.17	0.18	99.12	67.5
50.25	1.71	13.19	11.87	0.20	7.38	11.58	2.60	0.17	0.17	99.12	78.5
49.98	1.71	13.29	11.85	0.22	7.33	11.60	2.63	0.16	0.15	98.92	89.5
50.99	1.74	13.19	11.65	0.24	7.27	11.56	2.60	0.16	0.19	99.58	113.4
50.14	1.72	13.12	11.78	0.22	7.22	11.57	2.55	0.17	0.20	98.68	118.3
49.97	1.75	13.40	11.78	0.24	7.27	11.54	2.61	0.18	0.16	98.90	143.4
50.24	1.79	13.53	11.79	0.22	7.14	11.52	2.59	0.16	0.19	99.17	148.3
50.00	1.77	13.63	11.78	0.21	7.17	11.50	2.63	0.16	0.19	99.03	173.4
50.36	1.78	13.74	11.73	0.21	7.15	11.47	2.64	0.17	0.16	99.39	178.2
49.90	1.77	13.73	11.74	0.19	7.07	11.48	2.67	0.18	0.16	98.89	203.4
50.20	1.78	13.91	11.80	0.24	7.10	11.43	2.70	0.17	0.15	99.46	208.2
49.76	1.81	13.80	11.78	0.22	7.01	11.42	2.62	0.17	0.19	98.78	233.4
50.22	1.82	13.97	11.74	0.22	7.01	11.38	2.67	0.17	0.19	99.38	238.2
50.10	1.78	13.85	11.79	0.22	6.97	11.41	2.60	0.18	0.16	99.06	263.4
50.08	1.77	13.92	11.72	0.22	7.04	11.38	2.68	0.17	0.20	99.18	268.2
49.54	1.76	13.86	11.92	0.24	6.95	11.42	2.72	0.18	0.19	98.78	293.4
50.12	1.83	13.94	11.79	0.18	6.99	11.36	2.66	0.17	0.16	99.19	298.2
50.08	1.80	13.96	11.88	0.21	6.94	11.36	2.66	0.17	0.18	99.24	323.4
50.26	1.83	13.95	11.78	0.20	6.99	11.34	2.67	0.19	0.18	99.39	328.2
50.15	1.83	14.10	11.74	0.18	6.93	11.35	2.70	0.17	0.15	99.28	358.2
49.79	1.83	13.93	11.83	0.24	6.89	11.31	2.71	0.16	0.20	98.88	383.4
50.11	1.82	13.99	11.80	0.26	6.94	11.31	2.67	0.17	0.19	99.24	388.2
49.94	1.85	13.97	12.02	0.17	6.86	11.31	2.69	0.17	0.20	99.17	413.4
50.02	1.83	14.05	11.87	0.20	6.92	11.25	2.71	0.18	0.16	99.18	418.2
49.61	1.83	13.94	12.06	0.24	6.86	11.28	2.72	0.18	0.20	98.92	443.4
50.23	1.82	14.04	11.88	0.20	6.94	11.26	2.71	0.17	0.19	99.44	448.2
49.90	1.83	13.95	11.98	0.22	6.86	11.27	2.68	0.17	0.18	99.06	473.4
49.70	1.80	13.92	12.07	0.21	6.85	11.22	2.65	0.18	0.18	98.76	503.4
50.28	1.87	14.09	11.90	0.24	6.91	11.22	2.69	0.15	0.18	99.53	508.2
49.85	1.84	13.92	12.08	0.21	6.89	11.28	2.67	0.19	0.17	99.09	533.4
49.97	1.83	14.04	11.91	0.23	6.93	11.23	2.66	0.18	0.21	99.18	538.2
49.77	1.85	13.93	12.06	0.25	6.83	11.24	2.69	0.19	0.16	98.96	563.4
50.24	1.81	14.12	11.89	0.19	6.89	11.25	2.74	0.18	0.20	99.50	568.2
49.66	1.85	13.95	12.13	0.23	6.85	11.20	2.69	0.19	0.17	98.90	648.7
49.94	1.81	14.03	12.02	0.21	6.90	11.21	2.68	0.18	0.16	99.13	652.3
49.84	1.82	14.00	12.28	0.22	6.88	11.19	2.66	0.18	0.18	99.23	734.1
50.03	1.85	14.05	12.11	0.21	6.90	11.17	2.67	0.17	0.18	99.34	736.4
49.64	1.76	13.90	12.22	0.22	6.88	11.21	2.65	0.17	0.17	98.82	819.3

50.05	1.84	14.01	12.08	0.24	6.86	11.17	2.65	0.17	0.18	99.25	820.5
49.71	1.84	14.06	12.22	0.23	6.88	11.16	2.65	0.18	0.20	99.13	904.6
49.69	1.81	13.94	12.21	0.24	6.86	11.21	2.70	0.17	0.18	99.00	904.6
49.55	1.83	14.01	12.21	0.21	6.87	11.22	2.76	0.18	0.17	99.01	988.8
49.74	1.76	13.95	12.27	0.19	6.90	11.18	2.69	0.18	0.16	99.01	990.0
49.60	1.81	13.94	12.14	0.19	6.87	11.16	2.68	0.17	0.20	98.76	1072.8
49.48	1.85	13.96	12.23	0.23	6.91	11.20	2.65	0.18	0.18	98.88	1075.3
49.67	1.81	14.01	12.13	0.19	6.90	11.19	2.68	0.18	0.17	98.93	1156.9
49.82	1.82	13.98	12.17	0.22	6.90	11.18	2.64	0.18	0.17	99.08	1160.6

Exp 15

SiO2	TiO2	Al2O3	FeO	MnO	MgO	CaO	Na2O	K2O	P2O5	Total	d (um)
53.78	0.97	7.00	9.65	0.17	10.16	15.46	2.02	0.10	0.05	99.48	15.6
53.81	0.76	5.67	8.59	0.12	12.49	17.26	1.41	0.04	0.01	100.22	16.8
53.32	0.76	5.89	8.49	0.12	12.33	17.12	1.46	0.07	0.07	99.66	40.6
53.02	0.91	6.79	8.45	0.15	12.17	16.82	1.37	0.06	0.06	99.85	90.7
52.59	0.94	7.27	8.63	0.20	11.90	16.58	1.35	0.10	0.04	99.65	114.7
52.51	0.91	7.86	8.76	0.12	11.50	16.18	1.62	0.12	0.10	99.75	139.2
52.11	1.03	7.99	8.58	0.14	11.59	16.45	1.36	0.11	0.05	99.50	140.7
52.14	1.02	8.38	8.91	0.20	10.87	15.51	1.43	0.07	0.09	98.73	178.7
52.13	1.16	8.62	8.79	0.11	11.01	16.14	1.72	0.10	0.12	100.00	180.7
51.58	1.08	9.10	9.28	0.22	10.53	15.30	1.87	0.13	0.07	99.25	203.2
51.71	1.18	9.15	9.02	0.13	10.74	15.68	1.45	0.11	0.14	99.40	205.8
51.22	1.18	9.79	9.37	0.25	10.23	15.15	1.54	0.10	0.11	99.02	227.7
51.30	1.23	9.73	9.03	0.13	10.25	15.50	1.90	0.11	0.07	99.37	230.8
51.11	1.28	10.28	9.35	0.20	9.95	14.95	1.49	0.15	0.18	99.08	255.8
51.61	1.30	9.44	9.41	0.06	10.14	15.38	1.84	0.07	0.15	99.50	261.6
50.82	1.27	10.19	9.23	0.18	9.91	15.03	1.93	0.11	0.12	98.93	282.7
51.03	1.36	10.56	9.62	0.17	9.56	14.82	1.56	0.15	0.20	99.15	296.6
50.86	1.39	10.96	9.30	0.13	9.30	14.45	1.86	0.14	0.17	98.69	307.7
51.15	1.34	11.24	9.28	0.19	9.33	14.30	2.07	0.18	0.12	99.31	325.5
51.10	1.40	11.27	9.46	0.20	9.22	14.36	2.03	0.08	0.26	99.51	331.5
50.91	1.41	11.34	9.42	0.12	9.24	14.08	2.12	0.14	0.18	99.08	337.5
50.16	1.38	11.32	9.51	0.12	9.15	14.54	2.08	0.12	0.18	98.67	338.9
50.61	1.42	11.49	9.65	0.19	9.17	14.41	2.08	0.13	0.20	99.47	343.5
50.29	1.41	11.62	9.45	0.19	9.15	14.40	2.14	0.15	0.08	98.99	344.6
50.68	1.38	11.63	9.66	0.14	9.12	14.06	2.13	0.12	0.21	99.27	349.5
50.69	1.44	11.74	9.52	0.15	9.17	14.19	2.11	0.15	0.14	99.45	350.3
50.59	1.42	11.66	9.43	0.16	9.06	13.98	2.15	0.13	0.23	98.94	355.5
50.52	1.37	11.80	9.58	0.20	9.02	14.15	2.12	0.14	0.12	99.12	356.1
50.44	1.37	11.80	9.61	0.18	9.00	14.01	2.14	0.18	0.13	98.99	361.5
50.26	1.49	11.93	9.76	0.19	9.03	14.08	2.13	0.15	0.14	99.29	361.8
50.00	1.38	11.56	9.49	0.25	8.91	14.07	2.07	0.14	0.21	98.20	365.0
50.21	1.45	11.86	9.61	0.19	8.85	13.86	2.13	0.13	0.16	98.61	367.5
50.42	1.38	12.06	9.61	0.18	8.94	14.09	2.16	0.13	0.13	99.20	367.6
49.96	1.43	11.63	9.54	0.21	8.93	13.90	2.16	0.18	0.18	98.25	370.9
50.35	1.43	12.14	9.68	0.10	8.92	13.79	2.25	0.16	0.26	99.20	373.3
50.39	1.36	12.10	9.75	0.19	8.93	14.03	2.21	0.15	0.22	99.43	373.5
49.89	1.43	11.91	9.38	0.15	8.86	14.06	2.13	0.17	0.15	98.21	376.7
50.28	1.39	12.35	9.59	0.21	8.74	13.89	2.24	0.16	0.15	99.16	379.1
49.76	1.49	12.10	9.64	0.19	8.97	13.81	2.25	0.17	0.18	98.73	379.5
50.57	1.49	11.94	9.60	0.14	8.89	14.04	2.19	0.15	0.22	99.35	382.5
50.19	1.41	12.24	9.68	0.12	8.61	13.73	2.23	0.12	0.17	98.64	384.8
50.48	1.49	11.99	9.58	0.19	8.87	14.07	2.17	0.19	0.18	99.36	388.4
50.15	1.45	12.52	9.84	0.12	8.75	13.85	2.31	0.16	0.19	99.46	390.6
50.49	1.45	12.29	9.71	0.23	8.84	13.85	2.15	0.17	0.20	99.47	394.2
49.62	1.52	12.56	9.71	0.18	8.75	13.68	2.31	0.16	0.17	98.81	396.3
50.11	1.52	12.29	9.80	0.27	8.72	13.90	2.18	0.14	0.15	99.21	400.1
49.56	1.45	12.59	9.88	0.18	8.64	13.50	2.27	0.16	0.21	98.57	402.1

50.22	1.52	12.36	9.90	0.21	8.79	13.73	2.26	0.15	0.12	99.38	405.9
49.38	1.56	12.62	9.80	0.20	8.57	13.78	2.27	0.16	0.23	98.67	407.8
50.12	1.53	12.50	10.01	0.23	8.75	13.56	2.30	0.14	0.17	99.43	411.8
50.80	1.43	11.95	9.61	0.19	8.56	13.31	2.16	0.15	0.24	98.52	415.5
51.01	1.44	12.17	9.73	0.18	8.68	13.77	2.18	0.14	0.07	99.50	415.6
49.98	1.56	12.55	9.83	0.12	8.63	13.59	2.26	0.18	0.19	99.01	417.6
49.98	1.54	12.62	9.72	0.21	8.49	13.49	2.28	0.11	0.12	98.73	423.4
49.90	1.59	12.73	9.76	0.20	8.60	13.65	2.25	0.18	0.20	99.21	429.2
50.40	1.40	12.53	9.89	0.16	8.60	13.38	2.31	0.15	0.11	99.05	430.6
50.59	1.47	12.38	9.91	0.19	8.54	13.69	2.26	0.17	0.14	99.47	431.4
49.64	1.63	12.63	10.01	0.22	8.50	13.52	2.31	0.15	0.13	98.90	435.1
49.51	1.59	12.93	9.95	0.24	8.49	13.52	2.22	0.17	0.16	98.91	440.9
50.02	1.44	12.66	9.94	0.16	8.42	13.34	2.27	0.13	0.12	98.61	445.6
50.22	1.45	12.49	9.96	0.18	8.50	13.39	2.21	0.13	0.15	98.79	447.3
50.08	1.52	12.99	10.13	0.09	8.23	13.17	2.33	0.15	0.15	98.95	460.6
50.10	1.40	12.68	10.14	0.19	8.42	13.26	2.30	0.17	0.10	98.89	463.2
49.91	1.57	13.06	10.15	0.23	8.10	13.24	2.39	0.16	0.21	99.13	475.6
50.56	1.55	12.83	9.91	0.21	8.19	13.34	2.27	0.17	0.12	99.29	478.9
50.06	1.44	12.98	10.22	0.24	8.24	13.08	2.37	0.16	0.14	99.06	479.1
49.93	1.59	13.30	10.17	0.12	8.00	12.67	2.44	0.13	0.16	98.66	490.6
50.09	1.46	13.10	10.13	0.20	8.18	13.01	2.40	0.14	0.15	98.99	495.0
49.90	1.60	13.11	10.08	0.23	8.14	13.41	2.45	0.17	0.19	99.39	495.6
49.70	1.53	13.42	10.33	0.16	7.78	12.58	2.40	0.19	0.13	98.38	505.6
49.78	1.48	13.27	10.25	0.13	8.06	12.59	2.39	0.18	0.22	98.50	510.9
49.57	1.64	13.16	10.18	0.25	8.08	13.01	2.33	0.16	0.24	98.76	512.2
49.89	1.53	13.40	10.44	0.19	7.83	12.39	2.49	0.18	0.24	98.71	520.6
50.11	1.39	13.54	10.36	0.16	7.97	12.50	2.43	0.17	0.19	98.98	526.7
49.81	1.61	13.39	10.25	0.27	7.93	13.00	2.39	0.20	0.15	99.15	528.9
49.60	1.56	13.56	10.51	0.21	7.74	12.55	2.55	0.20	0.23	98.87	535.6
50.06	1.34	13.70	10.36	0.20	7.93	12.46	2.49	0.19	0.13	99.01	542.6
49.83	1.66	13.39	10.42	0.16	7.90	12.87	2.49	0.23	0.18	99.29	545.6
49.69	1.58	13.73	10.56	0.16	7.72	12.31	2.47	0.20	0.18	98.74	550.5
49.89	1.51	13.66	10.47	0.18	7.75	12.33	2.50	0.26	0.04	98.75	558.5
49.57	1.70	13.47	10.44	0.22	7.83	12.73	2.43	0.18	0.12	98.84	562.3
49.53	1.61	13.76	10.69	0.09	7.60	12.33	2.56	0.20	0.26	98.78	565.5
49.68	1.51	13.88	10.64	0.21	7.74	12.26	2.48	0.17	0.22	98.93	574.4
49.70	1.68	13.63	10.43	0.11	7.65	12.48	2.47	0.18	0.18	98.64	579.1
49.67	1.65	13.86	10.71	0.23	7.59	12.33	2.55	0.18	0.14	99.08	580.5
49.76	1.52	13.80	10.79	0.24	7.58	12.27	2.60	0.18	0.15	99.01	590.2
49.61	1.71	13.78	10.74	0.22	7.47	12.05	2.59	0.20	0.22	98.78	595.5
49.18	1.70	13.74	10.65	0.12	7.69	12.35	2.52	0.20	0.14	98.40	595.7
49.52	1.62	13.91	10.70	0.21	7.59	12.14	2.55	0.17	0.21	98.81	606.1
49.89	1.74	14.03	10.78	0.22	7.39	12.16	2.57	0.20	0.14	99.25	610.5
49.50	1.73	13.78	10.70	0.15	7.49	12.25	2.52	0.17	0.24	98.68	612.4
49.77	1.64	14.01	10.71	0.23	7.46	11.97	2.59	0.22	0.14	98.89	622.1
49.63	1.67	13.97	10.84	0.23	7.46	12.01	2.65	0.18	0.19	99.01	625.5
49.65	1.63	13.85	10.81	0.20	7.38	12.27	2.51	0.17	0.11	98.70	629.1
49.51	1.55	13.94	10.93	0.18	7.44	11.92	2.55	0.20	0.23	98.61	638.0
49.72	1.71	13.87	10.95	0.21	7.38	11.90	2.60	0.16	0.13	98.76	640.5

49.57	1.64	14.03	10.83	0.22	7.45	12.03	2.56	0.19	0.07	98.76	645.8
49.41	1.59	14.15	10.98	0.23	7.44	11.70	2.73	0.18	0.18	98.73	653.8
49.81	1.71	13.95	11.04	0.18	7.40	11.80	2.70	0.22	0.18	99.18	655.5
49.77	1.71	13.95	10.96	0.20	7.37	12.00	2.58	0.21	0.21	99.09	662.5
49.45	1.60	14.11	11.05	0.23	7.41	11.72	2.73	0.24	0.15	98.85	669.7
49.77	1.76	14.01	10.99	0.24	7.30	11.71	2.62	0.19	0.13	98.89	670.5
49.83	1.75	13.92	11.01	0.18	7.32	11.91	2.67	0.22	0.15	99.10	679.1
49.60	1.74	14.16	11.25	0.24	7.26	11.72	2.62	0.23	0.18	99.18	685.4
49.78	1.71	13.98	11.01	0.16	7.32	11.97	2.62	0.21	0.18	99.08	695.8
49.27	1.76	14.05	11.28	0.20	7.23	11.74	2.63	0.18	0.28	98.75	700.4
49.56	1.72	14.10	11.10	0.16	7.17	11.69	2.55	0.18	0.20	98.60	712.5
49.92	1.64	14.23	11.22	0.22	7.19	11.60	2.65	0.17	0.14	99.14	715.4
49.91	1.52	14.13	11.21	0.23	7.14	11.75	2.65	0.20	0.17	99.04	729.1
49.76	1.71	14.13	11.20	0.14	7.19	11.72	2.70	0.18	0.11	98.95	729.2
49.38	1.71	14.06	11.43	0.12	7.25	11.57	2.71	0.18	0.12	98.71	730.4
49.28	1.75	14.12	11.47	0.22	7.14	11.37	2.70	0.17	0.21	98.55	745.4
49.70	1.75	14.11	11.21	0.22	7.13	11.67	2.68	0.18	0.10	98.91	745.9
49.65	1.47	14.15	11.21	0.19	7.17	11.47	2.68	0.17	0.10	98.39	749.5
49.70	1.71	14.04	11.39	0.25	7.24	11.66	2.74	0.16	0.21	99.26	762.5
49.34	1.63	14.09	11.36	0.13	7.22	11.54	2.68	0.19	0.21	98.54	770.0
49.63	1.68	14.14	11.51	0.16	7.21	11.49	2.72	0.21	0.25	99.15	779.3
49.79	1.53	13.92	11.66	0.26	6.94	11.19	2.68	0.21	0.12	98.45	784.3
50.09	1.42	14.18	11.58	0.19	6.90	10.88	2.73	0.20	0.24	98.54	791.0
49.62	1.78	14.07	11.34	0.16	7.12	11.51	2.80	0.17	0.19	98.95	796.0
49.82	1.47	14.20	11.57	0.18	7.03	11.18	2.70	0.19	0.23	98.70	801.4
49.53	1.48	14.08	11.77	0.22	7.02	10.91	2.69	0.19	0.21	98.24	810.5
49.55	1.69	14.02	11.56	0.23	7.12	11.56	2.69	0.18	0.19	98.95	812.7
49.72	1.57	14.04	11.68	0.14	7.02	11.09	2.75	0.15	0.17	98.44	815.0
49.70	1.48	14.18	11.65	0.26	7.06	11.09	2.74	0.18	0.25	98.72	827.7
49.69	1.77	14.16	11.47	0.18	7.00	11.37	2.68	0.18	0.13	98.78	829.4
49.30	1.59	14.24	11.69	0.17	7.00	11.04	2.85	0.16	0.10	98.27	836.9
49.73	1.62	14.23	11.65	0.26	7.05	11.14	2.73	0.21	0.12	98.87	838.9
49.52	1.70	14.20	11.45	0.25	7.03	11.24	2.68	0.20	0.21	98.59	846.0
49.60	1.53	14.15	11.71	0.22	6.93	10.99	2.75	0.15	0.17	98.32	854.1
49.37	1.79	14.06	11.52	0.20	7.05	11.25	2.72	0.20	0.19	98.48	862.7
49.22	1.53	14.14	11.67	0.27	7.04	10.97	2.73	0.20	0.25	98.16	862.9
48.91	1.55	14.24	11.90	0.19	6.99	10.99	2.78	0.19	0.17	98.03	863.1
48.78	1.71	14.17	11.69	0.19	7.00	11.41	2.67	0.15	0.12	98.06	879.4
49.65	1.48	14.27	11.86	0.10	6.97	10.85	2.64	0.18	0.21	98.32	880.5
49.93	1.60	13.94	11.84	0.22	6.96	11.09	2.67	0.17	0.17	98.74	882.1
48.99	1.49	14.04	11.86	0.19	6.97	11.06	2.77	0.12	0.16	97.83	886.9
49.51	1.50	14.13	11.81	0.18	7.08	10.82	2.73	0.18	0.13	98.19	906.9
49.93	1.61	13.93	11.67	0.21	6.95	10.89	2.71	0.23	0.17	98.46	916.2
49.49	1.64	14.16	11.74	0.31	6.96	11.02	2.70	0.19	0.18	98.52	917.3
50.50	1.58	14.14	11.66	0.17	6.99	11.03	2.70	0.19	0.13	99.22	921.8
49.92	1.72	14.16	11.96	0.15	6.95	11.04	2.73	0.18	0.15	99.12	951.5
49.71	1.54	14.12	11.94	0.18	6.95	11.03	2.72	0.20	0.29	98.79	952.6
49.43	1.52	14.14	11.87	0.21	7.03	10.92	2.76	0.17	0.22	98.43	957.1
49.70	1.68	14.14	11.82	0.23	6.92	10.99	2.72	0.18	0.21	98.68	986.6

49.39	1.57	14.14	11.77	0.20	6.96	10.86	2.76	0.17	0.12	98.12	987.9
49.63	1.67	14.11	11.84	0.25	6.91	11.03	2.70	0.15	0.15	98.58	1021.9
49.62	1.68	14.09	11.93	0.21	6.85	11.09	2.74	0.16	0.16	98.67	1023.2
49.78	1.51	14.18	11.88	0.28	6.98	10.78	2.67	0.18	0.12	98.49	1027.6
49.59	1.62	14.21	12.05	0.14	6.92	11.12	2.66	0.17	0.22	98.85	1057.1
49.71	1.70	14.11	11.94	0.14	6.98	10.87	2.69	0.17	0.18	98.62	1058.4
49.46	1.49	14.05	11.86	0.27	6.93	10.66	2.72	0.16	0.25	97.96	1062.7
49.37	1.64	14.00	11.79	0.19	6.88	11.07	2.71	0.20	0.24	98.24	1092.4
49.69	1.55	14.19	11.83	0.20	6.84	11.12	2.67	0.16	0.10	98.50	1093.7
49.47	1.43	14.22	12.21	0.27	6.98	10.60	2.71	0.19	0.25	98.48	1098.0
49.57	1.64	14.19	12.06	0.24	6.98	10.97	2.76	0.19	0.09	98.87	1127.5
49.08	1.60	14.28	11.91	0.23	6.87	10.90	2.74	0.16	0.20	98.08	1129.0
49.78	1.49	14.08	11.93	0.28	6.99	10.93	2.75	0.16	0.12	98.66	1133.2
49.50	1.67	14.20	11.96	0.20	6.98	11.05	2.75	0.15	0.26	98.83	1162.8
49.61	1.59	14.13	12.10	0.25	6.90	10.90	2.70	0.20	0.19	98.72	1164.3
49.65	1.46	14.23	12.18	0.18	6.95	11.03	2.72	0.18	0.23	98.94	1168.5
49.37	1.66	14.18	12.13	0.22	6.93	10.99	2.71	0.15	0.15	98.62	1198.0
49.75	1.58	14.17	12.09	0.19	6.90	10.93	2.81	0.16	0.21	98.93	1203.6
49.53	1.58	14.20	12.08	0.22	7.02	10.82	2.73	0.18	0.15	98.62	1232.8
49.13	1.59	14.11	12.01	0.19	6.83	10.93	2.72	0.16	0.23	98.05	1267.7
49.64	1.51	14.06	12.00	0.22	6.97	10.96	2.77	0.19	0.15	98.58	1272.3
49.29	1.73	14.08	11.99	0.15	6.89	10.99	2.79	0.24	0.18	98.43	1301.4
49.48	1.48	14.15	12.02	0.22	7.00	10.78	2.70	0.17	0.23	98.38	1337.6
49.68	1.58	14.24	12.04	0.24	7.00	10.87	2.72	0.14	0.10	98.74	1341.0
49.46	1.65	14.04	11.96	0.12	6.95	10.90	2.68	0.19	0.26	98.34	1369.9
49.57	1.59	14.18	12.05	0.22	6.99	10.73	2.78	0.19	0.21	98.62	1407.3
49.50	1.56	14.07	12.08	0.18	6.93	10.76	2.77	0.17	0.18	98.33	1409.5
49.42	1.62	14.20	12.15	0.19	6.98	11.00	2.76	0.17	0.11	98.70	1438.5
49.34	1.56	14.06	11.97	0.28	6.99	10.92	2.72	0.17	0.21	98.35	1477.1
49.51	1.66	14.13	11.91	0.23	6.94	10.94	2.78	0.13	0.13	98.48	1478.2
49.59	1.51	14.17	12.04	0.25	7.01	10.72	2.77	0.18	0.21	98.62	1507.0
49.57	1.77	14.23	11.95	0.23	7.00	10.93	2.67	0.20	0.15	98.84	1546.7
49.44	1.51	14.16	11.92	0.23	6.99	10.83	2.73	0.23	0.18	98.36	1546.9
49.63	1.63	14.10	12.15	0.17	6.97	10.91	2.72	0.21	0.12	98.73	1575.6
49.37	1.50	14.16	12.04	0.13	6.98	10.80	2.68	0.18	0.21	98.18	1616.7

Appendix E
Fittings to Composition Profiles of Clinopyroxene Dissolution in Basalt

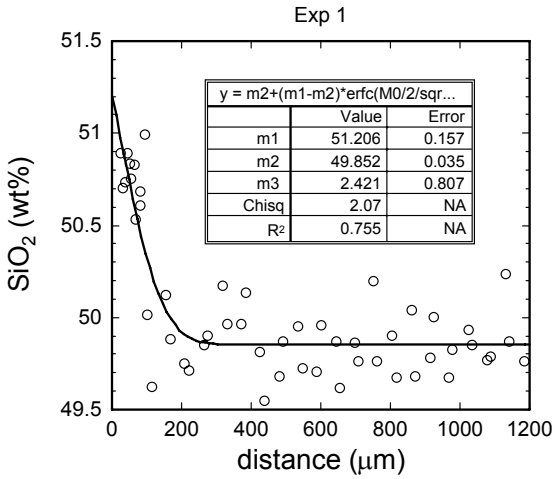

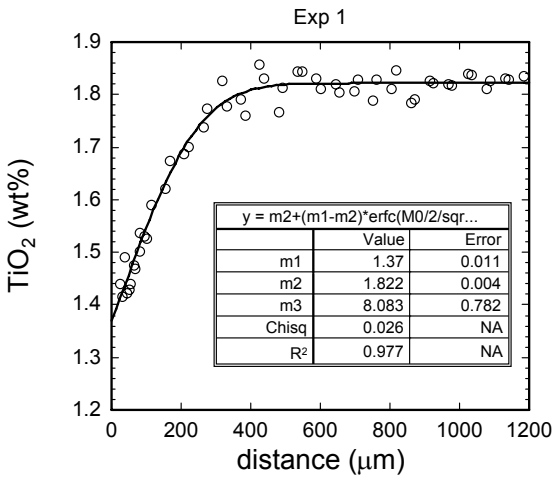

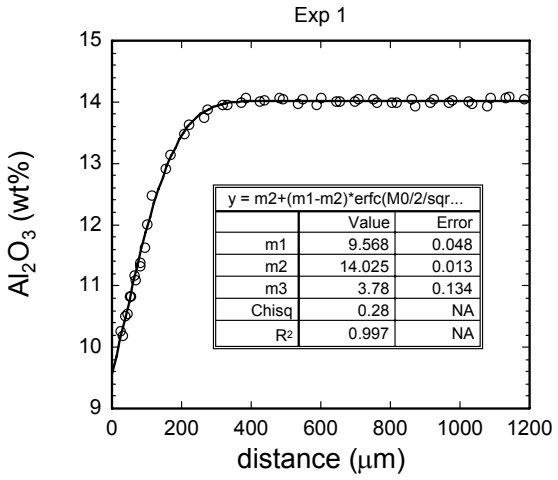

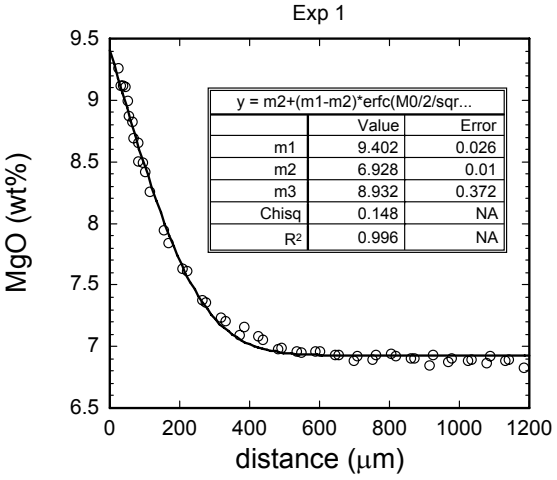

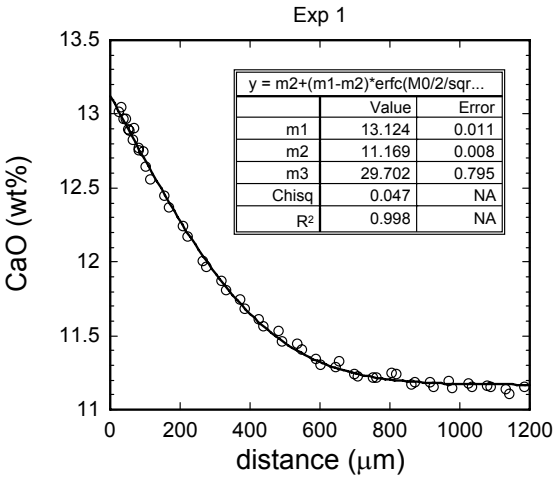

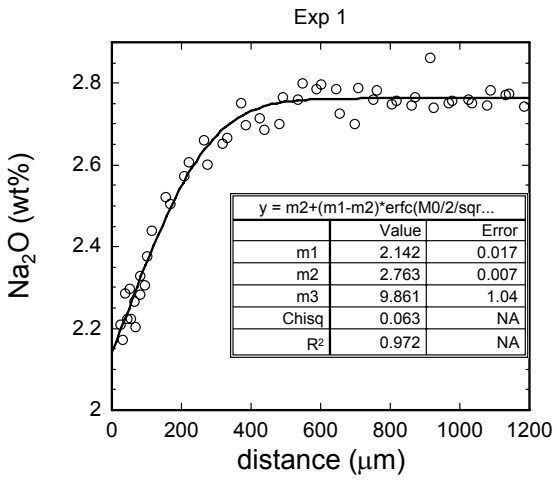

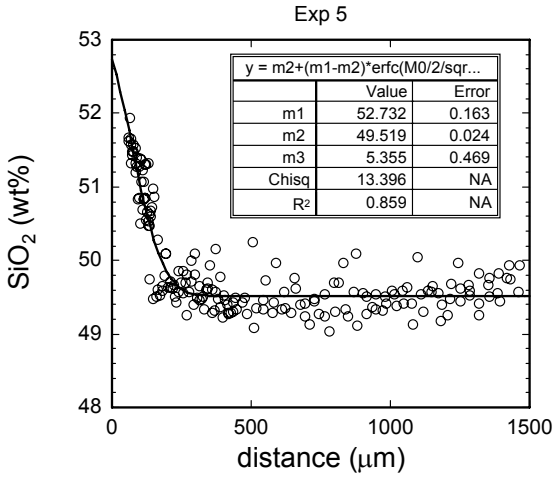
Exp 5
y = m2+(m1-m2)*erfc(M0/2/sqr...
Value Error
m1 52.732 0.163
m2 49.519 0.024
m3 5.355 0.469
Chisq 13.396 NA
R² 0.859 NA
SiO2 (wt%)
distance (μm)

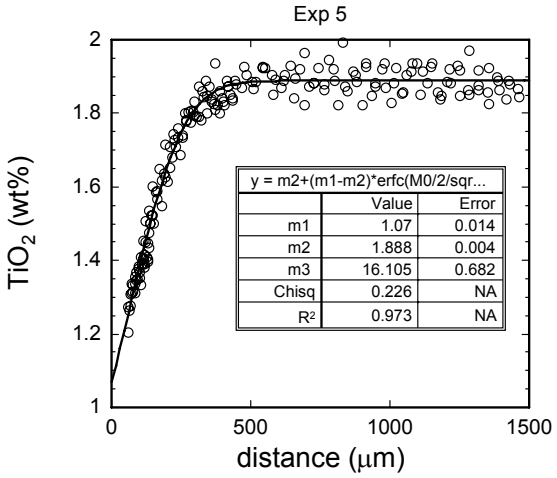
Exp 5
y = m2+(m1-m2)*erfc(M0/2/sqr...
Value Error
m1 1.07 0.014
m2 1.888 0.004
m3 16.105 0.682
Chisq 0.226 NA
R² 0.973 NA
TiO2 (wt%)
distance (μm)

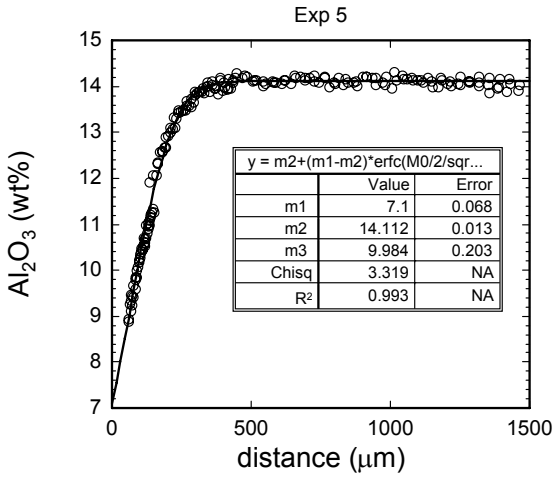
Exp 5
y = m2+(m1-m2)*erfc(M0/2/sqr...
Value Error
m1 7.1 0.068
m2 14.112 0.013
m3 9.984 0.203
Chisq 3.319 NA
R² 0.993 NA
Al2O3 (wt%)
distance (μm)

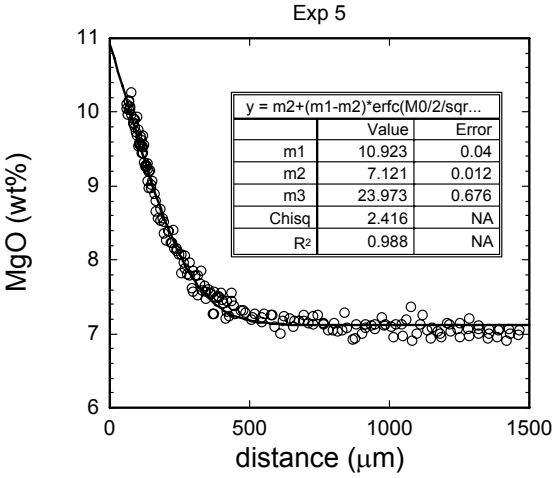
Exp 5
y = m2+(m1-m2)*erfc(M0/2/sqr...
Value Error
m1 10.923 0.04
m2 7.121 0.012
m3 23.973 0.676
Chisq 2.416 NA
R² 0.988 NA
MgO (wt%)
distance (μm)

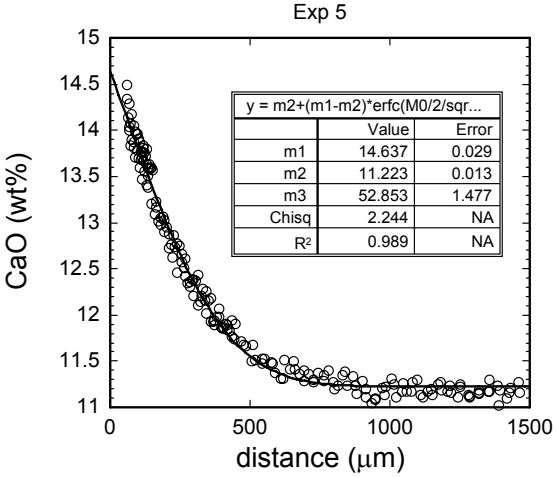
Exp 5
y = m2+(m1-m2)*erfc(M0/2/sqr...
Value Error
m1 14.637 0.029
m2 11.223 0.013
m3 52.853 1.477
Chisq 2.244 NA
R² 0.989 NA
CaO (wt%)
distance (μm)

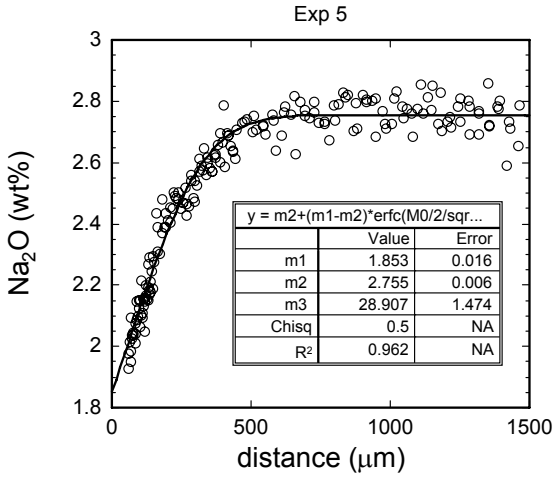
Exp 5
y = m2+(m1-m2)*erfc(M0/2/sqr...
Value Error
m1 1.853 0.016
m2 2.755 0.006
m3 28.907 1.474
Chisq 0.5 NA
R² 0.962 NA
Na2O (wt%)
distance (μm)

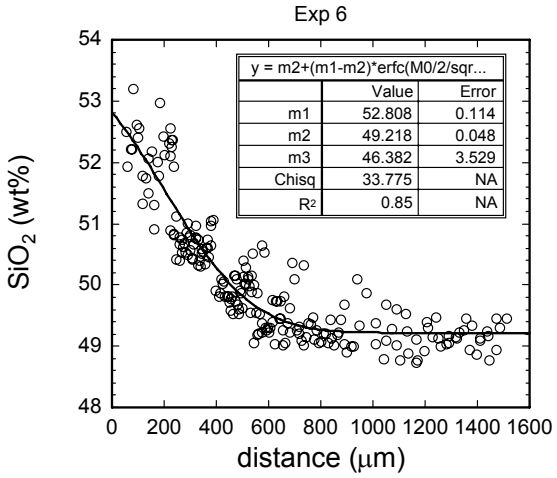
Exp 6
SiO2 (wt%)
distance (μm)
y = m2+(m1-m2)*erfc(M0/2/sqr...
Value Error
m1 52.808 0.114
m2 49.218 0.048
m3 46.382 3.529
Chisq 33.775 NA
R² 0.85 NA

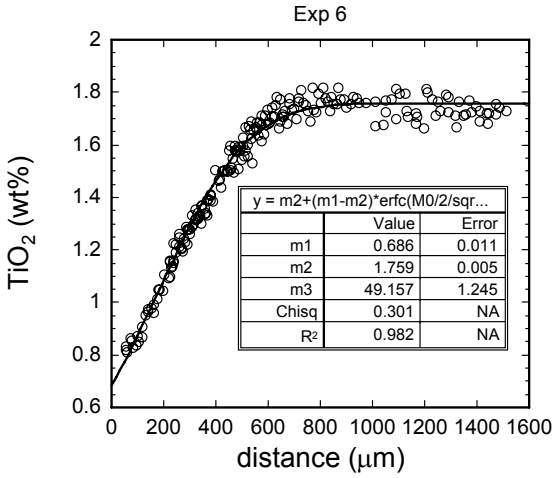
Exp 6
TiO2 (wt%)
distance (μm)
y = m2+(m1-m2)*erfc(M0/2/sqr...
Value Error
m1 0.686 0.011
m2 1.759 0.005
m3 49.157 1.245
Chisq 0.301 NA
R² 0.982 NA

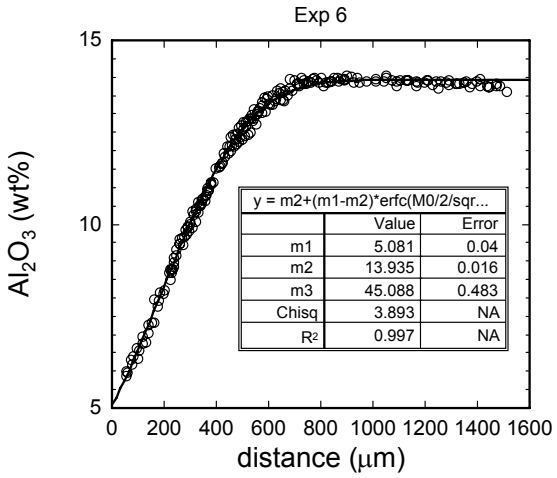
Exp 6
Al2O3 (wt%)
distance (μm)
y = m2+(m1-m2)*erfc(M0/2/sqr...
Value Error
m1 5.081 0.04
m2 13.935 0.016
m3 45.088 0.483
Chisq 3.893 NA
R² 0.997 NA

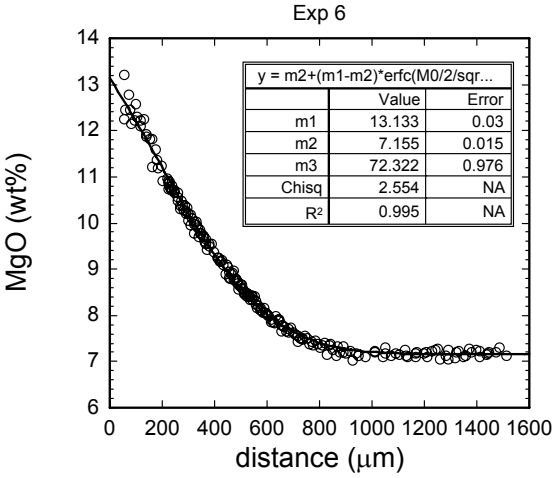
Exp 6
MgO (wt%)
distance (μm)
y = m2+(m1-m2)*erfc(M0/2/sqr...
Value Error
m1 13.133 0.03
m2 7.155 0.015
m3 72.322 0.976
Chisq 2.554 NA
R² 0.995 NA

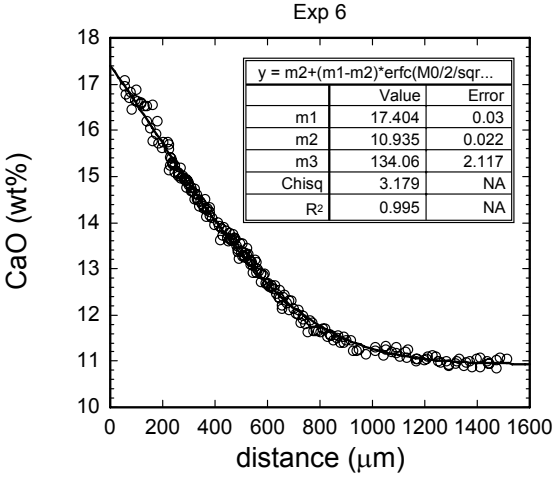
Exp 6
CaO (wt%)
distance (μm)
y = m2+(m1-m2)*erfc(M0/2/sqr...
Value Error
m1 17.404 0.03
m2 10.935 0.022
m3 134.06 2.117
Chisq 3.179 NA
R² 0.995 NA

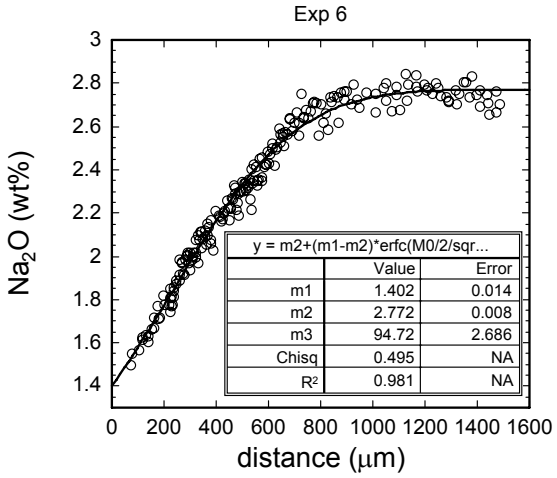
Exp 6
Na2O (wt%)
distance (μm)
y = m2+(m1-m2)*erfc(M0/2/sqr...
Value Error
m1 1.402 0.014
m2 2.772 0.008
m3 94.72 2.686
Chisq 0.495 NA
R² 0.981 NA

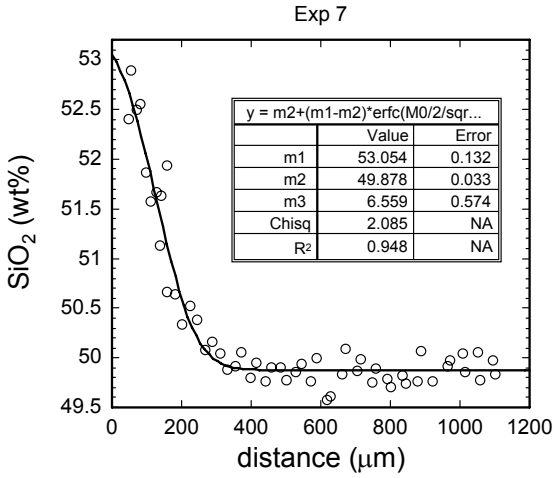
Exp 7
SiO2 (wt%)
distance (μm)
y = m2+(m1-m2)*erfc(M0/2/sqr...
Value Error
m1 53.054 0.132
m2 49.878 0.033
m3 6.559 0.574
Chisq 2.085 NA
R² 0.948 NA

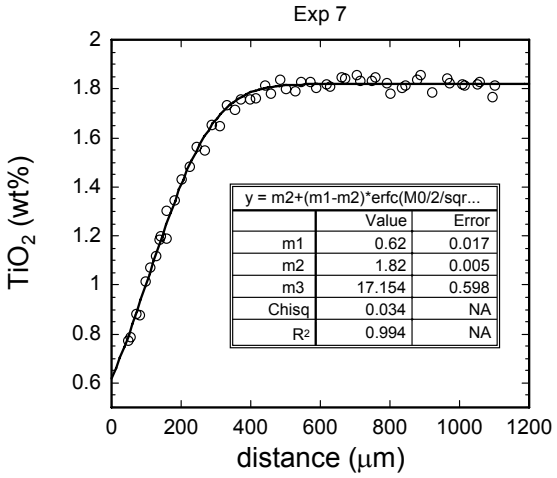
Exp 7
TiO2 (wt%)
distance (μm)
y = m2+(m1-m2)*erfc(M0/2/sqr...
Value Error
m1 0.62 0.017
m2 1.82 0.005
m3 17.154 0.598
Chisq 0.034 NA
R² 0.994 NA

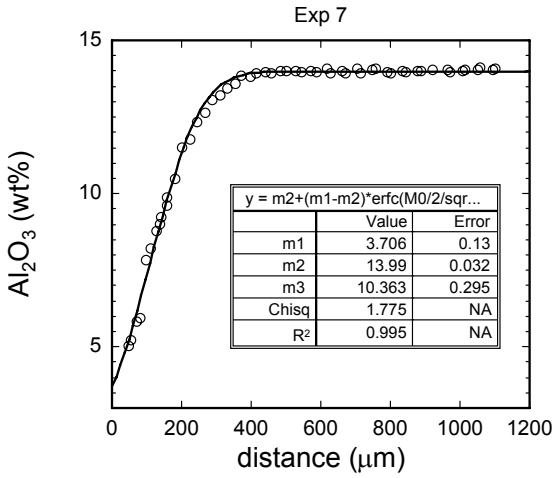
Exp 7
Al2O3 (wt%)
distance (μm)
y = m2+(m1-m2)*erfc(M0/2/sqr...
Value Error
m1 3.706 0.13
m2 13.99 0.032
m3 10.363 0.295
Chisq 1.775 NA
R² 0.995 NA

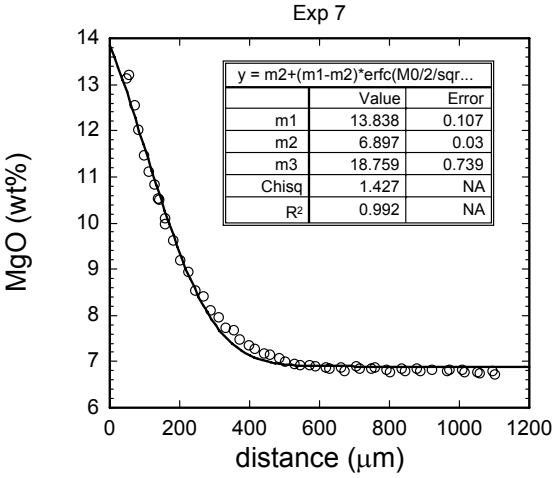
Exp 7
MgO (wt%)
distance (μm)
y = m2+(m1-m2)*erfc(M0/2/sqr...
Value Error
m1 13.838 0.107
m2 6.897 0.03
m3 18.759 0.739
Chisq 1.427 NA
R² 0.992 NA

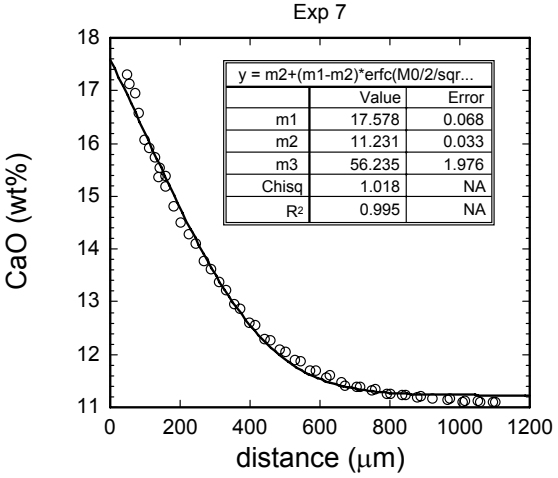
Exp 7
CaO (wt%)
distance (μm)
y = m2+(m1-m2)*erfc(M0/2/sqr...
Value Error
m1 17.578 0.068
m2 11.231 0.033
m3 56.235 1.976
Chisq 1.018 NA
R² 0.995 NA

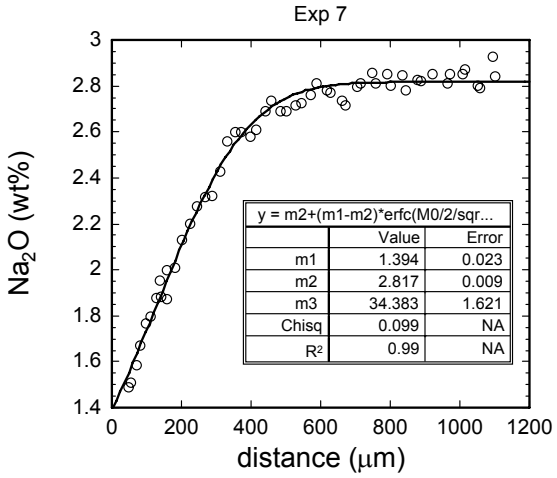
Exp 7
Na2O (wt%)
distance (μm)
y = m2+(m1-m2)*erfc(M0/2/sqr...
Value Error
m1 1.394 0.023
m2 2.817 0.009
m3 34.383 1.621
Chisq 0.099 NA
R² 0.99 NA

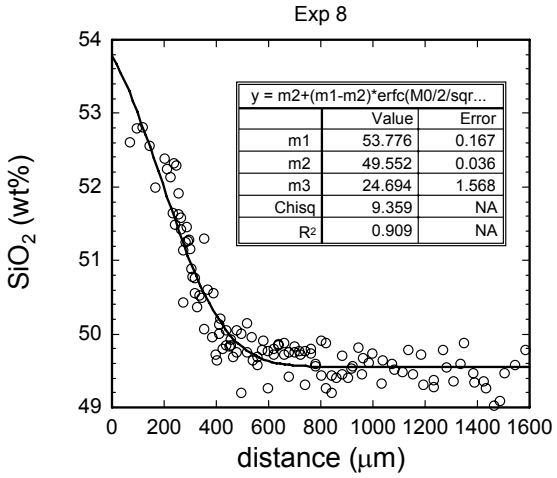
Exp 8
SiO2 (wt%)
distance (μm)
y = m2+(m1-m2)*erfc(M0/2/sqr...
Value Error
m1 53.776 0.167
m2 49.552 0.036
m3 24.694 1.568
Chisq 9.359 NA
R² 0.909 NA

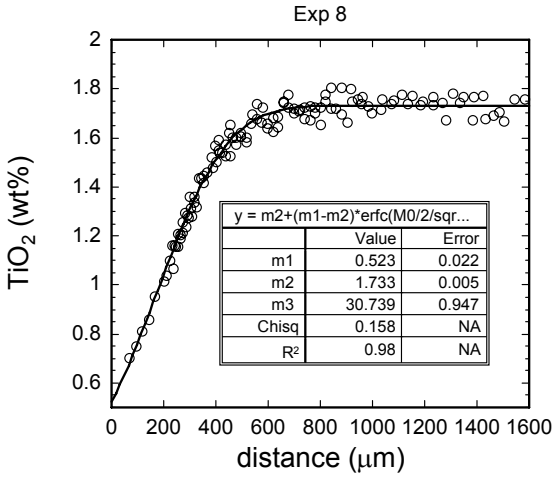
Exp 8
TiO2 (wt%)
distance (μm)
y = m2+(m1-m2)*erfc(M0/2/sqr...
Value Error
m1 0.523 0.022
m2 1.733 0.005
m3 30.739 0.947
Chisq 0.158 NA
R² 0.98 NA

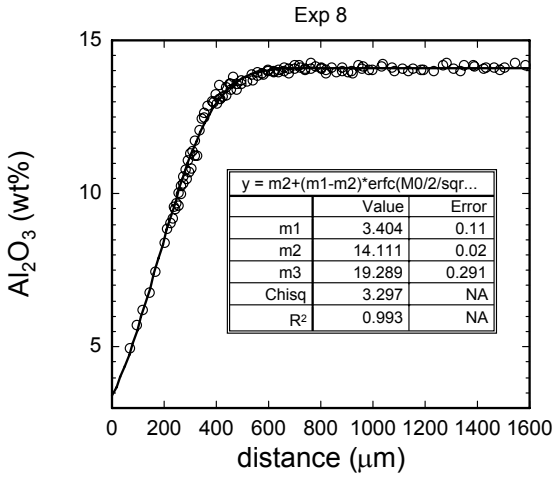
Exp 8
Al2O3 (wt%)
distance (μm)
y = m2+(m1-m2)*erfc(M0/2/sqr...
Value Error
m1 3.404 0.11
m2 14.111 0.02
m3 19.289 0.291
Chisq 3.297 NA
R² 0.993 NA

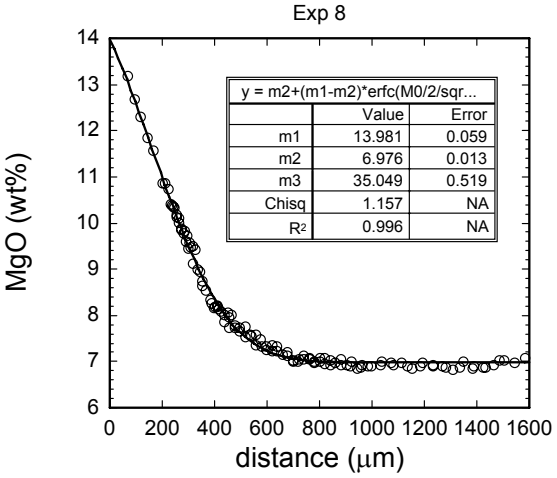
Exp 8
MgO (wt%)
distance (μm)
y = m2+(m1-m2)*erfc(M0/2/sqr...
Value Error
m1 13.981 0.059
m2 6.976 0.013
m3 35.049 0.519
Chisq 1.157 NA
R² 0.996 NA

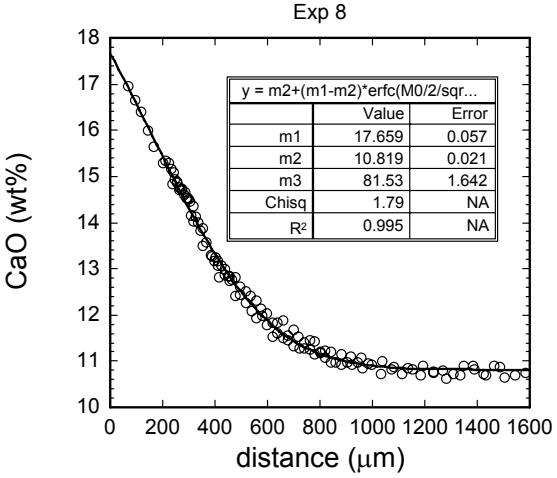
Exp 8
CaO (wt%)
distance (μm)
y = m2+(m1-m2)*erfc(M0/2/sqr...
Value Error
m1 17.659 0.057
m2 10.819 0.021
m3 81.53 1.642
Chisq 1.79 NA
R² 0.995 NA

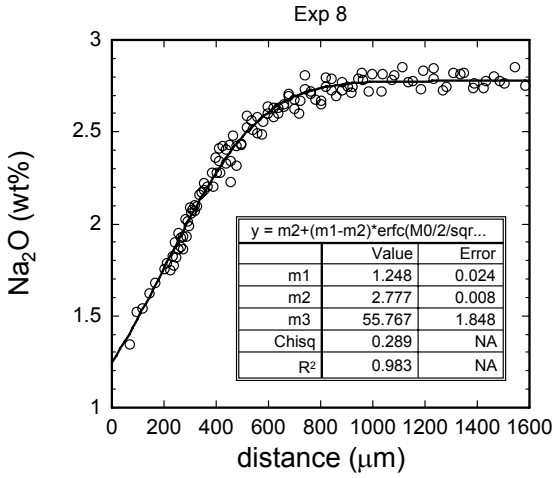
Exp 8
Na2O (wt%)
distance (μm)
y = m2+(m1-m2)*erfc(M0/2/sqr...
Value Error
m1 1.248 0.024
m2 2.777 0.008
m3 55.767 1.848
Chisq 0.289 NA
R² 0.983 NA

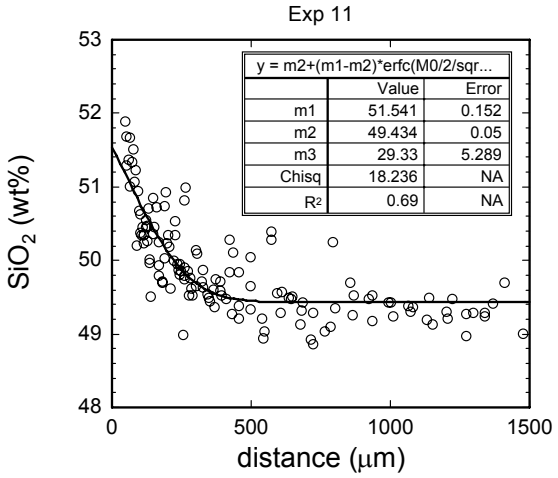
Exp 11
y = m2+(m1-m2)*erfc(M0/2/sqr...
Value Error
m1 51.541 0.152
m2 49.434 0.05
m3 29.33 5.289
Chisq 18.236 NA
R² 0.69 NA
SiO2 (wt%)
distance (μm)

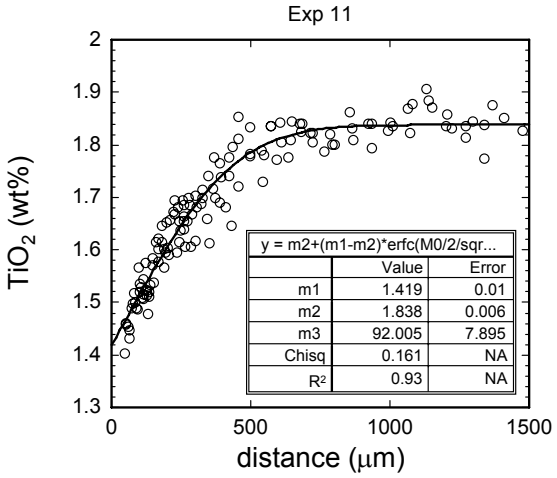
Exp 11
y = m2+(m1-m2)*erfc(M0/2/sqr...
Value Error
m1 1.419 0.01
m2 1.838 0.006
m3 92.005 7.895
Chisq 0.161 NA
R² 0.93 NA
TiO2 (wt%)
distance (μm)

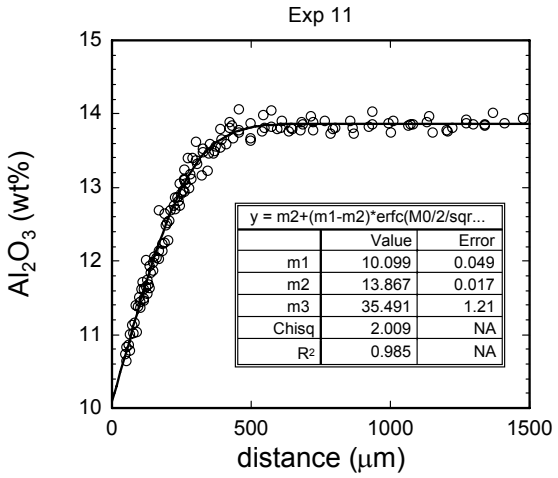
Exp 11
y = m2+(m1-m2)*erfc(M0/2/sqr...
Value Error
m1 10.099 0.049
m2 13.867 0.017
m3 35.491 1.21
Chisq 2.009 NA
R² 0.985 NA
Al2O3 (wt%)
distance (μm)

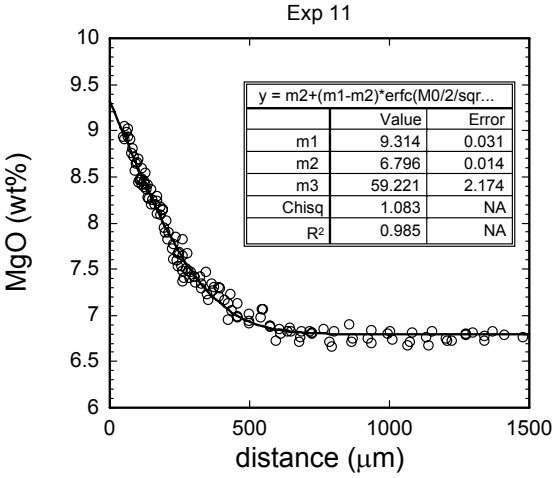
Exp 11
y = m2+(m1-m2)*erfc(M0/2/sqr...
Value Error
m1 9.314 0.031
m2 6.796 0.014
m3 59.221 2.174
Chisq 1.083 NA
R² 0.985 NA
MgO (wt%)
distance (μm)

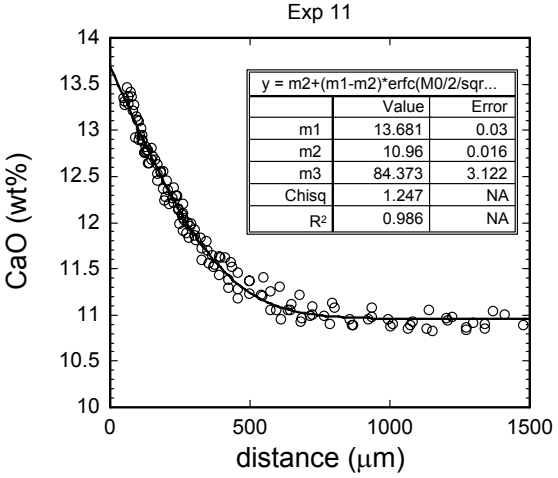
Exp 11
y = m2+(m1-m2)*erfc(M0/2/sqr...
Value Error
m1 13.681 0.03
m2 10.96 0.016
m3 84.373 3.122
Chisq 1.247 NA
R² 0.986 NA
CaO (wt%)
distance (μm)

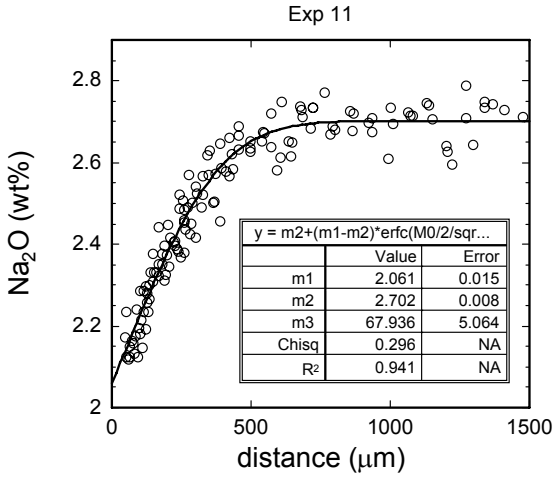
Exp 11
y = m2+(m1-m2)*erfc(M0/2/sqr...
Value Error
m1 2.061 0.015
m2 2.702 0.008
m3 67.936 5.064
Chisq 0.296 NA
R² 0.941 NA
Na2O (wt%)
distance (μm)

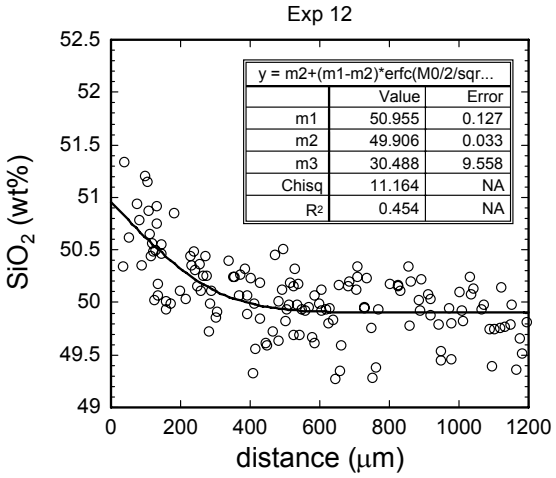
Exp 12
SiO2 (wt%)
distance (μm)
y = m2+(m1-m2)*erfc(M0/2/sqr...
Value Error
m1 50.955 0.127
m2 49.906 0.033
m3 30.488 9.558
Chisq 11.164 NA
R² 0.454 NA

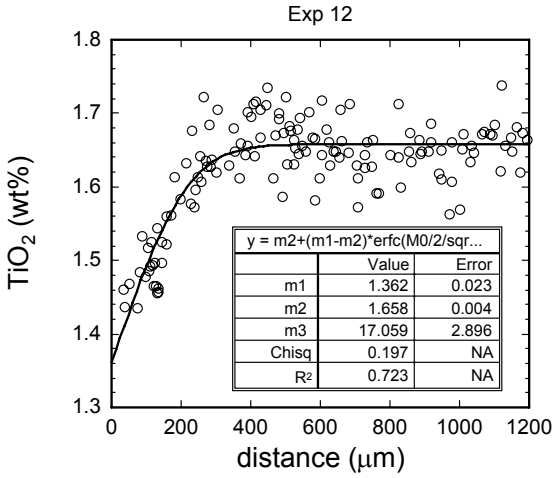
Exp 12
TiO2 (wt%)
distance (μm)
y = m2+(m1-m2)*erfc(M0/2/sqr...
Value Error
m1 1.362 0.023
m2 1.658 0.004
m3 17.059 2.896
Chisq 0.197 NA
R² 0.723 NA

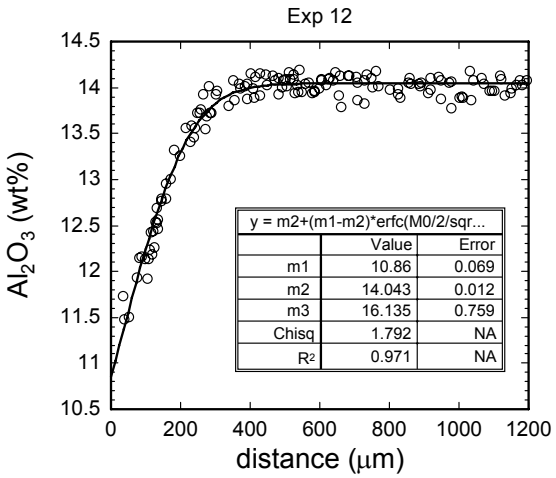
Exp 12
Al2O3 (wt%)
distance (μm)
y = m2+(m1-m2)*erfc(M0/2/sqr...
Value Error
m1 10.86 0.069
m2 14.043 0.012
m3 16.135 0.759
Chisq 1.792 NA
R² 0.971 NA

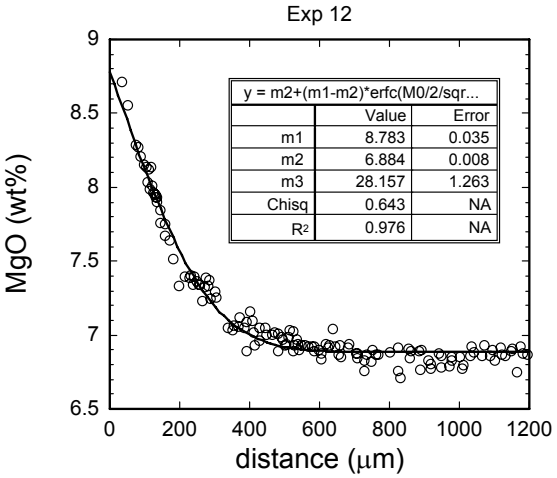
Exp 12
MgO (wt%)
distance (μm)
y = m2+(m1-m2)*erfc(M0/2/sqr...
Value Error
m1 8.783 0.035
m2 6.884 0.008
m3 28.157 1.263
Chisq 0.643 NA
R² 0.976 NA

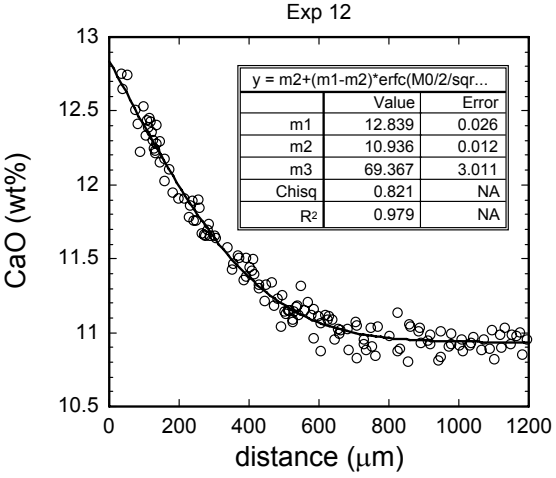
Exp 12
CaO (wt%)
distance (μm)
y = m2+(m1-m2)*erfc(M0/2/sqr...
Value Error
m1 12.839 0.026
m2 10.936 0.012
m3 69.367 3.011
Chisq 0.821 NA
R² 0.979 NA

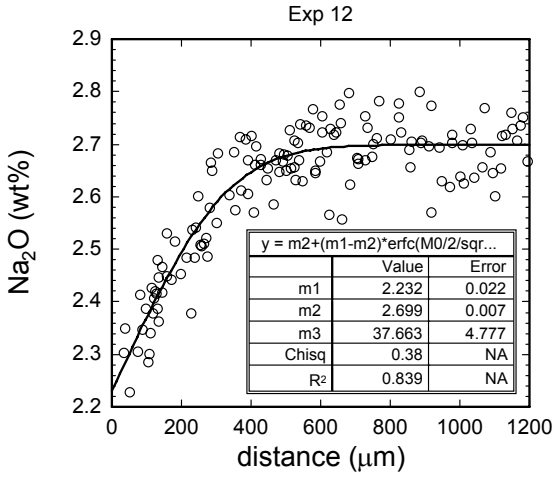
Exp 12
Na2O (wt%)
distance (μm)
y = m2+(m1-m2)*erfc(M0/2/sqr...
Value Error
m1 2.232 0.022
m2 2.699 0.007
m3 37.663 4.777
Chisq 0.38 NA
R² 0.839 NA

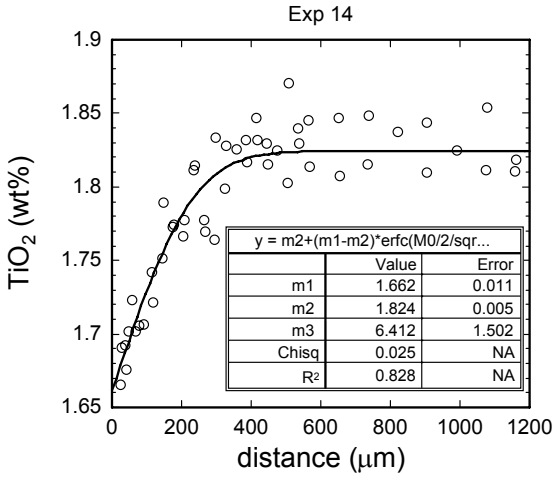
Exp 14
TiO2 (wt%)
distance (μm)
y = m2+(m1-m2)*erfc(M0/2/sqr...
Value Error
m1 1.662 0.011
m2 1.824 0.005
m3 6.412 1.502
Chisq 0.025 NA
R² 0.828 NA

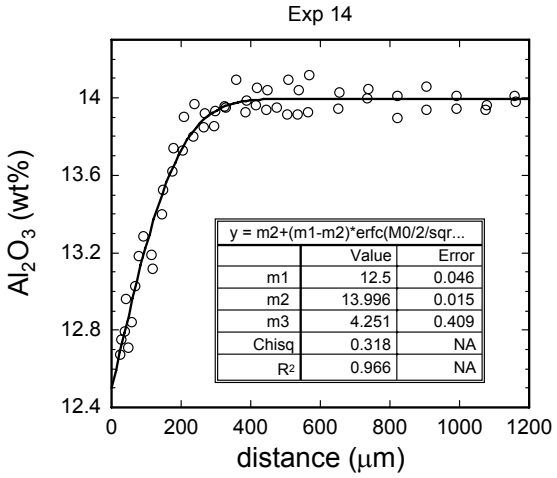
Exp 14
Al2O3 (wt%)
distance (μm)
y = m2+(m1-m2)*erfc(M0/2/sqr...
Value Error
m1 12.5 0.046
m2 13.996 0.015
m3 4.251 0.409
Chisq 0.318 NA
R² 0.966 NA

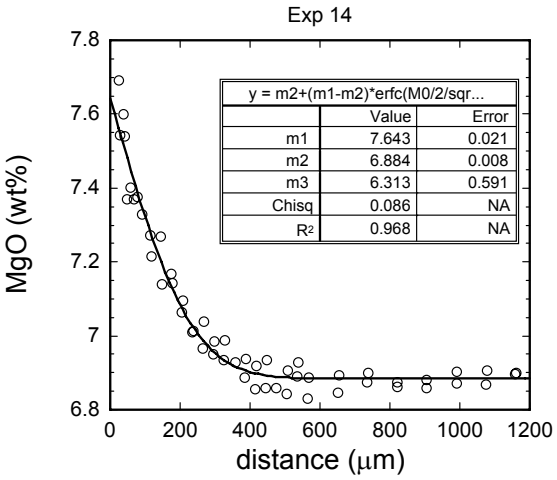
Exp 14
MgO (wt%)
distance (μm)
y = m2+(m1-m2)*erfc(M0/2/sqr...
Value Error
m1 7.643 0.021
m2 6.884 0.008
m3 6.313 0.591
Chisq 0.086 NA
R² 0.968 NA

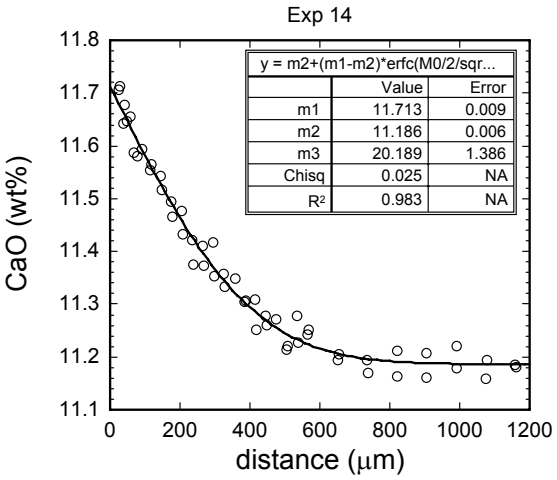
Exp 14
CaO (wt%)
distance (μm)
y = m2+(m1-m2)*erfc(M0/2/sqr...
Value Error
m1 11.713 0.009
m2 11.186 0.006
m3 20.189 1.386
Chisq 0.025 NA
R² 0.983 NA

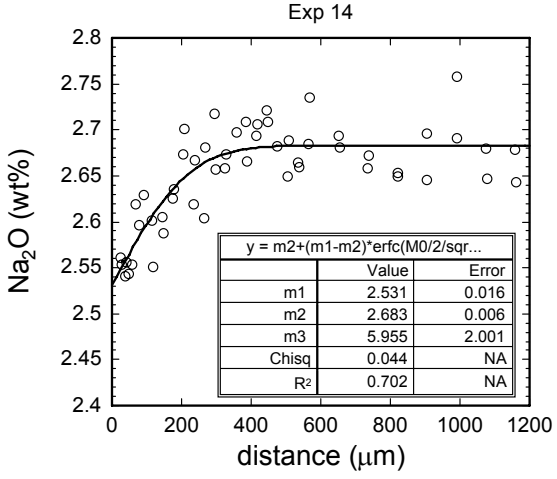
Exp 14
Na2O (wt%)
distance (μm)
y = m2+(m1-m2)*erfc(M0/2/sqr...
Value Error
m1 2.531 0.016
m2 2.683 0.006
m3 5.955 2.001
Chisq 0.044 NA
R² 0.702 NA

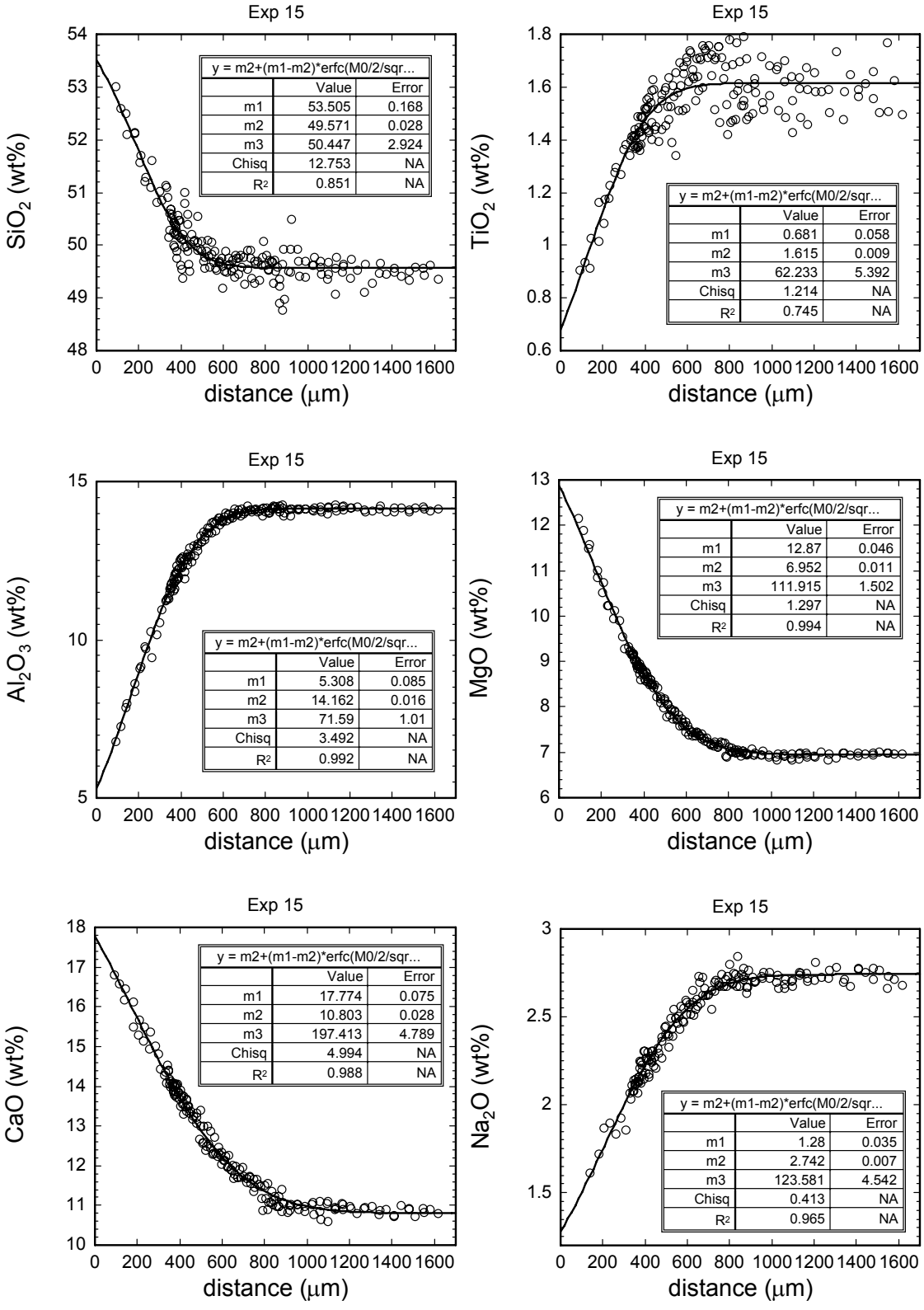
Exp 15
SiO2 (wt%)
distance (μm)
y = m2+(m1-m2)*erfc(M0/2/sqr...
Value Error
m1 53.505 0.168
m2 49.571 0.028
m3 50.447 2.924
Chisq 12.753 NA
R² 0.851 NA
Exp 15
TiO2 (wt%)
distance (μm)
y = m2+(m1-m2)*erfc(M0/2/sqr...
Value Error
m1 0.681 0.058
m2 1.615 0.009
m3 62.233 5.392
Chisq 1.214 NA
R² 0.745 NA
Exp 15
Al2O3 (wt%)
distance (μm)
y = m2+(m1-m2)*erfc(M0/2/sqr...
Value Error
m1 5.308 0.085
m2 14.162 0.016
m3 71.59 1.01
Chisq 3.492 NA
R² 0.992 NA
Exp 15
MgO (wt%)
distance (μm)
y = m2+(m1-m2)*erfc(M0/2/sqr...
Value Error
m1 12.87 0.046
m2 6.952 0.011
m3 111.915 1.502
Chisq 1.297 NA
R² 0.994 NA
Exp 15
CaO (wt%)
distance (μm)
y = m2+(m1-m2)*erfc(M0/2/sqr...
Value Error
m1 17.774 0.075
m2 10.803 0.028
m3 197.413 4.789
Chisq 4.994 NA
R² 0.988 NA
Exp 15
Na2O (wt%)
distance (μm)
y = m2+(m1-m2)*erfc(M0/2/sqr...
Value Error
m1 1.28 0.035
m2 2.742 0.007
m3 123.581 4.542
Chisq 0.413 NA
R² 0.965 NA